frontiers | Research Topics

Submarine canyons: Human connections to the deep sea

Edited by
Awantha Dissanayake, Veerle Ann Ida Huvenne, Jaime Selina Davies and Kostas Kiriakoulakis

Published in
Frontiers in Marine Science

ISSN 1664-8714
ISBN 978-2-8325-3991-0
DOI 10.3389/978-2-8325-3991-0

About Frontiers

Frontiers is more than just an open access publisher of scholarly articles: it is a pioneering approach to the world of academia, radically improving the way scholarly research is managed. The grand vision of Frontiers is a world where all people have an equal opportunity to seek, share and generate knowledge. Frontiers provides immediate and permanent online open access to all its publications, but this alone is not enough to realize our grand goals.

Frontiers journal series

The Frontiers journal series is a multi-tier and interdisciplinary set of open-access, online journals, promising a paradigm shift from the current review, selection and dissemination processes in academic publishing. All Frontiers journals are driven by researchers for researchers; therefore, they constitute a service to the scholarly community. At the same time, the *Frontiers journal series* operates on a revolutionary invention, the tiered publishing system, initially addressing specific communities of scholars, and gradually climbing up to broader public understanding, thus serving the interests of the lay society, too.

Dedication to quality

Each Frontiers article is a landmark of the highest quality, thanks to genuinely collaborative interactions between authors and review editors, who include some of the world's best academicians. Research must be certified by peers before entering a stream of knowledge that may eventually reach the public - and shape society; therefore, Frontiers only applies the most rigorous and unbiased reviews. Frontiers revolutionizes research publishing by freely delivering the most outstanding research, evaluated with no bias from both the academic and social point of view. By applying the most advanced information technologies, Frontiers is catapulting scholarly publishing into a new generation.

What are Frontiers Research Topics?

Frontiers Research Topics are very popular trademarks of the *Frontiers journals series*: they are collections of at least ten articles, all centered on a particular subject. With their unique mix of varied contributions from Original Research to Review Articles, Frontiers Research Topics unify the most influential researchers, the latest key findings and historical advances in a hot research area.

Find out more on how to host your own Frontiers Research Topic or contribute to one as an author by contacting the Frontiers editorial office: frontiersin.org/about/contact

Submarine canyons: Human connections to the deep sea

Topic editors

Awantha Dissanayake — University of Gibraltar, Gibraltar
Veerle Ann Ida Huvenne — University of Southampton, United Kingdom
Jaime Selina Davies — University of Plymouth, United Kingdom
Kostas Kiriakoulakis — Liverpool John Moores University, United Kingdom

Citation

Dissanayake, A., Huvenne, V. A. I., Davies, J. S., Kiriakoulakis, K., eds. (2023). *Submarine canyons: Human connections to the deep sea*. Lausanne: Frontiers Media SA.
doi: 10.3389/978-2-8325-3991-0

Table of contents

frontiers | Frontiers in Marine Science

TYPE Editorial
PUBLISHED 09 November 2023
DOI 10.3389/fmars.2023.1304429

OPEN ACCESS

EDITED AND REVIEWED BY
Ana Hilário,
University of Aveiro, Portugal

*CORRESPONDENCE
Awantha Dissanayake
Awantha.Dissanayake@unigib.edu.gi

RECEIVED 29 September 2023
ACCEPTED 24 October 2023
PUBLISHED 09 November 2023

CITATION
Dissanayake A, Davies JS, Kiriakoulakis K and Huvenne VAI (2023) Editorial: Submarine canyons: human connections to the deep sea.
Front. Mar. Sci. 10:1304429.
doi: 10.3389/fmars.2023.1304429

Editorial: Submarine canyons: human connections to the deep sea

Awantha Dissanayake[1]*, Jaime Selina Davies[1,2], Kostas Kiriakoulakis[3] and Veerle Ann Ida Huvenne[4]

[1]School of Marine & Environmental Sciences, University of Gibraltar, Gibraltar, Gibraltar, [2]School of Biological and Marine Sciences, University of Plymouth, Plymouth, United Kingdom, [3]Liverpool John Moores University, Liverpool, United Kingdom, [4]Ocean BioGeosciences, National Oceanography Centre, Southampton, United Kingdom

KEYWORDS

submarine canyon, deep sea, marine litter, faunal assemblage, anthropogenic impact

Editorial on the Research Topic
Submarine canyons: human connections to the deep sea

Submarine canyons are described as conduits to the deep sea where the interplay between oceanographic, biological/ecological processes, and bathymetric and topographical features have consequences on the functioning and associated diversity of both pelagic and benthic communities. Impacts from human activities range from fishing, resource extraction, and as transport 'sinks'. The true human connection to these important features is often unknown, under-reported, and/or poorly understood. In order to better address the various challenges submarine canyons face, there is a need to strengthen our understanding of the types of anthropogenic pressures on and threats to submarine canyons and their associated communities.

This Research Topic, *Submarine Canyons: Human Connections to the Deep Sea*, presents three review papers and eight original research papers from 20 different countries (70 authors), and presents research that spans the field of submarine canyons and the wider deep-sea area, providing insight into the links between anthropogenic activities and canyons. Here, we summarize some of the highlights derived from the 11 articles published in this Research Topic.

Marine litter

Marine litter or debris (hereafter marine litter) is, by far, one of the most prevalent and pervasive contaminant inputs found in submarine canyons. Four articles in this Research Topic delve into the issue of marine litter from a geoscience and transportation perspective as well as short and longer-term ecological perspectives. Pierdomenico et al. evaluate from the published literature various sources and transport mechanisms responsible for marine litter deposition within canyons, concluding that impacts from fishing gear are found to

accumulate on canyon heads and walls, whereas general debris items, mainly plastic, are subject to hydrodynamical processes within canyons and are generally linked to proximity to coastal riverine inputs.

A case study from southern Spain reports litter hotspots related to canyon morphological features such as rocky outcrops. Most of the debris found was attributed to coastal origin e.g., from beaches and nearly regional agricultural practices as well as fishing gear (Cerrillo-Escoriza et al.). Two review articles take a more policy-based approach to understanding marine litter impacts in canyons. Hernandez et al. highlight the need for a standardized framework of reporting of marine litter due to varying worldwide practices in identifying, enumerating, and classifying such items and only through an implemented standardized approach to reporting can patterns in use and, thus, submarine canyon vulnerability be identified. To attain an understanding of the true ecological effects, Bruemmer et al. have created a comprehensive, standardized Marine Litter-Faunal Interactions framework to qualify the types of litter interactions observed with marine fauna. The framework is applicable for use in all aquatic research, not just in studying submarine canyons. The framework is intentionally broad, providing six main categories of interactions, two of which also occur with abiotic features such as entanglement, ingestion, smothering, habitat provision, adaptive behavior, and encountering. Among publications that have reported litter-fauna (L-F) interactions in canyons, the large majority occur in the Mediterranean Sea, and the most reported interaction is of corals becoming entangled in fishing gear.

Sediments and transport

Paradis et al. evaluate the sediment transport and flux within the Palamós Canyon (NW Mediterranean) emanating from trawling activities during the trawling season (March – December) and seasonal closure (February). Using instrumented moorings deployed along the canyon axis and northern flank, it was found that fishing activities led to sediment flows at the canyon flank. Bottom trawling enhances the resuspension of degraded sediments and large particle fluxes within the canyon, the activity of which potentially affects canyon benthic communities. Tung et al. report on a case study on infaunal communities (meio- and macrofauna) within the Gaoping Submarine Canyon, Taiwan assessing the difference in biomass and body size, growth, metabolism, and size composition between canyon and adjacent continental slope. Larger individuals, both meio- and macrofauna, were observed within the slope than within the canyon. The dynamic nature of the canyon environment, with associated environmental conditions such as internal tides, bottom currents, and high sediment loading, are attributed to the lower community biomass, secondary production, and respiration rates.

Dobbs et al. assess how mobilization of sediments occurred across the Morro Bay continental slope (central California) from the Pleistocene to the present day. An integrated dataset encompassing multibeam bathymetry, sediment cores, radiocarbon samples, and isotope data was utilized. Results show that sediment deposition and clustering is predominantly due to lowstand sea-levels during the Last Glacial Maximum where canyons were directly connected to fluvial systems sequestered to the continental shelf. The implications for potential geohazards for offshore windfarm construction are discussed.

Faunal assemblages

Pearman et al. employ an interdisciplinary approach to evaluating faunal assemblages within the Whittard Canyon (North- East Atlantic). Using biological, hydrodynamic, and bathymetric datasets, a high- resolution analysis of the abiotic conditions within the biotic communities supports the hypothesis that spatial and temporal environmental heterogeneity from internal tides are an influencing factor of diversity on submarine canyon vertical walls. Brun et al. provide an insight into hydrodynamic processes with the Cassadaigne Canyon (Northwestern Mediterranean). As submarine canyons incise the continental shelf, they play a role in influencing hydrodynamic flows. Upwellings are induced by westerly/north-westerly winds in the region of speeds greater than 14 m s^{-1}. Current orientation near the canyon head and shelf is dependent on underlying topography, wind (speed and direction), and stratification. The mesoscale variability of the Northern Current, a feature of water circulation in the north-western Mediterranean Sea, can lead to its intrusion over the shelf and, in turn, to barotropic crosscurrents over the canyon. Turbidity currents were observed in this case study associated with upwellings, suggestive of its importance to shelf sedimentary processes in this area.

Filander et al. provide the first detailed description of species diversity and taxonomic description within and around the Cape Canyon, South Africa. This particular case study focused on two canyon and 13 non-canyon stations, evaluating biodiversity and hydrographic data to discern differences in species composition with substrate type and depth i.e. as predictors of distribution patterns. Thirteen species were found to be characteristic of canyon areas compared to three from non-canyon areas.

Bigham et al. report on the ecological recovery in a megafaunal community associated with the benthos within the Kaikōura Canyon following the 2016 earthquake (M_w 7.8). The megafauna community visible in seafloor imagery four years after the event appears to be resilient to the earthquake-triggered turbidity flow. Ecological productivity and thus recovery is now similar to the previous highly productive community present before the turbidity flow. Population growth models predict that the community could fully recover in a minimum of 4.5 years, though full recovery may take up to 12 years post- disturbance.

In summary, this Research Topic is of interest to the wider submarine canyon and deep-sea community and sheds light on the dynamic characteristics of canyons and the inextricable human connection to the deep sea.

Author contributions

AD: Writing – original draft, Writing – review & editing. JD: Writing – review & editing. KK: Writing – review & editing. VH: Writing – review & editing.

Funding

The author(s) declare financial support was received for the research, authorship, and/or publication of this article. VH was supported by the CLASS programme, funded by the Natural Environment Research Council, UK (Grant No NE/R015953/1).

Conflict of interest

The authors declare that the research was conducted in the absence of any commercial or financial relationships that could be construed as a potential conflict of interest.

Publisher's note

frontiers | Frontiers in Marine Science

TYPE Systematic Review
PUBLISHED 02 September 2022
DOI 10.3389/fmars.2022.965612

OPEN ACCESS

EDITED BY
Clara F. Rodrigues,
University of Aveiro, Portugal

REVIEWED BY
Fantina Madricardo,
National Research Council (CNR), Italy
Melanie Bergmann,
Alfred Wegener Institute Helmholtz Centre for Polar and Marine Research (AWI), Germany
Michela Angiolillo,
Istituto Superiore per la Protezione e la Ricerca Ambientale (ISPRA), Italy

*CORRESPONDENCE
Awantha Dissanayake
Awantha.Dissanayake@unigib.edu.gi

†These authors have contributed equally to this work and share senior authorship

SPECIALTY SECTION
This article was submitted to Deep-Sea Environments and Ecology, a section of the journal Frontiers in Marine Science

RECEIVED 09 June 2022
ACCEPTED 04 August 2022
PUBLISHED 02 September 2022

CITATION
Hernandez I, Davies JS, Huvenne VAI and Dissanayake A (2022) Marine litter in submarine canyons: A systematic review and critical synthesis. *Front. Mar. Sci.* 9:965612. doi: 10.3389/fmars.2022.965612

Marine litter in submarine canyons: A systematic review and critical synthesis

Ivan Hernandez[1], Jaime S. Davies[2†], Veerle A. I. Huvenne[3†] and Awantha Dissanayake[1*†]

[1]School of Marine Science, University of Gibraltar, Gibraltar, Gibraltar, [2]School of Marine Science and Engineering, University of Plymouth, Plymouth, United Kingdom, [3]Ocean BioGeosciences, National Oceanography Centre, Southampton, United Kingdom

The presence of marine litter is of concern in submarine canyons, although research in this area is still in its infancy. A critical synthesis and literature review selecting studies with primary data of benthic marine litter at depths of over 50 m revealed important gaps in the knowledge, with information on the impact of macroplastics in deep-sea environments still scarce. Less than 1% of medium to large submarine canyons mapped have been studied in any measure for marine litter, with over 91% of the canyon studies located in European waters. Imaging techniques are now the main tools used for sampling, overtaking trawling methods despite the continued growth of the latter for marine litter deep-sea research. Enumeration of litter was diverse with over 75% using abundance for quantification. Despite the existence of litter protocols available for deep-sea environments, over 73% of studies did not use any. There was no standardization in the implementation of established classification protocols, which were either not used in full or were customized in part. Fishing-related categories do not feature as a top-level category in the classification hierarchy in any of the protocols, yet over 50% of publications featured fishing materials as a main category, pointing to a more intuitive activity-based categorization of litter instead of a materials-led approach from the established protocols. Furthermore, interactions between litter and the surrounding environment and biota are very much underreported with little or no consensus between how the data are analyzed and expressed. There were no discernible patterns between litter density, composition and broad geographical location of canyons, with individual topographical characteristics, hydrodynamic regimes and anthropogenic activities being determining factors in how submarine canyons are affected by litter. Overall, there is no apparent framework to allow comparison of studies and due to the different methods of identifying, enumerating, quantifying and classifying marine litter, or lack of data on position and morphological setting within the canyon system. The evidence provided within this study highlights a 'call to action' for an urgent need to standardize and unify methodologies with new or established protocols to fully understand the impact of marine litter in submarine canyons.

KEYWORDS

submarine canyons, marine litter, plastic pollution, marine debris, macrolitter, benthic litter, deep-sea litter, deep-sea debris

Introduction

Marine litter

Marine litter, also known as marine debris, is defined by the UNEP as "any persistent, manufactured or processed solid material discarded, disposed of, or abandoned in the marine and coastal environment" (UNEP, 2009), and is found in all seas, at all depths, and regardless of proximity to densely populated regions. It has economic, cultural, public health and safety impacts, adding additional pressures to ecosystems and habitats already affected by other anthropogenic pressures. The terms 'marine litter' and 'marine debris' can be used interchangeably; the former, however, can infer greater attributability on littering behaviors by consumers instead of surging plastic production and/or waste mismanagement by wealthier nations. The term 'marine litter' is used in overarching programs such as the UNEP and within legal texts in Europe, such as the MSFD, where it is included in the list of descriptors to achieve GES (Good Environmental Status) by the European Commission, with the deep seafloor considered one of the largest litter accumulation zones in the ocean (European Commission, 2010; Galgani et al., 2013; Pham et al., 2014).

Most marine litter studies, thus far, have focused on the impacts on sea surface biota, beach ecosystem services, floating or coastal litter, and knowledge of benthic macrolitter (>25 mm in diameter) beyond coastal habitats is sparse (Spengler and Costa, 2008; Barboza et al., 2018; Consoli et al., 2018a; Napper and Thompson, 2019; Sinopoli et al., 2020; Suaria and Alani, 2014; Canals et al., 2021). Marine sources of litter are linked to shipping routes and activities (commercial and recreational), fishing activities, marine traffic, military activities, aquaculture, offshore installations, and dumping at sea (Ramirez-Llodra et al., 2013; Woodall et al., 2015). Sources of land-based litter include agriculture, recreational coastal use, ports, tourism, or shipyards, sewage outflows or river discharge, making the exact source of any item of litter almost impossible to identify (Stefatos et al., 1999; Galgani et al., 2000; Pham et al., 2014; Angiolillo, 2019). Land-based sources of marine litter, however, have been found to provide the major fraction of litter found on the coastline (Canals et al., 2021).

Plastics are the most prevalent type of litter; they are inexpensive, strong, lightweight, resistant to corrosion and taking many forms, with global production rising from 5 Mt per year in the 1950s to 438 Mt per year in 2017 and is projected to increase to 1.1 billion tonnes per year by 2050 (Jambeck et al., 2015; Napper and Thompson, 2019; Geyer, 2020). It has been estimated that 19 to 23 million metric tons (Mt) (11%, of plastic waste generated globally) entered aquatic ecosystems in 2016 alone, and taking into consideration ambitious commitments by some governments this could rise to 53 Mt per year by 2030, or to over 90 Mt per year under the current 'business as usual scenario' (Borrelle et al., 2020). There are thought to be over 5.25 trillion plastic particles > 5 mm in diameter floating on the sea surface alone, weighing over 240,000 tonnes (Eriksen et al., 2014). Plastics are long-lasting with yet unknown persistence timescales which require more data to be assessed effectively, but are largely dependent on the polymer properties aided by additives (Barnes et al., 2009; Ward and Reddy, 2020). In deep-sea benthic environments where oxygen levels are reduced and light required for photooxidation is absent, timescales could be considerably larger than on the surface (Barnes et al., 2009; Spedicato et al., 2019).

Impacts on biota

Ingestion is one of the main direct impacts that marine litter has on a wide range of biota, causing potential internal injuries, blockage in the digestive tract, decreased nutrient uptake or false sense of satiation, harm by toxicity such as deleterious effects on sexual reproduction and survival, or even death by accumulation (Kühn et al., 2015). Other threats include physical harm by entanglement, smothering, abrasion, breakage, necrosis, and suffocation. Observations of mechanical damage by fishing lines have been documented on sessile organisms in deep-sea environments, such as cold-water corals (CWCs) and sponges, and when they die the affecting debris can be released if structures do not remain intact, free to repeat the cycle on other organisms (Pham et al., 2013; Bo et al., 2014; Angiolillo et al., 2015; Cau et al., 2017; Angiolillo, 2019). Alien invasive species can use non-degradable litter objects as vectors for transportation horizontally over large distances (Kühn et al., 2015).

Derelict fishing gear (DFG) is one of the most abundant types of litter in rocky environments, and is responsible for ghost fishing; a type of entanglement that entraps and causes the death of a wide range of organisms by hindering their ability to breathe, feed or escape from predators (Lopez-Lopez et al., 2017; Melli et al., 2017; Angiolillo, 2019). The overall amount of DFG is unknown, although crude approximations point to 10% of all litter entering the marine environment consisting of ghost nets (Macfadyen et al., 2009). Other types of fishing gear such as traps and pots may also continue to "fish" passively for years after settlement in the environment (Ramirez-Llodra et al., 2011; Galgani et al., 2013; Consoli et al., 2020). It is estimated

Abbreviations: CWCs, Cold-water corals; DFG, Derelict fishing gear; EU, European Union; GES, Good Environmental Status; GS, Google Scholar; JAMSTEC, Japan Agency for Marine-Earth Science and Technology; LITTERBASE, Online Portal for Marine Litter; MEDITS, Mediterranean International Bottom Trawl Survey; MLI, Marine litter impacts; MSFD, Marine Strategy Framework Directive; OSPAR, Oslo Paris Convention; ROV, Remotely operated vehicle; SD, Science Direct; SFH, Seafloor features and habitats; TC, Towed camera; UN, United Nations; UNEP, United Nations Environmental Programme.

that DFG may contribute up to 98% of total litter where fishing activities represent an important economic sector (Angiolillo et al., 2015; Cau et al., 2017; Consoli et al., 2018b; Consoli et al., 2019). Impacts which may not necessarily be considered to be negative are also observed through increases in habitat and spatial heterogeneity at small scales, use as a substratum by some organisms to grow, refugia by prey and predator species, and even becoming biodiversity hotspots boosting population extensions of sessile and some free-living invertebrates (Watters et al., 2010; Miyake et al., 2011; Mordecai et al., 2011; Bergmann and Klages, 2012; Schlining et al., 2013; Woodall et al., 2015; Song et al., 2021).

Transport of litter into the deep sea

The buoyancy of plastics is highly variable and while it is estimated that 50% of plastics from municipal waste have a density greater than seawater and will sink quickly, the rest can float on the surface for large distances before changing in density by being fouled, waterlogged, leaching of additives or amassing too much fouling epibiota (Ye and Andrady, 1991; Barnes et al., 2009; Andrady, 2011; Engler, 2012; Pham et al., 2014; Avio et al., 2017; Fortibuoni et al., 2019; van Sebille et al., 2020). It is thought that 70% of floating litter eventually sinks although rates are largely unknown, with arrival on the seafloor potentially delayed for long periods of time (UNEP, 2005; Pham et al., 2014; Tekman et al., 2017). Spatial distribution of litter and accumulation are uneven and dependent on localised factors such as the route and amount of litter, the marine environment, local wind and hydrographic conditions, anthropogenic activities, population density, temporal environmental variations or catastrophic events, such as the Tohoku earthquake where litter density on the continental slope of north Japan increased substantially after the event, or flash floods in Sicily causing the highest litter accumulations in submarine canyons (and in the deep sea) recorded to date (Keller et al., 2010; Mordecai et al., 2011; Pham et al., 2013; Ramirez-Llodra et al., 2013; Pham et al., 2014; Tubau et al., 2015; Goto and Shibata, 2015; Shimanaga and Yanagi, 2016; Pierdomenico et al., 2020). Litter can also become trapped in areas of low circulation, high sedimentation, and high rugosity morphological settings (Galgani et al., 2000; Eriksen et al., 2014).

Hydrodynamic processes such as gravity currents, thermohaline currents, bottom currents, seafloor gyres and downwelling processes, are important for the transport and redistribution of marine litter on the seafloor, with entrainment of litter possible in turbulent flows that can cause higher litter densities in submarine canyons in comparison to the continental slope (Galgani et al., 2000; Ramirez-Llodra et al, 2011; Ioakeimidis et al., 2014; Tubau et al., 2015; Woodall et al., 2015; Buhl Mortensen and Buhl Mortensen, 2017; Kane and Clare, 2019; Pierdomenico et al., 2019b, Kane et al., 2020; Pierdomenico et al., 2020). Downwelling processes have been found to responsible for the vertical transport of litter in the South China Sea, where fishing activity is a notable source of pollution (Zhang et al., 2020). A substantial portion of plastic litter entering the ocean is now found deposited and/or buried in ocean sediments with marine sediments being a major sink of plastic pollution in the ocean (Kane and Fildani, 2021; Martin et al., 2022).

Submarine canyons

To date 9,477 medium-to-large-sized submarine canyons with a depth range of at least 1,000 m, a width/depth ratio of less than 150:1 and a canyon incision of at least 100 m, have been mapped on all continental margins, occupying a global ocean surface area of 11.2% of the continental slope (Harris and Whiteway, 2011; Harris et al., 2014). Submarine canyons are preferential conduits for nutrients, organic matter, and sediments to deep-sea environments, connecting the shallower continental shelf with deeper basins (Canals et al., 2006). They exhibit greater abundances and species richness when compared to adjacent slope areas as higher levels of associated primary productivity can lead to canyons to be hotspots of faunal productivity in the deep sea (De Leo et al., 2010). As such, submarine canyons are important regional sources of marine biodiversity and ecosystem function, and provide a wide range of ecosystem services (Fernandez-Arcaya et al., 2017). Sedimentary gravity flows such as turbidity currents, density currents, and oceanographic processes such as internal waves and upwelling/downwelling circulation patterns in shelf-incising canyons are thought to facilitate the transport of marine litter hundreds of kilometers from the coast at times, turning canyons into sinks that act as passive accumulation areas (Watters et al., 2010; Ramirez-Llodra et al., 2013; Schlining et al., 2013; Pham et al., 2014; Tubau et al., 2015; Fernandez-Arcaya et al., 2017; Pierdomenico et al., 2019b). There is no discernible pattern regarding the source of litter in submarine canyons, although marine sources are responsible for litter on the open slope close to major shipping routes and fishing lanes, with correlations established between these and the presence of heavy, fast-sinking objects (Ramirez-Llodra et al., 2013; Fiorentino et al., 2015; García-Rivera et al., 2017; Tekman et al., 2017; Parga Martinez et al., 2020).

Monitoring marine litter

Most marine litter protocols and frameworks are better suited to record floating, beach and coastal litter (Canals et al., 2021). Some have been designed to monitor marine litter regionally during fisheries surveys using trawling as their method of sampling, such as the MEDITS and OSPAR

protocols (MEDITS, 2017; OSPAR Commission, 2017). The latter incorporates the International Bottom Trawling Survey that has been running yearly surveys since 1970 in the North Sea, and the Baltic International Trawl Survey. The MEDITS protocol oversees collection of data at depths between 10 m and 800 m in five different strata on a yearly basis. The MSFD recommends Member States to use existing regional sea conventions, such as OSPAR (NE Atlantic Ocean), Barcelona Convention (Mediterranean Sea), Helsinki Convention (Baltic Sea), and the Bucharest Convention (Black Sea) as institutional cooperation structures to build upon existing programs and activities to achieve cohesion and coordination of strategies and even standardizes the OSPAR and MEDITS protocol within its overarching framework (European Commission, 2010; Galgani et al., 2013; MEDITS, 2017; OSPAR Commission, 2017). The MSFD has a large master list of litter categories and subcategories which are suitable for use in different environments, such as the sea surface, beaches, or the seabed, caters for item size in its classification system, is the only major official protocol that caters for imaging technology, and has an online photo catalogue to aid identification of litter types (Galgani et al., 2013; Fleet et al., 2021). Few protocols exist that specifically target macrolitter, benthic or deep-sea environments that can be used to assess the impacts of marine litter in submarine canyons. Alignment, synergies, and divergences in non-coastal benthic litter classification between the MSFD, MEDITS and OSPAR can be found in Supplementary Table 1.

This review aims to identify gaps in the knowledge to this effect, with one of the main objectives being to determine whether comparisons and coherent patterns can be derived in the identification, classification, enumeration, and quantification of marine litter in existing studies, as well as possible comparisons in litter trends in the literature. Another aim is to evaluate the need for unified and standardized parameters and practices when carrying out litter surveys in submarine canyons (although there is a need for a unified and standardized observational protocol for litter in the deep-sea as a whole), so that the true extent of litter pollution in submarine canyons can be fully understood, the transport, deposition, and biotic interactions can be investigated, and individual studies can be made compatible and comparable.

Materials and methods

A literature review and critical synthesis was conducted using Google Scholar (GS) and Science Direct (SD) and structured based on the PRISMA framework (Page et al., 2021). Using both discovery engines is supported by standard infometric methodologies as a way of countering bias from paywall services, with 95% of Web of Science citations and 92% of Scopus citations found on GS, which can be considered a superset of these services with substantially increased coverage (Moed et al., 2016; Halevi et al., 2017; Martín-Martín et al., 2018). Lexical units were selected from preliminary subject reading, forming two distinct groupings: seafloor features and habitats (SFH) and marine litter impacts (MLI), (Table 1). Searches per lexical unit were conducted for the period 1981-2020 at yearly intervals. Adequacy of using only GS was established for subsequent searches (Supplementary Table 2), and lexical units from both groups were combined for the discrete period 2001-2020 in a string of two parts using quotation marks around the components for greater specificity, to focus on the last two decades when most of the literature related to marine litter was seen to appear and was taken as the main limiting factor. A heatmap was produced to examine the weight of MLI in relation to SFH. Searches were carried out to determine the most mentioned submarine canyons using the term "submarine canyon" and a list of broad geographical areas (Table 1) between 2001-2020. Submarine canyons found in the top 100 search results were then searched by canyon name (allowing for syntax differences and name equivalences) combined with a selection of MLI terms (Table 1).

Exhaustive analyses of datasets produced from combinations of selected terms as indicated from Table 1 were carried out to produce a collection of studies on marine litter based on the criteria below, henceforth referred to as the corpus. The period 2001-2020 was used for the inclusion of data since this was taken as the limiting factor when combining lexical terms and made for a more efficient focus on the corpus analysis. The criteria for literature selection were:

- Inclusion of primary data on macrolitter identification, classification and quantification in submarine canyons or the seabed at depths > 50 m.
- Exclusion of data on beach, estuarine, riverine, floating litter, or microplastics.

Review publications and the LITTERBASE database were also queried for analysis of litter distribution and composition in the literature (Pham et al., 2014; Angiolillo, 2019; LITTERBASE, 2020).

Data were extracted from the corpus publications for geographical area and study sites, data type, acquisition methodology, morphological setting, impacts on biota, enumeration, quantification, litter protocols used, depth ranges, litter density and litter categories used (hierarchical tiers and nomenclature). Litter categories used were standardized to the minimum number of broad categories possible for the comparison of litter composition and classification systems, by grammatically harmonizing for use of singular and plural, use of punctuation, syntax variations of the

TABLE 1 List of marine litter impacts, seafloor features and habitats and broad geographical areas used to conduct searches.

Marine litter impacts (MLI)	Seafloor features and habitats (SFH)	Broad geographical areas
Marine litter *†	Submarine canyons *	Atlantic Ocean
Microplastics pollution	Cold water corals	Pacific Ocean
Marine debris *†	Ocean trench	Indian Ocean
Marine plastic debris *	Deep seabed *	Mediterranean Sea
Plastic pollution *†	Continental slope *	Arctic Ocean
Marine plastic litter *	Abyssal plain	Southern Ocean
Macroplastics *	Seamounts	Antarctica
Derelict fishing gear *	Marine sponges	Australia
Marine microplastics	Deep-sea corals	New Zealand
Microplastics	Deep water corals	
Ghost fishing *	Hydrothermal vent	

*Lexical terms from the MLI and SFHs groups combined for the analysis of datasets to select publications to produce a corpus.
†MLI terms combined with submarine canyon names derived from broad geographical area searches for the analysis of datasets to select publications to produce a corpus.

same object or term, and incorrect terminology, thus reducing the number of categories and subcategories while maintaining maximum diversity of discrete items where contextually and lexically possible. Categories and subcategories were not based on existing litter protocols pre-2020 since their top-level classification systems were insufficient to list all the main types of litter found in the corpus. Contextual groupings were made with categories that had evident links in type of material composition to determine the main types of litter found, such as plastic bottle, plastic sheet or plastic bag grouped into a wider artificial polymer group.

Geographical areas were standardized and grouped to establish links and patterns with study sites extracted with the corresponding number of surveys per site. If canyon and non-canyon features were cited for the same geographical area, these were listed separately. Number of surveys per site, differentiated between seafloor and submarine canyons were plotted in a map. Litter densities per canyon were recalculated to provide a mean value where canyon data were provided by more than one study (providing the data were in comparable formats, e.g. abundance per spatial area) or when data were combined in studies to give a single density figure for canyons in a broad geographical area (such as the Gulf of Lyon canyons), taking into account standard deviation and standard error. Interactions between litter and benthic fauna were also extracted from the corpus studies. The schematic representation of the overall analysis is summarized in Figure 1.

Results

Lexical term search results 1981-2020

Lexical groups showed a marked difference in the number of publications and the rate at which they appear over the forty-year period studied. The rate of increase in the number of publications was steady for most terms in the SFH group (Figure 2), in particular for the terms 'continental slope', 'seamounts', 'marine sponge' and 'hydrothermal vents' since the year 2000, with the latter having registered an increase of over 37% between 2019 and 2020, to 3,630 results returned by GS. Synonyms for CWCs were analyzed individually and cumulatively, showing a five-fold increase in results from 2003 to 1,197 results returned by GS in 2020. Number of results displayed for 'marine sponge' increased noticeably between 2010 and 2014 and showed almost three times as many results (3,270) as the three variations of CWCs combined, which may be indicative of the connection of CWC terms with deep-sea habitats whereas research on marine sponges could be from shallow waters. Progression in results on 'submarine canyons', 'deep seabed'/'deep seafloor', and 'abyssal plain' showed similar trajectories but with much smaller increases until 2019, with 'submarine canyons' showing over 48% more results (1,510) in 2020 than in the previous year.

The rate of increase in results shown by GS in the MLI group grew dramatically per year from 2013, in large part driven by research into microplastics and plastic pollution related terms (Figure 3), with an almost sixteen-fold increase between 2010 and 2020 to 29,494 results, suggesting an increase into the perception of topicality of MLI. Publications related to 'ghost fishing' and 'derelict fishing gear' show the least amount of growth. Even though these are amply referred to in the corpus as one of the biggest MLI in the sea, there are few dedicated research programs on these impacts specifically.

Lexical group combinations

A summary matrix was produced by combining terms from the MLI and SFH groups to depict and evaluate contextual clusters and hotspots from the lexical unit combinations for the period 2001-2020 and were compared to the results for single

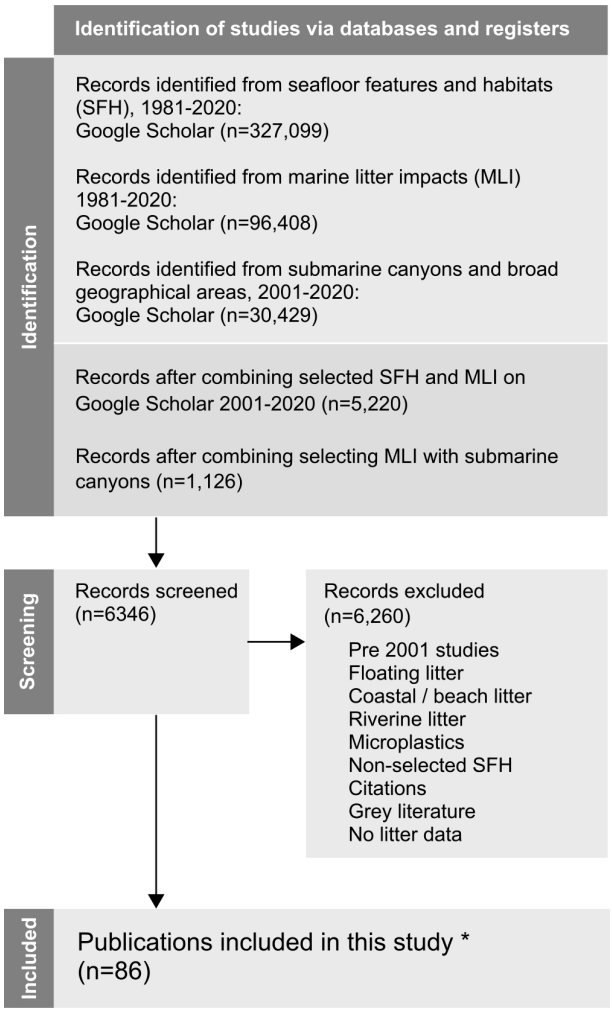

FIGURE 1
Schematic representation of the literature review and critical synthesis to produce a corpus.* Jeong et al., 2005; Lee at al., 2006; Koutsodendris et al., 2008; Barnes et al., 2009; Keller et al., 2010; Topçu and Öztürk, 2010; Watters et al., 2010; Miyake et al., 2011; Mordecai et al., 2011; Bergmann and Klages, 2012; Wei et al., 2012; Güven et al., 2013; Lefkaditou et al., 2013; Mifsud et al., 2013; Pham et al., 2013; Purser et al., 2013; Ramirez-Llodra et al., 2013; Sánchez et al., 2013; Schlining et al., 2013; Bo et al., 2014; Debrot et al., 2014; Eryaşar et al., 2014; Fabri et al., 2014; Ioakeimidis et al., 2014; Pham et al., 2014; Angiolillo et al., 2015; Fiorentino et al., 2015; Goto and Shibata, 2015; Ioakeimidis et al., 2015; Neves et al., 2015; Oliveira et al., 2015; Papadopoulou et al., 2015; Strafella et al., 2015; Tubau et al., 2015; Vieira et al., 2015; Woodall et al., 2015; Yamakita et al., 2015; Lastras et al., 2016; Moriarty et al., 2016; Pasquini et al., 2016; Shimanaga and Yanaghi., 2016; Buhl-Mortensen and Buhl-Mortensen, 2017; Cau et al., 2017; García-Rivera et al., 2017; Lopez-Lopez et al., 2017; Louald et al., 2017; Rodríguez and Pham, 2017; Tekman et al., 2017; van den Beld., 2017; Alvito et al., 2018; Baudrier et al., 2018; Cau et al., 2018; Chiba et al., 2018; Consoli et al., 2018b; Domingiez Carrió, 2018; Ferrigno et al., 2018; García-Rivera et al., 2018; Grøsvik et al., 2018; Kammann et al., 2018; Maes et al., 2018; Olguner et al., 2018; Urban-Malinga et al., 2018; Consoli et al., 2019; Fortibuoni et al., 2019; Gerigny et al., 2019; Giusti et al., 2019; Peng et al., 2019; Pierdomenico et al., 2019a; Pierdomenico et al., 2019b; Rhinane and Loulad, 2019; Spedicato et al., 2019; Strafella et al., 2019; Zablotski and Kraak, 2019; Alomar et al., 2020; Amon et al., 2020; Botero, et al., 2020; Consoli et al., 2020; Crocetta et al., 2020; Du Preez et al., 2020; Enrichetti et al., 2020; Garofalo et al., 2020; Grinyó et al., 2020; Kuroda et al., 2020; Mecho et al., 2020; Pierdomenico et al., 2020 and Ryan et al., 2020

lexical units in the MLI and SFH groups for the same period. Some SFH terms such as 'submarine canyons' (13.0%), or CWCs (16.4%), showed a much higher proportion of publications discussing MLI than others such as 'continental slope' (3.2%), 'hydrothermal vent' (1.5%) or 'marine sponge' (0.4%), despite these terms having the highest number of results per year when searched individually (Figure 4). Terms in the MLI group showed much higher proportions as a total of individual results relating to SFH than in reverse, especially in terms such as 'ghost fishing' (43.3%) and 'derelict fishing gear' (48.7%).

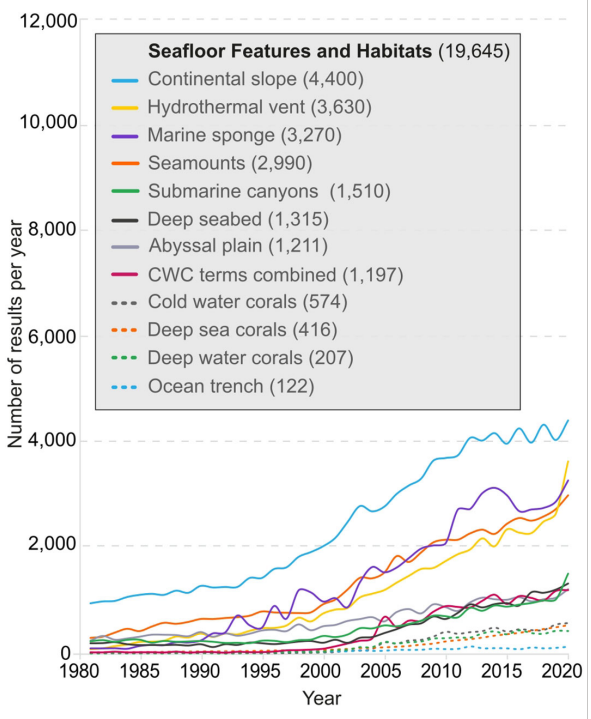

FIGURE 2
Number of publications per year listed in GS for the SFH lexical group, between 1981-2020. CWC terms (deep-water corals, deep-sea corals, cold-water corals) were plotted individually and as a combined count.

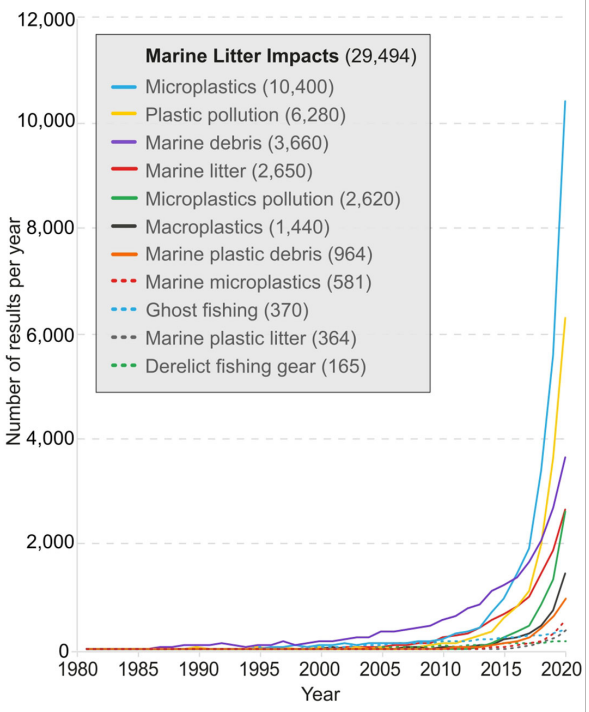

FIGURE 3
Number of publications listed per year in GS for the MLI lexical group, between 1981-2020.

Submarine canyons in the literature

Refining litter related searches to include canyon names shows a very high variability in the number of publications (Table 2). The volume of these results can be somewhat misleading as they do not represent studies of MLI in submarine canyons per se, but mentions of litter within the publication, including references. The canyons in the Gulf of Mexico (Green Canyon and Mississippi Canyon) have some of the lowest MLI percentages despite showing the highest number of overall results, whereas some of the canyons with the highest MLI ratios have much fewer total publications under their name. In contrast, the Monterey Canyon, has one of the highest counts by name and in numbers of MLI results, but is not within the top positions of MLIs as a percentage, indicative of a heavily researched canyon in other areas.

Corpus analysis

There were 86 publications (85 papers from scientific journals, one PhD thesis) identified using the selection criteria for inclusion in the corpus (Figure 5), of which 18 had data of litter in submarine canyons (either specifically or as part of a wider study with other non-canyon sites) and 68 had data solely on other seafloor features; 10 publications were specifically focussed on litter, with the other 76 including litter data among other data provided, 5 publications had other foci such as ecological surveys, and 3 publications had data reanalyzed for the purpose of quantifying marine litter in studies with data spanning a number of years from MEDITS trawls. It was not generally possible to ascertain whether publications that had marine litter as the focus acquired the data specifically for the purpose of analyzing litter, or whether the data were part of a larger contingent or multidisciplinary analysis, repackaged as a litter-focused study.

Trawled physical litter samples (henceforth referred to as 'samples') were used in 39 (45.3%) studies, equivalent to the number of studies that used trawls as the data acquisition method. Video and image data were used in conjunction in 7 (8.1%) studies despite the different ways used to acquire that data (ROV, drop camera, TC, or submersible). Samples, photographs, and video data were used in conjunction in 1 (1.2%) study.

Abundance of litter was used by 65 (75.7%) studies in different forms, such as abundance per area, per linear distance, per number of photographic frames or with no other criteria (Figure 6). Some studies used more than one way to acquire, record, and enumerate marine litter, with 17 (19.8%)

10.3389/fmars.2022.965612

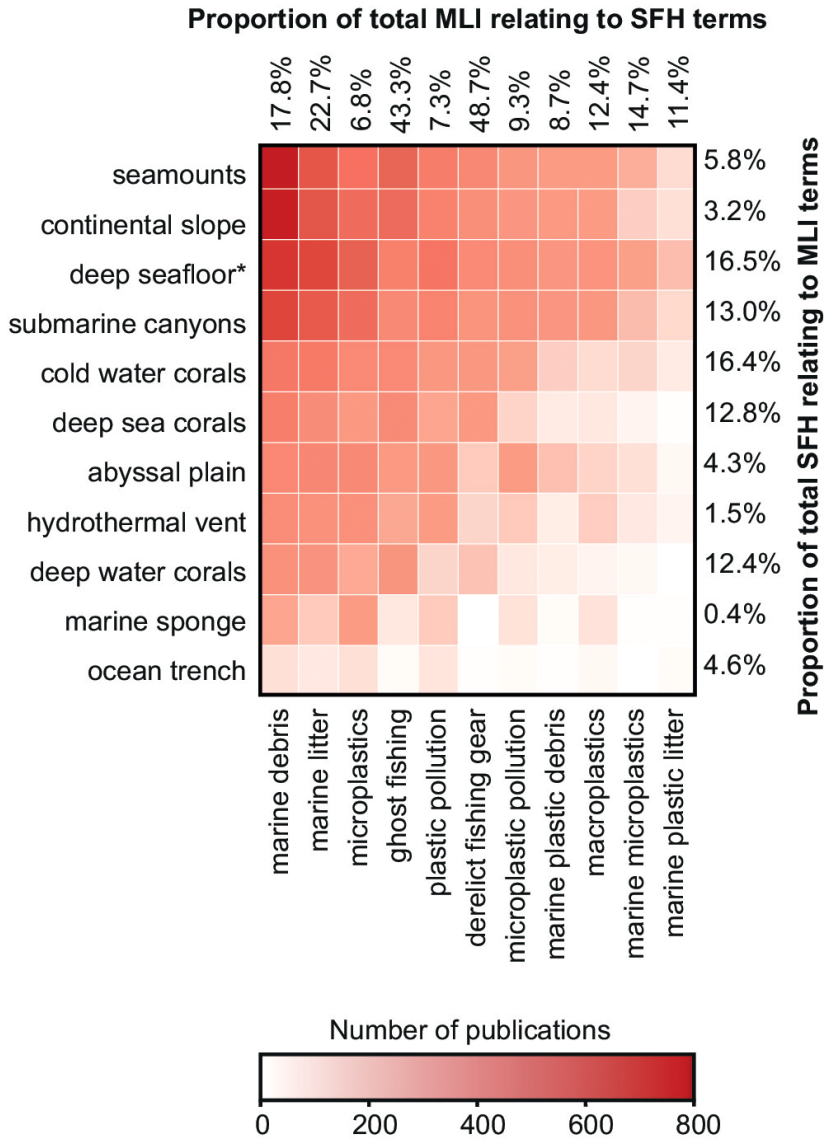

FIGURE 4
Heatmap for the cumulative number of publications for lexical unit combinations between lexical groupings, for the period 2001-2020 in Google Scholar. Proportion percentages were calculated as: MLI and SFH lexical unit combinations results 2001-2020 divided by single MLI or SFH lexical unit results 2001-2020. *Term equivalent for deep seafloor or deep seabed.

studies recording items both as weight and abundance in any of its different forms.

Litter protocols, classification systems and interactions

Official litter protocols were not used by 63 (73.3%) publications. Of those that did, 8 (34.5%) used MEDITS, 8 (34.5%) used the MSFD, 5 (20.7%) used OSPAR, with the remaining publications using other minor litter protocols as classification systems. Classification systems in litter protocols were not followed fully with substantial differences between protocols. Studies that followed MEDITS used on average 78.6% ± 38.2 of categories available in the protocol, and most included a 'general' or 'miscellaneous' category not listed in the protocol. Studies that followed OSPAR had the greatest amount of classification fidelity with 91.7% ± 16.7, and those that followed the MSFD had the least fidelity and greatest variance, with 44.6% ± 42.1. The number of subcategories used from the

10.3389/fmars.2022.965612

TABLE 2 A and B Submarine canyons most studied showing number of publications in Google Scholar when searched by name only for the period 2001-2020, and in combination with selected marine litter impacts terms ('marine litter', 'marine debris', 'plastic pollution').

Canyon	Publications	Litter impacts	% MLI	Canyon	Publications	Litter impacts	% MLI
São Vicente Canyon	100	39	39.00%	Mississippi Canyon	4,420	55	1.24%
Gioia Canyon	61	12	19.67%	Green Canyon	4,340	14	0.32%
Berenguera Canyon	17	3	17.65%	Monterey Canyon	2,620	229	8.74%
Lisbon Canyon	153	24	15.69%	Nazaré Canyon	1,509	156	10.34%
Blanes Canyon	380	55	14.47%	Hudson Canyon	1,500	36	2.40%
La Fonera Canyon	294	41	13.95%	Baltimore Canyon	1,130	8	0.71%
Albany Canyon	27	3	11.11%	Barrow Canyon	1,120	10	0.89%
Cap de Creus	658	70	10.64%	Keathley Canyon	869	2	0.23%
Nazaré Canyon	1,509	156	10.34%	Kaoping Canyon	725	12	1.66%
Dohrn Canyon	113	11	9.73%	Cap de Creus	658	70	10.64%
Subtotal of top 10 canyons by name only	3,312	414	12.5%	Subtotal of top 10 canyons by name only	18,891	592	3.13%
Total (from Supplementary Table 3)	30,429	1,126	3.70%	Total (from Supplementary Table 3)	30,429	1,126	3.70%
% Publications of top 10 canyons by name only	10.9%			% Publications of top 10 canyons by name only	62.1%		

Table 2a (right) shows canyons sorted by proportion of MLI. Table 2b (left) shows canyons sorted by name only. Full results can be found in Supplementary Table 3.

protocols were much lower in comparison with 24.6% ± 37.9 for MEDITS, 3.1% ± 8.8 for the MSFD and 32.7% ± 42.7 for OSPAR. There were 23 publications that had fishing gear subcategories under other broad categories, such as artificial polymer, metal, rubber, general, or even wood, but not under its own broad 'fishing materials' (or similar) category (Figure 7).

The resolution of litter classification systems was highly variable, with 54 (62.8%) having a primary classification

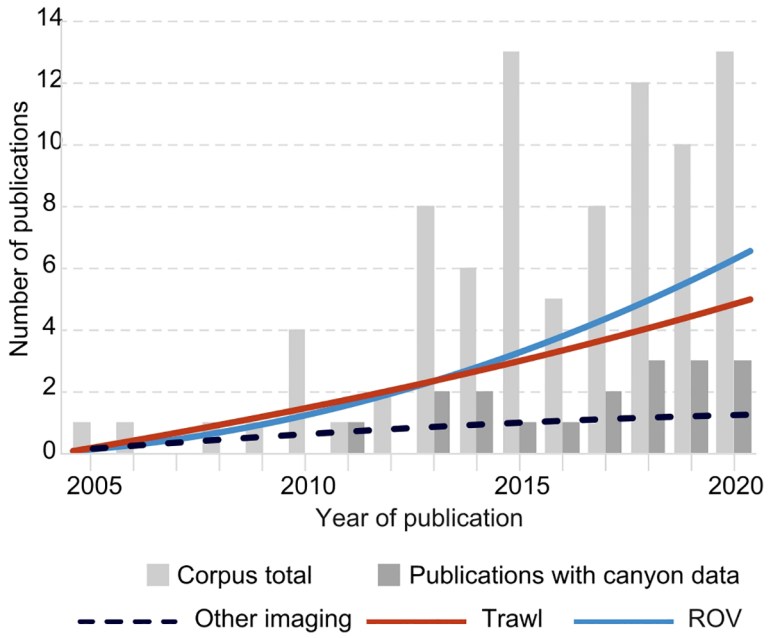

FIGURE 5
Total number of publications in the corpus per year for the period 2001-2020, and publications with canyon data, with polynomial trend lines (order 2) for different data acquisition methods. "Other imaging" techniques include submersible, TC and dropframe camera.

10.3389/fmars.2022.965612

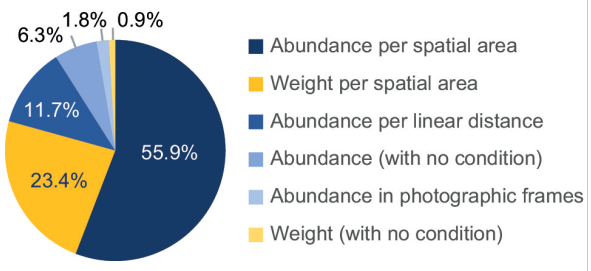

FIGURE 6
Types of enumeration used in the corpus.

system (categories) only, 28 (32.6%) including a secondary classification system (categories and subcategories) and 4 (4.7%) having neither. Additionally, 49 (56.9%) had <12 litter categories with no subcategories, and 33 (38.4%) had >12 categories and/or subcategories. The mean number of categories where a classification system existed was 7.3 ± 3.6 (n=82), and the mean number of hierarchical subcategories was 18.6 ± 11.6 (n=28).

Interactions between litter and organisms or the surrounding environment were mentioned in 25 (29.1%) publications. Entanglement was the most prevalent type of interaction with 13 (18.3%) of the total (Figure 8). Only 1 (1.4%) publication had an instance of 'not observed' and 4 publications (5.6%) included 'no impact' as an option, which in both cases can be taken as recording data of absence.

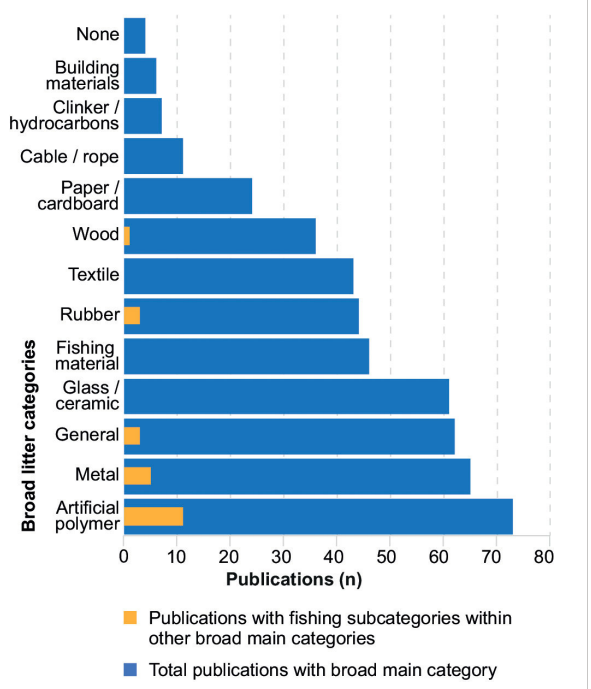

FIGURE 7
Number of publications in the corpus (n=86) that record data in each of the broad litter classification groupings (blue). Number of publications that included fishing materials as subcategories in other broad litter classification groups (yellow).

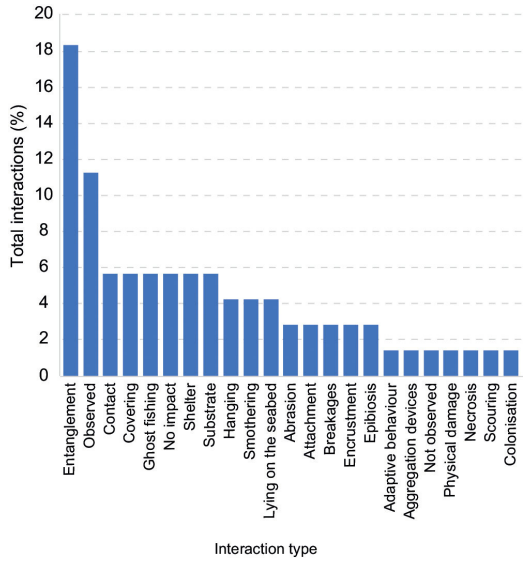

FIGURE 8
Instances of litter interactions (n=71) listed in the literature (25 out of 86 total publications).

Marine litter surveys, litter density and composition

Surveys in the corpus were conducted in 291 distinct sites with the Mediterranean basin accounting for 64.5% of the total. Submarine canyons encompassed 31.3% of the sites with 91.2% of these located in European waters (Figure 9). The high number of surveys in relation to number of sites is due to most publications having data on at least more than one survey over periods of time, or in different locations, with publications featuring over 600 surveys in the Gulf of Lyon, the Ligurian Sea and Corsica over a 24-year period (Gerigny et al., 2019).

The highest reported litter density by far was found in four channels of the Messina Canyon, with a mean density of 521,250 ± 117,100 items km^{-2}, over ten times higher than the next highest density recorded in the SY82 tributary canyon of the Xisha Trough (Peng et al., 2019; Pierdomenico et al., 2019b). Other heavily littered canyons in the western Mediterranean Sea and some of the most impacted canyons in the Bay of Biscay showed litter densities >10,000 items km^{-2}. There was much variability between canyons located in the same broad geographical area indicating localised factors driving these

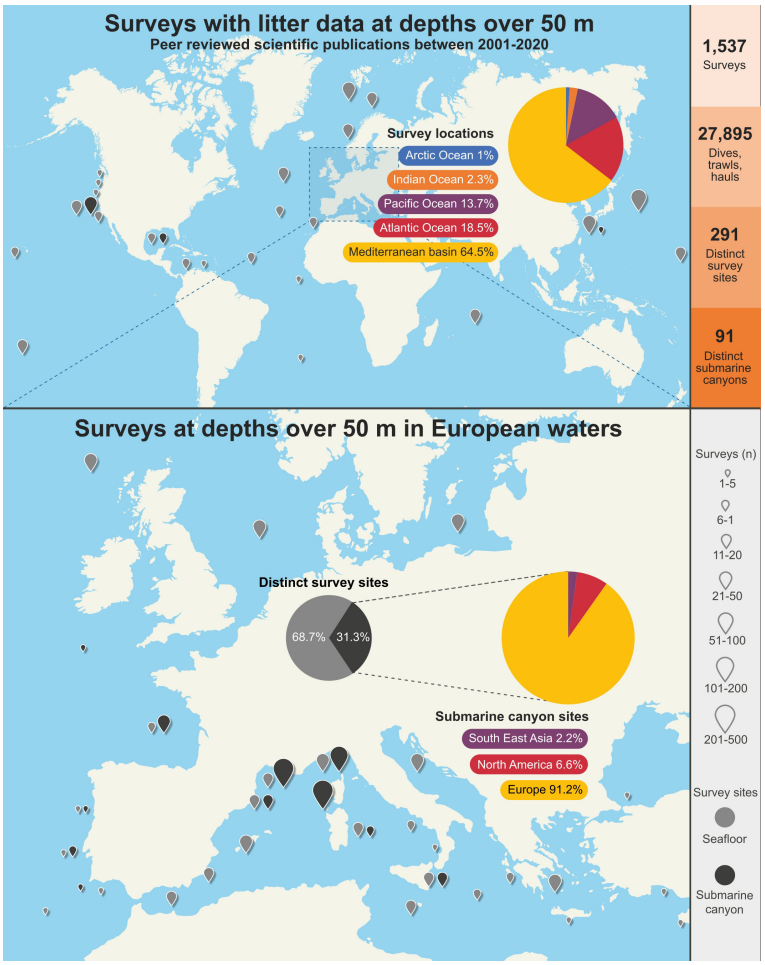

FIGURE 9
Surveys in the literature that contain marine litter data at depths >50 m worldwide and in European waters. Data in pie charts are representative of worldwide figures.

differences. Global budgets and per broad geographical region were calculated by standardizing the canyon means with a 95% confidence to remove outliers and provide conservative estimates. The number of canyons and mean canyon area per broad geographical region from Harris et al., 2014, were used to derive global and regional total litter value ranges. Global conservative budgets of 22488 ± 6897 items km^{-2} in the global ocean canyons were calculated using data from the Mediterranean Sea, North Atlantic Ocean, and North Pacific Ocean, giving a range of 7.0 to 13.7 million items of macrolitter in any one canyon, and a total figure of 68 to 128 billion items of macrolitter found as a total of all the ocean's canyons.

Litter composition was reduced to the lowest possible thematic resolution (based on the broad categories used in Figure 7), only including those groups of litter found in the canyon data (Figure 10). There are no discernible patterns between broad geographical area and litter composition, or with depth ranges either (Figure 11). Hydrographical and topographical features of individual canyons are the determining factors in the typology and distribution of litter. The Cap de Creus Canyon featured in different studies and had very different litter composition data; one study found a predominance of artificial polymers, and another found it to be fishing gear (Dominguez-Carrió, 2018; Gerigny et al., 2019).

Depth ranges available for litter studies in canyons in Figure 11 reveal a clear split between shallower ranges in the Mediterranean Canyons and those in the Atlantic Ocean especially. The exceptions are the canyons in the Catalan margin which have been sampled to considerably greater depths than other Mediterranean canyons, and the São Vicente Canyon which was sampled at much shallower depths than the other Portuguese canyons. Several studies only gave data on the mean survey depth which have been included for comparative reasons and labelled accordingly.

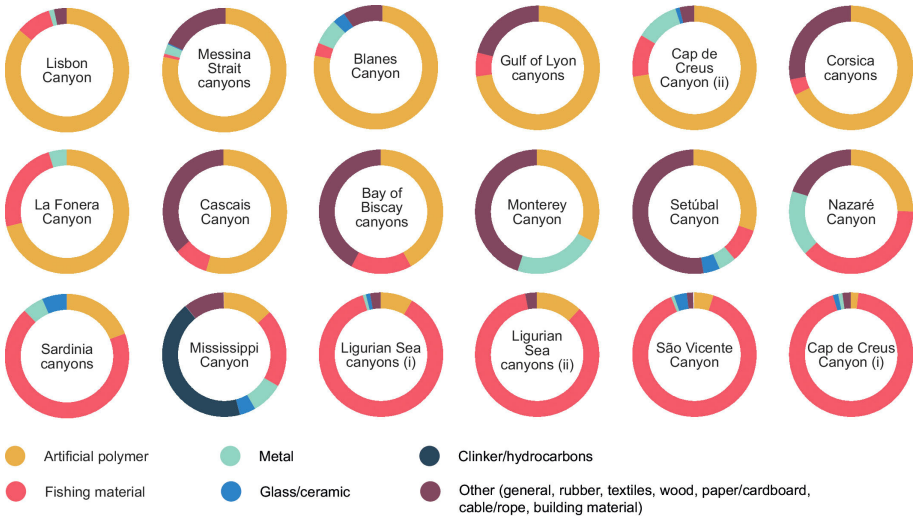

FIGURE 10
Low resolution litter composition in submarine canyons ordered by proportion of artificial polymer, adapted from the standardized custom 12 broad categories in Figure 7, where 'Other' represents building material, cable/rope, paper/cardboard, textile, rubber, wood and general/ miscellaneous, for brevity and clarity. Ligurian Sea canyons were detailed in two separate studies targeting different canyons within that broad geographical area. Cap de Creus studies were kept separate as they display distinctly different litter typologies for the same site.

Discussion

Analysis of canyon literature search results

Literature searches 1981-2020

There was a general increase in SFH literature over time, with CWC related publications increasing as from 2003, possibly due to technological developments making it easier to study these geomorphologically complex ecosystems. The inclusion of CWCs and marine sponges as a vulnerable marine ecosystem in UN resolution 61/105 in 2006 may have also prompted dedicated funding programs (e.g. EU framework programs) that have facilitated research into these areas (UN General Assembly, 2006). Results for submarine canyons showed a similar trajectory than CWCs, possibly for similar reasons stemming from the development of new technologies making them more attractive and feasible to study.

Searches into marine litter impacts in seafloor features and habitats

The high proportion of 'ghost fishing' or 'derelict fishing gear' publications that relate to SFH terms in Figure 4 (43% and 49% respectively) could be attributed to studies about their deleterious and nefarious consequences on habitats, and the damage to fishing gears associated with deep-sea trawling. The latter has been quantified for losses of over 1% of revenue from all fishing activities in the EU alone, (61.67M €), and although there is limited data on the damage of litter to fisheries, revenue lost from this economic activity could well be a driver for results in this area (Terzi and Seyhan, 2020). The hotspot around CWC terms combined with 'marine litter', 'marine debris' or 'ghost fishing' could be attributed to many studies focusing on the damage caused to CWCs by fishing activities, and because CWCs can snag litter and fishing gear (Purser et al., 2013; Lastras et al., 2016; Giusti et al., 2019; Pierdomenico et al., 2019a).

Research on deep-sea benthic macrolitter is not as prominent as other types of litter studies (such as floating, beach, or microlitter), and can be somewhat indicative of anthropocentric perspectives regarding impacts on the environment, with little regard for the effects on species and habitats far removed from direct view. Finding data on benthic deep-sea macrolitter is challenging and could benefit from promoting a central repository for recording data, such as the JAMSTEC Deep-Sea Debris database, or the LITTERBASE developed by the Alfred Wegener Institute, even if the former is more regional in nature (JAMSTEC, 2020; LITTERBASE, 2020).

Canyon searches

The top ten canyons mentioned in the literature (Table 2B) accounted for over 62% of all canyon publications found, in line with other findings where a small number of canyons dominated most of the canyon research with uneven geographical and thematical distribution (Matos et al., 2018). While the São Vicente Canyon had a sizeable proportion of the literature dedicated to selected MLI (39%), the mean overall canyon MLI

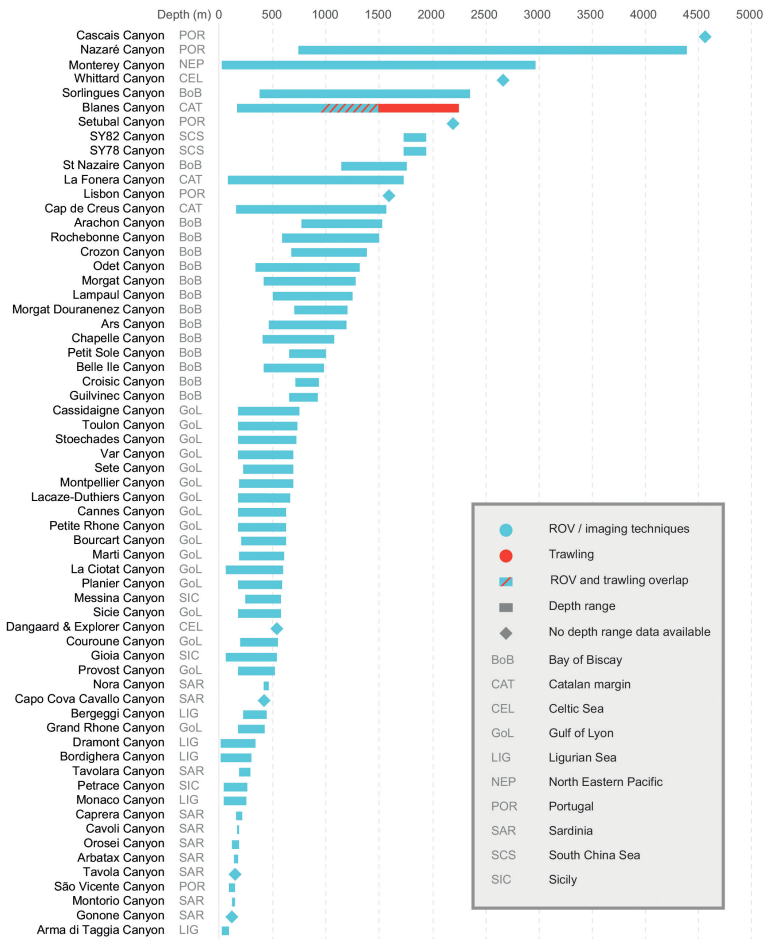

FIGURE 11
Depth ranges of litter surveys within canyons. Broad geographical areas for each canyon were added (codes can be found in the legend) including the main sampling technique used.

proportion was 3%. This is supported by observations that some canyons have specific research foci (Matos et al., 2018) Blanes Canyon is mostly studied for anthropogenic effects (including marine litter), Cap de Creus Canyon for CWCs, density gradients and sedimentation, Nazaré Canyon for biodiversity, or the Monterey Canyon for hydrodynamic modelling. Typically, once a canyon has been studied in a field, the accumulation of background information makes it easier to continue detailed studies in the same field, as patterns derived from a single canyon may not be easy to extrapolate to others (Huvenne and Davies, 2014; Matos et al., 2018).

The type of study conducted could be crucial for whether litter data is available, given that litter is not usually the primary focus of studies in submarine canyons. Thus, given that different canyons tend to be the focus of different research areas, it could help explain the geographical disproportion in litter studies in canyons to date, such as those in European waters versus submarine canyons elsewhere. The acquisition of data of high enough resolution to enumerate litter is dependent on the purpose of the survey. For example, a geological study using acoustic techniques to characterize the seafloor will not acquire imagery or sample data to allow quantification of litter, although acoustic surveys have been used to assess and recover large items of litter such as DFG using stakeholder cooperation (Havens et al., 2011; Sullivan et al., 2019). Biological or ecological studies, however, may conduct trawl surveys or use camera systems which could allow for identification and enumeration of litter even if the purpose of the study was another.

Litter study sites in submarine canyons and in the deep sea

As can be seen in Figure 9, a sizeable majority of deep-sea litter surveys occurred in European waters, especially in the Mediterranean Sea, with a disproportionate number carried out on the northern side (European waters) which is much more densely populated and industrialized than the southern side (African waters), possibly due to the explicit inclusion of marine litter as an indicator of GES in the MSFD. Regional litter protocols such as MEDITS that allow for litter data to be collected as part of fisheries assessments and of a time series may have also been a factor. Additionally, submarine canyons studied in the European side of the Mediterranean basin tend to be close to coastal areas and connected to well-known fishing grounds, which may make them logistically easier to study for marine litter. It could be argued that developed nations have greater resources for litter studies yet there is a general scarcity of data. In North American waters only canyons in the Monterey area and the Mississippi Canyon in the Gulf of Mexico have been surveyed for marine litter (Bo et al., 2014; Enrichetti et al., 2020). In the central South China Sea basin, only two tributary canyons in the Xisha Trough have been studied (Peng et al., 2019). Overall, there is a very large gap in the knowledge, with <1% of 9,477 mapped medium-to-large canyons studied for marine litter presence and impact (Harris et al., 2014).

Data type and data acquisition

There was alignment in data types between studies that used trawling and samples, and those that used equipment for visual analysis and photographs or video. There were several instances of overlaps using data from multiple methods such as ROV and trawls in studies that consolidated data from different sites and/or sources (Pham et al., 2014; Chiba et al., 2018; Gerigny et al., 2019; Strafella et al., 2019). Most studies that used ROVs also used video data, with only 20% using photographs. During surveys photographs are taken at regular intervals, unlike video data which is continuous. Even though an adequate and representative photographic sampling scheme should be as accurate as video data, there could be litter items missed along the transect leading to an underestimation of the true amount of litter if not enough ground is covered, often a limitation in deep-sea surveys. Additionally, the camera setup may also cause issues with the ability to compare data, as oblique angled cameras may introduce an error in area estimates and should be taken into account for comparative studies.

There are associated difficulties and costs to deep-sea sampling (logistics and equipment) when compared to shallower or coastal areas, as well as advantages and disadvantages for each sampling method (Cau et al., 2018). Image sampling is non-invasive and occurs in-situ, can detect more types of litter and smaller sized items, is not harmful to benthic environments and communities and allows for direct observation of the interactions between debris and epifauna, allows for identification of smaller-scale distribution/accumulation patterns (unlike trawls), and does not remove litter that can be assessed over time (Watters et al., 2010; Eryaşar et al., 2014; Ioakeimidis et al., 2015; Canals et al., 2021). Image-based techniques can thus be used to assess the impacts of interactions and entanglement by litter, especially DFG on areas dominated by sessile suspension feeders (also known as marine animal forests) and sponges (Galgani et al., 2018; Parga Martinez et al., 2020). Another advantage of ROVs and other imaging techniques (camera frames, drop frame cameras, or TCs) is that they are not limited to use on soft bottoms or by depth like trawls are, and have been used to detect litter in the deepest parts of the ocean (Miyake et al., 2011; Chiba et al., 2018; Peng et al., 2019). Disadvantages of using imaging technology include the limitation of transect length and higher costs in comparison to trawling, with the latter usually combined with fishing assessments to reduce overheads. Additionally, videos and photographs cannot detect items which are buried beneath the surface, can be of limited use in turbid conditions and the minimum size of litter that can be observed is dependent on the resolution of the cameras (Ioakeimidis et al., 2015; Canals et al., 2021).

Trawls have their own set of challenges, from damage to seafloor environments to loss of litter due the mesh size and opening of the cod end when retrieving the trawl net (Spengler and Costa, 2008). The lower depth limit of fishing trawls used to survey litter (currently 1,500 m), the inconclusive efficacy for sampling different types of litter, their limited spatial range conducted within fishing lanes, or not being able to be used on rocky bottoms or steep bottom slopes, can lead to possible underestimations of litter densities in these morphologies (Watters et al., 2010; Harris and Whiteway, 2011; Consoli et al., 2018b; Galgani et al., 2019; Garofalo et al., 2020). Large amounts of litter can be removed by commercial bottom trawling with underestimations and unexpected low instances of litter and/or fishing gear possible due to its continuous removal by these fishing activities (Ioakeimidis et al., 2015; Alomar et al., 2020). Correlations have been found between greater presence of litter (including fishing material) and slopes with gradients >40° out of reach of bottom trawls (Schlining et al., 2013) There has also been a shift in types of sampling method over time. A review of twenty-six litter studies in 2008 found trawling to be the most common type of sampling method (Spengler and Costa, 2008). The corpus in this review shows that even though use of trawling has increased through time, the use of ROVs is more widespread to date (Figure 5), whereas other imaging techniques have not increased much through the years. Regardless of the techniques used to acquire deep-sea litter data,

it is noteworthy that only 12% of studies in the corpus were focussed on marine litter, which is in accordance with the view that generally, litter tends to be studied opportunistically and not in its own right, relying on methodologies designed for other areas of research, such as the assessment of fish stocks (using bottom trawling), or image/video data from ecological or geological surveys that have been reanalyzed (Canals et al., 2021).

Enumeration of litter data

Over 75% of studies used abundance in some form for enumeration with the most frequent variation being per spatial area unit (n km^{-2}, n ha^{-1}). Abundance can be expressed when using trawls and imaging techniques, reflected in the large number of studies that use trawls and enumerated litter in both abundance and weight, similar to how biological data can be measured. Weight, however, is limited to trawling as it cannot be determined by visual means alone and was most frequently used per spatial area unit (kg km^{-2}), with some studies arguing that weight may be better overall for quantifying of marine litter (Zablotski and Kraak, 2019). This can be true when there are too many small pieces to count, but comparisons between studies if they use different parameters (such as weight per spatial area, or weight per haul) can be difficult (Canals et al., 2021).

Abundance per spatial area unit can be considered to be the most flexible type of enumeration allowing for direct comparisons between studies even with different area units. Linear units (e.g. n km^{-1}) may be used when the width of the field of view of the camera cannot be determined especially if there are no laser scales or when large debris items, such as fishing gears, appear to extend for hundreds of meters leading to possible overestimations in litter density if a conventional transformation to an area unit is performed (Dominguez Carrió, 2018). Comparisons using weight and abundance data are limited to using the same data types, although for monitoring purposes both can be treated as complementary. Coupling information from trawling (as a by-product of fishing operations or stock assessment) and imaging techniques, covering different substrates and depths within the same location, could give a more complete picture of the state of littering (Gerigny et al., 2019). The different ways of enumerating data given the difficulties in comparability between them denotes a lack of harmonization to the detriment of deep-sea research communities that could benefit from being able to compare and share data. Lack of standardization in litter quantification and distribution may be preventing hidden sinks and the true extent of litter impacts from being identified (Tekman et al., 2017). Thus, providing data in as many formats as possible especially since the practical problems in the comparability of data are yet to be solved, is particularly important as this research area is mostly at the baseline stage, with baseline concentrations yet to be agreed upon (Canals et al., 2021).

Litter densities in submarine canyons

Litter densities of over 100,000 items km^{-2} have historically been reported in areas of the Mediterranean Sea with high population density and close to anthropogenic inputs, influenced by a combination of currents, surface circulation variability and areas of high sedimentation rates (Galgani et al., 2000; Galgani, 2019). Caution must be exercised when looking at the density values in Table 3, as the data may only be representative of part of a canyon and not the whole site. A minority of studies detail where the transects took place and where samples were taken from, such as the canyon floor, thalweg, flank, or head. Most, however, do not provide that information, even if there are data from more than one dive or transect, or the depth of dives as a numerical value or site locations on a bathymetric map are provided. Conservative global budgets of up to 128 billion items of macrolitter have been estimated (Table 3) with the Mediterranean Sea canyons in total potentially having up to 46% (11.2 billion items) as much litter as the canyons in the North Pacific, which is a disproportionate amount given the size difference of the two geographical areas. Possible reasons for this could be the enclosed nature of the Mediterranean Sea and having a large number of canyons close to highly urbanized areas. These estimates, while useful, do come with important caveats, such as being based on a reduced number (36) of canyons out of 9,477 with data that was in a format of abundance per spatial area that was comparable, and the figures being representative of the entirety of the canyon areas.

The complex topographies, different morphologies, localised hydrodynamic processes, and pressures from marine litter impacts could explain the high degree of variability of litter densities, even within the same broad geographical area. The Messina Canyon shows the highest amount of litter density of all canyons studied with 521,500 items km^{-2} calculated from data provided from four different channels within the canyon area, ranging from a minimum of 121,000 items km^{-2} in the Sant'Agata channel (already twice the density of the next most littered canyon, SY82 Canyon, in Table 3) to one of the Tremestieri channels with over 1.3 million items km^{-2}, two orders of magnitude higher than even the other most littered canyons in the Mediterranean Sea. Localised conditions could be responsible for these extraordinary densities, such as the occurrence of violent flash floods in *fiumara* (short but steep ephemeral streams), that are exacerbated by a densely urbanized coastal area and poor or no waste management, generating sedimentary submarine gravity flows, seafloor erosion and slope failures that can transport large numbers of litter items (Pierdomenico et al., 2019b).

TABLE 3 Litter densities transformed to n km^{-2} with SD where available.

Canyon	Mean litter density (n km^{-2})	Litter items per canyon	Litter items in all canyons	Sampling method
SY82 (Xisha Trough) [6]	51,929			ROV
SY78 (Xisha Trough) [6]	36,818			ROV
Monterey Canyon [9]	473			ROV
North Pacific canyons	29,740	1.16×10^{7}	2.43×10^{10}	
Messina Canyon [8]	521,200 ± 117,100			ROV
La Fonera Canyon [10]	28,450 ± 45361			ROV
Cap de Creus Canyon [2, 10]	25,990 ± 6,312			ROV
Sardinia canyons [1]	17,500 ± 10,082			ROV
Bordighera Canyon [4]	12,138			ROV
Begeggi Canyon [4]	4,539			ROV
Arma di Taggia Canyon [4]	4,418			ROV
Blanes Canyon [7, 10]	3,574 ± 2,176			ROV, Trawl
Dramont Canyon [4]	2,564			ROV
Monaco Canyon [4]	2,135			ROV
Corsica canyons [3]	268 ± 315			ROV
Gulf of Lyon canyons [3, 7]	85 + 153			ROV
Mediterranean canyons	51,905 ± 20,606	6.26×10^{6}– 1.45×10^{7}	5.11×10^{9} – 1.18×10^{10}	
Belle-île Canyon [11]	19,072			TC
Arcachon Canyon [11]	14,358 ± 5,857			TC
Morgat Canyon [11]	13,431 ± 7,223			TC
Lisbon Canyon [5]	6,616			ROV
St. Nazaire Canyon [11]	5,873			ROV
Rochebonne Canyon [11]	5,654			ROV
Morgat - Douarnenez Canyon [11]	5,467			ROV
Guilvinec Canyon [11]	5,346 ± 5,620			ROV
Crozon Canyon [11]	3,695			ROV
Odet Canyon [11]	3,256 ± 843			TC
Setubal Canyon [5]	2,463			ROV
Lampaul Canyon [11]	2,349			ROV
Petit Sole Canyon [11]	2,076 ± 484			ROV
Chapelle Canyon [11]	1,684 ± 561			TC
Whittard Canyon [7]	1,400 ± 133			ROV
Ars Canyon [11]	1,206 ± 281			ROV, TC
Cascais Canyon [5]	1,058			ROV
Croisic Canyon [11]	769			ROV
Dangaard & Explorer Canyons [7]	720 ± 1791			ROV
Sorlingues Canyon [11]	592 ± 414			ROV
Nazare Canyon [5]	417 ± 568			ROV
North Atlantic canyons	4,643 ± 1,067	1.72×10^{6} – 2.74×10^{6}	2.66×10^{9} – 4.24×10^{9}	
Global ocean canyons	22,488 ± 6,897	7.17×10^{6} – 1.36×10^{7}	6.8×10^{10} – 1.28×10^{11}	

1. Cau et al., 2017; 2. Dominguez Carrió, 2018; 3. Gerigny et al., 2019; 4. Giusti et al., 2019; 5. Mordecai et al., 2011; 6. Peng et al., 2019; 7. Pham et al., 2014; 8. Pierdomenico et al., 2019b; 9. Schlining et al., 2013; 10. Tubau et al., 2015; 11. van den Beld et al., 2017

Mean density ranges for broad geographical regions and the global ocean were calculated using a 95% confidence interval to remove outliers.

Moreover, sediments in submarine canyons are transient and in flux, with episodic movements spanning tens to thousands of years before reaching their end points, which could help explain somewhat the density variability within canyons and between those in the same geographical area (Kane and Fildani, 2021). Recent studies looking at microplastics in deep-sea sediments point to intermediate depths (200 - 2000 m) and the continental rise (2000 – 4000 m) having 10 times greater loads of litter density than deeper parts of the seafloor, although trenches are known to be litter accumulation zones (Martin et al., 2022). These findings agree with other studies in two North Atlantic canyons (Norfolk Canyon and Baltimore Canyon) which show litter (both microplastics and macroplastics) to be more prevalent in the higher and intermediate sections of the canyons suggesting that macroplastics may be deposited earlier than microplastics by down-canyon currents (Jones et al., 2022). Given the timescales involved and that most canyons featured in this study (except for the Cascais Canyon and Nararé Canyon) have not been sampled at depths greater than 4000 m, it is yet unknown whether the results from studies on microplastics can be extrapolated to deeper areas of submarine canyons to show whether they remain less affected, accumulate less macroplastics or do so less rapidly than the intermediate continental slope, given the strong gravity flows that are known to occur in canyons (Kane et al., 2020).

Other localised hydrographic factors can translocate litter, as is the case of Corsica Island, that is affected by currents in the Gulf of Lyon, Ligurian Sea and Tyrrhenian Sea (Gerigny et al., 2019). The current reaching the north Tyrrhenian Sea creates a mesoscale eddy dividing the oceanic flow into two currents with opposing orientations (north and south), creating a litter accumulation zone to the north of the island (which can be aggravated by seasonal tourism activities) that cannot drain to Ligurian waters due natural topographic barriers on the seabed, whereas the southern current drains part of the litter debris to the south of Corsica (Gerigny et al., 2019). Off the French Mediterranean coast, low litter densities have been found on the continental shelf contrasting canyons adjacent to heavily urbanized areas such as Marseilles, suggesting localised hydrodynamic conditions possibly influenced by the discharge of the Rhône River, removing litter from the continental shelf into deeper areas (Galgani et al., 1996). In contrast, river flow may explain the relatively low litter densities generally recorded in some Gulf of Lyon canyons, such as high sedimentation rates in adjacent canyons of the Var River burying items of litter thus preventing them from being observed on imagery data (Galgani et al., 1996; Fabri et al., 2014; Pham et al., 2014; Gerigny et al., 2019). River discharge can be responsible for relatively high densities in some canyons in the Bay of Biscay, where the Belle-île Canyon shows the highest mean density and is believed to be heavily influenced by input from the Loire River despite being located on the widest part of the continental shelf of the Armorican margin (van den Beld et al., 2017).

In the Monterey Canyon hydrographic regimes are also thought to be responsible for litter accumulation zones, where debris swept off the continental shelf into the canyon is restricted by topographical barriers and is coupled with sediment transport processes that carry debris into deep habitats that characterize canyons as conduits for sediments and litter (Canals et al., 2006; Schlining et al., 2013). Similar patterns in movements have been observed in the South China Sea where large litter dumps are found in terrace scarps in the upper headless canyons of the Xisha trough, located approximately 150 km from land and with a favorable topography for litter to accumulate (Peng et al., 2019). The area is subject to frequent turbidity currents, receiving litter and sediment delivered by along-shelf currents, with turbidity currents having been found to transfer plastic down the canyon to the deeper parts of the ocean floor which may then be redistributed into accumulation zones (Zhong and Peng., 2021)

Strong bottom currents and periodic dense shelf water cascading events affect the Cap de Creus Canyon and could be responsible for temporal variations by moving and redistributing large amounts of litter to deeper areas where the canyon floor becomes an accumulation zone (Canals et al., 2006). Mean densities of 8,090-42,100 items km^{-2} in different studies have been recorded, where in one instance densities of >28,000 items km^{-2} were recorded at depths >1000 m, in another study the highest densities were observed at depths <400 m (Tubau et al., 2015; Dominguez-Carrió, 2018). These differences serve to demonstrate that there can be substantial variations within a canyon due to data being acquired at different depths, time periods where redistribution of litter may be taking place, or geomorphological settings within the canyon. Bottom currents have been shown to control the distribution of microplastics on the seafloor, especially those transported via submarine channels linked to terrestrial sources in the Tyrrhenian Sea, with stronger gravity currents in deeper areas capable of flushing them down the canyon even further, with greater implications for the translocation of macroplastics (Kane et al., 2020).

Litter composition in submarine canyons

There is no clear geographical separation in the litter composition affecting different canyons. Differences in enumeration were not a limiting factor when comparing litter composition between sites, as publications that used abundance in all forms, or weight as their measuring unit could be included. The distribution of DFG has been found to have a negative and non-linear effect on other types of benthic litter, dependent on the location of fishing grounds, type of fishing activities, and whether litter removal and redistribution to rocky bottoms outside of sampling capabilities takes place (Lopez-Lopez et al., 2017; Angiolillo, 2019).

As with litter density there can be marked variations in composition even within the same canyon, such as for the Cap de Creus Canyon in Figure 10 (Tubau et al., 2015; Dominguez Carrió, 2018). The land area adjacent to the canyon is a national park and is relatively unpopulated although there is considerable commercial fishing activity in the canyon with fishing concentrating along the flank areas at depths of 300–700 m. This may explain the high presence of DFG at shallower depths (Cap de Creus(i) in Figure 10), and a much greater proportion of plastic litter than fishing gear sampled at much greater depths (Cap de Creus (ii) in Figure 10), with trawling removing small items of litter from shallower depths coupled with deposition at greater depths by bottom currents and dense shelf water cascading events (Tubau et al., 2015; Dominguez Carrió, 2018). Other factors could include discharge from the Rhône River, despite being 160 km away from the canyon area, and aeolian transport by the Tramuntana winds, which can transport light items of litter from land onto the sea and cause litter accumulation in this canyon (Galgani et al., 2000; Tubau et al., 2015).

Socio-economic factors and anthropogenic activities must also be taken into account when considering differences in litter abundance and composition. Despite the relative geographical closeness of the Gulf of Lyon canyons to land, they were more affected by higher densities from fishing debris and trawling. Canyons in the Ligurian Sea, where there are smaller and more artisanal fishing fleets, saw higher densities of litter sourced from shipping and recreational activities (Fabri et al., 2014; Giusti et al., 2019). The presence of fisheries adjacent to or in canyon areas exerts a large influence on fishing litter found especially at shallower depths where fishing activities are unimpeded by depth or complex topographical terrains. This is observed in Sardinian canyons which are surrounded by a relatively low coastal population and thus a lower land-based litter input, yet small scale professional fisheries can account for up to three times higher DFG density when compared to other types of litter (Cau et al., 2017). Similarly, the "Sagres Bank" as it is known among local fishermen, can be found by the São Vicente Canyon where there is a high fishing activity correlating with a large proportion of DFG found in the canyon, although the sampling depth in this canyon was much shallower than the other Portuguese canyons (Figure 11) (Oliveira et al., 2015). The Lisbon and Setubal canyons were found to be markedly more impacted by plastic litter, due to their closer proximity to densely populated and highly industrialized areas, also receiving direct input from the Tagus River. The Nazaré Canyon appears to be much less affected by land-based litter and shows higher levels of fishing litter, in part due to the greater distance surveyed within the canyon from the coast, and greater maritime activity (Mordecai et al., 2011). Despite the Bay of Biscay being an area of high fishing activity there is a greater prevalence of plastic litter and categories combined under "other" in Figure 10. This can be partly explained by the large influence of land-based sources of litter from the Loire River and Gironde estuary, as well as the increased maritime activities from seasonal tourism in the area (Galgani et al., 2000). There is also evidence that unlike plastic litter, fishing litter is much less likely to be displaced by currents due to its size and weight since it is not found to preferentially aggregate around corals or complex habitats (van den Beld et al., 2017).

Depth ranges in canyon studies

Depth of surveys (when made available) showed a large overall range and a clear geographical separation (with some exceptions) between canyons sampled at shallower depths and those with deeper data (Figure 11). Except for the Blanes Canyon, all canyons where depth was provided were sampled using ROVs using video data mainly. An otter trawl and Agassiz trawl were used in the Blanes Canyon to depths of 2,700 m which were used for sampling megafauna, and not as part of fishing surveys as is common with other studies that use trawling on the continental shelf (Ramirez-Llodra et al., 2013). Depth ranges are largely dependent on the study in which they are conducted with some studies from the Sardinian and Ligurian Sea canyons sampling at shallower depths, whereas those off the coast of Portugal (except for São Vicente Canyon which was sampled on the canyon head and was not part of the same study) were sampled at great depths (Cau et al., 2017; Giusti et al., 2019; Mordecai et al., 2011). Caution must be exercised when trying to establish patterns between litter densities, composition, and depth ranges in different canyons unless the data are segmented accordingly, which is often not the case.

Marine litter interactions with biota

Over 29% of studies recorded interactions of marine litter with biota or the surrounding environment, with the level of observational detail varying greatly. Some studies detailed types of interactions and impacts observed (mainly studies that focussed on benthic biodiversity), whereas others only acknowledged that interactions were observed with no further comparative data provided, with little or no consistency between studies. It could be argued that studies that use trawling cannot directly view interactions that litter may have with its surroundings in-situ, unlike ROVs or other visual data-capture techniques, although some interactions like colonization, epibiosis or encrustation can still be observed on litter items collected.

Characteristics of biota, especially of coral skeletons in terms of flexibility or resistance to friction, can also play a role in the impacts endured, such as entanglement, smothering or partial necrosis (Bo et al., 2014; Kühn et al., 2015). The upright and rugose structure of biota such as corals and sponges, may render

them particularly vulnerable to entanglement or smothering by litter, hence why are considered sentinels (Galgani et al., 2018). Entanglement has been observed as an impact on thirty-four taxa (mostly cnidarians), predominantly caused by fishing gears, with abrasion being the most common action that can cause breakage of biotic structures and progressive removal of tissues, making them more vulnerable to disease and covering by epibionts (Angiolillo and Fortibuoni, 2020). Coral species that are breakable are frequently observed as having debris on the surrounding area following interaction with marine litter or fishing activities (Angiolillo et al., 2015). Interactions between benthic fauna and DFG and the consequences of these (such as ghost fishing, smothering or coverage) can cause significant modifications to the structure and functioning of reef ecosystems (Angiolillo and Fortibuoni, 2020). Indeed, there is a paucity of studies at population level over time assessing how many organisms in a population are affected by litter, providing valuable information, such as a study carried out at the HAUSGARTEN observatory in the Arctic Ocean (Parga Martinez et al., 2020). Interactions with microplastics and macroplastics under controlled conditions have also been found to be species specific, with potential implications for large changes within coral community composition and subsequent biodiversity in submarine canyons and deep-sea environments (Mouchi et al., 2019)

Negative interactions may be very much underestimated, and the pressure exerted by litter on the environment may be greater than thought, outweighing any positive interactions that may occur. Of the studies that used imaging data, over 54% did not list any impacts or interactions (or lack of thereof), suggesting an important gap in the data even when interaction identification is potentially possible. Having data on litter interactions can be as important as knowing how much litter is on the seafloor. Recording interactions helps identify stresses that debris could be exerting and can help determine long-term effects that are yet relatively unknown. Other interactions that may seem advantageous at first glance, such as increased substrate heterogeneity, increased availability as substrate for colonization, shelter, or even enhancing the presence of some species, may be less so since they involve changes in diversity patterns, making the true impact of litter on benthic fauna very difficult to quantify (Mordecai et al., 2011).

Litter classification systems and marine litter protocols for submarine canyons

Studies that did not use a protocol to classify litter were in the majority, with less than 27% doing so. The main official protocols available are regional in nature and are intended for use in European waters. Official litter protocols are much more than mere classification systems, with OSPAR and MEDITS detailing the methodology for sampling (trawling), use of equipment, identification, and enumeration (MEDITS, 2017, OSPAR Commission, 2017). These two protocols also prioritize using fishing expeditions that were originally designed to provide fish stock assessments to save costs, and is cheaper than acquiring visual data (OSPAR Commission, 2017; Spedicato et al., 2020). Trawling is no longer recommended for studying submarine canyons as it can alter natural sedimentary environments, cause sediment resuspension events and can be destructive towards benthic environments. MEDITS also establishes a framework for the annual sampling of macrolitter and collection of data providing temporal and spatial comparability (Ramirez-Llodra, et al., 2013; MEDITS, 2017; Paradis et al., 2017). Temporal scales of studies are important to determine whether marine litter is increasing or decreasing and by how much, with scales of ten years or more observed in eleven studies, of which only two were in submarine canyons, although not all the timespans observed in the studies from the corpus represented continuous intervals of data (Schlining et al, 2013; Gerigny et al., 2019).

Studies that encompass large time ranges can provide a wider knowledge of litter distribution, density, patterns, and trends required for a better understanding of the pressures of marine litter on the environment (Alomar et al., 2020). Most studies outside of European waters did not follow any litter protocols, possibly due to a lack of regional protocols suitable for deep-sea litter analysis or a lack of requirement like there is in European waters with the MSFD.

Litter classification systems were used by over 95% of studies in the corpus, with over 65% using a one-tier classification system only (categories), and over 34% using a two-tier system (categories and subcategories). The mean number of subcategories shows a much higher variability (18.6 ± 11.6) than categories, whereas the mean number of categories used (7.3 ± 3.6) is lower than the twelve standardized top-level category groups derived in this review based on observation from studies in the corpus to include all main litter types found (Figure 7). The number of categories used in the official protocols is lower than the mean in the corpus (7 for MSFD, 7 for MEDITS and 6 for OSPAR), although the mean number of subcategories in the protocols was substantially higher than in the corpus (52 for MSFD, 28 for MEDITS and 39 for OSPAR) (Galgani et al., 2013; MEDITS, 2017; OSPAR Commission, 2017). The higher variability in the corpus subcategories used indicates that whereas most publications used few or no subcategories, the minority that did follow the established protocols used an elevated number of subcategories, with some studies that used the OSPAR protocol listing up to 39 litter subcategories in their classification system. High variabilities can also be observed in the publications that did follow a protocol, seen in the number of studies that used fragments of the classification system instead of the full classification systems provided. Possible reasons could be that nothing was recorded in some of the categories/subcategories, in which case there would

be an underreporting of data of absence, or because items could not be identified. Many publications also added custom categories such as 'general' or 'miscellaneous' to those supplied in the protocols, especially those that followed the MSFD, indicating difficulty in placing some items of litter in any of the categories provided.

Fishing-specific top-level categories were included in over 40% of publications in the corpus (Figure 7), although fishing gear is not used as a category grouping in any of the official protocols and is usually included as a subcategory in plastics, metals, rubber, or general/miscellaneous categories. Over 10% of artificial polymer, metal and rubber subcategories in the corpus belong to fishing gear items, indicative of studies that follow the official protocols and how they methodically classify litter, with the first level classifying by material and the second level by item type. Corpus studies that do not follow any protocols may be categorizing litter in a more intuitive but less systematic manner. The discrepancy between how official protocols and how many corpus studies classify litter could point towards a difference in questions asked or prioritized. A more methodical materials-led approach may be more beneficial if trying to evaluate the physiochemical or toxicological impacts of litter. A more intuitive approach led by type of litter may be more appropriate if trying to assess possible sources or impacts derived from specific anthropogenic activities. Another possibility could be that the official protocol classification systems may not be sufficiently fitting in practice for the identification of the main types of litter found in the corpus studies, given the low adherence to the protocol classification systems available and the large number of studies that do not follow them. A separate and unified litter classification system independent of the litter sampling methods in the protocols could be used for deep-sea environments, irrespective of geographical location, maintaining a degree of flexibility to include new litter subcategories if required for types of litter that may be found in specific locations, as a solution to bridge the disconnect between the classification systems in the protocols and those used in studies.

The variety, variability, and resolution of classification systems in the corpus studies, and the loose adherence of classification systems provided by the protocols, could pose the question of the usefulness of using high-resolution classification systems, and whether doing so at a lower resolution could lead to easier litter classification. Higher-resolution data, however, allows types of litter pressures to be identified to a much greater precision allowing for specific problems caused by marine litter to be identified even if they are highly localised. At larger scales, lower resolutions may be more useful to allow comparability between studies if they are using the same, or at least similar classification systems. Recording litter data at a higher resolution, allows conversion to lower resolutions or reclassification depending on the criteria of the study, such as assessing the amount and impacts of fishing gear. Using a high-resolution system would allow for relevant subcategories within groups such as artificial polymers, metals, or rubber to be regrouped for this purpose to convert from a more methodical materials led approach to a more intuitive activity led approach. If, however, the initial recording is more intuitively led by associated activity (such as fishing gear) then it would be impossible to reclassify to estimate the amount of any given material on the seafloor, such as plastics. The lack of standardization to this respect could continue to make comparisons difficult, although having high resolution data allows for comparison between sites, such as in Figure 10 where lowering the overall thematic resolution allowed for comparison of litter composition in different submarine canyons.

Conclusions and recommendations

It is very difficult to ascertain how litter is affecting submarine canyons in different geographical areas when <1% have been studied for marine litter and only 36 canyons have data that can be used for comparative purposes to establish regional and global canyon litter budgets. Another difficulty lies in the accessibility of the data, where many studies did not comply with FAIR (Findability, Accessibility, Interoperability and Reuse) data principles, nor is data provided in accessible or comparable formats on many occasions. This is compounded by numerous knowledge gaps and lack of information of where the data was taken from within the submarine canyons, being incongruent with the acceptance of their varied topographic profiles. The following recommendations are put forward:

Standardization in classification

There is a need to standardize identification, enumeration, quantification, and classification of marine litter in deep-sea environments generally and especially within submarine canyons. At present there is no consensus on how data are reported or presented, making comparisons between studies very difficult which may preclude the true extent of litter impacts from being quantified or identified. Most studies seem to use litter classification systems based on their own findings and not based on any existing marine litter protocols available, with a dichotomy in litter classification systems. Established protocols take a more materials-based approach evident in the inclusion of fishing gear as subcategories of plastics, metal, and rubber, whereas many studies take a more intuitive functionality-based approach having fishing gear as a main category based on its prevalence and impact on benthic environments. This raises the point of whether the classification systems in the official protocols are useful or suitable for marine litter studies beyond floating, beach or coastal areas. It is not within the scope of this review to

evaluate different litter protocols to this effect although having a unified and standardized approach when identifying and classifying litter that considers different resolutions of litter identification, the impact of fishing gears and the materials they are composed of, could be very beneficial.

Standardization in enumeration and quantification

Enumeration methods are varied and diverse which can be problematic when attempting to derive spatial and temporal patterns and impacts. The most flexible form of enumeration for the purpose of comparison is that of abundance in a spatial area unit, although one potential pitfall is a possible underestimation of large fishing gear, where volume could give a more appropriate estimation. A unified method of enumerating benthic litter that takes into consideration the relative size of items to account for large fishing gears would be beneficial. Studies that use weight can also give data based on abundance and the coupling of both formats could be seen as complimentary and not mutually exclusive. Indeed, until standards are introduced and harmonization across studies is improved, it would be recommended to report data in as many dimensions as possible.

Litter interactions and impacts

Interactions between marine litter and the surrounding environment/biota are very much underreported and an aspect of the research that needs to be developed further. The relatively small number of studies that have data on litter interactions and the differences between these denote an urgent requirement for standardization in this area. While recognizing that the scope of many studies may not be identification of species or biological in nature, listing interactions with benthic fauna and or abiotic structures would be of much use when assessing the impacts and any possible underestimation of negative impacts. It would be advantageous to take a sentinel approach for monitoring purposes, and if studies rely on imagery, to quantify interactions at population level where possible. Unifying the types of interactions and impacts possible would be advantageous so that the extent of these impacts, temporally and spatially, can be evaluated.

Considerations when evaluating benthic marine litter

Submarine canyons are very diverse topographic structures and as such require careful consideration when trying to understand how affected they are by marine litter. Density and composition should be considered together in submarine canyons at least, as the complex processes that take place within and in different parts of canyons can determine the amount and type of litter found. When evaluating benthic litter in canyons it is important to consider that while canyons are regarded as conduits for the transport sediments and nutrients connecting the continental shelf with deeper basins, each canyon structure is unique and is affected by a set of circumstances that may not be transposable to another canyon, even if located in a close geographic setting. Their complexities require a holistic approach to study different parts within a canyon to have a greater understanding of litter impact on the canyon as a whole. Having a single density or composition data figure from a canyon may be useful at first glance especially when comparing with other sites but does not give a full or realistic picture, especially if it is not known which part of the canyon the data is pertinent to. When evaluating litter density and composition in canyons the following factors could be considered:

a. Hydrographic regimes that occur within the canyon and in the geographical area that may be responsible for the transport of litter. River discharge even at distance may have a considerable impact on litter in canyons and must be considered.
b. Seabed barriers and topography that may prevent litter from redistributing and create accumulation zones, related to hydrographic regimes.
c. The standard canyon geomorphic settings (head, flanks, thalweg, floor, mouth) as well as depth, for more accurate segmented results.
d. Proximity of submarine canyons to urban areas of high population density and deficiencies in waste management.
e. Shipping lanes and sources of litter (land or marine).
f. Fishing activities and seasonal variations that may explain the litter composition.
g. Conservation zones or marine protected areas close to submarine canyons and their enforcement.

Data availability statement

The original contributions presented in the study are included in the article/Supplementary Material. Further inquiries can be directed to the corresponding author.

Author contributions

IH, conceptualization, methodology, formal analysis, investigation, writing – original draft, and visualization. JD, conceptualization, methodology, validation, formal analysis,

investigation, resources, data curation, writing – review and editing, supervision, and project administration. VH, conceptualization, methodology, validation, formal analysis, resources, writing – review and editing, supervision, and project administration. AD, conceptualization, methodology, validation, resources, writing – review and editing, supervision, and project administration. All authors contributed to the article and approved the submitted version.

Conflict of interest

The authors declare that the research was conducted in the absence of any commercial or financial relationships that could be construed as a potential conflict of interest.

Publisher's note

Supplementary material

The Supplementary Material for this article can be found online at: https://www.frontiersin.org/articles/10.3389/fmars.2022.965612/full#supplementary-material

References

Alomar, C., Compa, M., Deudero, S., and Guijarro, B. (2020). Spatial and temporal distribution of marine litter on the seafloor of the Balearic islands (western Mediterranean Sea). *Deep-Sea Res. Part I: Oceanogr. Res. Papers* 155, 103178. doi: 10.1016/j.dsr.2019.103178

Alvito, A., Bellodi, A., Cau, A., Moccia, D., Mulas, A., Palmas, F., et al. (2018). Amount and distribution of benthic marine litter along sardinian fishing grounds (CW Mediterranean Sea). *Waste Manage.* 75, 131–140. doi: 10.1016/j.wasman.2018.02.026

Amon, D. J., Kennedy, B. R. C., Cantwell, K., Suhre, K., Glickson, D., Shank, T. M., et al. (2020). Deep-Sea debris in the central and Western pacific ocean. *Front. Mar. Sci.* 7. doi: 10.3389/fmars.2020.00369

Andrady, A. L. (2011). Microplastics in the marine environment. *Mar. Pollut. Bull.* 62 (8), 1596–1605. doi: 10.1016/j.marpolbul.2011.05.030

Angiolillo, M. (2019). *Chapter 14 - Debris in Deep Water,World Seas.Volume III: Ecological Issues and Environmental Impacts*, (*Second* Edition), Academic Press, (pp. 251–268). ISBN 9780128050521. doi: 10.1016/B978-0-12-805052-1.00015-2

Angiolillo, M., and Fortibuoni, T. (2020). Impacts of marine litter on Mediterranean Reef Systems: From shallow to deep waters. *Frontiers in Marine Science*, 7. doi: 10.3389/fmars.2020.581966

Angiolillo, M., Lorenzo, B., Farcomeni, A., Bo, M., Bavestrello, G., Santangelo, G., et al. (2015). Distribution and assessment of marine debris in the deep tyrrhenian Sea (NW Mediterranean Sea, Italy). *Mar. Pollut. Bull.* 92 (1–2), 149–159. doi: 10.1016/j.marpolbul.2014.12.044

Avio, C. G., Gorbi, S., and Regoli, F. (2017). Plastics and microplastics in the oceans: From emerging pollutants to emerged threat. *Mar. Environ. Res.* 128, 2–11. doi: 10.1016/j.marenvres.2016.05.012

Barboza, L. G. A., Cózar, A., Gimenez, B. C. G., Barros, T. L., Kershaw, P. J., and Guilhermino, L. (2018). Macroplastics pollution in the marine environment. In: C. Sheppard (eds) *World Seas: An Environmental Evaluation Volume III: Ecological Issues and Environmental Impacts*, Academic Press (pp. 305–328), ISBN 9780128050521. doi: 10.1016/B978-0-12-805052-1.00019-X

Barnes, D. K. A., Galgani, F., Thompson, R. C., and Barlaz, M. (2009). Accumulation and fragmentation of plastic debris in global environments. *Philos. Trans. R. Soc. B: Biol. Sci.* 364 (1526), 1985–1998. doi: 10.1098/rstb.2008.0205

Baudrier, J., Lefebvre, A., Galgani, F., Saraux, C., and Doray, M. (2018). Optimising French fisheries surveys for marine strategy framework directive integrated ecosystem monitoring. *Mar. Policy* 94, 10–19. doi: 10.1016/j.marpol.2018.04.024

Bergmann, M., and Klages, M. (2012). Increase of litter at the Arctic deep-sea observatory HAUSGARTEN. *Mar. Pollut. Bull.* 64 (12), 2734–2741. doi: 10.1016/j.marpolbul.2012.09.018

Bo, M., Bava, S., Canese, S., Angiolillo, M., Cattaneo-Vietti, R., and Bavestrello, G. (2014). Fishing impact on deep Mediterranean rocky habitats as revealed by ROV investigation. *Biol. Conserv.* 171, 167–176. doi: 10.1016/j.biocon.2014.01.011

Borrelle, S. B., Ringma, J., Law, K. L., Monnahan, C. C., Lebreton, L., McGivern, A., et al. (2020). Predicted growth in plastic waste exceeds efforts to mitigate plastic pollution. *Science* 369 (6510), 1515–1518. doi: 10.1126/science.aba3656

Botero, C. M., Zielinski, S., Pereira, C. I., León, J. A., Dueñas, L. F., and Puentes, V. (2020). The first report of deep-sea litter in the south-Western Caribbean Sea. *Mar. Pollut. Bull.* 157, 111327. doi: 10.1016/j.marpolbul.2020.111327

Buhl-Mortensen, L., and Buhl-Mortensen, P. (2017). Marine litter in the Nordic seas: Distribution composition and abundance. *Mar. Pollut. Bull.* 125 (1–2), 260–270. doi: 10.1016/j.marpolbul.2017.08.048

Canals, M., Pham, C. K., Bergmann, M., Gutow, L., Hanke, G., Van Sebille, E., et al. (2021). The quest for seafloor macrolitter: a critical review of background knowledge, current methods and future prospects. *Environ. Res. Lett.* 16, 023001. doi: 10.1088/1748-9326/abc6d4

Canals, M., Puig, P., de Madron, X. D., Heussner, S., Palanques, A., and Fabres, J. (2006). Flushing submarine canyons. *Nature* 444 (7117), 354–357. doi: 10.1038/nature05271

Cau, A., Alvito, A., Moccia, D., Canese, S., Pusceddu, A., Rita, C., et al. (2017). Submarine canyons along the upper sardinian slope (Central Western Mediterranean) as repositories for derelict fishing gears. *Mar. Pollut. Bull.* 123 (1–2), 357–364. doi: 10.1016/j.marpolbul.2017.09.010

Cau, A., Bellodi, A., Moccia, D., Mulas, A., Pesci, P., Cannas, R., et al. (2018). Dumping to the abyss: single-use marine litter invading bathyal plains of the sardinian margin (Tyrrhenian Sea). *Mar. Pollut. Bull.* 135, 845–851. doi: 10.1016/j.marpolbul.2018.08.007

Chiba, S., Saito, H., Fletcher, R., Yogi, T., Kayo, M., Miyagi, S., et al. (2018). Human footprint in the abyss: 30 year records of deep-sea plastic debris. *Mar. Policy* 96, 204–212. doi: 10.1016/j.marpol.2018.03.022

Company, J. B., Ramirez-llodra, E., Aguzzi, J., Puig, P., Canals, M., Calafat, A., et al. (2012) *Submarine canyons in the Catalan Sea (NW mediterranean): megafaunal biodiversity patterns and anthropogenic threats. Mediterranean submarine canyons: Ecology and governance*. Available at: https://www.researchgate.net/publication/235277627.

Consoli, P., Andaloro, F., Altobelli, C., Battaglia, P., Campagnuolo, S., Canese, S., et al. (2018b). Marine litter in an EBSA (Ecologically or biologically significant area) of the central Mediterranean Sea: Abundance, composition, impact on benthic species and basis for monitoring entanglement. *Environ. Pollut.* 236, 405–415. doi: 10.1016/j.envpol.2018.01.097

Consoli, P., Falautano, M., Sinopoli, M., Perzia, P., Canese, S., Esposito, V., et al. (2018a). Composition and abundance of benthic marine litter in a coastal area of the central Mediterranean Sea. *Mar. Pollut. Bull.* 136, 243–247. doi: 10.1016/j.marpolbul.2018.09.033

Consoli, P., Romeo, T., Angiolillo, M., Canese, S., Esposito, V., Salvati, E., et al. (2019). Marine litter from fishery activities in the Western Mediterranean Sea: The impact of entanglement on marine animal forests. *Environ. Pollut.* 249, 472–481. doi: 10.1016/j.envpol.2019.03.072

Consoli, P., Sinopoli, M., Deidun, A., Canese, S., Berti, C., Andaloro, F., et al. (2020). The impact of marine litter from fish aggregation devices on vulnerable marine benthic habitats of the central Mediterranean Sea. *Mar. Pollut. Bull.* 152, 110928. doi: 10.1016/j.marpolbul.2020.110928

Crocetta, F., Riginella, E., Lezzi, M., Tanduo, V., Balestrieri, L., and Rizzo, L. (2020). Bottom-trawl catch composition in a highly polluted coastal area reveals multifaceted native biodiversity and complex communities of fouling organisms on litter discharge. *Mar. Environ. Res.* 155, 104875. doi: 10.1016/j.marenvres.2020.104875

Debrot, A. O., Vinke, E., van der Wende, G., Hylkema, A., and Reed, J. K. (2014). Deepwater marine litter densities and composition from submersible video-transects around the ABC-islands, Dutch Caribbean. *Mar. Pollut. Bull.* 88 (1–2), 361–365. doi: 10.1016/j.marpolbul.2014.08.016

Dominguez Carrió, C. (2018) *ROV-based ecological study and management proposals for the offshore marine protected area of cap de creus (NW Mediterranean)*. Available at: www.tdx.cat.

de Leo, F. C., Smith, C. R., Rowden, A. A., Bowden, D. A., and Clark, M. R. (2010). Submarine canyons: Hotspots of benthic biomass and productivity in the deep sea. *Proceedings of the Royal Society B: Biological Sciences* 277 (1695), 2783–2792. doi: 10.1098/rspb.2010.0462

du Preez, C., Swan, K. D., and Curtis, J. M. R. (2020). Cold-water corals and other vulnerable biological structures on a north pacific seamount after half a century of fishing. *Front. Mar. Sci.* 7. doi: 10.3389/fmars.2020.00017

Engler, R. E. (2012). The complex interaction between marine debris and toxic chemicals in the ocean. *Environ. Sci. Technol.* 46 (22), 12302–12315. doi: 10.1021/es3027105

Enrichetti, F., Dominguez-Carrió, C., Toma, M., Bavestrello, G., Canese, S., and Bo, M. (2020). Assessment and distribution of seafloor litter on the deep ligurian continental shelf and shelf break (NW Mediterranean Sea). *Mar. Pollut. Bull.* 151, 110872. doi: 10.1016/j.marpolbul.2019.110872

Eriksen, M., Lebreton, L. C. M., Carson, H. S., Thiel, M., Moore, C. J., Borerro, J. C., et al. (2014). Plastic pollution in the world's oceans: More than 5 trillion plastic pieces weighing over 250,000 tons afloat at Sea. *PloS One* 9 (12), e111913. doi: 10.1371/journal.pone.0111913

Eryaşar, A. R., Özbilgin, H., Gücü, A. C., and Sakinan, S. (2014). Marine debris in bottom trawl catches and their effects on the selectivity grids in the north eastern Mediterranean. *Mar. Pollut. Bull.* 81 (1), 80–84. doi: 10.1016/j.marpolbul.2014.02.017

European Commission (2010). 'COMMISSION DECISION of 1 September 2010 on criteria and methodological standards on good environmental status of marine waters', (2010/477/Eu) *Commission Decision*, (2008), p. 11. https://eur-lex.europa.eu/LexUriServ/LexUriServ.do?uri=OJ:L:2010:232:0014:0024:EN:PDF

Fabri, M. C., Pedel, L., Beuck, L., Galgani, F., Hebbeln, D., and Freiwald, A. (2014). Megafauna of vulnerable marine ecosystems in French Mediterranean submarine canyons: Spatial distribution and anthropogenic impacts. *Deep-Sea Res. Part II: Topical Stud. Oceanogr* 104, 184–207. doi: 10.1016/j.dsr2.2013.06.016

Fernandez-Arcaya, U., Ramirez-Llodra, E., Aguzzi, J., Allcock, A. L., Davies, J. S., Dissanayake, A., et al. (2017). Ecological role of submarine canyons and need for canyon conservation: A review. *Front. Mar. Sci.* 4. doi: 10.3389/fmars.2017.00005

Ferrigno, F., Appolloni, L., Russo, G. F., and Sandulli, R. (2018). Impact of fishing activities on different coralligenous assemblages of gulf of Naples (Italy). *J. Mar. Biol. Assoc. U K* 98 (1), 41–50. doi: 10.1017/S0025315417001096

Fiorentino, F., Gancitano, V., Giusto, G. B., Massi, D., Sinacori, G., Titone, A., et al. (2015). Marine litter on trawlable bottoms of the Strait of Sicily/Rifiuti antropici marini sui fondi strascicabili dello strettottotto di Sicilia. *Biologia Marina Mediterranea* 22 (1), 225–228. https://www.proquest.com/docview/1819112565

Fleet, D., Vlachogianni, T., and Hanke, G. (2021). *A joint list of litter categories for marine macrolitter monitoring* (Luxembourg, European Union: EUR 30348 EN Publications Office of the European Union, JRC121708), 52. doi: 10.2760/127473

Fortibuoni, T., Ronchi, F., Mačić, V., Mandić, M., Mazziotti, C., Peterlin, M., et al. (2019). A harmonized and coordinated assessment of the abundance and composition of seafloor litter in the Adriatic-Ionian macroregion (Mediterranean Sea). *Mar. Pollut. Bull.* 139, 412–426. doi: 10.1016/j.marpolbul.2019.01.017

Galgani, F. (2019). Litter in the Mediterranean Sea, In: T. Komatsu, H. J. Ceccaldi, J. Yoshida, P. Prouzet and Y. Henocque (eds) *Oceanography Challenges to Future Earth: Human and Natural Impacts on our Seas* (Springer International Publishing), 55–67. doi: 10.1007/978-3-030-00138-4_6

Galgani, F., Hanke, G., Werner, S., Oosterbaan, L., Nilsson, P., Fleet, D., et al. (2013). *Guidance on Monitoring of Marine Litter in European Seas*. Joint Research Centre, Institute for Environment and Sustainability, Publications Office. doi: 10.2788/99475

Galgani, F., Leaute, J. P., Moguedet, P., Souplet, A., Verin, Y., Carpentier, A., et al. (2000). Litter on the sea floor along European coasts. *Mar. Pollut. Bull.* 40 (6), 516–527. doi: 10.1016/S0025-326X(99)00234-9

Galgani, F., Pham, C. K., Claro, F., and Consoli, P. (2018). Marine animal forests as useful indicators of entanglement by marine litter. *Mar. Pollut. Bulletin Elsevier* 135 (June), 735–738. doi: 10.1016/j.marpolbul.2018.08.004

Galgani, F., Souplet, A., and Cadious, Y. (1996). Accumulation of debris on the deep sea floor off the French Mediterranean coast. *Mar. Ecol. Prog. Ser.* 142, 225–234. doi: 10.3354/meps142225

García-Rivera, S., Lizaso, J. L. S., and Millán, J. M. B. (2017). Composition, spatial distribution and sources of macro-marine litter on the gulf of alicante seafloor (Spanish Mediterranean). *Mar. Pollut. Bull.* 121 (1–2), 249–259. doi: 10.1016/j.marpolbul.2017.06.022

García-Rivera, S., Lizaso, J. L. S., and Millán, J. M. B. (2018). Spatial and temporal trends of marine litter in the Spanish Mediterranean seafloor. *Mar. Pollut. Bull.* 137, 252–261. doi: 10.1016/j.marpolbul.2018.09.051

Garofalo, G., Quattrocchi, F., Bono, G., di Lorenzo, M., di Maio, F., Falsone, F., et al. (2020). What is in our seas? assessing anthropogenic litter on the seafloor of the central Mediterranean Sea. *Environ. Pollut.* 266, 115213. doi: 10.1016/j.envpol.2020.115213

Gerigny, O., Brun, M., Fabri, M. C., Tomasino, C., le Moigne, M., Jadaud, A., et al. (2019). Seafloor litter from the continental shelf and canyons in French Mediterranean water: Distribution, typologies and trends. *Mar. Pollut. Bull.* 146, 653–666. doi: 10.1016/j.marpolbul.2019.07.030

Geyer, R. (2020). Chapter 2 - Production, use, and fate of synthetic polymers. In: T. M. Letcher (eds) *Plast. Waste Recycling Elsevier*, 13–32. Academic Press. doi: 10.1016/B978-0-12-817880-5.00002-5

Giusti, M., Canese, S., Fourt, M., Bo, M., Innocenti, C., Goujard, A., et al. (2019). Coral forests and derelict fishing gears in submarine canyon systems of the ligurian Sea. *Prog. Oceanogr* 178, 102186 doi: 10.1016/j.pocean.2019.102186

Goto, T., and Shibata, H. (2015). Changes in abundance and composition of anthropogenic marine debris on the continental slope off the pacific coast of northern Japan, after the march 2011 tohoku earthquake. *Mar. Pollut. Bull.* 95 (1), 234–241. doi: 10.1016/j.marpolbul.2015.04.011

Grøsvik, B. E., Prokhorova, T., Eriksen, E., Krivosheya, P., Horneland, P. A., and Prozorkevich, D. (2018). Assessment of marine litter in the barents Sea, a part of the joint Norwegian-Russian ecosystem survey. *Front. Mar. Sci.* 5 (MAR). doi: 10.3389/fmars.2018.00072

Grinyó, J., lo Iacono, C., Pierdomenico, M., Conlon, S., Corbera, G., and Gràcia, E. (2020). Evidences of human impact on megabenthic assemblages of bathyal sediments in the alboran Sea (western Mediterranean). *Deep Sea Res. Part I: Oceanogr. Res. Papers* 165, 103369. doi: 10.1016/j.dsr.2020.103369

Güven, O., Gülyavuz, H., and Deval, M. C. (2013). Antalya körfezi (doğu akdeniz) batial zonunda bentik çöp birikimi. *Turkish J. Fish Aquat. Sci.* 13 (1), 43–49. doi: 10.4194/1303-2712-v13_1_06

Halevi, G., Moed, H., and Bar-Ilan, J. (2017). Suitability of Google scholar as a source of scientific information and as a source of data for scientific evaluation–review of the literature. *J. Informetrics* 11, 823–834. doi: 10.1016/j.joi.2017.06.005

Harris, P. T., Macmillan-Lawler, M., Rupp, J., and Baker, E. K. (2014). Geomorphology of the oceans. *Mar. Geol.* 352, 4–24. doi: 10.1016/j.margeo.2014.01.011

Harris, P. T., and Whiteway, T. (2011). Global distribution of large submarine canyons: Geomorphic differences between active and passive continental margins. *Mar. Geol.* 285 (1–4), 69–86. doi: 10.1016/j.margeo.2011.05.008

Havens, K., Bilkovic, D. M., Stanhope, D., and Angstadt, K. (2011). Fishery failure, unemployed commercial fishers, and lost blue crab pots: An unexpected success story. *Environ. Sci. Policy Elsevier Ltd 14(4)* pp, 445–450. doi: 10.1016/j.envsci.2011.01.002

Huvenne, V. A. I., and Davies, J. S. (2014). Towards a new and integrated approach to submarine canyon research. *Deep Sea Res. Part II: Topical Stud. Oceanogr* 104, 1–5. doi: 10.1016/j.dsr2.2013.09.012

Ioakeimidis, C., Papatheodorou, G., Fermeli, G., Streftaris, N., and Papathanassiou, E. (2015). *Use of ROV for assessing marine litter on the seafloor*

of saronikos gulf (Greece): A way to fill data gaps and deliver environmental education. SpringerPlus, 4, 463. doi: 10.1186/s40064-015-1248-4

Ioakeimidis, C., Zeri, C., Kaberi, H., Galatchi, M., Antoniadis, K., Streftaris, N., et al. (2014). A comparative study of marine litter on the seafloor of coastal areas in the Eastern Mediterranean and black seas. *Mar. Pollut. Bull.* 89 (1–2), 296–304. doi: 10.1016/j.marpolbul.2014.09.044

Jambeck, J. R., Geyer, R., Wilcox, C., Siegler, T. R., Perryman, M., Andrady, A., et al. (2015). Plastic waste inputs from land into the ocean. *Science* 347 (6223), 768–771. doi: 10.1126/science.1260352

JAMSTEC (2020) *Deep Sea debris database*. Available at: http://www.godac.jamstec.go.jp/catalog/dsdebris/e/.

Jeong, S.-B., Lee, D.-I., Cho, H. S., and Kim, Y.-J. (2005). Characteristics of marine litters distribution on the seabed of the East China Sea. *J. Korean Soc. Mar. Environ. Eng.* 8 (4), 220–226.

Jones, E. S., Ross, S. W., Robertson, C. M., and Young, C. M. (2022). Distributions of microplastics and larger anthropogenic debris in Norfolk Canyon, Baltimore Canyon, and the adjacent continental slope (Western North Atlantic Margin, U.S.A.). *Marine Pollution Bulletin* 174, 113047. doi: 10.1016/j.marpolbul.2021.113047

Kammann, U., Aust, M. O., Bahl, H., and Lang, T. (2018). Marine litter at the seafloor - abundance and composition in the north Sea and the Baltic Sea. *Mar. Pollut. Bull.* 127, 774–780. doi: 10.1016/j.marpolbul.2017.09.051

Kane, I. A., and Clare, M. A. (2019). Dispersion, accumulation, and the ultimate fate of microplastics in deep-marine environments: A review and future directions. *In Frontiers in Earth Science*, 7. doi: 10.3389/feart.2019.00080

Kane, I. A., Clare, M. A., Miramontes, E., Wogelius, R., Rothwell, J. J., Garreau, P., et al. (2020). Seafloor microplastic hotspots controlled by deep-sea circulation. *Science* 368 (6495), 1140–1145. doi: 10.1126/science.aba5899

Kane, I. A., and Fildani, A. (2021). Anthropogenic pollution in deep-marine sedimentary systems–a geological perspective on the plastic problem. *Geol.* 49 (5), 607–608. doi: 10.1130/focus052021.1

Keller, A. A., Fruh, E. L., Johnson, M. M., Simon, V., and McGourty, C. (2010). Distribution and abundance of anthropogenic marine debris along the shelf and slope of the US West coast. *Mar. Pollut. Bull.* 60 (5), 692–700. doi: 10.1016/j.marpolbul.2009.12.006

Koutsodendris, A., Papatheodorou, G., Kougiourouki, O., and Georgiadis, M. (2008). Benthic marine litter in four gulfs in Greece, Eastern mediterranean; abundance, composition and source identification. *Estuarine Coast. Shelf Sci.* 77 (3), 501–512. doi: 10.1016/j.ecss.2007.10.011

Kühn, S., Bravo Revolledo, E., and van Franeker, J. (2015). Deleterious effects of litter on marine life. In: M. Bergmann, L. Gutow and &M. Klages (eds) *Marine Anthropogenic Litter* (75–116). Springer, Cham. doi: 10.1007/978-3-319-16510-3

Kuroda, M., Uchida, K., Tokai, T., Miyamoto, Y., Mukai, T., Imai, K., et al. (2020). The current state of marine debris on the seafloor in offshore area around Japan. *Mar. Pollut. Bull.* 161, 111670. doi: 10.1016/j.marpolbul.2020.111670

Lastras, G., Canals, M., Ballesteros, E., Gili, J. M., and Sanchez-Vidal, A. (2016). Cold-water corals and anthropogenic impacts in la fonera submarine canyon head, northwestern Mediterranean Sea. *PloS One* 11 (5), e0155729. doi: 10.1371/journal.pone.0155729

Lee, D. I., Cho, H. S., and Jeong, S. B. (2006). Distribution characteristics of marine litter on the seabed of the East China Sea and the south Sea of Korea. *Estuarine Coast. Shelf Sci.* 70 (1–2), 187–194. doi: 10.1016/j.ecss.2006.06.003

Lefkaditou, E., Karkani, M., Anastasopoulou, A., Kavadas, S., Christidis, G., and Mytilineou, C. (2013). Litter composition on the shelf and upper slope of the argosaronikos region and the eastern Ionian Sea, as evidenced by MEDITS surveys 1995-2008. *ICES CM 2013/A* 3357, 1–3. Available at: https://www.ices.dk/sites/pub/CM%20Doccuments/CM-2013/Theme%20Session%20A%20contributions/A0613.pdf

LITTERBASE (2020) *Online portal for marine litter*. Available at: https://litterbase.awi.de/litter.

Lopez-Lopez, L., González-Irusta, J. M., Punzón, A., and Serrano, A. (2017). Benthic litter distribution on circalittoral and deep sea bottoms of the southern bay of Biscay: Analysis of potential drivers. *Continental Shelf Res.* 144, 112–119. doi: 10.1016/j.csr.2017.07.003

Loulad, S., Houssa, R., Rhinane, H., Boumaaz, A., and Benazzouz, A. (2017). Spatial distribution of marine debris on the seafloor of Moroccan waters. *Mar. Pollut. Bull.* 124 (1), 303–313. doi: 10.1016/j.marpolbul.2017.07.022

Macfadyen, G., Huntington, T., and Cappell, R. (2009) *Abandoned, lost or otherwise discarded fishing gear, FAO consutlants, lymington. united kingdom of great Britain and northern Ireland, FAO fisheries and aquaculture technical paper*. Available at: http://www.unep.org/regionalseas/marinelitter/publications/default.asp.

Maes, T., Barry, J., Leslie, H. A., Vethaak, A. D., Nicolaus, E. E. M., Law, R. J., et al. (2018). Below the surface: Twenty-five years of seafloor litter monitoring in coastal seas of north West europe 1992–2017). *Sci. Total Environ.* 630, 790–798. doi: 10.1016/j.scitotenv.2018.02.245

Martín-Martín, A., Orduna-Malea, E., Thelwall, M., and Delgado López-Cózar, E. (2018). Google Scholar, web of science, and scopus: A systematic comparison of citations in 252 subject categories. *J. Informetrics* 12 (4), 1160–1177. doi: 10.1016/j.joi.2018.09.002

Martin, C., Young, C. A., Valluzzi, L., and Duarte, C. M. (2022). Ocean sediments as the global sink for marine micro- and mesoplastics. *Limnology Oceanogr Lett.* 7 (3), 235–243. doi: 10.1002/lol2.10257

Matos, F. L., Ross, S. W., Huvenne, V. A. I., Davies, J. S., and Cunha, M. R. (2018). Canyons pride and prejudice: Exploring the submarine canyon research landscape, a history of geographic and thematic bias. *Prog. Oceanogr* 169, 6–19. doi: 10.1016/j.pocean.2018.04.010

Mecho, A., Francescangeli, M., Ercilla, G., Fanelli, E., Estrada, F., Valencia, J., et al. (2020). Deep-sea litter in the gulf of cadiz (Northeastern Atlantic, Spain). *Mar. Pollut. Bull.* 153, 110969. doi: 10.1016/j.marpolbul.2020.110969

MEDITS-Handbook. Version 9 (2017) *Instruction manual of Mediterranean international bottom trawl survey*. Available at: http://www.sibm.it/MEDITS2011/principaleproject.htm.

Melli, V., Angiolillo, M., Ronchi, F., Canese, S., Giovanardi, O., Querin, S., et al. (2017). The first assessment of marine debris in a site of community importance in the north-western Adriatic Sea (Mediterranean Sea). *Mar. Pollut. Bull.* 114 (2), 821–830. doi: 10.1016/j.marpolbul.2016.11.012

Mifsud, R., Dimech, M., and Schembri, P. J. (2013). Marine litter from circalittoral and deeper bottoms off the Maltese islands (Central Mediterranean). *Mediterr. Mar. Sci.* 14 (2), 298–308. doi: 10.12681/mms.413

Miyake, H., Shibata, H., and Furushima, Y. (2011). Deep-sea litter study using deep-sea observation tools. In: K. Omori, X. Guo, N. Yoshie, N. Fujii, I. C. Handoh, A. Isobe, et al (eds) *Interdisciplinary Studies on Environmental Chemistry - Marine Environmental Modeling and Analysis*, 261–269. TERRAPUB. https://www.researchgate.net/publication/266245893_Deep-Sea_Litter_Study_Using_Deep-Sea_Observation_Tools.

Moed, H. F., Bar-Ilan, J., and Halevi, G. (2016). A new methodology for comparing Google scholar and scopus. *J. Informetrics* 10 (2), 533–551. doi: 10.1016/j.joi.2016.04.017

Mordecai, G., Tyler, P. A., Masson, D. G., and Huvenne, V. A. I. (2011). Litter in submarine canyons off the west coast of Portugal. *Deep Sea Res. Part II: Topical Stud. Oceanogr* 58 (23–24), 2489–2496. doi: 10.1016/j.dsr2.2011.08.009

Moriarty, M., Pedreschi, D., Stokes, D., Dransfeld, L., and Reid, D. G. (2016). Spatial and temporal analysis of litter in the celtic Sea from groundfish survey data: Lessons for monitoring. *Mar. Pollut. Bull.* 103 (1–2), 195–205. doi: 10.1016/j.marpolbul.2015.12.019

Mouchi, V., Chapron, L., Per, E., Prusk, A. M., Meistertzhei, A. L., Vétio, G., et al. (2019). Long-term aquaria study suggests species-specific responses of two cold-water corals to macro-and microplastics exposure. *Environ. Pollut 253* pp, 322–329. doi: 10.1016/j.envpol.2019.07.024

Napper, I. E., and Thompson, R. C. (2019). Marine plastic pollution: Other than microplastic. In: T. M. Letcher and D. A. Vallero (eds) *Waste* (*Second* Edition), 425–442. Academic Press. doi: 10.1016/b978-0-12-815060-3.00022-0

Neves, D., Sobral, P., and Pereira, T. (2015). Marine litter in bottom trawls off the Portuguese coast. *Mar. Pollut. Bull.* 99 (1–2), 301–304. doi: 10.1016/j.marpolbul.2015.07.044

Olguner, M. T., Olguner, C., Mutlu, E., and Deval, M. C. (2018). Distribution and composition of benthic marine litter on the shelf of antalya in the eastern Mediterranean. *Mar. Pollut. Bull.* 136, 171–176. doi: 10.1016/j.marpolbul.2018.09.020

Oliveira, F., Monteiro, P., Bentes, L., Henriques, N. S., Aguilar, R., and Gonçalves, J. M. S. (2015). Marine litter in the upper são Vicente submarine canyon (SW portugal): Abundance, distribution, composition and fauna interactions. *Mar. Pollut. Bull.* 97 (1–2), 401–407. doi: 10.1016/j.marpolbul.2015.05.060

OSPAR Commission (2017) *'CEMP Guidelines on Litter on the Seafloor', OSPAR Agreement 2017-06. EIHA 17/9/1 Annex 12*. https://www.ospar.org/documents?d=37515

Page, M. J., McKenzie, J. E., Bossuyt, P. M., Boutron, I., Hoffmann, T. C., Mulrow, C. D., et al. (2021). The PRISMA 2020 statement: an updated guideline for reporting systematic reviews. *BMJ* 372, n71. doi: 10.1136/bmj.n71

Papadopoulou, K.-N., Smith, C. J., Apostolidis, C. H., and Karachle, P. K. (2015). Trawled up marine litter, first observations from Heraklion Bay. *11th Panhellenic Symposium on Oceanography and Fisheries*, 373–376. https://www.researchgate.net/publication/281118473

Paradis, S., Puig, P., Masqué, P., Juan-Díaz, X., Martín, J., and Palanques, A. (2017). Bottom-trawling along submarine canyons impacts deep sedimentary regimes. *Scientific Reports*, 7 (1), 43332. doi: 10.1038/srep43332

Parga Martínez, K. B., Tekman, M. B., and Bergmann, M. (2020). Temporal trends in marine litter at three stations of the HAUSGARTEN observatory in the Arctic deep Sea. *Front. Mar. Science 7(May)* pp. doi: 10.3389/fmars.2020.00321

Pasquini, G., Ronchi, F., Strafella, P., Scarcella, G., and Fortibuoni, T. (2016). Seabed litter composition, distribution and sources in the northern and central Adriatic Sea (Mediterranean). *Waste Manage.* 58, 41–51. doi: 10.1016/j.wasman.2016.08.038

Peng, X., Dasgupta, S., Zhong, G., Du, M., Xu, H., Chen, M., et al. (2019). Large Debris dumps in the northern south China Sea. *Mar. Pollut. Bull.* 142, 164–168. doi: 10.1016/j.marpolbul.2019.03.041

Pham, C. K., Gomes-Pereira, J. N., Isidro, E. J., Santos, R. S., and Morato, T. (2013). *Abundance of litter on condor seamount (Azores, Portugal, northeast Atlantic)* (Deep-Sea Research Part II: Topical Studies in Oceanography, 98(PA), 204–208). doi: 10.1016/j.dsr2.2013.01.011

Pham, C. K., Ramirez-Llodra, E., Alt, C. H. S., Amaro, T., Bergmann, M., Canals, M., et al. (2014). …Marine litter distribution and density in European seas, from the shelves to deep basins. *PloS One* 9 (4), e95839. doi: 10.1371/journal.pone.0095839

Pierdomenico, M., Cardone, F., Carluccio, A., Casalbore, D., Chiocci, F., Maiorano, P., et al. (2019a). Megafauna distribution along active submarine canyons of the central Mediterranean: Relationships with environmental variables. *Prog. Oceanogr* 171, 49–69. doi: 10.1016/j.pocean.2018.12.015

Pierdomenico, M., Casalbore, D., and Chiocci, F. L. (2019b). Massive benthic litter funnelled to deep sea by flash-flood generated hyperpycnal flows. *Sci. Rep.* 9 (1), 5330. doi: 10.1038/s41598-019-41816-8

Pierdomenico, M., Casalbore, D., and Chiocci, F. L. (2020). The key role of canyons in funnelling litter to the deep sea: A study of the gioia canyon (Southern tyrrhenian Sea). *Anthropocene* 30, 100237. doi: 10.1016/j.ancene.2020.100237

Purser, A., Orejas, C., Gori, A., Tong, R., Unnithan, V., and Thomsen, L. (2013). Local variation in the distribution of benthic megafauna species associated with cold-water coral reefs on the Norwegian margin. *Continental Shelf Res.* 54, 37–51. doi: 10.1016/j.csr.2012.12.013

Ramirez-Llodra, E., de Mol, B., Company, J. B., Coll, M., and Sardà, F. (2013). Effects of natural and anthropogenic processes in the distribution of marine litter in the deep Mediterranean Sea. *Prog. Oceanogr* 118, 273–287. doi: 10.1016/j.pocean.2013.07.027

Ramirez-Llodra, E., Tyler, P. A., Baker, M. C., Bergstad, O. A., Clark, M. R., Escobar, E., et al. (2011). Man and the last great wilderness: Human impact on the deep Sea. *PLoS One* 6 (8), e22588. doi: 10.1371/journal.pone.0022588

Rhinane, H., Houssa, R., and Loulad, S. (2019). *The seafloor marine debris on the north and the central part of the Moroccan Atlantic waters from tangier (35n) to sidi ifni (29n): composition, abundance, spatial distribution, sources and movement* (Remote Sensing and Spatial Information Sciences: ISPRS - International Archives of the Photogrammetry). doi: 10.5194/isprs-archives-xlii-4-w19-377-2019

Rodríguez, Y., and Pham, C. K. (2017). Marine litter on the seafloor of the faial-pico passage, Azores archipelago. *Mar. Pollut. Bull.* 116 (1–2), 448–453. doi: 10.1016/j.marpolbul.2017.01.018

Ryan, P. G., Weideman, E. A., Perold, V., Durholtz, D., and Fairweather, T. P. (2020). *A trawl survey of seafloor macrolitter on the south African continental shelf* (150: Marine Pollution Bulletin). doi: 10.1016/j.marpolbul.2019.110741

Sánchez, P., Masó, M., Sáez, R., De Juan, S., Muntadas, A., and Demestre, M.. (2013). Estudio de referencia sobre la distribución de basura marina en fondos blandos asociados a caladeros de pesca de arrastre en el Mediterráneo norte. *Scientia Marina* 77 (2), 247–255. doi: 10.3989/scimar03702.10A

Schlining, K., von Thun, S., Kuhnz, L., Schlining, B., Lundsten, L., Jacobsen Stout, N., et al. (2013). Debris in the deep: Using a 22-year video annotation database to survey marine litter in Monterey canyon, central California, USA. *Deep-Sea Res. Part I: Oceanogr. Res. Papers* 79, 96–105. doi: 10.1016/j.dsr.2013.05.006

Shimanaga, M., and Yanagi, K. (2016). The Ryukyu trench may function as a "depocenter". *anthropogenic Mar. litterJ. Oceanogr* 72 (6), 895–903. doi: 10.1007/s10872-016-0388-7

Sinopoli, M., Cillari, T., Andaloro, F., Berti, C., Consoli, P., Galgani, F., et al. (2020). *Are FADs a significant source of marine litter? assessment of released debris and mitigation strategy in the Mediterranean Sea* (253: Journal of Environmental Management). doi: 10.1016/j.jenvman.2019.109749

Song, X., Lyu, M., Zhang, X., Ruthensteiner, B., Ahn, I., Pastorino, G., et al. (2021). Large Plastic debris dumps: New biodiversity hot spots emerging on the deep-Sea floor. *Environ. Sci. Technol. Letters* 8(2), pp. 148–154. doi: 10.1021/acs.estlett.0c00967

Spedicato, M. T., Massutí, E., Mérigot, B., Tserpes, G., Jadaud, A., and Relini, G. (2020). The MEDITS trawl survey specifications in an ecosystem approach to fishery management. *Scientia Marina* 83 (S1), 9. doi: 10.3989/scimar.04915.11X

Spedicato, M. T., Zupa, W., Carbonara, P., Fiorentino, F., Follesa, M. C., Galgani, F., et al. (2019). Spatial distribution of marine macro-litter on the seafloor in the northern Mediterranean Sea: The MEDITS initiative. *Scientia Marina* 83 (S1), 257–270. doi: 10.3989/scimar.04987.14A

Spengler, A., and Costa, M. F. (2008). Methods applied in studies of benthic marine debris. *Mar. Pollut. Bull.* 56 (2), 226–230. doi: 10.1016/j.marpolbul.2007.09.040

Stefatos, A., Charalampakis, M., Papatheodorou, G., and Ferentinos, G. (1999). Marine debris on the seafloor of the Mediterranean Sea: Examples from two enclosed gulfs in Western Greece. *Mar. Pollut. Bull.* 38 (5), 389–393. doi: 10.1016/S0025-326X(98)00141-6

Strafella, P., Fabi, G., Despalatovic, M., Cvitković, I., Fortibuoni, T., Gomiero, A., et al. (2019). Assessment of seabed litter in the northern and central Adriatic Sea (Mediterranean) over six years. *Mar. Pollut. Bull.* 141, 24–35. doi: 10.1016/j.marpolbul.2018.12.054

Strafella, P., Fabi, G., Spagnolo, A., Grati, F., Polidori, P., Punzo, E., et al. (2015). Spatial pattern and weight of seabed marine litter in the northern and central Adriatic Sea. *Mar. Pollut. Bull.* 91 (1), 120–127. doi: 10.1016/j.marpolbul.2014.12.018

Suaria, G., and Aliani, S. (2014). Floating debris in the Mediterranean Sea. *Mar. Pollut. Bull.* 86 (1–2), 494–504. doi: 10.1016/j.marpolbul.2014.06.025

Sullivan, M., Straub, P., Reding, M., Robinson, N., and Zimmermann, E. (2019). Identification, recovery, and impact of ghost fishing gear in the mullica river-great bay estuary (New Jersey, USA): Stakeholder-driven restoration for smaller-scale systems. *Mar. Pollut. Bulletin Elsevier 138(November 2018)* pp, 37–48. doi: 10.1016/j.marpolbul.2018.10.058

Tekman, M. B., Krumpen, T., and Bergmann, M. (2017). Marine litter on deep Arctic seafloor continues to increase and spreads to the north at the HAUSGARTEN observatory. *Deep-Sea Res. Part I: Oceanogr. Res. Papers 120 (June* 2016), 88–99. doi: 10.1016/j.dsr.2016.12.011

Terzi, Y., and Syhan, K. (2020). Marine plastics in the fishing grounds in the Black Sea. In: Ü. Aytan, M. Pogojeva and A. Simeonova (eds) *Marine Litter in the Black Sea* (pp 151–160. Turkish Marine Research Foundation (TUDAV) Publication No: 56, Istanbul, Turkey, ISBN 978-975-8825-48-6

Topçu, E. N., and Öztürk, B. (2010). Abundance and composition of solid waste materials on the western part of the Turkish black sea seabed. *Aquat. Ecosystem Health Manage.* 13 (3), 301–306. doi: 10.1080/14634988.2010.503684

Tubau, X., Canals, M., Lastras, G., Rayo, X., Rivera, J., and Amblas, D. (2015). Marine litter on the floor of deep submarine canyons of the northwestern Mediterranean Sea: The role of hydrodynamic processes. *Prog. Oceanogr* 134, 379–403. doi: 10.1016/j.pocean.2015.03.013

UN General Assembly (2006). *Resolution 61/105 'Sustainable fisheries, including through the 1995 agreement for the implementation of the provisions of the united nations convention on the law of the Sea of 10 December 1982 relating to the conservation and management of straddling fish stocks and highly migratory fish stocks, and related instruments.* pp1–p21. https://documents-dds-ny.un.org/doc/UNDOC/GEN/N06/500/73/PDF/N0650073.pdf?OpenElement

UNEP (2005). *Marine litter: An analytical overview. intergovernmental oceanographic commission of the united nations educational, scientific and cultural organisation* Vol. 58 (Nairobi: UNEP).

UNEP (2009). 'Marine litter: A global challenge'. *Regional Seas U Nations Environ. Programme* p, 13. Available at: https://stg-wedocs.unep.org/bitstream/handle/20.500.11822/31632/MLAGC.pdf

Urban-Malinga, B., Wodzinowski, T., Witalis, B., Zalewski, M., Radtke, K., and Grygiel, W. (2018). Marine litter on the seafloor of the southern Baltic. *Mar. Pollut. Bull.* 127, 612–617. doi: 10.1016/j.marpolbul.2017.12.052

van den Beld, I. M. J., Guillaumont, B., Menot, L., Bayle, C., Arnaud-Haond, S., and Bourillet, J.-F. (2017). Marine litter in submarine canyons of the bay of Biscay. *Deep Sea Res. Part II: Topical Stud. Oceanogr* 145, 142–152. doi: 10.1016/j.dsr2.2016.04.013

van Sebille, E., Aliani, S., Law, K. L., Maximenko, N., Alsina, J. M., Bagaev, A., et al. (2020). The physical oceanography of the transport of floating marine debris the physical oceanography of the transport of floating marine debris. *Environ. Res. Letters 15(2)* p, 023003. doi: 10.1088/1748-9326/ab6d7d

Vieira, R. P., Raposo, I. P., Sobral, P., Gonçalves, J. M. S., Bell, K. L. C., and Cunha, M. R. (2015). Lost fishing gear and litter at gorringe bank (NE Atlantic). *J. Sea Res.* 100, 91–98. doi: 10.1016/j.seares.2014.10.005

Ward, C. P., and Reddy, C. M. (2020). We need better data about the environmental persistence of plastic goods. *Proc. Natl. Acad. Sci. U S A* 117 (26), 14618–14621. doi: 10.1073/pnas.2008009117

Watters, D. L., Yoklavich, M. M., Love, M. S., and Schroeder, D. M. (2010). Assessing marine debris in deep seafloor habitats off California. *Mar. Pollut. Bull.* 60 (1), 131–138. doi: 10.1016/j.marpolbul.2009.08.019

Wei, C. L., Rowe, G. T., Nunnally, C. C., and Wicksten, M. K. (2012). Anthropogenic "Litter" and macrophyte detritus in the deep northern gulf of Mexico. *Mar. Pollut. Bull.* 64 (5), 966–973. doi: 10.1016/j.marpolbul.2012.02.015

Woodall, L. C., Robinson, L. F., Rogers, A. D., Narayanaswamy, B. E., and Paterson, G. L. J. (2015). Deep-sea litter: A comparison of seamounts, banks and a ridge in the Atlantic and Indian oceans reveals both environmental and anthropogenic factors impact accumulation and composition. *Front. Mar. Sci.* 2 (FEB). doi: 10.3389/fmars.2015.00003

Yamakita, T., Yamamoto, H., Yokoyama, Y., Sakamoto, I., Tsuchida, S., Lindsay, D., et al. (2015). Distribution of the marine debris on seafloor from the primary report of five cruises after the great East Japan earthquake 2011. In: H. J. Ceccaldi, Y. Hénocque, Y. Koike, T. Komatsu, G. Stora, M. H. Tusseau-Vuillemin, et al (eds) *Marine Productivity: Perturbations and Resilience of Socio-ecosystems* (pp. 101–109). Springer, Cham. doi: 10.1007/978-3-319-13878-7_11

Ye, S., and Andrady, A. L. (1991). Fouling of floating plastic debris under Biscayne bay exposure conditions. *Mar. Pollut. Bull.* 22 (12), 608–613. doi: 10.1016/0025-326X(91)90249-R

Zablotski, Y., and Kraak, S. B. M. (2019). Marine litter on the Baltic seafloor collected by the international fish-trawl survey. *Mar. Pollut. Bull.* 141, 448–461. doi: 10.1016/j.marpolbul.2019.02.014

Zhang, F., Yao, C., Xu, J., Zhu, L., Peng, G., and Li, D. (2020). Composition, spatial distribution and sources of plastic litter on the East China Sea floor. *Sci. Total Environ Elsevier B.V* 742, 140525. doi: 10.1016/j.scitotenv.2020.140525

Zhong, G., and Peng, X. (2021). Transport and accumulation of plastic litter in submarine canyons–the role of gravity flows. *Geol.* 49 (5), 581–586. doi: 10.1130/G48536.1

frontiers | Frontiers in Marine Science

TYPE Original Research
PUBLISHED 26 October 2022
DOI 10.3389/fmars.2022.1017052

OPEN ACCESS

EDITED BY
Kostas Kiriakoulakis,
Liverpool John Moores University,
United Kingdom

REVIEWED BY
Manuel Vargas-Yáñez,
Spanish Institute of Oceanography (IEO), Spain
Mauro Celussi,
Istituto Nazionale di Oceanografia e di Geofisica Sperimentale, Italy

*CORRESPONDENCE
Sarah Paradis
sparadis@ethz.ch

SPECIALTY SECTION
This article was submitted to Deep-Sea Environments and Ecology, a section of the journal Frontiers in Marine Science

RECEIVED 11 August 2022
ACCEPTED 28 September 2022
PUBLISHED 26 October 2022

CITATION
Paradis S, Arjona-Camas M, Goñi M, Palanques A, Masqué P and Puig P (2022) Contrasting particle fluxes and composition in a submarine canyon affected by natural sediment transport events and bottom trawling. *Front. Mar. Sci.* 9:1017052. doi: 10.3389/fmars.2022.1017052

Contrasting particle fluxes and composition in a submarine canyon affected by natural sediment transport events and bottom trawling

Sarah Paradis[1,2,3]*, Marta Arjona-Camas[2], Miguel Goñi[4], Albert Palanques[2], Pere Masqué[1,5,6] and Pere Puig[2]

[1]Institute of Environmental Science and Technology (ICTA), Universitat Autònoma de Barcelona, Bellaterra, Spain, [2]Marine Sciences Institute, Consejo Superior de Investigaciones Científicas (ICM-CSIC), Barcelona, Spain, [3]Geological Institute, Department of Earth Sciences, Eidgenössische Technische Hochschule (ETH) Zürich, Zürich, Switzerland, [4]College of Earth, Ocean, and Atmospheric Sciences, Oregon State University, Corvallis, OR, United States, [5]School of Natural Sciences, Centre for Marine Ecosystems Research, Edith Cowan University, Joondalup, WA, Australia, [6]Marine Environment Laboratories, International Atomic Energy, Principality of Monaco, Monaco

Submarine canyons are important conduits of sediment and organic matter to deep-sea environments, mainly during high-energy natural events such as storms, river floods, or dense shelf water cascading, but also due to human activities such as bottom trawling. The contributions of natural and trawling-induced sediment and organic matter inputs into Palamós Canyon (NW Mediterranean) were assessed from three instrumented moorings deployed in the axis and northern flank of the canyon covering the trawling closure (February) and the trawling season (March-December) of 2017. During the trawling closure, large sediment fluxes with high contents of labile marine organic matter content were registered in the canyon axis, associated to storm resuspension on the shelf that coincided with dense shelf water cascading and high surface water productivity. Although no major natural sediment transport events occurred during the following spring and summer months, near-daily trawling-induced sediment gravity flows were recorded in the northern flank mooring, placed directly below a fishing ground, which sometimes reached the canyon axis. Compositionally, the organic matter transferred by trawling resuspension was impoverished in the most labile biomarkers (fatty acids, amino acids, and dicarboxylic acids) and had a high degree of degradation, which was similar to surficial sediment from the adjacent fishing ground. Trawling resuspended particles masked the transfer of organic matter enriched in labile biomarkers that naturally occur during the quiescent

summer months. Overall, bottom trawling enhances the magnitude of particle fluxes while modifying its organic carbon composition, increasing the re-exposure and transfer of degraded organic carbon and potentially affecting benthic communities that rely on the arrival of fresh organic matter.

KEYWORDS

submarine canyon, NW Mediterranean, surface sediment, sediment transport, carbon cycle, biomarkers, storms, bottom trawling

1 Introduction

Submarine canyons act as preferential conduits of particulate matter connecting the productive coastal shelf with the nutrient-limited abyss (Allen and Durrieu de Madron, 2009; Puig et al., 2014; Porter et al., 2016). The enhanced flux of organic matter into canyons combined with their heterogenous set of habitats makes these morphological features important nursery and refuge areas for diverse marine life (Vetter et al., 2010; De Leo et al., 2014; Fernandez-Arcaya et al., 2017). Consequently, several benthic species of commercial interest tend to congregate near submarine canyons, supporting many fishing grounds (Farrugio, 2012).

The ecological importance of submarine canyons relies on the transfer of organic matter to the canyon's interior, which is enhanced by natural processes that increase the flux of particulate matter into canyons (see review by Puig et al., 2014). These processes include river floods that deliver elevated amounts of suspended sediment to the margin and high-energy storm-waves, which resuspend sediment from shallower regions of the shelf. Combined, both processes can transport elevated amounts of suspended particulate matter into canyons as turbidity currents and/or hyperpycnal flows (Martín et al., 2011; Liu et al., 2012; Puig et al., 2014). Dense shelf water cascading (DSWC) events generated by cooling and/or evaporation of coastal surface waters can also transport large amounts of particulate matter into canyons. Their excess in density forces these waters to sink to greater depths through submarine canyons as gravity-driven currents that carry resuspended sediment until reaching neutral buoyancy (Durrieu de Madron et al., 2005; Canals et al., 2006; Palanques et al., 2012). Particulate fluxes derived from both storms and DSWC tend to be highest in the upper and middle canyon reaches, and decrease with depth as the hydrodynamic forces subside, rarely reaching the lower canyon (de Stigter et al., 2007; Palanques et al., 2012; Pedrosa-Pàmies et al., 2013). Sediment transported during storms and DSWC generally have relatively low particulate organic matter content and is composed of aged terrestrial organic carbon (OC) eroded from the continental shelf (Sanchez-Vidal et al., 2008; Tesi et al., 2010; Martín et al., 2011; Hsu et al., 2014; Sparkes et al., 2015). However, when these events occur in coincidence with phytoplankton blooms, particulate matter enriched with marine OC is transferred into submarine canyons (Fabres et al., 2008; Pasqual et al., 2010; Lopez-Fernandez et al., 2013a).

Anthropogenic activities can also modify the transport of sediment in submarine canyons. Several studies have proven that deep bottom trawling around submarine canyons can be a main driver of particulate matter transfer (Martín et al., 2006; Palanques et al., 2006; Puig et al., 2012; Martín et al., 2014a; Wilson et al., 2015; Arjona-Camas et al., 2019; 2021). This enhanced transferal of particulate matter has caused a general increase in sedimentation rates within the axes of several trawled submarine canyons (Martín et al., 2008; Puig et al., 2015; Paradis et al., 2017; 2018a; 2018b; 2021a), which has modified the abundance and biodiversity of meiobenthos (Pusceddu et al., 2014; Román et al., 2018). These shifts in meiobenthic community structures are attributed to a presumed alteration in both the amount and the composition of organic matter transferred into canyons, since bottom sediments from fishing grounds tend to be depleted in labile organic matter compounds (Martín et al., 2014b; Pusceddu et al., 2014; Paradis et al., 2021b) and the organic matter associated with local resuspended sediment tends to be highly degraded (Pusceddu et al., 2015; Wilson et al., 2015; Wu et al., 2016; Daly et al., 2018). However, the organic matter composition of downward particulate matter transferred antropogenically from fishing grounds into canyon axes have not been studied yet.

The NW Mediterranean margin is incised by several canyons that present large particle fluxes from both natural sediment transport processes and from bottom trawling activities, and Palamós Canyon (also known as La Fonera Canyon) is one of the most prominent of these. Northern storms are frequent and persistent in this margin, but they generate relatively small waves (~2 m) on the inner shelf that have limited capacity to resuspend sediment. In contrast, the rarer eastern storms generally present larger waves (> 4 m) and are accompanied by heavy rains and torrential river discharges carrying large amounts of sediment to the coast. In the case of Palamós Canyon, the Ter River is the closest to its canyon head and contributes significant amounts of terrigenous material to the system (Palanques et al., 2005). These eastern storms also resuspend sediments that are then intercepted by Palamós Canyon, supplying large amounts of OC-poor sediment into the canyon (Martín et al., 2006). DSWC in the NW Mediterranean margin originates in the Gulf of Lions during winter and generates a southward flow of cold dense water that reaches Palamós Canyon in

specific years, supplying large amounts of sediment into it (Ribó et al., 2011; Arjona-Camas et al., 2021).

Palamós Canyon supports important trawling grounds along its northern and southern flanks, named Sant Sebastià and Rostoll fishing grounds, respectively (Figure 1). These fishing grounds are concentrated at the 400-800 m depth range in accordance to the life-cycle of their most targeted commercial species, the highly coveted red-and-blue deep-sea shrimp *Aristeus antennatus* (Sardà et al., 1994; Tudela et al., 2003). Chronic bottom trawling activities along the canyon's flanks cause almost daily sediment resuspension evolving into gravity flows towards the canyon's interior (Palanques et al., 2006; Puig et al., 2012; Martín et al., 2014b), which can be detached as persistent nepheloid layers at the same depth range of the fishing grounds (Martín et al., 2014b; Arjona-Camas et al., 2021). Trawling-derived sediment gravity flows are then channeled through canyon flank tributaries, such as the Montgrí gully in the northern flank (Figure 1), and can reach the canyon axis, transporting eroded sediment with high silt content, as well as lower OC and opal content (Martín et al., 2006; Palanques et al., 2006). However, these studies have not assessed the variations in the composition of downward particulate organic matter transported by natural and trawling activities.

Hence, the aim of this study is to evaluate how sediment transport events linked to both natural processes and trawling activities influence the composition of downward particulate organic matter into Palamós Canyon, using biomarkers yielded from the oxidation of CuO which have been used to assess the origin and degree of degradation of organic matter transferred into canyons (Tesi et al., 2008; Goñi et al., 2013; Pasqual et al., 2010; 2013). To address this, three instrumented moorings were deployed in Palamós Canyon to measure the sedimentary dynamics and the downward particle fluxes and their composition from February to December 2017. Since 2013, a two-month trawling closure occurs in Palamós Canyon from early January to early March to allow the recruitment of shrimp juveniles and avoid the risk of overexploitation of the fishing stock (Bjørkan et al., 2020), providing a time-window to study natural particle fluxes in February and the effect of trawling activities for the remainder of the year. To identify the alteration of organic matter compounds transferred into the canyon by natural sediment transport processes and bottom trawling activities, we compared the sedimentological and biogeochemical composition of sediment trap samples along with the composition of surface sediment obtained on the adjacent trawling grounds.

2 Materials and methods

2.1 Fieldwork and instrumentation

To conduct this observational study, three moorings were deployed in Palamós Canyon: at 929 m water depth in the canyon axis (Axis-900), at 975 m water depth in the Montgrí tributary gully located ~0.5 km from Sant Sebastià trawling ground (Flank-1000), and at 1230 m water depth in the confluence of the tributary gully and the canyon axis, at ~2 km from the same fishing ground (Axis-1200), and ~4 km down-canyon from Axis-900 mooring (Figure 1). The moorings were deployed in three consecutive periods: from February 7 to June 5 and from June 9 to October 3 2017, and from October 3 2017 to March 5 2018, but this study was centered on data of 2017 (Figure S1).

Mooring Axis-900 was equipped with an autonomous hydrographic profiler (Aqualog), as well as a near-bottom autonomous turbidimeter (AQUA-logger 210TY) with a SeaPoint turbidity sensor set to record turbidity in Formazin Turbidity Unit (FTU) at 1-min intervals in auto-gain mode, placed at 5 m above the bottom (mab), and a current meter (Aquadopp, Nortek) coupled with a temperature sensor (SeaBird SBE-37) set to record at 5-min intervals and placed at 6 mab. The Aqualog only registered data from February 7 to April 7, and the results are explained in detail in Arjona-Camas et al. (2021). The current meter stopped some days before the end of the first and second deployments acquiring data from February 7 to May 20 and from June 9 to September 8, respectively, whereas it recorded data during all of the third deployment (Figure S1).

Mooring Flank-1000 had a string of 5 single-point autonomous turbidimeters (AQUA logger 210TY, AQUATEC) placed at 5, 10, 20, 50 and 80 mab, each one equipped with temperature, pressure, and a SeaPoint turbidity sensor set to record FTUs at 1-min sampling interval. The mooring line also held a downward-looking 300 kHz Teledyne RDI Acoustic Doppler Current Profiler (ADCP) placed above the turbidimeters, which provided current velocity and direction from 10 to 80 mab in 2-m bins at 5-min intervals. The turbidimeter at 20 mab from the first deployment presented increasing FTUs over time, indicating the effect of biofouling. Hence, data from this sensor were omitted (Figure S1).

Mooring Axis-1200 was equipped with a single-point autonomous turbidimeter (AQUA logger 210TY, AQUATEC) set to record at 1-min intervals in auto-gain mode, placed at 5 mab, and a current meter (Aquadopp, Nortek) paired with a conductivity and temperature sensor (SeaBird SBE-37) and a SeaPoint turbidimeter (0-25 FTU) set to record at 5-min intervals placed at 6 mab. The autonomous turbidity sensor of the first deployment did not work, so the turbidity data were extracted from the turbidimeter paired with the current meter, providing values up to 25 FTUs. Unfortunately, the current meter only acquired data from February 7 to March 21 and from June 6 to October 3 (Figure S1). Additionally, this mooring had a 24-cup sediment trap Technicap PPS3/3 model, with a 0.125 m^2 cylindrical opening and an aspect ratio of 2.5 (1 m long/0.4 m wide), placed at 22 mab and programmed to collect downward particulate fluxes at 7-day intervals, from Monday to Sunday, to assess the weekly particle fluxes. The sediment trap overfilled in

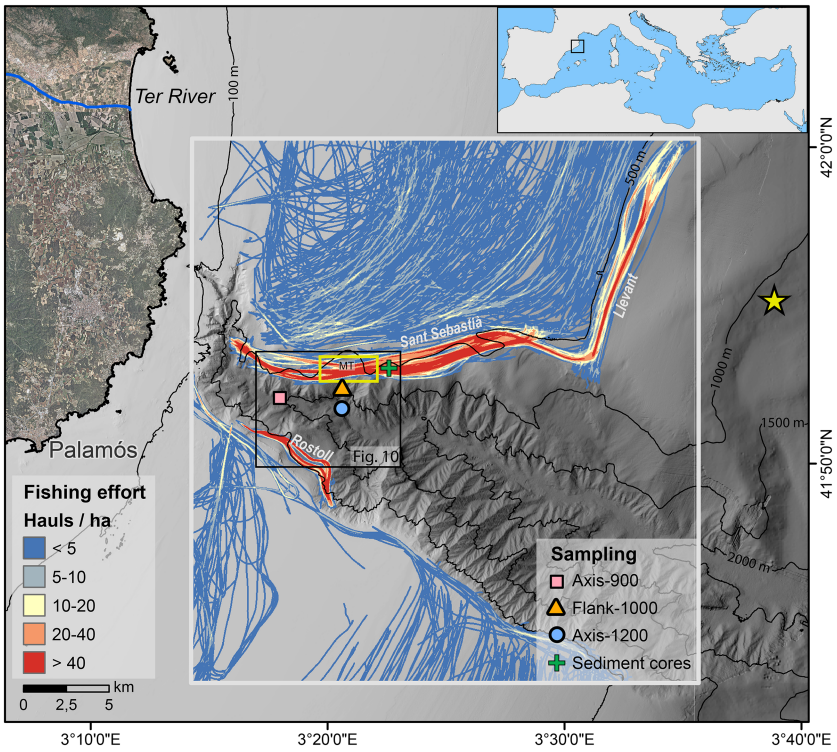

FIGURE 1
Bathymetric map of Palamós Canyon, with the location of Axis-900 (pink square) mooring at the canyon axis, Flank-1000 mooring (orange triangle) deployed in the Montgrí tributary gully (MT) and Axis-1200 mooring (blue circle) deployed in the confluence between MT and the canyon axis. The yellow rectangle above the Flank-1000 mooring delimits the section of the fishing ground where daily hauls were extracted for Figure 2. Composition of the sediment trap (Axis-1200) was compared with surficial composition of the sediment core collected in the trawled flank (green cross). Fishing effort is given as cumulative number of hauls per hectare obtained from AIS data from February to December 2017, identifying the main fishing grounds (Sant Sebastià, Rostoll, Llevant). The location of the Cap Begur buoy is given by a yellow star.

the 4th sample of the first deployment (March 6-13) and in the 8th sample of the third deployment (December 4-11), providing valid samples only from February 13 to March 9 and from June 12 to December 7 (Figure S1).

Current speeds and directions from the different current meters were decomposed in E-W and N-S current velocity components. In order to obtain the along- and across-canyon directions for the Axis-900 and Axis-1200 moorings, data from these moorings were rotated 70° clockwise to align their reference frames to the canyon axis orientation, converting the N-S velocity component into the along-canyon velocity component (positive up-canyon) and the E-W velocity component into the across-canyon velocity component (positive towards the NNE). Data of the Flank-1000 mooring were rotated 11° counterclockwise to align the reference frame to the canyon gully orientation, converting the N-S velocity component into the along-gully velocity component (positive up-gully), and the E-W velocity component into the across-gully velocity component (positive towards ESE). To make the three moorings comparable among them, all current direction components were reported with respect to the main canyon axis orientation: along-canyon (i.e. across-gully for Flank-1000) and across-canyon (i.e. along-gully for Flank-1000). FTUs from the different turbidimeters were converted to estimates of suspended sediment concentration (SSC; mg·L^{-1}) following the calibration described in Arjona-Camas et al. (2021). Cumulative sediment transport (kg·m^{-2}) in the across- and along-canyon direction were calculated through the cumulative sum of the product of the decomposed and rotated current speed and the SSC. Given the maximum acquisition of turbidity values of Axis-1200 in the first deployment and the missing data between mooring deployments, cumulative suspended sediment transport must be regarded as lower estimates.

In addition, three sediment cores were taken on the trawled northern flank of Palamós Canyon (Figure 1), at the time of the first deployment and during the mooring turnaround cruises: one during the temporal trawling close season in February 7, and two during the trawling season, in June 5 and in October 3. The cores were collected using a K/C Denmark multicorer at ~500-m depth (see Paradis et al. (2021b) for further details).

2.2 Sediment sample treatment and analytical procedure

Sediment trap samples were prepared and processed in the laboratory using the same method as described in Palanques and Puig (2018), obtaining sub-sample aliquots for each sample. Total mass flux (TMF; $g \cdot m^{-2} \cdot d^{-1}$) was calculated from the sample dry weight of two sub-sample aliquots, which were averaged and upscaled based on their dilution factor, and divided by the collecting area (0.125 m^2) and the sampling interval (7 days) of the sediment trap, with an average standard error of 2.4%.

Average grain size and the fraction of clay (< 4 μm), silt (4 – 63 μm), and sand (63 μm – 2 mm) in downward particulate fluxes were analyzed using a Horiba Partica LA-950 V2m particle-size analyzer by oxidizing approximately 1 g of sample using 20% H_2O_2 and disaggregating with 2.5% $P_2O_7^{4-}$.

Elemental analysis of total carbon (TC), organic carbon (OC) and total nitrogen (TN) contents were carried out with an elemental analyzer (Costech ECS Analyzer 4010), according to the procedure described by Nieuwenhuize et al. (1994). Prior to OC analysis, samples were first decarbonated through acid-fuming in the presence of 12 N HCl during 24 h and repeatedly adding 100 μL of 2 N HCl to the sample until effervescence ceased. Inorganic carbon, quantified as the difference between total carbon and organic carbon, was converted to $CaCO_3$ contents using the molecular mass ratio of 100/12, assuming all inorganic carbon present is in the form of $CaCO_3$. Opal (biogenic silica) was analyzed using a wet-alkaline extraction with sodium carbonate using the method described by Mortlock and Froelich (1989). Finally, the lithogenic fraction was calculated as the difference between the total mass and the main mass constituents ($CaCO_3$, organic matter, and opal), where organic matter content was estimated as twice the OC content.

Specific biomarkers yielded from the CuO oxidation of sediment trap samples were analyzed following the method described by Goñi and Montgomery (2000). Briefly, between 250 and 400 mg of homogenized ground sample was oxidized with CuO under basic conditions (2 N NaOH) in an oxygen-free atmosphere at 150°C for 90 min in a microwave. After oxidation, samples were spiked with ethyl vanillin and trans-cinnamic acid as recovery standards, after which the samples were acidified to 1 pH using small volumes of concentrated HCl, and subsequently extracted twice using ethyl acetate. Samples were then evaporated under a constant flow of nitrogen gas, reconditioned in pyridine, and derivatized by adding bistrimethylsilyltrifluoroacetamide (BSTFA) + 10% trimethylchlorosilane (TMCS). Specific reaction products (Table S1) were quantified by GC-MS (Hewlett Packard 6890 GC System) with DB1 column and the HP5973 mass selective detector through selective ion monitoring as previously described by Goni et al. (2009). CuO yields were grouped into specific compound classes that have distinct chemical precursors including those from specific terrestrial sources such as vascular plants (lignin phenols, cutin acids, and certain p-hydroxybenzenes), soil (certain benzoic acids), as well as compound classes (fatty-acids, di-carboxylic acids, amino acids) that can be of both marine and terrestrial origin (Table S1). Mean concentrations of the parameters were calculated as flux-weighted mean concentrations over the whole sampling period, as explained by Heussner et al. (1990).

Sediment samples from the sediment cores taken on the trawled northern flank of Palamós Canyon during the cruises were analyzed for grain size, OC, TN, $CaCO_3$, and CuO biomarkers, following the same procedure as the sediment trap samples. The procedures and the results of these analysis were published in Paradis et al. (2021b). For this study we use the results of the surface sediment samples (0-1 cm) of these cores to compare them with the results of the sediment trap samples.

2.3 Forcing conditions

Significant wave height (H_s) was obtained from the Cap de Begur buoy (3.65° E, 41.92° N), located ~10 km NE at the continental slope region next to Palamós Canyon (Figure 1), which is managed by the Spanish Ports Authority. Storms were defined as H_s greater than 2 m for more than 6 h (Mendoza and Jiménez, 2009) and eastern storms were identified when the wave direction was between 60° and 120°. Daily Ter River discharge was obtained from the Catalan Water Agency. Data of net primary productivity (NPP) were extracted from the Ocean Productivity database (http://www.science.oregonstate.edu/ocean.productivity/index.php). NPP data from this database are calculated using the Vertically Generalized Production Model, which uses both surface chlorophyll concentrations and sea surface temperature data extracted from satellite imagery (Behrenfeld and Falkowski, 1997).

Trawling activity was obtained from vessel Automatic Identification System (AIS) extracted from Shiplocus, the official Spanish Port System module that manages and evaluates maritime traffic data. AIS data were filtered following the method described by Paradis et al. (2021b) to obtain the number of hauls per hectare in each fishing ground. The number of hauls above Montgrí tributary gully was then extracted from the polygon delimited in Figure 1.

2.4 Statistical analyses

Principal Component Analysis (PCA) was performed on CuO biomarkers of downward particulate fluxes obtained from the sediment trap (Axis-1200) to reduce the dimensions of the dataset and maximize the variance between samples. PCA was performed using Python's Scikit-learn module (Pedregosa et al., 2011) by first normalizing the data. Based on this PCA, PC loadings of OC composition of surface sediment collected in the adjacent

trawling ground (Paradis et al., 2021b) were used to study its relationship with the composition of downward particulate fluxes.

3 Results

3.1 Forcing conditions

During the sampling period, natural forcing conditions (H_s, Ter River discharge, and NPP) followed a similar seasonal pattern, with generally stronger events occurring during the winter (January-March) and autumn (October-December) months (Figures 2A–C). Although the majority of the storms were caused by northern winds, exceptionally strong eastern storms occurred in January 19-23 and in February 12-15 with H_s reaching 6 m and 5 m respectively, and strong Ter River floods, reaching 133 $m^3 \cdot s^{-1}$ and 30 $m^3 \cdot s^{-1}$ respectively during each eastern storm (Figures 2A, B). Although NPP also followed this general seasonal pattern, values were low during the first eastern storm in January (550 mg $C \cdot m^{-2} \cdot d^{-1}$) but increased during the second eastern storm in February due to a late-winter phytoplankton bloom (1200 mg $C \cdot m^{-2} \cdot d^{-1}$) (Figure 2C).

During the more quiescent late-spring and summer months, these natural forcing conditions receded to background values (~1 m H_s, ~3 $m^3 \cdot s^{-1}$ Ter River discharge, and ~450 mg $C \cdot m^{-2} \cdot d^{-1}$ NPP) (Figures 2A–C). The general decrease of NPP was interrupted by a second phytoplankton bloom in early-June (870 mg $C \cdot m^{-2} \cdot d^{-1}$) (Figure 2C).

From October to December, H_s increased again due to seasonal autumn storms (Figure 2A). These events were generally dry storms caused by northern winds that did not lead to significant increases in Ter River discharges (Figures 2A, B). NPP steadily increased during autumn until reaching ~780 mg $C \cdot m^{-2} \cdot d^{-1}$ in late-November and decreased again to background values in the following winter months (Figure 2C).

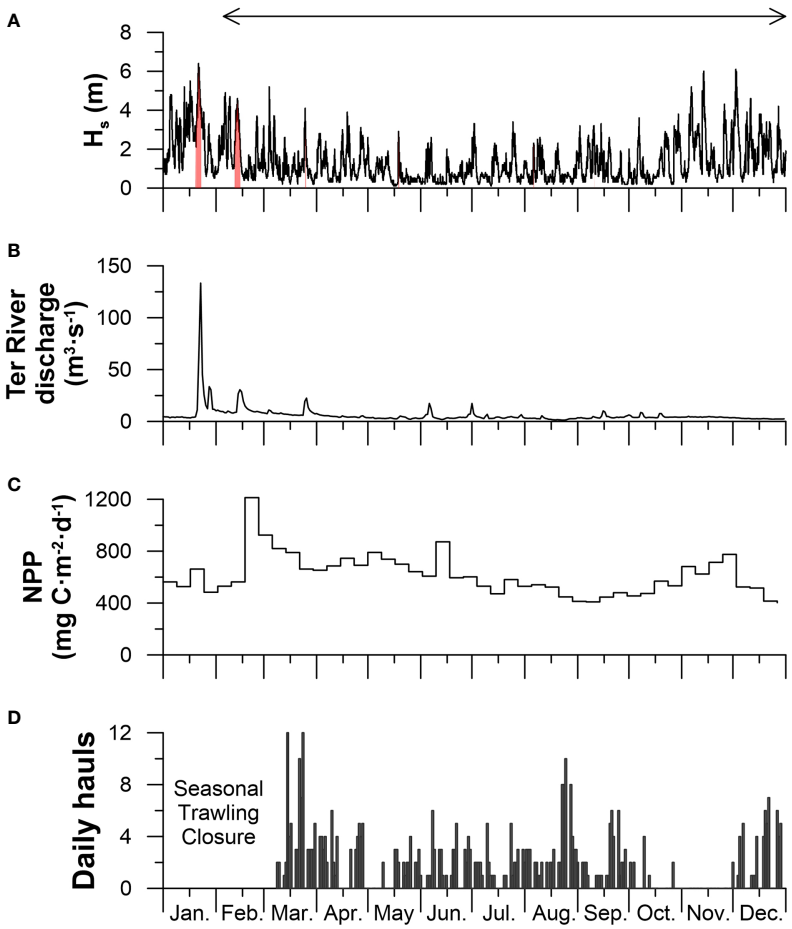

FIGURE 2
Forcing conditions in 2017. **(A)** Significant wave height (H_s) measured at the Cap de Begur buoy, where eastern storms are identified in red. **(B)** Ter River discharge. **(C)** 8-day average net primary productivity (NPP). **(D)** Daily hauls in the trawling ground above the Montgrí tributary gully (see yellow polygon in Figure 1). The horizontal arrow on top indicates the monitoring period.

Trawling effort in the Sant Sebastià fishing ground above the Montgrí tributary gully varied throughout the year (Figure 2D). No hauls were detected at the beginning of the year during the seasonal trawling closure, nor during the weekends or national holidays, when trawlers are not allowed to operate (Bjørkan et al., 2020). During working days, an average of 2 hauls per day were recorded, but trawling effort varied from 0 to 12 hauls per working day. Highest fishing effort occurred at the beginning of the trawling season in March, in late August, and again in late December, with 7 to 12 hauls per day (Figure 2D). During late October and throughout November, there was negligible trawling activity on the Sant Sebastià fishing ground (Figure 2D) since bottom trawlers had moved to shallower fishing grounds on the open slope (Figure S2).

3.2 Sediment transport in canyon axis (929 m water depth)

The time series of the Axis-900 mooring located in the canyon axis are presented in detail in Arjona-Camas et al. (2021), but described here briefly to contextualize the observed downward particle fluxes. Temperature recorded at 6 mab fluctuated between 13.2 and 13.6°C throughout the year, with a sharp drop to 12.6°C between February 13 and 15 (Figure 3A) due to an eastern storm concurrent with a DSWC event that caused a maximum peak in SSC of ~230 mg·L^{-1}. This event was initially directed down-canyon at 0.3 m·s^{-1}, but was followed by a quick up-canyon reversal of current direction reaching maximum values of 0.6 m·s^{-1} (Figure 3D), following the predominant up-canyon bottom current direction (~280°) at this site (Figure 3E).

Since the onset of trawling activities in March, several sporadic peaks of ~20 mg·L^{-1} were recorded only during weekdays, with exceptionally higher SSC of 190, 140, and 120 mg·L^{-1} at the end of July, in mid-August and at the end of September (Figure 3B). SSC was negligible during November, but small peaks of SSC (~60 mg·L^{-1}) resumed again in mid-December (Figure 3B). Current velocities presented fluctuating up-canyon and down-canyon flows (~0.15 m·s^{-1}), with increasing speeds of up to 0.4 m·s^{-1} towards the end of the year in November and December (Figure 3D). The predominant direction of near-bottom currents was up-canyon (~280°), although currents came from the northern flank during some high SSC events (Figure 3E).

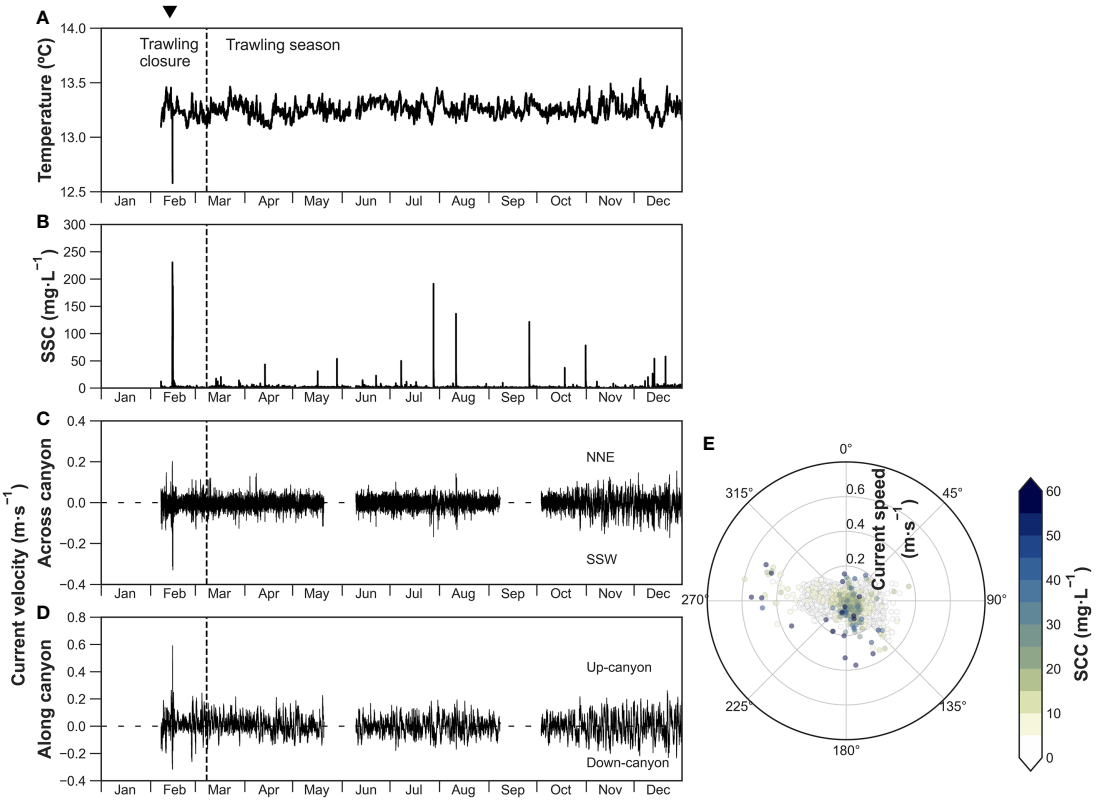

FIGURE 3
Axis-900 time-series of **(A)** temperature at 6 mab, **(B)** suspended sediment concentration (SSC), **(C)** across-canyon current velocity, and **(D)** along-canyon current velocity. **(E)** Polar plot of non-rotated current direction (angle), current speed (radius) and turbidity (color bar) at 5 mab. The inverted triangle on top indicates the occurrence of a dense shelf water cascading event. Note the different axis of along canyon and across canyon current speeds.

3.3 Sediment transport in the Montgrí tributary (975 m water depth)

In the Flank-1000 mooring located in the Montgrí tributary gully, temperatures at 5 mab fluctuated between 13.2 and 13.6°C during the whole sampling period, with no apparent change (Figure 4A). In contrast, recordings of SSC, current speed, and direction indicate frequent sediment transport events into the canyon's interior that follow a distinct temporal trend (Figures 4B-D). During the trawling closure in February, SSC was negligible at all depths, aside for a small near-bottom (5-10 mab) SSC peak of ~60 mg·L^{-1} as well as a sharp off-shore and down-flank increase in current speed of 0.4 m·s^{-1} and 0.2 m·s^{-1}, respectively, that occurred in coincidence with the eastern storm and DSWC event of mid-February (Figures 4B-D).

At the onset of the trawling period in March, peaks of near-bottom SSC (~400 mg·L^{-1}) and current speeds (~0.4 m·s^{-1}) caused by trawling-induced sediment gravity flows were recorded down-flank through the tributary (~190°; Figures 4B-D) on a daily basis, only during weekdays. The magnitude of these sediment transport events generally decreased throughout the year to SSC of ~50 mg·L^{-1} and were limited to between 5-20 mab (Figure 4B). Despite this general decreasing trend, exceptionally high sporadic near-bottom SSC of 250-770 mg·L^{-1} were observed in summer months that were accompanied with strong down-flank current speeds of between 0.25 m·s^{-1} to 0.6 m·s^{-1} (Figures 4C, D). Sediment gravity flows through the Montgrí tributary gully were absent in late October and throughout November when bottom trawlers moved to the open slope (Figure S2), but resumed again in December, with near-bottom SSC between 100 and 260 mg·L^{-1} and current speeds of ~0.2 m·s^{-1} (Figures 4B-D).

3.4 Sediment transport in canyon axis (1230 m water depth)

In the Axis-1200 mooring, temperature remained relatively constant, fluctuating between 13.1-13.4°C (Figure 5A) and did not present the sharp drop in temperature caused by the storm and DSWC event observed in the mooring further up-canyon

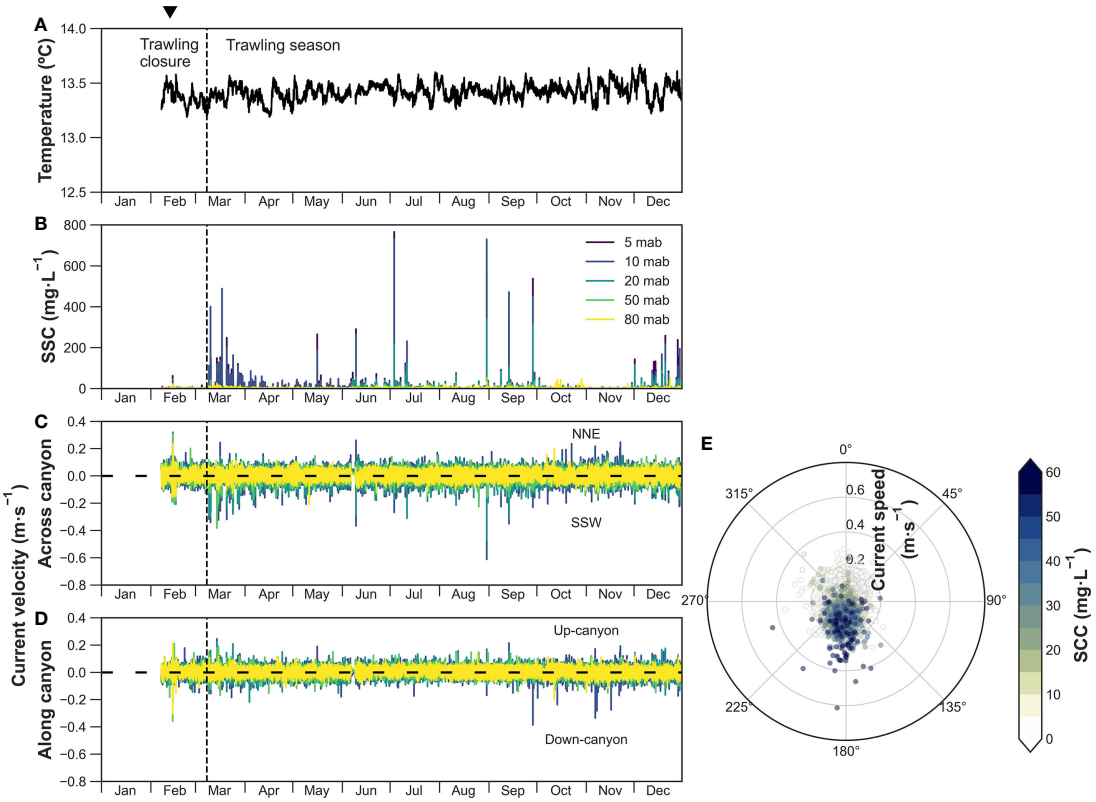

FIGURE 4
Flank-1000 time-series of **(A)** temperature at 5 mab, **(B)** suspended sediment concentration (SSC) at different water depths, **(C)** across-canyon current velocity at 10-80 mab, and **(D)** along-canyon current velocity at 10-80 mab. **(E)** Polar plot of non-rotated current direction (angle), current speed (radius) and turbidity (color bar) at 10 mab. The inverted triangle on top indicates the occurrence of a dense shelf water cascading event.

(Figure 3A). Instead, temperature presented a slight increase from 13.2 °C to 13.4 °C at the beginning of the event (Figure 5A) concurrent with an increase of near-bottom SSC >28.5 mg·L^{-1}, above the sensor range, and a peak of near-bottom current speed of 0.66 m·s^{-1} directed across-canyon and coming from the northern flank (Figures 5B, C). One day later, on February 15, a second peak of SSC >28.5 mg·L^{-1} was recorded, coinciding with another strong bottom current speed that reached 0.66 m·s^{-1} directed down-canyon (Figures 5B, D). A second sharp increase in SSC occurred on February 27, reaching the maximum turbidity reading values of >28.5 mg·L^{-1}, with strong across-canyon bottom current speed of 0.58 m·s^{-1} coming from the northern flank (Figures 5B, C). At the onset of bottom trawling in March, near-bottom SSC presented sharp increases of ~20 mg·L^{-1} only during weekdays (Figures 5A, B). Unfortunately, sensors in this first deployment stopped working on March 21.

During the second deployment in summer, frequent increases in SSC from ~1 mg·L^{-1} to between 60 and 230 mg·L^{-1} were recorded from June to early September, accompanied by increases in across-canyon current speed from 0.1 m·s^{-1} to 0.45 m·s^{-1} (Figures 5B–D). Some of these sediment gravity flows were directed towards the S and came from the Montgrí tributary gully (Figures 5C, E), occurring in coincidence to the sediment gravity flows recorded in the Flank-1000 mooring that had SSC exceeding 250 mg·L^{-1} (Figure 4). The remaining sediment gravity flows were directed towards the SSW and came from an adjacent tributary gully to the Montgrí, or towards the SE, coming from the upper canyon axis (Figure 5E). A strong sediment gravity flow was again registered in October 24, reaching high near-bottom SSC of 135 mg·L^{-1} coupled with strong down-canyon (0.25 m·s^{-1}) and NNW (0.15 m·s^{-1}) bottom currents (Figures 5B, D). Aside from the down-flank sediment gravity flows registered during the summer, the predominant bottom currents during the sampling period were essentially directed down-canyon (Figure 5E).

3.5 Downward particle fluxes and composition in canyon axis (1230 m water depth)

Downward TMF was highly variable during the whole sampling period, averaging 45.9 g·m^{-2}·d^{-1} but ranging from 7.4

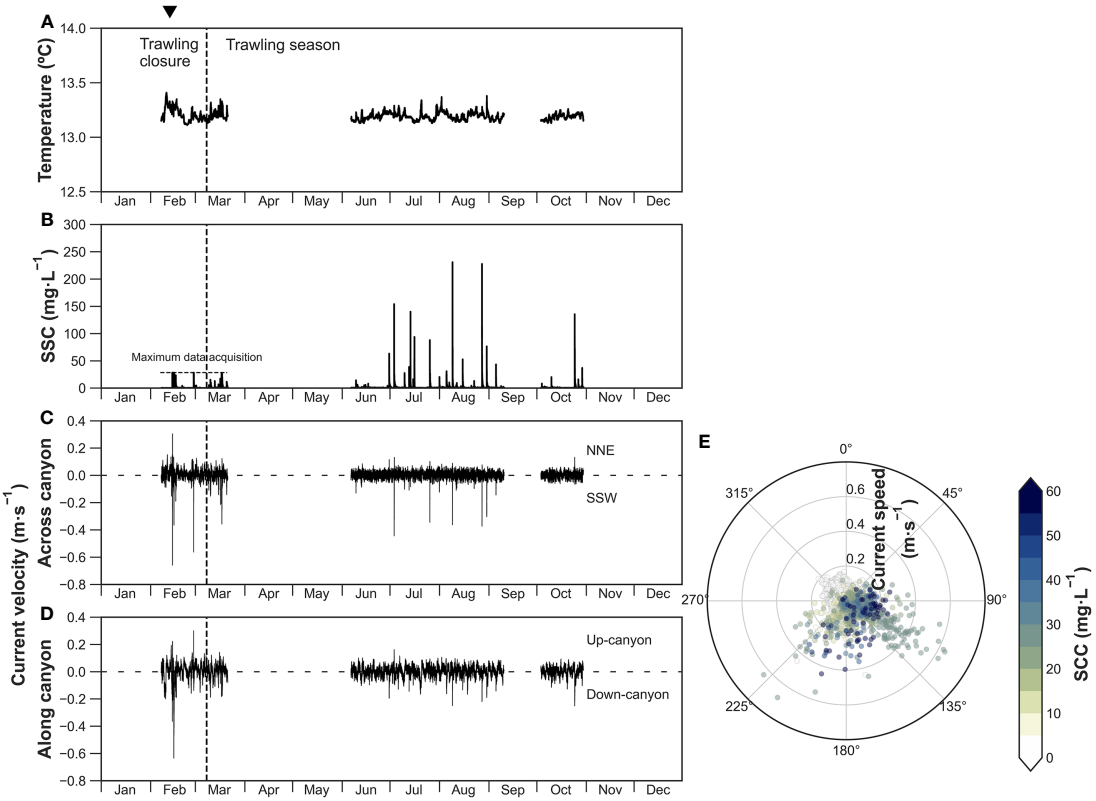

FIGURE 5
Axis-1200 time-series of **(A)** temperature, **(B)** suspended sediment concentration (SSC), **(C)** across-canyon current velocity, and **(D)** along-canyon current velocity. Note the maximum data acquisition for SSC in the first deployment. **(E)** Polar plot of non-rotated current direction (angle), current speed (radius) and turbidity (color bar) at 5 mab. The inverted triangle on top indicates the occurrence of a dense shelf water cascading event.

$g \cdot m^{-2} \cdot d^{-1}$ to >140 $g \cdot m^{-2} \cdot d^{-1}$ (Figure 6A). Due to the lack of data between March and June, a complete analysis of seasonal variability is not possible. At the beginning of the sampling period, TMF values increased from 29 $g \cdot m^{-2} \cdot d^{-1}$ in mid-February to >140 $g \cdot m^{-2} \cdot d^{-1}$ when the sediment trap overfilled in early March, at the onset of the bottom trawling season. Downward TMF presented sporadic increases from mid-June to late-September that ranged from approximately 50 $g \cdot m^{-2} \cdot d^{-1}$ to 125 $g \cdot m^{-2} \cdot d^{-1}$, which occurred in coincidence with sediment gravity flows coming from the northern flank (Figures 5A, 6A). Lower TMF values of approximately 14 $g \cdot m^{-2} \cdot d^{-1}$ were generally observed from October to early December, interrupted by a high TMF in late October (55 $g \cdot m^{-2} \cdot d^{-1}$) in coincidence with the sporadic sediment gravity flow coming from the southern canyon flank. The sediment trap overfilled in early December (>93 $g \cdot m^{-2} \cdot d^{-1}$), which resulted in an overfilled sample cup and the clogging of the sediment trap funnel.

The flux weighed average of the mean grain size was 12.8 μm during the whole sampling period, and ranged from 7.7 μm to 20.0 μm, generally following the patterns of TMF (Figure 6A). Sediment grain size consisted of mostly silt (71%) and clay (27%) fractions (Figure 6B), with slight increases in sand content from 0.5 to 6.5% during periods with highest TMF (> 40 $g \cdot m^{-2} \cdot d^{-1}$) (Figures 6A, B). The highest sand contents of 6.5% and 5.2% were detected in the overfilled sediment trap samples from March and December, respectively (Figure 6C). In comparison to surficial sediment from the adjacent trawled flank, sediment trap samples had finer grain size (Figures 6A, B). The predominant major constituents of the downward particle fluxes were lithogenic and $CaCO_3$ fractions with relatively constant values (average 70% and 26% respectively). Downward particle fluxes presented similar $CaCO_3$ contents as surficial sediment in the sediment core collected in the adjacent trawled site (Figure 6C).

The flux weighed mean of OC and TN contents was 0.91% and 0.11%, respectively, and followed a clear seasonal pattern with high contents at the beginning of the year (0.99% OC, 0.12% TN) that generally decreased in late-spring and summer to minimum values (0.86% OC, 0.10% TN), and increased again in autumn towards the end of the year (1.05% OC, 0.13% TN) (Figure 6D). The OC/TN molar ratio had a flux weighted mean of 8.2, and ranged from 7.2 to 10.2, with highest values occurring during high TMF in the summer (Figure 6E). Concentrations of OC and TN in the sediment trap samples during the winter months were 45 and 57% higher, respectively, than those quantified in the surficial sediment of the trawled sediment core, but presented similar values during the summer months (Figure 6D).

The composition of organic matter was investigated by calculating the OC-normalized contents of different types of biomarkers (in μg of biomarker per 100 mg of OC), which showed considerable variations throughout the sampling period (Figure 7). Terrestrial vanillyl phenols (VP) and syringyl phenols (SP) displayed low concentrations during the February storm and DSWC event (44 and 40 μg·100 mg^{-1} OC, respectively), but reached maximum concentrations in the overfilled sample in March at the beginning of the trawling season (65 and 50 μg·100 mg^{-1} OC, respectively), with values similar to those of the surface sediment from the adjacent trawled flank (Figure 7A). In contrast, terrigenous cinnamyl phenols (CP) and cutin acids (CA) presented relatively constant concentrations during this period (18 and 59 μg·100 mg^{-1} OC, respectively). During the summer, concentrations of terrestrial compounds were similar to those quantified in the surficial sediment of the core collected in the adjacent trawling flank, although small sporadic increases occurred in mid-July and early September (Figures 7A, B). Small increases in these compounds were also detected during the late-October sediment gravity flow, as well as the overfilled sediment trap in early-December. Ratios of SP/VP and CP/VP in the sediment trap ranged from 0.6 to 1.1 and from 0.2 to 0.4, respectively, whereas ratios of acid to aldehyde of vanillyl phenols (Vd/Vl) and syringyl phenols (Sd/Sl) ranged from 0.4 to 1.1 and from 0.2 to 0.8, respectively (Figure S3).

From the heterogenous compound classes, p-hydroxybenzenes (PB) and benzoic acids (BA) presented a similar pattern as VP and SP, with low concentrations during the February storm and DSWC event (31 and 9 μg·100 mg^{-1} OC, respectively) that peaked with the overfilling of the sediment trap in March (51 and 22 μg·100 mg^{-1} OC, respectively), reaching similar values as those from the surface sediment sampled in the adjacent trawled area (Figure 7C). Concentrations of PB and BA were initially high in early-summer (64 and 27 μg·100 mg^{-1} OC, respectively) and then decreased to similar values as those observed in the surficial sediment of the trawled site (Figure 7C). Towards the end of summer, concentrations of PB and BA increased again to 64 and 22 μg·100 mg^{-1} OC, respectively, but dropped to 35 and 8 μg·100 mg^{-1} OC, respectively, during the late-October sediment gravity flow (Figure 7C).

The fatty acid (FA), dicarboxylic acid (DA) and amino acid (AA) CuO products are highly enriched in marine organic matter sources (e.g., phytoplankton, zooplankton) relative to terrestrial plants (Goñi and Hedges, 1995). Given their high degradability, these compounds are rapidly transformed during their transport towards the seafloor, so presence of these compounds in downward particulate fluxes generally indicate the arrival of fresh marine organic matter, often derived from periods of high net primary productivity (Goni et al., 2009). These compounds presented higher OC-normalized concentrations during the mid-February eastern storm and DSWC event (89, 65 and 568 μg·100 mg^{-1} OC) and decreased during the following weeks (72, 52 and 390 μg·100 mg^{-1} OC) (Figures 7D, E). However, concentrations increased again in the overfilled sediment trap in March. The summer months generally presented lower concentrations (~55, ~40 and ~245 μg·100 mg^{-1} OC, respectively), similar to the surficial

sediment of the core collected in the trawled flank. Exceptionally high concentrations (103, 78 and 621 μg·100 mg^{-1} OC) were observed in early June, as observed with PB and BA, as well as in mid-July and mid-September. Concentrations remained low and similar to the surface sediment of the trawled area during the remaining sampling period, with another increase in concentration in the overfilled sediment trap in early December (68, 39 and 380 μg·100 mg^{-1} OC) (Figures 7D, E).

The variations in OC composition in downward particulate fluxes are summarized in a PCA, which in total explained 74% of the variance (Figure 8). Eigenvalue scores show that higher PC1 values reflect greater concentrations of all CuO compounds, consistent with the presence of organic matter with higher overall biomarker abundances, whereas different groups of CuO compounds are differentiated along the PC2 axis in terms of their general reactivity, as observed by Paradis et al. (2021b) (Figure 8A). With the exception of the last sediment

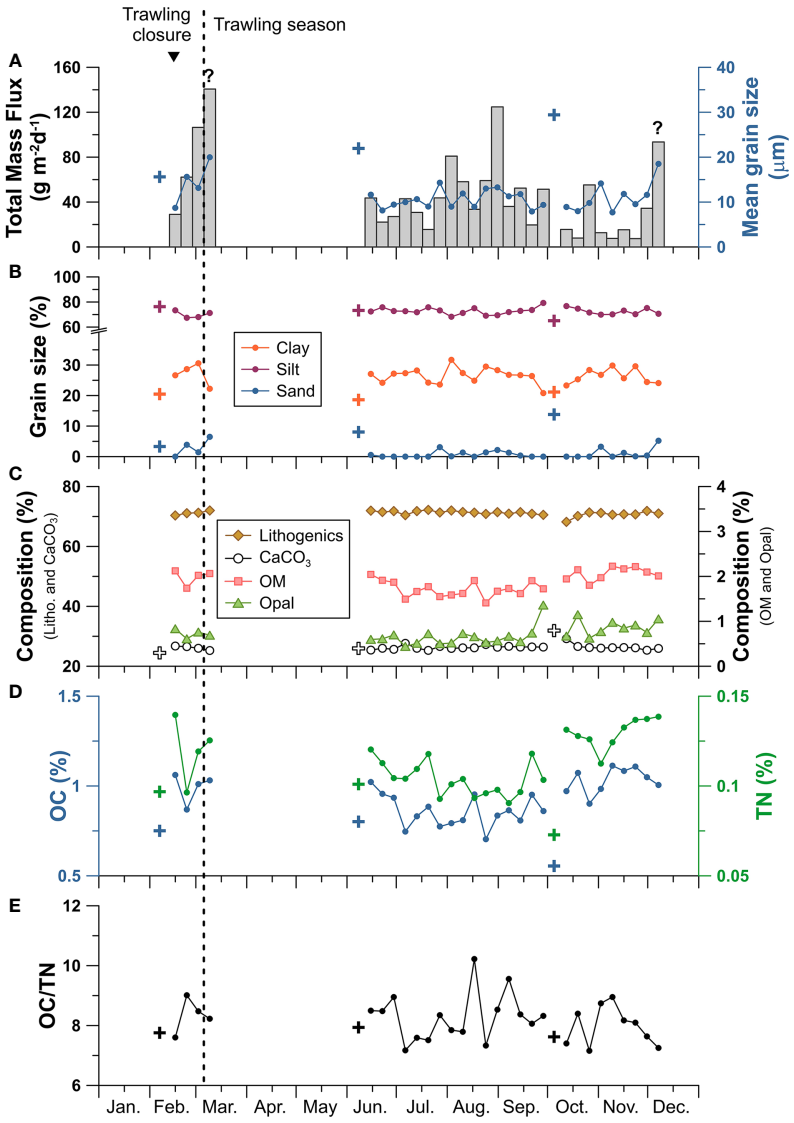

FIGURE 6
Axis-1200 time series of the sediment trap: **(A)** total mass flux (TMF) in grey bars and mean grain size in blue circles, **(B)** grain size classes, **(C)** relative concentration of the main mass composition: lithogenics (brown diamonds), calcium carbonate ($CaCO_3$, white circles), organic matter (OM, pink squares), and biogenic opal (green triangles), **(D)** organic carbon (OC) in blue and total nitrogen (TN) in green, and **(E)** OC/TN molar ratio. Question marks above TMF bars indicate that the sediment trap had overfilled in that sample and the inverted triangle indicates the occurrence of a dense shelf water cascading event. Mean values of grain size, $CaCO_3$, OC, and TN of surficial sediment of the sediment core retrieved on the trawled flank in February, June, and October (Paradis et al., 2021b) are given with crosses. Note the break in the axis of the grain size fraction **(B)**.

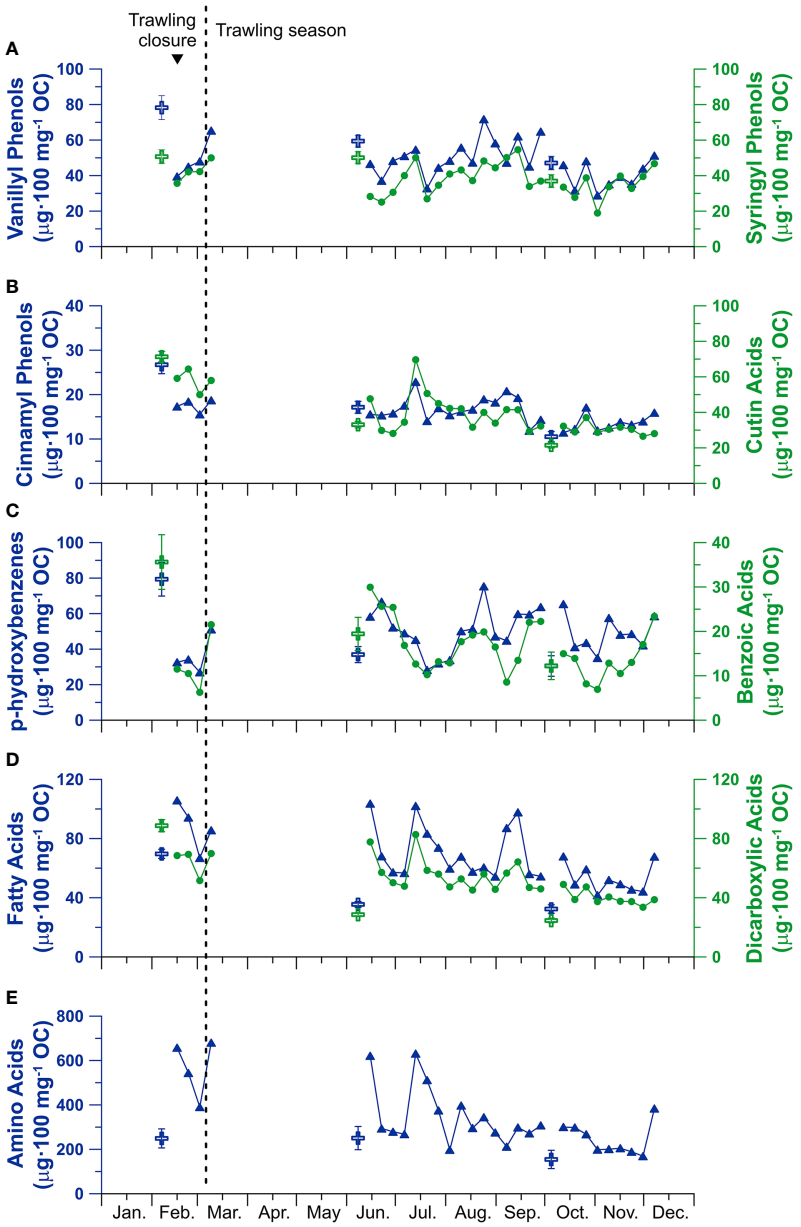

FIGURE 7
Temporal evolution of OC-normalized CuO compound classes in the sediment trap samples (Axis-1200). **(A)** terrestrial vanillyl (blue triangles) and syringyl (green circles) phenols, **(B)** terrestrial cinnamyl phenols (blue triangles) and cutin acids (green circles), **(C)** p-hydroxy benzenes (blue triangles) and benzoic acids (green circles), **(D)** fatty acids (blue triangles) and di-carboxylic acids (green circles), **(E)** amino acids (blue triangles). Values of surficial sediment of the sediment core retrieved on the trawled flank in February, June, and October (Paradis et al., 2021b) are given with crosses. Note the different scales for each compound classes. The inverted triangle on top indicates the occurrence of a dense shelf water cascading event.

trap sample from early-March, the temporal evolution of PC1 generally reflects higher values during the trawling closure than during the trawling season (Figure 8B). In contrast, during the trawling season, higher TMF values are normally associated to lower PC1 and PC2 values, similar to values of surficial samples from the adjacent trawling ground (Figures 8B, C).

4 Discussion

During the 2017 sampling period, several sediment transport events of both natural and anthropic origin were identified in Palamós Canyon. Storms occurred during winter and autumn months, characteristic of seasonal patterns of this margin

(Palanques et al., 2005; Zúñiga et al., 2009; Lopez-Fernandez et al., 2013b) with exceptionally strong eastern storms in mid-January and mid-February (Figures 2A, B). These natural forcing conditions abated during the spring and summer months, when bottom trawling activities were predominant in the surroundings of Palamós Canyon (Figure 2; Palanques et al., 2006; Puig et al., 2012; Martín et al., 2014a). Both storms and trawling activities transported sediment into the canyon through different pathways and with different sediment composition. The following sections describe and discuss in detail each of these events chronologically.

4.1 Winter storm and dense shelf water cascading (February)

An exceptionally strong eastern storm occurred a week prior to the mooring deployment in mid-January, causing a flash flood of the Ter River (Figures 2A, B). This flood event transported terrestrial organic matter to the margin and reached the northern flank of Palamós Canyon (Figure 1), which we sampled two weeks after this storm. The surface sediment recovered from this core had high concentrations of lignin phenols and cutin acids from vascular plants, reflecting fresh terrestrial inputs from the storm (Figures 7A, B; Paradis et al., 2021b).

This storm was followed by another eastern storm a week after the deployment of the moorings in mid-February that drove the cascading of dense shelf water into the upper Palamós Canyon axis, reaching the Axis-900 mooring, which registered a drop in temperatures (< 12.6°C), as well as an increase in turbidity (~230 mg·L^{-1}) and current speed (0.6 m·s^{-1}) (Figures 3A, B; Arjona-Camas et al., 2021). No drop of temperatures was observed either in Flank-1000 nor in Axis-1200, the latter mooring located ~4 km down-canyon from Axis-900, indicating that these dense waters had reached neutral buoyancy at shallower depths. However, this DSWC event prompted the transport of suspended sediment through the entire canyon. The Flank-1000 mooring registered SSC of ~50 mg·L^{-1} and current speeds of 0.4 m s^{-1}, while the Axis-1200 mooring registered SSC >28.5 mg·L^{-1} and current speeds of 0.6 m s^{-1} (Figure S4). However, the turbidimeter at Axis-1200 recorded maximum values during that event due to the sensor range limitation (28.5 mg·L^{-1}), and we expect that actual SSC were significantly higher given the simultaneous increases in SSC in all moorings (Figure S4).

The strong sediment transport event associated to DSWC in the Axis-1200 mooring did not lead to high downward sediment fluxes in the sediment trap (Figure 6A), which could indicate either a stronger horizontal rather than vertical sediment flux that would have bypassed the sediment trap, or that the sediment transport occurred close to the seafloor and was missed by the sediment trap located at 22 mab, as hypothesized in other studies (Bonnin et al., 2008; Rumín-Caparrós et al., 2016). Moreover, high current speeds can affect sediment trap collection efficiency (Baker et al., 1988; Heussner et al., 2006), so downward particulate fluxes during this event should be considered as semi-quantitative.

Downward sediment fluxes from the mid-February eastern storm and DSWC event had higher concentrations of OC and TN (1.1% and 0.14%, respectively) (Figure 6D) enriched in compound classes of marine origin (i.e. fatty acids,

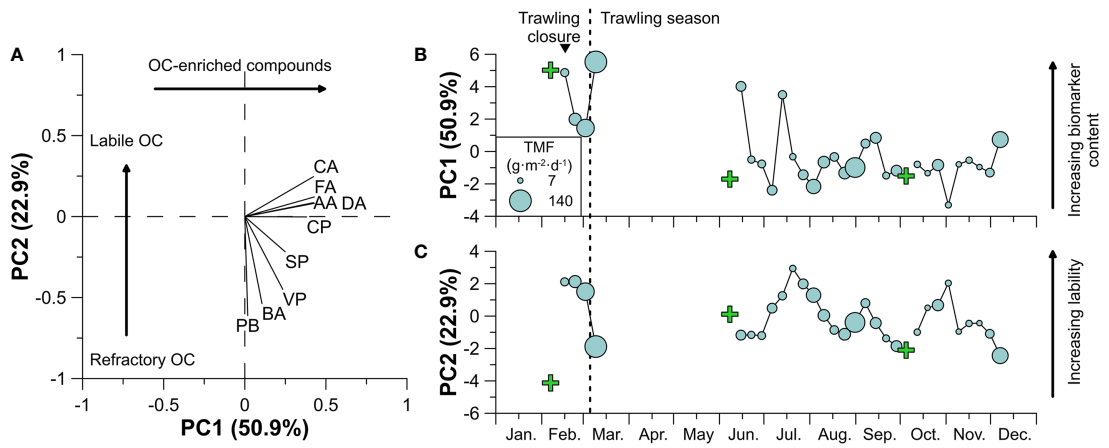

FIGURE 8
PCA results. **(A)** Eigenvalues of the PCA performed of OC-normalized CuO products in the sediment trap (Axis-1200). Temporal evolution of **(B)** PC1 and **(C)** PC2 values of the sediment trap samples, where the size of the circles refers to TMF and the green crosses show the PC value of surficial sediment of the sediment core retrieved on the trawled flank in February, June, and October (Paradis et al., 2021b). The inverted triangle on top indicates the occurrence of a dense shelf water cascading event.

dicarboxylic acids, and amino acids) (Figures 7D, E) in comparison to particulate matter accumulated during the following week (Figure S4). This peak in marine biomarkers coincided with elevated estimates of NPP that were consistent with a winter phytoplankton bloom. Although this storm caused high Ter River discharge (Figure 2B) that reached off-shore sediments on the Palamós northern flank (Paradis et al., 2021b), the organic matter in the sediment traps had low OC-normalized concentrations of terrestrial compounds because they were diluted by the enhanced contribution of fresh marine organic compounds from the phytoplankton bloom (Figure 2). Other studies have shown similar trends, where the usual transfer of OC-poor terrigenous organic matter into canyons during storms (Tesi et al., 2010; Sanchez-Vidal et al., 2012) is offset by the transfer of fresh marine organic matter during phytoplankton blooms (Fabres et al., 2008; Pasqual et al., 2010; Lopez-Fernandez et al., 2013a). Hence, these high-energy DSWC events can result in important drivers of fresh and labile organic matter from surface shelf and slope waters to deep-sea environments, while also transferring fluvial derived terrestrial material.

During the following 2 weeks, downward sediment fluxes in the sediment trap increased from ~30 to ~100 $g{\cdot}m^{-2}{\cdot}d^{-1}$ (Figure 6A), indicating the settling of sediment that had remained in suspension after the DSWC event (Arjona-Camas et al., 2021). These samples displayed lower OC and TN contents and decreasing OC-normalized concentrations of the most labile compounds (i.e. amino acids, fatty acids, dicarboxylic acids; Figures 7, 8), which indicate the resuspension and transfer of OC-poor sediment resuspended by the strong DSWC currents (Puig et al., 2008). Alternatively, these trends could also reflect a general degradation of these compounds given their long transit time in the water column before reaching the sediment trap.

4.2 Onset of trawling season (March)

Bottom trawling activities began on March 8, after 2 months of a trawling closure on the fishing grounds surrounding Palamós Canyon (BOE, 2017). At the onset of bottom trawling activities, high sediment fluxes were recorded at the Axis-900 mooring (Arjona-Camas et al., 2021), and sediment gravity flows with high SSC (200-400 $mg{\cdot}L^{-1}$) and strong bottom currents (~0.4 $m{\cdot}s^{-1}$) were channeled through the Montgrí tributary gully, recorded by the Flank-1000 mooring, some reaching the Axis-1200 mooring ~1.5 km further down-flank (Figure S5). The strong sediment gravity flows occurring on Thursday and Friday (March 10 and 11) that reached Axis-1200 with SSC between 10-20 $mg{\cdot}L^{-1}$ would have caused the overfilling of that week's sediment trap cup, with a total mass flux of >140 $g{\cdot}m^{-2}{\cdot}d^{-1}$ (Figure S5). Sediment transported at the onset of the trawling season had coarser grain size with higher sand content than the previous trap samples (Figures 6B, S5), as observed in trawling-induced sediment gravity flows from a sediment trap deployed in this same site in 2002 (Palanques et al., 2006).

Downward sediment flux during the onset of the trawling season was enriched in most biomarkers, including terrestrial compounds (lignin phenols) and labile marine compounds (fatty acids, di-carboxylic acids, and amino acids) in comparison to the previous trap sample (Figures 7, S5), with a similar overall composition to surficial sediment from the trawled flank (Figure 8; Paradis et al., 2021b). This confirms that bottom trawling is translocating sediment from the fishing grounds into the canyon. The higher terrestrial content was associated to the transfer of surficial sediment from the fishing ground which was enriched in these compounds due to the Ter River flash flood that occurred in January (Paradis et al., 2021b), while the higher marine compounds indicate the transferal of the remnants of the phytoplankton bloom (see section 4.1).

4.3 Trawling season (March-October)

Previous studies observed that bottom trawling during the summer causes almost-daily sediment gravity flows through the Montgrí tributary only during working days (Palanques et al., 2006; Puig et al., 2012; Martín et al., 2014a), which were also evident during this study (Figures S5, S6). The intensity of these sediment gravity flows in Flank-1000 mooring decreased as the trawling season unfolded, from ~500 $mg{\cdot}L^{-1}$ in early March to ~15 $mg{\cdot}L^{-1}$ in late October, although some large isolated peaks were still registered (Figure 4A). This decreasing trend proves a progressive depletion of sediment available for resuspension by bottom trawling gears during the trawling season, as hypothesized in previous studies (Martín et al., 2014a).

Although these sediment gravity flows were directed towards the canyon axis, only the exceptionally intense sediment gravity flows (SSC >250 $mg{\cdot}L^{-1}$) at Flank-1000 reached the Axis-1200 mooring, causing SSC and TMF to increase from ~1 to 60-230 $mg{\cdot}L^{-1}$ and from ~16 to 120 $g{\cdot}m^{-2}{\cdot}d^{-1}$ respectively (Figure S6), with similar magnitude as those registered during the summer months at the same site in 2001 (Martín et al., 2006). These sediment gravity flows mainly originated from the Montgrí tributary gully (~190°), but also from an adjacent tributary gully towards the NNE (~220°) (Figure S6), as hypothesized in previous studies (Martín et al., 2006; Palanques et al., 2006). This proves that the various tributary gullies along the flanks of Palamós Canyon (Lastras et al., 2011) would likely serve as pathways of resuspended sediment from the fishing grounds along the canyon flanks into the canyon axis (Figure 1), presumably leading to increases in sedimentation rates not only at 1750 m in depth, as reported in previous studies (Martín et al., 2008; Puig et al., 2015), but likely throughout the whole canyon axis, as observed in the adjacent Blanes Canyon (Paradis et al., 2018b).

Trawling-derived sediment gravity flows transported coarser grain sizes in comparison to periods with naturally low TMFs (Figure S6), as observed by Palanques et al. (2006). However,

downward particulate matter collected by the sediment trap had finer grain size than surface sediment of trawling grounds (Figures 7A, B) as a result of grain size sorting and winnowing of finer grained sediment by bottom trawling (Martín et al., 2014b; Paradis et al., 2021b). The flux weighed mean concentration of OC and TN during this period (March-October) was lower (0.84% OC, 0.10% TN) than during the rest of the study period (1.00% OC, 0.13% TN) (Figures 6D, S6), which also coincided with the periods with lower net primary productivity in the area (Figure 2C). This could indicate that marine productivity is the main driver increasing OC and TN contents sinking to the seafloor, where submarine canyons play an important role in its transfer to deeper environments (Fabres et al., 2008; Lopez-Fernandez et al., 2013a; Grinyó et al., 2017), and that bottom trawling does not alter the OC and TN content of the downward particulate matter fluxes. However, the composition of OC obtained from CuO oxidation indicates that periods with high downward particulate fluxes due to bottom trawling-derived sediment gravity flows transferred highly degraded terrestrial compounds and lower content of the most labile marine compound classes, and its biogeochemical composition was similar to surficial sediment from the adjacent trawling ground (Figures 8, S6). Despite the similar biogeochemical composition to the trawled site, in the majority of the samples, OC, TN and the most labile compound classes (i.e. fatty acids, di-carboxylic acids, and amino acids) had slightly higher content in the sediment trap than in the trawling ground (Figures 6, 7), which reveals that the downward particle flux consisted of a combination of eroded sediment transferred from fishing grounds with hemipelagic settling of particulate organic matter enriched in biomarkers of marine origin (Figure 7). In contrast, in the absence of trawling-derived sediment gravity flows during the summer, particulate organic matter had higher content of reactive marine compound classes, such as in early June, associated to the high NPP occurring then (Figures 2C, 7).

4.4 Intermission of trawling activities (November-December)

Throughout October and November, SSCs in all three moorings were negligible, while the downward sediment fluxes in the sediment trap were only ~10 $g{\cdot}m^{-2}{\cdot}d^{-1}$ (Figures 3-6) with the exception of an isolated sediment gravity flow in late-October (Figure S7). This reduced sediment flux occurred in the absence of fishing activities in the Sant Sebastià fishing ground (Figure S2), confirming the strong relationship between sediment transport into Palamós Canyon and this anthropogenic activity. During this low sediment flux period, sediment collected in the Axis-1200 trap had higher OC and TN contents (1.04% OC, 0.13% TN), than during the summer months (0.84% OC, 0.10% TN) when frequent trawling-derived sediment gravity flows were registered in the canyon axis (Figures 6D, S7). This was likely the result of increasing NPP (Figure 2C) and the lower dilution of organic matter due to lower lithogenic transport during this period in comparison to periods with trawling-derived sediment gravity flows. This is supported by the more labile organic matter during this period (Figures 7, S7), indicating the transferal of fresh material into the canyon in the absence of trawling activities.

An isolated late-October sediment gravity flow coming from the southern flank interrupted the low TMF during the absence of trawling activities, which led to high TMF of ~60 $g{\cdot}m^{-2}{\cdot}d^{-1}$ with high lithogenic fraction that diluted the OC contents (Figure S7). In contrast to trawling-derived sediment gravity flows coming from the northern flank (see section 4.3), organic matter presented higher lability (Figure 8C), indicating the transferal of fresh material, albeit diluted by the high lithogenic fraction, into the canyon. Therefore, this sporadic sediment gravity flow seems to be associated to a natural sediment destabilization from the untrawled southern canyon flank, as previously observed in deeper parts of this canyon (Martín et al., 2006; 2007).

After five weeks of trawling intermission in Sant Sebastià fishing ground, bottom trawlers resumed their activity in December (Figure S2), increasing near-bottom SSCs to 130-260 $mg{\cdot}L^{-1}$ in Flank-1000 and to ~50 $mg{\cdot}L^{-1}$ in Axis-900 during that month, while the sediment trap in Axis-1200 overfilled once more, attaining a TMF of at least 94 $g{\cdot}m^{-2}{\cdot}d^{-1}$ (Figure S8). This increase in sediment transport in all moorings confirm that the fishing ground was replenished with new erodible sediment during the fishing intermittence, generating large sediment gravity flows when trawling activities resumed, as was observed at the onset of trawling season in early March (see section 4.2). In both overfilled trap samples, the sediment transported into the canyon consisted of coarser particles with high terrigenous and marine OC (Figures 6-8, S8), indicating the translocation of freshly-deposited sediment with higher organic matter contents into the canyon. This corroborates that chronic trawling disturbance depletes organic matter from fishing grounds (Pusceddu et al., 2014), while short periods without trawling disturbance are insufficient to allow its recovery (Paradis et al., 2021b), which swiftly remove the most OC-rich surficial sediment from fishing grounds when trawling activities resume.

4.5 Annual sediment transport and composition in Palamós Canyon

Sediment transport into Palamós Canyon during 2017 was highly dynamic, dominated by natural high-energy events such as eastern storms and DSWC, as well as by bottom trawling, both of which transferred large volumes of sediment into the canyon. Sediment transport through the Montgrí tributary gully was dominated by trawling-induced sediment gravity flows, which accounted for ~1500 $kg{\cdot}m^{-2}$ sediment whereas the eastern storm

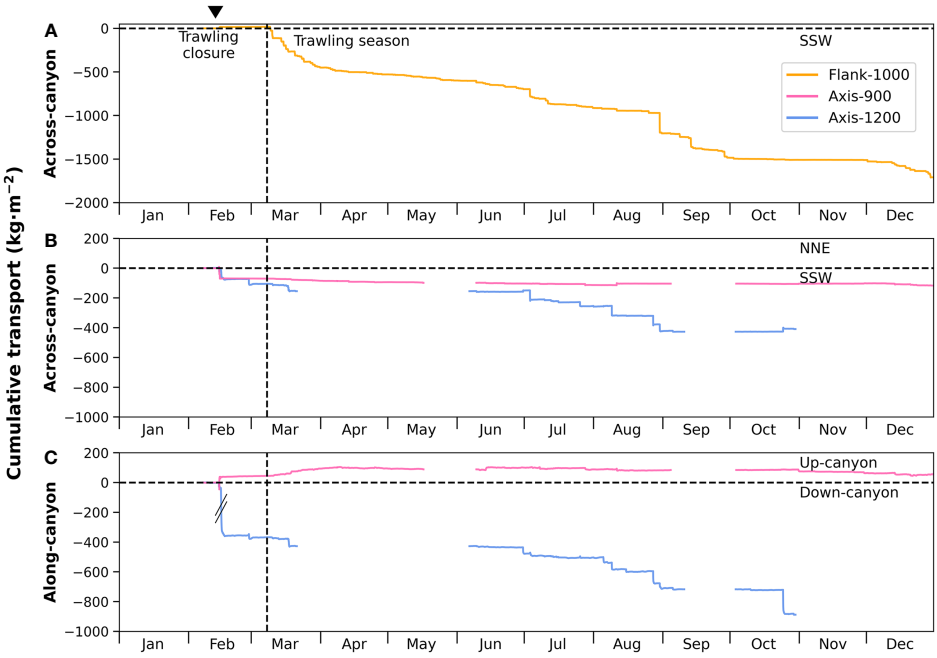

FIGURE 9
Time series of cumulative sediment transport at all moorings: **(A)** at the Flank-1000 mooring in the across-canyon direction (10 mab), **(B)** at Axis-900 and Axis-1200 in the across-canyon direction (5 mab) and **(C)** in the along-canyon direction (5 mab). Cumulative sediment transport for Axis-900 and Axis-1200 are highly underestimated due to their incomplete timeseries and the maximum data acquisition of the Axis-1200 turbidimeter during the first deployment (Figure 5). Note the different axes for the Flank-1000 cumulative sediment transport in comparison to the across-canyon and along-canyon transport of Axis-900 and Axis-1200. The inverted triangle on top indicates the occurrence of a dense shelf water cascading event.

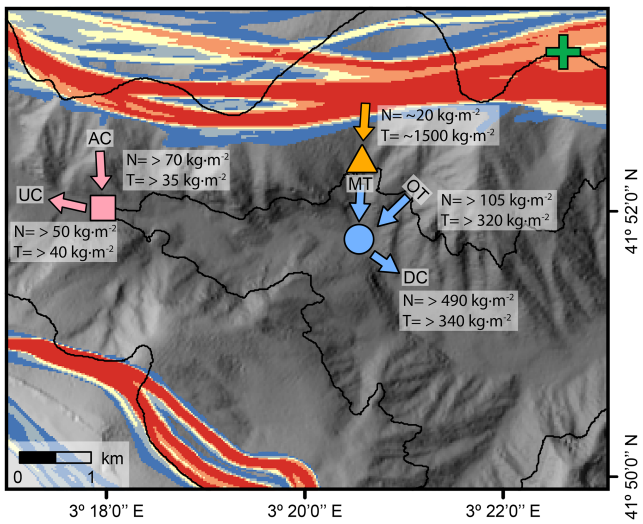

FIGURE 10
Map of main sediment transport pathways of the three mooring locations in Palamós Canyon: up-canyon (UC) and across-canyon (AC) for Axis-900 mooring (pink square), Montgrí tributary gully (MT) for Flank-900 mooring (orange triangle), other tributary gully (OT), and down-canyon (DC) for Axis-1200 mooring (blue circle). Annotated in the figure is the cumulative sediment transport for natural high-energy events (N) and trawling-derived events (T). Note that the across-canyon cumulative transport for the Axis-1200 mooring combines sediment transported through both tributaries (MT and OT).

and DSWC at the beginning of the year transported ~20 kg·m^{-2} of sediment through this tributary and into the canyon (Figures 9, 10). In the case of the moorings located along the canyon axis (Axis-900, Axis-1200), the magnitudes of sediment fluxes from natural and anthropogenic events were comparable (Figures 9, 10). In Axis-900, total sediment flux from storms and DSWC was at least ~120 kg·m^{-2} during 2017, while bottom trawling accounted for at least ~75 kg·m^{-2}. Further down-canyon, natural high-energy events transported at least ~600 kg·m^{-2} of sediment through Axis-1200 whereas trawling activities accounted for at least ~680 kg·m^{-2} of sediment (Figures 9, 10). Despite the comparable magnitude of sediment fluxes, natural events tend to be sporadic and seasonal, whereas bottom trawling causes continuous and persistent sediment fluxes into the canyon.

With regards to the composition of sediment transported into the canyon, it is worth noting that terrestrial compounds (i.e. lignin phenols and cutin acids) were detected during the whole sampling period (Figure 7), irrespectively of the sediment transport process, as observed in other submarine canyons nearby (Tesi et al., 2010; Pasqual et al., 2013), which confirms the role of submarine canyons as across-margin conduits of terrestrial organic matter towards deep-sea basins. The high acid to aldehyde ratio of vanillyl and syringyl phenols, SP/VP and CP/VP ratios (Figure S3) indicates that terrestrial organic matter was highly degraded and mostly originated from non-woody angiosperm leaves and grasses (Hedges and Mann, 1979; Goñi and Hedges, 1995). The highly degraded compositions are expected given the distance of the Axis-1200 mooring to the shore and the long transit times that promote its alteration (Pasqual et al., 2013). Presence of non-woody organic matter signatures is also expected given the association of these compounds to fine-grained sediment that can be more easily transported offshore than larger-sized woody detritus with high vanillyl phenol contents, which tend to accumulate in more nearshore environments (Gordon and Goñi, 2004; Pasqual et al., 2013; Zhang et al., 2014).

Bottom trawling-derived sediment fluxes in the canyon axis had lower OC content (~0.8%) and consisted of more degraded organic matter in comparison to downward sediment fluxes in the absence of bottom trawling during the summer, as well as in comparison to the sediment fluxes during the storms in February (~1% OC), since these natural processes occurred in coincidence with high net primary productivity in surface waters or an intermittence of fishing activities. The enhanced particulate matter fluxes of eroded sediment by bottom trawling modify the OC composition of downward particulate fluxes in submarine canyons from fresh marine organic matter to degraded and less reactive terrestrial organic matter. This alteration in the nutritional value of organic matter would affect the benthic community structure inhabiting submarine canyons, and could explain the lower diversity of meiofauna mainly consisting of opportunistic nematode species as observed within the axes of the studied canyon (Pusceddu et al., 2014) as well as in the adjacent Blanes Canyon (Román et al., 2018).

Despite the lower OC content of these trawling-derived sediment fluxes (~0.8%), the higher TMF associated to bottom trawling activities (>54 kg·m^{-2}; Figure 6A), indicate that a substantial amount of organic carbon is transferred into the canyon (> 0.43 kg OC·m^{-2}), where it will eventually be buried in the canyon axis. Since efficient OC burial is generally associated to high sedimentation rates (Blair and Aller, 2012; Bianchi et al., 2018), the enhanced sediment transfer and resulting increase in sedimentation rates in the canyon axis by bottom trawling activities (Martín et al., 2008; Puig et al., 2015) could lead to high OC burial in the canyon axis. However, this enhanced transport of OC by bottom trawling activities could partially offset the OC lost from fishing grounds (Martín et al., 2014b; Paradis et al., 2021b), and further studies will be necessary to properly quantify the sediment and the OC budgets in Palamós Canyon, and assess the potential effects on benthic communities.

5 Conclusion

High energy events such as river floods and storms are important mechanisms that enhance the transport of particulate matter into submarine canyons, but recent studies have emphasized that bottom trawling activities modify natural sedimentary dynamics within these geomorphological features. This study shows how bottom trawling is altering sedimentary dynamics in submarine canyons and reveals that the organic matter composition of down-canyon particulate matter is modified by this anthropogenic activity. While winter storms transport terrigenous and fresh marine organic matter into the canyon in the presence of phytoplankton blooms, trawling-induced sediment gravity flows transfer more degraded organic matter. Trawling events interrupt the naturally high concentrations of fresh and reactive organic matter compounds that are usually transferred during the calm summer months, which could affect benthic communities that inhabit the canyon and rely on the input of fresh organic matter. However, the higher downward particulate fluxes into the canyon by bottom trawling also increases organic carbon fluxes, urging to better constrain the sediment and organic carbon budgets in bottom trawling-affected submarine canyons.

Data availability statement

The raw data supporting the conclusions of this article will be made available by the authors, without undue reservation.

Author contributions

SP, MA-C, AP, and PP conceptualized the study design and performed the fieldwork. MA-C and SP analyzed sensor data from moorings. SP performed the laboratory analyses and interpreted the

results alongside MG. AP, PM, and PP provided funding for the study. SP wrote the manuscript with the contribution of all co-authors, who approve the submitted version.

Funding

The results presented in this study were obtained within the "Assessment of Bottom-trawling Impacts in Deep-sea Sediments" (ABIDES) Spanish Research Project (CTM2015-65142-R). Additional funds were provided by the Generalitat de Catalunya (2017 SGR-663 and SGR- 1588), by the Australian Research Council LIEF Project (LE170100219) and by the "Assessment of Bottom-trawling Resuspension Impacts in deep benthic Communities" (ABRIC) Spanish Research Project (RTI2018-096434-B-I00). This work is contributing to the ICTA's "Unit of Excellence" Maria de Maetzu (CEX2019-000940-M), and ICM-CSIC's "Center of Excellence" Severo Ochoa (CEX2019-000928-S). Open access funding provided by ETH Zurich.

Acknowledgments

We would like to thank the crew of the R/V García del Cid as well as Elena Martinez, Neus Maestro, and Silvia de Diago, who helped collect and process the samples. The IAEA is grateful for the support provided to its Environment Laboratories by the Government of the Principality of Monaco.

Conflict of interest

The authors declare that the research was conducted in the absence of any commercial or financial relationships that could be construed as a potential conflict of interest.

Publisher's note

Supplementary material

The Supplementary Material for this article can be found online at: https://www.frontiersin.org/articles/10.3389/fmars.2022.1017052/full#supplementary-material

References

Allen, S. E., and Durrieu de Madron, X. (2009). A review of the role of submarine canyons in deep-ocean exchange with the shelf. *Ocean Sci.* 5, 607–620. doi: 10.5194/os-5-607-2009

Arjona-Camas, M., Puig, P., Palanques, A., Durán, R., White, M., Paradis, S., et al. (2021). Natural vs. trawling-induced water turbidity and sediment transport variability within the palamós canyon (NW Mediterranean). *Mar. Geophys. Res.* 42, 38. doi: 10.1007/s11001-021-09457-7

Arjona-Camas, M., Puig, P., Palanques, A., Emelianov, M., and Durán, R. (2019). Evidence of trawling-induced resuspension events in the generation of nepheloid layers in the foix submarine canyon (NW Mediterranean). *J. Mar. Syst.* 196, 86–96. doi: 10.1016/j.jmarsys.2019.05.003

Baker, E. T., Milburn, H. B., and Tennant, D. A. (1988). Field assessment of sediment trap efficiency under varying flow conditions. *J. Mar. Res.* 46, 573–592. doi: 10.1357/002224088785113522

Behrenfeld, M. J., and Falkowski, P. G. (1997). Photosynthetic rates derived from satellite-based chlorophyll concentration. *Limnol. Oceanogr.* 42, 1–20. doi: 10.4319/lo.1997.42.1.0001

Bianchi, T. S., Cui, X., Blair, N. E., Burdige, D. J., Eglinton, T. I., and Galy, V. (2018). Centers of organic carbon burial and oxidation at the land-ocean interface. *Org. Geochem.* 115, 138–155. doi: 10.1016/j.orggeochem.2017.09.008

Bjørkan, M., Company, J. B., Gorelli, G., Sardà, F., and Massaguer, C. (2020). *When fishemen take charge: The development of a management plan for the red shrimp fishery in Mediterranean Sea (NE Spain)* (Cham: Springer), 159–178. doi: 10.1007/978-3-030-26784-1_10

Blair, N. E., and Aller, R. C. (2012). The fate of terrestrial organic carbon in the marine environment. *Ann. Rev. Mar. Sci.* 4, 401–423. doi: 10.1146/annurev-marine-120709-142717

BOE (2017). Resolución de 26 de enero de 2017, de la secretaría general de pesca, por la que se fija, para 2017, el periodo de veda establecido en la orden AAA/923/2013, de 16 de mayo, por la que se regula la pesca de gamba rosada (Aristeus antennatus) con arte de arrastre de fondo en determinadas zonas marítimas próximas a palamós. *Boletin Oficial del Estado* 30, 8169.

Bonnin, J., Heussner, S., Calafat, A., Fabres, J., Palanques, A., Durrieu de Madron, X., et al. (2008). Comparison of horizontal and downward particle fluxes across canyons of the gulf of lions (NW mediterranean): Meteorological and hydrodynamical forcing. *Cont. Shelf Res.* 28, 1957–1970. doi: 10.1016/j.csr.2008.06.004

Canals, M., Puig, P., de Madron, X. D., Heussner, S., Palanques, A., and Fabres, J. (2006). Flushing submarine canyons. *Nature* 444, 354. doi: 10.1038/nature05271

Daly, E., Johnson, M. P., Wilson, A. M., Gerritsen, H. D., Kiriakoulakis, K., Allcock, A. L., et al. (2018). Bottom trawling at whittard canyon: Evidence for seabed modification, trawl plumes and food source heterogeneity. *Prog. Oceanogr.* 169, 227–240. doi: 10.1016/j.pocean.2017.12.010

De Leo, F. C., Vetter, E. W., Smith, C. R., Rowden, A. A., and McGranaghan, M. (2014). Spatial scale-dependent habitat heterogeneity influences submarine canyon macrofaunal abundance and diversity off the main and Northwest Hawaiian islands. *Deep Sea Res. Part II Top. Stud. Oceanogr.* 104, 267–290. doi: 10.1016/j.dsr2.2013.06.015

de Stigter, H. C., Boer, W., de Jesus Mendes, P. A., Jesus, C. C., Thomsen, L., van den Bergh, G. D., et al. (2007). Recent sediment transport and deposition in the nazaré canyon, Portuguese continental margin. *Mar. Geol.* 246, 144–164. doi: 10.1016/j.margeo.2007.04.011

Durrieu de Madron, X., Ferré, B., Le Corre, G., Grenz, C., Conan, P., Pujo-Pay, M., et al. (2005). Trawling-induced resuspension and dispersal of muddy sediments and dissolved elements in the gulf of lion (NW Mediterranean). *Cont. shelf Res.* 25 (19-20), 2387–2409. doi: 10.1016/j.pocean.2004.08.004

Fabres, J., Tesi, T., Velez, J., Batista, F., Lee, C., Calafat, A., et al. (2008). Seasonal and event-controlled export of organic matter from the shelf towards the gulf of lions continental slope. *Cont. Shelf Res.* 28, 1971–1983. doi: 10.1016/j.csr.2008.04.010

Farrugio, H. (2012). "A refugium for the spawners of exploited Mediterranean marine species: the canyons of the continental slope of the gulf of lion," in *Mediterranean Submarine canyons: Ecology and governance*. Ed. M. Würtz (Gland, Switzerland: International Union for Conservation of Nature), 45–50.

Fernandez-Arcaya, U., Ramirez-Llodra, E., Aguzzi, J., Allcock, A. L., Davies, J. S., Dissanayake, A., et al. (2017). Ecological role of submarine canyons and need for canyon conservation: A review. *Front. Mar. Sci.* 4. doi: 10.3389/fmars.2017.00005

Goni, M. A., Aceves, H., Benitez-Nelson, B., Tappa, E., Thunell, R., Black, D. E., et al. (2009). Oceanographic and climatologic controls on the compositions and fluxes of biogenic materials in the water column and sediments of the cariaco basin over the late Holocene. *Deep Sea Res. Part I Oceanogr. Res. Pap.* 56, 614–640. doi: 10.1016/j.dsr.2008.11.010

Goñi, M. A., and Hedges, J. I. (1995). Sources and reactivities of marine-derived organic matter in coastal sediments as determined by alkaline CuO oxidation. *Geochim. Cosmochim. Acta* 59, 2965–2981. doi: 10.1016/0016-7037(95)00188-3

Goñi, M. A., and Montgomery, S. (2000). Alkaline CuO oxidation with a microwave digestion system: Lignin analyses of geochemical samples. *Anal. Chem.* 72, 3116–3121. doi: 10.1021/ac991316w

Goñi, M. A., O'Connor, A. E., Kuzyk, Z. Z., Yunker, M. B., Gobeil, C., and Macdonald, R. W. (2013). Distribution and sources of organic matter in surface marine sediments across the north American Arctic margin. *J. Geophys. Res. Ocean.* 118, 4017–4035. doi: 10.1002/jgrc.20286

Gordon, E. S., and Goñi, M. A. (2004). Controls on the distribution and accumulation of terrigenous organic matter in sediments from the Mississippi and atchafalaya river margin. *Mar. Chem.* 92, 331–352. doi: 10.1016/J.MARCHEM.2004.06.035

Grinyó, J., Isla, E., Peral, L., and Gili, J.-M. (2017). Composition and temporal variability of particle fluxes in an insular canyon of the northwestern Mediterranean Sea. *Prog. Oceanogr.* 159, 323–339. doi: 10.1016/j.pocean.2017.11.005

Hedges, J. I., and Mann, D. C. (1979). The characterization of plant tissues by their lignin oxidation products. *Geochim. Cosmochim. Acta* 43, 1803–1807. doi: 10.1016/0016-7037(79)90028-0

Heussner, S., Durrieu de Madron, X., Calafat, A., Canals, M., Carbonne, J., Delsaut, N., et al. (2006). Spatial and temporal variability of downward particle fluxes on a continental slope: Lessons from an 8-yr experiment in the gulf of lions (NW Mediterranean). *Mar. Geol.* 234, 63–92. doi: 10.1016/J.MARGEO.2006.09.003

Heussner, S., Ratti, C., and Carbonne, J. (1990). The PPS 3 time-series sediment trap and the trap sample processing techniques used during the ECOMARGE experiment. *Continent. Shelf Res.* 10, 943–958. doi: 10.1016/0278-4343(90)90069-X

Hsu, R. T., Liu, J. T., Su, C.-C., Kao, S.-J., Chen, S.-N., Kuo, F.-H., et al. (2014). On the links between a river's hyperpycnal plume and marine benthic nepheloid layer in the wake of a typhoon. *Prog. Oceanogr.* 127, 62–73. doi: 10.1016/j.pocean.2014.06.001

Lastras, G., Canals, M., Amblas, D., Lavoie, C., Church, I., De Mol, B., et al. (2011). Understanding sediment dynamics of two large submarine valleys from seafloor data: Blanes and la fonera canyons, northwestern Mediterranean Sea. *Mar. Geol.* 280, 20–39. doi: 10.1016/j.margeo.2010.11.005

Liu, J. T., Wang, Y.-H., Yang, R. J., Hsu, R. T., Kao, S.-J., Lin, H.-L., et al. (2012). Cyclone-induced hyperpycnal turbidity currents in a submarine canyon. *J. Geophys. Res. Ocean.* 117, C04033. doi: 10.1029/2011JC007630

Lopez-Fernandez, P., Bianchelli, S., Pusceddu, A., Calafat, A., Sanchez-Vidal, A., and Danovaro, R. (2013a). Bioavailability of sinking organic matter in the blanes canyon and the adjacent open slope (NW Mediterranean Sea). *Biogeosciences* 10, 3405–3420. doi: 10.5194/bg-10-3405-2013

Lopez-Fernandez, P., Calafat, A., Sanchez-Vidal, A., Canals, M., Mar Flexas, M., Cateura, J., et al. (2013b). Multiple drivers of particle fluxes in the blanes submarine canyon and southern open slope: Results of a year round experiment. *Prog. Oceanogr.* 118, 95–107. doi: 10.1016/j.pocean.2013.07.029

Martín, J., Palanques, A., and Puig, P. (2006). Composition and variability of downward particulate matter fluxes in the palamós submarine canyon (NW Mediterranean). *J. Mar. Syst.* 60, 75–97. doi: 10.1016/j.jmarsys.2005.09.010

Martín, J., Palanques, A., and Puig, P. (2007). Near-bottom horizontal transfer of particulate matter in the palamós submarine canyon (NW Mediterranean). *J. Mar. Res.* 65, 193–218. doi: 10.1357/002224007780882569

Martín, J., Palanques, A., Vitorino, J., Oliveira, A., and de Stigter, H. C. (2011). Near-bottom particulate matter dynamics in the nazaré submarine canyon under calm and stormy conditions. *Deep Sea Res. Part II Top. Stud. Oceanogr.* 58, 2388–2400. doi: 10.1016/j.dsr2.2011.04.004

Martín, J., Puig, P., Masqué, P., Palanques, A., and Sánchez-Gómez, A. (2014a). Impact of bottom trawling on deep-sea sediment properties along the flanks of a submarine canyon. *PloS One* 9, e104536. doi: 10.1371/journal.pone.0104536

Martín, J., Puig, P., Palanques, A., Masqué, P., and García-Orellana, J. (2008). Effect of commercial trawling on the deep sedimentation in a Mediterranean submarine canyon. *Mar. Geol.* 252, 150–155. doi: 10.1016/j.margeo.2008.03.012

Martín, J., Puig, P., Palanques, A., and Ribó, M. (2014b). Trawling-induced daily sediment resuspension in the flank of a Mediterranean submarine canyon. *Deep Sea Res. Part II Top. Stud. Oceanogr.* 104, 174–183. doi: 10.1016/j.dsr2.2013.05.036

Mendoza, E. T., and Jiménez, A. A. (2009). "Vulnerability assessment to coastal storms at a regional scale," in *Coastal engineering 2008*, vol. vol 5. , 4154–4166.

Mortlock, R. A., and Froelich, P. N. (1989). A simple method for the rapid determination of biogenic opal in pelagic marine sediments. *Deep Sea Res. Part A. Oceanogr. Res. Pap.* 36, 1415–1426. doi: 10.1016/0198-0149(89)90092-7

Nieuwenhuize, J., Maas, Y. E. M., and Middelburg, J. J. (1994). Rapid analysis of organic carbon and nitrogen in particulate materials. *Mar. Chem.* 45, 217–224. doi: 10.1016/0304-4203(94)90005-1

Palanques, A., García-Ladona, E., Gomis, D., Martín, J., Marcos, M., Pascual, A., et al. (2005). General patterns of circulation, sediment fluxes and ecology of the palamós (La fonera) submarine canyon, northwestern Mediterranean. *Prog. Oceanogr.* 66, 89–119. doi: 10.1016/j.pocean.2004.07.016

Palanques, A., Martín, J., Puig, P., Guillén, J., Company, J. B., and Sardà, F. (2006). Evidence of sediment gravity flows induced by trawling in the palamós (Fonera) submarine canyon (northwestern Mediterranean). *Deep Sea Res. Part I Oceanogr. Res. Pap.* 53, 201–214. doi: 10.1016/j.dsr.2005.10.003

Palanques, A., and Puig, P. (2018). Particle fluxes induced by benthic storms during the 2012 dense shelf water cascading and open sea convection period in the northwestern Mediterranean basin. *Mar. Geol.* 406, 119–131. doi: 10.1016/j.margeo.2018.09.010

Palanques, A., Puig, P., Durrieu de Madron, X., Sanchez-Vidal, A., Pasqual, C., Martín, J., et al. (2012). Sediment transport to the deep canyons and open-slope of the western gulf of lions during the 2006 intense cascading and open-sea convection period. *Prog. Oceanogr.* 106, 1–15. doi: 10.1016/j.pocean.2012.05.002

Paradis, S., Goñi, M., Masqué, P., Durán, R., Arjona-Camas, M., Palanques, A., et al. (2021b). Persistence of biogeochemical alterations of deep-Sea sediments by bottom trawling. *Geophys. Res. Lett.* 48, e2020GL091279. doi: 10.1029/2020GL091279

Paradis, S., lo Iacono, C., Masqué, P., Puig, P., Palanques, A., Russo, T., et al. (2021a). Evidence of large increases in sedimentation rates due to fish trawling in submarine canyons of the gulf of Palermo (SW Mediterranean). *Mar. pollut. Bull.* 172, 112861. doi: 10.1016/j.marpolbul.2021.112861

Paradis, S., Masqué, P., Puig, P., Juan-Díaz, X., Gorelli, G., Company, J. B., et al. (2018a). Enhancement of sedimentation rates in the foix canyon after the renewal of trawling fleets in the early XXIst century. *Deep Res. Part I Oceanogr. Res. Pap.* 132, 51–59. doi: 10.1016/j.dsr.2018.01.002

Paradis, S., Puig, P., Masqué, P., and Juan-Diáz, X. (2017). Bottom-trawling along submarine canyons impacts deep sedimentary regimes. *Sci. Rep.* 7, 43332. doi: 10.1038/srep43332

Paradis, S., Puig, P., Sánchez-Vidal, A., Masqué, P., García-Orellana, J., Calafat, A., et al. (2018b). Spatial distribution of sedimentation-rate increases in blanes canyon caused by technification of bottom trawling fleet. *Prog. Oceanogr.* 169, 241–252. doi: 10.1016/j.dsr.2018.01.002

Pasqual, C., Goñi, M.A., Tesi, T., Sanchez-Vidal, A., Calafat, A., and Canals, M. (2013). Composition and provenance of terrigenous organic matter transported along submarine canyons in the gulf of lion (NW Mediterranean Sea). *Prog. Oceanogr.* 118, 81–94. doi: 10.1016/j.pocean.2013.07.013

Pasqual, C., Sanchez-Vidal, A., Zúñiga, D., Calafat, A., Canals, M., Durrieu de Madron, X., et al. (2010). Flux and composition of settling particles across the continental margin of the gulf of lion: the role of dense shelf water cascading. *Biogeosciences* 7, 217–231. doi: 10.5194/bg-7-217-2010

Pedregosa, F., Varoquaux, G., Gramfort, A., Michel, V., Thirion, B., Grisel, O., et al. (2011). Scikit-learn: Machine learning in Python. *J. Mach. Learn. Res.* 12, 2825–2830.

Pedrosa-Pàmies, R., Sanchez-Vidal, A., Calafat, A., Canals, M., and Durán, R. (2013). Impact of storm-induced remobilization on grain size distribution and organic carbon content in sediments from the blanes canyon area, NW Mediterranean Sea. *Prog. Oceanogr.* 118, 122–136. doi: 10.1016/j.pocean.2013.07.023

Porter, M., Inall, M. E., Hopkins, J., Palmer, M. R., Dale, A. C., Aleynik, D., et al. (2016). Glider observations of enhanced deep water upwelling at a shelf break canyon: A mechanism for cross-slope carbon and nutrient exchange. *J. Geophys. Res. Ocean.* 121, 7575–7588. doi: 10.1002/2016JC012087

Puig, P., Canals, M., Company, J. B., Martín, J., Amblas, D., Lastras, G., et al. (2012). Ploughing the deep sea floor. *Nature* 489, 286–289. doi: 10.1038/nature11410

Puig, P., Martín, J., Masqué, P., and Palanques, A. (2015). Increasing sediment accumulation rates in la fonera (Palamós) submarine canyon axis and their relationship with bottom trawling activities. *Geophys. Res. Lett.* 42, 8106–8113. doi: 10.1002/2015GL065052

Puig, P., Palanques, A., and Martín, J. (2014). Contemporary sediment-transport processes in submarine canyons. *Ann. Rev. Mar. Sci.* 6, 53–77. doi: 10.1146/annurev-marine-010213-135037

Puig, P., Palanques, A., Orange, D. L., Lastras, G., and Canals, M. (2008). Dense shelf water cascades and sedimentary furrow formation in the cap de creus canyon, northwestern Mediterranean Sea. *Cont. Shelf Res.* 28 (15), 2017–2030. doi: 10.1016/j.csr.2008.05.002

Pusceddu, A., Bianchelli, S., and Danovaro, R. (2015). Quantity and biochemical composition of particulate organic matter in a highly trawled area (Thermaikos gulf, Eastern Mediterranean Sea). *Adv. Oceanogr. Limnol.* 6, 21–32. doi: 10.4081/aiol.2015.5448

Pusceddu, A., Bianchelli, S., Martin, J., Puig, P., Palanques, A., Masque, P., et al. (2014). Chronic and intensive bottom trawling impairs deep-sea biodiversity and ecosystem functioning. *Proc. Natl. Acad. Sci.* 111, 8861–8866. doi: 10.1073/pnas.1405454111

Ribó, M., Puig, P., Palanques, A., and Lo Iacono, C. (2011). Dense shelf water cascades in the cap de creus and palamós submarine canyons during winters 2007 and 2008. *Mar. Geol.* 284, 175–188. doi: 10.1016/j.margeo.2011.04.001

Román, S., Vanreusel, A., Ingels, J., and Martin, D. (2018). Nematode community zonation in response to environmental drivers in blanes canyon (NW Mediterranean). *J. Exp. Mar. Bio. Ecol* 502, 111–128. doi: 10.1016/j.jembe.2017.08.010

Rumín-Caparrós, A., Sanchez-Vidal, A., González-Pola, C., Lastras, G., Calafat, A., and Canals, M. (2016). Particle fluxes and their drivers in the avilés submarine canyon and adjacent slope, central cantabrian margin, bay of Biscay. *Prog. Oceanogr.* 144, 39–61. doi: 10.1016/j.pocean.2016.03.004

Sanchez-Vidal, A., Canals, M., Calafat, A. M., Lastras, G., Pedrosa-Pàmies, R., Menéndez, M., et al. (2012). Impacts on the deep-Sea ecosystem by a severe coastal storm. *PloS One* 7, e30395. doi: 10.1371/journal.pone.0030395

Sanchez-Vidal, A., Pasqual, C., Kerhervé, P., Calafat, A., Heussner, S., Palanques, A., et al. (2008). Impact of dense shelf water cascading on the transfer of organic matter to the deep western Mediterranean basin. *Geophys. Res. Lett.* 35, L05605. doi: 10.1029/2007GL032825

Sardà, F., Cartes, J. E., and Norbis, W. (1994). Spatio-temporal structure of the deep-water shrimp aristeus antennatus (Decapoda: Aristeidae) population in the western Mediterranean. *Fish. Bull.* 92, 599–607.

Sparkes, R. B., Lin, I.-T., Hovius, N., Galy, A., Liu, J. T., Xu, X., et al. (2015). Redistribution of multi-phase particulate organic carbon in a marine shelf and canyon system during an exceptional river flood: Effects of typhoon morakot on the gaoping river–canyon system. *Mar. Geol.* 363, 191–201. doi: 10.1016/J.MARGEO.2015.02.013

Tesi, T., Langone, L., Goñi, M. A., Turchetto, M., Miserocchi, S., and Boldrin, A. (2008). Source and composition of organic matter in the bari canyon (Italy): Dense water cascading versus particulate export from the upper ocean. *Deep Sea Res. Part I Oceanogr. Res. Pap.* 55, 813–831. doi: 10.1016/j.dsr.2008.03.007

Tesi, T., Puig, P., Palanques, A., and Goñi, M. A. (2010). Lateral advection of organic matter in cascading-dominated submarine canyons. *Prog. Oceanogr.* 84, 185–203. doi: 10.1016/J.POCEAN.2009.10.004

Tudela, S., Sardà, F., Maynou, F., and Demestre, M. (2003). Influence of submarine canyons on the distribution of the deep-water shrimp, *Aristeus antennatus* (Risso 1816) in the NW Mediterranean. *Crustaceana* 76, 217–225. doi: 10.1163/156854003321824567

Vetter, E. W., Smith, C. R., and De Leo, F. C. (2010). Hawaiian Hotspots: Enhanced megafaunal abundance and diversity in submarine canyons on the oceanic islands of Hawaii. *Mar. Ecol.* 31, 183–199. doi: 10.1111/j.1439-0485.2009.00351.x

Wilson, A. M., Kiriakoulakis, K., Raine, R., Gerritsen, H. D., Blackbird, S., Allcock, A. L., et al. (2015). Anthropogenic influence on sediment transport in the whittard canyon, NE Atlantic. *Mar. pollut. Bull.* 101, 320–329. doi: 10.1016/j.marpolbul.2015.10.067

Wu, Y., Liu, Z., Hu, J., Zhu, Z., Liu, S., and Zhang, J. (2016). Seasonal dynamics of particulate organic matter in the changjiang estuary and adjacent coastal waters illustrated by amino acid enantiomers. *J. Mar. Syst.* 154, 57–65. doi: 10.1016/j.jmarsys.2015.04.006

Zhang, Y., Kaiser, K., Li, L., Zhang, D., Ran, Y., and Benner, R. (2014). Sources, distributions, and early diagenesis of sedimentary organic matter in the pearl river region of the south China Sea. *Mar. Chem.* 158, 39–48. doi: 10.1016/j.marchem.2013.11.003

Zúñiga, D., Flexas, M. M., Sanchez-Vidal, A., Coenjaerts, J., Calafat, A., Jordà, G., et al. (2009). Particle fluxes dynamics in blanes submarine canyon (Northwestern Mediterranean). *Prog. Oceanogr.* 82, 239–251. doi: 10.1016/j.pocean.2009.07.002

frontiers | Frontiers in Marine Science

TYPE Original Research
PUBLISHED 18 November 2022
DOI 10.3389/fmars.2022.1025113

OPEN ACCESS

EDITED BY
Jaime Selina Davies,
University of Plymouth,
United Kingdom

REVIEWED BY
Daniel Pech,
El Colegio de la Frontera Sur, Mexico
Alvar Carranza,
Universidad de la República, Uruguay

*CORRESPONDENCE
Zoleka Filander
zfilander@gmail.com

SPECIALTY SECTION
This article was submitted to Deep-Sea Environments and Ecology, a section of the journal Frontiers in Marine Science

RECEIVED 22 August 2022
ACCEPTED 10 October 2022
PUBLISHED 18 November 2022

CITATION
Filander Z, Smith ANH, Cawthra HC and Lamont T (2022) Benthic species patterns in and around the Cape Canyon: A large submarine canyon off the western passive margin of South Africa.
Front. Mar. Sci. 9:1025113.
doi: 10.3389/fmars.2022.1025113

Benthic species patterns in and around the Cape Canyon: A large submarine canyon off the western passive margin of South Africa

Zoleka Filander[1]*, Adam N. H. Smith[2,3], Hayley C. Cawthra[4,5] and Tarron Lamont[1,6,7]

[1]Department of Forestry, Fisheries, and Environment, Oceans and Coasts Research, Cape Town, South Africa, [2]Plymouth Routines in Multivariate Ecological Research (PRIMER-e), Quest Research Limited, Auckland, New Zealand, [3]School of Mathematical and Computational Sciences, Massey University, Auckland, New Zealand, [4]Geophysics and Remote Sensing Unit, Council for Geoscience, Bellville, South Africa, [5]African Centre for Coastal Palaeoscience, Nelson Mandela University, Gqeberha/Port Elizabeth, South Africa, [6]Bayworld Centre for Research and Education, Constantia, Cape Town, South Africa, [7]Marine Research Institute and Department of Oceanography, University of Cape Town, Rondebosch, South Africa

Although submarine canyons are internationally recognized as sensitive ecosystems and reported to be biological hotspots, regional studies are required to validate this consensus. To this end, hydrographic and benthic biodiversity data were collected during three cruises (2016-2017) to provide insights on the benthic patterns within South African canyon and non-canyon offshore areas. A total of 25 stations, sampled at 200-1000 m depth range, form the basis of the multivariate analysis. Diversity gradients were calculated and then differences were compared across substrate types and depth zones represented within 12 canyon and 13 non-canyon stations. Significant differences in both substrate and depth were evident, despite measures being highly variable. This observation of varying diversity in different substrates is in line with previous studies. No clear pattern was observed for species diversity (delta+). However, non-canyon stations overall showed a higher diversity in comparison to canyon stations. A notable peak in diversity is observed in canyon areas in the 401-500 m depth zone. Species richness followed an opposing pattern, as it decreased with depth and was consistently higher in canyon areas. These results align with the well-defined influence of depth-related variables on the distribution of taxonomic groups and the substrate available, at various scales. The eutrophic characteristic of the Benguela region may have attributed to the insignificant diversity differences between canyon and non-canyon stations. To assess the benthic species structure in canyon and non-canyon areas, we converted the 108 benthic species into a gamma+ matrix. We then modelled the biological response to predictor variables (substrate and depth). Although the canyon and non-canyon areas have an overlapping species composition, the main effects (canyon vs. non-canyon, depth, and substrate) showed significant

differences. Thirteen species were characteristic of canyon areas, whilst only three distinguished non-canyon areas. The region has a long history of anthropogenic activities, so the observed benthic profiles may already be altered. The current study therefore provides the first detailed taxonomic description and analysis of benthic species profiles in the Cape Canyon, and advances important baseline information necessary for understanding the ecological importance of the Cape Canyon.

KEYWORDS

biodiversity, deep-sea, depth, substrate, species profiles

1 Introduction

Submarine canyons are complex systems that host a range of substrate types and habitats, from mud banks to exposed rocky walls (De Leo et al., 2014; Fernandez-Arcaya et al., 2017). Additional factors such as the unique oceanographic signatures (Allen and Durrieu De Madron, 2009; Quattrini et al., 2015), sedimentology processes and rates, nutrient input (influenced by proximity to river outflows, among other features) (Duros et al., 2014; Lo Iacono et al., 2014; Hawie et al., 2019), morphology, bathymetry, and depth-associated hydrographic variables collectively contribute to submarine canyon heterogeneity (Duffy et al., 2014). The rich variety of habitats and environmental conditions found in canyons may contribute substantially to benthic biodiversity (De Leo et al., 2010; Di Bella et al., 2017; Bianchelli and Danovaro, 2019; Pierdomenico et al., 2019; Bertolino et al., 2019).

Patterns of benthic biodiversity in submarine canyons in the Northern Hemisphere are well documented. These studies showed that relationships between benthic biodiversity and environmental variables in submarine canyons differ among benthic taxonomic groups at various scales. For example, Quattrini et al. (2015) showed the varying degrees to which three taxonomic groups (demersal fish, decapod crustaceans, and corals) were influenced by broad-scale habitat features (canyons, seamounts, seeps, etc.) in the North Atlantic. They found that the species richness of demersal fish and decapod crustaceans declined with depth, and the turnover of species of all three groups was greatest on lower to middle slope areas where there were major boundaries between water masses. A similar result of megafaunal communities being influenced by depth-related variables, where species richness steadily increased with depth between 200-700 m before declining at deeper depths, was reported by a study on five Pacific canyons (Duffy et al., 2014). Statistical differences in benthic community structure between canyon and surrounding areas and across various substrata, were not observed (Duffy et al., 2014). Compelling evidence in their study, however, suggested that the slope of the seafloor influences species composition (Duffy et al., 2014). In the Hawaiian archipelago, submarine features in the Pacific showed that megafaunal communities in canyons differ significantly from those in nearby slope habitats at all depths (Vetter et al., 2010). An increased species richness and diversity trend was generally observed within the canyons. Notably, canyon species diversity and richness patterns are by no means consistent or universal; the canyon size and morphology, bathymetry, local anthropogenic impacts, and oceanography are some of the factors that collectively influence biodiversity patterns.

Despite the recent increase in scientific interest in submarine canyons (Huvenne and Davies, 2013), to date, there have been only a few studies of canyon ecosystems in the Southern Hemisphere. This is particularly true around South Africa, where over 40 submarine canyons have been identified from low-resolution global bathymetric datasets and from sporadic higher resolution investigations. These include: two significant canyons on the western margin (Cape Canyon and Cape Point Valley); three (Sundays, Addo, and Rocks Canyon) off the southern margin, and many more off the eastern margin between East London and Sodwana Bay. Recent fine-scale regional work in the southwestern Cape identified 14 previously unknown submarine canyon systems off the western margin between the Cape Canyon and Cape Agulhas (Palan, 2017). Research to date has focused primarily on canyons in the eastern margin at depths of ca. 150 m, as these are more accessible on the narrow continental shelf and thus more easily sampled (Bang, 1968; Sink et al., 2006; Green and Uken, 2008; Wiles et al., 2013; Green, 2011), and are home to the rare coelacanth (Venter et al., 2000; Green et al., 2009). Comparatively little is known, however, about the Cape Canyon system on the western margin.

There have been studies of the geology (Simpson and Forder, 1968; Dingle, 1973; Wigley and Compton, 2006), oceanography (Shannon and Nelson, 1996; Lamont et al., 2014; Jarre et al., 2015; Lamont et al., 2015; Barlow et al., 2018; Lamont et al., 2018; Veitch et al., 2018; Kersaleí et al., 2019), fisheries (Shannon

et al., 2004; Shannon et al., 2010; Travers et al., 2010; Yemane et al., 2014; Mbatha et al., 2019), and vulnerable habitats (Sink et al., 2019) in the region, but little is known about benthic distributions (Atkinson et al., 2011; Lange, 2012; Karenyi et al., 2016; Sink et al., 2019). Deep-water (>200 m) benthic studies that focus on community structure are limited to investigations on the effects of trawling on benthic fauna at a large scale (i.e., from southern Namibia to Cape Town) (Atkinson et al., 2011), the use of demersal by-catch data to determine the distribution of soft-bottom macrofaunal assemblages (Lange, 2012), and defining unconsolidated shelf seascapes (Karenyi et al., 2016). Of interest are the epifaunal diversity patterns highlighted by Lange (2012), whereby the environmental conditions of the Benguela region (western margin) yielded distinctively lower species richness (but high biomass) in comparison to the Agulhas region (southern margin). Although there was no clear relationship between diversity patterns and depth-related environmental variables, along with sediment type (Lange, 2012), the highest number of species was recorded at 300-399 m and the lowest at 500-599 m.

Building on these Southern Benguela Upwelling regional studies is a conservation plan undertaken in 2011, which identified offshore priority conservation areas by collating the best available data at the time (Sink et al., 2011). Such a priority selection analysis developed numerical targets in consultation with stakeholders and produced nine planning scenarios, which ranged from seabed protection to pelagic biodiversity and considered industry activities. At the least cost to primary industry (e.g., fisheries and mining), the Cape Canyon head was identified as one of the areas which warrant protection. Thus, following the Operation Phakisa National Development Plan launched in 2014, research focused on the offshore conservation areas identified by Sink et al. (2011). Amongst these research plans was the three-year Cape Canyon project, which yielded datasets to support the declaration of the Cape Canyon Head as a Marine Protected Area (Department of Environmental Affairs, 2019).

Nonetheless, research focused on the Cape Canyon benthic data has not been carried out, apart from exploratory mining surveys within an area that overlaps with the canyon (see Wigley, 2004; Wigley and Compton, 2006). Here, we present the first detailed study of the benthic distributional patterns in the largest known submarine canyon in South African territory, which lies in the Benguela upwelling system – the Cape Canyon (Figure 1). Our overarching aim was to compare and characterize invertebrate benthic patterns in relation to

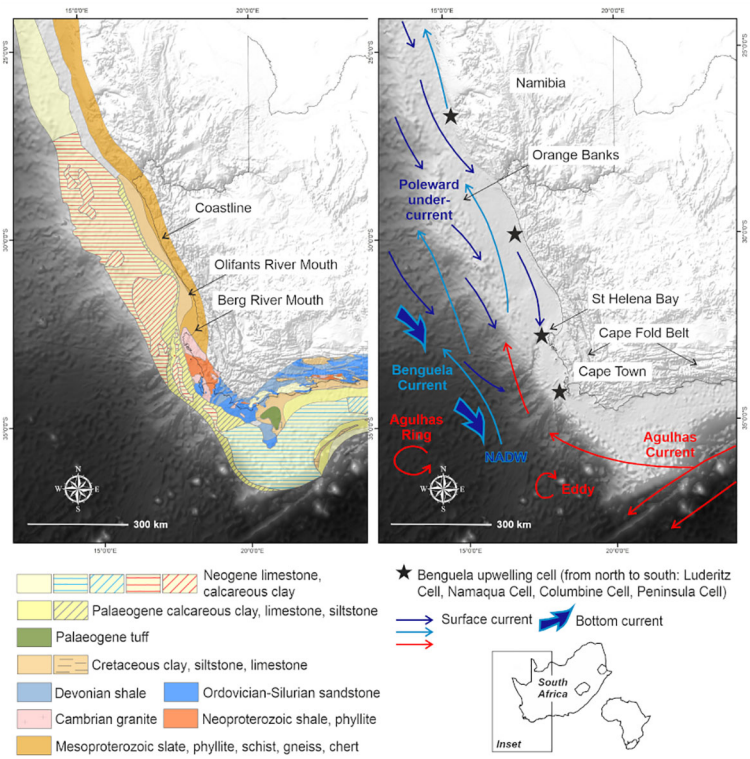

FIGURE 1
Map showing the South African western margin, in relation to the African continent, with underlying geology and circulation patterns of the Benguela region.

oceanographic and bathymetric features within Cape Canyon and adjacent areas. More specifically, we compared the diversity gradients and structure of benthic distribution between canyon and non-canyon habitats and examined how these patterns change with varying environmental conditions (depth, bottom temperature, and dissolved oxygen), and among different lithological classes of substrate.

2 Materials and methods

2.1 Regional settings

This study focuses on the passive western margin of South Africa, in the Benguela upwelling system (Figure 1). The western margin of South Africa is considered unusual because it has two shelf breaks. It is broad and relatively deep and descends into the Cape Basin in the Southeast Atlantic from a depth of ~500 m (Du Plessis et al., 1972; Birch, 1975). The outer shelf between Cape Town and the Orange Banks is characterized by a rocky, erosional surface composed of seaward-dipping Neogene-Paleogene carbonate hardgrounds with patchy Quaternary sand cover less than 0.5 m thick (Birch, 1975; Rogers, 1977; Rogers and Bremner, 1991; Compton et al., 2002). The narrow and rugged continental shelf and steep continental slope south of St Helena Bay reflect the buoyant continental margin above the Columbine–Agulhas Arch (Dingle, 1979; Dingle et al., 1983). As highlighted by Wigley and Compton (2006), the seaward extent of the inner-shelf platform is marked by a steep edge. Furthermore, the knick point of the inner shelf occurs at water depths of 90 to 150 m and is partially filled by the Holocene mudbelt (Birch, 1975). Seaward-dipping Cretaceous sediments, with a thin Quaternary veneer occur in the middle shelf region (Figure 1).

The Benguela region is characterized by seasonal wind-driven upwelling (Lamont et al., 2018), which transports cold nutrient-rich waters to the surface (Shannon and Nelson, 1996), increasing primary production (Lamont et al., 2014; Barlow et al., 2018). These nearshore upwelling pathways are further complemented by shelf-edge jet currents and highly variable offshore mesoscale eddies (Veitch et al., 2017; Kersaleí et al., 2019). Spatially variable and persistent low-oxygen cells have also been reported in nearshore regions off the St Helena Bay escarpment (Jarre et al., 2015; Lamont et al., 2015) (Figure 1).

The behavior of water masses in the vicinity is influenced by the local bathymetry, which is characterized by a relatively broad continental shelf where the Cape Canyon incises and gradually extends offshore (de Wet, 2013) (Supplementary: Image 1). The Cape Canyon cuts obliquely across the narrow continental shelf south of St Helena Bay (Figure 1), and has a longitudinal extent of at least 200 km. This feature, being the most profound in the western continental shelf, incises up to the middle shelf. The head of the Cape Canyon lies immediately seaward of the southernmost extent of the Holocene mudbelt and the Columbine upwelling cell, centered over St Helena Bay (Figure 1). It forms a well-developed trench on the continental shelf, which is 100 m deep and 4 km wide, gradually extending to depths of up to 3600 m and becoming progressively broader. Two perennial rivers, the Berg and Olifants, have catchments that extend from the Cape Fold Belt Mountains to the coastal plain and discharge into St Helena Bay (Figure 1).

2.2 Sampling and data sources

During 2016-2018, the *RS Algoa* was used to conduct multidisciplinary cruises across the Southern Benguela region. Bathymetry and other environmental data, together with epibenthic samples, were collected to characterize the distribution of benthic assemblages within the Cape Canyon and adjacent areas.

2.2.1 Bathymetry

A SIMRAD EK60 system was used to collect split-beam bathymetric data during continuous steaming (at a constant speed of 6 knots) along regularly spaced (4 km) transects, which were orientated perpendicular to the coast and extended 65 km offshore. The processing of the collected split-beam echo-sounder data followed that outlined in de Wet (2013) but differs in that only the data from three transducers (120 kHz, 200 kHz and 38 kHz) were averaged, and the vessel's draught was accounted for in the ES70 software before surveying the area. Prior to analysis, geographic coordinates were converted to decimal degrees, deleting entries with values of zero, and converting positive values of depth to negative values (for easier expression in the software). A grid was then created from a total of 399413 data points through a kriging method, using Golden Software Surfer. A blanking file was created to crop the area surveyed. After blanking, the resulting grid output was filtered using a low pass filter for better visualization. The bathymetric data complemented the existing topographic knowledge on the Cape Canyon (Supplementary: Image 2) and was also used to classify station data as being located either inside or outside of the canyon for subsequent analyses.

de Wet (2013) produced an updated gridded bathymetric map of the South African seafloor, assimilating available existing datasets. In this dataset, details of the inner shelf's rocky platform were clearer and structural features can be resolved (Supplementary: Image 2B, D, right representing de Wet and Compton, 2021). In our dataset, these details were less apparent, but the terraced transition separating the inner and mid continental shelf was more apparent (Supplementary: Image 2A, C, left representing data collected through this project). While our data resolution is lower in deeper water due to the limitations of the instruments used, the inner-canyon structures are much clearer.

2.2.2 Benthic sampling and processing

Benthic epi-fauna was collected during each cruise. A stratified random design was followed, whereby stations were identified based on depth zones and whether they were located within or outside of the canyon. However, due to challenging sampling conditions, these efforts yielded an unbalanced design with 12 stations representing canyon areas and 13 non-canyon stations. Despite the unbalanced design, these 25 stations were all located in the 201-1000 m depth range and provided a total of 581 species records, significantly increasing the existing benthic species observations in the region (Supplementary: Data Sheet 1, meta-data) (Figure 2).

All epi-benthic sampling was conducted using a customized dredge with a mouth opening of 30 cm × 100 cm and mesh-lining of 1 cm^2. To standardize sampling effort, dredge transects had a bottom-time of 15 to 20 minutes and constant speed of 0.5 knots. Specimens were identified to the lowest possible taxonomic level using the recently published offshore field guide (Atkinson and Sink, 2018) and expert opinion. When identification was not possible (e.g., polychaetes, sponges, ascidians, etc.) organisms were separated according to broad morpho-types. Thus, a total of 180 taxonomically distinct specimens were identified (Supplementary: Data Sheet 1, sample collection). Samples were fixed and preserved in molecular-graded ethanol for long-term storage at the National Department of Forestry, Fisheries, and Environment (DFFE). The associated higher taxonomic classifications of the 108 species/morpho-types were extracted from the World Register of Marine Species batch match online function (Supplementary: Data Sheet 1, taxonomic attributes) (WoRMS Editorial Board, 2022).

2.2.3 Other environmental data

During each cruise, profiles of temperature, salinity, and dissolved oxygen were collected throughout the water column using multiple SBE911 Conductivity-Temperature-Depth (CTD) systems. In 2016, the CTD grid focused on the canyon head and surrounding areas (48 stations). This grid was extended further south during the 2017 survey, yielding data from 131 stations, while in 2018 additional transects (191 stations in total) were added in the northern part of the region, to better capture oceanographic conditions in the upper reaches of the canyon. All CTD casts were taken from the surface to within 5–10 m of the seafloor. Dissolved oxygen concentrations (DO) of discrete seawater samples from selected depths were determined by Winkler titrations and used to calibrate the dissolved oxygen profiles. For this study, we used only bottom temperature, salinity, and dissolved oxygen measurements, which were averaged across the cruises at overlapping stations. The averaged oceanographic bottom data (Supplementary: Data Sheet 2) and bathymetry were used as environmental variables of interest for subsequent analyses.

The most recent geological spatial layer, which characterizes substrate types, was also considered. There are two published regional classifications for this area. First, Dingle and Siesser

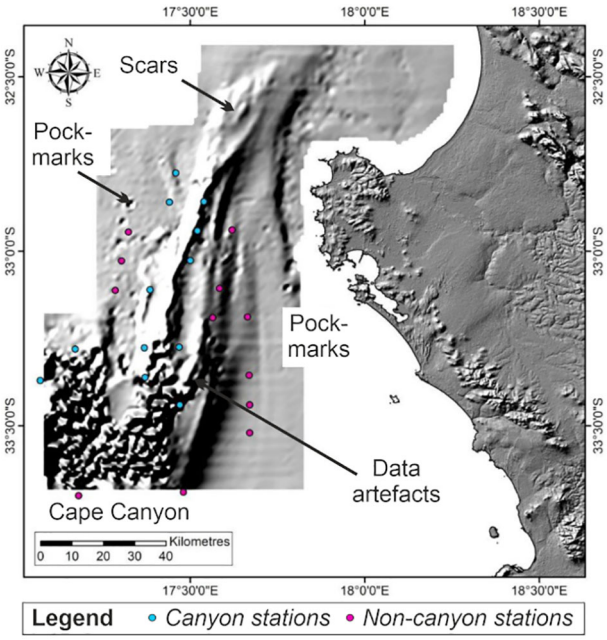

FIGURE 2
Map showing canyon vs. non-canyon stations overlaid onto bathymetry data (grey shading) collected through this project.

(1975) produced a regional-scale geological map of the coastal and seafloor areas and focused on the basement geology. These lithologies are mantled with unconsolidated sediment which was first published as a regional sediment map (Dingle et al., 1987) and is the basis of the National Biodiversity Assessment (Sink et al., 2019). Their recent assessment highlighted the difficulties in classifying canyon substrate types with their nested-hierarchical methodology (Sink et., 2019). Thus, for the purposes of correlating benthic habitats to substrate, we applied the geological seafloor classification data, i.e., Dingle's (1975) lithology groups, as substrates.

To match biotic data to environmental data, the starting points of each of the 25 dredge stations were related to the nearest coverage point of each of the three spatial environmental datasets (temperature, salinity, DO, bathymetry, and substrate) by applying the Near Function in ArcGis 10.6.1. The full resulting dataset therefore included biotic data (occurrences of 180 taxa) and associated physical and hydrographic variables, including substrate type, bottom averaged temperature, bottom averaged DO, depth, and the canyon (C)/non-canyon (NC) classification, at each of the 25 stations (Figure 2). Two substrate classes characterized the 25 stations, and these include a: CCSL =Calcareous clay, siltstone, limestone; and **LCC** = Limestone, Calcareous Clay. The order of sediment type within these substrate groups represents the proportion of each within a combination (Supplementary: Data Sheet 1, associated physical variables).

2.2.4 Sampling bias and assumptions

This study was based on qualitative biological (presence-absence) data, which was collected using an unbalanced sampling strategy and lacks rigorous terrain seabed features (e.g., slope aspect, micro-habitat). Although attempts to standardize sampling effort were prioritized (i.e., 15-20 min bottom time and speed 0.5 knots), weather conditions and seabed topography were irregular and led to sampling biases. For example, an estimated distance of 200 to 300 meters was anticipated for each dredge operation but some deployments covered a third of the total anticipated distance (i.e., stations on canyon margin). In addition, underlying geology (lithology classes) was used as a proxy for substrate type and such delineations may not accurately represent the current seafloor characteristics. Whilst these lithology classes are the best available sediment attribute data in our area of interest, the inability of epibenthic dredges to provide point specific specimen and substrate information exacerbates the existing sampling biases. CTD casts did not require such consideration, as these deployments are point specific and stations were represented by 5 x 5 nautical mile (nmi) grid. Our study therefore assumes that a dredge operation within the 5 x 5 nmi is associated to the CTD cast within that radius.

2.3 Data analysis

2.3.1. Diversity measures in canyon and non-canyon sites across substrate and depth ranges

Data on the presence and absence of 108 benthic taxa at 25 stations (Supplementary: Data Sheet 1, presence-absence matrix) were analyzed in PRIMER v7 with the PERMANOVA+ add-on package (Anderson et al., 2008; Clarke et al., 2014). We firstly calculated various measures of diversity for each station, including species richness (S) and average taxonomic distinctiveness (delta+) to examine whether diversity gradients existed within the substrate type and depth groups represented in the canyon vs. non-canyon stations. The associated dredge data was grouped according to 100 m incremental zones. These depth zones, along with the canyon vs. non-canyon and substrate classifications (see section 2.2.1. and 2.2.3.; respectively) were added as factors to the presence-absence matrix. We then tested for significant differences across the substrate types and depth groups (within the canyon vs. non-canyon comparison) by converting the diversity measures into a fourth-rooted Euclidean distance matrix. A two-way PERMANOVA (Anderson, 2001) on each fixed factor within the canyon vs. non-canyon comparison was used to test the response of diversity measures to substrate type and depth zone.

To further investigate the factors that influenced diversity we aggregated the presence-absence matrix to family level then summed it according to the combined factors. We thereafter computed a group average SIMPROF cluster analysis on the square rooted Bray-Curtis resemblance matrix of the aggregated and summed output. A shaded plot was then superimposed with SIMPROF hierarchical clusters and showed the distribution of phyla across the groups in question.

2.3.2 Relating epibenthic benthic species profiles to environmental variables

Following the above exploratory analysis, we quantified the taxonomic dissimilarity of each pair of stations, using the "Gamma+" measure (Clarke et al., 2006). The Gamma+ measure uses taxonomic information (Supplementary: Data Sheet 1, taxonomic attributes) on the species common to both samples. For species found only in one sample, a contribution to the dissimilarity is made according to its closest relative in the other sample. Two samples that share the same and/or closely related species have dissimilarity near zero, while two samples with species that share only distantly related species have a dissimilarity near one.

The matrix of among-sample Gamma+ dissimilarities was visualized with a non-metric Multi-Dimensional Scaling (nMDS) plot. We analyzed the matrix as a multivariate response using PERMANOVA to test our hypotheses regarding differences in the taxonomic composition of benthic patterns (Anderson, 2001). To achieve this, we modelled taxonomic composition according to a suite of predictor

variables relating to depth, bottom temperature, bottom dissolved oxygen, and substrate type. The predictor variables were not highly skewed, so no transformation was applied. Bottom temperature and bottom dissolved oxygen were both highly correlated with depth (Pearson measure between -0.7 to 0.7), so we used depth as a predictor variable. We used a three-factor PERMANOVA to test for effects of the canyon (inside vs. outside the canyon), substrate, and depth on taxonomic composition of benthic species. All factors were treated as fixed. A SIMPER analysis showed species characteristics of canyon vs. non-canyon groups.

3 Results

3.1 Diversity measures in canyon and non-canyon sites across substrate and depth groups

Overall, the two diversity measures (species richness S and average taxonomic distinctiveness Delta+) had a skewed distribution within groups, in which non-canyon and canyon stations represented both of these substrate classes (Figures 3, 4) across depth classes in range of 201-1000 m (Figures 5, 6). The

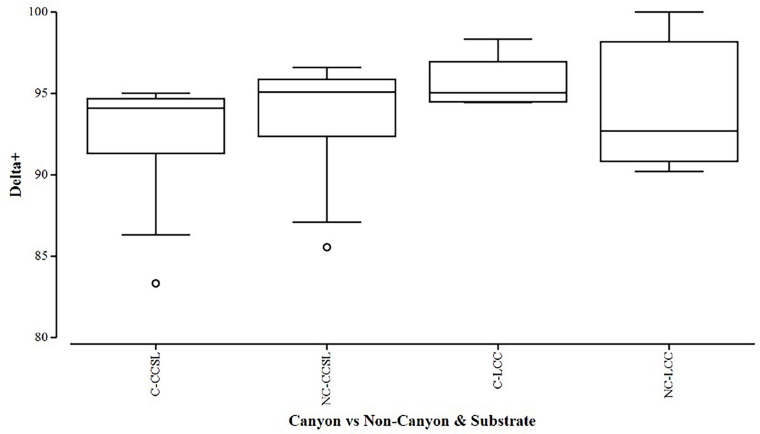

FIGURE 3
Box plot showing the average taxonomic distinctiveness represented within each canyon (C) vs. non-canyon (NC) substrate type group: where CCSL represents Calcareous clay, siltstone, limestone; and LCC, Limestone, Calcareous Clay.

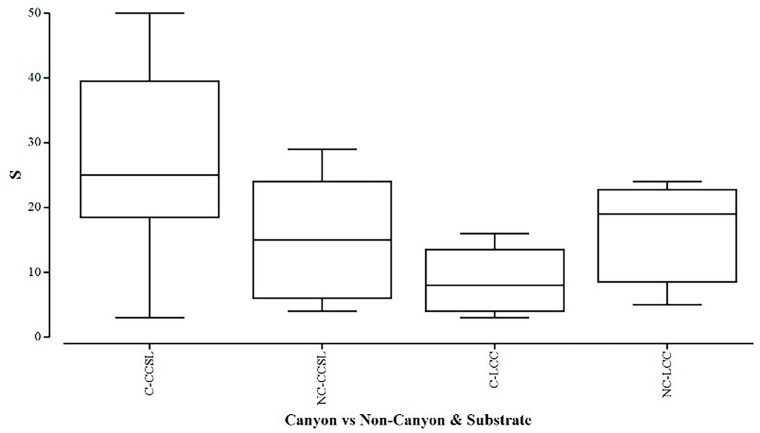

FIGURE 4
Box plot showing the species richness represented within each canyon (C) vs. non-canyon (NC) substrate type group: where CCSL, represents Calcareous clay, siltstone, limestone; and LCC, Limestone, Calcareous Clay.

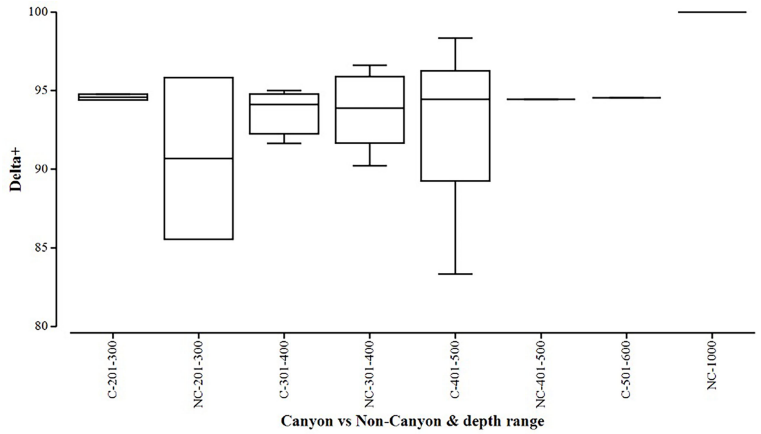

FIGURE 5
Box plot showing average taxonomic distinctiveness (denoted by delta+) represented within each canyon (C) vs. non-canyon (NC) depth class within the range of 201-1000 m.

highest average taxonomic distinctness (denoted by delta +) was recorded at the calcareous clay, siltstone (CCSL) stations; for which majority of the canyon CCSL stations fell within the lower quartile (Figure 3). Outliers in both the canyon and non-canyon CCSL groups were evident. Variability in species richness also peaked in CCSL stations, whereby the non-canyon CCSL areas fell in the lower quartile (Figure 4). The PERMANOVA showed significant differences in the diversity measures between the substrate groups (DF=1, pseudo-F= 7.249, P(Perm)= 0.009), but none for the canyon vs. non-canyon groups (DF=1, pseudo-F= 1.229, P(Perm)= 0.276) (Table 1).

When comparing diversity measures between canyon and non-canyon stations across various depth classes (Figures 5, 6), diversity was highly variable in the 201-300 m depth range in which the canyon stations are represented in the higher quantile. Of note, is the consistently higher diversity in non-canyon sites up to the 401-500 m depth range. In this depth range (401-500 m) the canyon diversity measure peaks and is highly variable (Figure 5). Species richness patterns show an opposing trend, where richness was highest in canyon stations with increasing depth (Figure 6). The most variable richness measure was observed at the 201-300 m depth, in which canyon and non-canyon sites did not overlap. An outlier was evident at the 301-400 m non-canyon stations. The two-way PERMANOVA showed significant differences in diversity when comparing the depth ranges (DF=5, pseudo-F= 5.927, P(Perm)= 0.008) (Table 2).

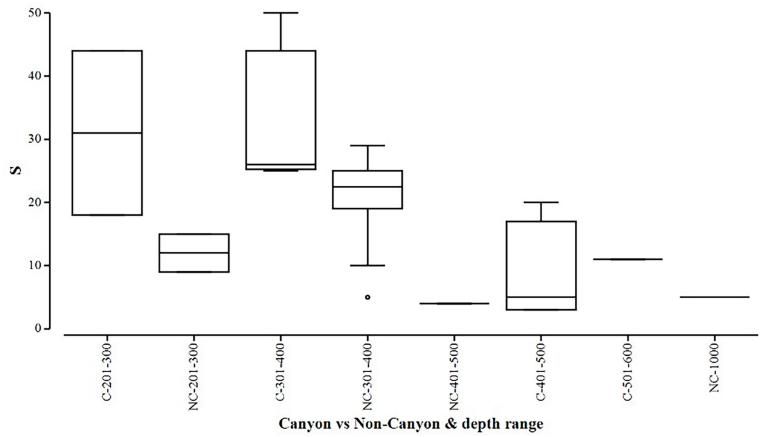

FIGURE 6
Box plot showing species richness (denoted by S) represented within each canyon (C) vs. non-canyon (NC) depth class within the range of 201-1000 m.

TABLE 1 PERMANOVA, Type1 (sequential) fixed effects on a permutation of residuals under a reduced model (9999 number of permutations), results of diversity measures in substrate groups represented in the canyon and non-canyon stations - where * shows significant values.

Source	df	SS	MS	Pseudo-*f*	P (perm)
Canyon effect	1	1.556	1.556	1.229	0.277
Substrate	1	9.175	9.175	7.249	0.009*
Canyon effect x Substrate	2	1.474	1.474	1.164	0.284
Residual	21	26.577	2626.4		
Total	24	38.782			

The aggregated data confirmed that 11 phyla were unevenly distributed in the study area, three of which dominated (Arthropoda, Mollusca, and Echinodermata). Phyla additionally followed a depth gradient in which molluscs were abundant at 200-400 m, whilst echinoderms dominated the 401-500m depth range (Figure 7). A high number of arthropods were observed at 300-401 m, with depths deeper than 501 m showing a low number of species (less than 4) representing the three dominating phyla. SIMPROF results, superimposed on the shaded plot, gave two major distinctive groups at the various levels of similarity (Figure 7). The first cluster comprised of CCSL areas at 201-400 m, followed by larger group comprising of overlapping taxa across the two substrate types at a 401-1000m range. Interestingly, benthic profiles at 401-500 m formed a distinctive cluster irrespective of different substrates (Figure 7).

3.2 Epibenthic patterns and potential environmental drivers

The non-metric MDS plot of the gamma+ resemblance matrix showed a separation between canyon and non-canyon stations, though a relatively high number of these are rather similar in species composition (Figure 8). Significant differences between the main effects were confirmed by the three-factor PERMANOVA, with canyon vs. non-canyon, depth, and substrate as fixed factors. These results indicated that the interaction of substrate and depth (DF=1, pseudo-F= 2.63, P (Perm)= 0.010), along with that of canyon vs. non-canyon and depth (DF=3, pseudo-F= 2.45, P(Perm)= 0.004), significantly contributed to the differences observed in the benthic patterns. Furthermore, all the main effects- canyon vs. non-canyon (DF=1, pseudo-F= 3.03, P(Perm)= 0.005), substrate (DF=1, pseudo-F= 2.99, P(Perm)= 0.006) and depth (DF=5, pseudo-F= 2.32, P(Perm)= 0.003) as individual factors significantly influenced benthic species profiles (Table 3, and Plate 1).

SIMPER results (Supplementary: Data Sheet 1, SIMPER results) confirmed that both the canyon and non-canyon stations had variable species within each category (an average similarity being 10% and 11%, respectively). Three brittle stars (*Ophiura (Ophiura) trimeni* Bell, 1905, *Ophiolycus dentatus* (Lyman, 1878), *Ophiothamnus remotus* Lyman, 1878) and one crab (*Dorhynchus thomsoni* C. W. Thomson, 1873) contributed the most (< 6%) to canyon stations; whilst one sea urchin (*Brissopsis lyrifera capensis* Mortensen, 1907) and two bivalves (*Lucinoma capensis* and *Limopsis*belcheri (Adams & Reeve, 1859)) were more dominant (> 12%) at non-canyon stations. When comparing the two groups, a higher number of species (13 species- *Pasiphaea* sp 1 Savigny, 1816, *Neopilumnoplax heterochir* (Studer, 1883), Hydrozoa sp 3 Owen, 1843, *Ophiothrix fragilis* (Abildgaard in O.F. Müller, 1789), *Hemiocnus insolens* (Théel, 1886), *Ophiactis carnea* Ljungman, 1867, *Parapontophilus gracilis* (Smith, 1882), Tanaididae sp Nobili, 1906, M*iersiograpsus kingsleyi* (Miers in Tizard et al., 1885), *Onchoporella bombycina* Bock, 2022, Kraussinidae sp Dall, 1870, Sipuncula sp 2 Stephen, 1965, *Parapagurus bouvieri* Stebbing, 1910) occurred exclusively at canyon stations, whilst only three species (*Virgularia* sp 1 Lamarck, 1816, *Asychis* sp 1 Kinberg, 1867, *Mursia cristata* H. Milne Edwards, 1834–1940) characterized non-canyon stations. Overall, species observed in both canyon and non-canyon areas exhibited varying numbers of feeding techniques, in which the non-canyon areas had a higher feeding method to species ratio (canyon = 0.23 vs. non-canyon areas = 0.66).

TABLE 2 PERMANOVA, Type1 (sequential) fixed effects on a permutation of residuals under a reduced model (9999 number of permutations), results of diversity measures in depth zones represented in the canyon and non-canyon stations - where * shows significant values.

Source	df	SS	MS	Pseudo-*f*	P (perm)
Canyon effect	1	1.556	1.556	1.229	0.167
Depth	5	22.843	4.569	7.249	0.007*
Canyon effect x Depth	3	2.822	0.940	1.164	0.332
Residual	15	11.562	0.770		
Total	24	38.782			

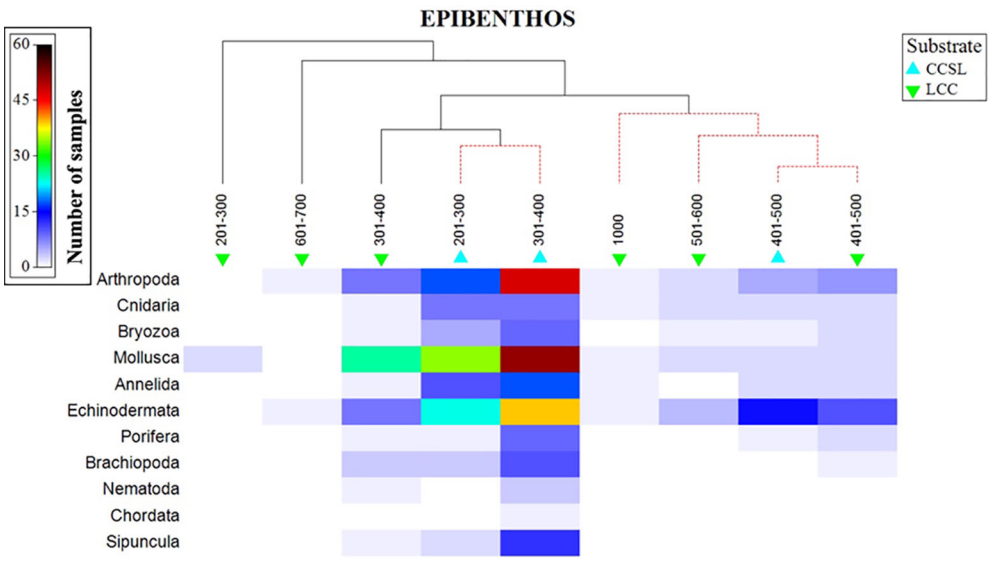

FIGURE 7
Shaded plot, superimposed with a SIMPROF cluster of the aggregated and summed Bray-Curtis resemblance matrix (square-rooted), showing the phyla represented in the depth and substrate groups.

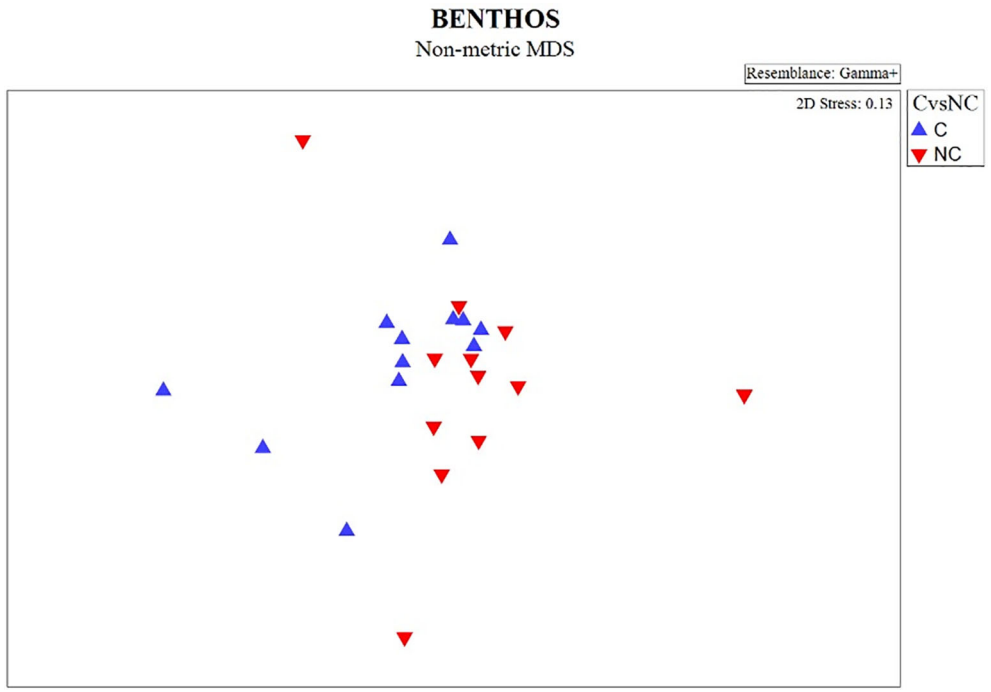

FIGURE 8
nMDS plot showing the gamma+ resemblance of benthic composition between canyon **(C)** and non-canyon **(NC)** stations.

TABLE 3 PERMANOVA, Type1 (sequential) fixed effects on a permutation of residuals under a reduced model (9999 number of permutations), results of differences in benthic assemblages in canyon (canyon vs. non-canyon), substrate, and depth groups - where * shows significant values.

Source	df	SS	MS	Pseudo-*f*	P (perm)
Canyon (C)	1	4939.1	4939.1	3.031	0.0051*
Substrate (S)	1	4882.8	4882.8	2.997	0.0059*
Depth (D)	5	18931	3786.1	2.324	0.0003*
C x S	1	2072.9	2072.9	1.272	0.2650
C x D	3	11957	3985.7	2.446	0.0039*
S x D	1	4294.4	4294.4	2.6354	0.0101*
C x S x D	0	0		NO TEST	
Residual	12	19554	1629.5		
Total	24	66631			

Suspension feeders were represented in both canyon vs. non-canyon areas. In addition, mobile species exhibiting deposit feeding and scavenger techniques (*N. heterochir, P. bouvieri)* were observed in canyon areas, whilst a detritus feeder/predator/scavenger combination (*M. cristata*) was noted in non-canyon areas.

4 Discussion

Although our results showed no significant diversity differences between canyon and the surrounding non-canyon areas, significant differences (p-value > 0.04) between the substrate types and depth zones were clearly observed. The absence of a significant difference between canyon and non-canyon stations, is likely attributed to the homogenous environment observed in both areas, in which identical substrate classes were recorded. Additionally, the overall upwelling characteristics of the Benguela region are known to generally harbor low diversity, but high biomass species profiles (Lange, 2012). Thus, even though large-scale spatio-temporal variations in upwelling patterns exist (Lamont et al., 2018), the fact that upwelling takes place along and across the entire shelf results in more or less uniform environmental conditions in the bottom layers, especially in the mid-shelf to offshore regions. This may limit spatial variability in the benthos unless different substrates are present. The unbalanced dataset provided limited replicates for each factor (i.e., substrate within depth classes), which may also have also contributed to the lack of the canyon effect. Whilst the samples collected at a depth range of 401-500 m clustered together irrespective of the different substrate types, the distinctively different diversity profiles (both species richness and average taxonomic distinctiveness) between substrate class are in line with the well-established theory that sediment characteristics influence species patterns (Levin et al., 2001; Ramirez-Llodra et al., 2010; Lins et al., 2016). Thus, despite the two classes being predominantly unconsolidated, there is variability in the grain size of classes. Using lithology classes as a substrate proxy should nonetheless also be considered in this pattern and therefore better substrate classifications may yield different results.

In terms of depth gradients, the increase of species richness (S) in the 200-400 m depth range agrees with previous local studies (Lange, 2012) that observed highest richness at depths of 300-399 m. Our results, however, contrast with the Duffy et al. (2014) submarine canyon observations of species richness steadily increasing with depth between 200-700 m. This may be an artifact of the low number of samples (n < 11) represented in the 501-700 m range, as species richness is dependent on sampling effort (Clarke and Warwick, 1998; 1999; Bevilacqua et al., 2021). The average taxonomic distinctiveness index (delta +), on the other hand, showed a fluctuation and opposing trend, whereby the lowest measure was identified at 201-300 m (the second most speciose depth) and the highest at 601-1000 m (least species richness). In other words, the 200-300 m depth range encompasses a higher number of distantly related species across six taxonomic families and can be considered as highly diverse as opposed to the 601-1000 m zone which constitutes five families with one species recorded. The properties of average taxonomic distinctiveness are unbiased by sampling effort (Clarke and Warwick, 1998; 1999) and are therefore demonstrated by this inverse relationship between the delta+ and S measures. Irrespective, the observed gradual decrease in diversity at 401-1000 m in our results agrees with the previous accounts of depth-dependent diversity patterns (Hernández-Ávila et al., 2018; Levin et al., 2001). Such a pattern is linked to food availability, amongst other variables, and the change in depth-related parameters (e.g., temperature) in deeper environments (Howell et al., 2002; Ramirez-Llodra et al., 2010) which may in turn influence other processes (e.g., resource partitioning) (Levin et al., 2001).

Despite the comparatively insignificant differences in diversity measures between canyon vs. non-canyon areas, a clear variation in the benthic species profiles was observed. Canyon areas were defined by higher species richness and diversity as compared to non-canyon areas. Even though

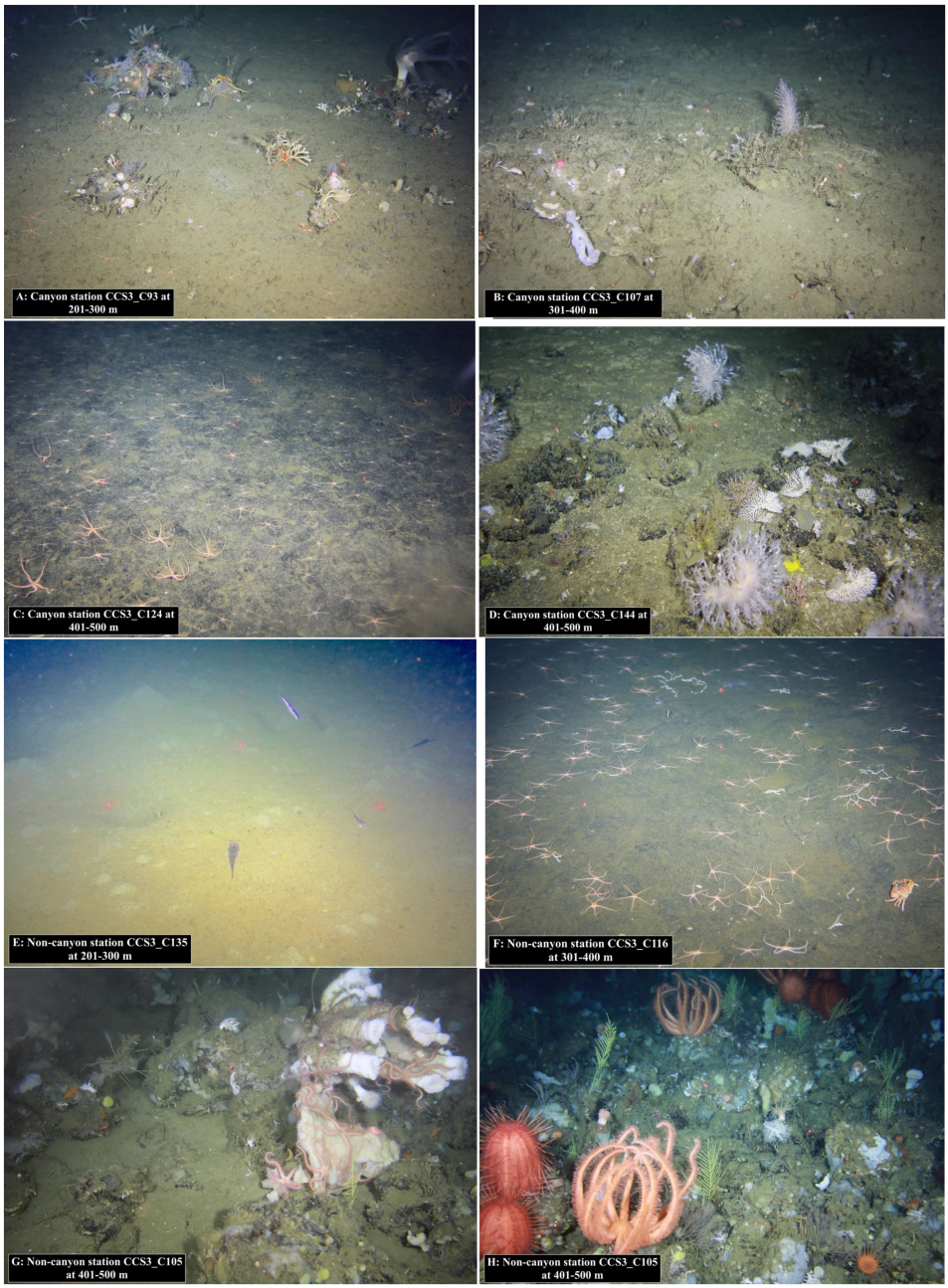

PLATE 1
Examples of canyon **(A–D)** and non-canyon **(E–H)** habitats observed at a 201-500 m depth range.

sampling biases occurred, the use of gamma+ as the basis of testing multivariate responses to predictor variables accounted for this by considering taxonomic relationships of species at all levels (Clarke et al., 2006; Bevilacqua et al., 2021). Nonetheless, high species variability at both the canyon and non-canyon stations was documented in which taxonomic groups discriminating the comparison were present. These distinguishing species represent overlapping and diverse feeding modes, with three feeding strategies being exhibited by the 13 species characteristic of canyon areas, whilst the three non-canyon species deployed only two feeding strategies. The latter consequently represents a higher feeding method to species ratio. It is however worth noting that the mode categorizations were adopted from a range of sources (MacDonald et al., 2010; Demopoulos et al., 2017; Puccinelli et al., 2018; O'Hara, pers comm; Marine Species Traits editorial

board, 2022) which may not be a true reflection of local feeding patterns. Nonetheless, converging presence of suspension feeders noted in both canyon (ophiuroids, holothuroids, and bryozoans) and non-canyon stations (one octocoral and a polychaete) may be driven by the overall upwelling conditions of the Benguela region. An even number of suspension feeders were observed in both canyon and non-canyon areas, thereby further demonstrating the masking effect of the wide-spread eutrophic characteristic of the region.

In addition, the overlapping presence of mobile scavengers in the study domain may be a result of the dynamic natural environmental regimes driving continuous sediment movement (e.g., upwelling/downwelling processes and sedimentary funneling). Furthermore, anthropogenic activities such as demersal trawling have a historical footprint that dates to the 19th century. However, it was only in the 1921 that the commercial offshore enterprise kicked off (Sink et al., 2012). Such impacts, alongside offshore diamond mining and petroleum activities, within the Cape Canyon vicinity (Atkinson et al, 2011; Sink et al., 2019), may also be influencing the feeding behavior and biological distribution patterns. However, the lack of benthic species data prior to the onset of trawling makes it impossible to determine this with any certainty. In essence, the correlation between environmental variation and biota is difficult to measure in the presence of other human-induced activities. Apart from these superimposed non-linear relationships, the benthic patterns are a result of a longer time scale which may not necessarily be reflected in the oceanographic bottom profiles averaged over 3 years. Irrespective, substrate type and depth collectively underpin the heterogeneity of the study area. It therefore comes as no surprise that benthic assemblages have responded to these predictor variables (in addition to the canyon effect). The significant canyon-depth along with the depth-substrate interaction results complement the findings of Mello-Rafter et al. (2021) who identified salinity, depth, and substrate to be environmental conditions that shaped submarine canyon benthic assemblages.

The work presented here therefore represents one of the first detailed studies documenting the benthic biology of the Cape Canyon, a feature extending 200 km offshore and reaching the abyss (~3 km deep), located within the Benguela upwelling system off the South African western margin. The study tested the hypothesis that significant differences in benthic diversity should be observed within submarine canyon ecosystems, as compared to the surrounding shelf habitats. Whereas the unbalanced and homogenous nature of the study area prevented significant diversity differences between canyon and non-canyon sites, we confirmed that different benthic patterns characterize the Cape Canyon compared to the surrounding shelf areas, for which depth and substrate type were indeed significant predictors of benthic distributional patterns. In addition, we have demonstrated the importance of accounting for taxonomic relationships when exploring diversity gradients. The application of taxonomic measures (e.g., average taxonomic distinctiveness and taxonomic dissimilarity matrix), that are independent of sampling biases, gave way to understanding taxonomic lineages in relation to biological profiles. Our analysis therefore principally serves as a baseline towards understanding the ecological function of the Cape Canyon in relation to its surrounding areas. We therefore recommend future quantitative studies to build on these findings and apply biodiversity frameworks which consider abundance and biomass indices. The refinement of substrate classifications is also of research gap that warrants attention.

Data availability statement

The original contributions presented in the study are included in the article/Supplementary Material. Further enquiries should follow the formal data request avenues, at data@ocean.gov.za, as per the South African Promotion of Access to Information Act.

Ethics statement

Ethical approval was not required for the collection of samples as per the section 83 of the Marine living resources Act, 1998 (ACT NO. 18 OF 1998) permit conditions highlighted in RES2016/DEA, RES2017/83-DEA, and RES2018/89-DEA.

Author contributions

ZF and TL conceptualized project and sampling design. ZF and HC processed the biological data and bathymetry data; respectively. TL validated oceanographic data. HC created all the maps. ZF and AS conducted the analysis and drafted the results and methodology section. ZF drafted the full version of manuscript. All authors contributed to the revision of the full manuscript and have approved submission to journal.

Funding

This was project funded by the Department of Environmental Affairs: DEA (now merged to Department of Forestry, Fisheries, and Environment) and the at-sea expeditions were supported under the Operation Phakisa Research surveys (cruise identification: ALG225 (March 2016); ALG236 (March 2017); ALG247 (March 2018).

Acknowledgments

We would like to thank Dr Sandra Brook (Florida State University: Coastal and Marine Lab) for her support and guidance in tow-camera sampling techniques. Prof Kerry Sink (SANBI) and Dr Lara Atkinson (SAEON) for expedition planning advice on the first survey in 2016. Prof Amanda Lombard (Nelson Mandela University) and Dr Lauren Williams (Department of Fisheries, Forestry, and Environment) are recognized for the ArcGIS technical assistance. The at-sea technical support provided by Mr Marcel van den Berg, Mr Mfundo Lombi, Mr Mbulelo Makhetha, Mr Gavin Tutt, Mr Gavin Louw, Mr Leon Jacobs, Mr Baxolele Mdokwana, and Mr Laurenne Snyders (Department of Forestry, Fisheries and Environment), all of which are co-authors for data analyzed herein, was instrumental throughout the project. This three-year multi-disciplinary research expedition, which forms the basis of this study, would have not been possible without the African Marine Solutions crew members onboard the *R/V Algoa* and all cruise participants. Taxonomic inputs and species associated knowledge was provided by Dr David Herbert (Department of Natural Sciences, National Museum Wales), Prof Charles Griffiths (University of Cape Town), Dr Christopher Mah (Department of Invertebrate Zoology, Smithsonian Institution), Dr Timothy O'Hara (Museum Victoria Museum: Australia), Dr Jennifer Olbers (WildTrust), Ms Robyn Payne (Anchor Environmental), Dr Jannes Landschoff (Sea Change), and Mr Dylan Clark (Research and Exhibitions Department, Iziko South African Museum), and therefore authorship of the associated biological data is granted. Dr Carl Palmer (Alliance of Collaboration in Climate and Earth System Science), Dr Jeroen Ingels (Florida State University: Coastal and Marine Lab), and Prof Marti Anderson (PRIMER-e. Quest Research Limited) are acknowledged for proof-reading earlier manuscript drafts. Mr Carlos Fonseca (OceanX) is thanked for the thought provoking conversations, in the early days of drafting this manuscript. The reviewers are also thanked for their input, which has improved the overall manuscript.

Conflict of interest

Dr. AS was employed by PRIMER-e. Quest Research Limited during the initial drafting of this manuscript.

The remaining authors declare that the research was conducted in the absence of any commercial or financial relationships that could be construed as a potential conflict of interest.

Publisher's note

Supplementary material

The Supplementary Material for this article can be found online at: https://www.frontiersin.org/articles/10.3389/fmars.2022.1025113/full#supplementary-material

SUPPLEMENTARY FIGURE 1
Plot showing the bottom temperature (°C) gradient in relation to the Cape Canyon, where 100 m isobaths distinguish the canyon from surrounding areas. Dataset is representative of the averaged bottom temperature measured on the 2016, 2017, and 2018 surveys.

SUPPLEMENTARY FIGURE :2
Comparison between the **(A, C).** Gridded split-beam bathymetric data collected for this study and **(B, D).** de Wet (2013) gridded regional bathymetry. **(A)** Gridded using the Kriging statistical method, with a node spacing of 0.33 decimal degrees. **(C)** Frame A. close-up of the Cape Canyon and surrounding shelf areas. **(B)** de Wet (2013) bathymetry clipped to the same blanking file used on the Cape Canyon dataset. **(D)** Frame **(B)**. close-up of the Cape Canyon and surrounding shelf area.

References

Adams, A., and Reeve, L. A.. (1848–1850) Mollusca. *The zoology of the voyage of H.M.S. Samarang, under the command of Captain Sir Edward Belcher, C.B., F.R.A.S., F.G.S., during the years 1843-1846*A. Adams (x + 87 pp., 24 pls. [Pt. I. Preface to Mollusca (iii–x, by Adams only), 1–24, pls. 1–9, 1 November 1848; Pt. II, 25–44, pls. 10–17, 1 May 1850; Pt. III, Preface and plate explanations (i-xv), 45–87, pls. 18–24, 1 September 1850.].) Reeve & Benham, London, available online at https://www.biodiversitylibrary.org/page/39770936

Allen, S. E., and Durrieu De Madron, X. (2009). A review of the role of submarine canyons in deep-ocean exchange with the shelf. *Ocean Sci.* 5 (4), 607–620. doi: 10.5194/os-5-607-2009

Anderson, M. J. (2001). A new method for non-parametric multivariate analysis of variance. *Austral Ecol.* 26 (1), 32–46. doi: 10.1111/j.1442-9993.2001.01070.pp.x

Anderson, M. J., Gorley, R. N., and Clarke, K. R. (2008). *PERMANOVA+ for PRIMER: guide to software and statistical methods* (Plymouth, UK: PRIMER-E).

Atkinson, L. J., Field, J. G., and Hutchings, L. (2011). Effects of demersal trawling along the west coast of southern Africa: multivariate analysis of benthic assemblages. *Mar. Ecol. Prog. Ser.* 430, 241–255. doi: 10.3354/meps08956

Atkinson, L. J., and Sink, K. J. (2018). Field guide to the offshore marine invertebrates of South Africa. *Malachite Marketing and Media: Pretoria*. 498. doi: 10.15493/SAEON.PUB.10000001

Bang, N. D. (1968). Submarine canyons off the natal coast. *South Afr. Geographical J.* 50 (1), 45–54. doi: 10.1080/03736245.1968.10559431

Barlow, R., Lamont, T., Louw, D., Gibberd, M. J., Airs, R., and van der Plas, A. (2018). Environmental influence on phytoplankton communities in the northern benguela ecosystem. *Afr. J. Mar. Sci.* 40 (4), 355–370. doi: 10.2989/1814232X.2018.1531785

Bell, F. J. (1905). Echinoderma. III. ophiuroidea. *Mar. Invest. S. Afr.* 3, 255–260.

Bertolino, M., Ricci, S., Canese, S., Cau, A., Bavestrello, G., Pansini, M., et al. (2019). Diversity of the sponge fauna associated with white coral banks from two

sardinian canyons (Mediterranean Sea). *J. Mar. Biol. Assoc. United Kingdom* 99 (8), 1735–1751. doi: 10.1017/S0025315419000948

Bevilacqua, S., Anderson, M. J., Ugland, K. I., Somerfield, P. J., and Terlizzi, A. (2021). The use of taxonomic relationships among species in applied ecological research: Baseline, steps forward and future challenges. *Austral Ecol.* 46 (6), 950–964. doi: 10.1111/aec.13061

Bianchelli, S., and Danovaro, R. (2019). Meiofaunal biodiversity in submarine canyons of the Mediterranean Sea: A meta-analysis, progress in oceanography. *Elsevier 170 (October* 2018), 69–80. doi: 10.1016/j.pocean.2018.10.018

Birch, G. F. (1975). *Sediments on the continental margin off the west coast of south Africa [Doctoral dissertation]* ([South Africa]: University of Cape Town).

Bock, P. (2022). World List of Bryozoa. *Onchoporella bombycina Busk* 1884. Available at: https://www.marinespecies.org/aphia.php?p=taxdetails&id=1429790 on 2022-11-07

Clarke, K. R., Gorley, R. N., Somerfield, P. J., and Warwick, R. M. (2014). Change in marine communities: an approach to statistical analysis and interpretation. *Primer-E Ltd.* 256.

Clarke, K. R., Somerfield, P. J., and Chapman, M. G. (2006a). On resemblance measures for ecological studies, including taxonomic dissimilarities and a zero-adjusted bray–Curtis coefficient for denuded assemblages. *J. Exp. Mar. Biol. Ecol.* 330 (1), 55–80. doi: 10.1016/j.jembe.2005.12.017

Clarke, K. R., and Warwick, R. M. (1998). A taxonomic distinctness index and its statistical properties. *J. Appl. Ecol.* 35 (4), 523–531. doi: 10.1046/j.1365-2664.1998.3540523.x

Clarke, K. R., and Warwick, R. M. (1999). The taxonomic distinctness measure of biodiversity: weighting of step lengths between hierarchical levels. *Mar. Ecol. Prog. Ser.* 184, 21–29. doi: 10.3354/meps184021

Compton, J. S., Mulabisana, J., and McMillan, L. K. (2002). Origin and age of phosphorite from the last glacial maximum to Holocene transgressive succession off the orange river, south Africa. *Mar. Geology* 186, 243–261. doi: 10.1016/S0025-3227(02)00211-6

Dall, W. H. (1870). A revision of the terebratulidae and lingulidae, with remarks on and descriptions of some recent forms. *Am. J. Conchology* 6 (2), 88–168. https://www.biodiversitylibrary.org/page/6991665.

Department of Environmental Affairs (2019). *National Gazette No 42478 of 23-May*, 647. Available at: https://cer.org.za/wp-content/uploads/2019/05/MPA-declarations.pdf

De Leo, F. C., Smith, C. R., Rowden, A. A., Bowden, D. A., and Clark, M. R. (2010). Submarine canyons: Hotspots of benthic biomass and productivity in the deep sea. *Proc. R. Soc. B: Biol. Sci.* 277 (1695), 2783–2792. doi: 10.1098/rspb.2010.0462

De Leo, F. C., Vetter, E. W., Smith, C. R., Rowden, A. A., and McGranaghan, M. (2014). Spatial scale-dependent habitat heterogeneity influences submarine canyon macrofaunal abundance and diversity off the main and Northwest Hawaiian islands. *Deep Sea Res. Part II: Topical Stud. Oceanography* 104, 267–290. doi: 10.1016/j.dsr2.2013.06.015

Demopoulos, A. W., McClain-Counts, J., Ross, S. W., Brooke, S., and Mienis, F. (2017). Food-web dynamics and isotopic niches in deep-sea communities residing in a submarine canyon and on the adjacent open slopes. *Mar. Ecol. Prog. Ser.* 578 (Elton 1927), 19–33. doi: 10.3354/meps12231

de Wet, W. M., and Compton, J. S. (2021). Bathymetry of the South African continental shelf. *Geo-Mar ine Letters* 41, 40. doi: 10.1007/s00367-021-00701-y

de Wet, W. M. (2013). *Bathymetry of the south African continental shelf. [Masters thesis]* ([South Africa]: University of Cape Town. South Africa). Available at: http://hdl.handle.net/11427/28970.

Di Bella, L., Pierdomenico, M., Porretta, R., Chiocci, F. L., and Martorelli, E. (2017). "Living and dead foraminiferal assemblages from an active submarine canyon and surrounding sectors: the gioia canyon system (Tyrrhenian Sea, southern Italy)," in *Deep-Sea research part I: Oceanographic research papers*, vol. 123. (Elsevier Ltd), 129–146. doi: 10.1016/j.dsr.2017.04.005

Dingle, R. V. (1973). Regional distribution and thickness of post-Palaeozoic sediments on the continental margin of southern Africa. *Geological Magazine* 110 (2), 97–102. doi: 10.1017/S001675680004783X

Dingle, R. V. (1979). Sedimentary basins and basement structures on the continental margin of southern Africa. *Bull. Geological Survey South Afr.* 63, 29–43.

Dingle, R. V., and Siesser, W. G. (1975). *Geology of the continental margin between Walvis bay and ponta do ouro* (Government Printer).

Dingle, R. V., Birch, G. F., Bremner, J. M., De Decker, R. H., Du Plessis, A., Engelbrecht, J. C., et al (1987). Deep-sea sedimentary environments around southern Africa (south- east Atlantic and south-west Indian Oceans). *Annals of the South African Museum*, 98, 1–27

Dingle, R. V., Siesser, W. G., and Newton, A. R. (1983). *Mesozoic and tertiary geology of southern Africa* (Rotterdam: AA Balkema).

Duffy, G. A., Lundsten, L., Kuhnz, L. A., and Paull, C. K. (2014). A comparison of megafaunal communities in five submarine canyons off southern California, USA. *Deep Sea Res. Part II: Topical Stud. Oceanography* 104, 259–266. doi: 10.1016/j.dsr2.2013.06.002

Du Plessis, A., Scrutton, R. A., Barnaby, A. M., and Simpson, E. S. W. (1972). Shallow structure of the continental margin of southwestern Africa. *Mar. Geology* 13 (2), 77–89. doi: 10.1016/0025-3227(72)90047-3

Duros, P., Jorissen, F. J., Cesbron, F., Zaragosi, S., Schmidt, S., Metzger, E., et al. (2014). Benthic foraminiferal thanatocoenoses from the cap-ferret canyon area (NE atlantic): a complex interplay between hydro-sedimentary and biological processes. *Deep Sea Res. Part II: Topical Stud. Oceanography* 104, 145–163. doi: 10.1016/j.dsr2.2013.09.024

Fernandez-Arcaya, U., Ramirez-Llodra, E., Aguzzi, J., Allcock, A. L., Davies, J. S., Dissanayake, A., et al. (2017). Ecological role of submarine canyons and need for canyon conservation: A review. *Front. Mar. Sci*. 4:5. doi: 10.3389/fmars.2017.00005

Green, A. (2011). Submarine canyons associated with alternating sediment starvation and shelf-edge wedge development: Northern KwaZulu-natal continental margin, south Africa. *Mar. Geology* 284 (1-4), 114–126. doi: 10.1016/j.margeo.2011.03.011

Green, A., Ukena, R., Ramsayb, P., Leuci, R., and Perritt, S. (2009). Potential sites for suitable coelacanth habitat using bathymetric data from the western Indian ocean: research letters. *South Afr. J. Sci.* 105 (3), 151–154. doi: 10.4102/sajs.v105i3/4.68

Green, A., and Uken, R. (2008). Submarine land sliding and canyon evolution on the northern KwaZulu-natal continental shelf, south Africa, SW Indian ocean. *Mar. Geology* 254 (3-4), 152–170. doi: 10.1016/j.margeo.2008.06.001

Hawie, N., Covault, J. A., and Sylvester, Z. (2019). Grain-size and discharge controls on submarine-fan depositional patterns from forward stratigraphic models. *Front. Earth Sci.* 7 (December). doi: 10.3389/feart.2019.00334

Hernández-Ávila, I., Guerra-Castro, E., Bracho, C., Rada, M., Ocaña, F. A., and Pech, D. (2018). Variation in species diversity of deep-water megafauna assemblages in the Caribbean across depth and ecoregions. *PloS One* 13 (8), e0201269. doi: 10.1371/journal.pone.0201269

Howell, K. L., Billett, D. S., and Tyler, P. A. (2002). Depth-related distribution and abundance of seastars (Echinodermata: Asteroidea) in the porcupine seabight and porcupine abyssal plain, NE Atlantic. *Deep Sea Res. Part I: Oceanographic Res. Papers* 49 (10), 1901–1920. doi: 10.1016/S0967-0637(02)00090-0

Huvenne, V. A., and Davies, J. S. (2013). Towards a new and integrated approach to submarine canyon research. *Deep Sea Res. Part II: Topical Stud. Oceanography* 104, 1–5. doi: 10.1016/j.dsr2.2013.09.012

Jarre, A., Hutchings, L., Kirkman, S. P., Kreiner, A., Tchipalanga, P. C., Kainge, P., et al. (2015). Synthesis: climate effects on biodiversity, abundance, and distribution of marine organisms in the benguela. *Fisheries Oceanography* 24, 122–149. doi: 10.1111/fog.12086

Karenyi, N., Sink, K., and Nel, R. (2016). Defining seascapes for marine unconsolidated shelf sediments in an eastern boundary upwelling region: the southern benguela as a case study. *Estuarine Coast. Shelf Sci.* 169, 195–206. doi: 10.1016/j.ecss.2015.11.030

Kersalé, M., Perez, R. C., Speich, S., Meinen, C. S., Lamont, T., Le Hénaff, M., et al. (2019). Shallow and deep eastern boundary currents in the south Atlantic at 34.5 s: Mean structure and variability. *J. Geophysical Research: Oceans* 124 (3), 1634–1659. doi: 10.1029/2018JC014554

Kinberg, J. G. H. (1867). *Annulata nova. [Continuatio.]* (Stockholm: Öfversigt af Königlich Vetenskapsakademiens förhandlingar) 23 (9), 337–357. Available at: http://biodiversitylibrary.org/page/32287795.

Lamarck, J. B. M. de. (1816). *Histoire naturelle des animaux sans vertèbres. tome second* (Paris: Verdière), 568. Available at: http://www.biodiversitylibrary.org/item/47698.

Lamont, T., Barlow, R. G., and Kyewalyanga, M. S. (2014). Physical drivers of phytoplankton production in the southern benguela upwelling system. *Deep-Sea Res. Part I: Oceanographic Res. Papers. Elsevier* 90 (1), 1–16. doi: 10.1016/j.dsr.2014.03.003

Lamont, T., García-Reyes, M., Bograd, S. J., van der Lingen, C. D., and Sydeman, W. J. (2018). Upwelling indices for comparative ecosystem studies: Variability in the benguela upwelling system. *J. Mar. Syst.* 188, 3–16. doi: 10.1016/j.jmarsys.2017.05.007

Lamont, T., Hutchings, L., van den Berg, M., Goschen, W. S., and Barlow, R. G. (2015). Hydrographic variability in the st. Helena bay region of the southern benguela ecosystem. *J. Geophys. Res. Oceans* 120, 2920–2944. doi: 10.1002/2014JC010619

Lange, L. (2012). *Use of demersal bycatch data to determine the distribution of soft-bottom assemblages off the West and south coasts of south africa. [Doctoral thesis]* ([South Africa]: University of Cape Town).

Levin, L. A., Etter, R. J., Rex, M. A., Gooday, A. J., Smith, C. R., Pineda, J., et al. (2001). Environmental influences on regional deep-sea species diversity. *Annu. Rev. Ecol. systematics* 32 (1), 51–93. doi: 10.1146/annurev.ecolsys.32.081501.114002

Lins, L., Leliaert, F., Riehl, T., Ramalho, S. P., Cordova, E. A., Esteves, A. M., et al. (2016). Species variability and connectivity in the deep sea: evaluating effects of spatial heterogeneity and hydrodynamics. *Biogeosciences Discuss* 2016, 1–33. doi: 10.1146/annurev.ecolsys.32.081501.114002

Ljungman, A. (1867). Ophiuroidea viventia huc usque cognita enumerat. *Öfversigt af* kgl. *Vetenskaps-Akademiens Förhandlingar 1866* 23 (9), 303–336. https://www.biodiversitylibrary.org/page/32287761.

Lo Iacono, C., Sulli, A., and Agate, M. (2014). Submarine canyons of north-western Sicily (Southern tyrrhenian sea): Variability in morphology, sedimentary processes, and evolution on a tectonically active margin. *Deep Sea Res. Part II: Topical Stud. Oceanography* 104, 93–105. doi: 10.1016/j.dsr2.2013.06.018

Lyman, T. (1878). "Ophiuridae and astrophytidae of the "Challenger" expedition. part I," in *Bulletin of the museum of comparative zoology*, vol. 5. (Cambridge, Mass: Harvard College), 65–168, 10. Available at: https://www.biodiversitylibrary.org/page/28876644#page/85/mode/1up.

Macdonald, T. A., Burd, B. J., Macdonald, V. I., and van Roodselaar, A. (2010). "Taxonomic and feeding guild classification for the marine benthic macroinvertebrates of the strait of Georgia, British Columbia," in *Fisheries and oceans Canada* (Canada: Pêches et océans).

Marine Species Traits editorial board (2022). *Marine Species Traits* Accessed at http://www.marinespecies.org/traits on 2022

Mbatha, F. L., Yemane, D., Ostrowski, M., Moloney, C. L., and Lipiński, M. R. (2019). Oxygen and temperature influence the distribution of deepwater cape hake merluccius paradoxus in the southern benguela: a GAM analysis of a 10-year time-series. *Afr. J. Mar. Sci.* 41 (4), 413–427. doi: 10.2989/1814232X.2019.1688681

Mello-Rafter, K., Sowers, D., Malik, M., Watling, L., Mayer, L. A., and Dijkstra, J. A. (2021). Environmental and geomorphological effects on the distribution of deep-Sea canyon and seamount communities in the Northwest Atlantic. *Front. Mar. Sci.* 1326. doi: 10.3389/fmars.2021.691668

Milne Edwards, H. (1834-1840). *Histoire naturelle des crustacés, comprenant l´ Anatomie, la physiologie et la classification de ces animaux* Vol. III (Paris: Encyclopédique Roret), 1-638, pls. 1–42. Available at: http://www.biodiversitylibrary.org/bibliography/16170#/summary.

Mortensen, T. (1907) The Danish Ingolf-Expedition 1895–1896. Vol. 4. No. 2. *Echinoidea*. Part 2. B. Luno, (Copenhagen), 200

Müller, O. F. (1789). *Zoologia danica seu animalium daniae et norvegiae rariorum ac minus notorum descriptiones et historia*. Ed. N. Möller (Copenhague: Havniae), 81–120. Available at: http://gdz.sub.uni-goettingen.de/dms/load/img/?PPN=PPN614794331.

Nobili, G. (1906). Diagnoses préliminaires de crustacés, décapodes et isopodes nouveaux recueillis par m. le dr. g. seurat aux îles touamotou. *Bull. du Muséum Natl. d'Histoire naturelle.* 12 (12), 256–270. doi: 10.5962/bhl.part.4097

Owen, R. (1843)Lectures on the comparative anatomy and physiology of the invertebrate animals. Available at: https://archive.org/stream/lecturesoncompar00owe#page/82/mode/2up.

Palan, K. J. (2017). *Submarine canyon evolution of the southwest cape continental margin. [Doctoral dissertation]* ([South Africa]: University of KwaZulu-Natal).

Pierdomenico, M., Cardone, F., Carluccio, A., Casalbore, D., Chiocci, F., Maiorano, P., et al. (2019). Megafauna distribution along active submarine canyons of the central Mediterranean: Relationships with environmental variables. *Prog. Oceanography* 171, 49–69. doi: 10.1016/j.pocean.2018.12.015

Puccinelli, E., McQuaid, C. D., and Ansorge, I. J. (2018). Factors affecting trophic compositions of offshore benthic invertebrates at a sub-Antarctic archipelago. *Limnology Oceanography* 63 (5), 2206–2228. doi: 10.1002/lno.10934

Quattrini, A. M., Nizinski, M. S., Chaytor, J. D., Demopoulos, A. W., Roark, E. B., France, S. C., et al. (2015). Exploration of the canyon-incised continental margin of the northeastern united states reveals dynamic habitats and diverse communities. *PloS One* 10 (10), 1–32. doi: 10.1371/journal.pone.0139904

Ramirez-Llodra, E., Brandt, A., Danovaro, R., De Mol, B., Escobar, E., German, C. R., et al. (2010). Deep, diverse and definitely different: unique attributes of the world's largest ecosystem. *Biogeosciences* 7 (9), 2851–2899. doi: 10.5194/bg-7-2851-2010

Rogers, J. (1977). Sedimentation on the continental margin of the orange river and the namib desert. *Bull. Joint Geological Survey: Univ. Cape Town Mar. Geosci. Group* 7, 1–162.

Rogers, J., and Bremner, J. M. (1991). The benguela ecosystem. part vn. marine-geological aspects. *Oceanography Mar. Biology: Annu. Rev.* 29, 1–85.

Savigny, J. C. (1816). Memoires sur les animaux sans vertebres. *Paris.* 2, 1–239. doi: 10.5962/bhl.title.9154

Shannon, L. J., Christensen, V., and Walters, C. J. (2004). Modelling stock dynamics in the southern benguela ecosystem for the period 1978–2002. *Afr. J. Mar. Sci.* 26 (1), 179–196. doi: 10.2989/18142320409504056

Shannon, L. J., Jarre, A. C., and Petersen, S. L. (2010). Developing a science base for implementation of the ecosystem approach to fisheries in south Africa. *Prog. Oceanography* 87 (1-4), 289–303. doi: 10.1016/j.pocean.2010.08.005

Shannon, L. V., and Nelson, G. (1996). "The benguela: large scale features and processes and system variability," in *The south Atlantic* (Berlin, Heidelberg: Springer). doi: 10.1007/978-3-642-80353-6_9

Simpson, E. S. W., and Forder, E. (1968). The cape submarine canyon. *Fisheries Bull. South Africa.* 5, 35–38.

Sink, K. J., Attwood, C. G., Lombard, A. T., Grantham, H., Leslie, R., Samaai, T., et al. (2011). "Spatial planning to identify focus areas for offshore biodiversity protection in south Africa," in *Final report for the offshore marine protected area project* (Cape Town: South African National Biodiversity Institute). Available at: https://www.sadstia.co.za/assets/uploads/Benthic-report-2012.pdf

Sink, K. J., Boshoff, W., Samaai, T., Timm, P. G., and Kerwath, S. E. (2006). Observations of the habitats and biodiversity of the submarine canyons at sodwana bay: Coelacanth research. *South Afr. J. Sci.* 102 (9), 466–474.

Sink, K., van der Bank, M., Majiedt, P., Harris, L., Atkinson, L., Kirkman, S., et al. (2019). *South African national biodiversity assessment 2018 technical report volume 4: Marine realm* (Pretoria. South Africa: South African National Biodiversity Institute). Available at: http://hdl.handle.net/20.500.12143/6372.

Sink, K. J., Wilkinson, S., Atkinson, L., Sims, P., Leslie, R., and Attwood, C. G. (2012). The potential impacts of south africa's demersal hake trawl fishery on benthic habitats: Historical perspectives, spatial analyses, current review, and potential management actions.

Smith, S. I. (1882) . *Reports on the results of dredging under the supervisión of Alexander Agassiz, on the east coast of the United States during the summer of 1880, by the U.S. Coast Survey Steamer "Blake", Commander J.R. Bartlett, U.S.N., commanding.* (Bulletin of the Museum of comparative Zoology at Harvard College) 10 (1), 1–108.

Stebbing, T. R. R. (1910). "General catalogue of south African Crustacea (Part v. @ of s. a. Crustacea, for the marine investigations in south Africa)," in *Annals of the south African museum*, vol. 6. , 281–593. doi: 10.5962/bhl.part.15558

Stephen, A. C. (1965). A revision of the classification of the phylum sipuncula. *Ann. Magazine Natural History. (Series 13)* 7 (80), 457–462. doi: 10.1080/00222936408651485

Studer, T. (1883). *Verzeichnis der während der crustaceen, welche während der reise S.M.S. "Gazelle" an der westküste von afrika, ascension un dem cap der guten hoffnung gesammelten crustaceen* Vol. 2 (Berlin: Abhandlungen der königlichen Akademie der Wissenschaften), 1–32.

Théel, H. (1886). Report on the holothurioidea collected by H.M.S. challenger during the years 1873-76. part II. report on the scientific results of the voyage of H.M.S. challenger during the years 1873–76. *Zoology* 14 (part 39), 1–2901–16. http://19thcenturyscience.org/HMSC/HMSC-Reports/Zool-39/htm/doc.html.

Thomson, C. W. (1873). The depths of the Sea: An account of the general results of the dredging cruises of HMSS" porcupine" and" lightning" during the summers of 1868, 1869, and 1870. *Macmillan*. 527 doi: 10.5962/bhl.title.19314

Tizard, T. H., Moseley, H. N., Buchanan, J. Y., and Murray, J. (1885). Narrative of the cruise of H.M.S. challenger, with a general account of the scientific results of the expedition. *Rep. Sci. Results Voyage H.M.S. Challenger during years 1873–1876.* 1 (1-2), i–liv, 1-1110. https://www.biodiversitylibrary.org/page/49431318.

Travers, M., Watermeyer, K., Shannon, L. J., and Shin, Y. J. (2010). Changes in food web structure underscenarios of overfishing in the southern benguela: comparison of the ecosim and OSMOSE modelling approaches. *J. Mar. Syst.* 79 (1-2), 101–111. doi: 10.1016/j.jmarsys.2009.07.005

Veitch, J., Hermes, J., Lamont, T., Penven, P., and Dufois, F. (2018). Shelf-edge jet currents in the southern benguela: A modelling approach. *J. Mar. Syst.* 188, 27–38. doi: 10.1016/j.jmarsys.2017.09.003

Venter, P., Timm, P., Gunn, G., Le Roux, E., Serfontein, C., Smith, P., et al. (2000). Discovery of a viable population of coelacanths (Latimeria chalumnae smit at sodwana bay, south Africa. *South Afr. J. Sci.* 96 (11-12), 567–568.

Vetter, E. W., Smith, C. R., and De Leo, F. C. (2010). Hawaiian Hotspots: enhanced megafaunal abundance and diversity in submarine canyons on the oceanic islands of Hawaii. *Mar. Ecol.* 31 (1), 183–199. doi: 10.1111/j.1439-0485.2009.00351.x

Wigley, R. A., and Compton, J. S. (2006). Late Cenozoic evolution of the outer continental shelf at the head of the cape canyon, south Africa. *Mar. Geology* 226 (1–2), 1–23. doi: 10.1016/j.margeo.2005.09.015

Wigley, R.A. (2004). Sedimentary facies from the Head of the Cape Canyon: Insights into the Cenozoic evolution of the western margin of South Africa. [Doctoral thesis]. (South Africa: University of Cape Town). Available at: https://open.uct.ac.za/handle/11427/4232

Wiles, E., Green, A., Watkeys, M., Jokat, W., and Krocker, R. (2013). The evolution of the tugela canyon and submarine fan: a complex interaction between margin erosion and bottom current sweeping, southwest Indian ocean, south Africa. *Mar. Petroleum Geology* 44, 60–70. doi: 10.1016/j.marpetgeo.2013.03.012

WoRMS Editorial Board (2022) *World register of marine species*. Available at: https://www.marinespecies.org (Accessed 2022-06-02).

Yemane, D., Kirkman, S. P., Kathena, J., N'siangango, S. E., Axelsen, B. E., and Samaai, T. (2014). Assessing changes in the distribution and range size of demersal fish populations in the benguela current Large marine ecosystem. *Rev. Fish Biol. Fisheries* 24 (2), 463–483. doi: 10.1007/s11160-014-9357-7

frontiers | Frontiers in Marine Science

TYPE Original Research
PUBLISHED 06 February 2023
DOI 10.3389/fmars.2023.1078831

OPEN ACCESS

EDITED BY
Veerle Ann Ida Huvenne,
University of Southampton,
United Kingdom

REVIEWED BY
Francesco Marcello Falcieri,
Department of Earth System Sciences and Technologies for the Environment (CNR),
Italy
Rob Hall,
University of East Anglia, United Kingdom

*CORRESPONDENCE
Lénaïg Brun
lenaig.brun@ifremer.fr

SPECIALTY SECTION
This article was submitted to Deep-Sea Environments and Ecology, a section of the journal Frontiers in Marine Science

RECEIVED 24 October 2022
ACCEPTED 10 January 2023
PUBLISHED 06 February 2023

CITATION
Brun L, Pairaud I, Jacinto RS, Garreau P and Dennielou B (2023) Strong hydrodynamic processes observed in the Mediterranean Cassidaigne submarine canyon. *Front. Mar. Sci.* 10:1078831. doi: 10.3389/fmars.2023.1078831

Strong hydrodynamic processes observed in the Mediterranean Cassidaigne submarine canyon

Lénaïg Brun[1]*, Ivane Pairaud[1], Ricardo Silva Jacinto[2], Pierre Garreau[1] and Bernard Dennielou[2]

[1]Ifremer, University of Brest, UMR 6523 CNRS, IRD, Laboratoire d'Océanographie Physique et Spatiale, Plouzané, France, [2]Ifremer, Geo-Ocean, University of Brest, CNRS, UMR 6538, Plouzané, France

Introduction: Submarine canyons are incisive morphologies that play an important role in the exchange between shallow and deep waters. They interact with the general circulation and induce a specific circulation locally oriented by the morphology. The characteristics of the physical processes at play, the way they interact with each other and the influence of extreme events is still an open question as few observations are available. To answer this question and to improve the representation of submarine canyons in numerical models, it is key to understand the specific circulation patterns and their transitions in these specific environments.

Methods: This paper presents observations of currents, temperature and turbidity along the Cassidaigne canyon, northwestern Mediterranean Sea. Two oceanographic cruises carried out in 2017 and 2019 gathered data from the outer shelf and canyon head at 100-400 m depth to the base of the continental slope at 1900 m depth.

Results and Discussion: The circulation in the Cassidaigne area is subject to upwelling and downwelling-favorable winds, to the Northern Current and its associated mesoscale structures and is oriented by the local morphology. Upwellings occur both during stratified and non-stratified conditions. They are triggered by a wind forcing higher than 14 m s^{-1} and their consecutive relaxations are marked by a counter-current. Near the canyon head and on the shelf, the current orientation depends on the stratification, the wind, the bottom morphology and the general circulation. The mesoscale variability of the Northern Current can lead to its intrusion over the shelf leading to barotropic cross currents over the canyon. At 1700 m depth, a quasi-permanent residual up-canyon flow is observed in a narrow gorge area and can be extrapolated to the canyon body. Finally, turbidity currents were observed for the first time in connection with upwelling events, suggesting the key role of canyons' internal hydrodynamics on shelf sedimentary processes.

KEYWORDS

circulation, submarine canyon, Cassidaigne, Mediterranean Sea, upwelling, Northern Current, turbidity current, morphology

1 Introduction

Submarine canyons incising continental slopes constitute key oceanic morphologies favoring the exchange of organic matter, carbon, heat or pollutants between the continental shelf and the deep sea (Ceramicola et al., 2015). These specific morphologies favor the generation of local complex hydrodynamic processes whose impact, interactions and relaxations have not been fully investigated due to the small scales involved and the laborious *in-situ* measurements. Understanding the circulation patterns in submarine canyons is a first step to characterize the interaction between hydrodynamic and sedimentary processes, benthic and pelagic habitat development, connectivity or contaminant transfer in canyons and slopes. It will also contribute to improving the representation of canyons in numerical models. In the northwestern sector of the Mediterranean Sea, the Gulf of Lions is one of the oceanic margins with the highest density of submarine canyons in the world with 3 to 4 canyons per 100 km (Allen and Durrieu de Madron, 2009; Würtz, 2012). The easternmost canyon of this area is the Cassidaigne submarine canyon (Figure 1).

While other canyons of the Gulf of Lions are sedimentary marine constructions (Mauffrey, 2015), the Cassidaigne submarine canyon is characterized by a steep, narrow and aerial morphology due to its particular origin (Ceramicola et al., 2015). During the Messinian salinity crisis, the level of the Mediterranean Sea was at least 1500 m lower than today (Gargani and Rigollet, 2007). As the head of the Cassidaigne canyon was exposed to the open air, it was initially eroded by winds and rivers before being further incised by currents after reflooding of the Mediterranean Sea. Unlike other canyons that gradually widen downstream, the Cassidaigne canyon of 6 km wide in its middle part is characterized by a narrowing of about 2 km wide at 1700 m depth downstream (Fabri et al., 2017). This specific morphology restricts and controls the local circulation. Fabri et al. (2017) identified maximum current velocities to the west part of the canyon head, but also at 1900 m depth at the canyon gorge and along its axis near the sea floor, in most confined areas with narrow morphologies.

The western part of the Gulf of Lions is well documented (Baztan et al., 2005; Jordi et al., 2005; Rennie, 2005; DeGeest et al., 2008; Lofi and Berné, 2008; Palanques et al., 2008; Ahumada-Sempoal et al., 2015) but the eastern region is not well known in terms of sedimentary geology. The Cassidaigne canyon is located in a microtidal area far from the Rhone, with negligible input of freshwater and sediments such as the karstic underwater flow coming from the Vallat des Brayes (Cavalera et al., 2010) and the discharge of the wastewater treatment plant of Cortiou near the surface (Oursel et al., 2014)). For 48 years, between 1967 and 2015, 30 megatons of red mud (bauxite residues) have been artificially discharged by the Gardanne plant at 400 m depth in the eastern canyon head (Alteo environnement Gardanne 2017 and Dauvin, 2009). The red mud flowed and spread along and across the canyon down to 2500 m depth. Although chemically inert, the remaining sediments cover the canyon bottom and act as flow tracers contributing to the characterization of hydrodynamic processes and sediment transport in the canyon. The interaction between sedimentary

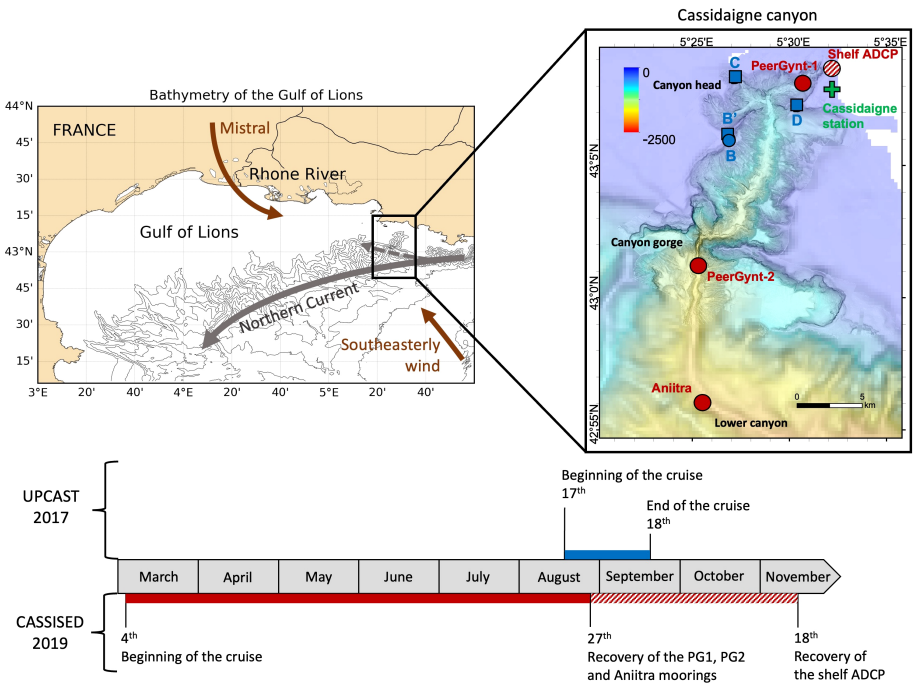

FIGURE 1
Bathymetry of the Gulf of Lions (top left), located between 42°N and 43.5°N of latitude and between 3°E and 6°E of longitude in the Mediterranean Sea, a semi-enclosed microtidal sea linked with the Atlantic Ocean by the Strait of Gibraltar. Its depth varies from 76 m on average on the shelf to 2500 m in the open sea. The gray arrow corresponds to the general circulation of the NC and the dashed gray arrow refers to its intrusion over the Gulf of Lions. Bathymetry of the Cassidaigne submarine canyon (m, right), the easternmost canyon in the Gulf of Lions, located 7 km away from the coast of Cassis. The squares refer to the position of the Mastodon-2d thermistor lines and the circles correspond to the ADCP current moorings for both UPCAST 2017 (in blue) and CASSISED 2019 (in red) cruises. Their deployment time is specified on the time lines (bottom). The green cross refers to the T-MedNet Cassidaigne station.

and hydrodynamic processes remains an open question. In most previous studies, the processes were analyzed separately.

Hydrodynamic processes in canyons such as upwelling or downwelling are relatively well known. Many studies were performed on the shelf or in idealized submarine canyons through numerical models and considering a simplified permanent forcing (She and Klinck, 2000; Kämpf, 2006; Allen and Durrieu de Madron, 2009; Saldías and Allen, 2020). The presence of submarine canyons incising the shelf modifies the structure of wind-induced upwellings and downwellings. In general, downwellings are characterized by down-canyon flows that tend to move away from the upstream edge of the canyon (i.e. the first edge met by the along-shore flow) and exit along the downstream edge (i.e. the last edge met by the along-shore flow). Upwellings are characterized by up-canyon flows along the upstream canyon rim and with an outflow of water masses on the downstream side (Allen and Durrieu de Madron, 2009). During an upwelling event, the flow crosses isobaths, stretching the water column and thus generating a cyclonic circulation within the canyon and an anticyclonic flow at the downstream edge (Hickey, 1997). Upwelling and downwelling can be separated into three phases: a time-dependent response of the water column to wind forcing, a non-linear established advection driven flow and consequently a relaxation phase (Allen and Durrieu de Madron, 2009). During the second phase, the response of the water column depends on its stratification and the canyon's morphology. Up to now, upwelling and downwelling have been mainly studied under stratified conditions. Studies on the Barkley and Astoria canyons demonstrated that non-linear terms and transient movements during set-up at short time scales within the canyon cause a break in the geostrophic balance, which is approximately in equilibrium on the shelf (Hickey, 1997; Allen et al., 2001; Allen and Hickey, 2010). Finally, the relaxation phase of upwelling and downwelling produces notable but less documented responses (Allen and Durrieu de Madron, 2009 and Hickey, 1997).

In the Gulf of Lions, upwellings are characterized by the movement of cold water from deeper levels to the surface. They lead to a drop of surface temperature in stratified conditions and a general increase in salinity in the water column (Millot, 1979; Millot, 1990; Odic et al., 2022 and Millot, 1997; Millot and Taupier-Letage, 2005). Upwellings are induced by westerly winds (Tramontane) and north-westerly winds (Mistral). The Mistral is characterized by intense (i.e. 25 m s^{-1}) episodes lasting several weeks in winter and weaker episodes (i.e. 10 to 15 m s^{-1}) during summer (Millot, 1990; Albérola and Millot, 2003; Millot, 2005 and Fabri et al., 2017). It generates six upwelling cells along the Gulf of Lions' margin, the strongest being close to the Cassidaigne canyon. Downwellings are induced by easterly winds. Both westerly and easterly winds' occurrence, speed and duration depend on the season. These winds blow in a succession of isolated storms generating transient movements and quasi-inertial oscillations (Petrenko, 2003). During fall, storm occurrence increases and upwellings and downwellings contribute to the homogenization of the water column (Fabri et al., 2017).

The Cassidaigne submarine canyon is also influenced by the Northern Current (NC), the northern branch of the general circulation in the northwestern Mediterranean Sea. It forms a surface slope current flowing from the Ligurian to the Catalan sea, characterized by a seasonal variability ranging from 1 m s^{-1} in winter to 0.3 m s^{-1} in summer (Conan and Millot, 1995; Flexas et al., 2002; Albérola and Millot, 2003; Petrenko, 2003; Guihou et al., 2013). The mesoscale variability of the NC manifests itself in the form of meanders which are particularly important in winter when it is the most unstable (Millot, 1997; Petrenko, 2003; Rubio et al., 2009). The NC usually flows along the shelf break front off the Gulf of Lions. During some south-easterly storms (Petrenko, 2003; Millot, 2005), intermittent Mistral's periods or relaxation of strong Mistral's events (Millot and Wald, 1980), up to 30% of its flow can separate from the main branch and enter the shelf mainly at the eastern entrance of the Gulf of Lions (Conan and Millot, 1995; Petrenko, 2003; Guihou et al., 2013) and potentially above the canyon (Pairaud et al., 2011). The impact of the NC on the water column has been mainly studied in the Grand-Rhone canyon (Durrieu de Madron, 1994 and Durrieu de Madron et al., 1999) or on the shelf (Rubio et al., 2009; Ross et al., 2016) but its interaction with the Cassidaigne canyon is not well documented. NC intrusion induces a vertical structure reorganization of the currents and a variation in surface temperature. Ross et al. (2016) studied the intrusion of the NC in the bay of Marseilles. The cold, nutrient-rich water brought to the surface during upwelling events is gradually replaced by warm, nutrient-poor water, in the observed 70 meters upper layer.

The variety and complexity of forcing processes around the Cassidaigne canyon implies taking into account their interaction and the transitions between regimes which are still not well-known in this region. The flow is forced both by the wind (generating upwelling, downwelling and inertia currents) and by the NC. It is also constrained by the seabed morphology. The knowledge of the Cassidaigne canyon area has been improved by previous oceanographic cruises (Pairaud et al., 2017; Danioux, 2018; Dennielou, 2019; Pairaud and Fuchs, 2021). In this paper, the shelf dynamics during strong upwelling events is analyzed using data gathered in 2017 over a period of 1 month. The behavior of residual currents on the shelf and within the canyon is analyzed with a second dataset collected in 2019 over a period of 6 to 8 months. The use of data from oceanographic campaigns allowed deepening the understanding of hydrodynamic and sedimentary processes in the Cassidaigne canyon. It also allowed the definition of a relevant study strategy. The paper is organized as follows: Section 2 introduces the materials and methods, i.e., the collection of *in-situ* and wind data and the data processing methods. Section 3 focuses on the main results considering periods of both non-stratified and stratified conditions. A focus on significant transient events (NC intrusions, upwellings) and occasional events (turbidity currents) is discussed in relation to previous studies in Section 4.

2 Materials and methods

2.1 Observations and modeling

Hydrological and hydrodynamic data were obtained during several monitoring periods (from 1 to 8 months) in and around the Cassidaigne canyon. Instruments were deployed along mooring lines

or mounted on benthic structures during two oceanographic cruises (Pairaud, 2017; Dennielou, 2019).

2.1.1 UPCAST 2017 campaign

In 2017, a one-month time-series of current and temperature data were acquired during the UPCAST 2017 oceanographic cruise from August 17th to September 18th 2017. The campaign was carried out in the northwestern Mediterranean Sea between the Calanques of Marseilles and the Hyéres islands (south of Toulon) on the RV Thetys II (Pairaud, 2017). The aim was to carry out physical and biogeochemical measurements to understand the interaction of the upwelling of Cassis with the local circulation in the Cassidaigne canyon and with the general circulation.

In addition to en-route measurements from the ship, a 300 kHz ADCP recording upward was moored on the shelf west of the canyon head at 125 m depth (B on Figure 1, Table 1). It was configured with a sampling rate of 10 min and measured currents in the water column from 8 to 108 m depth above the seabed using bins of 5 m size.

Three Mastodon-2d thermistor lines were deployed (Figure 1, Table 2, Figure S1): (i) on the shelf west of the canyon (B') at 125 m depth, (ii) at the canyon head (C) at 193 m depth and (iii) on the shelf east of the canyon (D) at 190 m depth. A Mastodon-2d thermistor line is a low-cost moored line (Lazure et al., 2015) used to record temperature and pressure along the water column. Pressure sensors were key to check the behavior of the line as it could be affected and bent by currents. It resulted in temperature measurements with a precision of 0.1°C.

2.1.2 CASSISED 2019 campaign

In the same area, the CASSISED oceanographic field experiment (Dennielou, 2019) was led from March 4th to August 30th 2019 (spring-summer). The aim of this campaign was to understand the transfer of particles from the continental shelf to the deep sea through the Cassidaigne canyon. The red mud injected in the canyon was considered as sediment flux tracers. The goal was also to estimate the

TABLE 1 Position and setting of each ADCP mooring used during the UPCAST 2017 and CASSISED 2019 cruises.

Mooring	B	Shelf	PG1	PG2	Aniitra
Deployment date	17 Aug 2017	4 March 2019	5 March 2019	5 March 2019	5 March 2019
Recovery date	18 Sept 2017	10 Nov 2019	26 Aug 2019	27 August 2019	27 Aug 2019
Latitude	N43°06,2220	N43°08,7780	N43°08,2367	N43°01,3409	N42°56,1653
Longitude	E5°26,8620	E5°32,2440	E5°30,7570	E5°25,3316	E5°25,5704
Depth of seabed (m)	125	86	422	1628	1906
Distance to seabed (m)	0	0	100	100	300
Ping frequency (kHz)	300	300	300	300	75
Sampling period (min)	10	15	10	10	10
Bin size (m)	5	4	4	4	4
Number of bins	24	20	24	19	72
Bin range from the seabed (m)	8-123	7-83	0-93	0-72	0-286
Number of pings per ensemble	50	50	60	60	60

TABLE 2 Position and setting of the thermistor lines and pressure and temperature sensors of each Mastodon-2d used during the UPCAST 2017 cruise.

Mastodon-2d	B'					C					D				
Deployment date	17 Aug 2017					17 Aug 2017					17 Aug 2017				
Recovery date	18 Sept 2017					18 Sept 2017					18 Sept 2017				
Latitude	N43°06,2096					N43°08,453					N43°07,3953				
Longitude	E5°26,8616					E5°27,140					E5°30,3355				
Depth of seabed (m)	125					193					190				
Sampling period (min)	5					5					5				
Averaged vertical resolution (m)	12.71					15.01					20.18				
Precision (°C)	0.1					0.1					0.1				
Number of sensors	10					10					10				
Mean sensors depth from the seabed (m)	0	9	18	29	43	0	10	25	44	69	0	10	24	50	75
	59	74	89	104	114	96	121	146	161	172	100	126	151	171	181

influence of upwellings, gravity currents and NC on particle movements with the aim of improving knowledge of the turbiditic channel, end lobes and contourites.

On the shelf, a 300 kHz ADCP looking upward, hereafter referred to as "shelf ADCP" (Figure 1, Table 1, Figure S1), was moored at 86 m bottom depth northeast of the canyon head. It sampled at a rate of 15 min part of the water column from 7 to 75 m depth above the seabed using bins of 4 m size. Due to a dysfunction of the acoustic release, this ADCP was recovered later on November 18th 2019. In the canyon, two 300 kHz ADCPs recording downward (PeerGynt moorings PG1 at the canyon head and PG2 embedded in the turbiditic channel at the outlet of the gorge) were immersed 100 m above the seafloor which was at 422 m depth for PG1 and 1628 m depth for PG2. They sampled at a rate of 10 min part of the water column from 13 to 93 m above the seabed and from 32 to 72 m depth above the seabed respectively using bins of 4 m size. A 75 kHz ADCP scanning downward (Aniitra mooring) was located 300 m above the 1906 m depth seafloor along the sedimentary ridge. It sampled at a rate of 10 min part of the water column using bins of 4 m size. The PG1 and PG2 moorings were equipped with STBD 6000 turbidimeters.

In deeper water layers, the measurements made by the 75 kHz Aniitra mooring were noisy. They had a lower resolution and velocity precision as they were configured to track turbidity currents, with higher speeds and particle charges than the background flows. Due to the ADCP configuration (4 m cell size), there was a high standard deviation in the data (0.047 m s^{-1}), which was of the order of magnitude of the measured velocity data. Data were often missing, especially at the beginning of the time series when too few particles were present in the water column. In the first half of the sampled water column, the nearest of the Aniitra mooring, the gaps were in the range of 10 to 30 min on average. The closer to the seabed, the more gaps in the data, sometimes of more than 24 h, resulting in very unreliable data. From March 5th to June 14th, a lot of data were missing from the seabed to 198 m above the seabed. From June 15th to August 27th, a lot of data were missing from the seabed to 149 m above the seabed. Therefore, only the upper part of the water column, from 198 to 269 m above the seabed, was exploited for the long-term residual current analysis. Moving means with a 30-minute window were first applied to the data to smooth the measurements and to reduce the noise in the velocity time series. Then, nearest-neighbor interpolations had to be carried out to fill isolated data gaps. This methodology generates a continuous time series but prevents from analyzing the signal at a period of less than 1 hour. Finally, the entire water column was analyzed for the turbidity current study.

Two temperature profiles in October 2019 were provided by the regional temperature observation network T-MEDNet (www.t-mednet.org) at the Cassidaigne station (43°08.740'N, 5°32.742'E, Figure 1) managed by Dorian Guillemain (MIO, Marseilles, France). Nine temperature sensors were attached to a rocky wall from 5 to 45 m depth. Data were acquired using temperature sensor HOBO Pro V2 Temp U22-001 (Accuracy ± 0.2°C).

2.1.3 Numerical models

The nearest meteorological station (Marignane airport) is separated from the canyon area by a remarkable orography (the Calanques massif) and is not sufficiently relevant in the area. In this approach, wind data were provided by the wind derived AROME (1.3 km resolution) modeling developed by the French Meteorological Office. The MARS3D (3D hydrodynamical Model for Applications at Regional Scale) model was used to simulate the coastal and regional circulation (developed by Lazure and Dumas, 2008; revised by Duhaut et al., 2008). For this study, the operational configuration "MENOR" of the MARS3D model (Garnier et al., 2014), which extends from the Balearic Islands to the Gulf of Lions and the Ligurian Sea (0°E 16°E, 39.5°N 44.5°N) was used. The model has a horizontal resolution of 1.2 km. The vertical resolution is defined using a generalized sigma coordinate system with 60 vertical levels on the order of ten centimeters near the surface, ten meters in the middle of the water column and a few meters near the bottom for a depth in the range of 200-1000 m.

2.2 Data processing strategy

2.2.1 Local circulation

The ADCP provided the zonal (u) and meridional (v) components of the horizontal velocity on a sampled portion of the water column. On the shelf, these velocities were analyzed considering a surface and a bottom layer separately. A characteristic surface layer depth of 65 ± 6 m has been defined empirically using either the thermocline depth or the current shear in order to best fit the observations. In order to do so, wind data were used together with current data (speed, stickplots…) provided by the shelf ADCPs and temperature data provided by the Mastodon-2d thermistor lines at all depths.

The non-stratified period was defined from March to early May, when Hovmöller diagrams showed a homogeneous water column (with almost the same current speed at the surface and the bottom) and temperature data were not characterized by important variations (of less than 0.2°C). In addition, the regional temperature observation network T-MEDNet showed an onset of stratification in early May.

The dynamical response to the offshore Ekman transport can produce a coastal upwelling. The horizontal fluxes deduced from the zonal and meridional components of the Ekman transport in steady state conditions were computed as:

$$U_{ek} = \frac{\tau_y}{\rho_e f} \quad (1)$$

$$V_{ek} = -\frac{\tau_x}{\rho_e f} \quad (2)$$

where ρ_e= 1025 kg m^{-3} is the water volumetric mass and f=10^{-4} rad s^{-1} is the Coriolis parameter at the Cassidaigne canyon. τ_x and τ_y are the zonal and meridional component of the wind stress $\tau = \rho_a C_D \mathbf{U_{10}}^2$ where ρ_a=1.2 kg m^{-3} is the air volumetric mass, C_D=1.5×10^{-3} is the air-sea friction coefficient and $\mathbf{U_{10}}$ is the wind velocity at 10 m above the sea surface given by the AROME model.

In the canyon, the along-canyon V_{along} and cross-canyon V_{cross} velocities were calculated from u and v. V_{along} is positive up-canyon and V_{cross} is positive to the west when looking up-canyon. The V_{along} direction was determined by an angle α clockwise from north at each mooring in the canyon (PG1, PG2 and Aniitra from the CASSISED 2019 cruise): α_{PG1} = 22°, α_{PG2} = 357° and $\alpha_{Aniitra}$=322°. The Fourier transform of V_{along} and V_{cross} were calculated (S2).

2.2.2 Upwelling detection

To detect upwelling events, favorable westerly local winds were first identified using the meteorological model (Figure 2). In stratified conditions, upwellings were then characterized by a temperature decrease ΔT (Figure 2) on the shelf near the sea floor where ADCP temperature sensors were located. Comparison of wind and temperature variability allowed to determine the temperature drops associated with Mistral events. However, this method was less effective under non-stratified conditions. In this case, the ADCPs provided information on the current direction and shear. During upwelling events, the current was characterized by an offshore component near the surface and an onshore component near the sea floor.

To provide a quantitative analysis of the role of wind forcing in displacing water masses, the maximum current speed vertically averaged on the part of the water column measured by the ADCP was estimated for each upwelling event. It was related to the maximum wind speed.

2.2.3 Northern current intrusion

NC intrusions on the shelf were identified using operational results from the MARS3D MENOR and AROME models. Favorable southeast storms or Mistral's relaxation events were first identified using the meteorological model hindcasts. Then, a qualitative estimation of NC intrusion events was made by observing the direction of the surface currents from the MENOR forecasts. Finally, a quantitative estimation of these intrusions was performed following the approach described by Casella et al. (2020). This method is based on the evaluation of the onshore volume flux F crossing through the 200 m isobath at eastern entrance of the Gulf of Lions. The flux is normalized:

$$F_n = \frac{F - \bar{F}}{\sigma_F} \quad (3)$$

where $\bar{F}$ is the temporal mean and σ_F is the standard deviation of the flux, both evaluated over a 10-year period with 3-hourly model outputs. Considering the NC intrusion as an event of infrequent and strong intensity, a threshold of F_n>1 is considered to characterize it.

3 Results

3.1 Shelf circulation in the canyon area

Shelf circulation in the vicinity of the Cassidaigne submarine canyon is modulated by the wind, by the regional circulation and by its underlying complex morphology. Both surface and bottom currents may differ, depending on the stratification. The local shelf circulation is presented hereafter considering separately the surface and bottom water layers under non-stratified or stratified conditions.

3.1.1 Westerly wind-induced upwellings and consecutive transients

During the non-stratified period (from March to early May, CASSISED 2019 cruise), Mistral and south-easterlies alternated (Figure 3). Upwellings were found to require Mistral events of more than 18.3 ± 4 m s^{-1} to be generated. During Mistral events, the shelf mooring north-east of the canyon (Figure 3) recorded 7 days of upwelling events in March and 11 days between April and early May. It led to a mean estimation of 9 days of upwelling per month. This short period of observation suggested a relatively high occurrence of upwelling under non-stratified conditions. Upwellings were

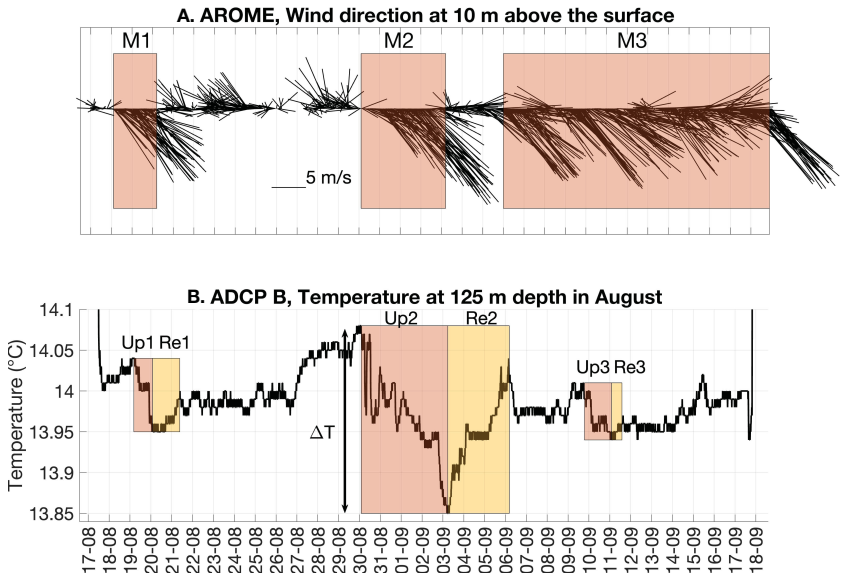

FIGURE 2
(A) Wind direction determined using the AROME meteorological model hindcasts during the UPCAST 2017 cruise. The stickplots point in the direction of the wind. Stickplots directed towards south-east to east (red boxes '*M1*', '*M2*' and '*M3*') correspond to Mistral events. **(B)** Temperature record (°C) measured at 125 m depth by the ADCP B (UPCAST 2017 cruise) under stratified conditions. Upwelling (red boxes '*Up1*', '*Up2*' and '*Up3*') generated by '*M1*', '*M2*' and '*M3*' respectively induce a decrease of temperature ΔT in the water column. Their corresponding relaxation '*Re1*', '*Re2*' and '*Re3*' are represented by the yellow boxes.

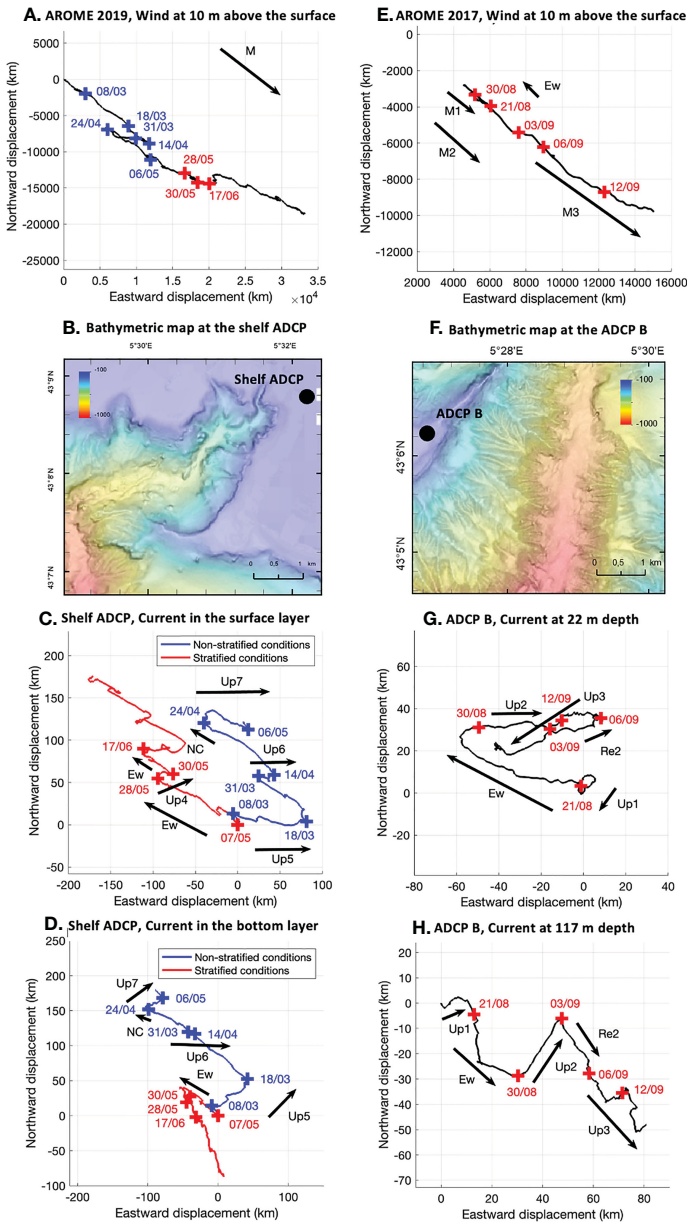

FIGURE 3
(A) Hodograph of the wind determined by the AROME meteorological model at 10 m above the surface during the CASSISED 2019 measurement period. '*M*' refers to the direction of the Mistral. **(B)** Bathymetric map at the shelf ADCP (m). Hodograph of the eulerian current measured by the shelf ADCP averaged on: **(C)** the surface layer of 65 m depth and **(D)** on the bottom layer. '*Up4*', '*Up5*', '*Up6*' and '*Up7*' correspond to upwelling events. '*Ew*' refers to easterly wind. '*NC*' corresponds to Northern Current intrusion. Blue crosses and lines refer to events in non-stratified conditions and red crosses and lines refer to events in stratified conditions. **(E)** Hodograph of the wind determined by the AROME meteorological model at 10 m above the surface during the UPCAST 2017 measurement period. '*M1*', '*M2*' and '*M3*' correspond to Mistral events. '*Ew*' refers to easterly wind. **(F)** Bathymetric map at the ADCP B (m). Hodograph of the eulerian current measured by the ADCP B: **(G)** at 22 m depth and **(H)** at 117 m depth. '*Up1*', '*Up2*' and '*Up3*' correspond to upwelling events. '*Re2*' is the relaxation phase of the '*Up2*' upwelling event.

represented on Figures 3C and D ('Up5', 'Up6' and 'Up7'). Upwellings were identified between the 8th and 18th of March (period 'Up5'). Other upwellings were identified between March 31st and April 14th (period 'Up6'). A last event was recorded between April 26th at 16:00 and May 6th at 06:00 (period 'Up7'). The surface layer (Figure 3) exhibited an eastward to southeastward (SE) direction of the current (i.e. along-shore) during Mistral events. Current speeds varied between 0.1 and 0.2 m s^{-1}. Near the seabed (Figure 4), the current direction was northeastward (NE, i.e. onshore) during upwelling events. Current speeds were in the range of 0.05 to 0.2 m s^{-1}. Thus, under non-stratified conditions, the wind controlled the circulation over almost the entire water column. Near the seabed, the current was also influenced by the presence of the Cassidaigne canyon further south, which orientated the flow NE along its axis.

While very few upwellings could be identified during the non-stratified period based on the temperature record at the shelf edge, they emerged clearly in the Hovmöller diagram of v (Figure 4). The vertical shear of meridional (i.e., across-shore) current associated with the upwelling showed a 2-layer water column. The shearing interface was located between 40 and 70 m depth.

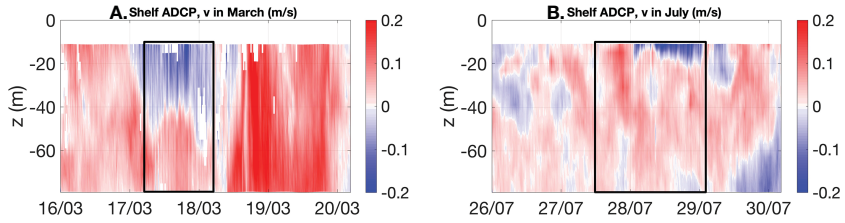

FIGURE 4
Meridional current (m s^{-1}) measured by the shelf ADCP: **(A)** in March and **(B)** in July. The boxes indicate upwelling events.

Under stratified conditions (from May to October), upwellings were observed for Mistral forcing of more than 14 m s^{-1} both during the 2017 and 2019 cruises. 5 days per month of upwelling events were recorded on average. In August-September 2017, three strong Mistral events able to trigger upwelling occurred from August 18th to August 21st, from August 30th to September 3rd and from September 6th till the end of the cruise ('M1', 'M2' and 'M3' on Figures 2, 3E). Over the same period, three upwellings have been identified on the shelf west of the canyon (Figure 3 and 'Up1', 'Up2' and 'Up3' on Figures 2, 3G, H). In particular, the 'Up3' upwelling was generated by the 'M3' Mistral event disrupted by short-time southerly wind pulses. It resulted in a temperature oscillation (Figure 2) on the shelf making it difficult to precisely identify the duration of the upwelling. It probably lasted more than 15 days. Thus, it was a particularly long phenomenon compared to other processes generally observed in the region.

Near the surface, currents on the shelf both west and northeast of the canyon orientated quickly to the wind direction during stratified conditions. Northeast of the canyon, currents were directed NE and varied between 0.1 and 0.2 m s^{-1}. West of the canyon, currents were either southwestward (SW, i.e. offshore, 'Up1' and 'Up3') or eastward (i.e. along-shore, 'Up2') and varied between 0.03 and 0.1 m s^{-1}. Near the bottom, the canyon impacts the local circulation. Northeast of the canyon, a SE residual current was recorded. It probably corresponded to an upwelling jet induced by an outflow from the eastern lobe of the canyon. Currents varied between 0.03 and 0.15 m s^{-1}. West of the canyon, the 'Up1' and 'Up2' upwelling events were characterized by a NE (i.e. onshore) current as a probable channelization of the flow in the vicinity of the canyon. Currents varied between 0.01 and 0.1 m s^{-1}. While current speeds were almost the same in the surface and the bottom layer in non-stratified conditions, they are weaker in the bottom layer in stratified conditions. The stratification restricts vertical mixing and hence the development of the Ekman Layer and the impact of wind in the bottom layer. The maximum contribution of upwelling processes to offshore surface layer velocity both to the west and to the northeast of the canyon can be evaluated using equations 1 and 2 in the range of 0.008 m s^{-1}. This result, estimated in a simplified case considering a constant wind, provides an estimate of magnitude of the current created by offshore winds. It is estimated to be negligible compared to the transient coastal currents generated by the wind.

Under stratified conditions, the shear pattern was not evident to detect as the offshore component of the current was confined in the surface mixed layer and was beyond the range of the ADCP (Figure 4). However, upwellings led to a drop in surface temperature (Figure 5). The most important temperature decrease was recorded during the 'Up2' upwelling event with a drop of 10°C at 11 m depth as found by Fabri et al. (2017) for a similar event in 2013.

Following an upwelling event under stratified conditions, the water column whose temperature initially decreased tends to warm up again to a threshold value. This transition phase is the relaxation from the upwelling. From the current hodographs (Figures 3G) and stickplots (Figures 5A), the currents reversed their direction from upwellings' active phase during the relaxation phase ('Re1', 'Re2' and 'Re3' on Figures 2, 3G, H, 5).

3.1.2 Easterly winds and NC intrusion events

In general, NC intrusion events are more frequent in autumn-winter than in spring-summer. In 2019, the MENOR model indicated an occurrence of 4 days per month of NC intrusion in stratified conditions and 9 days per month in non-stratified conditions as shown by Casella et al. (2020). NC intrusions occur under easterlies or during the relaxation of Mistral events. Near the surface, the northwestward (NW) direction of the current recorded by the shelf ADCP (CASSISED 2019) northeast of the canyon head was due either to easterlies or to NC intrusions ('Ew' and 'NC' on Figures 3C) both under stratified and non-stratified conditions. For example, a NC intrusion event 'NC' occurred on April 22nd 2019 (i.e. in non-stratified conditions) under easterlies. At the same time, the shelf ADCP recorded maximum current speeds of 0.41 m s^{-1} at 14:00 in the surface layer and 0.4 m s^{-1} at 23:00 in the bottom layer (not shown).

On October 24th (i.e. under stratified conditions), the strongest NC intrusion event observed in 2019 was recorded (Figure 6). This event occurred after a south-easterly storm of more than 15 m s^{-1} from October 22nd to October 23rd. The NC intrusion led to a supply of warm water at 86 m depth on the shelf leading to an increase of the temperature from 20 to 20.25°C near the surface and from 17.9 to 20.25°C at the deepest water layers (Figures 6B). This event also contributed to a homogenization of the current recorded along the 80 m depth of the water column at the measurement location (Figures 6D). The shelf ADCP recorded maximum current speeds of 0.36 m s^{-1} at 12:00 in the surface layer and 0.3 m s^{-1} at 14:00 in the bottom layer. NC intrusion events contributed to facilitate the vertical mixing even in stratified conditions.

3.2 Circulation inside the canyon

The CASSISED 2019 experiment provided a unique opportunity to study the currents in the deeper water layers along the canyon. Three locations were investigated: the canyon head, the canyon gorge

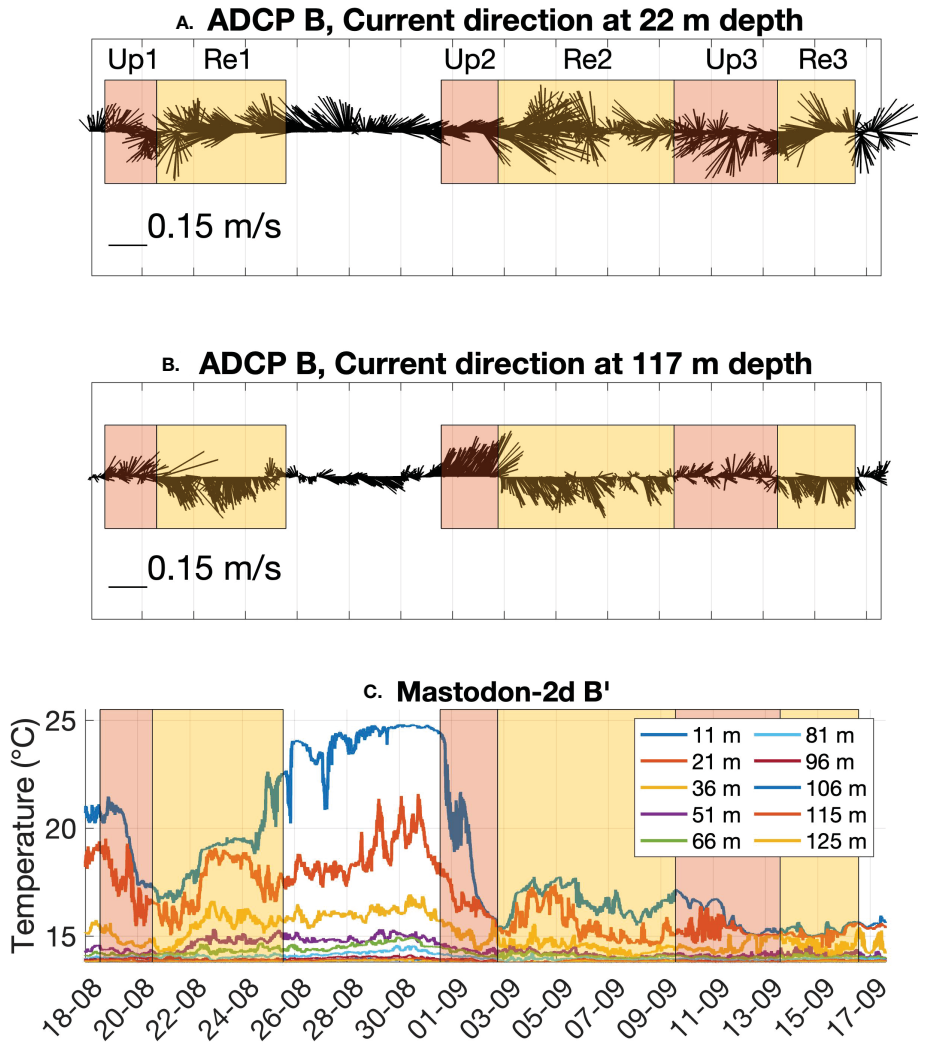

FIGURE 5
Current direction and speed measured by the ADCP B: **(A)** at 22 m depth and **(B)** at 117 m depth. The stickplots point in the direction of the current. **(C)** Temperature records (°C) measured by the Mastodon-2d B' thermistor line during the UPCAST 2017 cruise for each sensor. The red boxes '*Up1*', '*Up2*' and '*Up3*' correspond to upwelling events. The yellow boxes '*Re1*', '*Re2*' and '*Re3*' refer to the corresponding relaxation phases.

and the lower canyon. Averaged Eulerian hodographs were plotted at each location to evaluate the direction of residual currents and their fluctuations (Figure 7).

3.2.1 In the canyon head

The canyon head was studied using the PG1 mooring (from 13 to 93 m above the sea floor at 422 m depth, Figure 7, Table 1). It was located at the northeastern branch of the canyon head in a constrained area of about 1 or 2 km wide. Along-canyon currents V_{along} ranged from 0.04 to 0.08 m s^{-1}. Cross-canyon currents V_{cross} were slightly weaker and ranged from 0.03 to 0.06 m s^{-1}.

The orientation of the current was evaluated under non-stratified and stratified conditions (Figure 7). Under non-stratified conditions, a residual NW (i.e. cross-canyon) current was recorded. Under stratified conditions, the circulation was characterized by a residual northward current in May and an up-canyon residual NE (i.e. along-canyon) current during the rest of the measurement period. Finally, the high frequency components of the current were oriented in the same direction as the canyon axis. These results suggest that the local circulation at the canyon head is strongly dependent on the stratification. The current seemed to be mainly modulated by the general circulation or by oscillatory current under non-stratified conditions. Under stratified conditions, water masses movements were limited by the density differences between the surface and the seabed. Currents at the canyon head appeared to be mainly modulated by the canyon morphology, favoring an upward or downward along-canyon flow. It suggests that the canyon favors vertical mixing under stratified conditions.

The Fourier transform of V_{cross} and V_{along} (see Figures S2A, S2B) showed dominant peaks around 0.7 day period (17 h) under non-stratified conditions. The same result was obtained for V_{along} under stratified conditions. The flow at the canyon head was strongly modulated by along-canyon near-inertial fluctuations as figured in Figures 7, 8A, B and on the V_{along} averaged over the water column in March (Figure 9). This result is consistent with the findings of Flexas et al. (2002) on near-inertial currents at 240 m depth on the shelf. Conversely, V_{cross} Fourier transform under stratified conditions

showed a clear peak at 2.6 days period, as a probable impact of the NC mesoscale activity (Conan and Millot, 1995; Flexas et al., 2002).

3.2.2 In the canyon gorge

The canyon gorge was studied using the PG2 mooring (from 32 to 72 m above the seafloor at 1628 m depth, Figure 7, Table 1). It was located in a 2 km wide narrowing area. A constant up-canyon component was recorded during the entire measurement period (Figure 7). It was generally reinforced during upwelling events (Figure 8). Under non-stratified conditions, residual currents were characterized by a NW displacement of 80 km in 2 months resulting in a residual current of about 0.015 m s^{-1}. Under stratified conditions, residual currents were weaker. They were marked by a NW displacement of about 100 km in 4 months resulting in a residual current of about 0.01 m s^{-1}. V_{along} speed varied in the range 0.02 to 0.1 m s^{-1}.V_{cross} speed varied in the range of 0.02 to 0.08 m s^{-1}. Then, residual currents under stratified conditions represented almost 10% of the V_{along} and V_{cross} transient oscillation amplitude.

At some short occasions, the mean flow was reversed and directed down-canyon during relaxation of strong upwellings (e.g. after April 15th), south-easterlies (e.g. on August 5th) or NC intrusions both in non-stratified and stratified conditions. During these events, SE currents were recorded by the PG2 mooring (zoom on Figure 7). This inversion of the flow was also observable on the along-canyon Hovmöller diagram shown in Figures 8C.

The Fourier transform analysis of V_{cross} and V_{along} (see Figures S2C, S2D) indicated similar results in non-stratified and stratified conditions. V_{cross} was marked by dominant peaks of about 2.5 days period. V_{along} was marked by dominant peaks of 5 to 6 days period. These results, combined with the V_{along} averaged over the water column in March (Figure 9) suggested that the circulation at the canyon gorge was influenced by the general circulation (between 2 and 6 days period as mentioned by Flexas et al., 2002), near-diurnal oscillations (24 h, March 20th to March 24th) or near-inertial fluctuations (17 h, March 8th to March 12th). The signal at 24 h was less expected as the northern part of the Mediterranean Sea is generally referred to as a mixed semi-diurnal tidal regime.

3.2.3 In the lower canyon

The lower canyon was observed using the Aniitra mooring (from 198 to 269 m above the sea floor at 1906 m depth, Figure 7, Table 1). It was located along the canyon's sedimentary ridge where both V_{along} and V_{cross} currents were weaker than at shallower locations of other ADCPs (Figures 8E, F). Above the abyssal plain, the residual velocity was westward (Figure 7) in the range of 0.003 m s^{-1} in non-stratified period and 0.004 m s^{-1} in stratified period. Additionally, the velocity exhibited a strong variability, with NW (i.e. up-canyon) and SE (i.e., down-canyon) oscillations, partially constrained by the channel, both under non-stratified and stratified conditions. In detail, cycloidal patterns were present, suggesting the transit of eddies. In March and April, the area probably experienced cyclonic structures traveling westward while during summer weaker anticyclonic structures dominated. The turbulent mesoscale bottom circulation, characterized by these eddies,

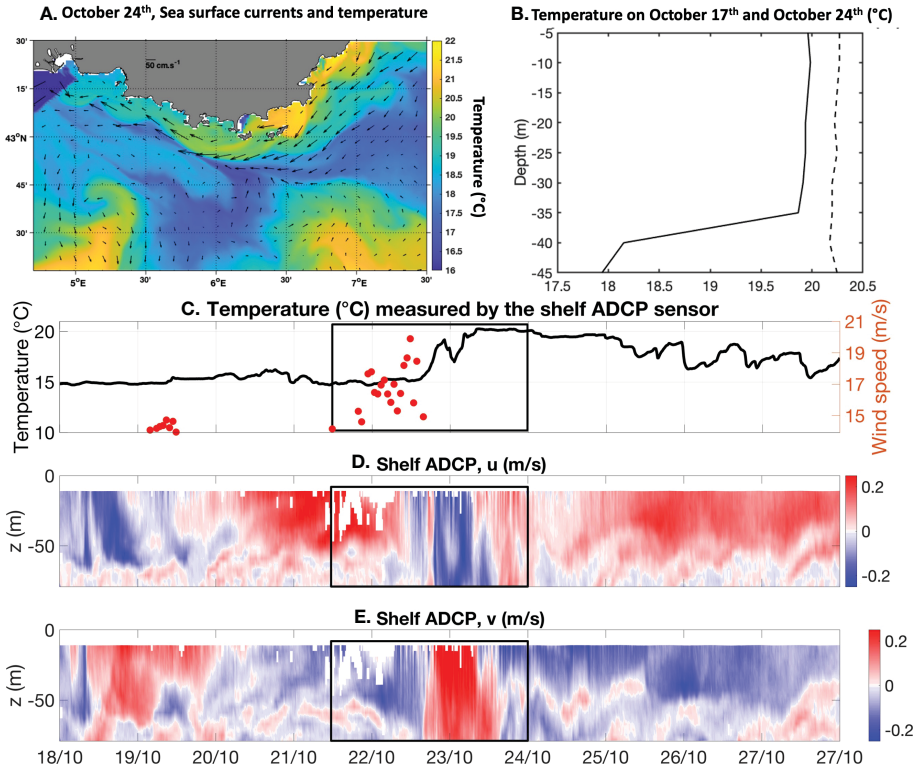

FIGURE 6
(A) Sea surface velocity currents (arrows) and temperature (°C, colors) estimated by the MARS3D MENOR 1200 model on October 24th 2019 at 12:00. **(B)** Temperature profiles measured by temperature sensors at the T-MedNet Cassidaigne station on October 17th at 12:00 (continuous line) before a NC intrusion over the Gulf of Lions and on October 24th at 12:00 (dashed line) during a NC intrusion over the Gulf of Lions. **(C)** Temperature (black line, °C) measured by the shelf ADCP at 86 m depth and wind speed (red dots) estimated by the AROME meteorological model. An easterly storm of more than 15 m s^{-1} started on October 22nd 2019, inducing a NC intrusion event from October 23rd to October 24th 2019. **(D)** Zonal and **(E)** meridional currents (m s^{-1}) measured by the shelf ADCP (CASSISED 2019) from October 18th to October 28th. Both the easterly storm and the NC intrusion event are included in the boxes.

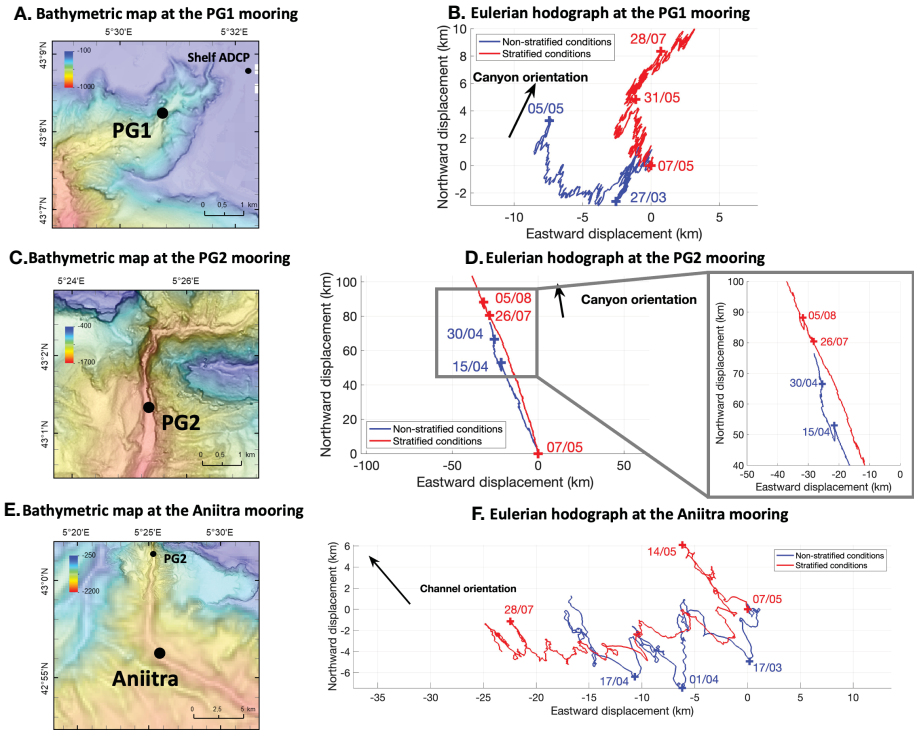

FIGURE 7
(A) Bathymetric map at the PG1 mooring (m). **(B)** Hodograph of the eulerian mean velocity in the bottom layer measured by the PG1 mooring. **(C)** Bathymetric map at the PG2 mooring (m). **(D)** Hodograph of the eulerian mean velocity in the bottom layer measured by the PG2 mooring and zoom on some inversion of the current direction. **(E)** Bathymetric map at the Aniitra mooring (m). **(F)** Hodograph of the eulerian mean velocity in the bottom layer measured by the Aniitra mooring. Blue lines and crosses correspond to non-stratified conditions. Red lines and crosses correspond to stratified conditions.

did not affect the rest of the canyon as there were no such fluctuations on the hodograph at PG2 (Figure 7).

The Fourier transform analysis of V_{cross} and V_{along} (see Figures S2E, S2F) indicated dominant peaks of 3 to 6 days period. Thus, the circulation along the canyon's sedimentary ridge is mainly influenced by the regional circulation.

3.3 Extreme events

From March 9th at 05:00 to March 11th 2019 at 19:00, an upwelling associated with maximum current's intensities of 0.21 m s^{-1} on the shelf was forced by a Mistral event of 17.4 m s^{-1}. During the relaxation of the upwelling, on March 11th at 19:00, the turbidimeter

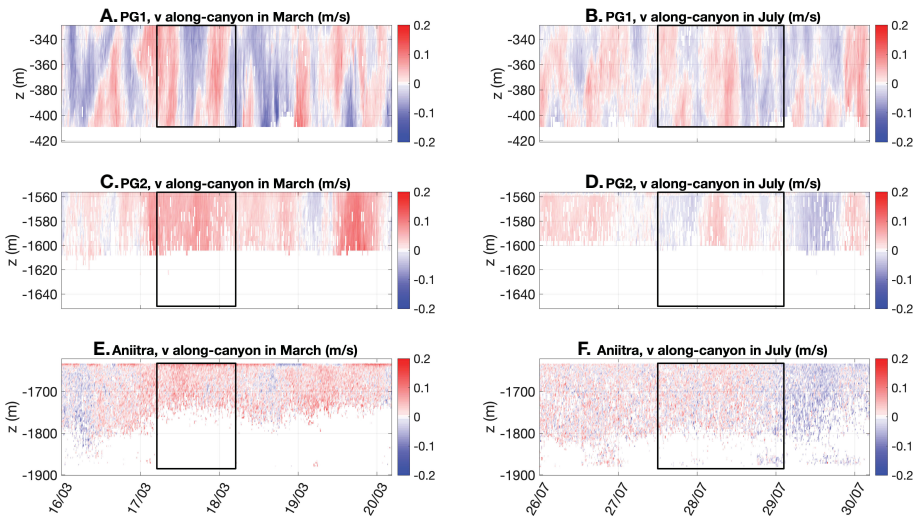

FIGURE 8
Along-canyon current (m s^{-1}) measured by the PG1 mooring: **(A)** in March and **(B)** in July. Along-canyon current (m s) measured by the PG2 mooring: **(C)** in March and **(D)** in July. Along-canyon current (m s^{-1}) measured by the Aniitra mooring: **(E)** in March and **(F)** in July. The boxes indicate upwelling events.

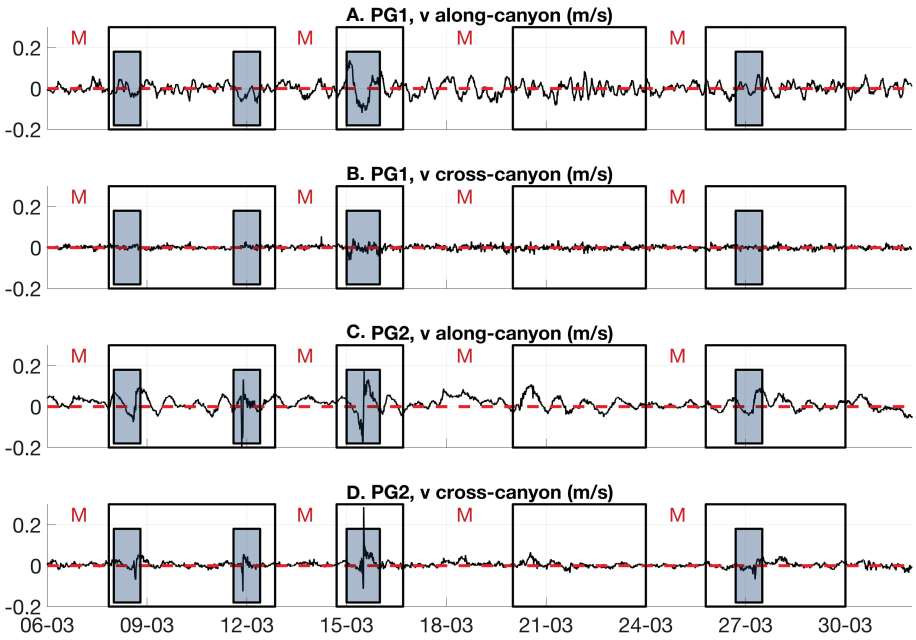

FIGURE 9
Averaged **(A)** along-canyon and **(B)** cross-canyon currents (m s^{-1}) measured by the PG1 mooring in March. Averaged **(C)** along-canyon and **(D)** cross-canyon currents (m s^{-1}) measured by the PG2 mooring in March. The filled gray boxes refer to specific events. The black boxes correspond to the relaxation of Mistral events. 'M' refers to Mistral events occurring over the periods preceding the boxes.

at the canyon head (PG1) did not record any significant event but the turbidimeter at the gorge outlet (PG2) measured a turbid event of 760.5 NTU (Figure 10). The echo intensity signal of the ADCP at PG2 was also strongly affected (Figure 10), revealing a signal characterized by particle entrainment near the sea floor and suspended particles around 1580 m depth for about 20 h from the start of the event. The vertically averaged along-channel current (V_{along}, Figure 9, Table 3) on the bottom layer at the canyon gorge was characterized by a maximum downward velocity of -0.2 m s^{-1} followed immediately by a weaker upward velocity in the range of 0.15 m s_{-1}. A similar pattern was also observed on the cross-channel current (V_{cross}, Figure 9, Table 3) with a decrease reaching -0.13 m s^{-1} (i.e. eastward) followed immediately by an increase reaching 0.06 m s^{-1} (i.e. westward). This turbid event was also detected 6 hours later on the backscatter signal of the deeper Aniitra mooring (Figure 10). As the PG2 and Aniitra moorings were separated by about 11.33 km, the sediment front flowed with a mean velocity of about 0.52 m s^{-1} (Figures 10C).

From March 13th at 07:00 to March 16th at 08:00, another upwelling associated with a maximum current speed of 0.34 m s^{-1} was recorded on the shelf during a Mistral event of 19.8 m s^{-1}. On March 15th at 12:00, a turbid event of lower intensity (turbidity of 5 NTU) was recorded at PG2 (Figures 10F). This event was associated with strong along-canyon and

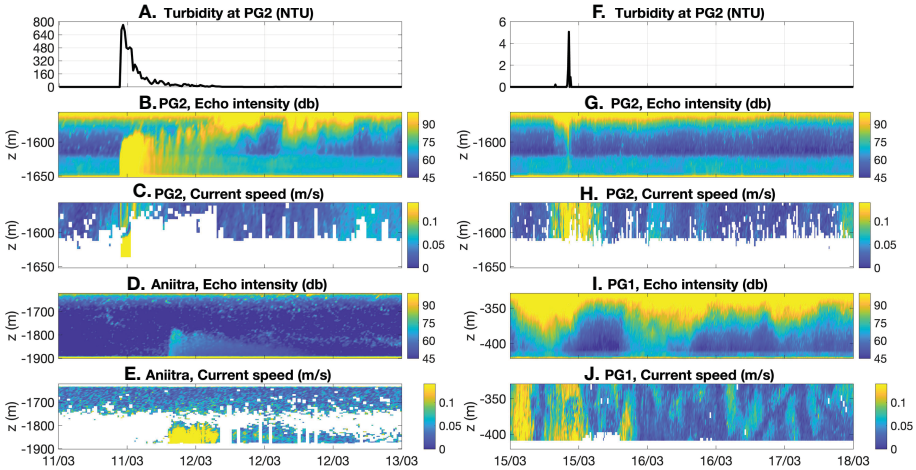

FIGURE 10
From March 11th to March 13th: **(A)** Turbidity (NTU), **(B)** echo intensity (db) and **(C)** current speed (m s-1) measured by the PG2 mooring and **(D)** echo intensity (db) and **(E)** current speed (m s-1) measured by the Aniitra mooring. From March 15th to March 18th: **(F)** Turbidity (NTU), **(G)** echo intensity (db) and **(H)** current speed (m s-1) measured by the PG2 mooring and **(I)** echo intensity (db) and **(J)** current speed (m s-1) measured by the PG1 mooring.

cross-canyon velocities (Figures 9C, Table 3). The V_{along} velocity was first marked by a decrease reaching -0.18 m s^{-1} (i.e. down-canyon) from March 15th at 00:00 to March 15th at 12:00 and then by an increase reaching 0.17 m s^{-1} (i.e. up-canyon). The V_{cross} velocity was characterized by a more important oscillation with a decrease reaching -0.14 m s^{-1} (i.e. eastward direction), and then an increase reaching 0.296 m s^{-1} (i.e. westward direction). An event of strong currents was also recorded on March 15th at 02:00 by the PG1 mooring (Figures 9, 10J). The V_{along} velocity was first marked by an increase reaching 0.12 m s^{-1} (i.e. up-canyon) from March 14th at 17:00 to March 15th at 02:00 and then by a decrease reaching -0.12 m s^{-1} (i.e. down-canyon) until March 15th at 11:00. Although no turbid event was measured by the turbidimeter of PG1, unlike at PG2, the V_{along} velocities measured at the canyon head and gorge (Figures 9A) indicated a co-occurring hydrodynamic process. Moreover, the PG1 backscatter signal experienced high variability in the upper part of the water column (Figure 10). These signals might correspond to suspended particles coming from the shelf and oscillating at near-inertial frequencies in the canyon at the PG1 mooring location, which was found to be mainly influenced by wind forcing (section 3.2.1).

During these two turbid events, both V_{along} and V_{cross} of PG2 were characterized by hourly peaks (Figures 9C).V_{along} and V_{cross} showed a few other velocity pulses that lasted up to one hour. As the sampling rate was 10 min, these peaks were not associated with noise signals. Such an isolated and short time scale event do not correspond to a purely hydrodynamic process. It suggests an interaction with the sedimentary movements despite an increase in the associated turbidity which remained much lower than for the extreme event of March 11th.

4 Discussion

4.1 Residual circulation in the canyon

On the shelf, the current direction in the vicinity of the Cassidaigne canyon head is forced by westerly and easterly winds. It coincides with the wind direction on the entire water column in non-stratified conditions and on the surface layer in stratified conditions (Figure 3). This result complements observations made by Albérola and Millot (2003) in stratified conditions, highlighting the relation of current to wind direction. The wind is able to generate along-shore currents whose direction may induce upwelling or downwelling event in canyons. Previous simulations and numerical approaches compiled by Klinck (1996) emphasized the asymmetry of the geostrophic imbalance effect regarding the along-shore current direction. A left-bounded along-shore current (i.e., southeastward over the Cassidaigne canyon during the Mistral) generates an upward movement in the canyon. Conversely, a right-bounded current (i.e., northwestward during south-easterly winds) contributes to a downward motion in the canyon. On the shelf northeast of the Cassidaigne canyon head near the sea floor and at the canyon head, the along-shore northwestward (i.e., cross-canyon) residual current dominates from March to April, resulting in a weak and vanishing residual downward circulation. During summer, the bottom flow on the shelf northeast of the canyon head is directed southeastward, resulting in an up-canyon (i.e. northeastward) dynamics at the canyon head (Figures 3C , Figures 7A).

At the canyon gorge at 1600 m depth, currents are characterized by a quasi-permanent up-canyon flow both in non-stratified and stratified conditions (Figures 7C). Previous numerical experiments in idealized canyons led by Allen et al. (2001); Kämpf (2006) and Klinck (1996) explained this up-canyon flow as a geostrophic adjustment to barotropic pressure gradient when the current direction is opposed to the Kelvin waves propagation. Thus, having up-canyon flows at the canyon gorge in stratified conditions was expected. The narrow morphology of the Cassidaigne canyon induces a break in the geostrophic balance producing an unbalanced cross-shore (i.e. northeastward) pressure gradient, as mentioned by Allen et al. (2001), which favors up-canyon flows both in non-stratified and stratified conditions. Moreover, the quasi-permanent up-canyon flow observed at the canyon gorge suggests that upward flows can be extrapolated to the canyon body and contrasts with the observations made by Durrieu de Madron (1994), who noticed a dominant down-canyon flow in the Grand-Rhone canyon, due to the right-bounded NC flow. As upwellings are associated with upward movement of water masses, this observation suggests that upwelling may occur in the entire Cassidaigne canyon, from 1600 m depth to the shelf. This result complements numerical analysis led by Kämpf (2006) on an idealized canyon. Kämpf (2006) identified upwellings in most areas of the canyon generating a channeled up-canyon flow from up to 400 m depth onto the shelf. Moreover, Hickey (1997) mentioned a maximum upwelling phase characterized by a permanent up-canyon flow in the full Astoria canyon.

4.2 Transient upwelling and downwelling

Mistral events of more than 15 m s^{-1} in speed generate multiple transient upwellings in the Cassidaigne canyon. Upwellings induce temperature decrease at the surface of up to 10°C (Figure 5). These results agree with the observations made by Hickey (1997) in the Astoria submarine canyon. The author noticed the generation of maximum upwellings, characterized by minimum temperature above the canyon rim, during stronger large-scale left-bounded along-shore winds. First, Hickey (1997) defined a transitory phase characterized by an increasing upwelling inducing a cyclonic flow in the canyon. In our study, there is a lack of data in the inner part of the Cassidaigne

TABLE 3 Maximum current speeds (m s^{-1}) recorded on the shelf and maximum along-canyon V_{along} and cross-canyon Vcross speeds (m s^{-1}) recorded at the canyon gorge during two turbid events on March 11th and March 15th.

Current speeds on March 11th (m s^{-1})					Current speeds on March 15th (m s^{-1})				
Shelf	PG2-V_{along}		PG2-V_{cross}		Shelf	PG2-V_{along}		PG2-V_{cross}	
	Down-canyon	Up-canyon	Eastcanyon	Westward		Down-canyon	Up-canyon	Eastcanyon	Westward
0.21	-0.2	0.15	-0.13	0.06	0.34	-0.18	0.17	-0.14	0.296

canyon to observe the possible deep cyclonic dynamics generated by the stretching of the tube vortex under an upwelling-prone onshore current, as modeled by Kämpf (2006). A numerical modeling of the Cassidaigne canyon at high resolution, using both realistic and idealized cases (bathymetry, forcing) will contribute to the understanding of the impact of hydrodynamic processes on the local circulation of the canyon. It should be noticed that the time scale involved in such processes (e.g. five days for She and Klinck (2000)) and the narrowness of the canyon gorge do not favor the establishment of this characteristic pattern. Second, on the shelf northeast of the Cassidaigne canyon head, a SE trend of the bottom current was recorded under stratified conditions (Figure 3). The separation of the bottom layer from the surface layer results in the generation of a baroclinic upwelling jet, as mentioned by Saldías and Allen, 2020 and Allen et al., 2001. Finally, Hickey (1997) characterized upwelling's relaxation phase by an inversion of the current and a down-canyon flow, as observed in this study (Figures 3G, Figures 5A).

This study showed the dependence of upwelling and downwelling response on stratification and wind direction and speed, both seasonally variable, and the role of upwellings in vertical mixing by bringing cold water to the surface. As stated by Fraysse et al. (2013), from an ecological point of view, upwellings also contribute to the development of benthic and pelagic ecosystems in the canyon. Depending on their duration and associated speed, upwellings contribute to a supply of nutrients at the head of the canyon and can induce phytoplankton blooms.

Even though many studies have already been carried out on upwelling and downwelling in submarine canyons, the *in-situ* measurements conducted in the Cassidaigne canyon bring new information in a regional context, from the shelf at 86 m depth to the deep sea at 1906 m depth. However, the lack of data in non-stratified conditions does not allow to entirely characterize upwelling and downwelling processes in the Cassidaigne canyon. In a global context, these results emphasize the key role of submarine canyons in the generation of small-scale and mesoscale cross-shelf processes that interact with the along continental margin circulation. Depending on the time scales, the strength of the dynamics and the characteristics of the advected material, transport can be upward or downward in canyons. The morphology of submarine canyons is key in the modulation of local bottom circulation. Submarine canyons promote vertical mixing between the deep sea and the continental shelf during upwelling and downwelling events.

4.3 Inertial oscillations

The local circulation in and around the Cassidaigne canyon is modulated by wind forcing. Currents in the canyon head are marked by near-inertial fluctuations around 350 m depth (Figures 8A, Figure 9, Figure S2). In most of the literature, inertial currents were studied on the shelf break under atmospheric forcing (Pollard, 1970; Millot and Crépon, 1981; Font et al., 1995; Flexas et al., 2002; Gonella, 1971 and Petrenko (2003)). Flexas et al. (2002) studied the circulation on the shelf edge and the continental slope off Marseilles. They found more important near-inertial fluctuations at the shelf break than on the shelf at 240 m depth. The borders of the narrow and steep Cassidaigne canyon may favor near-inertial current fluctuations. Under stratified conditions, Petrenko (2003) and Millot and Crépon (1981) observed the generation of two-layer baroclinic inertial currents in the Gulf of Lions under strong wind forcing. Font et al. (1995) also noticed the repeated presence of clockwise current at the near-inertial frequency in the NC at 100 m depth. However, near-inertial fluctuations are observed at the canyon head both under non-stratified and stratified conditions. As the Cassidaigne canyon is located in a microtidal area, the inertia is an important component of the dynamics in the canyon. Unexpectedly, intermittent near-inertial fluctuations are also observed in the along-canyon currents at the canyon gorge, around 1600 m depth (Figure 9, Figure S2). Observation of inertial motion at such depth suggests that the wind also has an impact on the deeper water layers. As the canyon gorge is narrower (almost 2 km width) than the canyon body (almost 6 km width), the Cassidaigne canyon guides and amplifies the inertial waves towards the deep sea inducing stronger flows.

4.4 Northern current intrusion

Near the surface, NC intrusions favor a NW direction of the current on the shelf northeast of the canyon head both under non-stratified and stratified conditions with a seasonally variable occurrence and duration (Figures 3C). This result is similar to the findings by Fabri et al. (2017), who identified NW currents on the eastern part of the shelf around the Cassidaigne canyon due to NC intrusions. The Fourier transform at the canyon head and gorge and near the seabed, revealed the presence of peaks between 2 and 6 days periods which correspond to mesoscale and synoptic variability of the NC as observed by Sammari et al. (1995); Flexas et al. (2002) and Conan and Millot (1995). Near the sea floor, the local circulation may also be influenced by the propagation of bottom topographic Rossby waves characterized by periods longer than 2.5 days, as mentioned by Sammari et al. (1995). In contrast to the circulation in the Grand-Rhone canyon described by Durrieu de Madron (1994; 1999), the NC has a sporadic influence on the Cassidaigne canyon circulation and does not drive downward residual currents but only short lived ones. In addition, during NC intrusion events over the Gulf of Lions, the lower end of the upper Cassidaigne canyon is characterized by a narrowing, preventing any partial intrusion of the NC in the canyon as observed for the other canyons of the Gulf of Lions (Petrenko, 2003).

In a global context, submarine canyons are ubiquitous on continental margins. Residual circulation, transient dynamics and extreme events are all involved in the transport of carbon, heat, nutrients or micro-plastics between the shelf and the deep sea. Submarine canyons are expected to play a key role in the global circulation and in the generation of hydrodynamic processes. The results obtained in the Cassidaigne canyon emphasized an interaction between the canyon and the general circulation, modulated by the canyon's morphology.

4.5 Turbidity current

During the CASSISED 2019 cruise, two turbidity currents were directly observed for the first time at the canyon gorge on March 11th and March 15th (Figure 10). They both occurred during the relaxation

of upwelling events suggesting an interaction between hydrodynamic and sedimentary processes. Even if there is an average up-canyon flow at the canyon gorge, upwelling events tend to reinforce the current speed. They also favor a down-canyon flow during their relaxation, carrying away the sediments to the deep sea. According to Fabri et al. (2017), particles require currents of 0.2 to 0.4 m s^{-1} to be resuspended. At the canyon gorge, along-canyon and cross-canyon currents recorded during these two turbidity currents could reach maximum values between 0.1 and 0.3 m s^{-1} (Table 3) as modelled by Kämpf (2006). Thus, upwelling events occurring at the Cassidaigne canyon are able to move the local sediment in the canyon. The regional circulation may also be able to modify and control the movement of particles near the seabed. Results previously mentioned demonstrated an impact of NC intrusions or bottom Rossby topographic waves near the sea floor.

The turbidity current observed on March 11th is relatively short-lived (2 h at PG2) and propagates with a low velocity of 0.52 m s^{-1} which is comparable to peak velocities observed for flood induced turbidity current in the Mediterranean Var canyon (Heerema et al., 2022). A stronger (1.5 m s^{-1}) and short-lived (6 min) turbidity current was observed under dilute river plume conditions by Hage et al. (2019). As shown by Talling et al. (2022) in the Congo submarine canyon, extreme turbidity events may reach propagations of up to 5 to 8 m s^{-1}. Even if relatively weak, the turbidity current generated in the Cassidaigne canyon under wind relaxation is able to effectively transport sediment stocked in the canyon to the deep sea in an upwelling dominated environment.

The western Gulf of Lions is marked by recurrent dense water cascading events during winter (Estournel et al., 2003 and Ulses et al., 2008) which could also occur in the Cassidaigne canyon. However, the Cassidaigne canyon is located in a small shelf area, which is not favorable to the generation of dense water cascading. The vicinity of the NC inhibits the formation of dense cold water east of the Gulf of Lions and upwelling events are also unfavorable to the accumulation of dense water near the coast.

In a global context, this paper demonstrated that sedimentary processes can be triggered by hydrodynamic processes controlling local sediment transport near the seabed. As submarine canyons are sediment-rich morphologies, the likely link between internal sedimentary and hydrodynamic processes in the Cassidaigne submarine canyon could be extended to other canyons. Fonnesu et al. (2019) found that the bottom circulation will rework the deposits and the transport of the sediments previously brought by turbidity currents in submarine canyons in a general context.

5 Conclusion

The Cassidaigne submarine canyon is located in an active circulation area where water masses are modulated by the wind, the regional circulation and the bottom morphology. The eastern Gulf of Lions is marked by recurrent westerly and easterly winds. On the one hand, south-easterly winds or Mistral's relaxation may favor right-bounded along-shore current, associated with down-canyon flows and NC intrusion events over the Gulf of Lions. NC intrusions lead to a homogenization of the water column in the vicinity of the Cassidaigne canyon. On the other hand, Mistral events of more than 14 m s^{-1} generate left-bounded along-shore current associated with up-canyon flows.

Upwellings are observable throughout the canyon until 1600 m depth. They lead to strong transient dynamics and upwelling-relaxation cycles which are characterized by down-canyon counter currents. In the presence of the canyon, upwelling events promote vertical mixing between the deep sea and the continental shelf by bringing cold water to the surface. In addition, the increase in bottom currents during transients appears to be strong enough to resuspend particles and trigger extreme events such as turbidity currents. This highlights the forcing of sedimentary processes by hydrodynamic processes in submarine canyons.

The Cassidaigne canyon has an atypical morphology that modulates the local circulation. On the shelf near the bottom, the canyon morphology leads to a channelization of the flow under stratified conditions. It also orientates currents in the canyon head under stratified conditions and at the canyon gorge and along the sedimentary ridge independently of the stratification. Both the canyon head and gorge are marked by near-inertial fluctuations. Moreover, the circulation at the canyon gorge, observed for the first time, is characterized by a constant up-canyon flow, stronger under non-stratified conditions, and by near-diurnal oscillations. Unlike other canyons that gradually widen toward the seabed, the Cassidaigne canyon is characterized by a narrow constricting gorge. Thanks to this restricted outlet, a local amplification of currents allowed the observation of quasi-inertial waves in the deep part of the canyon. The canyon acts as a near-inertial wave-trap and downwards guide for the oscillations generated at the surface by the wind.

The observations carried out in the Cassidaigne canyon show the important role of canyons on both local and regional circulation. This knowledge will contribute to improve the understanding of sedimentary processes in the bottom layer, the characterization of benthic and pelagic habitats or the understanding of exchanges between the shelf and the seabed. It will also contribute to improving the representation of submarine canyons in numerical models and thus to deepen their study.

Data availability statement

The raw data supporting the conclusions of this article are available as: Brun Lenaig, Pairaud Ivane, Silva Jacinto Ricardo, Garreau Pierre, Dennielou Bernard (2023). Hydrodynamic dataset from the UPCAST and CASSISED campaigns in the Cassidaigne canyon (NW Mediterranean Sea). SEANOE. https://doi.org/10.17882/92820.

Author contributions

IP carried out the UPCAST 2017 cruise and BD, IP, and RS carried out the CASSISED 2019 cruise. BD realized the bathymetric maps. LB analyzed the data, interpreted the results, designed the figures and wrote the manuscript with critical feedback and help to shape the analysis and the manuscript from all authors. Previous processing of the data were led by IP and RS. All authors contributed to the article and approved the submitted version.

Funding

Ifremer funded the PhD of LB.

Acknowledgments

The authors acknowledge the technical team of the French Oceanographic Fleet (FOF) and the crews of the R/V THETYS II and R/V L'EUROPE for their contribution to the field experiments. The authors also thank Valérie Garnier, Christophe Ravel, Deny Malengros and Christel Pinazo for their help during the UPCAST campaign and Ronan Apprioual, Mikaël Roudaut and Jérémie Gouriou for the mooring deployments during the CASSISED cruise.

Conflict of interest

The authors declare that the research was conducted in the absence of any commercial or financial relationships that could be construed as a potential conflict of interest.

Publisher's note

Supplementary material

The Supplementary Material for this article can be found online at: https://www.frontiersin.org/articles/10.3389/fmars.2023.1078831/full#supplementary-material

References

Ahumada-Sempoal, M. A., Flexas, M. M., Bernardello, R., Bahamon, N., Cruzado, A., and Reyes-Hernández, C. (2015). Shelf-slope exchanges and particle dispersion in blanes submarine canyon (NW Mediterranean sea): A numerical study. *Continental Shelf Res.*, 109:35–45. doi: 10.1016/j.csr.2015.09.012

Albérola, C., and Millot, C. (2003). Circulation in the French mediterranean coastal zone near Marseilles: the influence of wind and the northern current. *Continental Shelf Res.* 23, 587–610. doi: 10.1016/S0278-4343(03)00002-5

Allen, S. E., and Durrieu de Madron, X. (2009). A review of the role of submarine canyons in deep-ocean exchange with the shelf. *Ocean Sci.* 5, 607–620. doi: 10.5194/os-5-607-2009

Allen, S. E., and Hickey, B. M. (2010). Dynamics of advection-driven upwelling over a shelf break submarine canyon. *J. Geophys Res.* 115. doi: 10.1029/2009JC005731

Allen, S., Vindeirinho, C., Thomson, R., Foreman, M., and Mackas, D. (2001). Physical and biological processes over a submarine canyon during an upwelling event. *Can. J. Fisheries Aquat. Sci.* 58, 671–684. doi: 10.1139/cjfas-58-4-671

Alteo environnement Gardanne, A. E (2017). *Gestion/réduction/arrêt*. https://alteo-environnement-gardanne.fr/-Gestion-Reduction-Arret-

Baztan, J., Berné, S., Olivet, J. L., Rabineau, M., Aslanian, D., Gaudin, M., et al. (2005). Axial incision: The key to understand submarine canyon evolution (in the western gulf of lion). *Mar. Petroleum Geology* 22, 805–826. doi: 10.1016/j.marpetgeo.2005.03.011

Casella, D., Meloni, M., Petrenko, A. A., Doglioli, A. M., and Bouffard, J. (2020). Coastal current intrusions from satellite altimetry. *Remote Sens.* 12, 3686. doi: 10.3390/rs12223686

Cavalera, T., Gilli, E., Mamindy-Pajany, Y., and Marmier, N. (2010). Mechanism of salt contamination of karstic springs related to the messinian deep stage. the speleological model of port miou (France). *Geodynamica Acta* 23, 15–28. doi: 10.3166/ga.23.15-28

Ceramicola, S., Amaro, T., Amblas, D., Cağatay, N., Carniel, S., Chiocci, F. L., et al. (2015). Submarine canyon dynamics - executive summary (Monaco: CIESM publisher), vol. 47 of. *CIESM Monograph.*, 47:7–20.

Conan, P., and Millot, C. (1995). Variability of the northern current off Marseilles, western Mediterranean Sea, from February to June 1992. *Oceanologica Acta* 18, 193–205.

Danioux, N. (2018). *2017 French oceanographic cruises report - bilan des campagnes océanographiques francaises 2017 (Ifremer)*. doi: 10.13155/55723 https://archimer.ifremer.fr/doc/00446/55723/

Dauvin, J.-C. (2009). Towards an impact assessment of bauxite red mud waste on the knowledge of the structure and functions of bathyal ecosystems: The example of the cassidaigne canyon (north-western Mediterranean Sea). *Mar. pollut. Bull.* 60, 197–206. doi: 10.1016/j.marpolbul.2009.09.026

DeGeest, A., Mullenbach, B., Puig, P., Nittrouer, C., Drexler, T., Durrieu de Madron, X., et al. (2008). Sediment accumulation in the western gulf of lions, France: The role of cap de creus canyon in linking shelf and slope sediment dispersal systems. *Continental Shelf Res.* 28, 2031–2047. doi: 10.1016/j.csr.2008.02.008

Dennielou, B. (2019). *CASSISED 2019 - 1-3 cruise, L'Europe R/V*. doi: 10.17600/18000904 https://campagnes.flotteoceanographique.fr/campagnes/18000904/

Duhaut, T., Honnorat, M., and Debreu, L. (2008). *Développements numériques pour le modèle MARS*. https://mars3d.ifremer.fr/content/download/49831/file/2008_05_30_INRIA_debreu_final.pdf

Durrieu de Madron, X. (1994). Hydrography and nepheloid structures in the grand-rhône canyon. *Continental Shelf Res.* 14, 457–477. doi: 10.1016/0278-4343(94)90098-1

Durrieu de Madron, X., Radakovitch, O., Heussner, S., Loye-Pilot, M., and Monaco, A. (1999). Role of the climatological and current variability on shelf-slope exchanges of particulate matter: Evidence from the rhône continental margin (NW Mediterranean). *Deep Sea Res. Part I: Oceanographic Res. Papers* 46, 1513–1538. doi: 10.1016/S0967-0637(99)00015-1

Estournel, C., Durrieu de Madron, X., Marsaleix, P., Auclair, F., Julliand, C., and Vehil, R. (2003). Observation and modeling of the winter coastal oceanic circulation in the gulf of lion under wind conditions influenced by the continental orography (FETCH experiment). *J. Geophys Res: Oceans* 108, 8059. doi: 10.1029/2001JC000825

Fabri, M.-C., Bargain, A., Pairaud, I., Pedel, L., and Taupier-Letage, I. (2017). Cold-water coral ecosystems in cassidaigne canyon_ an assessment of their environmental living conditions. *Deep-Sea Res. II* 137, 436–453. doi: 10.1016/j.dsr2.2016.06.006

Flexas, M., Durrieu de Madron, X., Garcia, M., Canals, M., and Arnau, P. (2002). Flow variability in the gulf of lions during the MATER HFF experiment (March–may 1997). *J. Mar. Syst.* 33-34, 197–214. doi: 10.1016/S0924-7963(02)00059-3

Fonnesu, M., Palermo, D., Galbiati, M., Bonamini, E., and Bendias, D. (2019). A new world-class deep-water play-type, deposited by the syndepositional interaction of turbidity flows and bottom currents: The giant Eocene coral field in northern Mozambique. *Mar. Petroleum Geology* 111, 179–201. doi: 10.1016/j.marpetgeo.2019.07.47

Font, J., Garcia-Ladona, E., and Gorriz, E. G. (1995). The seasonality of mesoscale motion in the northern current of the western Mediterranean: several years of evidence. *Oceanologica Acta* 18, 207–219.

Fraysse, M., Pinazo, C., Faure, V., Fuchs, R., Lazzari, P., Raimbault, P., et al. (2013). Development of a 3D coupled physical-biogeochemical model for the marseille coastal area (NW Mediterranean sea): What complexity is required in the coastal zone? *PloS One*, 18. doi: 10.1371/journal.pone.0080012

Gargani, J., and Rigollet, C. (2007). Mediterranean Sea Level variations during the messinian salinity crisis. *Geophys Res. Lett.* 34. doi: 10.1029/2007GL029885

Garnier, V., Pairaud, I. L., Nicolle, A., Alekseenko, E., Baklouti, M., Thouvenin, B., et al. (2014). MENOR: a high-resolution (1.2 km) modeling of the north-western mediterranean sea routinely run by the previmer operational forecast system. *Mercator Ocean Quaterly Newslett.* 49.

Gonella, J. (1971). A local study of inertial oscillations in the upper layers of the ocean. *Deep-Sea Res.* 18, 775–788. doi: 10.1016/0011-7471(71)90045-3

Guihou, K., Marmain, J., Ourmières, Y., Molcard, A., Zakardjian, B., and Forget, P. (2013). A case study of the mesoscale dynamics in the north-Western Mediterranean Sea: a combined data–model approach. *Ocean Dynamics* 63, 793–808. doi: 10.1007/s10236-013-0619-z

Hage, S., Cartigny, M., Summer, E., Clare, M., Clarke, J., Talling, P., et al. (2019). Direct monitoring reveals initiation of turbidity currents from extremely dilute river plumes. *Geophys Res. Lett.* 46, 11310–11320. doi: 10.1029/2019GL084526

Heerema, C., M.J.B., C., Silva Jacinto, R., Simmons, S., Apprioual, R., and Talling, P. (2022). How distinctive are flood-triggered turbidity currents? *J. Sedimentary Res.* 92, 1–11. doi: 10.2110/jsr.2020.168

Hickey, B. M. (1997). The response of a steep-sided, narrow canyon to time-variable wind forcing. *J. Phys. Oceanogr* 27, 697–726. doi: 10.1175/1520-0485(1997)027<0697:TROASS>2.0.CO;2

Jordi, A., Orfila, A., Basterretxea, G., and Tintoré, J. (2005). Shelf-slope exchanges by frontal variability in a steep submarine canyon. *Prog. Oceanogr* 66, 120–141. doi: 10.1016/j.pocean.2004.07.009

Kämpf, J. (2006). Transient wind-driven upwelling in a submarine canyon: A process-oriented modeling study. *J. Geophys Res.* 11. doi: 10.1029/2006JC003497

Klinck, J. M. (1996). Circulation near submarine canyons: A modeling study. *J. Geophys Res.* 101, 1211–1223. doi: 10.1029/95JC02901

Lazure, P., and Dumas, F. (2008). An external-internal mode coupling for a 3d hydrodynamical model for applications at regional scale (mars). *Adv. Water Resour.* 31, 233–250. doi: 10.1016/j.advwatres.2007.06.010

Lazure, P., Le Berre, D., and Gautier, L. (2015). Mastodon mooring system to measure seabed temperature data logger with ballast, release device at European continental shelf. *Sea Technol.* 56 (10), 19–21.

Lofi, J., and Berné, S. (2008). Evidence for pre-messinian submarine canyons on the gulf of lions slope (Western Mediterranean). *Mar. Petroleum Geology* 25, 804–817. doi: 10.1016/j.marpetgeo.2008.04.006

Mauffrey, M.-A. (2015). *Impact des variations du climat et du niveau marin sur les canyons sous-marins du golfe du lion (France) et de la marge de l'Ebre (Catalogne) au cours du plio-quaternaire* (UniversitÃ© de Perpignan, via Domitia). Ph.D. thesis. https://hal.science/tel-01300859/

Millot, C. (1979). Wind induced upwellings in the gulf of lions. *Oceanologica Acta* 2, 261–274.

Millot, C. (1990). The gulf of lions' hydrodynamics. *Continental Shelf Res.* 10, 885–894. doi: 10.1016/0278-4343(90)90065-T

Millot, C. (1997). Circulation in the Western Mediterranean Sea. *J. Mar. Syst.* 20, 423–442. doi: 10.1016/S0924-7963(98)00078-5

Millot, C. (2005). Circulation in the Mediterranean Sea: evidences, debates and unanswered questions. *Scientia Marina* 69, 5–21. doi: 10.3989/scimar.2005.69s15

Millot, C., and Crépon, M. (1981). Inertial oscillations on the continental shelf of the gulf of lions - observations and theory. *J. Phys. Oceanogr* 11, 639–657. doi: 10.1175/1520-0485(1981)011<0639:IOOTCS>2.0.CO;2

Millot, C., and Taupier-Letage, I. (2005). Circulation in the Mediterranean Sea. *Handb. Environ. Chem.* 5, 29–66. doi: 10.1007/b107143

Millot, C., and Wald, L. (1980). The effect of mistral wind on the ligurian current near provence. *Oceanologica Acta* 3, 399–402.

Odic, R., Bensoussan, N., Pinazo, C., Taupier-Letage,, and Rossi, V. (2022). Sporadic wind-driven Upwelling/Downwelling and associated Cooling/Warming along northwestern Mediterranean coastlines. *Continental Shelf Res.* 250 doi: 10.1016/j.csr.2022/104843

Oursel, B., Garnier, C., Pairaud, I., Omanovic, D., Durrieu, G., Syakti, A. D., et al. (2014). Behaviour and fate of urban particles in coastal waters: Settling rate, size distribution and metals contamination characterization. *Estuarine Coast. Shelf Sci.* 138, 14–26. doi: 10.1016/j.ecss.2013.12.002

Pairaud, I. (2017). *UPCAST oceanographic cruise, Thétys II R/V*. doi: 10.17600/17009500 https://campagnes.flotteoceanographique.fr/campagnes/17009500/

Pairaud, I., and Fuchs, R. (2021). *Rapport des campagnes TURBIDENT Leg1 (Mai 2018) et Leg2 (Octobre 2018)*. doi: 10.13155/78596 https://archimer.ifremer.fr/doc/00674/78596/

Pairaud, I., Garnier, V., Ravel, C., Berre, D. L., Leizour, S., and Lazure, P. (2017). "Mastodon-2D deployment in Mediterranean Sea during upcast field experiment," in *Mongoos workshop "Mediterranean Sea observing system"*(Athens, Greece).

Pairaud, I., Gatti, J., Bensoussan, N., Verney, R., and Garreau, P. (2011). Hydrology and circulation in a coastal area off marseille: Validation of a nested 3D model with observations. *J. Mar. Syst.* 88, 20–33. doi: 10.1016/j.jmarsys.2011.02.010

Palanques, A., Guillén, J., Puig, P., and Durrieu de Madron, X. (2008). Storm-driven shelf-to-canyon suspended sediment transport at the southwestern gulf of lions. *Continental Shelf Res.* 28, 1947–1956. doi: 10.1016/j.csr.2008.03.020

Petrenko, A. A. (2003). Variability of circulation features in the gulf of lion NW Mediterranean sea. importance of inertial currents. *Oceanologica Acta* 26, 323–338. doi: 10.1016/S0399-1784(03)00038-0

Pollard, R. T. (1970). On the generation by winds of inertial waves in the ocean. *Deep-Sea Res.* 17, 795–812. doi: 10.1016/0011-7471(70)90042-2

Rennie, S. J. (2005). *Oceanographic processes in the Perth canyon and their impact on productivity* (Curtin University of Technology). Ph.D. thesis. https://espace.curtin.edu.au/handle/20.500.11937/1904

Ross, O., Fraysse, M., Pinazo, C., and Pairaud, I. (2016). Impact of an intrusion by the northern current on the biogeochemistry in the eastern gulf of lion, NW Mediterranean. *Estuarine Coast. Shelf Sci.* 170, 1–9. doi: 10.1016/j.ecss.2015.12.022

Rubio, A., Tailandier, V., and Garreau, P. (2009). Reconstruction of the mediterranean northern current variability and associated cross-shelf transport in the gulf of lions from satellite-tracked drifters and model outputs. *J. Mar. Syst.* 78, S63–S78. doi: 10.1016/j.jmarsys.2009.01.011

Saldías, G., and Allen, S. (2020). The influence of a submarine canyon on the circulation and cross-shore exchanges around an upwelling front. *J. Phys. Oceanogr* 50, 1677-1698. doi: 10.1175/JPO-D-19-0130.1

Sammari, C., Millot, C., and Prieur, L. (1995). Aspects of the seasonal and mesoscale variabilities of the northern current in the western Mediterranean Sea inferred from the PROLIG-2 and PROS-6 experiments. *Deep-Sea Res.* 42, 893–917. doi: 10.1016/0967-0637(95)00031-Z

She, J. M., and Klinck, J. (2000). Flow near submarine canyons driven by constant winds. *J. Geophys Res: Oceans* 105, 28671–28694. doi: 10.1029/2000jc900126

Talling, P., Baker, M., Pope, E., Ruffell, S., Silva Jacinto, R., Heijnen, M., et al. (2022). Longest sediment flows yet measured show how major rivers connect efficiently to deep sea. *Nat. Commun.* 13. doi: 10.1038/s41467-022-31689-3

Ulses, C., Estournel, C., Bonnin, J., Durrieu de Madron, X., and Marsaleix, P. (2008). Impact of storms and dense water cascading on shelf-slope exchanges in the gulf of lion (NW Mediterranean). *J. Geophys Res.* 113. doi: 10.1029/2006JC003795

Würtz, M. (2012). *Mediterranean Submarine canyons: Ecology and governance* (Gland, Switzerland and Malaga, Spain: IUCN).

frontiers | Frontiers in Marine Science

TYPE Original Research
PUBLISHED 16 February 2023
DOI 10.3389/fmars.2023.1099472

OPEN ACCESS

EDITED BY
Veerle Ann Ida Huvenne,
University of Southampton,
United Kingdom

REVIEWED BY
Xiwu Luan,
Qingdao National Laboratory for Marine Science and Technology, China
Chris Goldfinger,
Oregon State University, United States
Elda Miramontes,
University of Bremen, Germany

*CORRESPONDENCE
Stephen C. Dobbs
scdobbs@stanford.edu

SPECIALTY SECTION
This article was submitted to Deep-Sea Environments and Ecology, a section of the journal Frontiers in Marine Science

RECEIVED 15 November 2022
ACCEPTED 06 February 2023
PUBLISHED 16 February 2023

CITATION
Dobbs SC, Paull CK, Lundsten EM, Gwiazda R, Caress DW, McGann M, Coholich MM, Walton MAL, Nieminski NM, McHargue T and Graham SA (2023) Sediment gravity flow frequency offshore central California diminished significantly following the Last Glacial Maximum. *Front. Mar. Sci.* 10:1099472. doi: 10.3389/fmars.2023.1099472

Sediment gravity flow frequency offshore central California diminished significantly following the Last Glacial Maximum

Stephen C. Dobbs[1]*, Charles K. Paull[2], Eve M. Lundsten[2], Roberto Gwiazda[2], David W. Caress[2], Mary McGann[3], Marianne M. Coholich[1], Maureen A. L. Walton[4], Nora M. Nieminski[5], Tim McHargue[1] and Stephan A. Graham[1]

[1]Department of Earth and Planetary Sciences, Stanford Doerr School of Sustainability, Stanford University, Stanford, CA, United States, [2]Monterey Bay Aquarium Research Institute, Moss Landing, CA, United States, [3]Pacific Coastal and Marine Science Center, U.S. Geological Survey, Menlo Park, CA, United States, [4]Ocean Sciences Division, U.S. Naval Research Laboratory, Stennis Space Center, MS, United States, [5]Pacific Coastal and Marine Science Center, U.S. Geological Survey, Santa Cruz, CA, United States

A high-resolution multibeam survey from a portion of the San Simeon Channel (offshore Morro Bay, California) captured a zone of recurring troughs and ridges adjacent to prominent submarine meander bends. Through an integrated study using surveying data, sediment core analysis, radiocarbon dating, and stable isotope measurements, we hypothesize that turbidity current event frequency was higher during the late Pleistocene than at present conditions. We speculate that the rise in sea-level following the Last Glacial Maximum sequestered sedimentation largely to the shelf during the Holocene. This work suggests that the occurrence of sediment gravity flows in this region, particularly away from any submarine channels, is appreciably lower than at times of continental shelf subaerial exposure.

KEYWORDS

submarine channels, offshore California, sediment gravity flows, Last Glacial Maximum, marine geology

1 Introduction

The continental slope offshore Morro Bay (central California; Figure 1) is a proposed site for offshore wind energy development due to its high resource potential from high offshore wind speeds and its proximity to power grid infrastructure (Bureau of Ocean Energy Management (BOEM), 2018). Studies by the Bureau of Ocean Energy Management and the U.S. Geological Survey provided geophysical assessments of offshore fault systems (Walton et al., 2021) and biological habitat characterization (Kuhnz et al., 2021; Cochrane et al., 2022a; Kuhnz et al., 2022) in the region. As noted by Walton et al. (2021), there

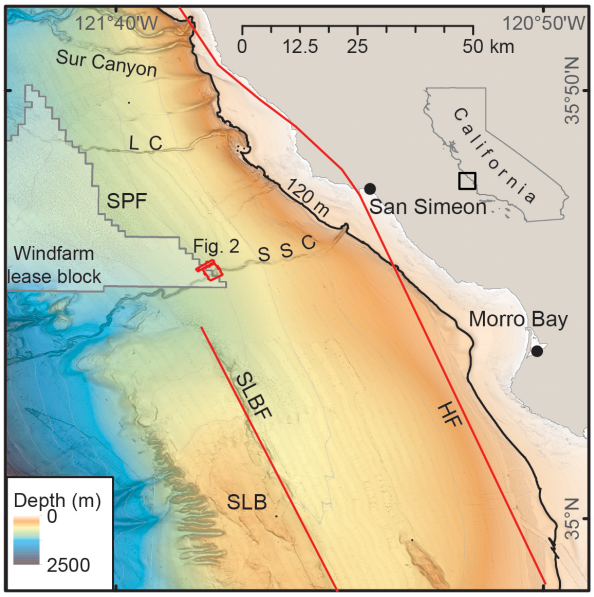

FIGURE 1
Regional map of the Morro Bay continental slope. SSC, San Simeon Channel; LC, Lucia Chica Channel; SPF, Sur Pockmark Field; SLB, Santa Lucia Bank; SLBF, Santa Lucia Bank Fault; HF, Hosgri Fault. Red lines are approximate locations of labeled faults. High-resolution survey and paired sub-bottom profiles of the San Simeon Channel bend highlighted in red outline (Figure 2). Gridded gray polygon outlines the proposed leasing block for offshore windfarm development.

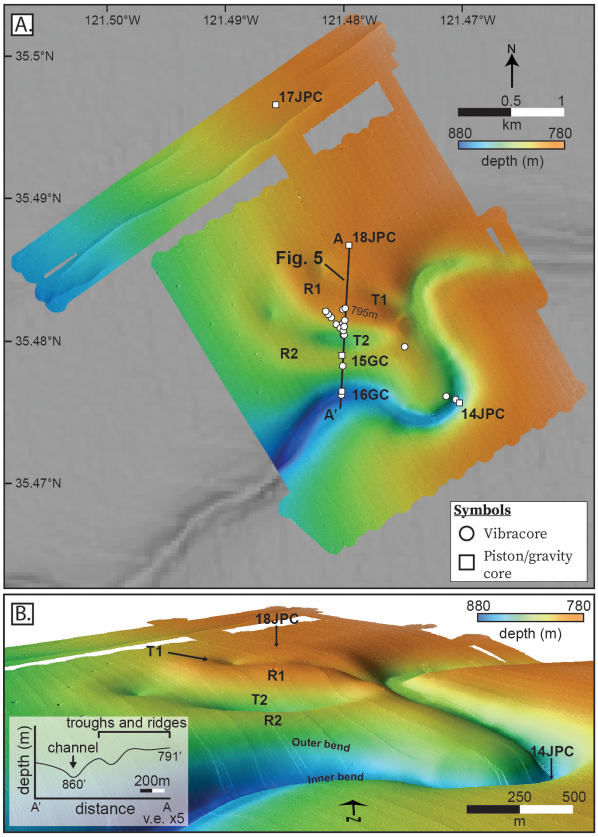

FIGURE 2
(A) Local 1m resolution bathymetric survey of the San Simeon Channel meander bend and adjacent troughs (T1–T2) and ridges (R1–R2). **(B)** Perspective view looking north (vertical exaggeration = 5x) highlighting both the meanders and the trough-and-ridge bathymetry. A-A′ bathymetric profile of trough-and-ridge bathymetry and channel (chirp profile shown in Figure 5).

remains a critical need for understanding the sediment dynamics of the region to evaluate the structural feasibility of offshore wind farm development in the area.

We present an integrated dataset of high-resolution multibeam bathymetry, sub-bottom profiles, sediment core analysis, radiocarbon dates, and stable isotope analysis of seafloor sediments to assess the sedimentation history of the Morro Bay continental slope. Specifically, we focus on a survey that images a meander bend of the San Simeon Channel (Figures 1, 2) and use sediment cores collected in this area to speculate as to the recurrence of sediment gravity flows in the region from the late Pleistocene to present.

2 Geologic Background

The San Simeon Channel is located offshore central California on the northern margin of the Santa Maria basin (McCulloch, 1987; McCulloch, 1989). The structural basin is bounded to the northeast by the Hosgri Fault (Wagner, 1974) and to the southwest by the Santa Lucia Bank Fault that parallels the narrow Santa Lucia Bank structural high (McCulloch, 1989). The San Simeon Channel bisects the southeastern margin of the Sur Pockmark field (Figure 1; Paull et al., 2002). The channel system heads on the outer continental shelf approximately 10 km southwest from the town of San Simeon. The San Simeon Channel appears to be a single confined channel that transects the continental slope until its intersection with a submarine canyon at the edge of the continental slope (Figure 1).

While much of the existing work in this area has focused on the tectono-stratigraphic history of the offshore California margin (e.g., Hoskins and Griffiths, 1971; Irwin and Dennis, 1979; Page et al., 1979; Ross and McCulloch, 1979; Saleeby, 1986; McCulloch, 1987; McCulloch, 1989) and the dextral slip history of the offshore Neogene San Gregorio-Hosgri Fault zone (e.g., Graham and Dickinson, 1978; Dickinson et al., 2005; Johnson et al., 2018), little is known about the submarine geomorphology and sediment transport processes occurring in the area (Paull et al., 2002; Maier et al., 2011; Maier et al., 2012; Maier et al., 2013; Dobbs et al., 2020; Dobbs et al., 2021; Walton et al., 2021).

3 Methods

3.1 Ship-based and AUV mapping and sub-bottom profiling

Prior to 2017, the morphology and structure of the continental slope offshore California from San Simeon to Morro Bay was poorly known. Multibeam, chirp sub-bottom profile, and sparker seismic reflection surveys by the National Oceanic and Atmospheric

Administration (NOAA) hydrographic survey vessels *Rainier* and *Fairweather* during 2017-2019 (Cochrane et al., 2022b) greatly improved the bathymetric model shown in Figure 1. The ship-based bathymetric resolution varies with seafloor depth from about 3 m at the 120 m deep shelf edge to about 20 m at 2000 m depth. Survey-capable autonomous underwater vehicles (AUVs) provide higher resolution topography and sub-bottom profiler data in deep water by operating at a constant low altitude. During 2018-2019, the Monterey Bay Aquarium Research Institute (MBARI) conducted 18 surveys (Kennedy et al., 2021) with its Dorado-class Mapping AUVs (Caress et al., 2008) along the Morro Bay continental slope from R/V *Rachel Carson*. The AUVs were equipped with 400 kHz Reson 7125 multibeam and 1-6 kHz sweep Edgetech chirp sub-bottom profiler sonars. The surveys were flown at a 50 m altitude with a 150 m survey line spacing, producing 1 m lateral resolution bathymetry and sub-bottom profiles penetrating up to 40 m of the subsurface with ~10 cm vertical resolution. Multibeam, sidescan, and sub-bottom profiler data were processed using the open-source software MB-System (Caress et al., 2008), which is capable of processing and displaying swath mapping sonar data. Data processing include editing of multibeam bathymetry, pitch and roll bias adjustment, and various corrections related to tides, navigation and sidescan data. This paper utilizes AUV survey mission 20180427m1 (Figure 2), which maps a bend of the San Simeon Channel.

3.2 Coring surveys

Vibracoring and groundtruthing surveys were conducted from the MBARI R/V *Western Flyer* using the *Doc Ricketts* ROV. Sea-bed video, shallow (<30 cm) push cores, and 1.5 m long vibracores were acquired from the seafloor with the ROV between February and November 2019. Additionally a cruise the R/V *Bold Horizon* collected deep-penetrating (up to seven meters of penetration) piston and gravity cores in September 2019. Three piston cores (14JPC, 17JPC, 18JPC) and two gravity cores (15GC, 16GC) were collected from the San Simeon Channel at the 800 mwd survey (Figure 2). These cores were processed at the U.S. Geological Survey core laboratory in Santa Cruz, California. Cores were cut into 150-cm sections and then ran through a multi-sensor core logger (MSCL) system that measured core depth and width, gamma density, p-wave velocity, loop sensor magnetic susceptibility, and electrical resistivity at 1-cm intervals. Cores were then split and photographed using the MSCL camera. Detailed sedimentological core descriptions were made using these data for each core, which were then sub-sampled for radiocarbon, grain size measurements, and stable isotope analyses.

3.3 Radiocarbon dating

A total of 33 sediment samples were collected for radiocarbon age dating. Sample sites were selected either at equal intervals or directly underneath turbidite horizons to provide a maximum depositional age of sediment gravity flow events. Mixed planktonic or benthic foraminifera were picked from 2-cm thick intervals of sediment. Foraminifera were analyzed at the National Ocean Sciences Accelerator Mass Spectrometry facility at the Woods Hole Oceanographic Institute. The global-average marine record of radiocarbon is ~650 years from 0–11.6 Ka and 750-1000 years further back in time (Heaton et al., 2020). A 59 ± 134-year regional marine radiocarbon reservoir correction (ΔR20) was used for the planktic foraminiferal samples based on 40 samples located from 35° N-40°N in the 14CHRONO Marine 20 Reservoir Database (http://calib.org/marine/), and 1100 ± 200 years for the benthic foraminiferal samples (reinterpretation of Kienast and McKay, 2001 based on Heaton et al., 2020). The CALIB 8.2 software was used to calibrate the ages using the reservoir-corrected values (Stuiver et al., 2022). All ages are reported in calendar years before present. Radiocarbon data associated with this article are compiled in McGann et al. (2023).

3.4 Stable isotope geochemistry and grain size measurements

Piston and gravity cores were sampled for paired grain size and stable isotope analyses. Downcore samples were collected every 50 cm. Where present, selected sand-rich event beds were also sampled at as little as 1 cm spacing. Samples were analyzed for weight percent organic nitrogen ($\delta^{15}N_{organic}$) and total weight percent carbon (TC) by combusting them in tin capsules. The same materials were prepared in silver capsules, acidified with 1N hydrochloric acid to dissolve any inorganic carbon, and remeasured to obtain total weight percent organic carbon (TOC) and $\delta^{13}C_{organic}$.Total inorganic carbon (IC) was calculated as the difference between TC and TOC. Analyses were performed on a Thermo Scientific EA IsoLink IRMS System with a Delta V Advantage coupled to a SmartFlash EA *via* ConfloIV interface at Stanford University. Data were standardized using reference material IAEA-600 (caffeine, -27.771 ± 0.043 ‰VPDB; Coplen et al., 2006). Bulk carbonate $\delta^{13}C$ and $\delta^{18}O$ were measured on a Thermo Scientific MAT252 mass spectrometer coupled to a Kiel III carbonate device. Bulk carbonate $\delta^{13}C$ and $\delta^{18}O$ are reported with respect to VPBD, and $\delta^{15}N$ with respect to air. Accuracy of the isotopic measurements was ensured by using reference material NBS19 (limestone, +1.95 ‰VPDB; Coplen et al., 2006) as a standard.

We used a Beckman-Coulter LS 13320 Laser Particle Size Analyzer (LPSA) at the San José State University Moss Landing Marine Laboratories to measure the distribution of grain sizes in each sample. This instrument analyzes small amounts (0.5–2 g) of sediment and uses combined principles of laser diffraction and polarized intensity differential scattering to resolve grain sizes between 0.04–2000 µm (Beckman Coulter Inc, 2003). These data were then compared between samples by plotting them as frequency distributions.

4 Results

4.1 Bathymetry

The AUV bathymetric survey imaged a portion of the San Simeon Channel from 770–875 mwd (Figure 2). The image reveals a

single confined, moderately sinuous (sinuosity coefficient = 1.48) submarine channel that is approximately 200 m wide. In the upper portion of the survey, channel thalweg to levee relief is ~15 m while the lower portion of the survey reaches reliefs of ~32 m. Three prominent meanders are captured in the survey region, with approximate orthogonal bends in channel directions. Adjacent to the channel between 790-832 mwd is a series of bathymetric troughs and ridges that make up an area measuring ~1.5 km^2 (labeled T1-R1 and T2-R2; Figure 2A). The shallowest trough (T1; maximum relief = 11 m; average side slopes = 5°; Figure 2A) is followed by the most prominent ridge (R1) and trough (T2) pair between 792-832 mwd, which has a maximum ridge-to-trough relief of 38 m and an average side slope 18° (Figure 2A). One more ridge is present in this area (R2), which has a maximum ridge-to-trough relief of 14 m, an average side slope ~7°, and abuts the outer bend of the lowermost meander in the survey. All side slopes are appreciably greater than the regional gradient, which is ~3°.

4.2 Subsurface profiles

A grid of chirp subsurface profiles was oriented approximately orthogonal to the regional gradient, which captured ~40 m of sub-bottom stratigraphy. We divide these reflections based on variations of acoustic properties. The shallowest level of reflections is primarily an acoustically transparent unit ranging from 0–0.01 s (~0–9 m) in thickness (Figure 3). This unit tends to drape over bathymetry in greater thickness where local relief is at a minimum and thins where relief is higher (e.g., toward the ridges and troughs). Below the drape layer is a combination of continuous, high amplitude acoustic reflections that are interbedded with acoustically transparent layers (Figure 3). This acoustic facies makes up most of the out-of-channel stratigraphy. This facies tends to thin away from the channel axis (Figures 3A, B). In some instances, the relatively younger interbedded reflections near the channel appear to have aggraded on top of the relatively older interbedded units (Figures 3C, D). The final acoustic facies is defined by poorly imaged, discontinuous packages of reflections that appear near or at the current channel's location (Figures 3A, B, E–G). This unit appears to be bound to regions proximal to the channel and does not appear in the out-of-channel stratigraphy.

Several important geometric relationships are noted in these profiles. The outer bend of the shallowest meander displays truncation of older, interbedded reflections and is overlain by younger reflections (Figures 3A, B). While the shallowest meander's inner bend records erosion at the margin of the channel that has subsequently been infilled by a combination of discontinuous and interbedded, flat-lying reflections. Interbedded packages near the channel are either truncated at the edge of the channel or dip toward the channel axis. Away from the channel, these interbedded units appear to be either sub-horizontal (Figures 3A, G) or moderately dip away from the channel margins (Figure 3B). The latter case appears to be most common on the side of the channel where the trough-and-ridge bathymetry exists, suggesting that the bathymetric influence of these features may propagate into the regions above and below the zone of troughs and ridges.

Subsurface profiles across the trough-and-ridge bathymetry reveal zones of deformation and truncation. At depths just above T1 near the channel margin, strata appear to be moderately deformed, which then onlap onto truncated, interbedded stratigraphy moving away from the channel (Figure 3C). This deformed unit is overlain by aggradational, interbedded reflections adjacent to the current location of the channel axis (Figures 3C, D). Chirp profiles that capture the maximum relief between the trough-ridge pairs reveal that strata making up the R1-T2 slope appear to be truncated at or near the modern surface of the seafloor (Figures 3D, E). The reflections making up the R2-T2 slope appear to be back-tilted in the direction away from the location of the channel, and onlap on the truncation surface of the R1-T2 slope (Figures 3D, E). At depths below the zone of highest relief created by the ridges and troughs, a truncated surface overlain by interbedded reflections can still be identified propagating into the subsurface (Figure 3F). On the southeastern side of channel, making up an inner bend of a meander, interbedded reflections appear to be truncated and infilled by flat-lying, interbedded reflections (Figures 3E, F). At depths below the bathymetric influence of the ridges and troughs, channel levees appear to be flat lying and do not show signs of deformation (Figure 3G).

4.2.1 Bathymetric and subsurface profile interpretations

We first use the variation in acoustic properties across groupings of the subsurface reflections to make inferences as to the sedimentological character of the subsurface stratigraphy and then make interpretations of the channel's history based on observed geometric relationships. The draping geometry of the acoustically transparent packages making up the shallowest level of stratigraphy suggests that this is a drape layer made up primarily of mud derived from hemipelagic fall out of fine-grained material from the water column (Figure 3). Sediment cores from these layers (discussed in section 4.3) are homogeneously mud. This suggests that the area has received predominantly hemipelagic sediments in recent times and few sediment gravity flows from the channel, an observation noted in other regions across the California continental slope (Paull et al., 2002; Maier et al., 2011; Walton et al., 2021). The interbedded acoustic reflections making up most of the strata are most likely a function of imaging sediment layers with contrasting acoustic impedances such as couplets of sand and mud. These reflections are a most likely a combination of channel levee and overbank deposits. Sediment cores taken from this unit are composed of interbedded fine-grained sand and mud (Figure 3D; section 4.3). The observation that these facies tend to thin away from the channel suggests these are levee and overbank deposits derived from overspilt or unconfined turbidity currents moving down the San Simeon Channel. Discontinuous strata near the channel axis are most likely coarser-grained channel fill facies derived from the densest parts of turbidity currents flowing through the San Simeon Channel. This observation comports with the discovery of coarse-grained shell hash from sediment

10.3389/fmars.2023.1099472

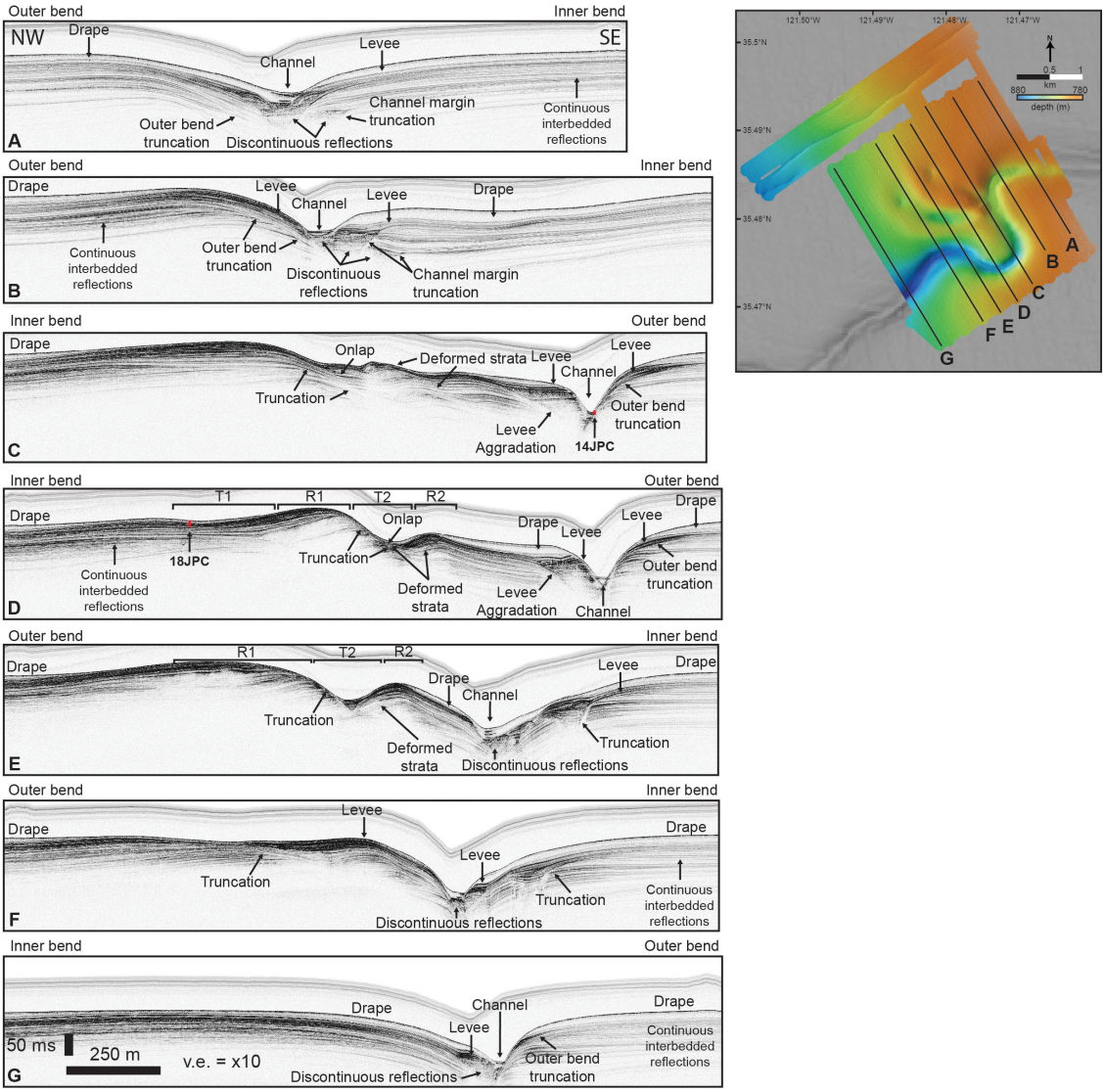

FIGURE 3
Annotated chirp profiles and map view locations from the AUV bathymetric survey. Locations of 14JPC and 18JPC (Figure 5) and approximate penetration depths are noted by the red rectangles. All profiles from left to right trend from northwest to southeast. **(A–G)** refer to the location of the cross sections relative to the plan view survey image (right).

cores sampling the channel thalweg (Figure 3C; section 4.3). Location of channel fill facies appears to have migrated away from the inner bends of meanders, causing an increase in channel sinuosity over time (Figures 3A, B). This is also indicated by the presence of truncated levee strata at the outer bends of channel meanders (Figures 3A–D) and aggradational levee facies on the inner bends (Figures 3C, D). These observations combined suggest that channel movement was accommodated *via* deposition on the inner bends and erosion on the outer bends.

The presence of deformed levee and overbank deposits and a zone of truncated strata at the R1-T2 slope suggests that some amount of structural deformation has occurred in this location. Back tilting and onlapping of R2 strata onto the R1-T2 slope and the difference in height of R2 relative to the crest height of R1 suggest that normal fault movement may be responsible for the current trough-and-ridge bathymetry (Figures 3C–F). Truncation of levee strata making up an inner bend of a meander in the deeper portion of the San Simeon Channel survey may be a channel cut that was later infilled with flat-lying levee deposits (Figures 3E, F). Alternatively, this feature could be a surface where channel-wall failure occurred. For a more detailed discussion as to the possible origin of these features, please refer to the supplemental text.

4.3 Sedimentology and radiocarbon age results

Sediment cores collected throughout the San Simeon Channel survey reveal that the continuous, interbedded acoustic reflections captured from chirp profiles are associated with interbedded fine-grained sand beds and muds while transparent reflections draping the upper portion of the surface are made up of muds. Piston core

14JPC penetrated ~4.5 m of sediment within the axis of the channel (Figure 3C). Three prominent sand beds were identified in this core, ranging from 10–23 cm in thickness (Figure 4). These sands are defined by sharp basal contacts that fine-upward, which are characteristic of turbidite sequences (Bouma, 1962). The lowermost sand bed is interbedded with fine-grained sand and medium to coarse-grained shell hash material. Occasional mud-filled burrows and mottled textures found within these units suggest that these beds were moderately bioturbated (Figure 4). A calibrated radiocarbon age of 5.72 Ka below the first sand bed provides a Holocene maximum depositional age for this event. The two other sand beds are bracketed by Pleistocene radiocarbon ages at 19.1 and 33.5 Ka, respectively.

Both a vibracore transect and two piston cores were taken outside of the channel to characterize the sedimentology of the ridges and troughs (Figures 2A, 4). Piston core 18JPC penetrated ~7 m of sediment at the bathymetric high of the trough-and-ridge bathymetry (Figures 2A, 3D, 4). This core contained at least 42 individually identified sand beds ranging from <1 to 10 cm in thickness. Many of these beds have sharp boundaries into underlying muddy units. Sand beds and overlying muds commonly have mottled textures suggestive of extensive mixing from bioturbation. We interpret these sand beds to be of sediment gravity flow in origin due to their sharp bases and grain size. Six calibrated radiocarbon ages sampled underneath sand beds constrain the timing of events to the Pleistocene (13.8–37.5 Ka). Vibracores collected down a transect of the exposed strata on the R1-T2 slope reveal that, similarly to 18JPC, these sediments are made up of interbedded muds and fine-grained turbidites (Figure 5). The calibrated radiocarbon ages of samples from underneath sand beds become progressively older down-dip of the exposed strata, which range from 18.8 Ka at the crest of R1 to >50 Ka midway down the R1-T2 slope (Figure 5). Piston core 17JPC penetrated ~7 m of subsurface stratigraphy near the northern edge of the survey. This core is made up entirely of mud and clay, with no obvious signs of sedimentation styles other than hemipelagic deposition. This observation is consistent with the chirp profiles, which identified the drape dominant layer as being up to 9 m thick in this region. Three calibrated radiocarbon ages sampled at 0.36 m, 3.5 m, and 7.0 m yield ages of 1.02 Ka, 12.9 Ka, and 21.9 Ka, respectively.

To provide an approximate sedimentation rate for each core, we used a linear regression of depth versus age for each sediment core with ≥2 radiocarbon samples. Modeled ages were extrapolated from the regression to assign age estimations of sediment intervals in the cores. The radiocarbon results from both sand-rich and mud-rich cores from the San Simeon piston and gravity cores yield an average sedimentation rate of 19 cm/ky, which is similar to the results from other samples taken from the Morro Bay slope (18 cm/ky; Figure 6; Coholich et al., 2022; Lundsten et al., 2022). Within uncertainty, there is no observed variation in sedimentation rates between sandy and muddy cores, and rates appear to be approximately linear.

4.4 Stable isotope geochemistry

We report 129 analyses of bulk sediment samples for stable isotopic analysis of total organic carbon (TOC), $\delta^{15}N_{organic}$, $\delta^{13}C_{organic}$, C:N values, and bulk carbonate values of $\delta^{13}C_{carbonate}$ and $\delta^{18}O_{carbonate}$ from piston and gravity cores 14JPC, 15GC, 16GC, 17JPC, and 18JPC. Mean weight percent organic carbon from all analyses is 1.6%. At each site TOC values decrease with depth. Isotopic $\delta^{15}N_{organic}$ values range from 3.51–8.56‰, with an average value of 6.09‰. In addition, $\delta^{15}N_{organic}$ values tend to decrease down core. Analyses of $\delta^{13}C_{organic}$ range from -23.46 to -21.69‰ with an average of -22.45‰. On balance, $\delta^{13}C_{organic}$ values become more negative down core. Ratios of C:N range between 8.37–23.02 with a mean value of 11.20. Delta $^{13}C_{carbonate}$ and $\delta^{18}O_{carbonate}$ values range from -7.96‰ to -0.04‰ and -6.54‰ to 2.64‰, respectively. Values of $\delta^{13}C_{carbonate}$ tend to become less negative downcore while $\delta^{18}O_{carbonate}$ becomes more positive.

5 Discussion

5.1 Sand frequency variation between the Holocene and Pleistocene

Sand beds were counted in each core and assigned an age according to their modeled regression age and then plotted as a histogram and kernel density estimate function of sand bed occurrences from all the sediment cores with age data (Figure 7). We test the null hypothesis that the above sand occurrence distribution is not significantly different from a randomly distributed Poisson function. A χ^2 test statistic measuring the difference between a Poisson distribution centered at the mean of observed sand bed occurrences returns a p-value < 1 x 10^{-15}. Thus, we can reject the null hypothesis that these data are not significantly different from each other.

The peak of these data is centered at approximately 23 Ka, with ~70% of all sand intervals between 18–25 Ka. This corresponds with the most recent sea-level lowstand, the Last Glacial Maximum. Widely used sequence-stratigraphic models (e.g., Vail et al., 1977) suggest that submarine canyon and fan deposition will occur in its greatest amounts during sea-level lowstands, when continental shelves are subaerially exposed and fluvial systems are able to connect directly with submarine canyons at the shelf edge. Several exceptions, however, have been noted wherein submarine canyon and fan systems are able to continue to deposit material during the most recent highstand (e.g., La Jolla Fan, southern offshore California; Covault et al., 2007; Normark et al., 2009; Sharman et al., 2021). This depends on several factors, including the width of the continental shelf, canyon-head intersection with littoral current cells, and/or the amount of sediment flux from fluvial sources for canyon systems to persist throughout sea-level highstands. The shelf edge distance from shore is relatively far at approximately 8 km from the head of the San Simeon Channel (Figure 1). Moreover, likely fluvial sources for the San Simeon Channel are small coastal catchments a part of the Santa Lucia Range, which do not include sources from large, regional rivers. Combined, this suggests that the limiting factor to channel activity at the San Simeon Channel is access to a terrestrial source. Given that the shelf only begins to widen a short distance (~30 km) north of the San Simeon Channel, it is unlikely that south-directed littoral cells are robust enough to

10.3389/fmars.2023.1099472

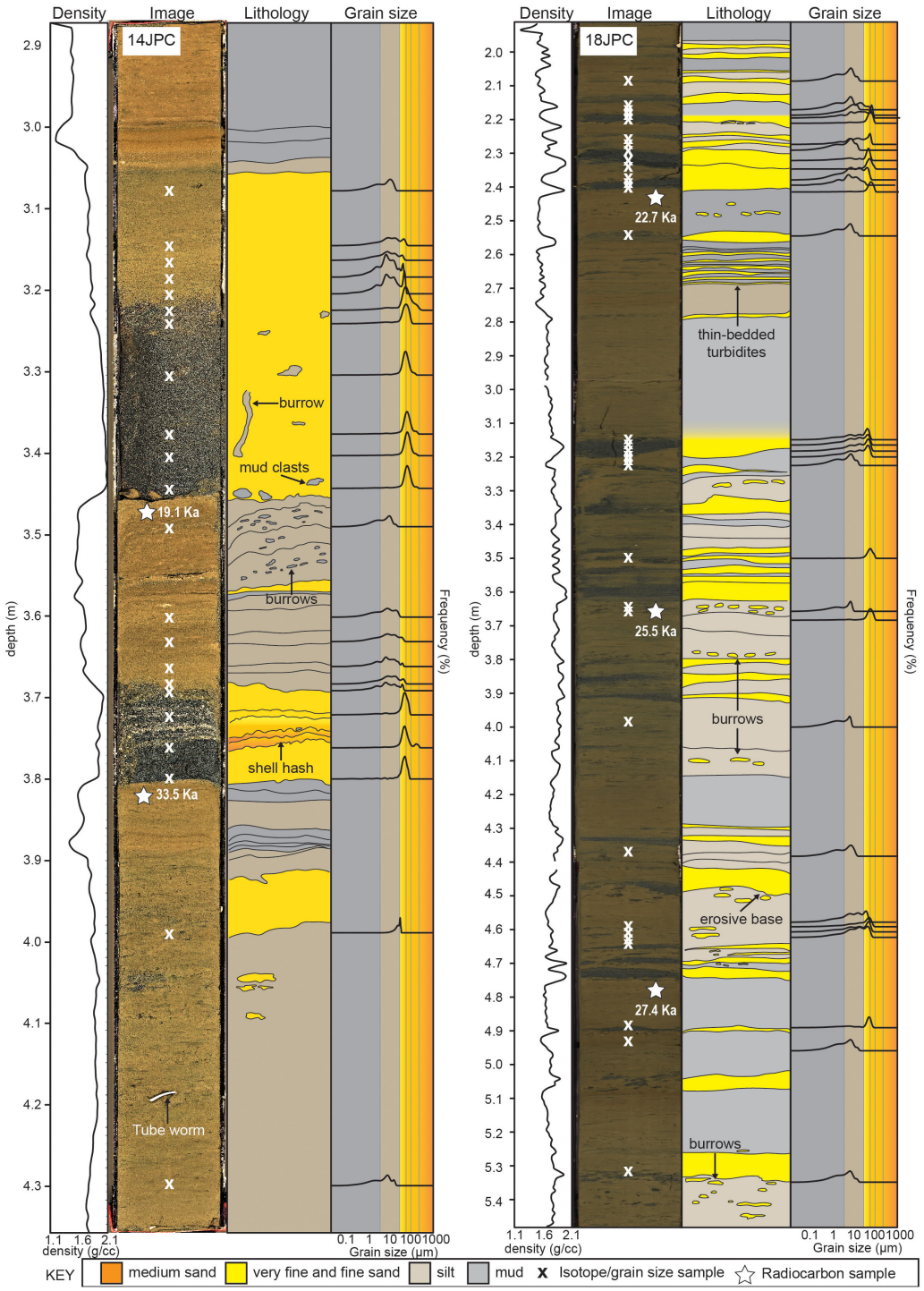

FIGURE 4
Density logs, photographs, descriptions, and grain size frequency plots of jumbo-piston cores 14JPC and 18JPC. Xs mark the sample location for both grain size and isotopic analyses. Stars mark radiocarbon sample locations. Note these are selected portions of the cores, not the entire cores. The apparent variation in core color between 14JPC and 18JPC is a function of camera settings when photographs were collected and not indicative of difference between material.

move sufficient quantities of sediment to maintain Holocene channel activity that is noted in other channel systems (e.g., Delgada Canyon; Smith et al., 2018). Canyon-fan systems within the Southern California Borderland of similar source catchment size and shelf-edge width have been shown to be most sensitive to fluvial connectivity in order to maintain channel activity (Carlsbad and Oceanside Fans; Sharman et al., 2021). Thus, we suggest that enhanced sand bed frequency during the latest lowstand in the San Simeon Channel is evidence for a sea-level control on sediment gravity flow rates in this region (Figure 8).

10.3389/fmars.2023.1099472

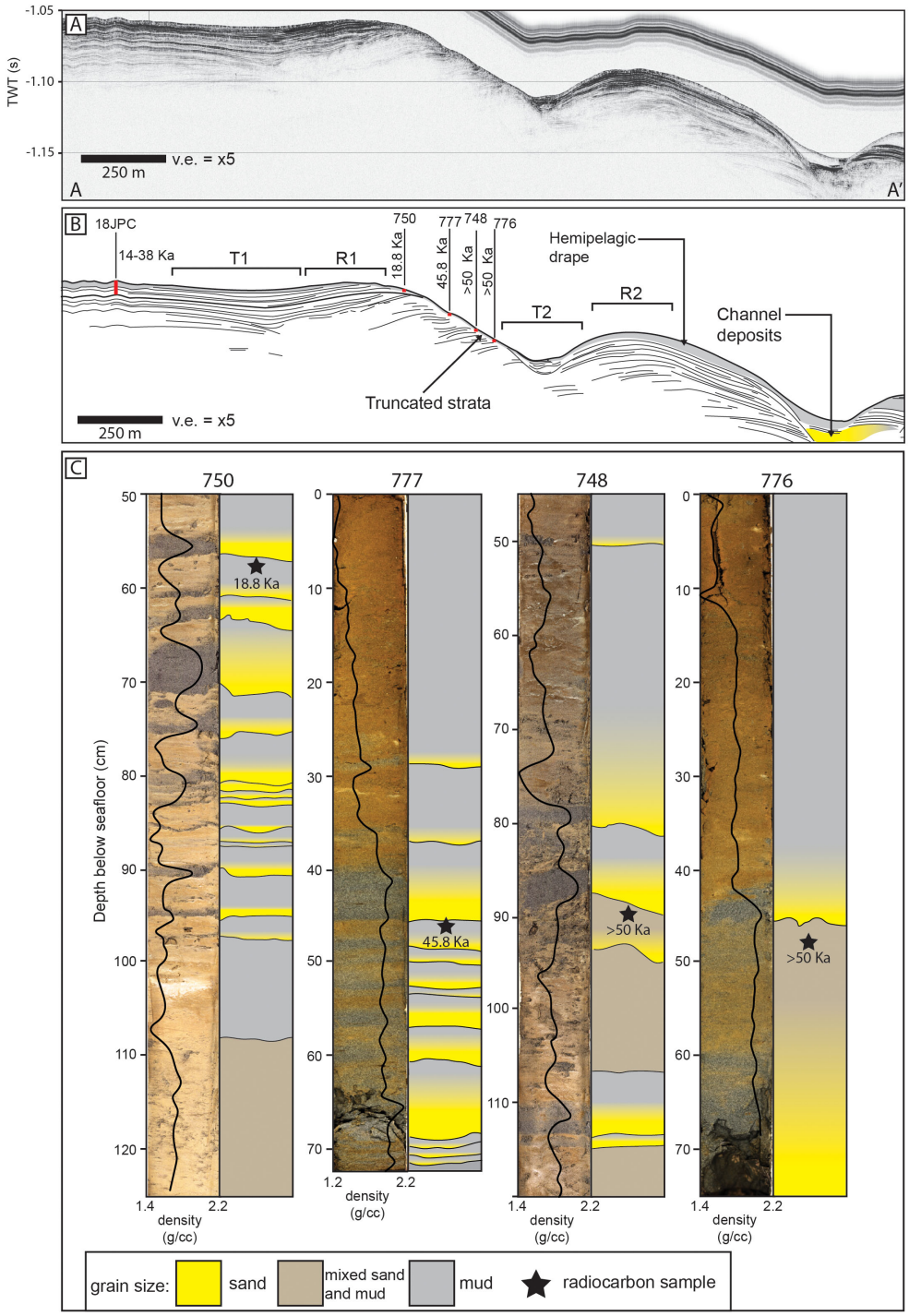

FIGURE 5
(A) Chirp profile perpendicular to approximate strike of the troughs and ridges (vertical exaggeration = x5). Location shown in Figure 2A (A-A'). **(B)** Annotated interpretation of subsurface acoustic reflections from above chirp profile with locations of vibracores (750, 777, 748, 776) and jumbo-piston core 18JPC. Locations of cores and approximate penetration depths are noted by the red rectangles. Note the zone of truncation at the R1-T2 slope that exposes Pleistocene-aged turbidites. **(C)** Images, density logs, and grain size interpretation of vibracores exposed along a R1-T2 surface shown in **(A, B)** Note the high amount of sand beds in all cores. T1, Trough 1; R1, Ridge 1; T2, Trough 2; R2, Ridge 2.

This observed correlation relies on the assumption that our age model accurately reflects the true age distribution of the turbidites. By sampling hemipelagic muds directly below turbidite beds, we have opted to measure a maximum depositional age for the above deposits. However, it is difficult to omit the possibility of varying amounts of erosion of hemipelagic materials by the overlying flows, which can yield artificially older ages (Urlaub et al., 2013). We address this potential complication by plotting our stable isotopic data from hemipelagic samples versus regressed age and comparing their results to local and global isotopic trends (Figure 9). These

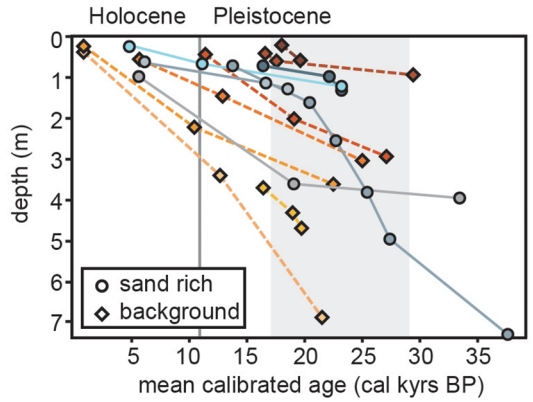

FIGURE 6
Plot of mean calibrated radiocarbon ages versus sample depth. A regression of all ages results in an average sedimentation rate of 19 cm/ky. Gray rectangle indicates approximate timing of the Last Glacial Maximum.

data are from piston and gravity cores taken from the study area, as well as an additional piston core from the Sur Pockmark Field (Figures 1, 2). In these data we see a consistent shift in $\delta^{13}C_{carbonate}$ and $\delta^{18}O_{carbonate}$ commonly associated with the boundary between marine isotope stages 1 and 2 at the termination of the Last Glacial Maximum and the start of sea-level transgression (e.g., Shakun et al., 2015). This same trend is observed in late Pleistocene benthic oxygen and carbon isotopic records offshore central and southern California at ODP sites 1011, 1012, and 1018 (Andreasen et al., 2000). Weight percent of total organic carbon (TOC) also predictably increases ~1% C by weight at the regressed age boundary between MIS 1–2, which is commonly cited as an effect of increased marine derived organics following sea-level rise at the start of the Holocene. The shift to more positive $\delta^{13}C_{organic}$ and $\delta^{15}N_{organic}$ values and a lower mean C:N ratio in younger sediments is indicative of increased sourcing from marine organic matter as the continental shelves became inundated during the Holocene

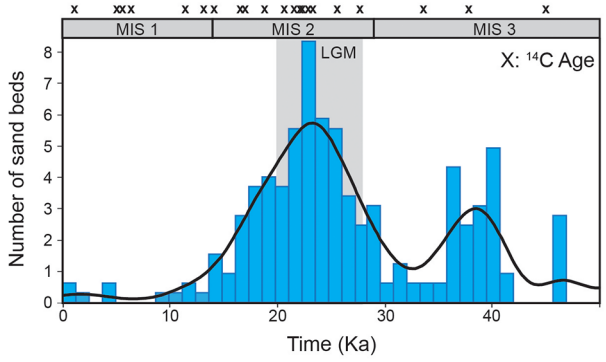

FIGURE 7
Kernel density estimate and histogram of sand occurrences over time from all sediment cores from the San Simeon Channel. Xs mark locations of radiocarbon ages used to calibrate the age regression for the sand beds. Note the increase in sand occurrences centered around the Last Glacial Maximum (gray rectangle; LGM). MIS 1–3, Marine Isotope Stages 1–3.

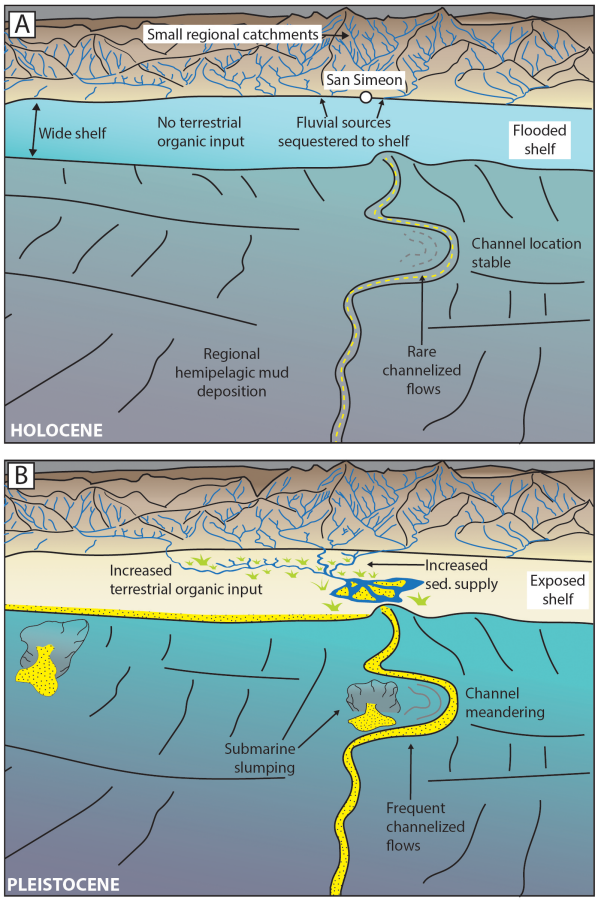

FIGURE 8
Schematic depiction of variation in Morro Bay continental slope sedimentation dynamics between the Pleistocene and Holocene. **(A)** Holocene style sedimentation. Sea-level transgression flooded the continental shelf, preventing deposition onto the slope. A regional hemipelagic drape of mud covered the slope. **(B)** Pleistocene style sedimentation. Lowered sea levels exposed the continental shelf, allowing for fluvial systems to propagate to the shelf edge. Higher rates of sedimentation led to more active channel activity.

transgression (Meyers, 1994). We argue, given our regressed age data appear to match the global paleoenvironmental isotopic trends observed at the Pleistocene–Holocene boundary, that our radiocarbon age data from several sediment cores across Morro Bay can be regressed into a reasonably sound age model. These observations also bolster the hypothesis that the head of the San Simeon Channel had been sequestered to the flooded continental shelf edge by the early Holocene, which lowered the rate of sediment gravity flow occurrence through the system.

Large (M ≥ 7) earthquakes may lead to destabilization of the continental slope and subsequent coeval turbidity currents (Goldfinger et al., 2012). The San Simeon Channel heads near San Gregorio-Hosgri Fault, which has an estimated generative potential of a M7.8 earthquake (Wells and Coppersmith, 1994). Recent geophysical efforts by Walton et al. (2021) offshore Morro Bay found no evidence of Quaternary slip along the Santa Lucia Bank Fault. However, the presence of turbidites captured from sediment cores

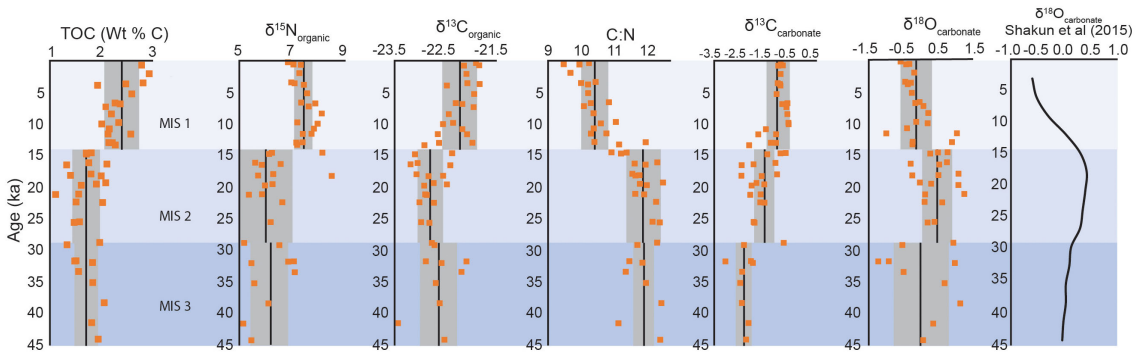

FIGURE 9
Isotopic data of all planktonic foraminifera measured in this study plotted versus regressed radiocarbon ages. Varying hues of blue divide the Marine Isotope Stages 1–3 (MIS 1–3). Averages (black centerlines) and ±1 standard deviation (gray rectangles) are presented for each isotopic stage. Note that the ~1‰ negative shift in $\delta^{18}O_{carbonate}$ corresponds to globally calibrated records of temperature-corrected planktonic isotope curves generated by others (e.g., Shakun et al., 2015).

down slope the eastern flank of the of Santa Lucia Bank (Figure 1)—a zone without a direct connection to submarine channels—suggests that shaking *via* the proximal Quaternary fault systems such as the San Andreas or San Gregorio-Hosgri Faults could have acted as a trigger for mass sediment transport in the region (Walton et al., 2021). Yet, radiocarbon dating of turbidites in the region presented herein did not identify any modern deposits that align with known local and historical earthquakes, such as the 1927 Lompoc, Calif, M7.0 or 1952 Piedras Blancas M6.2 earthquakes (Mueller, 2018). Thus, the lack of correlation between dated turbidites and historical earthquakes precludes any discussion regarding a paleoseismic control on turbidite distributions. Such a hypothesis awaits a broader study that incorporates regional age data from multiple channels on the Morro Bay slope in order to be tested.

5.2 Turbidity current geohazard potential offshore Morro Bay

Sediment gravity flow event frequency has diminished greatly since the Pleistocene. During the Holocene, channelized flows are rare and confined to the San Simeon and Lucia Chica Channels. The predominant sedimentation style during the Holocene is hemipelagic fallout of mud. Thus, the history of the Morro Bay continental slope during the Holocene, away from any submarine channels, has been mostly quiescent. However, a small portion of the proposed wind farm leasing blocks does intersect the San Simeon Channel (Figure 1), which has experienced Holocene flow events.

6 Conclusions

We use an integrated dataset of multibeam bathymetry, sediment cores, radiocarbon samples, and isotopic data to assess how sediment has been mobilized across the Morro Bay continental slope from the latest Pleistocene to present. We note that sand bed distributions counted from sediment cores from the San Simeon Channel cluster around the Last Glacial Maximum. We argue the most likely control for this turbidite clustering is lowstand sea-level during the Last Glacial Maximum. Lowered sea-levels exposed the continental shelf, incentivizing fluvial incisement of the shelf and propagation of shelf-edge deltas. The change in sedimentation style between the Holocene and Pleistocene suggests that modern sediment gravity flow events are rare and restricted to channels.

Data availability statement

The original contributions presented in the study are included in the article/Supplementary Material, further inquiries can be directed to the corresponding author/s.

Author contributions

CP and SG were the primary advisors of the project and were involved in all portions of the manuscript. TM and MC were involved in the sediment core analysis and seismic data interpretation. MM was involved in radiocarbon analysis and sediment core processing. NN and MW were involved in sediment core analysis. MW was also involved in the seismic data interpretation. RG and EL were involved in sediment core processing and data reduction for stable isotopic analyses. EL also produced figure 1 and was integral to data management for the entire project. DC was the primary scientist and engineer responsible for acquiring AUV bathymetry data. All authors contributed to the article and approved the submitted version.

Funding

Support for this work was provided by the David and Lucile Packard Foundation and the Stanford Project on Deep-water Depositional Systems.

Acknowledgments

Thanks to Dave Mucciarone for stable isotopic analyses, the R/Vs *Western Flyer*, *Bold Horizon*, *Rachel Carson*, and the NOAA ship *Rainer* crews, ROV pilots, and AUV operators. Additional thanks to Don Lowe for his assistance with sediment core interpretation. The US Bureau of Ocean Energy Management in part funded the acquisition of sediment cores for this project. Three reviews and three USGS internal reviews improved the quality and clarity of the manuscript. Any use of trade, firm, or product names is for descriptive purposes only and does not imply endorsement by the U.S. Government.

Conflict of interest

The reviewer [CG] declared a past co-authorship with the author [MW] to the handling Editor.

Supplementary material

The Supplementary Material for this article can be found online at: https://www.frontiersin.org/articles/10.3389/fmars.2023.1099472/full#supplementary-material

SUPPLEMENTARY FIGURE 1
(A) Annotated perspective view looking northwest at submarine slump scarp and deposit. Vertical exaggeration = x5. **(B)** Subsurface chirp line Z-Z′ imaging the slip surface and folded allochthonous mass. The presence of a minor depression above the primary slip surface may be evidence of a secondary retrogressive failure surface. **(C)** Enhanced view of inset rectangle in B. Note the contact between the slip surface and slump, which shows potential drag folds.

References

Andreasen, D. H., Flower, M., Harvey, M., Chang, S., and Ravelo, A. C. (2000). ""Data report: late pleistocene oxygen and carbon isotopic records from sites 1011, 1012, and 1018"," in *Proceedings of the ocean drilling program*. Eds. M. Lyle, I. Koizumi, C. Richter and T. C. Moore Jr (College Station, TX: Ocean Drilling Program), 141–144. doi: 10.2973/odp.proc.sr.167.225.2000

Beckman Coulter Inc (2003). *LS 13 230 particle size analyzer manual PN 7222061A* (Miami, Florida: Particle Characterization Group).

Bouma, A. H. (1962). "Sedimentology of some flysch deposits," in *A graphic approach to facies interpretation* (Amsterdam: Elsevier), 168 p.

Bureau of Ocean Energy Management (BOEM). (2018). *Commercial leasing for wind power development on the outer continental shelf (OCS) offshore California (Call for information and nominations) in federal register 83:203 (October 19, 2018) p. 53096* (Camarillo, California: Bureau of Ocean Energy Management. OCS Study BOEM 2021-044), 56 p.

Caress, D. W., Thomas, H., Kirkwood, W. J., McEwen, R., Henthorn, R., Clague, D. A., et al. (2008). "High-resolution multibeam, sidescan, and subbottom surveys using the MBARI AUV", in *Marine habitat mapping technology for Alaska*. Eds. J. R. Reynolds and H. G. Greene (Fairbanks, AK: Alaska Sea Grant for North Pacific Research Board), 47–69. doi: 10.4027/mhmta.2008.04

Cochrane, G. R., Kuhnz, L. A., Dartnell, P., Gilbane, L., and Walton, M. A. (2022b). *Multibeam echosounder, video observation, and derived benthic habitat data offshore of south-central California in support of the bureau of ocean energy management Cal DIG I, offshore alternative energy project* (Santa Cruz, CA: U.S. Geological Survey data release). doi: 10.5066/P9QQZ27U

Cochrane, G. R., Kuhnz, L. A., Gilbane, ,. L., Dartnell, P., Walton, M. A. L., and Paull, C. K. (2022a). *California Deepwater investigations and groundtruthing (Cal DIG) I, volume 3–benthic habitat characterization offshore morro bay, California: U.S. geological survey open-file report 2022–1035* (Reston, VA: Bureau of Ocean Energy Management OCS Study BOEM 2021–045), 18 p. doi: 10.3133/ofr20221035

Coholich, M. M., Paull, C. K., Walton, M. A., Caress, D., McGann, M., Lundsten, E. M., et al. (2022). Mechanisms of sand deposition within the Lucia chica submarinechannel system, offshore California, U.S.A. SEPM virtual bouma conference. (Bouma Deep Water Geoscience Conference: Society of Sedimentary Geology).

Coplen, T. B., Brand, W. A., Gehre, M., Groning, M., Meijer, H. A. J., Toman, B., et al. (2006). New guidelines for delta c-13 measurements. *Anal Chem.* 78 (7), 2439–2441. doi: 10.1021/ac052027c

Covault, J. A., Normark, W. R., Romans, B. W., and Graham, S. A. (2007). Highstand fans in the California borderland: The overlooked deep-water depositional systems. *Geology* 35 (9), 783–786. doi: 10.1130/G23800A.1

Dickinson, W. R., Ducea, M. N., Rosenberg, L. I., Greene, F. G., Graham, S. A., Clark, J. C., et al. (2005). Net dextral slip, neogene San Gregorio-hosgri fault zone, coastal California: Geologic evidence and tectonic implications. *Geol Soc. America Special Paper* 391, 43. doi: 10.1130/SPE391

Dobbs, S. C., Addison, J. A., Cochrane, G. R., Gwiazda, R., Lorenson, T. R., Lundsten, E. M., et al. (2020). Submarine waveform field records enhanced frequency of sediment transport event during the pleistocene, offshore morro bay, California. *Am. Geophys Union*. AGU Fall Meeting Abstracts, EP065-11.

Dobbs, S. C., Addison, J. A., Coholich, M. M., Gwiazda, R., Lundsten, E. M., McGann, M., et al. (2021). Increased frequency of out-of-channel sediment gravity flows are coincident with late pleistocene falling sea-level offshore morro bay, California. *Int. network submarine canyon Invest. Sci. exchange Conf.* 5, 11.

Goldfinger, C., Nelson, C. H., Morey, A. E., Johnson, J. R., Patton, J., Karabanov, E., et al. (2012). *Turbidite event history–methods and implications for Holocene paleoseismicity of the cascadia subduction zone* (Reston, VA: U.S. Geological Survey Professional Paper 1661–F), 170 p.

Graham, S. G., and Dickinson, W. R. (1978). Evidence for 115 kilometers of right slip on the San Gregorio-hosgri fault trend. *Science* 199 (4325), 179–181. doi: 10.1126/science.199.4325.179

Heaton, T. J., Kohler, P., Butzin, M., Bard, E., Reimer, R. W., Austin, W. E. N., et al. (2020). Marine20 – the marine radiocarbon age calibration curve (0–55,000 ca BP). *Radiocarbon* 62(4), 779–820. doi: 10.1017/RDC.2020.68

Hoskins, E. G., and Griffiths, J. R. (1971). Hydrocarbon potential of northern and central California offshore. *Am. Assoc. Petroleum Geologists Memoir* 15, 212–228. doi: 10.1306/M15370C16

Irwin, W. P., and Dennis, M. D. (1979). "Geologic structure section across southern klamath mountains, coast ranges and seaward from point delgada, California," in *Geological society of America map and chart series MC-28D, scale 1:250,000*. (Boulder, Colo: Geological Society of America).

Johnson, S. Y., Watt, J. T., Hartwell, S. R., and Kluesner, J. W. (2018). Neotectonics of the big sur bend, San Gregorio-hosgri fault system, central California. *Tectonics* 37, 1930–1954. doi: 10.1029/2017TC004724

Kennedy, D. J., Walton, M. A. L., Cochrane, G. R., Paull, C. K., Caress, D. W., Anderson, K., et al. (2021). "Donated AUV bathymetry and chirp data collected during Monterey bay aquarium research institute cruises in 2018-2019 offshore of south-central California," in *U.S. geological survey data release*. (Santa Cruz, CA: US Geological Survey). doi: 10.5066/P97QM7NF

Kienast, S. S., and McKay, J. L. (2001). Sea Surface temperatures in the subarctic northeast pacific reflect millennial-scale climate oscillations during the last 16 kyrs. *Geophys Res. Lett.* 28, 1563–1566. doi: 10.1029/2000GL012543

Kuhnz, L. A., Gilbane, L., Cochrane, G. R., and Paull, C. K. (2021). *California Deepwater investigations and groundtruthing (Cal DIG) I, volume 1–biological site characterization offshore morro bay, camarillo (CA): Bureau of ocean energy management outer continental shelf (OCS) study BOEM 2021–037*. (Santa Cruz, CA: US Geological Survey), 67 p.

Kuhnz, L. A., Gilbane, L., Cochrane, G. R., and Paull, C. K. (2022). Multi-factor biotopes as a method for detailed site characterization in diverse benthic megafaunal communities and habitats in deep-water off Morro Bay, California. *Deep Sea Research Part I: Oceanographic Research Papers* 190, 103872. doi: 10.1016/j.dsr.2022.103872.

Lundsten, E., Paull, C. K., Caress, D. W., Gwiazda, R., Kuhnz, L., Walton, M., et al. (2022). One of north america's largest pockmark fields offshore big sur, California is maintained over time by intermittent, non-channelized gravity flow events. *Particulate Gravity Currents Environ. conference.*

Maier, K. L., Fildani, A., McHargue, T. R., Paull, C. K., Graham, S. A., and Caress, D. W. (2012). Punctuated deep-water channel migration: High-resolution subsurface data from the Lucia chica channel system, offshore California, U.S.A. *J. Sedimentary Res.* 82 (1), 1–8. doi: 10.2110/jsr.2012.10

Maier, K. L., Fildani, A., Paull, C. K., Graham, S. A., McHargue, T. R., Caress, D. W., et al. (2011). The elusive character of discontinuous deep-water channels: New insights from Lucia chica channel system, offshore California. *Geology* 39 (4), 327–330. doi: 10.1130/G31589.1

Maier, K. L., Fildani, A., Paull, C. K., McHargue, T. R., Graham, S. A., and Caress, D. W. (2013). Deep-sea channel evolution and stratigraphic architecture from inception to abandonment from high-resolution autonomous underwater vehicle surveys offshore central California. *Sedimentology* 60 (4), 935–960. doi: 10.1111/j.1365-3091.2012.01371

McCulloch, D. S. (1987). ""Regional geology and hydrocarbon potential of offshore central california"," in *Geology and resource potential of the continental margin of Western north America and adjacent oceans Beaufort Sea to Baja California: Houston, Texas*, vol. 6 . Eds. A. Grantz and J. G. Vedder (Washington, DC (United States: Circum-Pacific Council for Energy and Mineral Resources), 353–401.

McCulloch, D. S. (1989). ""Evolution of the offshore central California margin"," in *The Eastern pacific ocean and Hawaii*. Eds. E. L. Winterer, D. M. Hussong and R. W. Decker (Boulder, CO: Geological Society of America), 439–470. doi: 10.1130/DNAG-GNA-N.439

McGann, M., Paull, C. K., Lundsten, E. M., Gwiazda, R., Walton, M. A. L., Nieminski, N. M., et al. (2023). *Radiocarbon age dating of biological material from cores collected off morro bay* (California. U.S: Geological Survey data release). doi: 10.5066/P9FWTKZQ

Meyers, P. A. (1994). Preservation of elemental and isotopic source identification of sedimentary organic matter. *Chem. Geology* 144, 289–302. doi: 10.1016/0009-2541(94)90059-0

Mueller, C. S. (2018). Earthquake catalogs for the USGS national seismic hazard maps. *Seismol. Res. Lett.* 90(1), 251–261. doi: 10.1785/0220170108.

Normark, W. R., Piper, D. J. W., Romans, B. W., Covault, J. A., Dartnell, P., and Sliter, R. W. (2009). ""Submarine canyon and fan systems of the California continental borderland"," in *Earth science in the urban ocean: The southern California continental borderland*, vol. 454 . Eds. H. J. Lee and W. R. Normark (Boulder, CO: Geological Society of America), 141–168. doi: 10.1130/2009.2454(2.7

Page, B. M., Wagner, H. C., McCulloch, D. S., Silver, E. A., and Spotts, J. H. (1979). Geologic cross section of the continental margin off San Luis obispo, and southern coast ranges, and the San Joaquin valley, California. *Geol Soc. America Map Chart Ser. MC-28G*. 12 p., 1 map, scale 1:250,000.

Paull, C. K., Ussler, I. I. I. W., Maher, N., Greene, H. G., Rehder, G., Lorenson, T., et al. (2002). Pockmarks off big sur, California. *Mar. Geology* 181 (4), 323–335. doi: 10.1016/S0025-3227(01)00247-X

Ross, D. C., and McCulloch, D. S. (1979). Cross section of the southern coast ranges and San Joaquin valley from offshore point sur to madera, California. *Geol Soc. America Map Chart Ser*. MC 28-B, 4 p.

Saleeby, J. B. (1986). C-2 central California offshore to Colorado plateau. *Geol Soc. America*. Centennial Continent/Ocean Transect 10, 2 sheets with text, scale 1:500,000. C-2, p. 1–63. doi: 10.1130/DNAG-COT-C-2

Shakun, J. D., Lea, D. W., Lisiecki, L. E., and Raymo, M. E. (2015). An 800-kyr record of global surface ocean δ18O and implications for ice volume-temperature coupling. *Earth Planetary Sci. Lett.* 426, 58–68. doi: 10.1016/j.epsl.2015.05.042

Sharman, G. R., Covault, J. A., Stockli, D. F., Sickmann, Z. T., Malkowski, M. A., and Johnstone, S. A. (2021). Detrital signals of coastal erosion and fluvial sediment supply during glacio-eustatic sea-level rise, southern California, USA. *Geology* 49 (12), 1501–1505. doi: 10.1130/G49430.1

Smith, M. E., Werner, S. H., Buscombe, D., Finnegan, N. J., Sumner, E. J., and Mueller, E. R. (2018). Seeking the shore: Evidence for active submarine canyon head incision due to coarse sediment supply and focusing of wave energy. *Geophys Res. Lett.* 45, 12,403–12,413. doi: 10.1029/2018GL080396

Stuvier, M., Reimer, P. J., and Reimer, R. W. (2022). CALIB radiocarbon calibration, CALIB rev. 8. *Radiocarbon* 35, 215–230.

Urlaub, M., Talling, P. J., and Masson, D. G. (2013). Timing and frequency of large submarine landslides: Implications for understanding triggers and future geohazard. *Quaternary Sci. Rev.* 72, 63–82. doi: 10.1016/j.quascirev.2013.04.020

Vail, P. R., Mitchum, R. M.Jr., and Thompson, S.III (1977). Seismic stratigraphy and global changes of Sea level, part 4: Global cycles of relative changes of Sea level," in Seismic stratigraphy — applications to hydrocarbon exploration. Ed. C. E. Payton (Tulsa, OK: The American association of petroluem geologists.), 83–97. doi: 10.1306/M26490C6

Wagner, H. C. (1974). Marine geology between cape San martin and pt. Sal, south-central California offshore. *U.S. Geol Survey Open-File Rep.* 74–252, 1–17. doi: 10.3133/ofr74252

Walton, M. A. L., Paull, C. K., Cochrane, G., Addison, J., Caress, D., Gwiazda, R., et al. (2021). *California Deepwater investigations and groundtruthing (Cal DIG) I, volume 2: Fault and shallow geohazard analysis offshore morro bay* (Camarillo (CA: U.S. Department of the Interior, Bureau of Ocean Energy Management. OCS Study BOEM 2021-044), 56 p.

Wells, D. L., and Coppersmith, K. J. (1994). New empirical relationships among magnitude, rupture length, rupture width, rupture area, and surface displacement. *Bull. Seismological Soc. America* 84, 974–1002. doi: 10.1785/BSSA0840040974

frontiers | Frontiers in Marine Science

TYPE Original Research
PUBLISHED 24 February 2023
DOI 10.3389/fmars.2023.1098927

OPEN ACCESS

EDITED BY
Veerle Ann Ida Huvenne,
University of Southampton,
United Kingdom

REVIEWED BY
Marie-Claire Fabri,
Ifremer Centre de Méditerranée, France
Peter Townsend Harris,
Grid-Arendal, Norway

*CORRESPONDENCE
Javier Cerrillo-Escoriza
javier.cerrillo@csic.es

SPECIALTY SECTION
This article was submitted to
Deep-Sea Environments and Ecology,
a section of the journal
Frontiers in Marine Science

RECEIVED 15 November 2022
ACCEPTED 07 February 2023
PUBLISHED 24 February 2023

CITATION
Cerrillo-Escoriza J, Lobo FJ,
Puga-Bernabéu Á, Rueda JL, Bárcenas P,
Sánchez-Guillamón O, Serna Quintero JM,
Pérez Gil JL, Murillo Y,
Caballero-Herrera JA, López-Quirós A,
Mendes I and Pérez-Asensio JN (2023)
Origin and driving mechanisms of marine
litter in the shelf-incised Motril, Carchuna,
and Calahonda canyons (northern
Alboran Sea).
Front. Mar. Sci. 10:1098927.
doi: 10.3389/fmars.2023.1098927

Origin and driving mechanisms of marine litter in the shelf-incised Motril, Carchuna, and Calahonda canyons (northern Alboran Sea)

Javier Cerrillo-Escoriza[1,2]*, Francisco José Lobo[1], Ángel Puga-Bernabéu[2], José Luis Rueda[3], Patricia Bárcenas[3], Olga Sánchez-Guillamón[3], José Miguel Serna Quintero[3], José Luis Pérez Gil[3], Yelvana Murillo[2], José Antonio Caballero-Herrera[3], Adrián López-Quirós[2,4], Isabel Mendes[5] and José Noel Pérez-Asensio[2]

[1]Marine Geosciences, Instituto Andaluz de Ciencias de la Tierra (IACT), Spanish National Research Council (CSIC), and University of Granada (UGR), Armilla, Granada, Spain, [2]Departamento de Estratigrafía y Paleontología, Facultad de Ciencias, University of Granada, Granada, Spain, [3]Centro Oceanográfico de Málaga, Instituto Español de Oceanografía (IEO), Spanish National Research Council (CSIC), Fuengirola, Málaga, Spain, [4]Department of Geoscience, Aarhus University, Aarhus, Denmark, [5]Centre for Marine, and Environment Research – CIMA, Universidade do Algarve, Faro, Portugal

Introduction and methods: Marine litter density, distribution and potential sources, and the impact on canyon seafloor habitats were investigated in the Motril, Carchuna and Calahonda canyons, located along the northern margin of the Alboran Sea. During the ALSSOMAR-S2S oceanographic survey carried out in 2019, canyon floor imagery was collected by a Remotely Operated Vehicle along 5 km in the Motril Canyon, 10 km in the Carchuna Canyon, and 3 km in Calahonda Canyon, together with 41 surficial sediment samples. Additionally, coastal uses, maritime traffic and fishing activity data were analyzed. A 50 m resolution multibeam bathymetry served as base map.

Results: In the Motril and Calahonda canyons, the density of marine litter was low and the material was dispersed, very degraded and partially buried. In contrast, the Carchuna Canyon contained a greater amount and variety of litter. The Carchuna Canyon thalweg exhibited a density of marine litter up to 8.66 items·100 m^{-1}, and litter hotspots with a density of up to 42 items·m^2 are found along the upper reaches of the canyon thalweg.

Discussion: Low litter abundances found in the studied canyons most likely reflect low population densities and the absence of direct connections with streams in the nearby coasts. The high shelf incision of the Carchuna Canyon and its proximity to the coastline favor littoral sediment remobilization and capture as well as the formation of gravity flows that transport the marine litter along the thalweg toward the distal termination of the channel. Litter hotspots are favored by the canyon morphology and the occurrence of rocky outcrops. Most debris is of coastal origin and related to beach occupation and agricultural practices in the

adjacent coastal plain. A third origin was represented by fishing gear in the study area. Fishing activity may be producing an impact through physical damage to the skeletons of the colonial scleractinians located in the walls of the Carchuna Canyon. In contrast, the Motril and Calahonda canyons can be considered passive systems that have mainly acted as depositional sinks in the recent past, as evidenced by buried marine litter.

KEYWORDS

submarine canyons, marine litter, seafloor imagery, litter hotspots, marine litter-habitats interaction, fishing gear, fishing effort, Alboran Sea

Introduction

The occurrence and accumulation of litter in the marine realm is an environmental problem with potential consequences for marine and coastal ecosystems (Richmond, 1993; Adams, 2005). Of particular importance is the long-lasting presence of plastic litter in the oceans, which exhibits high concentrations and has accumulated in diverse seafloor features, such as submarine canyons, channels and sedimentary drift deposits (Goldberg, 1997; Thompson et al., 2004; Kane and Fildani, 2021). Considering the global trends in plastic production, the increased fluxes and areal coverage of plastics can impact the seafloor and alter its nature, therefore affecting its habitats and associated benthic communities (Goldberg, 1997; Thushari and Senevirathna, 2020).

Studies on litter composition provide information about its origin. Plastics usually come from coastal and land sources, whereas other types of marine debris —such as those coming from fishing gears— may indicate human activity in the marine realm (Pham et al., 2014a; Vieira et al., 2015; Alves et al., 2021; Morales-Caselles et al., 2021). On continental margins, litter density, distribution, and composition are variable at different scales (Sánchez et al., 2013). Specifically, the spatial distribution of litter is influenced by a multiplicity of factors, including waves and oceanographic currents, seafloor geomorphology, anthropogenic activities, shipping routes, and river inputs (Galgani et al., 2000; Ramirez-Llodra et al., 2013; Pham et al., 2014b; Angiolillo et al., 2015; Angiolillo, 2019; Gerigny et al., 2019; Dominguez-Carrió et al., 2020; Canals et al., 2021; Bergmann et al., 2022; Hernandez et al., 2022). Interactions of litter artefacts with the seafloor biota are very complex and may have an impact on benthic and demersal organisms, since litter can provide habitat or coverage for diverse marine species (e.g., Goldberg, 1997; Sánchez et al., 2013; Mecho et al., 2020).

Channeled seafloor features such as submarine canyons may display significantly higher concentrations of marine debris (Galgani et al., 2000; Pham et al., 2014b), and tend to show patchy but pervasive distributions (Pierdomenico et al., 2019). Canyon heads, incised in the shelf at a short distance from the coast, can act as sinks of diverse types of land-derived litter (Wei et al., 2012; Ramirez-Llodra et al., 2013; Mecho et al., 2020); for this reason, coastal urbanization, population density, and fluvial inputs would be critical factors in determining litter concentrations in shelf-incised canyons (Mordecai et al., 2011; Neves et al., 2015; Tubau et al., 2015). In shelf-incised submarine canyons located at longer distances from the coast, litter is mainly marine-sourced (Mordecai et al., 2011). Yet submarine canyons can locally receive human discards from ships if they are located along shipping routes (Wei et al., 2012; van den Beld et al., 2017).

Along submarine canyons, litter can be entrained by diverse deep-water flows, such as downslope near-bottom currents (Tubau et al., 2015; Pierdomenico et al., 2020) or turbidity currents with strong erosional activity (Zhong and Peng, 2021). In addition, geomorphological canyon complexity may favor litter accumulations along the pathway of the submarine canyons (Tubau et al., 2015).

Because of the high densities of marine litter usually found in submarine canyons, some benthic habitats and species found in these seafloor features are particularly vulnerable, and interactions between marine debris and sessile organisms are varied, including physical contact and entanglements (Mordecai et al., 2011; Oliveira et al., 2015). Major disturbances to Vulnerable Marine Ecosystems (VMEs) of submarine canyons such as cold-water coral banks or gorgonian aggregations appear to be caused by different types of lost fishing gear (Fabri et al., 2014).

The Alboran Sea is a narrow and elongated basin located in the westernmost part of the Mediterranean Sea (Figures 1A, B) that receives moderate amounts of marine plastic litter (García-Rivera et al., 2018; Liubartseva et al., 2018). The occurrence of marine litter in the northern margin of the Alboran Sea is high by the coast at 0–50 m water depths and in open waters at 500–800 m water depths (García-Rivera et al., 2018). It is hypothesized that the abrupt character of the northern margin, with a narrow shelf and the sculpting of specific sectors by submarine canyons and other valley systems (Vázquez et al., 2015), is conducive to a relatively efficient seaward dispersal of marine litter. The Motril, Carchuna, and Calahonda shelf-incised submarine canyons lie in the central sector of the northern Alboran Sea margin (Figures 1B, C). In this study, marine litter has been observed along the canyon floor and the flanks of the three submarine canyons.

This study aims to analyze the litter distribution, density and origin in the Motril, Carchuna, and Calahonda shelf-incised

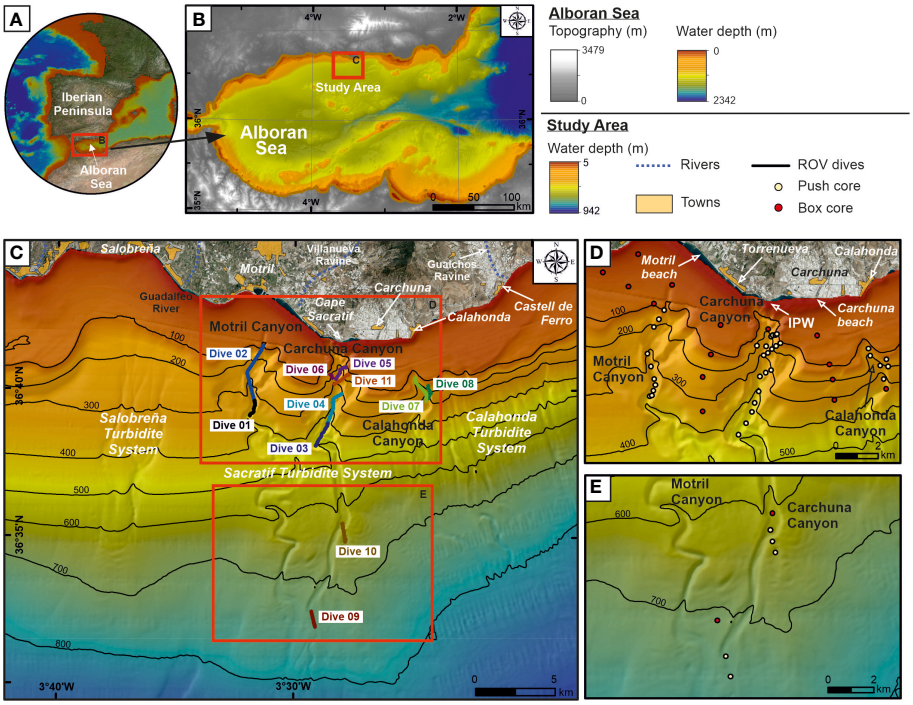

FIGURE 1
(A) Geographic location of the study area in the southern Iberian Peninsula. **(B)** Overview topo-bathymetric map of the Alboran Sea indicating the location of the study area on the northern margin. **(C)** Bathymetric map ("Ministerio de Pesca, Agricultura y Alimentación", Spanish government) of the study area showing the three studied submarine canyons and the location of the ROV underwater dives (Dives 01 to 11) executed along the canyon thalwegs and flanks. Inland aerial photography shows the streams and towns. **(D, E)** Zoomed-in bathymetric maps of the study area showing the location of sediment cores collected in the canyons during the oceanographic survey ALSSOMAR-S2S 2019. IPW, infralittoral prograding wedges. Bathymetric contours in meters.

submarine canyons. The specific objectives of this study are: (1) to characterize and quantify litter type and density in Motril, Carchuna and Calahonda canyons and, in view of other worldwide submarine canyons, to understand the major factors behind litter accumulation; (2) to understand the factors that control the distribution of marine litter in the studied submarine canyons; (3) to discern the litter origin (land- versus marine-sourced); and (4) to analyze the potential impact of litter on the benthic habitats and communities in the three studied submarine canyons.

Regional setting

The coastal domain

Sediment supply to the coastlines of the northern Alboran Sea is mainly provided via relatively short, mountainous rivers (Liquete et al., 2005) and ephemeral creeks, active during autumn and winter (Stanley et al., 1975; Fabres et al., 2002; Palanques et al., 2005). Inshore of the submarine canyons, there is no significant river or creek-delta system at present (Liquete et al., 2005). Only two small dry streams of a torrential character in the rainy season debouch in the proximity of the study area: Villanueva Ravine inland from the Motril Canyon, and Gualchos Ravine east of the study area (Figure 1C). These ravines are short (<20 km) and feature high slopes (>3.6°), and they occur in small basins (<120 km^2) (Bárcenas and Macías, 2009). The Guadalfeo River is a major regional fluvial system located west of the study area (Figure 1C), with an average water discharge of 23.4 $m^3 \cdot s^{-1}$ and an average sediment load of 83 $kg \cdot s^{-1}$ (Liquete et al., 2005; Bárcenas et al., 2015).

The coastal geomorphology of the study area is characterized by beaches and coastal plains that are unusual on this stretch of coast, where the mountains and the sea are in contact (Godoy et al., 2020). The coastal sedimentary record in the study area contains alluvial fans (Lario et al., 1999; Fernández-Salas et al., 2009), along with sandy deposits, such as spit bars and infralittoral prograding wedges (IPW) that constitute major progradational phases separated by erosional gaps, generated by coastal drift during the Holocene (Lario et al., 1999; Fernández-Salas et al., 2009; Bárcenas et al., 2011).

Submarine geomorphology, deposits, and processes

The northern Alboran Sea shelf is narrow (2-15 km) and the shelf break is located at an average water depth of 115 m (Ercilla et al., 1994; Vázquez, 2001). The study area comprises the narrowest shelf (2 km) of the entire northern margin, with a gradient <1° (Figures 1B, C) (Ercilla et al., 1994; Fernández-Salas et al., 2009). The western shelf of the study area is characterized by the south-

eastward thinning of the Guadalfeo River deltaic wedge (Figure 1C) (Bárcenas and Macías, 2009; Lobo et al., 2015). Infralittoral prograding wedges (defined according to Hernández-Molina et al., 2000) have been identified in the eastern shelf off the coastal segment fed by ephemeral streams between Carchuna and Calahonda towns (Figure 1D) (Ortega-Sánchez et al., 2014).

The shelf-to-slope transition around the study area is marked by diverse erosive features. The Motril Canyon is located 3 km south-east of the Guadalfeo River mouth at 70 m water depth and its main valley exhibits a sinuous morphology on the slope (Figures 1C-E). The straight Carchuna Canyon (Figures 1C-E) crosses the shelf and is located 200 m off Cape Sacratif at 25 m water depth. Both canyons debouch into large lobes fed by distributary channels (Pérez-Belzuz and Alonso, 2000; Pérez-Belzuz et al., 2000). The Calahonda Canyon (Figures 1C, D) is a shelf-incised canyon located 2.5 km south of Calahonda town with a sinuous valley along the slope.

Oceanographic setting

The Carchuna Canyon head (25-250 m water depths) influences the coastal swell and storm-related processes as it increases nearshore wave heights, particularly of westerly waves, favoring long-term coastal erosion due to energy concentration (Ortega-Sánchez et al., 2014). The shelf around the Carchuna Canyon head is affected by relatively high current velocity values (above 0.1 $m{\cdot}s^{-1}$) in the upper layer, under easterlies dominance, which causes high values of shear stress. Under westerlies dominance, a northeastward flow of <0.1 $m{\cdot}s^{-1}$ occurs in the upper layer of the water column (Bárcenas et al., 2011). A bottom flow distinct from the wind-driven surface flow has been detected in the Carchuna Canyon; in the bottom layer, the currents tend to flow downcanyon, particularly during easterlies dominance, where bottom flow velocities are between 20-30 $cm{\cdot}s^{-1}$ (Serrano et al., 2020).

Seafloor habitats and biota

The cliffs and marine bottoms along the rocky coastlines between Calahonda and Castell de Ferro towns constitute the Special Area of Conservation (SAC) "*Acantilados y Fondos Marinos de Calahonda-Castell de Ferro*" (Cliffs and Marine Bottoms of Calahonda-Castell de Ferro) (ES6140014) since 2015 (Mateo-Ramírez et al., 2021). The SAC covers an area of ca. 9 km^2 between the coastline and ca. 65 m water depth, and contains some littoral habitats, e.g., sandbanks (Habitat Code [HC] 1110 from the EU Habitat Directive), *Posidonia* beds (HC 1120), large shallow inlets and bays (HC 1160), reefs (HC 1170), and submerged or partially submerged sea caves (HC 8330) (Mateo-Ramírez et al., 2021). Knowledge of the habitats and associated communities of bathyal areas where the three studied canyons are located is very scarce, except for general studies on fish, decapod and mollusc assemblages of the northern Alboran Sea (Abelló et al., 2002; García-Ruiz et al., 2015; Ciércoles et al., 2018; Ciércoles et al., 2022).

Anthropogenic activity

The beaches located along the coast of the northern Alboran Sea exhibit high plastic item percentages (ca. 88% on the coast of Málaga and ca. 80% on the coast of Almería) (Ministerio para la Transición Ecológica y el Reto Demográfico (MITECO-DGCM), 2021). Inland the study area, most litter is composed of plastics in Carchuna beach (Figure 1D): 62.4% of >50 cm size items and 80.9% of <50 cm size items. In the vicinity of the study area, Motril beach (Figure 1D) exhibits a microplastic concentration of ca. 32 $particles{\cdot}kg^{-1}$ (Godoy et al., 2020). In addition, the massive use of agricultural activities (greenhouses and farming) along the coast in the study area can generate large amounts of waste that are not always managed correctly, and can undoubtedly lead to greater pollution of beaches (Junta de Andalucía. Consejería de Medio Ambiente, 2019). The Port of Motril accounts for 5.3% of artisanal vessels of the total number of vessels (318) along the northern coast of the Alboran Sea (Baro et al., 2021). In the Port of Motril, the most relevant fishing techniques are bottom trawl (67.1%), artisanal activity (21.7%), purse seine (10%) and surface longline activity (1.2%) (Baro et al., 2021).

Materials and methods

Recent datasets, submarine imagery and sediment samples were collected during the ALSSOMAR-S2S multidisciplinary expedition carried out from 29 August to 19 September 2019 on board the RV "Sarmiento de Gamboa". The bathymetric, coastal uses, and fishing activity data were acquired from different Spanish governmental sources.

Submarine imagery

Acquisition of the optical submarine imagery was carried out with the Remotely Operating Vehicle (ROV) Luso (EMEPC—Portuguese Task Group for the Extension of the Continental Shelf) during the ALSSOMAR-S2S oceanographic cruise (2019). The ROV Luso was equipped with an Argus HD-SDI 1/3" standard definition video camera. The high-resolution photos and video footage obtained amount to a total of 70 hours of video recording. The ROV Luso was equipped with two parallel laser beams at a fixed width of 62 cm that provided a reference scale to measure targets during subsequent video analysis. Besides, the ROV was equipped with an ultra-short baseline positioning system (USBL) to ensure detailed records of the ROV tracks where the device moved at an average speed of 0.3 knots.

Eleven submarine video dives explored almost 18 km track length of the seafloor in the Motril, Carchuna, and Calahonda canyons (Figure 1C; Table 1). Two dives covering a total length of ~5 km were conducted in the upper reaches of the Motril Canyon along the thalweg and the western flank at a water depth range of 106-388 m (Table 1). Seven dives covering a total length of ~10 km were conducted in the Carchuna Canyon in a 107-740 m water

TABLE 1 Summary of ROV dives used in this study including their water depth range, length, the amount of litter detected, and litter density recorded in each dive.

Dive	Submarine canyon	Date	Coordinates				Water depth range (m)		Transect length (m)	Number of items	Litter density (items·100 m^{-1})
			Start		End		Min	Max			
			Latitude (N)	Longitude (W)	Latitude (N)	Longitude (W)					
01-02a	Motril (T)	08/30/2019 08/31/2019	36°39'6.17"	3°31'53.53"	36°40'22.14"	3°31'57.78"	294	388	2534	3	0.12
02b	Motril (F)	08/31/2019	36°40'22.14"	3°31'57.78"	36°41'30.35"	3°31'21.2"	106	294	2520	13	0.52
07	Calahonda (T)	09/04/2019	36°39'36.69"	3°24'26.64"	36°40'26.82"	3°24'57.28"	152	324	1860	21	1.13
08	Calahonda (F)	09/04/2019	36°39'42.71"	3°24'24.27"	36°40'9.34"	3°24'22.55"	127	316	1055	2	0.19
03-04	Carchuna (T)	09/01/2019 09/02/2019	36°38'5.05"	3°29'6.63"	36°39'51.57"	3°28'1.48"	313	480	4407	382	8.66
05a	Carchuna (T)	09/03/2019	36°40'21.57"	3°28'16.59"	36°40'42.01"	3°28'5.25"	227	283	715	3	0.42
05b	Carchuna (F)	09/03/2019	36°40'42.01"	3°28'5.25"	36°40'47.01"	3°27'50.76"	120	150	552	12	2.30
11	Carchuna (F)	09/06/2019	36°40'10.58"	3°28'20.52"	36°40'33.27"	3°27'44.15"	107	307	1420	5	0.35
6	Carchuna (F)	09/03/2019	36°40'24.31"	3°28'25.14"	36°40'31.15"	3°28'31.31"	140	260	374	7	1.87
10a	Carchuna (D)	09/05/2019	36°34'49.56"	3°27'50.61"	36°35'12.73"	3°27'55.28"	624	649	878	1	0.11
10b	Carchuna (T)	09/05/2019	36°35'20.02"	3°27'56.12"	36°35'27.96"	3°27'57.24"	631	636	510	2	0.40
09	Carchuna (T)	09/05/2019	36°31'56.02"	3°29'6.19"	36°32'28.39"	3°29'15.70"	730	740	1016	3	0.30

T, canyon thalweg; F, canyon flank; D, lateral deposit.

10.3389/fmars.2023.1098927

depth range (Table 1). Finally, two dives covering a total length of ~3 km were conducted in the upper reaches of the Calahonda Canyon along its eastern flank and thalweg in the 127-324 m water depth range (Table 1).

The submarine imagery was used to characterize and quantify marine litter type and density, and to analyze the potential impact of litter on the benthic habitats in the three submarine canyons. The length of the ROV dives was calculated and the total number of items for each dive was converted and quantified as linear litter density, in items·100 m^{-1}. Subsequently, the identified marine litter was georeferenced in ArcGIS™. Marine litter classification was based on the protocol of the Guidance on Monitoring of Marine Litter in European Seas put forth by the Technical Subgroup on Marine Litter (MSFD) (European Commission of the European Union, 2013). A standardized litter classification considers five main categories of material (Table 2): plastic, metal, rubber, glass/ceramics, and textiles/natural fibers; and four additional categories in the Mediterranean Sea: wood, paper/cardboard, other, unspecific.

Seafloor habitats displaying the greatest concentrations of anthropogenic activity were characterized by combining the substrate type and the dominant habitat-structuring species identified in ROV underwater images. Annotations of the type of substrate were made every time a substrate change was detected along the dive transects and in some sedimentary areas, substrate type annotations from the underwater images were calibrated with data coming from grain size analyses from the sediment cores from the push corer and box corer. Six categories of substrates were identified and compared with the surficial sediment samples and grain-size analysis whenever possible (rock, detritic sediment with bioclasts, sand, muddy sand, sandy mud, and mud). The habitat-structuring taxa (mainly megabenthic taxa) and other associated taxa observed in the video dives were ranked using a system to quantify them (0 = absence of species; 1 = 1 individual of that taxa; 2 = 2-5 individuals; 3 = 5-25 individuals; 4 = 25-100 individuals; 5 >100 individuals). Those taxa showing the highest average rank along sections of the same dive were interpreted as dominant, but only the dominant habitat-structuring taxa were selected to determine the biological component of the seafloor habitat type. Habitat characterization and nomenclature was carried out whenever it was possible by combining depth, substrate type and dominant taxa information. In some cases, facies (interpreted as subtypes or varieties) of the same habitat were detected in some of the underwater images. Habitat classification and nomenclature followed the Reference List of Marine Habitats located in Spain (Templado et al., 2013), which follows a similar hierarchical habitat classification scheme to the EUNIS pan-European habitat identification system from the European Environment Agency. Whenever possible, some habitat types were also linked to the habitat classification of the Barcelona Convention and/or the EU Habitats Directive (Council Directive 92/43/EEC).

Seafloor sediment samples

A total of 25 sediment cores up to 30 cm long were collected during the ALSSOMAR-S2S oceanographic cruise (2019) with a push corer mounted on the ROV and handled by a plier arm (Figures 1D, E). Additionally, 16 sediment cores up to 50 cm long were collected by deploying a box corer from the vessel (Figures 1D, E). Grain size analysis was executed in the uppermost centimeter of 41 sediment cores (Supplementary Table 1) using 10-15 g of dried sediment (60°C) pre-treated with 20% H_2O_2 to remove organic matter, and sodium hexametaphosphate as a dispersing agent. Samples were wet sieved to separate the coarse fraction (gravel) using a 2 mm mesh size sieve. Particle sizes <2 mm (sand, silt and clay) were determined using a laser diffraction analyzer (Mastersizer 3000, Malvern®). Textural classification of the sediments was based on Folk (1954) ternary diagrams.

Bathymetric data

A 50 m resolution multibeam bathymetric grid ("Ministerio de Pesca, Agricultura y Alimentación", Spanish government) was imported in a geographic information system using ArcGIS™ (Figures 1C-E) and QPS Fledermaus™ software to serve as base

TABLE 2 Litter categories of the Guidance on Monitoring of Marine Litter in Mediterranean Sea (European Commission of the European Union, 2013).

Type of litter	Examples
Plastics	Bags, bottles, food wrappers, sheets, other plastic objects, fishing nets, fishing lines, other fishing related, ropes/strapping bands, sanitaries (diapers, etc.)
Rubber	Tyres, others (gloves, shoes, etc.)
Metals	Beverage cans, other food cans/wrappers, middle size containers, large metallic objects, cables, fishing related
Glass/Ceramics	Bottles, pieces of glass, ceramic jars, large objects
Textiles / natural fibers	Clothing (clothes, shoes), large pieces (carpets, etc.), natural ropes
Wood (processed)	Construction timbers, pallets, fragments
Paper/cardboard	Magazines, boxes
Other (specify)	–
Unspecified	–

maps where the rest of the data could be integrated. The multibeam bathymetry acquisition took place in 2002 during cruise Alborán-03 aboard the R/V Vizconde de Eza in the framework of the project entitled Fishing Charts of the Mediterranean (CAPERMA), carried out by the Spanish Institute of Oceanography (IEO) and the General Secretary of Maritime Fisheries (SGPM). These surveys were carried out using a Simrad EM 300 multibeam echosounder in conjunction with differential GPS and the inertial aided system Seapath 200. The slope parameter was calculated from the bathymetric grid to describe the flanks, lateral deposits and axial channels of the studied submarine canyons. The terminology defined by Paull et al. (2013) was used to describe the major geomorphic features of the studied submarine canyons (Figure 2).

Coastal uses data

Land use data regarding the coastal plain adjacent to the study area ("Consejería de Agricultura, Ganadería, Pesca y Desarrollo Sostenible, Junta de Andalucía", regional government) were mapped in ArcGIS™. These datasets extend from the Guadalfeo River delta to the east of Calahonda town and cover an extension of 8706 ha. Eleven land uses were considered for classification purposes: beaches, forest, farming, scrubs and pastures, wet areas, areas with low vegetation coverage, greenhouses, roads, industrial infrastructures, mining extraction, and urban. These data were analyzed by calculating the area of each individual use and the minimal distance from each use to the coastline in order to help us to explain the origin of marine litter.

Maritime traffic data (AIS)

A maritime traffic density map of the number of routes·km^{-2} in the study area for the year 2018 was downloaded from the MarineTraffic© website (www.marinetraffic.com). This website provides information about the current geographic positions of ships, ship characteristics, and weather conditions, among other data. This map was imported and georeferenced in the ArcGIS™ project to describe the position of the ships and the major maritime routes in the study area.

Fishing activity data (VMS)

Vessel Monitoring System (VMS) data of the main fishing fleets operating in the study area were assessed for the period 2018-2019 ("Ministerio de Pesca, Agricultura y Alimentación", Spanish government). The VMS database covers the geographic position, date, time (approximately every two hours), and instantaneous velocity of each boat. The VMS data included separate data organized by fishing gear of each fleet type, including vessels with licenses for a single gear. Fishing fleets in the study area include artisanal fishing boats, bottom trawling, purse seine, and longline fishing boats. For this study, the fishing activity could only be analyzed for bottom trawling, purse seine, and longline fishing boats, as VMS data were not available for the remaining fishing fleets. The three studied fishing fleets are responsible for the largest landings in the Port of Motril, which is the main one in the study area.

This VMS database was imported and georeferenced in the ArcGIS™ project to describe the fishing activity along the studied canyons. The fishing activity in the study area was quantified in five sectors, from west to east: Western Sector, the Motril Canyon, Carchuna Canyon, Calahonda Canyon, and Eastern Sector. Depth ranges within each sector included the shelf (0-100 m water depths), shelf edge and uppermost slope (100-200 m water depths), upper slope (200-500 m water depths), and middle slope (below 500 m water depth). The fishing effort was estimated as the average number of fishing days per km^2 in 2018 and 2019.

Results

Overall geomorphology and sedimentology of submarine canyons

The shelf in the study area is up to 3 km wide, narrowing due to the occurrence of shelf-incised canyon heads (Figures 1, 2). Shelf surface sediments vary from coarse silts close to fine sands on the shelf edge (Figure 2).

Three geomorphological segments were identified in the Motril Canyon. The upper segment is defined by a 4.3 km wide amphitheater-like canyon head incised in the outer shelf and upper slope. The canyon head is located 2 km off the coastline and connects to a 950 m long and 140 m wide short and straight shelf channel (Figures 1C, 2). The canyon valley is bounded by gentle flanks (ca. 3°), and it widens and increases in sinuosity downward to 400 m water depth. Surface sediment grain size decreases down the canyon thalweg, from very fine sands to medium silts (Figure 2). The middle segment is characterized by an abrupt change in the direction of the valley from N-S to NW-SE down to 500 m water depth. The canyon valley shows a sinuous path with a gentle south-western flank (ca. 2°), whereas the north-eastern flank is steeper (ca. 8°) (Figure 2). The lower segment is characterized by a meandering channel limited by steep walls with continuous adjacent deposits over the slope.

Two geomorphological segments were identified in the Carchuna Canyon. In the upper segment, the canyon is deeply incised in the shelf, as its head is located just 200 m off the coastline. It is characterized by a 100 m wide narrow axial channel with large steep flanks (Figures 1C, 2). The straight canyon increases its width up to 430 m water depth and it is bounded by a narrow and steep eastern flank and large terraces in the western flank. The axial channel in the upper segment is characterized by fine sands in the canyon head that change downslope to coarse silts, while the flanks are characterized by fine sands (Figure 2). The landward tip of the lower segment is marked by an abrupt change of orientation of the canyon from NE-SW to WNW-ESE. This lower segment has a straight and wide valley (up to 550 m) bounded by steep walls (ca. 20°) and continuous lateral slope deposits. Grain sizes in the lower segment range from very fine sands in the axial channel to medium silts in lateral deposits (Figure 2).

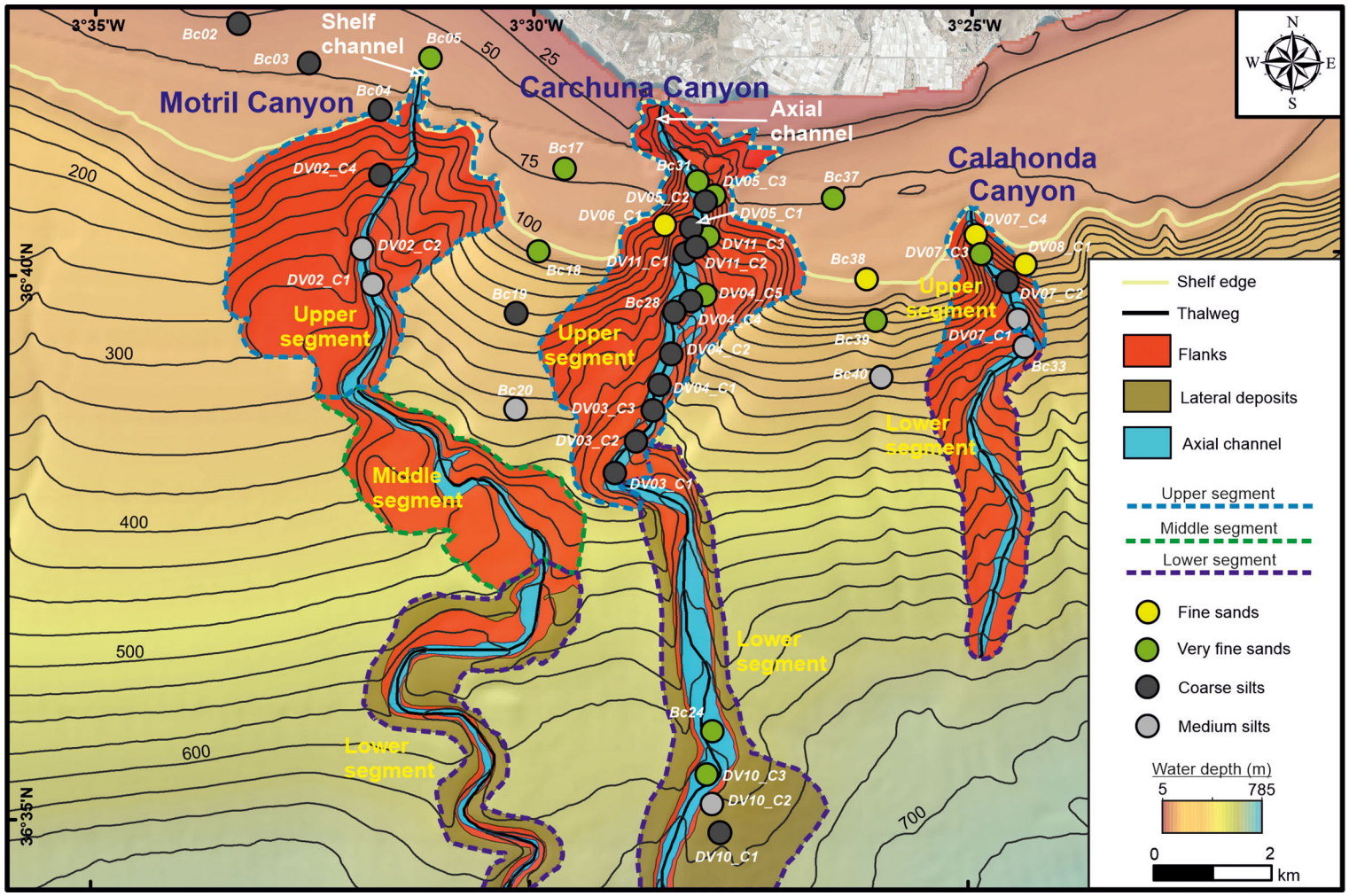

FIGURE 2
Geomorphologic map of the Motril, Carchuna and Calahonda submarine canyons showing the segment distribution within each canyon and the texture of surficial sediment samples. Bathymetric contours in meters. See Supplementary Table 1 in which location and depth of the sediment cores sampled for grain size analysis are included.

10.3389/fmars.2023.1098927

Two geomorphological segments were identified in the Calahonda Canyon. In the upper segment, the canyon incises the shelf edge, where the canyon head is located 2.5 km off the coastline (Figures 1C, 2). The canyon head is 150 m wide at the shelf edge and has steep flanks. In the lower segment, the canyon exhibits a meandering pattern and is bounded by smooth flanks. The axial channel is characterized by fine sands in the canyon head that change downslope to medium silts, while the eastern flank is characterized by fine sands (Figure 2).

Marine litter distribution

A total of 454 litter items were observed in the 11 ROV video dives (Figure 3A; Table 1). Plastics predominate (almost 75% of occurrences), and they include bottles, bags, fishing nets, sheets, seedbeds and other objects with sizes from centimeters to meters. Other minor components of marine litter in the studied canyons include metal items, building material, and rubber items (Figures 3A, 4). Overall, the marine litter is partially buried, covered by a thin layer of mud and in a degraded state.

The lowest average abundances of litter were found in the Motril and Calahonda canyons (Figures 3B, 4; Table 1). In the Motril Canyon, the litter density along the thalweg was 0.12 items·100 m^{-1}. A higher litter density (0.52 items·100 m^{-1}) was observed along the western flank of the canyon (Figure 4). Marine litter in the upper segment of the Motril Canyon included plastics (60%), metals (6.67%), and unspecified items (33.33%) (Figures 3B, 4). The litter appeared dispersed, degraded and frequently broken, both in the thalweg (Figure 5A) and the western flank.

In the Calahonda Canyon, litter density was higher along the thalweg (1.13 items·100 m^{-1}) than in the eastern flank (0.19 items·100 m^{-1}) (Figure 4; Table 1). Marine litter in the Calahonda Canyon was composed of plastics (almost 70%), metals, building material, and unspecified items in the upper segment of the canyon (Figures 3C, 4). Marine litter generally occurred as 2-5 item

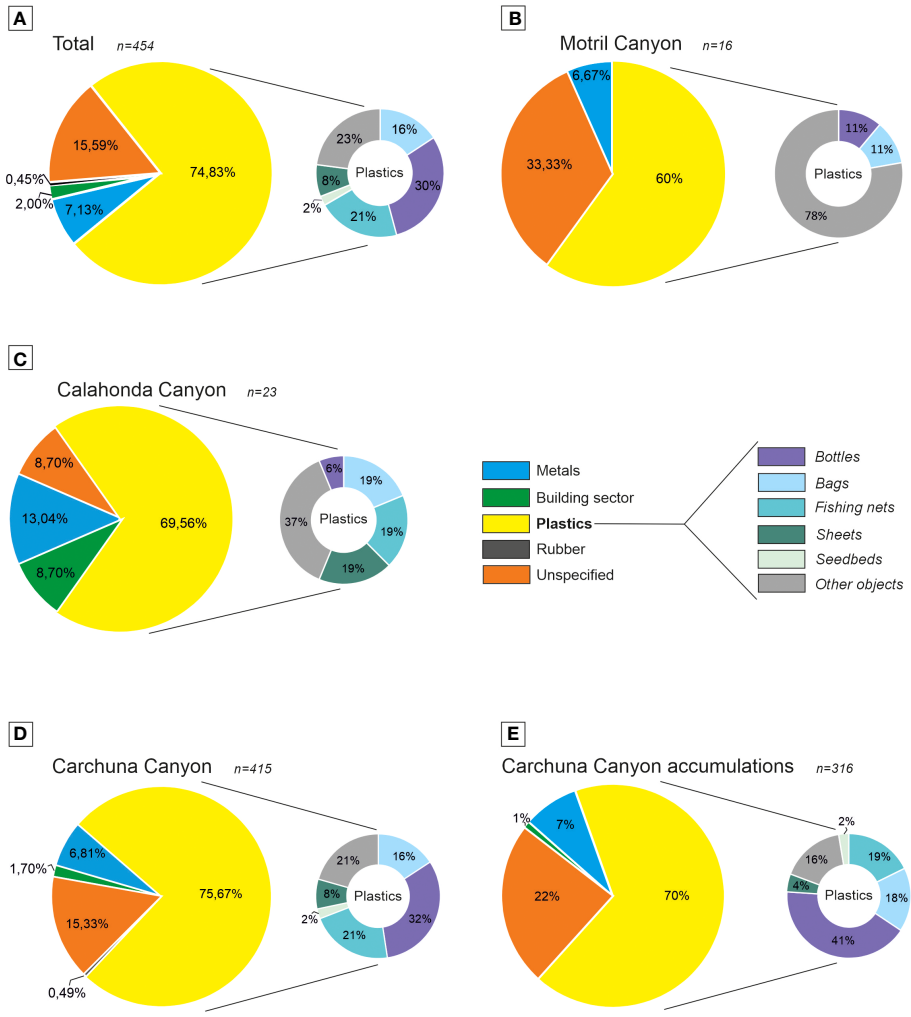

FIGURE 3
Litter composition in the three studied submarine canyons. Percentages of litter items are divided into five litter categories and six plastic subcategories as defined by the Guidance on Monitoring of the Marine Litter in the Mediterranean Sea (European Commission of the European Union, 2013): **(A)** studied submarine canyons; **(B)** upper segment of Motril Canyon; **(C)** upper segment of Calahonda Canyon; **(D)** Carchuna Canyon; and **(E)** Carchuna Canyon accumulations. n: total number of litter items counted.

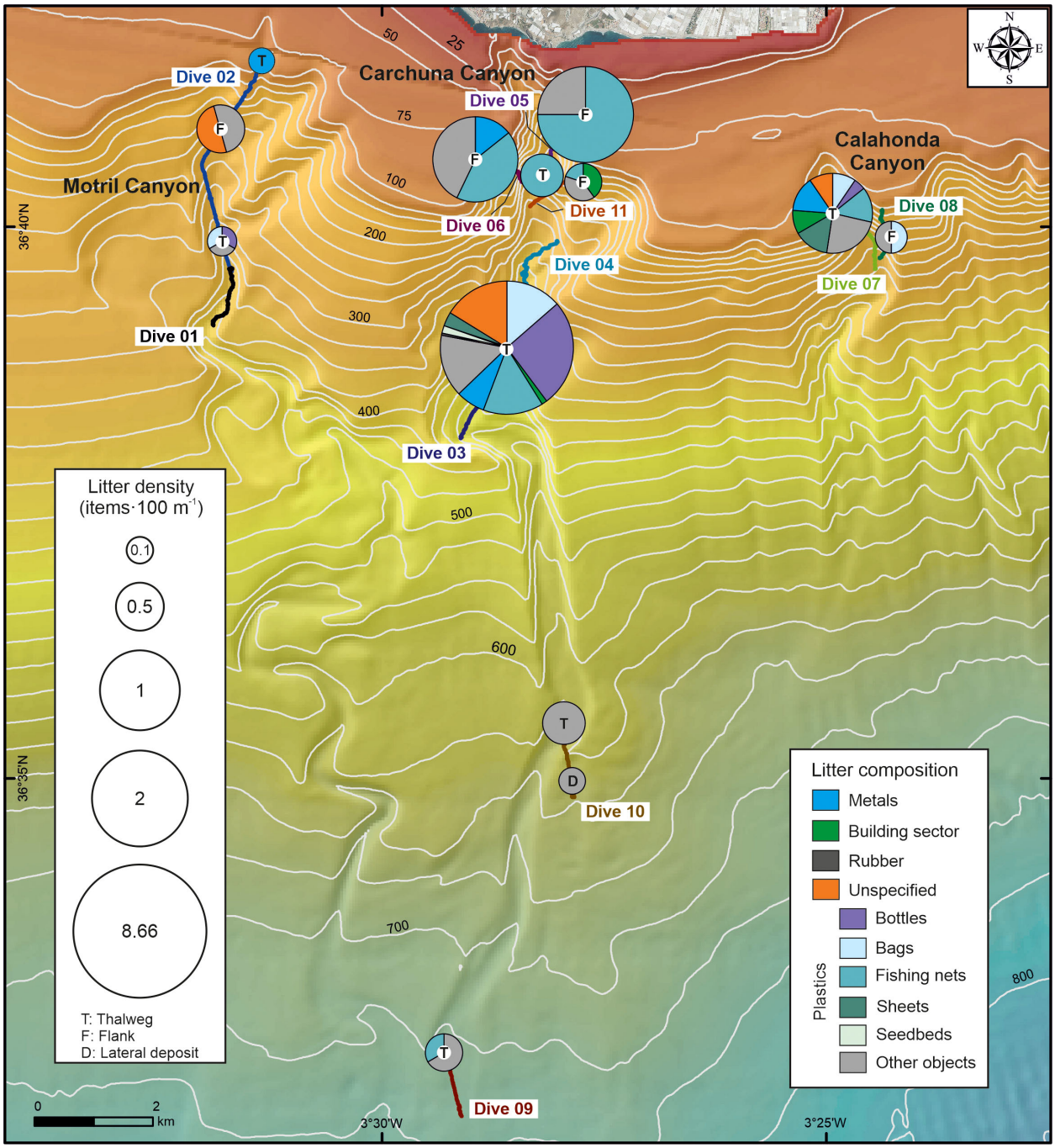

FIGURE 4
Spatial distribution and composition of marine litter along the canyon thalwegs and flanks of the three studied submarine canyons. The size of the pie charts is proportional to the abundance of litter (expressed as number of items·100 m^{-1}). The maximum litter density (8.66 items·100 m^{-1}) was found in the thalweg of the Carchuna Canyon. Bathymetric contours in meters.

accumulations (Figure 5B) or dispersed along the thalweg and eastern canyon flank. Marine litter on the seafloor was found degraded and partially buried.

The highest litter abundance was detected in the Carchuna Canyon (Figures 3D, 4; Table 1). Litter densities along the flanks of the upper segment varied between 0.35 and 2.3 items·100 m^{-1}. The highest litter density was detected along the thalweg in the upper canyon with 8.66 items·100 m^{-1}. In contrast, the lowest densities of marine litter occurred in the lower canyon up to 0.35 items·100 m^{-1} in the thalweg and the lateral deposits (Figure 4). In the Carchuna Canyon, marine litter was made up of plastics (almost 76%), metals, building material, rubber, and unspecified items (Figures 3D, 4). Plastic items mainly included bottles, fishing nets, bags, sheets, and seedbeds (Figures 3D, 4). Marine litter on the flanks was composed of plastics such as fishing nets (Figure 5C), and dispersed and degraded building items (Figure 5D). In the lower canyon, marine

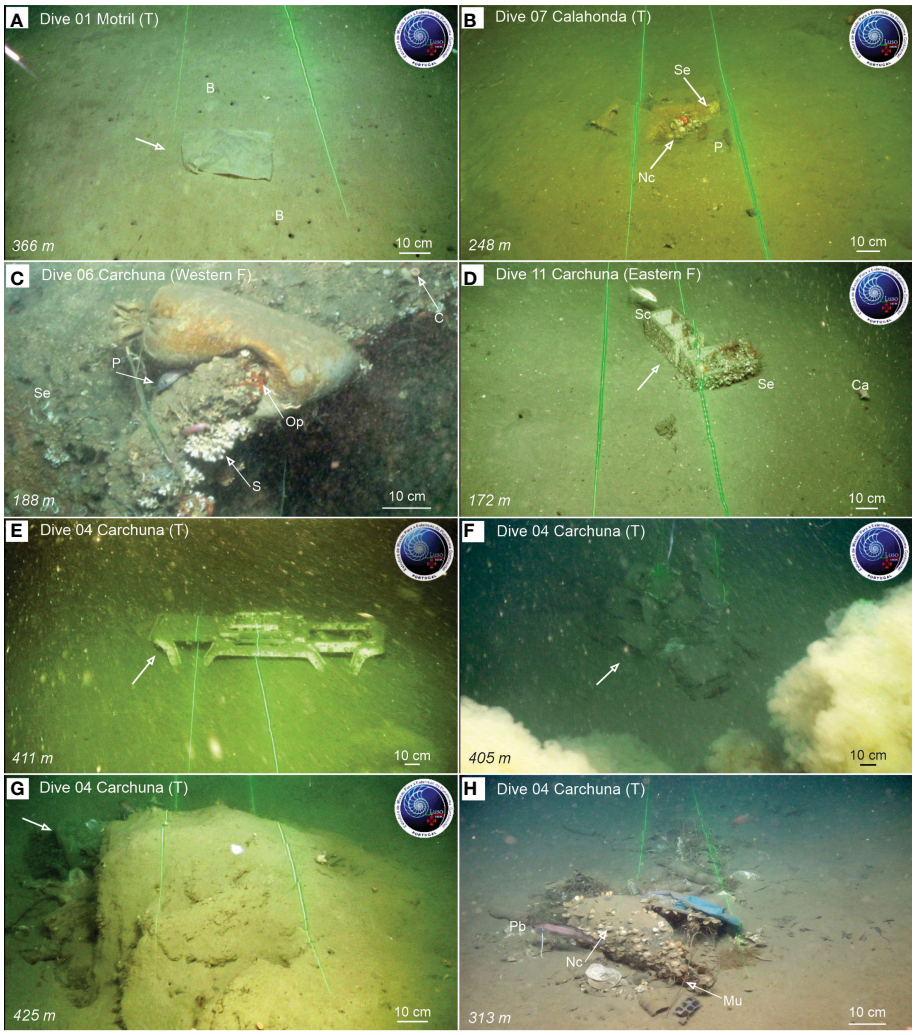

FIGURE 5
Examples of litter items observed during ROV dives in the Motril, Calahonda, and Carchuna canyons, and litter accumulations found in Dive 04 along the thalweg of the Carchuna Canyon. Dive number, water depth and relative location within the canyons (T, canyon thalweg; F, canyon flank) are indicated. **(A)** Plastic bag (arrow) on the thalweg of the Motril Canyon. **(B)** Two concrete blocks used in longline fishing as weights, colonized by serpulid polychaetes and *N. cochlear* aggregations, together with two *P. bogaraveo* individuals as well as a soda can and small plastic fragments on the thalweg of the Calahonda Canyon. **(C)** A filled plastic bag (used as weight in longline fishing) on rocks colonized by unidentified colonial scleractinians, serpulid polychaetes and *Ophiotrix* sp., together with individuals of the black-spot seabream *Pagellus bogaraveo* (one of the target species of longline fishing). **(D)** Two bricks colonized by serpulids on the eastern flank of the Carchuna Canyon, with some fishes (*Serranus cabrilla* and *Capros aper*). **(E)** Sunbed over the seafloor on the thalweg of the Carchuna Canyon. **(F)** Accumulation characterized by a large number of bottles. **(G)** Accumulation composed of bottles, bags and fishing nets blocked behind a seafloor rocky outcrop. **(H)** Accumulation with bricks, a broken sheet, various bags and bottles, fishing nets, a metal tube and diverse plastic items, some of them colonized by *N. cochlear*, but also providing shelter to the greater forkbeard *Phycis blennoides* and *Munida* sp. B, Burrows made by decapods; C, *Caryophyllia* sp.; Ca, *Capros aper*; Mu, *Munida* sp.; Nc, *Neopycnodonte cochlear*; Op, *Ophiothrix* sp.; P, *Pagellus bogaraveo;* S, Scleractinians; Sc, *Serranus cabrilla*; Se, Serpulid polychaetes.

litter was largely composed of very degraded and buried plastic items.

In the Carchuna Canyon, marine litter mainly occurred as large accumulations or litter hotspots of up to 6 m^2 (Accumulations 17, 18, and 20) in extent or containing up to 42 items·m^{-2} (Accumulation 19) (Table 3) that alternate with isolated items (Figure 5E). Three different types of accumulations were observed along the canyon thalweg: (1) marine litter accumulated in smooth canyon floor depressions (Figure 5F); (2) marine litter accumulated by rocky floor blocking (Figure 5G); (3) marine litter accumulated by tangling of fishing nets (Figure 5H). These accumulations were composed of plastics (70%), metals, building material, and unspecified items (Figure 3E) and they were detected along the canyon thalweg between 339-493 m water depths (Figure 6). Overall, the marine litter accumulations appeared degraded and partially buried.

Other seafloor bottom anthropogenic marks

Ten straight, regular, and continuous bottom trawling marks were detected on the seafloor of the studied canyons: six in the Motril Canyon (370-180 m water depths), two in the Carchuna

TABLE 3 Characterization of litter accumulations found in the Carchuna Canyon in terms of extent, item density and number of items.

Accumulation number	Size (m^2)	Density ($items \cdot m^{-2}$)	Items
1	0.8	15	12
2	0.72	2.78	2
3	0.96	7.29	7
4	0.64	4.68	3
5	0.72	27.7	20
6	0.24	33.3	8
7	4	9.5	38
8	3	7.67	23
9	3	3.33	10
10	2.5	3.2	8
11	0.3	20	6
12	4.5	2.89	13
13	3.6	5	18
14	1	30	30
15	0.4	5	2
16	4	4.75	19
17	6	2.17	13
18	6	3.83	23
19	0.5	42	21
20	6	6.67	40

Canyon (450-400 m water depths), and two in the Calahonda Canyon (290 m water depth) (Supplementary Table 2). These marks were more frequent in the thalweg and the western flank of the Motril Canyon, but they were also detected in the thalwegs of Calahonda and Carchuna canyons (Figures 7A, B). Some bottom trawling marks exhibited a well-defined groove having straight marks with an extensive and lateral continuous mound (Figure 7A). In some places, irregular broken fragments of organisms were observed over the muddy seafloor of the grooves (Figure 7A). Other mark types were smoother, comprising various parallel lines with straight margins, which may correspond to marks of the weights attached to the bottom part of the opening of bottom trawling nets (Figure 7B).

Anthropogenic activity regarding the main seafloor habitats

A total of 13 habitat types have been detected in the 11 ROV video dives, however, 6 of those habitats may represent facies of the detected habitats but occur at differents depths (e.g., Circalittoral and bathyal detritic bottom *vs.* Bathyal detritic bottom with bivalve and cold-water coral remains) and sediment types (e.g., Bathyal muddy sand and sandy mud bottom with burrowing megafauna *vs.* Bathyal sandy silt bottom with burrowing megafauna). The detected habitats ranged from highly complex ones with a high biogenic component (e.g., Bathyal rocky bottom with scleractinians) to habitats with low complexity and low biogenic component (e.g., Bathyal sandy mud bottom with burrowing megafauna) (Figures 7, 8). Regarding the main habitats detected, the most common ones in the explored canyons (based on their length along the analysed video transects) were: (1) bathyal muddy sand and sandy mud bottom with burrowing megafauna (including the different facies) (Total Length = 8420 m, %Length of all habitats = 50.4%); (2) circalittoral and bathyal sandy silt bottoms with alcyonaceans (mainly dominated by *Alcyonum palmatum*) (2964 m, 17.7%) (Figure 7C); (3) bathyal sandy silt bottoms with ceriantharians (1739 m, 10.4%) (Figure 7D); (4) bathyal sandy mud and muddy sand with ceriantharians and *Funiculina quadrangularis* (mainly dominated by *Cerianthus* spp.) (1279 m, 7.7%) (Figure 7E); and (5) circalittoral and bathyal detritic bottom (1154 m, 6.9%). Data on the length of the different habitats and their facies as well as the percentage of the habitat length within each dive and submarine canyon are given in Figure 8, together with annotations of the main dominant taxa of each habitat.

The habitats that displayed the highest average densities of anthropogenic activity indicators when combining all density values obtained in the same habitat at different canyons and sectors of the canyon (i.e., the 18 km of survey track) were (Figure 8): (1) bathyal

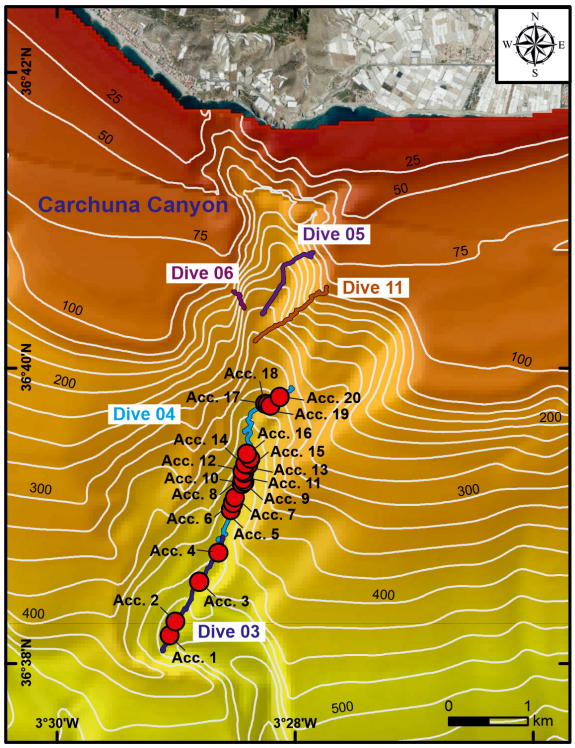

FIGURE 6
Zoomed-in bathymetric map of the study area ("Ministerio de Pesca, Agricultura y Alimentación", Spanish government) showing the location of the litter accumulations found in the Carchuna Canyon. Bathymetric contours in meters.

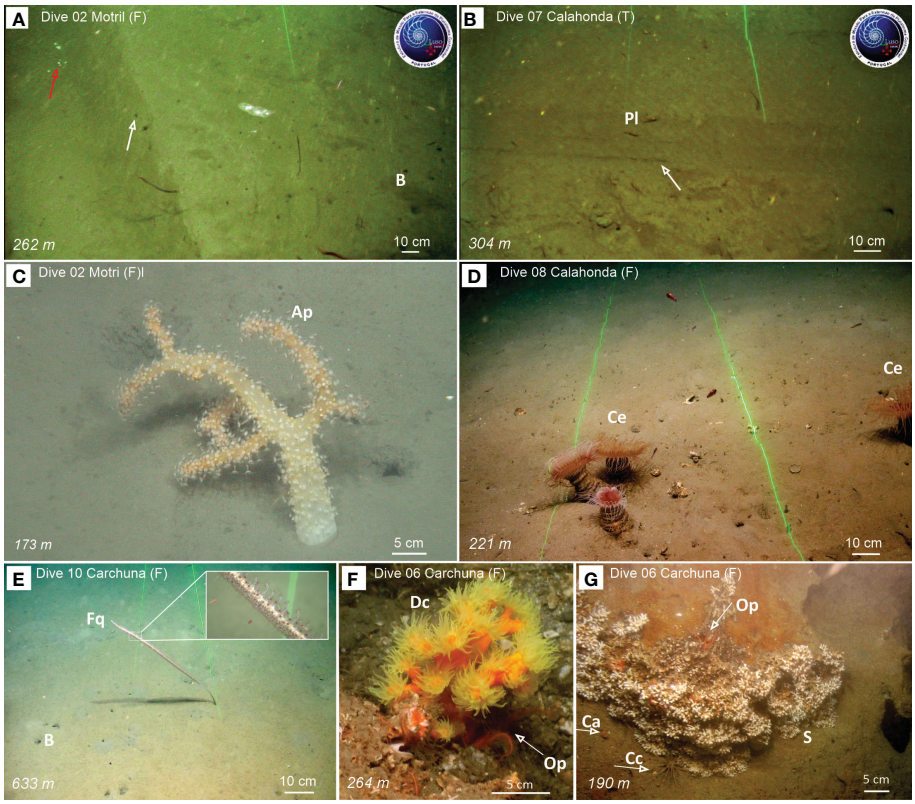

FIGURE 7
Examples of seafloor trawling marks observed during ROV dives along the flank of the Motril Canyon **(A)** and the thalweg of the Calahonda Canyon **(B)**, and benthic and demersal fauna detected in Motril **(C)**, Calahonda **(D)** and Carchuna **(E-G)** canyons. **(A)** Seafloor groove made by the otter board of a bottom trawling gear with broken fragments (red arrow) and a lateral mound (white arrow) on the western flank of the Motril Canyon. **(B)** Seafloor groove made by the otter board of a bottom trawling gear on the thalweg of the Calahonda Canyon. The bottom trawling marks seen on video footage collected by the ROV in the three submarine canyons is shown in Figure 10D. **(C)** The soft octocoral *Alcyonum palmatum*. **(D)** Aggregation of the cerianthiid *Cerianthus* sp. **(E)** Muddy bottoms with decapod burrows and the sea-pen *Funiculina quadrangularis*, with a detail of its polyps. **(F)** The colonial scleractinian *Dendrophyllia cornigera* providing shelter to the ophiurid *Ophiothrix* sp. **(G)** Aggregation of unidentified colonial scleractinians, together with solitary *Caryophyllia* sp. and individuals of the echinoid *Cidaris cidaris* and the ophiuroid *Ophiothrix* sp. Ap, *Alcyonum palmatum*; B, Burrows made by decapods; Ca, *Caryophyllia* sp.; Cc, *Cidaris cidaris*; Ce, *Cerianthus* sp.; Dc, *Dendrophyllia cornigera*; Fq, *Funiculina quadrangularis*; Op, *Ophiothrix* sp.; Pl, *Plesionika* sp.; S, unidentified colonial scleractinians.

detritic bottoms (occurring at the head of the three canyons, ca. 100-200 m water depths) (average 2.14 items·100 m^{-1}), which mainly contained plastics and fishing nets; (2) bathyal sandy mud and muddy sand bottoms with burrowing megafauna (generally in the thalwegs of the studied canyons, ca. 200-500 m water depths) (2.13 items·100 m^{-1}) affected by plastics, bottom trawling marks and fishing nets, among others; and (3) bathyal rocky bottoms with scleractinians (western flank of the Carchuna Canyon head, 193-222 m water depths) (2.1 items·100 m^{-1}) that mainly contained bags (Figures 5C, 7F, G, 8). In contrast, the habitats that displayed the lowest average densities of anthropogenic activity indicators were (Figure 8): (1) bathyal muddy sand and sandy mud bottoms with alcyonaceans (at the flanks of the three canyons, 100-250 m water depths) (average 0.44 items·100 m^{-1}), mostly containing plastics, bottom trawling marks, cables, and fishing nets; (2) bathyal sandy mud and muddy sand bottoms with large echinoderms as well as bathyal sandy mud and muddy sand bottoms with ceriantharians and *Funiculina quadrangularis* (deep part of the Carchuna thalweg, 630-730 m water depths) (0.34 items·100 m^{-1}) mainly containing plastics; and (3) bathyal sandy mud bottoms with ceriantharians (Motril and Calahonda canyon thalwegs, 273-377 m water depths) (0.15 items·100 m^{-1}) with plastics and bottom trawling marks (Figures 5, 7, 8).

Mapping of the coastal domain

Prevailing land uses along the coasts adjacent to the study area (approximate area of 8706 ha) are agricultural (ca. 48%): farming (ca. 34%) and greenhouses (ca. 13%); scrubs and pastures (ca. 25%); and urban (ca. 8%) (Figure 9A). Motril Town is located 2 km north of the coastline, with a population density of 567.68 people·km^{-2} ("Instituto de Estadística y Cartografía de Andalucía, Junta de Andalucía", regional government) and at least 83% of the population residing in the town. Motril Town is surrounded by pastures, industrial infrastructures and greenhouses and crops that extend up to the coastline.

The Motril Canyon head is located 2 km offshore the Port of Motril. The Carchuna Canyon head is located off a small bay limited laterally by beaches, greenhouses and Torrenueva and Carchuna

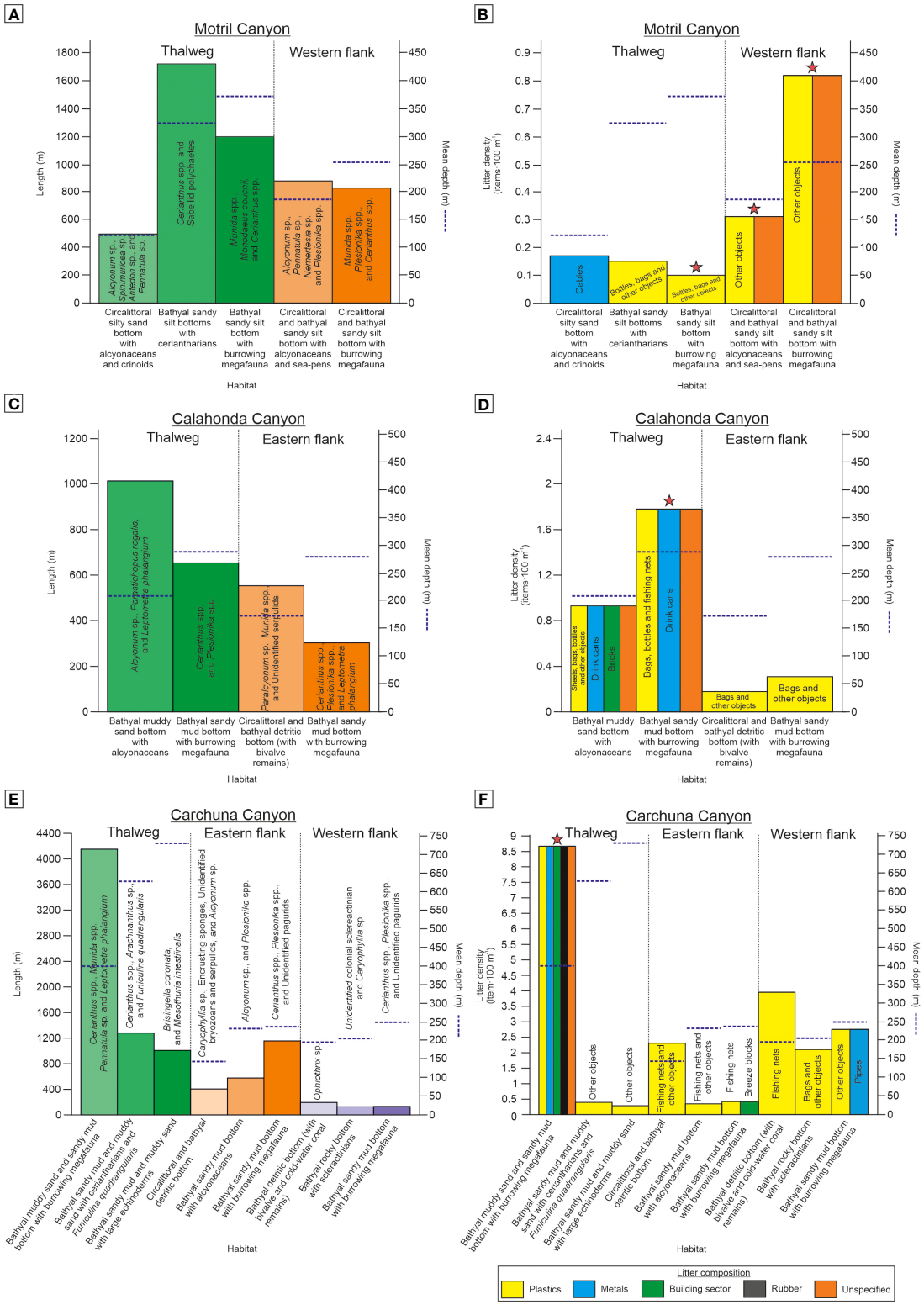

FIGURE 8
Types and length (in ROV underwater image transects) of habitats detected along the Motril **(A)**, Calahonda **(C)**, and Carchuna **(E)** canyons, with annotations of the dominant taxa and mean water depth (blue dotted line) of each habitat. Litter density and types of litter and other anthropic activity indicators along the Motril **(B)**, Calahonda **(D)**, and Carchuna **(F)** canyons is also shown. Stars indicate the presence of seafloor marks from bottom trawling in a particular habitat.

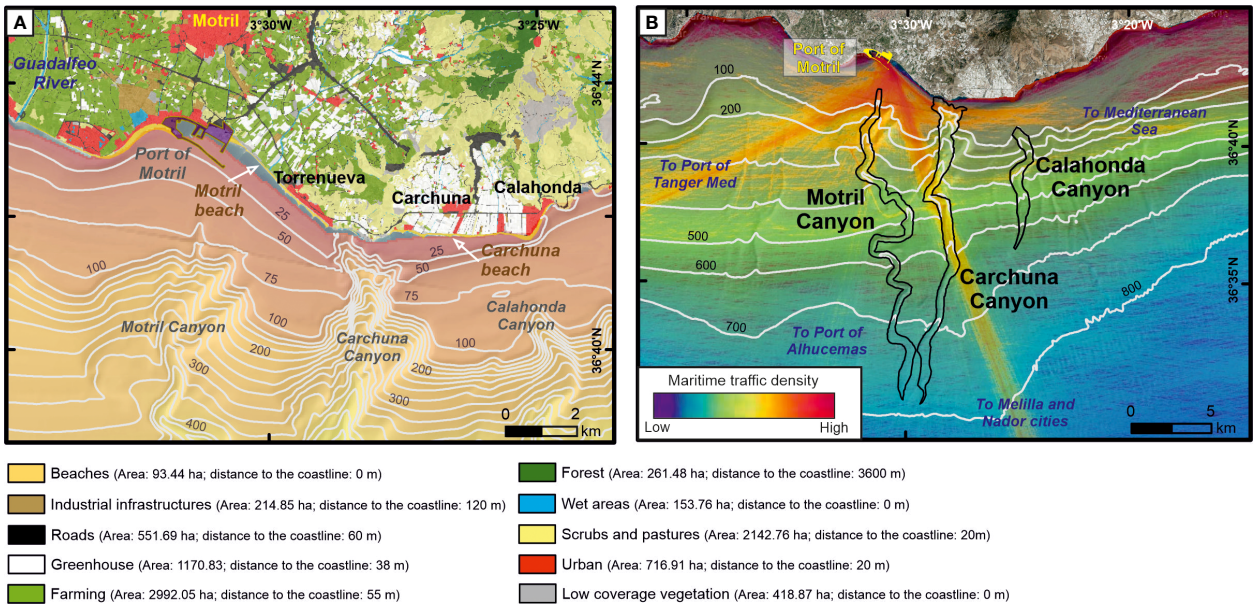

FIGURE 9
Depiction of coastal uses and maritime traffic in the study area. **(A)** Mapping of main land uses in the adjacencies of the three studied submarine canyons ("Consejería de Agricultura, Ganadería, Pesca y Desarrollo Sostenible, Junta de Andalucía", regional government). The area and the minimum distance to the coastline of each land use are shown in the legend. **(B)** Density (number of routes·0.08 $km^{-2}·y^{-1}$) of maritime traffic in 2018 (www.marinetraffic.com) with the drawing axial channel of the three studied submarine canyons. Bathymetric contours in meters.

towns. The Calahonda Canyon head is located 2.5 km off the beach of Calahonda Town. The coastline close to the studied canyons is mainly composed of gravel beaches interrupted by the Port of Motril (200,000 m^2) and its surrounding industrial area, some greenhouses (mostly concentrated between Calahonda and Carchuna towns) and urban land uses (Torrenueva, Carchuna and Calahonda towns). The population density in Torrenueva Town is 432 people·km^{-2} while Carchuna and Calahonda towns have lower densities (72 and 53 people·km^{-2}, respectively) ("Instituto de Estadística y Cartografía de Andalucía, Junta de Andalucía", regional government). Urban land uses on the coastline are typical of a touristic area, with summerhouses and various commercial uses, absorbing a duplication in population during summer that causes a triplication of urban litter (Ayuntamiento de Motril. Medio Ambiente Urbano, 2021).

Maritime traffic routes

The Port of Motril is an important commercial and fishing infrastructure offering freight and passenger traffic between Spain and northern Africa. The port has four maritime connections crossing the Alboran Sea (Figure 9B): (1) a south-southeast route that crosses the Carchuna Canyon towards Melilla and Nador cities; (2) a south-west route that crosses the Motril Canyon head towards the Port of Tanger Med; (3) a south-southwest route that crosses the upper segment of the Motril Canyon towards the Port of Alhucemas; and (4) an east route that crosses the Carchuna Canyon head towards the Mediterranean Sea. Additional straight and short routes with north-south and west-east orientations along the slope can be identified in the study area.

Mapping of the fishing activity

The fishing fleet of Motril Port comprised ca. 53 fishing boats in 2019 (from the 640 fishing boats operating in GSA1- Northern Alboran Sea fishing area). The main fishing fleets were artisanal fishing boats (ca. 50%) using set gillnets, trammel nets and traps, followed by bottom otter trawling (ca. 26%), purse seine (ca. 22%), and set longline (ca. 2%) fishing boats.

The spatial distribution of purse seine fishing, bottom trawling, and longline fishing displayed contrasting patterns (Figure 10). Purse seine fishing was mainly detected on the shelf outside the canyons (Figures 10A, B). Bottom trawling was higher in the shelf areas affected by the submarine canyons and in the upper slope of the Motril and Calahonda canyons (Figures 10C, D), where bottom trawling marks were identified (Figure 10D; Supplementary Table 2). Longline fishing showed a very low number of records due to a low number of boats and their highly seasonal trend (mainly in summer and autumn), but the highest activity was detected on the shelf close to the Motril Canyon head (Figures 10E, F).

Gillnet fishing boats operated at 0-100 m water depths. Cadufo fishing boats generally operated at ca. 50 m depth. Crab pot fishing boats operated in upper and middle slope areas are different from those used by bottom trawling boats. Some of these areas could be located within the submarine canyons, where large numbers of individuals of the main target species —the deep-water pandalid shrimp *Plesionika edwardsii*— were detected in the underwater images.

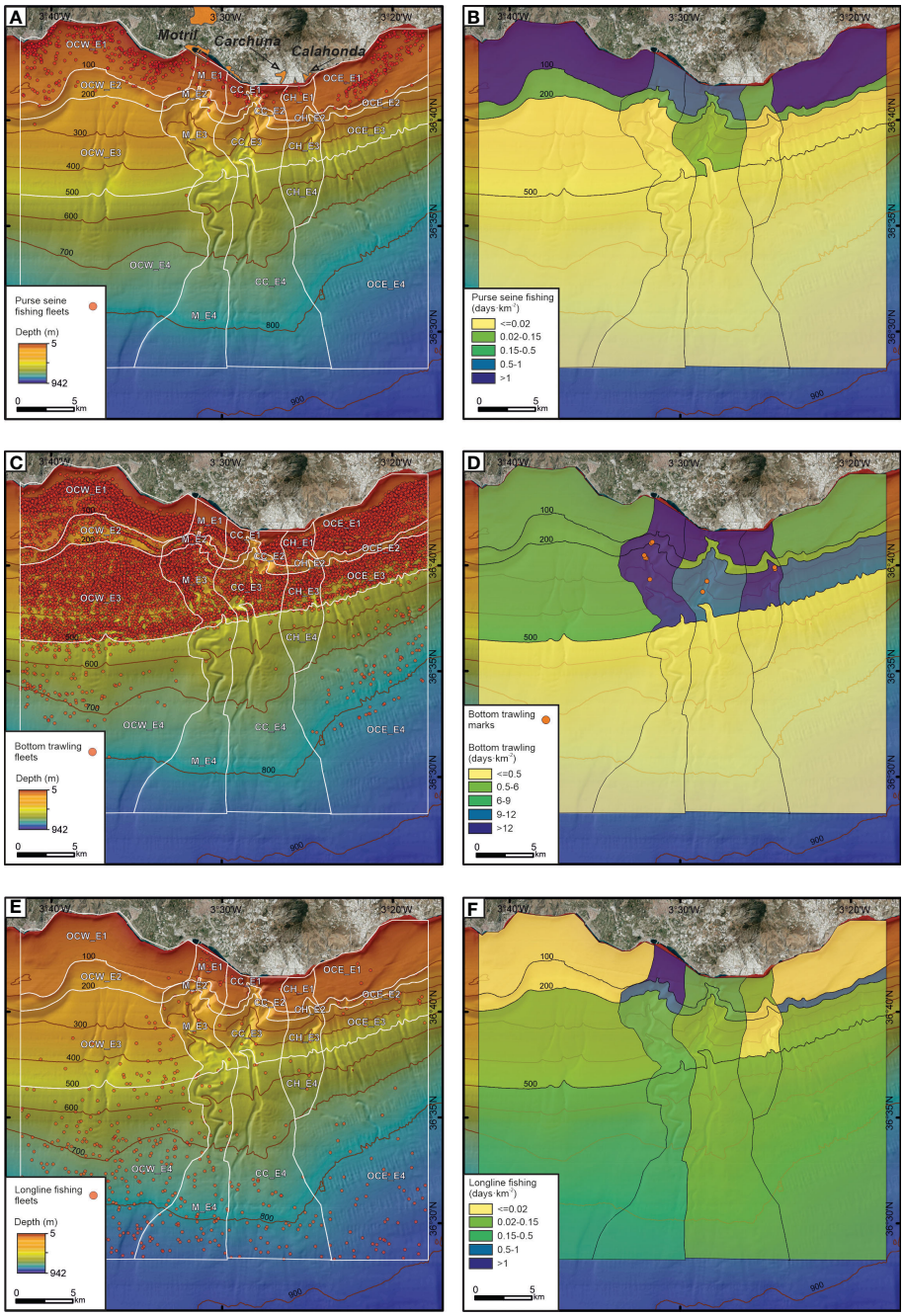

FIGURE 10
Data from Vessel Monitoring System during 2018-2019 ("Ministerio de Pesca, Agricultura y Alimentación", Spanish government). Spatial distribution of purse seine fishing fleets **(A)**, bottom trawling **(C)** and longline fishing **(E)**. Fishing effort (in days·km^{-2}) for purse seine fishing **(B)**, bottom trawling **(D)** and longline fishing **(F)**. The bottom trawling marks seen on video footage collected by the ROV in the three submarine canyons is shown **(D)**. See Supplementary Table 2 to location and depth of the bottom trawling marks and Figures 7A, B for examples of seafloor trawling marks along the flank of Motril Canyon and the thalweg of Calahonda Canyon. OCW, Western sector of the study area; M, Motril Canyon; CC, Carchuna Canyon; CH, Calahonda Canyon; OCE, Eastern sector of the study area; E1: Shelf; E2: Outer shelf-uppermost slope; E3: Upper slope; E4: Middle slope. Bathymetric contours in meters.

Discussion

Drivers of the litter abundance

In the study area of the Northern Alboran Sea, average values of marine litter density in the Motril, Calahonda and Carchuna canyons (0.32, 0.66, and 1.8 items·100 m^{-1}, respectively) are lower than most of the values found in Mediterranean canyons (Table 4), where noteworthy amounts of marine litter have been reported, particularly as large accumulations or litter hotspots along the thalwegs (e.g., Pham et al., 2014b; Tubau et al., 2015; Pierdomenico et al., 2020). The values of marine litter found in

TABLE 4 Values of density of marine litter reported in linear measurements in different submarine canyons of the Atlantic Ocean and the Mediterranean Sea.

Region	Submarine canyon	Items·100 m^{-1}	Plastic (%)	Fishing related (%)[a]	Mean water depth (m)	Reference
Study area	Motril	0.12-0.52	60	0	200	This study
	Calahonda	0.19-1.13	69.6	13.2	238	This study
	Carchuna	0.11-8.66	75.7	15.9	396	This study
Portugal coast	Lisbon	1.32	86	9	1602	Mordecai et al., 2011
	Setúbal	0.49	30	8.6	2194	Mordecai et al., 2011
	Cascais	0.21	54	9	4574	Mordecai et al., 2011
	Nazaré	0.083	25	37	3144	Mordecai et al., 2011
	São Vicente	0.58-3.31	15.9	80.5	230	Oliveira et al., 2015
Gulf of lion	Grand Rhône	0.5	25	20	345	Fabri et al., 2014
Ligurian Sea	Toulon	1.3	10	5	412	Fabri et al., 2014
Catalan coast	Cap de Creus	0.7-8.6	72.7	11.1	1210	Tubau et al., 2015
	La Fonera	0.3-18	71.1	24	701	Tubau et al., 2015
	Blanes	0.2-1.6	78.1	3.1	1509	Tubau et al., 2015
Bay of Biscay	Cap Ferret	0.69[b]	65	25	1392	van den Beld et al., 2017
	Guilvec	0.32[b]	72	12	877	van den Beld et al., 2017
	Belle-Île	0.86[b]	55	25	682	van den Beld et al., 2017
Calabria	Gioia	0.77-56.3	88	3	581	Pierdomenico et al., 2020
	Petrace	3.94-41.9	80	0	612	Pierdomenico et al., 2020
Sardinia	Sardinia canyons	1.01-3.06	88	42	302	Cau et al., 2017

[a]Percentage of litter related to fishing.
[b]Abundance reported as linear measurement (items·100 m^{-1}) by Cau et al., 2017.

Italian, Calabrian and Sardinian canyons are much higher than values found in Spanish and French canyons. Litter density values in the studied canyons are in the range of the values found in the Portuguese canyons (0.083-3.31 items·100 m^{-1}; Mordecai et al., 2011; Oliveira et al., 2015), French Atlantic canyons (0.32-0.86 items·100 m^{-1}; van den Beld et al., 2017), and French Mediterranean canyons (0.5-1.3 items·100 m^{-1}; Fabri et al., 2014) (Table 4). Within the study area, the upper segment of the Carchuna Canyon displayed a relatively high litter density (8.6 items·100 m^{-1}), which is similar to the values registered in the Cap de Creus Canyon off the Catalan coast (up to 8.6 items·100 m^{-1}; Tubau et al., 2015) (Table 4).

The study area has a population density of up to 567 inhabitants·km^{-2}, and over 80% of the population around the study area is located 2 km inshore from the coastline. Such population density is low in comparison with other areas featuring submarine canyons close to the coastline which exhibit higher densities of marine litter. For example, the heads of the Blanes, La Fonera and Cap de Creus canyons are located on the Catalan margin with a coastal population density of up to 1091 inhabitants·km^{-2}, and exhibit marine litter densities of up to 18 items·100 m^{-1} (Tubau et al., 2015). As an extreme case, the Messina Strait and Gioia canyons have the highest densities of marine litter in the Mediterranean Sea (up to 56.3 items·100 m^{-1}; Pierdomenico et al., 2020; Table 4), and exhibit a coastal population density of up to 800 inhabitants·km^{-2}. As high densities of marine litter generally display a strong correlation with the proximity of canyon heads to densely populated coasts (Hernandez et al., 2022; Taviani et al., 2023), we interpret that in the study area the relatively low amounts of litter found in the studied canyons are primarily determined by low coastal population densities.

Another factor that needs to be considered in explaining marine litter densities is the connectivity of submarine canyons to fluvial streams. The studied canyons are not directly connected to fluvial systems, and the nearby creeks exhibit very reduced dimensions and seasonal patterns (Liquete et al., 2005; Liquete et al., 2009). In contrast, very high litter densities have been registered in shelf-incised submarine canyons with heads connected to fluvial systems or with subaerial streams, for example, up to 130 items·100 m^{-1} in the Messina Strait canyons (Pierdomenico et al., 2019). Therefore, the relatively low litter densities detected in the studied canyons are interpreted as the result of a combination of the low coastal population densities and the lack of connection of canyon heads with major streams (Figures 1C, 2). These regional conditions broadly resemble those of canyons located off the Catalan coast (Table 4), which incise narrow shelves and generally have heads

near the coast, where population densities are relatively low and seasonally variable (Tubau et al., 2015).

The proximity of the Carchuna Canyon head to the coastline (<200 m) implies that the litter density in this canyon is considerably higher than in the Motril and Calahonda canyons, located >2 km from the coastline. This observation agrees with reports from other Mediterranean canyons, where the highest marine litter densities occur in shelf-incised submarine canyons with canyons dissecting the entire shelf (e.g., Calabria coast; Pierdomenico et al., 2020), or in shelf-incised canyons located in very narrow shelves (e.g., Sardinia western coast; Cau et al., 2017). In contrast, the lowest values of marine litter density occur in canyons incised in wide shelves and distant from the coastline (e.g., Gulf of Lion; Fabri et al., 2014). Therefore, we also suggest that differences in marine litter densities observed among the three studied submarine canyons should mainly reflect the distance between canyon heads and the coastline.

Drivers of the litter distribution

The transport and/or accumulation of litter along submarine canyons is considered to be determined by two major factors, downcanyon gravity flows (Dominguez-Carrió et al., 2020; Angiolillo et al., 2021; Zhong and Peng, 2021), and canyon geomorphological settings (Gerigny et al., 2019; Mecho et al., 2020; Pierdomenico et al., 2020).

The identification of litter hotspots along the upper segment of the Carchuna Canyon, the identification of marine litter along the thalweg in the lowest segment, even at the termination of the canyon (740 m water depth), and the occurrence of very fine sands in the lower segment canyon floor, are regarded as compelling evidences of the occurrence of deep transport by gravity flows along the Carchuna Canyon thalweg. Such sediment transport pulses in this canyon may be driven by downslope bottom flows, described during easterlies dominance (Serrano et al., 2020). Therefore, we consider that the Carchuna Canyon is an active system —it acts preferentially as a conduit, favouring the transport of marine litter from the deeply incised shelf (25 m water depth) to the termination of the channel in the transition towards a distal lobular deposit (740 m water depth) (Figure 1). In contrast to the Carchuna Canyon, evidences of gravity flow activity in the Motril and Calahonda canyons are lacking. Instead, the low densities of mainly buried litter by muddy sediments in those canyons can be interpreted as evidence that the canyons have behaved as sinks of marine litter along their thalweg and flanks, possibly because of their relatively high distance from the coastline.

The geomorphological setting of the Carchuna Canyon seems also to have played a role in litter transport and/or accumulation in two ways, inducing the generation of (1) the above-mentioned gravity flows, and (2) litter accumulations along its course. On the one hand, the fact that the canyon head is located very close to the coast has been previously related to energy concentration in the canyon head due to coastal waves and storm focusing (Ortega-Sánchez et al., 2014). Those processes have been observed in other canyon heads close to coastlines, where they lead to increased shear stress that frequently mobilizes coarse-grained sediments (Smith et al., 2018). A similar situation is plausible in the Carchuna Canyon head, where energy concentration in the canyon head could erode proximal sandy infralittoral prograding wedges (IPW; Figure 1D) defined along the coastline, providing a coarse-grained sediment source for the development of gravity flows.

On the other hand, litter hotspots are identified in the upper segment of the Carchuna Canyon favoured by geomorphological features such as smooth seafloor depressions and rocky outcrops blocking the thalweg (Figures 5F-H, 6; Table 3). We consider that those evidences indicate the generation of litter sinks in the Carchuna Canyon, as evidenced elsewhere (Galgani et al., 1996; Galgani et al., 2000; Watters et al., 2010; Miyake et al., 2011; Schlining et al., 2013). In canyon depressions, litter accumulations result from changes in the morphodynamic conditions of bottom currents (Carvajal et al., 2017; Zhong and Peng, 2021), whereas rocky bottoms may act as obstacles to litter items carried by gravity flows (Galgani et al., 2000; Watters et al., 2010; Schlining et al., 2013).

Litter origin: Coastal uses and marine activities

Coastal sources

Marine litter in the studied submarine canyons is overwhelmingly dominated by plastics, accounting for 75% of the total litter (Figures 3, 4). This value is similar to the plastic percentages registered in most Mediterranean canyons (Table 4), and suggests a dominant coastal origin (at least 50%) in the studied canyons. Of the different coastal uses in the study area, the influence of coastal recreational uses linked to beaches and coastal urbanization would appear to be outstanding. In fact, most of the coastal fringe at both sides of the Carchuna Canyon head is delineated by several kilometers long beaches, such as Motril and Carchuna beaches (Figure 9A). Although these beaches are periodically cleaned, because they are deemed suitable for tourism, abundant litter can be found on them (Godoy et al., 2020; Martín-Lara et al., 2021; MITECO-DGCM, 2021). Therefore, deficiencies in waste management in the beaches of the study area can increase the total amount of marine litter that can be eventually trapped by the canyons. The fact that 35% of marine litter in the studied canyons is made up of plastic bottles and bags constituted compelling evidence for coastal recreational origin. Several metal items, including beverage and food cans, can also be unequivocally attributed to beach occupation.

Almost 8% of marine litter in the study area consists of plastic sheets connected with remote pieces of greenhouses infrastructures, and seedbeds derived from agricultural practices. Both plastic types can be linked to the greenhouses and farming exploitations in the adjacent coastal plain, the main land use in the coastal domain surrounding the beaches (ca. 48%). Specifically, greenhouses are widespread in the backshore of Carchuna Beach, which is closer to the Carchuna Canyon head, whereas greenhouses in the backshore of Motril Beach are more scattered and they alternate with the farming land uses that are located backshore between the Guadalfeo River and Torrenueva town (Figure 9A). This interpretation is supported by several additional evidences that attest to the

occurrence of litter derived from agricultural practices on the northern coast of the Alboran Sea. For example, microplastics found by Godoy et al. (2020) on the beaches of the coast of Granada are low-density polyethylene, high-density polyethylene, polypropylene, and high-strength polystyrene, all common plastic types used in agriculture. In addition, whales consuming greenhouse marine litter items have been found off Almeria and Granada coasts, which are severely occupied by the greenhouse industry (de Stephanis et al., 2013).

Finally, we consider that sporadic inputs of litter from creeks mainly draining farming areas (Figure 9A) would provide marine litter from both urban and agriculture uses due to the torrential behaviour of the ravines close to the Carchuna Canyon head (Liquete et al., 2005). The coast of the Carchuna Canyon head is moreover affected by long-term erosion associated with extreme events (Ortega-Sánchez et al., 2014) and by relatively high current velocity values, causing high values of shear stress (Bárcenas et al., 2011); both processes would favour the transport of marine litter to the Carchuna Canyon head. In contrast, fluvial influence should be minor in the Motril Canyon head, as this submarine feature is relatively far (i.e., several kilometers) from the Guadalfeo River mouth; in any case, the lateral redistribution of Guadalfeo River sediment plumes under westerlies dominance (Bárcenas et al., 2011) could eventually lead to moderate amounts of marine litter from urban uses, considering the occurrence of several urban areas in the vicinity of the Port of Motril.

Marine activities

Submarine canyons can also locally receive human discards from ships if they are located along shipping routes (Stefatos et al., 1999; Wei et al., 2012; van den Beld et al., 2017; Morales-Caselles et al., 2021). In the study area, marine litter such as sunbeds and pipes found in the upper segment of the Carchuna Canyon can be attributed to shipping traffic because of the large size of these items and the fact that the canyon segment is crossed by a south-southeast shipping route (Figure 9B).

The high number of unspecified items found in the Motril Canyon makes it difficult to discern the origin of marine litter. However, the marine litter found in the upper segment of the Motril Canyon coincides with a high concentration of maritime traffic owing to the proximity of the Port of Motril and the junction of both south-west and south-southwest routes above the canyon (Figure 9B). Considering the distance between the Motril Canyon and the coastline (ca. 2 km), we infer that the marine litter in this canyon is mostly marine sourced.

Some evidence suggests the influence of fishing activities in the accumulation of marine litter in the studied canyons, considering that other types of marine debris, such as fishing gear, indicate an origin linked to marine extractive activities (Pham et al., 2014a; Vieira et al., 2015; Hernandez et al., 2022). Indeed, nearly 16% of marine litter is related to fishing activities in the study area, i.e., fishing nets and gear used by the artisanal fishing fleet. In addition, rubber items related to the floating defence of fishing boats and building items that are used as support for longline fishing can be found.

Fishing activity apparently produces a differential effect on the studied canyons, due to their distinctive geomorphological and sedimentological characteristics. The upper and middle segments of the Motril Canyon and the entire Calahonda Canyon contain smooth flanks and muddy bottoms that favour fishing activities; this is reflected by abundant evidence of high fishing efforts by bottom trawling, purse seine and longline fishing in those canyons (e.g., numerous marks by bottom trawling in the upper segment of the Motril Canyon; Figures 7A, B, 10D). However, in the Motril and Calahonda canyons, no marine litter derived from fishing activities (e.g., fishing nets) was observed. This likely indicates an efficient sediment burial and subsequent alteration in muddy environments. In contrast, fishing effort, especially bottom trawling, is lower in the Carchuna Canyon (Figure 10D) owing to the abrupt seafloor morphology, featuring very steep flanks and the local occurrence of rocky outcrops. These seafloor features might favour purse seine and longline fishing practices in the upper segment of the Carchuna Canyon. This is reflected by abundant evidence of high fishing efforts of purse seine and longline fishing (Figures 10B, F). In addition, it is evidenced by the high number of fishing nets, with several building and rubber items related to the fishing activities, found along both flanks and thalweg of the upper segment of the Carchuna Canyon (Figures 4, 11). Indeed, the tangling of fishing nets along the canyon thalweg favours the formation of litter hotspots (Figure 5H).

Interactions of anthropogenic activity indicators with marine habitats and species

The interaction of anthropogenic activities with marine habitats, and especially with certain species, may entail both positive and negative effects (Katsanevakis et al., 2007; Gregory, 2009; Browne et al., 2015; Deudero and Alomar, 2015). Such effects were identified in the study area. Among the positive ones, some litter items provide a hard substrate and refuge for specific sessile (e.g., the bivalve *Neopycnodonte cochlear*, hydrozoans) and mobile species (e.g., the decapod *Munida* sp., the greater forkbeard *Phycis blennoides*) on the sedimentary bottoms of the studied canyons (Figure 5H). The role of some types of litter as artificial hard substrates for sessile species is widely known —particularly floating objects that may act as vectors of dispersion for some species, including indigenous invasive species (Thiel and Gutow, 2005). Among the species settling and growing on these artificial substrates (e.g., *N. cochlear*), some are generally considered 'opportunistic' and may represent pioneering species in the colonization of new natural substrates in circalittoral and bathyal bottoms (Sotomayor-García et al., 2019). The provision of refuge made by litter for mobile species has scarcely been investigated, although an increase in the total abundance and the number of species in soft bottoms with litter has been linked to litter that created refuge or reproduction sites for mobile species (Katsanevakis et al., 2007). In the submarine canyons studied here, some large pieces of litter served as refuge for squat lobsters *Munida* spp. or the greater forkbeard *Phycis blennoides* (Figure 5H). These species seem to benefit from the crevices and complexity provided by litter items, because they play a role similar to that of isolated rocks or coral rubble in sedimentary habitats (Uiblein et al., 2003; Poore et al., 2011; Rueda et al., 2021). The use of litter as a refuge by squat lobsters could be related to the

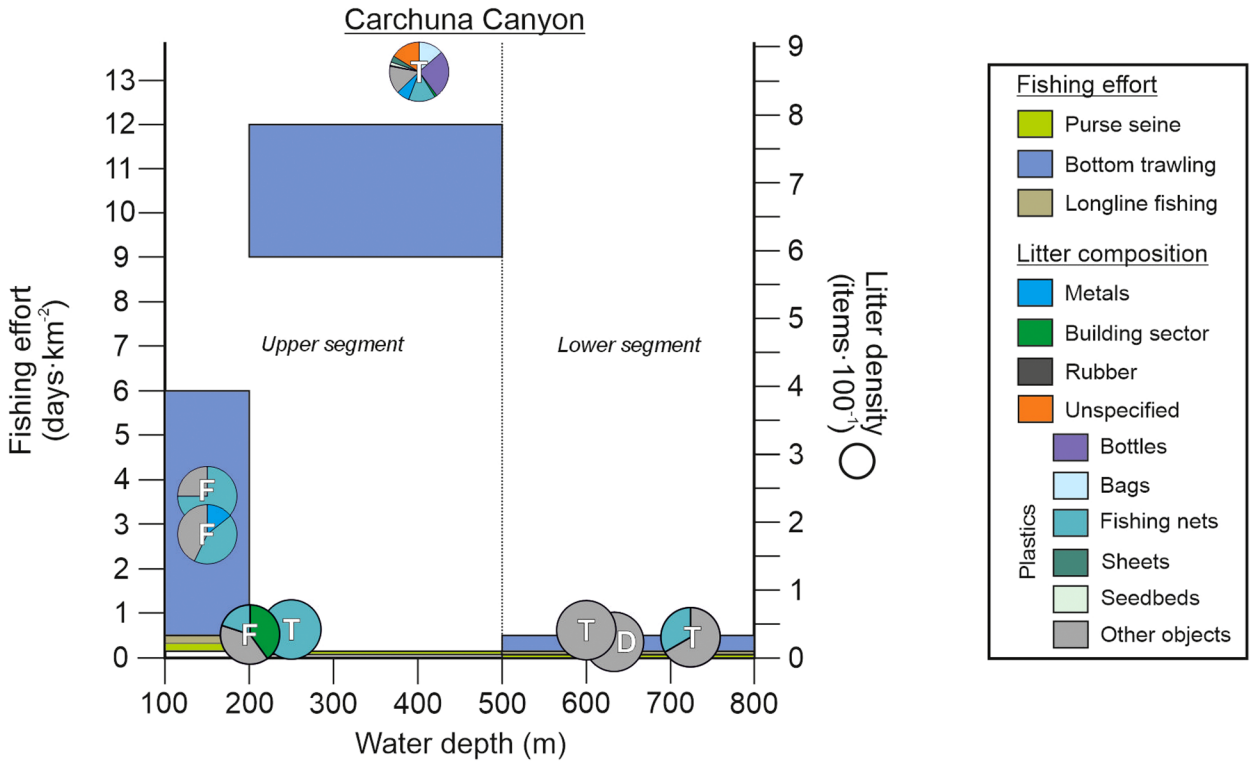

FIGURE 11
Chart showing the ranges of fishing effort (days·km^{-2}) for each of the Carchuna Canyon sections (see Figure 10). Litter density (expressed as number of items·100 m^{-1}), and litter composition (as pie charts) are also shown. T, canyon thalweg; F, canyon flank; D, lateral deposit.

fact that they commonly live in burrows or are associated with large sessile invertebrates, which would influence their resistance to physical pressures and their protection against predation and/or acquisition of food (Trenkel et al., 2007; Poore et al., 2011). In the case of the greater forkbeard, large litter affords cavities for these active station holders with an effective foraging strategy for capturing their main prey, such as epibenthic and benthopelagic crustaceans (Du Buit, 1978; Mauchline and Gordon, 1984; Uiblein et al., 2003).

Negative effects of anthropogenic activities on the seabed are widely known, and may include physical abrasion, damage, entanglement, and/or burial of sessile and mobile species, chemical transfer (including microplastics) to organisms and the food chain, as well as declines of important commercial stocks, among others (Gregory, 2009; Ramirez-Llodra et al., 2011; Browne et al., 2015; Clark et al., 2016; Trestrail et al., 2020). Fishing activity in submarine canyons was described as the main source of impacts on their seafloor and associated biota, whether habitat-forming species or those with important economic value (Puig et al., 2015; Cau et al., 2017; Fernandez-Arcaya et al., 2017; Oberle et al., 2018; Giusti et al., 2019; Paradis et al., 2021). Some of the indirect impacts from bottom trawling are generally caused by the resuspension of shelf (and nearby) fine sediments during the trawling operations and their deposition in the seabed of the underlying canyons, which may cause siltation of some sessile habitat-forming species (Puig et al., 2012; Martín et al., 2014). Indeed, in the analyzed underwater images, some of these benthic species seemed to be silted up in different parts of the canyon. In the present study, the largest average densities of anthropogenic activity indicators were detected in some of the shallowest habitats, including detritic bottoms and scleractinian aggregations (Figure 5C), considered vulnerable habitats with high ecological importance (Bellan-Santini et al., 2007; Rueda et al., 2021). Detritic bottoms host a biocoenosis of great diversity and abundance (Bellan-Santini et al., 2007; Rueda et al., 2021). The biocoenosis is favoured by the mixture of different substrate types, which enhances the substrate heterogeneity and the diversification of organisms and food sources. Despite their unquestionable species richness, detritic bottoms do not benefit from any kind of formal protection other than being included in marine protected areas designated for other components. Perspectives for specific protection are scant because these bottoms are a major target for trawling and because they can be very extensive (Figures 7A, B). Meanwhile, scleractinian aggregations in hard substrates correspond to Habitat 1170 "Reefs" from the EU Habitat Directive (92/43/EEC), and this study detected them in the western wall of the Carchuna Canyon head, together with a high number of cloth bags and lines generally used in local longline fisheries (Figure 5C). Interaction of longline fishing with benthic fauna can be very localized to specific areas but still can cause a severe impact on slow-growing species that provide a high three-dimensional complexity (e.g., aggregations of colonial scleractinians) (Fabri et al., 2014; Tubau et al., 2015; Ragnarsson et al., 2017). Longline fishing might alter the seabed to a lesser extent than bottom trawling, in view of its much narrower bottom

mark (Pham et al., 2014a; Fabri et al., 2022). A negative impact may stem from the cloth bags filled with sediments or stones used as weights for the longline fisheries, and which, together with the lines, can easily break the skeletons of the scleractinians, inducing the decline and final loss of the habitat they conform (Fosså et al., 2002; Clark et al., 2016). In this sense, urgent protection measures are needed to preserve this vulnerable habitat structured by colonial scleractinians in the studied submarine canyons. Finally, it is important to mention that this study did not provide information on the potential ingestion of microplastics by the detected taxa. It is known that microplastic ingestion in some organisms (e.g., invertebrates) reduces somatic and reproductive growth (Trestrail et al., 2020). Considering this, further studies should provide information on those taxa that may contain high rates of microplastics in their bodies as well as on the potential negative effects on them.

Conclusion

The detailed analysis of the origin and driving mechanisms of marine litter density and distribution and of the interactions between anthropogenic impacts and marine habitats and species, in this case in the Motril, Carchuna, and Calahonda canyons (northern margin of the Alboran Sea), stands as a contribution to cataloguing marine litter in submarine canyons worldwide, and to understanding the role of submarine canyons as conduits or sinks for litter, with its subsequent impact on benthic habitats. The main conclusions of this study are:

1. The Motril, Calahonda and Carchuna canyons exhibit low litter densities in comparison with other submarine canyons located in the Mediterranean Sea, due to the combination of relatively low coastal population densities and the lack of connection of canyon heads to major streams. The proximity of the Carchuna Canyon head (<200 m) to the coastline implies that the litter density in this canyon is considerably higher than in the Motril and Calahonda canyons, at longer distances from the coast.
2. The Motril and Calahonda canyons can be considered passive systems that have acted as mainly depositional sinks in the recent past, as evidenced by the occurrence of buried marine litter and mostly muddy sediments on the canyon floors. In contrast, the high shelf incision of the Carchuna Canyon and its proximity to the coastline favour the capture of littoral sediment transport, and the formation of gravity flows that transport the marine litter downslope, evidenced by marine litter along the thalweg (up to the termination of the canyon; 740 m water depth) and the occurrence of very fine sand in the lower segment; litter hotspots are favoured by the canyon morphology and the occurrence of rocky outcrops.
3. The main sources of marine litter in the study area (at least 35%) can be traced to coastal recreational uses, such as beaches and coastal urbanization as well as the pressure from tourism. Another coastal origin of the marine litter in the study area could be linked to agricultural practices (at least 8%) that is the main land use in the study area and characterized by greenhouse exploitation in the adjacent coastal plain. A third origin is related to fishing techniques and litter discards from ships. The Motril and Calahonda canyons have smooth flanks and muddy bottoms that favour fishing activities, as opposed to the Carchuna Canyon, having an abrupt seafloor morphology.
4. In the studied canyons, some large pieces of litter are used as refuges by some species against predation and/or for food acquisition. In contrast, fishing activity involving the use of cloth bags, gears, and lines may be producing an impact through entanglement and physical damage to erect benthic fauna, including some aggregations of colonial scleractinians on the walls of the Carchuna Canyon.

Data availability statement

The original contributions presented in the study are included in the article/Supplementary Material. Further inquiries can be directed to the corresponding author.

Author contributions

JC-E wrote the manuscript draft and elaborated most of the figures. FL and ÁP-B provided the conceptual framework of the study and rewrote extensively the manuscript. JR wrote sections of the manuscript. PB performed the grain size analysis. OS-G, AL-Q, IM, JP-A, and JC-H contributed to figure making. JS, JP, IM, JP-A and YM performed the statistical analysis. All authors contributed to manuscript revision, reading, and approved the submitted version.

Funding

This research was funded by the projects Alboran Shelf-Slope cOupling processes and deep sediMent trAnsfeR: Source To Sink approaches and implications for biodiversity-ALSSOMAR S2S (CTM2017-88237-P) (Ministerio de Economía y Competitividad, Spanish goverment), and Sediment gravity flows and ANthropogenic Impacts in a MEDiterranean deltaic-and-canyon environment: Causal relationships and consequences-SANIMED (PID2021-125489OB-I00) (Ministerio de Ciencia e Innovación, Spanish goverment). This study is also part of Cerrillo-Escoriza's PhD project, which is supported by Grant PRE2018-084812 funded by MCIN/AEI/10.13039/501100011033 and FSE Invierte en tu futuro.

Acknowledgments

The authors wish to thank the captain and crew of R/V Sarmiento de Gamboa for their dedication and constant support for the execution of activities onboard, and to the participants of the ALSSOMAR-S2S expedition for their help during data acquisition. Multibeam bathymetry and fishing activity data were provided by the "Ministerio de Pesca, Agricultura y Alimentación", Spanish government. Land use data were provided by the "Consejería de Agricultura, Ganadería, Pesca y Desarrollo Sostenible, Junta de Andalucía", regional government. JR acknowledges partial support from the 18-ESMARES2-CIRCA project of the Instituto Español de Oceanografía (IEO-CSIC), under the framework of the tasks commissioned to the IEO by the Ministerio de Transición Ecológica y Reto Demográfico (MITERD) of the Spanish government for the application of the Marine Strategy Framework Directive (MSFD) in Spanish waters. IM acknowledges to Fundação para a Ciência e a Tecnologia for Research Assistant contract DL57/2016/CP1361/CT0009 and project UID/0350/2020 CIMA. Very constructive and detailed reviews of an initial manuscript version were provided by two reviewers and by Guest Associate Editor Veerle Huvenne. We are grateful to Jean Sanders for correcting the English text.

Conflict of interest

The authors declare that the research was conducted in the absence of any commercial or financial relationships that could be construed as a potential conflict of interest.

Publisher's note

Supplementary material

The Supplementary Material for this article can be found online at: https://www.frontiersin.org/articles/10.3389/fmars.2023.1098927/full#supplementary-material

References

Abelló, P., Carbonell, A., and Torres, P. (2002). Biogeography of epibenthic crustaceans on the shelf and upper slope off the Iberian peninsula Mediterranean coasts: Implications for the establishment of natural management areas. *Sci. Mar.* 66, 183–198. doi: 10.3989/scimar.2002.66s2183

Adams, S. M. (2005). Assessing cause and effect of multiple stressors on marine systems. *Mar. Pollut. Bull.* 51, 649–657. doi: 10.1016/j.marpolbul.2004.11.040

Alves, T. M., Kokinou, E., Ekström, M., Nikolaidis, A., Georgiou, G. C., and Miliou, A. (2021). Scientific, societal and pedagogical approaches to tackle the impact of climate change on marine pollution. *Sci. Rep.* 11, 1–15. doi: 10.1038/s41598-021-82421-y

Angiolillo, M. (2019). *Chapter 14 - debris in deep water, world Seas.Volume III: Ecological issues and environmental impacts. 2nd ed.* (Cambridge: Academic Press), 251–268. doi: 10.1016/B978-0-12-805052-1.00015-2

Angiolillo, M., di Lorenzo, B., Farcomeni, A., Bo, M., Bavestrello, G., Santangelo, G., et al. (2015). Distribution and assessment of marine debris in the deep tyrrhenian Sea (NW Mediterranean Sea, Italy). *Mar. Pollut. Bull.* 92, 149–159. doi: 10.1016/j.marpolbul.2014.12.044

Angiolillo, M., Gérigny, O., Valente, T., Fabri, M. C., Tambute, E., Rouanet, E., et al. (2021). Distribution of seafloor litter and its interaction with benthic organisms in deep waters of the ligurian Sea (Northwestern Mediterranean). *Sci. Total Environ.* 788, 147745. doi: 10.1016/j.scitotenv.2021.147745

Ayuntamiento de Motril. Medio Ambiente Urbano (2021). Anexo 2: Residuos urbanos y asimilables a urbanos. *Motril Agenda* 21, 45–73.

Bárcenas, P., Lobo, F. J., Macías, J., Fernández-Salas, L. M., and Díaz del Río, V. (2011). Spatial variability of surficial sediments on the northern shelf of the alboran Sea: the effects of hydrodynamic forcing and supply of sediment by rivers. *J. Iber. Geol.* 37, 195–214. doi: 10.5209/rev_JIGE.2011.v37.n2.8

Bárcenas, P., Lobo, F. J., Macías, J., Fernández-Salas, L. M., López-González, N., and Díaz del Río, V. (2015). Submarine deltaic geometries linked to steep, mountainous drainage basins in the northern shelf of the alboran Sea: Filling the gaps in the spectrum of deltaic deposition. *Geomorphology* 232, 125–144. doi: 10.1016/j.geomorph.2014.11.028

Bárcenas, P., and Macías, J. (2009). Estudio morfométrico comparativo entre las ondulaciones de los prodeltas de los ríos de andalucía oriental. *Rev. Soc Geol. Esp.* 22, 43–56.

Baro, J., García-Jiménez, T., and Serna-Quintero, J. M. (2021). "Description of artisanal fisheries in northern alboran Sea," in *Alboran Sea - ecosystems and marine resources*, vol. 15 . Eds. J. C. Báez, J. T. Vázquez, J. A. Camiñas and M. Malouli Idrissi (Cham: Springer), 524–542.

Bellan-Santini, D., Bellan, G., Bitar, G., Harmelin, J. G., and Pergent, G. (2007). *Handbook for interpreting types of marine habitat for the selection of sites to be included in the national inventories of natural sites of conservation interest* Vol. 168 (Tunisia: UNEP-MAP RAC/SPA).

Bergmann, M., Collard, F., Fabres, J., Gabrielsen, G. W., Provencher, J. F., Rochman, C. M., et al. (2022). Plastic pollution in the Arctic. *Nat. Rev. Earth Environ.* 3, 323–337. doi: 10.1038/s43017-022-00279-8

Browne, M. A., Underwood, A. J., Chapman, M. G., Williams, R., Thompson, R. C., and Van Franeker, J. A. (2015). Linking effects of anthropogenic debris to ecological impacts. *Proc. R. Soc B.* 282, 20142929. doi: 10.1098/rspb.2014.2929

Canals, M., Pham, C. K., Bergmann, M., Gutow, L., Hanke, G., Van Sebille, E., et al. (2021). The quest for seafloor macrolitter: A critical review of background knowledge, current methods and future prospects. *Environ. Res. Lett.* 16, 023001. doi: 10.1088/1748-9326/abc6d4

Carvajal, C., Paull, C. K., Caress, D. W., Fildani, A., Lundsten, E., Anderson, K., et al. (2017). Unraveling the channel-lobe transition zone with high-resolution AUV bathymetry: Navy fan, offshore Baja California, Mexico. *J. Sediment. Res.* 87, 1049–1059. doi: 10.2110/jsr.2017.58

Cau, A., Alvito, A., Moccia, D., Canese, S., Pusceddu, A., Rita, C., et al. (2017). Submarine canyons along the upper sardinian slope (Central Western Mediterranean) as repositories for derelict fishing gears. *Mar. Pollut. Bull.* 123, 357–364. doi: 10.1016/j.marpolbul.2017.09.010

Ciércoles, C., García-Ruíz, C., Abelló, P., Hidalgo, M., Torres, P., González, M., et al. (2022). Decapod crustacean assemblages on trawlable grounds in the northern alboran Sea and gulf of Vera. *Sci. Mar.* 86, e039. doi: 10.3989/scimar.05265.039

Ciércoles, C., García-Ruiz, C., González-Aguilar, M., Ortiz de Urbina Gutiérrez, J., López-González, N., Urra-Recuero, J., et al. (2018). Molluscs collected with otter trawl in the northern alboran Sea: main assemblages, spatial distribution and environmental linkage. *Mediterr. Mar. Sci.* 19, 209–222. doi: 10.12681/mms.2124

Clark, M. R., Althaus, F., Schlacher, T. A., Williams, A., Bowden, D. A., and Rowden, A. A. (2016). The impacts of deep-sea fisheries on benthic communities: A review. *Ices J. Mar. Sci.* 73, 51–69. doi: 10.1093/icesjms/fsv123

de Stephanis, R., Giménez, J., Carpinelli, E., Gutierrez-Exposito, C., and Canadas, A. (2013). As main meal for sperm whales: Plastics debris. *Mar. Pollut. Bull.* 69, 206–214. doi: 10.1016/j.marpolbul.2013.01.033

Deudero, S., and Alomar, C. (2015). Mediterranean Marine biodiversity under threat: Reviewing influence of marine litter on species. *Mar. Pollut. Bull.* 98, 58–68. doi: 10.1016/j.marpolbul.2015.07.012

Dominguez-Carrió, C., Sanchez-Vidal, A., Estournel, C., Corbera, G., Riera, J. L., Orejas, C., et al. (2020). Seafloor litter sorting in different domains of cap de creus continental shelf and submarine canyon (NW Mediterranean Sea). *Mar. Pollut. Bull.* 161, 111744. doi: 10.1016/j.marpolbul.2020.111744

Du Buit, M. (1978). Alimentation de quelques poissons téléostéens de profondeur dans la zone du seuil de wyville Thomson. *Oceanol. Acta* 1, 129–134.

Ercilla, G., Alonso, B., and Baraza, J. (1994). Post-calabrian sequence stratigraphy of the northwestern alboran Sea (southwestern Mediterranean). *Mar. Geol.* 120, 249–265. doi: 10.1016/0025-3227(94)90061-2

European Commission of the European Union (2013). *MSDF guidance on monitoring marine litter* (Luxembourg: Publications Office of the European Union).

Fabres, J., Calafat, A., Sanchez-Vidal, A., Canals, M., and Heussner, S. (2002). Composition and spatio-temporal variability of particle fluxes in the Western alboran gyre, Mediterranean Sea. *J. Mar. Syst.* 33–34, 431–456. doi: 10.1016/S0924-7963(02)00070-2

Fabri, M. C., Dugornay, O., de la Bernardie, X., Guerin, C., Sanchez, P., Arnaubec, A., et al. (2022). 3D-representations for studying deep-sea coral habitats in the lacaze-duthiers canyon, from geological settings to individual specimens. *Deep. Res. Part I. Oceanogr. Res. Pap.* 187, 103831. doi: 10.1016/j.dsr.2022.103831

Fabri, M. C., Pedel, L., Beuck, L., Galgani, F., Hebbeln, D., and Freiwald, A. (2014). Megafauna of vulnerable marine ecosystems in French mediterranean submarine canyons: Spatial distribution and anthropogenic impacts. *Deep-sea Res. Pt. II.* 104, 184–207. doi: 10.1016/j.dsr2.2013.06.016

Fernandez-Arcaya, U., Ramirez-Llodra, E., Aguzzi, J., Allcock, A. L., Davies, J. S., Dissanayake, A., et al. (2017). Ecological role of submarine canyons and need for canyon conservation: A review. *Front. Mar. Sci.* 4. doi: 10.3389/fmars.2017.00005

Fernández-Salas, L. M., Dabrio, C. J., Goy, J. L., Díaz del Río, V., Zazo, C., Lobo, F. J., et al. (2009). Land-sea correlation between late Holocene coastal and infralittoral deposits in the SE Iberian peninsula (Western Mediterranean). *Geomorphology* 104, 4–11. doi: 10.1016/j.geomorph.2008.05.013

Folk, R. L. (1954). The distinction between grain size and mineral composition in sedimentary rock nomenclature. *J. Geol.* 62, 344–359. doi: 10.1086/626171

Fosså, J. H., Mortensen, P. B., and Furevik, D. M. (2002). The deep-water coral lophelia pertusa in Norwegian waters: Distribution and fishery impacts. *Hydrobiologia* 471, 1–12. doi: 10.1023/A:1016504430684

Galgani, F., Leaute, J. P., Moguedet, P., Souplet, A., Verin, Y., Carpentier, A., et al. (2000). Litter on the Sea floor along European coasts. *Mar. Pollut. Bull.* 40, 516–527. doi: 10.1016/S0025-326X(99)00234-9

Galgani, F., Souplet, A., and Cadiou, Y. (1996). Accumulation of debris on the deep sea floor off the French Mediterranean coast. *Mar. Ecol. Prog. Ser.* 142, 225–234. doi: 10.3354/meps142225

García-Rivera, S., Lizaso, J. L. S., and Millán, J. M. B. (2018). Spatial and temporal trends of marine litter in the Spanish Mediterranean seafloor. *Mar. Pollut. Bull.* 137, 252–261. doi: 10.1016/j.marpolbul.2018.09.051

García-Ruiz, C., Lloris, D., Rueda, J. L., García-Martínez, M. C., and Gil de Sola, L. (2015). Spatial distribution of ichthyofauna in the northern alboran Sea (western Mediterranean). *J. Nat. Hist.* 49, 1191–1224. doi: 10.1080/00222933.2014.1001457

Gerigny, O., Brun, M., Fabri, M. C., Tomasino, C., Le Moigne, M., Jadaud, A., et al. (2019). Seafloor litter from the continental shelf and canyons in French Mediterranean water: Distribution, typologies and trends. *Mar. Pollut. Bull.* 146, 653–666. doi: 10.1016/j.marpolbul.2019.07.030

Giusti, M., Canese, S., Fourt, M., Bo, M., Innocenti, C., Goujard, A., et al. (2019). Coral forests and derelict fishing gears in submarine canyon systems of the ligurian Sea. *Prog. Oceanogr.* 178, 102186. doi: 10.1016/j.pocean.2019.102186

Godoy, V., Prata, J. C., Blázquez, G., Almendros, A. I., Duarte, A. C., Rocha-Santos, T., et al. (2020). Effects of distance to the sea and geomorphological characteristics on the quantity and distribution of microplastics in beach sediments of Granada (Spain). *Sci. Total Environ.* 746, 142023. doi: 10.1016/j.scitotenv.2020.142023

Goldberg, E. D. (1997). Plasticizing the seafloor: An overview. *Environ. Technol.* 18, 195–201. doi: 10.1080/09593331808616527

Gregory, M. R. (2009). Environmental implications of plastic debris in marine settings- entanglement, ingestion, smothering, hangers-on, hitch-hiking and alien invasions. *Phil. Trans. R. Soc B.* 364, 2013–2025. doi: 10.1098/rstb.2008.0265

Hernandez, I., Davies, J. S., Huvenne, V. A. I., and Dissanayake, A. (2022). Marine litter in submarine canyons: A systematic review and critical synthesis. *Front. Mar. Sci.* 9. doi: 10.3389/fmars.2022.965612

Hernández-Molina, F. J., Fernández-Salas, L. M., Lobo, F., Somoza, L., Díaz-del-Río, V., and Alveirinho Dias, J. M. (2000). The infralittoral prograding wedge: A new large-scale progradational sedimentary body in shallow marine environments. *Geo-Mar. Lett.* 20, 109–117. doi: 10.1007/s003670000040

Junta de Andalucía, Consejería de Medio Ambiente, A. Y. P. (2019). *Plan director territorial de gestión de residuos no peligrosos de andalucía 2010–2019*. Junta de Andalucía, BOJA 168, 5–6.

Kane, I. A., and Fildani, A. (2021). Anthropogenic pollution in deep-marine sedimentary systems–a geological perspective on the plastic problem. *Geology* 49, 607–608. doi: 10.1130/focus052021.1

Katsanevakis, S., Verriopoulos, G., Nicolaidou, A., and Thessalou-Legaki, M. (2007). Effect of marine litter on the benthic megafauna of coastal soft bottoms: A manipulative field experiment. *Mar. Pollut. Bull.* 54, 771–778. doi: 10.1016/j.marpolbul.2006.12.016

Lario, J., Zazo, C., and Goy, J. L. (1999). Fases de progradación y evolución morfosedimentaria de la flecha litoral de calahonda (Granada) durante el holoceno. *Estud. Geol.* 55, 247–250. doi: 10.3989/egeol.99555-6164

Liquete, C., Arnau, P., Canals, M., and Colas, S. (2005). Mediterranean River systems of Andalusia, southern Spain, and associated deltas: A source to sink approach. *Mar. Geol.* 222-223, 471–495. doi: 10.1016/j.margeo.2005.06.033

Liquete, C., Canals, M., Ludwig, W., and Arnau, P. (2009). Sediment discharge of the rivers of Catalonia, NE Spain, and the influence of human impacts. *J. Hydrol.* 366, 76–88. doi: 10.1016/j.jhydrol.2008.12.013

Liubartseva, S., Coppini, G., Lecci, R., and Clementi, E. (2018). Tracking plastics in the Mediterranean: 2D Lagrangian model. *Mar. Pollut. Bull.* 129, 151–162. doi: 10.1016/j.marpolbul.2018.02.019

Lobo, F. J., Goff, J. A., Mendes, I., Bárcenas, P., Fernández-Salas, L. M., Martín-Rosales, W., et al. (2015). Spatial variability of prodeltaic undulations on the guadalfeo river prodelta: Support to the genetic interpretation as hyperpycnal flow deposits. *Mar. Geophys. Res.* 36, 309–333. doi: 10.1007/s11001-014-9233-9

Martín, J., Puig, P., Palanques, A., and Ribó, M. (2014). Trawling-induced daily sediment resuspension in the flank of a Mediterranean submarine canyon. *Deep. Res. Part II. Top. Stud. Oceanogr.* 104, 174–183. doi: 10.1016/j.dsr2.2013.05.036

Martín-Lara, M. A., Godoy, V., Quesada, L., Lozano, E. J., and Calero, M. (2021). Environmental status of marine plastic pollution in Spain. *Mar. Pollut. Bull.* 170, 112677. doi: 10.1016/j.marpolbul.2021.112677

Mateo-Ramírez, Á., Marina, P., Moreno, D., Valero, Alcántara, Aguilar, R., Báez, J. C., et al. (2021). "Marine protected areas and key biodiversity areas of the alboran Sea and adjacent areas," in *Alboran Sea – ecosystems and marine resources*, vol. 25 . Eds. J. C. Báez, J. T. Vázquez, J. A. Camiñas and M. Malouli Idrissi (Cham: Springer), 819–923.

Mauchline, J., and Gordon, J. D. (1984). Feeding and bathymetric distribution of the gadoid and morid fish of the rockall trough. *J. Mar. Biol. Assoc. Uk.* 64, 657–665. doi: 10.1017/S0025315400030320

Mecho, A., Francescangeli, M., Ercilla, G., Fanelli, E., Estrada, F., Valencia, J., et al. (2020). Deep-sea litter in the gulf of cadiz (Northeastern Atlantic, Spain). *Mar. Pollut. Bull.* 153, 110969. doi: 10.1016/j.marpolbul.2020.110969

Ministerio para la Transición Ecológica y el Reto Demográfico (MITECO-DGCM) (2021). Programa de seguimiento de basuras marinas en playas. Informe de resultados. Dirección general de la costa y el mar, 290 pp.

Miyake, H., Shibata, H., and Furushima, Y. (2011). "Deep-sea litter study using deep-sea observation tools," in *Interdisciplinary studies on environmental chemistry — marine environmental modeling and analysis*. Eds. K. Omori, X. Guo, N. Yoshie, N. Fujii, I. C. Handoh, A. Isobe and S. Tanabe (Tokyo: TERRAPUB), 261–269.

Morales-Caselles, C., Viejo, J., Martí, E., González-Fernández, D., Pragnell-Raasch, H., González-Gordillo, J. I., et al. (2021). An inshore–offshore sorting system revealed from global classification of ocean litter. *Nat. Sustain.* 4, 484–493. doi: 10.1038/s41893-021-00720-8

Mordecai, G., Tyler, P. A., Masson, D. G., and Huvenne, V. A. I. (2011). Litter in submarine canyons off the west coast of Portugal. *Deep-sea Res. Pt. II.* 58, 2489–2496. doi: 10.1016/j.dsr2.2011.08.009

Neves, D., Sobral, P., and Pereira, T. (2015). Marine litter in bottom trawls off the Portuguese coast. *Mar. Pollut. Bull.* 99, 301–304. doi: 10.1016/j.marpolbul.2015.07.044

Oberle, F. K. J., Puig, P., and Martín, J. (2018). "Fishing activities," in *Submarine geomorphology*. Eds. A. Micallef, S. Krastel and A. Savini (Cham: Springer), 503–534.

Oliveira, F., Monteiro, P., Bentes, L., Henriques, N. S., Aguilar, R., and Gonçalves, J. M. S. (2015). Marine litter in the upper são Vicente submarine canyon (SW portugal): Abundance, distribution, composition and fauna interactions. *Mar. Pollut. Bull.* 97, 401–407. doi: 10.1016/j.marpolbul.2015.05.060

Ortega-Sánchez, M., Lobo, F. J., López-Ruiz, A., Losada, M. A., and Fernández-Salas, L. M. (2014). The influence of shelf-indenting canyons and infralittoral prograding wedges on coastal morphology: The carchuna system in southern Spain. *Mar. Geol.* 347, 107–122. doi: 10.1016/j.margeo.2013.11.006

Palanques, A., El Khatab, M., Puig, P., Masqué, P., Sánchez-Cabeza, J. A., and Isla, E. (2005). Downward particle fluxes in the guadiaro submarine canyon depositional system (north-western alboran Sea), a river flood dominated system. *Mar. Geol.* 220, 23–40. doi: 10.1016/j.margeo.2005.07.004

Paradis, S., Lo Iacono, C., Masqué, P., Puig, P., Palanques, A., and Russo, T. (2021). Evidence of large increases in sedimentation rates due to fish trawling in submarine canyons of the gulf of Palermo (SW Mediterranean). *Mar. Pollut. Bull.* 172, 112861. doi: 10.1016/j.marpolbul.2021.112861

Paull, C. K., Caress, D. W., Lundsten, E., Gwiazda, R., Anderson, K., McGann, M., et al. (2013). Anatomy of the la Jolla submarine canyon system; offshore southern California. *Mar. Geol.* 335, 16–34. doi: 10.1016/j.margeo.2012.10.003

Pérez-Belzuz, F., and Alonso, B. (2000). Evolución sedimentaria reciente de dos sistemas turbidíticos del área de motril (NE alborán). parte II: sistema turbidítico de sacratif. *Geotemas* 1, 207–211.

Pérez-Belzuz, F., Alonso, B., and Ercilla, G. (2000). Modelos de sistemas turbidíticos en el Área de motril (NE alborán). *Geotemas* 1, 213–216.

Pham, C. K., Diogo, H., Menezes, G., Porteiro, F., Braga-Henriques, A., Vandeperre, F., et al. (2014a). Deep-water longline fishing has reduced impact on vulnerable marine ecosystems. *Sci. Rep.* 4, 4837. doi: 10.1038/srep04837

Pham, C. K., Ramirez-Llodra, E., Alt, C. H. S., Amaro, T., Bergmann, M., Canals, M., et al. (2014b). Marine litter distribution and density in European seas, from the shelves to deep basins. *PloS One* 9, e95839. doi: 10.1371/journal.pone.0095839

Pierdomenico, M., Casalbore, D., and Chiocci, F. L. (2019). Massive benthic litter funnelled to deep sea by flash-flood generated hyperpycnal flows. *Sci. Rep.* 9(5330). doi: 10.1038/s41598-019-41816-8

Pierdomenico, M., Casalbore, D., and Chiocci, F. L. (2020). The key role of canyons in funnelling litter to the deep sea: A study of the gioia canyon (Southern tyrrhenian Sea). *Anthropocene* 30, 100237. doi: 10.1016/j.ancene.2020.100237

Poore, G. C. B., Ahyong, S. T., and Taylor, J. (2011). The biology of squat lobsters. *CSIRO* 363 p. doi: 10.1071/9780643104341

Puig, P., Canals, M., Company, J. B., Martín, J., Amblas, D., Lastras, G., et al. (2012). Ploughing the deep sea floor. *Nature* 489, 286–289. doi: 10.1038/nature11410

Puig, P., Martín, J., Masqué, P., and Palanques, A. (2015). Increasing sediment accumulation rates in la fonera (Palamós) submarine canyon axis and their relationship with bottom trawling activities. *Geophys. Res. Lett.* 42, 8106–8113. doi: 10.1002/2015GL065052

Ragnarsson, S.Á., Burgos, J. M., Kutti, T., van den Beld, I., Egilsdóttir, H., Arnaud-Haond, S., et al. (2017). "The impact of anthropogenic activity on cold-water corals," in *Marine animal forests: the ecology of benthic biodiversity hotspots*. Eds. S. Rossi, L. Bramanti, A. Gori and C. Orejas (Cham: Springer), 989–1023.

Ramirez-Llodra, E., De Mol, B., Company, J. B., Coll, M., and Sardà, F. (2013). Effects of natural and anthropogenic processes in the distribution of marine litter in the deep Mediterranean Sea. *Prog. Oceanogr.* 118, 273–287. doi: 10.1016/j.pocean.2013.07.027

Ramirez-Llodra, E., Tyler, P. A., Baker, M. C., Bergstad, O. A., Clark, M. R., Escobar, E., et al. (2011). Man and the last great wilderness: Human impact on the deep sea. *PloS One* 6, e22588. doi: 10.1371/journal.pone.0022588

Richmond, R. H. (1993). Coral reefs: Present problems and future concerns resulting from anthropogenic disturbance. *Integr. Comp. Biol.* 33, 524–536. doi: 10.1093/icb/33.6.524

Rueda, J. L., Gofas, S., Aguilar, R., de la Torriente, A., García Raso, J. E., Lo Iacono, C., et al. (2021). "Benthic fauna of littoral and deep-Sea habitats of the alboran Sea: A hotspot of biodiversity BT," in *Alboran Sea – ecosystems and marine resources*, vol. 9 . Eds. J. C. Báez, J. T. Vázquez, J. A. Camiñas and M. Malouli Idrissi (Cham: Springer), 285–358.

Sánchez, P., Masó, M., Sáez, R., de Juan, S., Muntadas, A., and Demestre, M. (2013). Baseline study of the distribution of marine debris on soft-bottom habitats associated with trawling grounds in the northern Mediterranean. *Sci. Mar.* 77, 247–255. doi: 10.3989/scimar03702.10A

Schlining, K., von Thun, S., Kuhnz, L., Schlining, B., Lundsten, L., Jacobsen Stout, N., et al. (2013). Debris in the deep: Using a 22-year video annotation database to survey marine litter in Monterey canyon, central California, USA. *Deep-sea Res. Pt. I.* 79, 96–105. doi: 10.1016/j.dsr.2013.05.006

Serrano, M. A., Díez-Minguito, M., Valle-Levinson, A., and Ortega-Sanchez, M. (2020). Circulation in a short, microtidal submarine canyon in the alborán Sea. *J. Coast. Res.* 95, 1531–1535. doi: 10.2112/SI95-295.1

Smith, M. E., Werner, S. H., Buscombe, D., Finnegan, N. J., Sumner, E. J., and Mueller, E. R. (2018). Seeking the shore: Evidence for active submarine canyon head incision due to coarse sediment supply and focusing of wave energy. *Geophys. Res. Lett.* 45, 12,403–12,413. doi: 10.1029/2018GL080396

Sotomayor-García, A., Rueda, J. L., Sánchez-Guillamón, O., Urra, J., Vázquez, J. T., Palomino, D., et al. (2019). First macro-colonizers and survivors around tagoro submarine volcano, canary islands, Spain. *Geosciences* 9, 52. doi: 10.3390/geosciences9010052

Stanley, D. J., Kelling, G., Vera, J. A., and Sheng, H. (1975). Sands in the alboran Sea: A model of input in a deep marine basin. *Sm. C. Earth Sc.* 15, 1–51. doi: 10.5479/si.00810274.15.1

Stefatos, A., Charalampakis, M., Papatheodorou, G., and Ferentinos, G. (1999). Marine debris on the seafloor of the Mediterranean Sea: Examples from two enclosed gulfs in western Greece. *Mar. Pollut. Bull.* 38, 389–393. doi: 10.1016/S0025-326X(98)00141-6

Taviani, M., Foglini, F., Castellan, G., Montagna, P., McCulloch, M. T., and Trotter, J. A. (2023). First assessment of anthropogenic impacts in submarine canyon systems off southwestern Australia. *Sci. Total Environ.* 857, 159243. doi: 10.1016/j.scitotenv.2022.159243

Templado, J., Ballesteros, E., Galparsoro, I., Borja, Á., Serrano, A., Martín, L., et al. (2013). Guía interpretativa. Inventario Español de Hábitats Marinos. Ministerio de Agricultura, Alimentación y Medio Ambiente, Spain, 230 pp.

Thiel, M., and Gutow, L. (2005). The ecology of rafting in the marine environment. II. the rafting organisms and community. *Oceanogr. Mar. Biol.* 43, 279–418. doi: 10.1201/9781420037449.ch7

Thompson, R. C., Olsen, Y., Mitchell, R. P., Davis, A., Rowland, S. J., John, A. W. G., et al. (2004). Lost at Sea: Where is all the plastic? *Science* 304, 838. doi: 10.1126/science.1094559

Thushari, G. G. N., and Senevirathna, J. D. M. (2020). Plastic pollution in the marine environment. *Heliyon* 6, e04709. doi: 10.1016/j.heliyon.2020.e04709

Trenkel, V. M., Le Loc'h, F., and Rochet, M. J. (2007). Small-scale spatial and temporal interactions among benthic crustaceans and one fish species in the bay of Biscay. *Mar. Biol.* 151, 2207–2215. doi: 10.1007/s00227-007-0655-7

Trestrail, C., Nugegoda, D., and Shimeta, J. (2020). Invertebrate responses to microplastic ingestion: Reviewing the role of the antioxidant system. *Sci. Total Environ.* 734, 138559. doi: 10.1016/j.scitotenv.2020.138559

Tubau, X., Canals, M., Lastras, G., Rayo, X., Rivera, J., and Amblas, D. (2015). Marine litter on the floor of deep submarine canyons of the northwestern Mediterranean Sea: The role of hydrodynamic processes. *Prog. Oceanogr.* 134, 379–403. doi: 10.1016/j.pocean.2015.03.013

Uiblein, F., Lorance, P., and Latrouite, D. (2003). Behaviour and habitat utilisation of seven demersal fish species on the bay of Biscay continental slope, NE Atlantic. *Mar. Ecol. Prog. Ser.* 257, 223–232. doi: 10.3354/meps257223

van den Beld, I. M. J., Guillaumont, B., Menot, L., Bayle, C., Arnaud-Haond, S., and Bourillet, J. F. (2017). Marine litter in submarine canyons of the bay of Biscay. *Deep-sea Res. Pt. II.* 145, 142–152. doi: 10.1016/j.dsr2.2016.04.013

Vázquez, J. T. (2001). Estructura del margen continental del mar de alborán. PhD Thesis (Madrid: Universidad Complutense de Madrid).

Vázquez, J. T., Ercilla, G., Alonso, B., Juan, C., Rueda, J. L., Palomino, D., et al. (2015). "Submarine canyons and related features in the alboran Sea: continental margins and major isolated reliefs," in *Submarine canyon dynamics*, vol. 47 . Ed. F. Briand (Italy: CIESM Workshop Monographs), 183–196.

Vieira, R. P., Raposo, I. P., Sobral, P., Gonçalves, J. M. S., Bell, K. L. C., and Cunha, M. R. (2015). Lost fishing gear and litter at gorringe bank (NE Atlantic). *J. Sea Res.* 100, 91–98. doi: 10.1016/j.seares.2014.10.005

Watters, D. L., Yoklavich, M. M., Love, M. S., and Schroeder, D. M. (2010). Assessing marine debris in deep seafloor habitats off California. *Mar. Pollut. Bull.* 60, 131–138. doi: 10.1016/j.marpolbul.2009.08.019

Wei, C. L., Rowe, G. T., Nunnally, C. C., and Wicksten, M. K. (2012). Anthropogenic "Litter" and macrophyte detritus in the deep northern gulf of Mexico. *Mar. Pollut. Bull.* 64, 966–973. doi: 10.1016/j.marpolbul.2012.02.015

Zhong, G., and Peng, X. (2021). Transport and accumulation of plastic litter in submarine canyons–the role of gravity flows. *Geology* 49, 581–586. doi: 10.1130/G48536.1

frontiers | Frontiers in Marine Science

TYPE Original Research
PUBLISHED 29 March 2023
DOI 10.3389/fmars.2023.1091855

OPEN ACCESS

EDITED BY
Chiara Romano,
University of Gastronomic Sciences, Italy

REVIEWED BY
Lorenzo Angeletti,
IRBIM-CNR, Italy
Henrique Queiroga,
University of Aveiro, Portugal

*CORRESPONDENCE
Tabitha R. R. Pearman
Tabitha.Pearman@noc.ac.uk

SPECIALTY SECTION
This article was submitted to Deep-Sea Environments and Ecology, a section of the journal Frontiers in Marine Science

RECEIVED 07 November 2022
ACCEPTED 27 February 2023
PUBLISHED 29 March 2023

CITATION
Pearman TRR, Robert K, Callaway A, Hall RA, Mienis F, Lo Iacono C and Huvenne VAI (2023) Spatial and temporal environmental heterogeneity induced by internal tides influences faunal patterns on vertical walls within a submarine canyon. *Front. Mar. Sci.* 10:1091855. doi: 10.3389/fmars.2023.1091855

Spatial and temporal environmental heterogeneity induced by internal tides influences faunal patterns on vertical walls within a submarine canyon

Tabitha R. R. Pearman[1,2,3]*, Katleen Robert[4], Alexander Callaway[5,6], Rob A. Hall[7], Furu Mienis[8], Claudio Lo Iacono[9] and Veerle A. I. Huvenne[1]

[1]Ocean BioGeosciences, National Oceanography Centre (NOC), Southampton, United Kingdom, [2]Ocean and Earth Science, University of Southampton, Southampton, United Kingdom, [3]South Atlantic Environmental Research Institute (SAERI), Stanley, Falkland Islands, [4]School of Ocean Technology, Memorial University, Newfoundland, NL, Canada, [5]Habitat Mapping and Human, Activities Team, Marine Ecology Group Centre for Environment, Fisheries and Aquaculture Science (Cefas), Lowestoft, United Kingdom, [6]Fisheries and Aquatic Ecosystems Branch, Environment and Marine Sciences Division, Agri-Food and Biosciences Institute (AFBI), Belfast, United Kingdom, [7]School of Environmental Sciences, University of East Anglia, Norwich, United Kingdom, [8]Department of Ocean Systems, The Royal Netherlands Institute for Sea Research (NIOZ), Texel, Netherlands, [9]Marine Sciences Institute, CSIC, Barcelona, Spain

Vertical walls of submarine canyons represent features of high conservation value that can provide natural areas of protection for vulnerable marine ecosystems under increasing anthropogenic pressure from deep-sea trawling. Wall assemblages are spatially heterogeneous, attributed to the high environmental heterogeneity over short spatial scales that is a typical feature of canyons. Effective management and conservation of these assemblages requires a deeper understanding of the processes that affect faunal distribution patterns. Canyons are recognised as sites of intensified hydrodynamic regimes, with focused internal tides enhancing near-bed currents, turbulent mixing and nepheloid layer production, which influence faunal distribution patterns. Faunal patterns also respond to broad-scale hydrodynamics and gradients in water mass properties (e.g. temperature, salinity, dissolved oxygen concentration). Oscillating internal tidal currents can advect such gradients, both vertically and horizontally along a canyon's walls. Here we take an interdisciplinary approach using biological, hydrodynamic and bathymetry-derived datasets to undertake a high-resolution analysis of a subset of wall assemblages within Whittard Canyon, North-East Atlantic. We investigate if, and to what extent, patterns in diversity and epibenthic assemblages on deep-sea canyon walls can be explained by spatial and temporal variability induced by internal tides. Vertical displacement of water mass properties by the internal tide was calculated from autonomous ocean glider and shipboard CTD observations. Spatial patterns in faunal assemblage structure were determined by cluster analysis and non-metric Multi-Dimensional Scaling plots. Canonical Redundancy Analysis and Generalised Linear

10.3389/fmars.2023.1091855

Models were then used to explore relationships between faunal diversity and assemblage structure and a variety of environmental variables. Our results support the hypothesis that internal tides influence spatial heterogeneity in wall faunal diversity and assemblages by generating both spatial and temporal gradients in hydrodynamic properties and consequently likely food supply.

KEYWORDS

cold-water coral, deep-sea, submarine canyon, hydrodynamics, internal tides

1 Introduction

Submarine canyons are complex geomorphological features that incise continental margins to form pathways between the shelf and deep sea. (Huvenne and Davies, 2014; Amaro et al., 2016). The movement of water masses, sediments and organic matter over varying temporal scales through the canyon generates environmental gradients of physico-chemical properties that occur both horizontally, i.e. along or across the canyon axis, and vertically (Obelcz et al., 2014; Fernandez-Arcaya et al., 2017; Hall et al., 2017; Ismail et al., 2018). As a result, environmental conditions can vary over short spatial scales, such that different branches within a single canyon, or even opposing walls of the same branch may have different seafloor characteristics, and experience different hydrodynamic and sedimentary regimes (McClain and Barry, 2010; Aslam et al., 2018; Bargain et al., 2018; Ismail et al., 2018; Pearman et al., 2020). The high spatial and temporal heterogeneity in environmental conditions often results in enhanced regional and local productivity, biodiversity, and faunal abundance (De Leo et al., 2010; Vetter et al., 2010; De Leo et al., 2014).

Submarine canyons are listed by the FAO (2009) as topographic features that may support vulnerable marine ecosystems (VMEs). Vertical walls situated within submarine canyons are features of high conservation value, providing natural areas of protection for VMEs under increasing anthropogenic pressure from deep-sea trawling (Huvenne et al., 2011; Johnson et al., 2013). Vertical walls support a range of faunal assemblages (which make up VMEs) that exhibit high diversity (Robert et al., 2015; Robert et al., 2017; Pearman et al., 2020). Examples are walls supporting dense aggregations of reef forming scleractinian corals, *Lophelia pertusa* (recently synonymised to *Desmophyllum pertusum* (Addamo et al., 2016)) (Huvenne et al., 2011; Brooke and Ross, 2014; Fabri et al., 2014) and *Madrepora oculata* (Fabri et al., 2014), the stony coral *Desmophyllum dianthus*, the octocorals *Paragorgia arborea* and *Duva florida* (Brooke et al., 2017), the deep-sea oyster, *Neopycnodonte zibrowii* (Van Rooij et al., 2010; Fabri et al., 2014), and the fire clam, *Acesta excavata* (Johnson et al., 2013). On the other hand, other sections of vertical walls can be devoid of life (Robert et al., 2015; Pearman et al., 2020). Consequently, vertical walls contribute to a canyon's habitat diversity in various ways.

Desmophyllum pertusum reefs and coral gardens are listed as 'threatened or declining' under Annex V of the Oslo-Paris convention agreement (OSPAR, 2008), under Annex 1 of the Habitats Directive (92/43/EEC, 1992) and as VMEs (FAO, 2008), requiring protection. Effective spatial management and conservation of vertical wall assemblages requires a deeper understanding of the processes that generate the observed faunal distribution patterns (Huvenne and Davies, 2014). However, despite the likely importance of vertical walls in supporting and protecting diversity hotspots and protected habitats, few ecological studies of wall fauna have been conducted (Robert et al., 2017; Robert et al., 2020) and our understanding of the processes that generate spatial patterns along them is limited.

Our limited understanding is, in part, attributed to the challenge of sampling deep-sea vertical walls and measuring the local environmental characteristics. As a result, vertical walls stayed largely unsampled prior to recent advancements in remote technologies (e.g. Remotely Operated Vehicles (ROVs)) (Huvenne and Davies, 2014). Additionally, the limitations in the resolution of ship-borne bathymetry prevents accurate delineation of vertical walls (Huvenne et al., 2011; Robert et al., 2017). Consequently, despite their likely importance, vertical walls remain under-represented and under-sampled environments of canyons, limiting our knowledge of canyon ecology. This is further confounded by the predominance of canyon studies which only model the probability of epibenthic species presence-absence (Robert et al., 2015; Bargain et al., 2018; Lo Iacono et al., 2018) or univariate faunal responses that condense faunal information into a single diversity index (Robert et al., 2015; Ismail et al., 2018), rather than representing wider, multivariate species assemblage data.

In general, the responses of canyon fauna are regulated by a complex interplay of multiple factors acting at different scales. Environmental factors (water mass properties, seafloor characteristics and food supply) are most likely to explain species patterns at broader spatial scales (McClain and Barry, 2010; Robert et al., 2015; Ismail et al., 2018) while biotic processes (e.g. competition) more often act at finer spatial scales (Robert et al., 2020). Stochastic events (disturbance) act at multiple scales (Pierdomenico et al., 2016). The interaction of these processes across different spatial and temporal scales makes identifying key factors that drive faunal patterns within heterogeneous canyon landscapes challenging.

Canyons are recognised as sites of intensified hydrodynamics, including energetic internal waves and internal tides

(Liu et al., 2010; Hall et al., 2017). Internal (baroclinic) waves occur when there is a perturbation to the interface between layers of the water column with different temperatures, salinities, and thus densities. The perturbation is restored by local buoyancy, forming oscillations (waves) that propagate along the interface. In a continuously stratified water column, such as the open ocean, the waves propagate vertically as well as horizontally. Internal waves generated by tidal motions, and thus oscillating at tidal frequencies (e.g. semidiurnal), are termed internal tides (Wunsch, 1975). In canyons, internal tides are generated when surface (barotropic) tidal currents flow across steep canyon topography (Allen and Durrieu De Madron, 2009; Vlasenko et al., 2016; Hall et al., 2017). Internal wave–topographic interactions (e.g. generation, reflection and breaking) are determined by multiple factors, including wave frequency, buoyancy frequency (i.e. stratification) and latitude. These determine the slope of internal wave propagation (s_{wave}) which can be compared to the local bathymetric slope (s_{bathy}) to predict wave behaviour. Canyon walls are typically steep compared to the slope of semidiurnal internal tides ($\alpha = s_{bathy}/s_{wave} > 1$), a state known as supercritical, so these internal waves approaching a wall are reflected back into deep water and towards the canyon floor. Conversely, the floors of canyons often have a gentler slope than semidiurnal internal tides ($\alpha < 1$), a state known as subcritical, so these internal waves approaching from offshore are reflected up the canyon towards its head. These processes combine to focus internal tide energy towards the canyon boundaries (its walls and floor), intensifying near-bed tidal currents (Hall and Carter, 2011; Hall et al., 2014). Where the local bathymetric slope is equal or near-equal to the internal wave slope ($\alpha \simeq 1$), the wave is trapped near the boundary, often leading to breaking – similar to surface waves breaking on a beach – which increases the turbulent mixing of heat, salt, nutrients, and particulate matter between the layers of the water column.

Internal tides are increasingly advocated as key environmental factors influencing species patterns in the deep sea (Huvenne et al., 2011; Johnson et al., 2013; Van Haren et al., 2017; Davison et al., 2019; Pearman et al., 2020). For example, research focussing on scleractinian cold-water coral (CWC) assemblages has highlighted the importance of local hydrodynamics (including internal tides) in supplying nutrients and food to sustain CWC populations and preventing sedimentation on the hard substratum that the corals colonise (Frederiksen and Westerberg, 1992; Thiem et al., 2006; Davies et al., 2009; Mienis et al., 2009; White and Dorschel, 2010). Through interactions with sloping topography, internal tides occurring within canyons may enhance near-bed currents and turbulent mixing, forming efficient food supply mechanisms to benthic communities (Johnson et al., 2013). For example, the aggregation of organic matter by internal tide driven resuspension and mixing is postulated to play an important role in supporting high densities of *M. oculata* on the southern wall of Cap de Creus Canyon (Orejas et al., 2009).Internal tides also influence the resuspension and advection of suspended material in nepheloid layers (White et al., 2005; Liu et al., 2010; Puig et al., 2014; Wilson et al., 2015), where enhanced amounts of suspended matter (including particulate organic matter) are observed, representing an important food source for deep-sea fauna (Demopoulos et al., 2017). Internal tide modulation of nepheloid layers can result in replenishment of food to the benthos over the tidal cycle (Davies et al., 2009) and has been linked to spatial distributions of antipatharians and gorgonians in canyons of the Bay of Biscay (Van Den Beld et al., 2017).

The vertical displacement of the water column strata, associated with internal tides, also results in temporal variability of water mass properties (including temperature, salinity, dissolved oxygen concentration) along the canyon walls. Fauna respond to such changes in water mass properties and hydrodynamics (Levin et al., 2001; Howell et al., 2002; Dullo et al., 2008; Fabri et al., 2017). In addition, spatial and temporal hydrodynamic variability has been linked to species richness and assemblage patterns on the Hebrides Terrace Seamount (Henry et al., 2014). Hydrodynamic variability of internal tides generates environmental heterogeneity in near-bed sheer stress and nutrient and sediment fluxes (Frederiksen and Westerberg, 1992), which are proposed to influence CWC coral mound formation in the North-East Atlantic (White and Dorschel, 2010). On the other hand, modelling indicates internal tide hydrodynamic variability is an important factor influencing larval dispersal on the Rosemary Bank Seamount (Stashchuk and Vlasenko, 2021). However, to date no studies investigating faunal responses to internal tide induced environmental heterogeneity have been conducted in submarine canyons.

Here for the first time we investigate if spatial and temporal gradients in hydrodynamic properties, induced by the internal tide, can explain variation in spatial patterns of faunal diversity and assemblage composition on deep-sea canyon walls. We utilise biological, hydrodynamic and bathymetry-derived datasets in an integrated approach to undertake a high-resolution analysis of wall assemblages within Whittard Canyon, North-East Atlantic. We ask the following questions: (1) Does epibenthic megafaunal assemblage composition change across hydrodynamic and substratum gradients on vertical walls and (2) which environmental variables exert the strongest influence on epibenthic megafaunal diversity and assemblage structure?

2 Materials and methods

2.1 Study area

Whittard Canyon extends over >200 km and incises the shelf break of the passive Celtic Margin, south-west of the British Isles in the Northern Bay of Biscay, starting at a depth of ~200 m (Figure 1). It is a dendritic canyon system comprised of four main tributaries, the Western, Western Middle, Eastern Middle and Eastern branches that coalesce at 3700 – 3800 m water depth. The Whittard Channel continues to a depth of ~4500 m, where it joins the Celtic Fan that leads onto the Porcupine Abyssal Plain (Hunter et al., 2013; Amaro et al., 2016). This study focusses on the Eastern branch of Whittard Canyon (Figure 1).

Several water masses occur in the region, defined by absolute salinity (SA) and conservative temperature (Θ). These include: Eastern North Atlantic Water (ENAW) (~100 – 600 m, SA = 35.8 – 36.3 g kg^{-1}, Θ = 12.2 – 14.8°C), the Mediterranean Outflow Water (MOW) (800 – 1200 m, SA = 36.35 – 36.65 g kg^{-1}, Θ = 9.5 – 10.5°C)

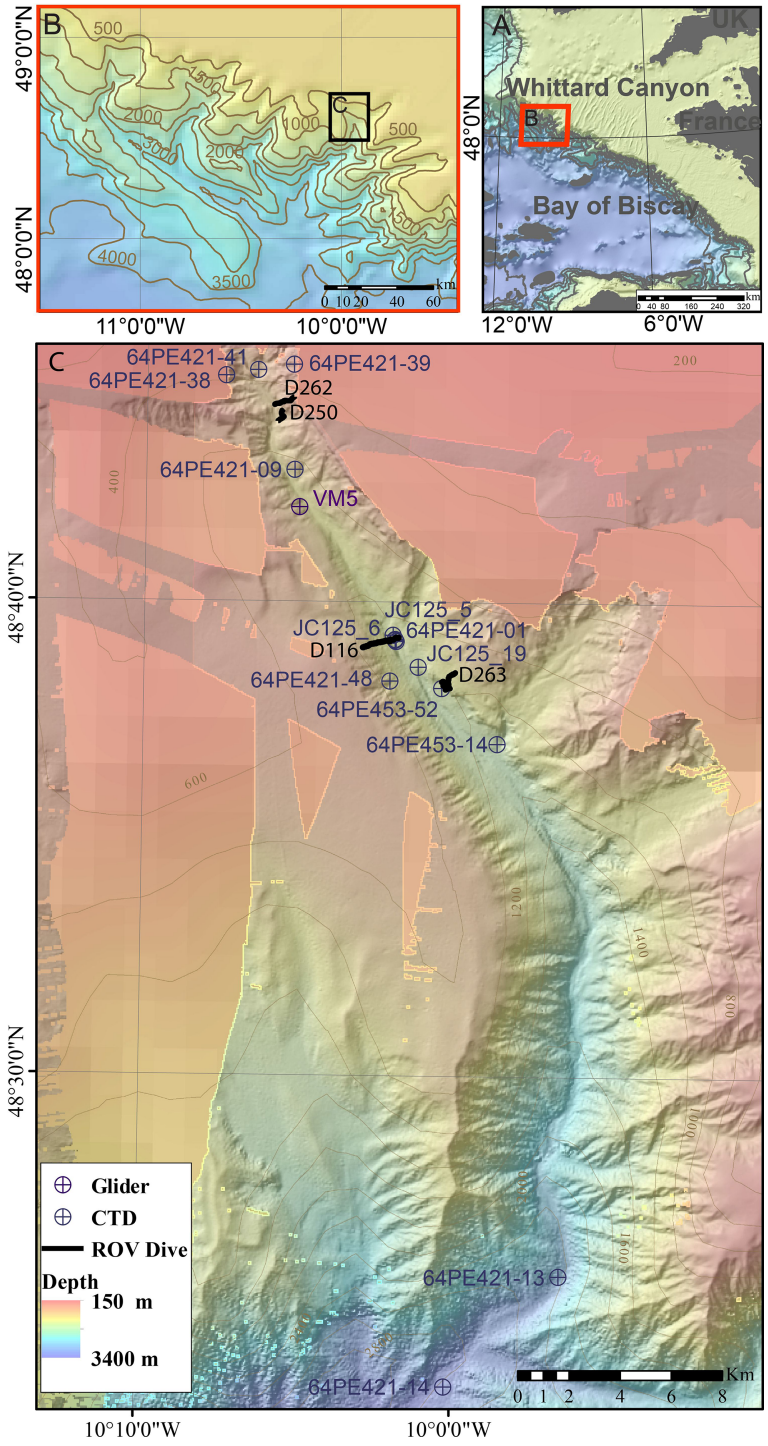

FIGURE 1
Location map of **(A)** Whittard Canyon and **(B)** the Eastern branch of Whittard Canyon **(C)** data acquired from the Eastern branch during the J036, JC125, 64PE421 and 64PE435 cruises. Background bathymetry from JC125 and GEBCO compilation group (2019).

and the Northeast Atlantic Deep Water (NEADW) (1500 – 3000 m, SA = 35.11 – 35.13 g kg $^{-1}$, Θ = 2.6 – 3.0°C) (Pollard et al., 1996; Van Aken, 2000). The influence of the ENAW and MOW water mass decreases up-canyon as depth decreases and mixing increases toward the head of the branch (Hall et al., 2017).

Intensified near-bed currents and internal tides have been documented from Whittard Canyon (Reid and Hamilton, 1990; Hall et al., 2017; Aslam et al., 2018) and attributed to generating spatial heterogeneity in environmental conditions (Wilson et al., 2015; Hall et al., 2017; Aslam et al., 2018; Pearman et al., 2020). Semidiurnal internal tides with amplitudes up to 80 m have been observed, with implications of 1°C temperature fluctuations and dissolved oxygen concentration changes of 12 µmol kg^{-1} along certain sections of the canyon's walls (Hall et al., 2017).

Additionally, dissipation of the observed energetic internal tide is expected to drive enhanced turbulent mixing, which is associated with increased concentrations of resuspended particulate organic matter (POM) and nepheloid layer formation within the canyon (Wilson et al., 2015; Hall et al., 2017; Aslam et al., 2018; Haalboom et al., 2021). Resuspension by intensified near-bed currents (including internal tides) and local slope failures within the canyon source fine grained material (Reid and Hamilton, 1990; Amaro et al., 2015; Amaro et al., 2016; Hall et al., 2017) which is transported down-canyon *via* turbidity currents and mud-rich sediment gravity flows (Cunningham et al., 2005; Amaro et al., 2016; Carter et al., 2018). There is also evidence that internal tides may act to transport material up-canyon (Wilson et al., 2015; Lo Iacono et al., 2020).

Whittard Canyon is characterised by complex geomorphology and variable substrata that differ along the canyon axis and between branches (Stewart et al., 2014; Robert et al., 2015; Amaro et al., 2016; Ismail et al., 2018). The distribution of substrata is linked to the canyon geomorphology: increasingly finer-grained sedimentary substrata are associated with flat terrain whilst hard substrata are mostly associated with steep slopes (Stewart et al., 2014; Ismail et al., 2018). The hard substrata constitute bedrock outcrops and escarpments (vertical walls) as well as boulders and smaller fractions of hard rock originating from slope failures (Carter et al., 2018). Due to the remobilisation and deposition of sediment in the canyon, hard substratum is often coated in a sediment veneer of varying thickness.

2.2 Data acquisition

Data used in this study were acquired during a number of cruises (Table 1) and derived from global and regional ocean models.

2.2.1 Acoustic data acquisition and processing, and extraction of terrain derivatives

Multibeam echosounder (MBES) data were acquired during the MESH, JC035 and JC125 cruises (Table 1) (Davies et al., 2008; Masson, 2009; Huvenne et al., 2016). Bathymetry data were processed utilising CARIS HIPS & SIPS v.8 and combined utilising the mosaic to new raster tool in ArcGIS 10.4.1(RRID: SCR_011081), to produce a new grid at a resolution of 50 m (WGS1984, UTM Zone 29N). The terrain derivatives slope, aspect and rugosity were derived from the bathymetry data using the ArcGIS extension Benthic Terrain Modeler v. 3.0 (Walbridge et al., 2018) with a neighbourhood of 3 x 3 pixels. Rugosity is the ratio of the surface area to the planar area (Wilson et al., 2007). Slope is a measure of change in elevation over distance. Aspect (subsequently converted to eastness and northness) measures the compass orientation of the direction of maximum slope. The terrain derivatives were chosen as they have previously been shown to be informative explanatory variables of canyon fauna distribution within Whittard Canyon (Robert et al., 2015; Price et al., 2019; Pearman et al., 2020). Bathymetric slope criticality to the dominant semidiurnal internal tide (α) was calculated from INFOMAR bathymetry (INFOMAR, http://www.infomar.ie) gridded at 200 m and potential density derived from a ship-based CTD cast during JC125 interpolated to 50 m resolution by kriging using the Spatial Analyst toolbox in ArcGIS (Supplementary materials 1.1). The environmental variables were exported as rasters at 50 m resolution (Supplementary Materials Figure 1).

2.2.2 Model-derived hydrodynamic variables

Tidal current variables were extracted from a 500 m horizontal resolution regional hydrodynamic model (a modified version of the Princeton Ocean Model) used to simulate the semidiurnal internal tide in Whittard Canyon (see Aslam et al. (2018) for further details).

TABLE 1 Details of data used in this study, acquired from different cruises within Whittard Canyon.

Cruise	Vessel	Cruise Dates	Data type	Description
MESH	R.V. *Celtic Explorer*	June 2007	Multibeam echosounder	Multibeam bathymetry acquired with shipboard Kongsberg Simrad EM1002 MBES system at 25 m resolution
JC035_JC306	RRS *James Cook*	June 2009	Multibeam echosounder	Multibeam bathymetry acquired with shipboard Kongsberg Simrad EM120 MBES at 50 m resolution
			ROV footage	ROV footage: dive 116
JC125	RRS *James Cook*	August-September 2015	Multibeam echosounder	Multibeam bathymetry acquired with shipboard Kongsberg Simrad EM120 MBES at 50 m resolution
			Ocean Glider data	1 station: Temperature, salinity, dissolved oxygen concentration (µmol kg-1), and optical backscatter at two wavelengths (470 nm and 700 nm)
			Shipboard CTD data	3 stations: Temperature, salinity, dissolved oxygen concentration (µmol kg^{-1}) and turbidity (NTU)
			ROV footage	ROV footage: dive 250, 262 and 263
64PE421	R.V. *Pelagia*	May 2017	Shipboard CTD data	9 stations: Temperature, salinity, dissolved oxygen concentration (µmol kg^{-1}) and turbidity (NTU)
64PE453	R.V. *Pelagia*	June 2019	Shipboard CTD data	2 stations: Temperature, salinity, dissolved oxygen concentration (µmol kg^{-1}) and turbidity (NTU)

Three variables were extracted: barotopic current speed, near-bottom baroclinic current speed, and near-bottom total (barotropic plus baroclinic) current speed. In each case, the variable is the root mean squared (r.m.s.) speed over a single semidiurnal tidal cycle. To match the resolution of the terrain derivatives, tidal current speeds were horizontally interpolated into rasters with 50 m resolution (Supplementary Figure 1). Interpolation was undertaken by kriging using the Spatial Analyst toolbox in ArcGIS, and based upon spatial variograms calculated in Golden Software Surfer V 8. To account for discrepancies in bathymetric depth over small topographic features between the hydrodynamic model grid and the 50 m MBES bathymetry, modelled current speed values were extracted from the vertical level nearest to that of the MBES bathymetry.

2.2.3 Observed hydrodynamic variables

Hydrographic data along the Eastern canyon branch were collected using an autonomous ocean glider and shipboard CTD surveys (Figure 1). The glider data were acquired with an iRobot 1KA Seaglider operating in virtual mooring mode around station VM5 (Figure 1) for 43 hours, during which it completed 22 full-depth dive cycles (see in Hall et al. (2017) for further details). During each dive two profiles of temperature, salinity and dissolved oxygen concentration (μmol kg^{-1}), were measured. Temperature and salinity were sampled every 5 seconds; oxygen concentration was sampled every 5 seconds in the upper 200 m and every 30 seconds between 200 m and 1000 m (or the seabed). All the glider data were quality controlled and averaged (median value) in 5 m depth bins before further analysis. The CTD data were acquired with a Seabird Electronics Sea-Bird SBE 911plus at 14 stations within the Eastern branch (Figure 1). Profiles of temperature, salinity and dissolved oxygen concentration were sampled at 24 Hz and averaged in 1 m depth bins. Accurate oxygen concentration measurement with a CTD is difficult and data was not calibrated by Winklers. However, the observed variability, which is the focus of this study, is accurate. Conservative temperature (°C), absolute salinity (g kg^{-1}), and potential density (kg m^{-3}), were calculated from the glider and CTD data using the Gibbs Sea Water Oceanographic Toolbox in Matlab (McDougall and Barker, 2011) (RRID: SCR_001622).

The CTD data were used to assess spatial and temporal variability within the dataset and confirm consistency between stations in close proximity but occupied at different times. As all ROV dives went below the seasonal thermocline, consistency at these depths allowed multiple CTD casts in close proximity to an ROV dive (Figure 1) to be averaged and linearly extrapolated to the maximum depth of the dive (Supplementary Figures 2 and 3). The averaged and extrapolated profiles were then used to derive environmental variables at the ROV dive sites for the multivariate analysis.

2.2.3.1 Semidiurnal vertical isopycnal displacement and water mass property variability

Both the glider and CTD data were used to calculate vertical isopycnal displacement caused by the semidiurnal internal tide. At sites toward the canyon head, above 900 m depth, glider data from VM5 were used; at mid-canyon sites, below 900 m CTD data from stations JC125_05, JC125_06 and JC125_19, deployed on the 16/08/2016, 20/8/2015 and 6/9/2015, were used. Density anomaly, $\rho'(z, t) = \rho(z, t) - \overline{\rho}(z)$, where ρ is measured potential density and $\overline{\rho}$ is time-average potential density, is calculated first, followed by vertical isopycnal displacement, $\xi(z, t) = -\rho'(\partial\overline{\rho}/\partial z)^{-1}$. An M_2 (the dominant semidiurnal tidal constituent, with a period of 12.42 hours) harmonic analysis was applied to vertical isopycnal displacement on each depth level using t-tide (Pawlowicz et al., 2002) to yield M_2 amplitudes for vertical isopycnal displacement ($\xi_A^{M_2}$). To justify the use of vertical isopycnal displacement derived from different datasets, consistency between the density profiles was confirmed (Supplementary Figures 2, 3).

The glider and CTD data were also used to infer the temporal variability of water mass properties due to vertical advection by the semidiurnal internal tide. At each location and on each depth level that harmonic analysis was applied, the resulting M_2 vertical isopycnal displacement amplitude was compared to time-average profiles of water mass properties (conservative temperature, absolute salinity, potential density, and dissolved oxygen concentration). The range of water mass properties within the vertical envelope defined by isopycnal displacement was considered the range of properties that would be experienced by an organism at that depth due to vertical advection.

2.2.4 Seafloor imagery

2.2.4.1 Imagery data acquisition

Video data were acquired during the JC036 and JC125 cruises (Table 1), using the remotely operated vehicle (ROV) Isis. During JC036 Isis was equipped with a standard definition video camera (Pegasus, Insite Tritech Inc. with SeaArc2 400 W, Deep sea Power&- Light illumination) and stills camera (Scorpio, Insite Tritech Inc., 2048 x 1536 pixels). For the JC125 cruise, the ROV Isis was equipped with a dual high definition stills and video camera (Scorpio, Insite Tritech Inc., 1920 x 1080 pixels). Positional data were derived from the ROV's ultra-short baseline navigation system (Sonardyne USBL). A total of four dives encompassing vertical walls were completed in the Eastern branch to depths of 1420 m (Figure 1 and Table 2) (Robert et al., 2015). Epibenthic morphospecies (visually distinct taxa) >10 mm were annotated from the video, using a laser scale with parallel beams positioned 10 cm apart to estimate organism size. Those sections where the seabed was out of view for extended periods, prohibiting annotations, were noted by time and excluded from subsequent analysis.

Composition of substrata was visually assessed and assigned a class based on the CATAMI classification (Althaus et al., 2015) (Table 3). Additionally, occurrences of coral reef and dead coral reef framework were annotated (example images are provided in Supplementary Figure 4). Due to the patchy distribution of substrata, substratum type was coded based upon the dominant substratum type followed by the subordinate, for example hard substratum with coral rubble was coded as H_CR. Vertical walls were identified visually from video data, and defined as topography oriented at an angle >50° to horizontal, and of a height >3 m.

TABLE 2 Characteristics of ROV dives in Whittard Canyon analysed in the study: Cruise number, total transect length (m), transect length (m) coincident with vertical walls, maximum and minimum water depth (m) coincident with vertical walls and number of samples extracted from each dive that represent vertical walls.

Dive	Cruise	Total Transect Length (m)	Transect Length (m) (V. wall)	Min Depth (m) (V. wall)	Max Depth (m) (V. wall)	Samples used in models (V. wall)
262	JC125	1205	390	486	836	21
htt250	JC125	783	400	753	895	15
116	JC036	1929	490	1291	1369	29
263	JC125	2296	552	1260	1420	50
Total		6213	1832			115

2.2.4.2 Imagery data analysis

Annotations from the JC036 (previously annotated by Robert et al. (2015)) and JC125 cruises were combined into a single data matrix and nomenclature standardised. Transects were subdivided into 10 m length sections and the morphospecies records within each section consolidated. Species richness and Simpson's reciprocal index (1/*D*) (Simpson, 1949) were calculated for each 10 m section sample. A 10 m sample length was chosen after data exploration revealed that distinct bands of fauna usually occurred in linear events <50 m so that 10 m sample units would enable structure in assemblages on walls to be identified (Borcard et al., 2011).

2.2.5 ROV derived depth

ROV derived depth was calculated to provide a higher resolution dataset than available from shipborne bathymetry (Robert et al., 2017). For approximately horizontal terrain, depth values for the seabed were derived by combing the ROV's altitude and depth records to obtain a seabed depth value (m). The ROV attitude data were cross-referenced with annotations to identify sections of vertical wall and for these sections ROV depth alone was used in the calculation. A smoothing average with a temporal window size of 3 seconds was applied to the new depth variable.

2.3 Statistical analyses

Univariate and multivariate analysis techniques were used to identify spatial patterns in faunal diversity and assemblages on canyon walls. Highly mobile taxa such as fish that can be 'double counted' were removed prior to analysis. Samples with <2 taxa present were also excluded from multivariate analysis. Environmental data coincident with the midpoint co-ordinate of each fauna sample were extracted from the rasters and combined with CTD data extracted from depth profiles coincident with the depth of the sample. Samples D263_108 and D263_109 were removed as CTD data did not extend to the water depths of these samples. Data exploration was undertaken following the protocol described in Zuur et al. (2010).

Generalised Linear Models (GLMs) were used to explore the relationships between diversity (species richness and 1/*D*) and the environmental variables. Species richness and 1/*D* were assessed using GLMs with link functions based on an exponential relationship between the response variable and the environmental predictor variables (Zuur et al., 2014b). A Poisson distribution was assumed for species richness and a Gamma distribution was assumed for 1/*D*, based upon the distribution of the response variable, together with a log link function. Environmental variables were selected by forward selection under parsimony

TABLE 3 Substratum classification used in annotation of image data.

CATAMI Classification				Annotation classification	
Level 2	Level 3	Level 4	Level 5	Substratum Description	Substratum Code
Unconsolidated (soft)	Sand/mud (<2 mm)	Coarse sand (with shell fragments)		Sand	S
		Fine sand (no shell fragments)			
		Mud/silt (<64 μm)		Mud	M
	Pebble/gravel	Biogenic	Shellhash	Biogenic gravel	BG
			Coral rubble	Coral rubble	CR
Consolidated (hard)				Dead coral reef framework	DCRF
				Coral reef	CRF
				Veneer	V
	Rock			Hard	H

Substratum was annotated based upon the CATAMI classification (Althaus et al., 2015). Additionally, coral reef and dead coral reef framework were added.

10.3389/fmars.2023.1091855

after Pearson's correlation and Variance Inflation Factor (VIF) scores were used to remove highly correlated variables (absolute correlation coefficients >0.7) (Zuur et al., 2014b). Model assumptions were verified by plotting residuals versus fitted values, versus each covariate in the model and each covariate not in the model. Residuals were assessed for spatial dependency *via* variograms (Zuur et al., 2014a). To further account for inherent spatial autocorrelation in the data, the residual autocovariate (RAC) was calculated for the optimal model. The RAC represents the similarity between the residual from the optimal model at a location compared with those of neighbouring locations. This method can account for spatial autocorrelation without compromising model performance (Crase et al., 2012).

Multivariate species data were assessed with non-metric Multi-Dimensional Scaling (nMDS) and hierarchal cluster analysis with group-averaged linkage, using a Hellinger dissimilarity matrix derived from the Hellinger transformed data matrix. Data were Hellinger transformed to enable the use of linear ordination methods (Legendre and Gallagher, 2001; Legendre and Legendre, 2012). The optimal number of interpretable clusters was determined with fusion level and mean silhouette widths (Legendre and Legendre, 2012). Characteristic morphospecies contributing to similarity among clusters were identified using the Similarity Percentage analysis (SIMPER) routine (Clarke, 1993).

Canonical Redundancy Analysis (RDA) was used to explore relationships between the multivariate species data and the different environmental variables. RDA combines the outputs of multiple regression with ordination (Legendre and Legendre, 2012). Prior to RDA, environmental data were standardised (i.e. transformed to zero mean, and unit variance). Forward selection was then carried out on the environmental variables to obtain the most parsimonious model and Pearson's correlation together with VIF scores were used to exclude environmental variables that showed strong collinearity with others present within the model (absolute correlation coefficients >0.7) (Borcard et al., 2011).

Spatial correlation in the multivariate species data was assessed by incorporating sample coordinates into the RDA of species data and by means of a Mantel correlogram on the detrended species data. Variance partitioning was then performed to assess how much of the variance explained in the species data by the environmental variables was spatially structured. Variance partitioning was performed using the environmental variables from the parsimonious model and sample coordinates, after forward selection (Legendre and Legendre, 2012).

During model selection for GLM and RDA, high collinearity was observed between certain environmental variables and depth. Depth per se does not influence fauna, but in canyons depth is correlated with measured and unmeasured environmental factors (e.g. current speed and water mass properties) that have been shown to influence faunal patterns (Robert et al., 2015; Pearman et al., 2020). Consequently, depth was retained in analysis, for ease of interpretation though in later sections we also discuss potential effects of correlated environmental factors.

All statistical analyses were conducted using the open source software R (R_CORE_TEAM, 2014), packages "Packfor" "vegan", "cluster", "ape", "ade4", "gclus", "AEM", "spdep" and "MASS".

3 Results

3.1 Spatial and temporal gradients in canyon oceanography

Glider and CTD measurements showed several water masses in the Eastern branch of Whittard Canyon (Figure 2 and Supplementary Figure 6). The ENAW (σ range: 27.1 – 2 7.25 kg m^{-3}) occurs below the seasonally warmed surface waters to approximately 600 m water depth (Figure 2). The influence of the MOW (σ range 27.5 – 27.6 kg m^{-3}), seen as a salinity maximum, can be observed from measurements taken further down the canyon axis, between 800 – 1200 m water depth, but is absent from those towards the canyon head (Figure 2). Similarly, large gradients in dissolved oxygen concentration that are observed from measurements taken further down the canyon axis are absent from those toward the canyon head (Supplementary Figure 6).

Vertical isopycnal displacement derived from the glider (Hall et al., 2017) and CTD data showed variability along the Eastern branch and with depth. The highest displacement amplitude from the glider data (VM5, upper canyon) was 53 m at 617 m water depth (Figure 3), resulting in tidal temperature variations of 0.53°C, salinity variations of 0.004 g kg^{-1}, potential density variations of 0.09 kg m^{-3} and dissolved oxygen variations of 9.2 µmol kg^{-1}. The highest amplitude calculated from the CTD data (mid canyon) was 140 m at 942 m water depth (Figure 3), resulting in tidal temperature variations of 1.55°C, salinity variations of 0.1 g kg^{-1}, potential density variations of 0.16 kg m^{-3} and dissolved oxygen variations of 5.8 µmol kg^{-1}.

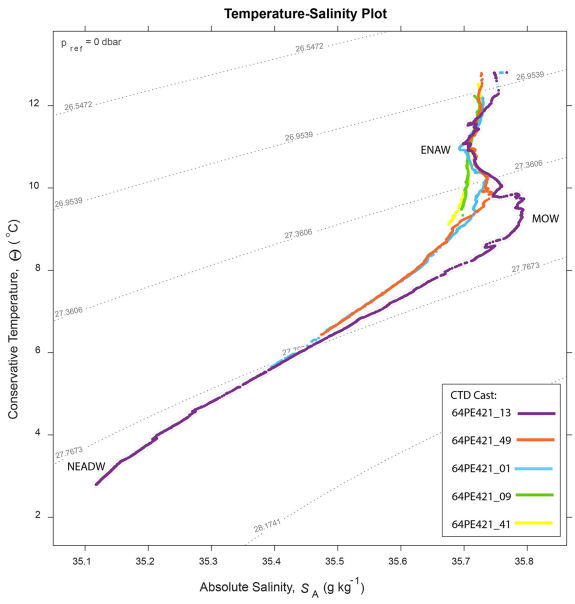

FIGURE 2
Temperature – salinity plot for 5 CTD casts along the canyon branch axis, collected during the 64PE21 cruise. See Supplementary Materials Figure 5 for CTD locations. The influence of the MOW decreases toward the head of the canyon.

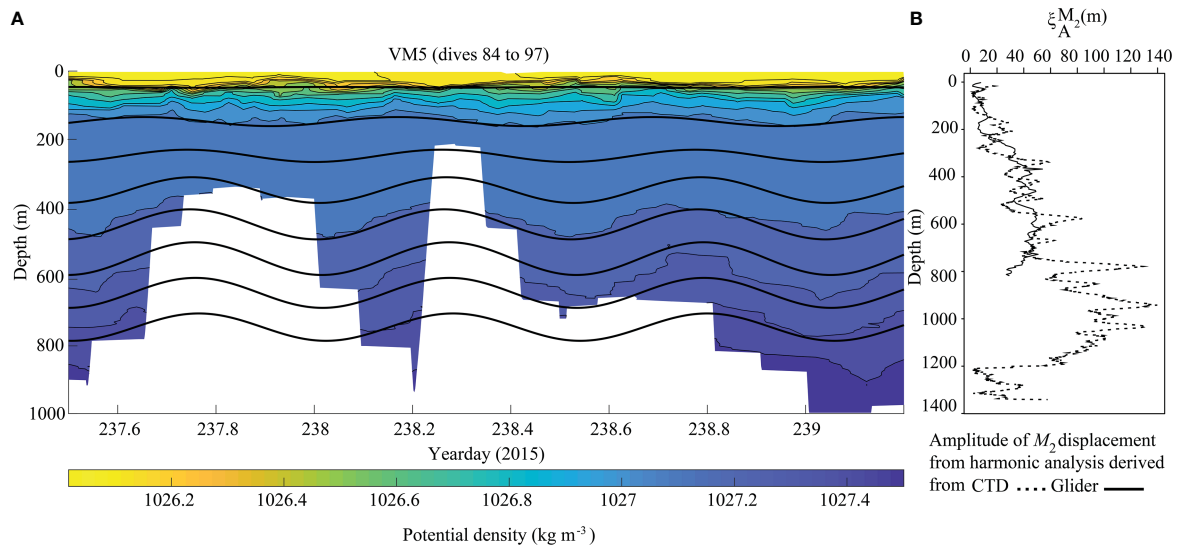

FIGURE 3
Time series of potential density overlaid with M_2 harmonically filtered vertical isopycnal displacement every 100 m calculated from **(A)** VM5. When operating in virtual mooring mode the glider stayed within 2.5 km of the station, but this imperfect geolocation over the steep canyon bathymetry resulted in a range of dive depths (white background). **(B)** Amplitude of M_2 displacement from the harmonic analysis derived from CTD (dashed lines) and glider data (Solid lines).

3.2 Spatial patterns of faunal diversity and assemblage composition on deep-sea canyon walls

A total of 14701 individuals assigned to 150 morphospecies were annotated. Most morphospecies were rare, whilst others were abundant in specific locations and occurred at low density across the rest of the samples. The most abundant morphospecies was Brachiopoda sp. 1 (4440). The most common morphospecies recorded across dives was Caryophylliidae sp. 1 (in 69.2% of total samples). Highest species richness (29/10 m transect) and $1/D$ (10.87) was observed from dive 262 on hard substratum vertical wall with coral rubble.

Walls toward the head of the canyon (dives 262 and 250) were steep and comprised of an alternation of geological strata resistant to erosion, and friable, less competent sedimentary units of varying thickness with occasional ledges, all of which was covered in a mud veneer of varying thickness. The bivalves *Neopycnodonte* sp. 1 and *Acesta excavata*, stony corals *Madrepora oculata* and Caryophylliidae sp. 1 and crinoids were observed to aggregate beneath ledges (Figure 4). On other sections of wall, the black coral Antipathidae sp. 1 or the basket star Brisingidae sp.1 reached relatively high abundances (Figure 4) and Cerianthidae sp. 1 occurred where soft sediment accumulated (Figure 4). The walls toward the canyon head were supercritical to the M_2 tide and although the area is exposed to relatively weaker currents 0.17 – 0.23 m s^{-1} (Supplementary Figure 1) it experienced similar short-term temporal variability of water mass properties to that of walls sampled in the mid canyon (dives 116 and 263), despite the water temperature being up to 5°C warmer.

Dense aggregations of *D. pertusum* framework were observed between 1301 and 1369 m water depth (dive 116) from walls comprised of alternations of strong and weak, thinly bedded sedimentary units that resulted in a 'stepped' relief (Figure 4) and that were covered in a mud veneer of varying thickness. The walls were supercritical to the M_2 tide in a region exposed to high current speeds of 0.42 – 0.46 m s^{-1}.

Brachiopods, large erect sponges and arborescent gorgonians were observed between 1261 – 1406 m water depth (dive 263) from walls that comprised brown rocky strata resistant to erosion and covered in a mud veneer of varying thickness (Figure 4). The walls were critical to the M_2 tide and experienced currents of 0.27 – 0.29 m s^{-1}.

3.3 Statistical analysis results

High collinearity was present within the environmental dataset. Density, temperature, salinity and current speed were highly correlated with depth, as on occasion were values for the M_2 amplitude and associated ranges in density, temperature and salinity. As a result, only M_2 amplitude, depth, criticality and substratum type were retained for the final RDA and depth, slope and substratum type retained in the final GLM model.

3.3.1 Species diversity

The GLM analysis of the vertical wall dataset identified slope, depth and substratum as significant variables explaining 39% deviance in species richness across the dives and 43% deviance in $1/D$ across dives. Species richness showed a weak positive relationship with slope and a weak negative relationship with depth and increasing soft sediment, biogenic gravel and coral reef framework. On the other hand, $1/D$ showed a weak negative relationship with slope and a weak positive relationship with depth, increasing soft sediment (Table 4).

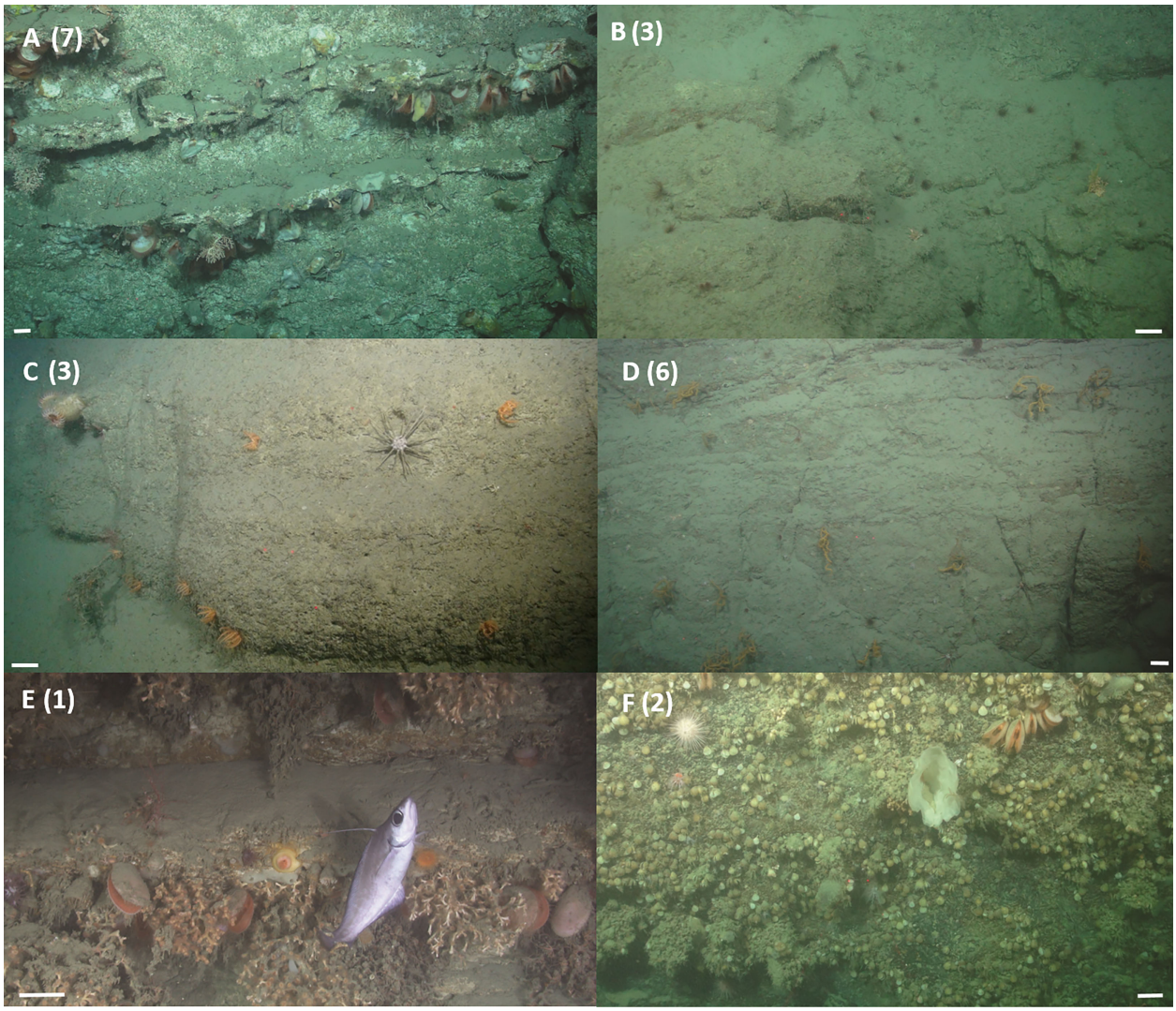

FIGURE 4
Example images of vertical wall assemblages observed from ROV video data. **(A)** The deep water oyster *Neopycnodonte* sp. 1 and the deep water bivalve *Acesta excavata*, the stony corals *Madrepora oculata* and Caryophylliidae sp. 1, the squat lobster Munididae sp. 1, the urchin *Cidaris cidaris* and crinoids, were observed aggregating beneath ledges, image taken during dive 262 at 637 m. **(B)** The anemone Cerianthidae sp. 1 occurs wherever there is sufficient soft sediment, image taken during dive 250 at 849 m. **(C)** The urchin *C. cidaris* and the seastar Brisingidae sp. 1, the anemone *Phelliactis* sp. 1, image taken during dive 262 at 826 m. **(D)** The black coral Antipathidae sp. 1, the urchin *C. cidaris*, the anemone Cerianthidae sp. 1, image taken during dive 262 at 733 m. **(E)** The stony coral *Desmophyllum pertusum*, the deep water bivalve *A. excavata*, the coral morphospecies Anthozoa sp. 1, the anemones morphospecies Actinaria sp. 2 and *Actinernus michaelsarsi*, and the fish *Lepidion eques*, image taken during dive 116 at 1362 m. **(F)** Brachiopoda sp. 1, sponge morphospecies chalice sponge, the deep water bivalve *A. excavata*, the holothurian *Psolus squamatus*, the stony coral Caryophylliidae sp. 1 and the urchin *Echinus* sp. 1, image taken during dive 263 at 1344 m. Scale bars = 10 cm. Numbers denote cluster membership after cluster analysis.

3.3.2 Canyon wall assemblages

Hierarchical clustering identified nine clusters (Figure 5, Table 5 and Supplementary Figure 7) that separated into three regions of the nMDS plot (Figure 5). From review of clustering (Figure 5) and SIMPER results (Table 5 and Supplementary Table 1) it is likely that clusters 1, 2 and 3 represent the three main assemblages with the remaining clusters representing transitionary components.

Cluster 1 represents the *D. pertusum* assemblage observed from dive 116, cluster 2 (and transitionary cluster 5) represents the Brachiopoda sp. 1 assemblage observed from dive 263 and cluster 3 (and transitionary clusters 4, 6 and 7) represents the general mixed assemblage comprised of Cerianthidae sp.1, *Cidaris cidaris* and Antipathidae sp. 1 observed from dives 262 and 250 (Figures 4, 5 and Table 5). Clusters 8 and 9 were only represented by a single sample, limiting conclusions that can be drawn and so are omitted from further discussion (Figure 4 and Table 5).

Walls toward the head of the canyon (between 500 - 900 m) support a wider variety of assemblages with some observed across both dive 250 and dive 262 (Figures 5-7). In contrast, lower down the canyon at approximately 1350 m, different single assemblage types dominated opposite canyon walls (dives 116 and 263) (Figures 5-7).

The RDA analysis demonstrated assemblage-environment relationships, showing that species aggregations are driven by

10.3389/fmars.2023.1091855

TABLE 4 Results from Generalised Linear Model for species richness and the selected environmental variables.

Model	Environmental Variables		Deviance explained
S	Slope	0.0199470 ***	0.39
	Depth	-0.0004673 *	
	RAC	1.4144485 ***	
	Substrate:		
	H_V.MS	-0.2589899 **	
	H_V.MS_BG	-0.1892338	
	H_V.MS_R	0.0163835	
	V.MS_CRF	-0.9036104 **	
1/D	Slope	-0.006666 ***	0.43
	Depth	0.0001939 ***	
	RAC	-1.767***	
	Substrate:		
	H_V.MS	0.0654 •	
	H_V.MS_BG	0.05817	
	H_V.MS_R	0.042	
	V.MS_CRF	0.07071	

Significance of individual terms ***p ≤ 0.001, **p ≤ 0.01, *p ≤ 0.05, • p ≤ 0.1.

depth, M_2 amplitude, criticality of the slope and substratum type (Adjusted R_2 48%) (Figure 7 and Table 6). The first axis of the RDA plot represents a gradient from reef to non-reef substrata and from supercritical to critical conditions, and the second axis represents a gradient in depth and M_2 amplitude (Figure 7).

The vectors representing species scores (Figure 7) separate into three subgroups. The upper left quadrant, characterized by the predominance of the anemone Cerianthidae sp. 1, the urchin *C. cidaris*, the deep water oyster *Neopycnodonte* sp. 1, the black coral Antipathidae sp. 1, the squat lobster Munididae sp. 1, the basket star Brisingidae sp. 1 and the stony coral *M. oculata*; within which there was further differentiation depending on the relative abundance of Cerianthidae sp. 1, Antipathidae sp. 1, *Neopycnodonte* sp. 1 and Brisingidae sp. 1. The lower right quadrant was represented by a predominance of Brachiopoda sp. 1, the stony coral Caryophylliidae sp. 1, Isididae sp. 3, the holothurian *Psolus squamatus*, the chalice sponge and the urchin *Echinus* sp. 1. The lower left quadrant was characterised by the predominance of the stony coral *D. pertusum*, the deep water bivalve *A. excavata*, the anemone morphospecies Actiniaria sp. 10, two coral morphospecies (Anthozoa sp. 1 and Cnidaria sp. 129) and Crinoidea sp. 11.

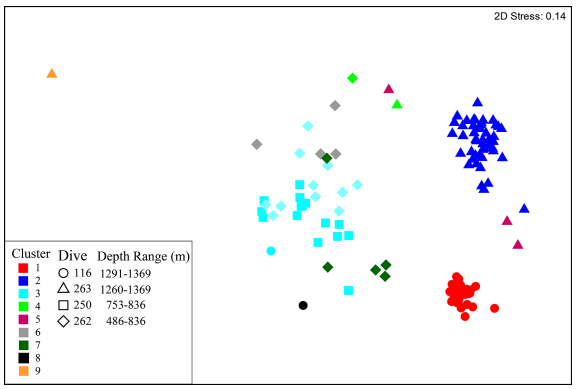

FIGURE 5
nMDS plot of multivariate Hellinger transformed species data. Samples are coloured to represent the nine clusters identified by hierarchal clustering analysis. Shapes denote the dive from which samples were collected.

The clustering and nMDS plots showed a similar trend by identifying nine clusters that separated into three regions of the nMDS plots (Figures 5, 7) comprised of the same characterising morphospecies as those in the RDA plot (Table 5). Cluster 1 relates to the lower left quadrant; cluster 2 relates to the lower right quadrant and cluster 3 relates to the upper left quadrant, with cluster 6 representing the increasingly Antipathidae sp. 1 dominated assemblage to the central upper left quadrant and cluster 4 representing the *Neopycnodonte* sp. 1 dominated assemblage.

Results of the spatial analysis show that fauna samples are spatially structured showing both a general trend at a broad scale and then greater similarity at distances <200 m and dissimilarity at distances >450 m that represents the difference between dives (Supplementary Figure 9). Variance partitioning shows 45.3% of variance explained in species data by environmental variables is also spatially structured in relation to the sample coordinates (Figure 8). Together these results suggest spatial patterns in species are driven

10.3389/fmars.2023.1091855

TABLE 5 Clusters identified from multivariate hierarchal clustering analysis with associated environmental parameters, number of samples represented by each cluster and SIMPER results identifying the morphospecies that characterise the clusters (70% accumulative contribution cut off).

Cluster	Characterising Species	Water Depth (m)	Substrate	Criticality	M_2 Amplitude (m)	Current Speed (ms^{-1})	Temp range and Average M_2 induced daily variation (°C)	N samples
1	*Desmophyllum pertusum, Acesta excavata*, coral morphospecies Anthozoa sp. 1 and Cnidaria sp. 129, Actiniaria sp. 10	1301-1369	H.CRF.V.M	Supercritical	0-58	0.42-0.46	5.6-7.1 (0.35)	26
2	Brachiopoda sp.1, Caryophylliidae sp. 1, *Psolus squamatus*, Isididae sp. 3, Porifera morphospecies chalice sponge	1261-1406	H.V.M, H_V.MS_BG	Critical	0-42	0.27-0.29	5.7-7.3 (0.31)	47
3	Cerianthidae sp. 1, *Cidaris cidaris*, Antipathidae sp. 1, Ophiuroidea	514-636	H_V.M, H_V.M_R	Supercritical	0-44	0.17-0.23	9.6-10.9 (0.24)	27
4	Caryophylliidae sp. 1	659 and 1330	H_V.M	Supercritical	27 and 45	0.19 and 0.28	5.8-6.9 (0.53) and9.5-10.6 (0.55)	2
5	*Echinus* sp. 1, *Acanella* sp. 1	1323-1368	H_V.M	Supercritical	0-28	0.28-0.29	5.7-6.9 (0.31)	3
6	Porifera sp. 15, Antipathidae sp. 1, Actinaria sp. 14, *Cidaris cidaris, Serpulidae* sp. 1,Cyclostomatidae sp. 1, Cerianthidae sp. 1	660-731	H_V.M_R, H_V.M	Supercritical	44-47	0.19	9.2-10.6 (0.51)	4
7	*Neopycnodonte* sp. 1, Crinoidea sp. 13, Munididae sp. 1, Caryophylliidae sp. 1, *Cidaris*, *Madrepora oculata*, Asterinidae sp. 1, Porifera sp. 11	486-666	H_V.M_R, H_V.M	Supercritical	32-44	0.17-0.19	9.4-11.0 (0.30)	4
8	Penatulacea sp. 1, *Actinoscyphia* sp. 1	1317	V.MS_CRF	Supercritical	13	0.4	6.4-6.4 (0.15)	1
9	Asteriodea sp. 1, Actiniidae sp. 5	1363	H_V.M	Critical	0	0.29	6.2 (0)	1

by environmental variables, which themselves are spatially organised and so exhibit a degree of induced spatial dependence.

4 Discussion

A number of studies have examined environmental drivers of faunal patterns in submarine canyons (Robert et al., 2015; Sigler et al., 2015; Pierdomenico et al., 2016; Domke et al., 2017; Bianchelli and Danovaro, 2019; Pierdomenico et al., 2019; Pearman et al., 2020) but until now, no study of canyon wall assemblages integrating both spatial and temporal oceanographic variability induced by the internal tide has been conducted. Using a multi-disciplinary approach, we have been able to further quantify spatial patterns in environmental variables and wall faunal assemblages in canyon settings.

Canyons are highly heterogeneous environments and the influence of spatial patterns in the environmental variables, coupled with the sample design of locations at two very different depths, makes it difficult to pull apart the role of environment vs the role of location (as illustrated by the strong significance of the RAC in the GLM and the overlap in variance partitioning in the RDA). Still, the nMDS and RDA results illustrate that faunal assemblages are not simply determined by ROV dive or sampling location since several assemblage clusters were observed from multiple dives (Figures 5, 7 and Table 5). Furthermore, the RDA analyses identified depth, slope, substratum and proxies of internal tide dynamics as important factors driving faunal patterns on canyon walls (Figure 7 and Table 6). The GLMs for species richness and $1/D$ also identified slope, depth and substrate characteristics as influencing faunal diversity, but not any of the proxies of internal tide dynamics (Table 4). Diversity metrics condense multivariate information (faunal composition and/or abundance) into a single measure that is not representative of species composition. In our data, areas of high diversity (species richness and $1/D$) supported different faunal compositions, demonstrating that the sole use of diversity metrics to represent faunal variability may miss key aspects of species – environment relationships in canyons and so limit our understanding of processes driving faunal distributions. As such these results indicate that other environmental factors (in this case proxies of internal tide dynamics), in addition to those traditionally highlighted by studies modelling diversity (i.e. depth, slope and substrate) (Robert et al., 2014; Ismail et al., 2018), are likely acting to determine assemblage composition in canyons. Additional sampling of other vertical walls in this part of Whittard Canyon would certainly help to obtain a clearer insight into the role of the environmental conditions in influencing faunal distributions.

Our spatial analysis revealed that the environmental variables investigated were spatially organised in relation to depth which was identified as an important factor influencing faunal patterns (Figure 8 and Tables 4, 6). Within Whittard Canyon we found

10.3389/fmars.2023.1091855

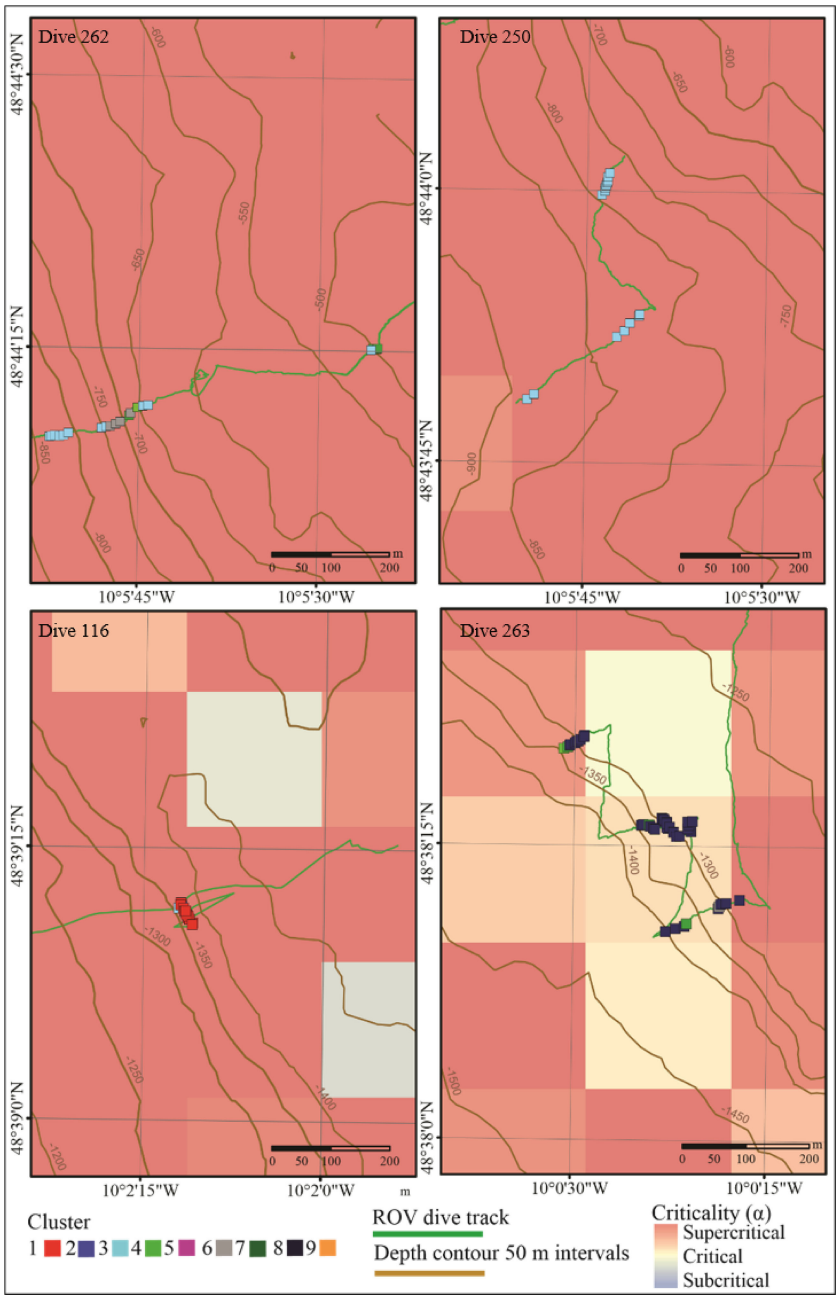

FIGURE 6
Spatial plot of sites (samples) from vertical walls across all dives plotted over bathymetric criticality to the M_2 tide. Samples are coloured to represent the nine clusters identified by hierarchal clustering analysis.

several oceanographic gradients (temperature, salinity and dissolved oxygen) that were correlated with depth and varied in intensity along the canyon (Figures 2, 3 and Supplementary Figures 2, 3, 6). Broad- scale environmental gradients of physico-chemical properties act to determine faunal patterns (Levin et al., 2001; Kenchington et al., 2014; Mcclain and Lundsten, 2015; Robert et al., 2015; Du Preez et al., 2016; Ismail et al., 2018) and are likely driving the difference in assemblages observed between walls of the upper and mid canyon (Figure 7 and Table 5). However, the observation from our study of different assemblages from similar depth ranges (Figures 5, 7, and Table 5) suggests that other processes, such as internal tides and substratum are working in concert at smaller spatial scales to drive spatial patterns in species assemblages on canyon walls.

Canyons are sites of intensified hydrodynamics including internal tides, which our study has shown generate spatial and temporal heterogeneity in water properties (temperature, salinity, density and dissolved oxygen concentration) (Figure 3) and near-bed current speeds (Supplementary Figure 1). In Whittard Canyon, short term temporal variability induced by the vertical isopycnal displacement of the M_2 internal tide (represented by the variable M_2 amplitude) was found to be a significant factor driving faunal

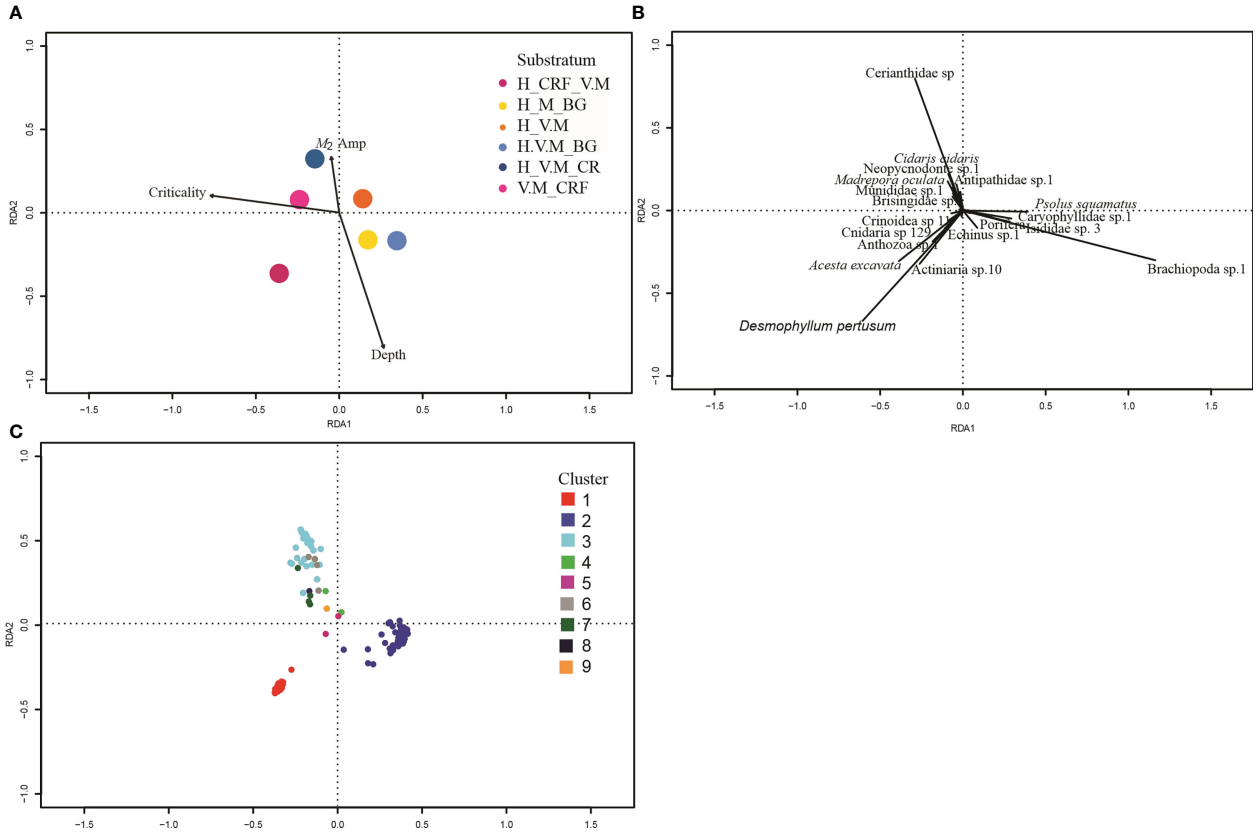

FIGURE 7
Canonical Redundancy Analysis of Hellinger transformed species data and selected environmental variables. For clarity, the triplot is displayed in three separate plots. **(A)** Environmental variables. The vector arrowheads represent high, the origin averages, and the tail (when extended through the origin) low values of the selected continuous environmental variables, centroids of categorical variables substratum shown as points colour coded by substratum type. **(B)** Species data with only species with strongest effect labelled. **(C)** Sites coloured by cluster following cluster analysis. Sites close to one another tend to have similar faunal structure than those further apart. Substratum codes: BG, Biogenic gravel; CR, Coral rubble; CRF, Coral reef framework; S, Sand; M, Mud; H, Hard; V, Veneer.

assemblages on canyon walls (Figure 7 and Table 6). Short-term variability in temperature, salinity and oxygen also drove differences in faunal assemblages on the Hebrides Terrace Seamount (Henry et al., 2014). Short-term internal tide induced variability in water properties may influence faunal distributions *via* species physiological constraints that limit their bathymetric distributions (Hutchins, 1947; Rowe and Menzies, 1969; Tietjen, 1971; Menzies and George, 1972; Van Den Hoek, 1982; Jeffree and Jeffree, 1994; Southward et al., 1995). The comparatively low variance explained by the vertical isopycnal displacement of the M_2 internal tide in our study may reflect the restricted environmental range that was sampled. For example, despite local amplitudes of up to 140 m calculated for the M_2 tide resulting in maximum tidal temperature variations of 1.55°C, these areas of high temporal variability did not coincide with data collected from vertical walls. Consequently, the temporal variability in oceanographic variables experienced by wall fauna was relatively consistent between dives, even if the absolute values differed (Table 5).

The M_2 vertical isopycnal elevation amplitudes diagnosed here may also reflect spatial and temporal variation in internal tide kinetic energy and associated turbulent mixing (Van Haren et al., 2022). In Whittard Canyon, peaks in turbulent kinetic energy dissipation have been linked with resuspension of material, nepheloid formation and sediment movement (Van Haren et al., 2022) that indirectly influences fauna by resuspending and concentrating POM (Dell'anno et al., 2013; Demopoulos et al., 2017; Pearman et al., 2020). Additionally, internal tide kinetic energy influences fauna directly by elevating near-bed current

TABLE 6 Results from Canonical Redundancy Analysis of Hellinger transformed species data and selected environmental variables.

Model	Environmental Variables - Significance of individual terms by ANOVA	Adjusted R^2	Significance of RDA Plot by ANOVA	
			F-value	p- value
V.Walls	Depth***, M_2.Amp***, Criticality ***, Substrate***	48	14.305, df= 8,105	0.001

Significance of individual terms by analysis of variance (ANOVA) on RDA including spatial structure. ***p ≤ 0.001.

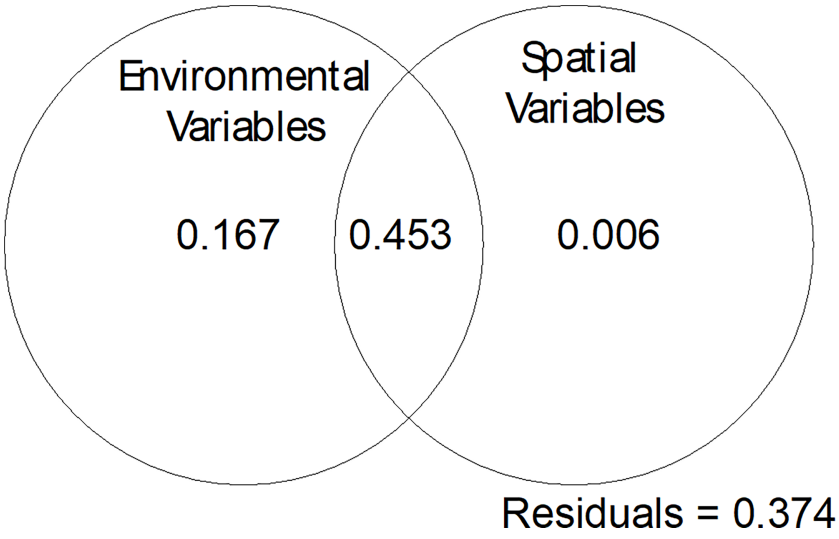

FIGURE 8
Variation partitioning plot for the Hellinger transformed species data, the selected environmental variables (depth, substratum, bathymetric criticality to the M_2 tide and amplitude of the M_2 tide) and spatial variables (sample coordinates).

speeds and associated physical stress (Weinbauer and Velimirov, 1996; Johnson et al., 2013; Orejas et al., 2016) and variation in internal tide kinetic energy has been correlated with fish larvae richness, abundance and assemblage composition in the Midrift Archipelago Region of the Tiburon Basin, Gulf of California (Ruvalcaba-Aroche 2019). Future observational campaigns, including moored Acoustic Doppler Current Profilers (ADCPs) and microstructure profiler surveys, will allow full diagnosis on internal tide energetics and associated turbulent mixing rates to quantitatively assess their influence on canyon fauna.

Internal tide–topographic interactions (indicated by bathymetric slope criticality to the dominant semidiurnal internal tide) are also linked to spatial heterogeneity in turbulent mixing (Wilson et al., 2015; Hall et al., 2017; Van Haren et al., 2017; Aslam et al., 2018) and near-bed current speeds both of which are linked to resuspension of POM (Thomsen and Gust, 2000; Wilson et al., 2015; Hall et al., 2017; Aslam et al., 2018). Deep-sea fauna predominantly rely upon the consumption of surface derived POM and internal tides interacting with supercritical slopes have been shown to form efficient food supply mechanisms capable of delivering high quality POM from surface waters to benthic assemblages at depth (Johnson et al., 2013; Mohn et al., 2014). Conversely, internal tides interacting with critical slopes may result in wave breaking and resuspension, and the mobilisation of older material from the seafloor that is often degraded and reworked material of lower quality POM. In Whittard Canyon, slope criticality was found to be a significant factor driving faunal assemblages on canyon walls, and it was mainly linked to assemblages that correlated with coral reef substrata (Figure 7 and Table 5). Dives 116 and 263, conducted at similar depths, differed in slope criticality and assemblages observed (Figure 6). On dive 263, brachiopods, large sponges and arborescent gorgonians were observed on walls where the slope was near critical (Table 5 and Figures 4, 6 and 7). In contrast, on dive 116, an assemblage characterised by *D. pertusum* was observed at similar depth, from a wall that was supercritical (Table 5 and Figures 4, 6 and 7). Isotopic analysis shows that *D. pertusum* has a broad trophic niche (Mueller et al., 2014; Demopoulos et al., 2017) having been known to feed on POM, zooplankton (Duineveld et al., 2007; Duineveld et al., 2012), bacteria and dissolved organic matter (Mueller et al., 2014) with a preference for high quality POM. On the other hand, isotopic signatures indicative of lower quality POM have been documented from brachiopods (Valls, 2017). Could the different spatial distributions of these assemblages be driven by the trophic niches of the characterising taxa that are able to capitalize on heterogeneity in POM influenced by the internal tide interacting with complex topography? Variability in the quality and amount of food supply is known to influence canyon faunal distributions (De Leo et al., 2010; McClain and Barry, 2010; Cunha et al., 2011; Chauvet et al., 2018). Furthermore, hydrodynamic and geomorphological processes have previously been proposed as factors influencing the supply and resuspension of particulate organic carbon to canyon environments and thus driving trophic structure, faunal assemblage composition and diversity (Dell'anno et al., 2013; Demopoulos et al., 2017). However, to confirm the role of the internal tide in generating spatial heterogeneity in food availability to which fauna respond, further trophic analysis of nepheloid layers in proximity to faunal assemblages in relation to internal tide dynamics would be required.

Near-bed current speed is also an important factor influencing food supply (Thomsen and Gust, 2000). Although R.M.S near-bottom baroclinic, barotropic and total current speed was removed from statistical analysis (due to collinearity with depth), data exploration showed that assemblages were distributed along a gradient of baroclinic (internal) current speed (Supplementary Figure 8). Separation of species along a gradient of current speed could reflect feeding and morphological adaptations. Species vary in their feeding strategies and efficiency under different hydrodynamic regimes (Järnegren and Altin, 2006; Van Oevelen et al., 2016). Species may exploit exposed areas to increase food encounter rates (Davies et al., 2009; Howell et al., 2011; Rengstorf et al., 2013; Mohn

et al., 2014; Van Oevelen et al., 2016; Bargain et al., 2018), or conversely avoid areas with high current speeds that may exceed food capture rates, damage feeding apparatus (Johnson et al., 2013; Orejas et al., 2016) or topple large arborescent species (Weinbauera and Velimirov, 1996). Current speed is a primary driver of coral distributions (De Clippele et al., 2018) and in our study the *D. pertusum* assemblage occurred in an area exposed to the highest speeds, which is consistent with published observations (Davies et al., 2009; Rengstorf et al., 2013; Mohn et al., 2014) including those from vertical walls (Brooke and Ross, 2014). On the other hand, larger gorgonians and sponges were observed in areas exposed to lower current speeds. Intensified currents are also linked to resuspension and increased turbidity, which both brachiopods and *D. pertusum* are noted to tolerate (James et al., 1992; Brooke et al., 2009) and may enable them to exploit these conditions. Corals also benefit from strong currents that reduce sediment settlement on corals, which in turn reduces cost expenditure associated with cleaning polyps (Brooke et al., 2009; Larsson and Purser, 2011).

The ability to exploit substrata may also influence faunal distributions in canyons. Canyon walls not only vary in their slope criticality but in their geological formation and fine scale structural complexity provided by ledges and organisms themselves. CWC species including arborescent gorgonians and scleractinians are considered ecosystem engineers capable of forming complex structures, which act to promote increased species richness by providing substratum for settlement, refuge, modification of local sedimentation and subsequent food availability (Buhl-Mortensen et al., 2010; Guihen et al., 2013), resulting in increased fine-scale environmental heterogeneity (Buhl-Mortensen et al., 2010) and diversity of associated species (Frederiksen and Westerberg, 1992; Henry and Roberts, 2007; Lessard-Pilon et al., 2010). In our study, species richness was highest where coral substrata co-occurred with mud on vertical walls with 'step-wise' substrata, whereby accumulations of mud supported additional soft sediment species, further increasing diversity (Figure 4E). The overall negative relationship between species richness and coral reef framework modelled by the GLM as opposed to the positive relationship between coral reef framework and $1/D$ likely represents the increased evenness among species on vertical walls that are dominated by *D. pertusum* and *A. excavata*. *Desmophylum pertusum* reefs will promote species richness to a point after which *D. pertusum* dominates, so that fewer species occur but those that do are relatively evenly represented resulting in increased $1/D$ (Henry and Roberts, 2007). Small-scale geomorphological features, such as ledges also appear to influence faunal distributions on walls (Figures 4A, E). In our study, certain species were observed aggregating in association with ledges (Figures 4A, E). Similar observations have been made from other vertical wall environments where the increased fine-scale structural complexity provided by ledges is proposed to contribute to fine-scale environmental heterogeneity and so promote niche differentiation (Robert et al., 2020). The fragile nature of the ledges has also been proposed as a limiting factor on maximum colony size of corals observed (Brooke et al., 2017; Robert et al., 2020). This postulation could explain the occurrence of the *D. pertusum* assemblage on the wall with wider stronger 'steps', observed from dive 116 (Figure 4E) that are capable of supporting greater weight and higher coral densities, compared to the thinner ledges observed elsewhere (Figure 4A). However, the existence of different communities associated with ledges in ours (dive 262, 250 and 116) and other studies of Whittard Canyon (Johnson et al., 2013; Robert et al., 2020), suggests that these features act to influence species patterns at fine spatial scales whilst other factors beyond substratum availability (e.g. depth, food supply and internal tide dynamics) influence assemblage patterns across walls at the canyon scale.

The findings of our research can be applied to other settings where internal tides interact with complex topography to generate spatial-temporal gradients in environmental conditions (i.e. seamounts, coral mounds and ridges) (Frederiksen and Westerberg, 1992; White and Dorschel, 2010). The importance of internal tides in inducing temporal variability in water properties and/or influencing food availability to sustain benthic assemblages in otherwise hostile conditions (i.e. oxygen minimum zones) have been reported from steep shelf (Hanz et al., 2019) and seamount environments (Van Haren et al., 2017). Internal tides are also considered important phenomena influencing cold-water coral mound development (White and Dorschel, 2010). However, few studies have explicitly incorporated the influence of internal tides (Van Haren et al., 2017). In light of our findings research in other complex settings should endeavour to incorporate internal tide data into their analysis.

5 Conclusion

Our results show that faunal patterns on vertical walls in submarine canyons are driven by broad-scale environmental gradients that co-vary with depth, but also has highlighted the role of the internal tide in generating environmental heterogeneity at a finer scale (via vertical isopycnal displacement of the M_2 internal tide and associated short term temporal variability in water mass properties, topography tide interactions and current speed) and how this might influence faunal distributions within the context of the larger depth related environmental gradients. As sites of intensified hydrodynamics, where internal tides generate spatial-temporal gradients in environmental variables, incorporating internal tide data is necessary to fully understand the processes that influence faunal patterns in canyons (including vertical walls).

We demonstrate that multivariate analysis of species data provides greater sensitivity than univariate indices, providing further insight into how the environmental factors interact at different scales to generate variability in environmental conditions that control species abundances and ultimately which species become characteristic of assemblages. Specifically, we highlight the likely link between internal tides and their associated vertical displacement in generating both spatial and temporal gradients in water mass properties that in turn influence faunal patterns on canyon walls.

Data availability statement

The raw data supporting the conclusions of this article will be made available by the authors, without undue reservation.

Author contributions

Conceptualization of paper, TP and VH, Methodology: CTD data provision FM, image annotation TP and KR, oceanographic data processing and analysis TP and RH, statistical analysis TP, Writing- original draft preparation TP, writing, reviewing and editing TP, AC, KR, RH, FM and VH. All authors contributed to the article and approved the submitted version.

Funding

This work was based on data collected from various expeditions. JC125 was funded by the ERC CODEMAP project (Starting Grant no 258482) and the NERC MAREMAP programme, the JC035_JC036 expedition was funded by the NERC core programme OCEANS2025, the EU FP7 IP HERMIONE; the 64PE421, 64PE453 and 64PE437 expeditions were funded by the NICO initiative by NWO and NIOZ and the NWO-VIDI, grant agreement 016.161.360 and MESH Joint copyright© 2007 Defra, JNCC, Marine Institute, BGS, UoP data were recorded during a collaborative survey (MESH Cruise 01-07-01) involving the Joint Nature Conservation Committee, the Marine Institute, the British Geological Survey and the University of Plymouth. The Department of the Environment, Fisheries and Rural Affairs (Defra) Natural Environmental Group Science Division (CRO361) made a significant financial contribution to this work. The MESH work contributed to the MESH project (www.searchmesh.net) that received European Regional Development Funding through the INTERREG III B Community Initiative (www.nweurope.org). TP was a PhD student in the NERC-funded SPITFIRE Doctoral Training Programme (Grant number NE/L002531/1) and received further funding from the National Oceanography Centre and the CASE partner CEFAS. VH was funded by the ERC Starting Grant project CODEMAP (Grant No 258482), by the NERC National Capability programme CLASS (Grant No NE/R015953/1), and the EU H2020 research and innovation programme project iAtlantic (grant agreement No 818123). During the final preparation stages of this manuscript she enjoyed a Fellowship from the Hanse-Wissenschaftskolleg Institute for Advanced Study. FM is supported by the innovational research scheme NWO-VIDI, grant agreement 016.161.360

Acknowledgments

The authors would like to thank the Captains, crews, and scientific parties of the various expeditions. Authors are particularly grateful to the Isis ROV team for the collection of groundtruthing data in the challenging submarine canyon terrain. We would also like to thank Tim Le Bas and Catherine Wardell for help with the bathymetry data processing, Dr. Brett Hosking for code to extract values from CTD casts and Michael Faggetter for his support with Matlab. We also thank the reviewers for their supportive reviews.

Conflict of interest

The authors declare that the research was conducted in the absence of any commercial or financial relationships that could be construed as a potential conflict of interest.

Publisher's note

Supplementary material

The Supplementary Material for this article can be found online at: https://www.frontiersin.org/articles/10.3389/fmars.2023.1091855/full#supplementary-material

References

92/43/EEC (1992). Council directive 92/43/EEC of 21 may 1992 on the conservation of natural habitats and of wild fauna and flora.

Addamo, A. M., Vertino, A., Stolarski, J., Garcia-Jimenez, R., Taviani, M., and Machordom, A. (2016). Merging scleractinian genera: The overwhelming genetic similarity between solitary *Desmophyllum* and colonial *Lophelia*. *BMC Evol. Biol.* 16, 108. doi: 10.1186/s12862-016-0654-8

Allen, S. E., and Durrieu De Madron, X. (2009). A review of the role of submarine canyons in deep-ocean exchange with the shelf. *Ocean Sci.* 5, 607–620. doi: 10.5194/os-5-607-2009

Althaus, F., Hill, N., Ferrari, R., Edwards, L., Przeslawski, R., Schonberg, C. H., et al. (2015). A standardised vocabulary for identifying benthic biota and substrata from underwater imagery: The CATAMI classification scheme. *PloS One* 10, e0141039. doi: 10.1371/journal.pone.0141039

Amaro, T., Huvenne, V. A. I., Allcock, A. L., Aslam, T., Davies, J. S., Danovaro, R., et al. (2016). The whittard canyon – a case study of submarine canyon processes. *Prog. Oceanography* 146, 38–57. doi: 10.1016/j.pocean.2016.06.003

Amaro, T., Stigter, H., Lavaleye, M., and Duineveld, G. (2015). Organic matter enrichment in the whittard channel; its origin and possible effects on benthic megafauna. *Deep-Sea Res. Part I: Oceanographic Res. Papers* 102, 90–100. doi: 10.1016/j.dsr.2015.04.014

Aslam, T., Hall, R., and Dyea, S. (2018). Internal tides in a dendritic submarine canyon. *Prog. Oceanography* 169, 20–32. doi: 10.1016/j.pocean.2017.10.005

Bargain, A., Foglini, F., Pairaud, I., Bonaldo, D., Carniel, S., Angeletti, L., et al. (2018). Predictive habitat modelling in two Mediterranean canyons including hydrodynamic variables. *Process Oceanography* 169, 151–168. doi: 10.1016/j.pocean.2018.02.015

Bianchelli, S., and Danovaro, R. (2019). Meiofaunal biodiversity in submarine canyons of the Mediterranean Sea: A meta-analysis. *Prog. Oceanography* 170, 69–80. doi: 10.1016/j.pocean.2018.10.018

Borcard, D., Gillet, F., and Legendre, P. (2011). *Numerical ecology with r* (New York: Springer-Verlag), 1–306.

Brooke, S., Holmes, M. W., and Young, C. M. (2009). Sediment tolerance of two different morphotypes of the deep-sea coral *Lophelia pertusa* from the gulf of Mexico. *Mar. Ecol. Prog. Ser.* 390, 137–144. doi: 10.3354/meps08191

Brooke, S., and Ross, S. W. (2014). "First observations of the cold-water coral," in Lophelia pertusa in mid-Atlantic canyons of the USA. *Deep-Sea Research II*. 104, 245–251. doi: 10.1016/j.dsr2.2013.06.011

Brooke, S. D., Watts, M. W., Heil, A. D., Rhode, M., Mienis, F., Duineveldd, G. C. A., et al. (2017). "Distributions and habitat associations of deep-water corals in Norfolk and Baltimore canyons," in *Mid-Atlantic bight*, vol. 137. (USA: Deep-Sea Research II), 131–147.

Buhl-Mortensen, L., Vanreusel, A., Gooday, A. J., Levin, L. A., Priede, I. G., Buhl-Mortensen, P., et al. (2010). Biological structures as a source of habitat heterogeneity and biodiversity on the deep ocean margins. *Mar. Ecol.* 31, 21–50. doi: 10.1111/j.1439-0485.2010.00359.x

Carter, G., Huvenne, V., Jennifer, G., Lo Iacono, C., Marsh, L., Ougier-Simonine, A., et al. (2018). Ongoing evolution of submarine canyon rockwalls; examples from the whittard canyon, celtic margin (NE Atlantic). *Prog. Oceanography* 169, 79–88. doi: 10.1016/j.pocean.2018.02.001

Chauvet, P., Metaxas, A., Hay, A., and Matabos, M. (2018). Annual and seasonal dynamics of deep-sea megafaunal epibenthic communities in barkley canyon (British Columbia, canada): A response to climatology, surface productivity and benthic boundary layer variation. *Prog. Oceanography*. 169, 89–105. doi: 10.1016/j.pocean.2018.04.002

Clarke, (1993). Non parametrc multivariate analysis of change. *Aust. J. Ecol.* 18, 117–143. doi: 10.1111/j.1442-9993.1993.tb00438.x

Crase, B., Liedloff, A. C., and Wintle, B. A. (2012). A new method for dealing with residual spatial autocorrelation in species distribution models. *Ecography* 35, 879–888. doi: 10.1111/j.1600-0587.2011.07138.x

Cunha, M. R., Paterson, G. L. J., Amaro, T., Blackbird, S., De Stigter, H. C., Ferreira, C., et al. (2011). Biodiversity of macrofaunal assemblages from three Portuguese submarine canyons (NE Atlantic). *Deep Sea Res. Part II: Topical Stud. Oceanography* 58, 2433–2447. doi: 10.1016/j.dsr2.2011.04.007

Cunningham, M. J., Hodgson, S., Masson, D. G., and Parson, L. M. (2005). An evaluation of along- and down-slope sediment transport processes between goban spur and brenot spur on the celtic margin of the bay of Biscay. *Sedimentary Geol.* 179, 99–116. doi: 10.1016/j.sedgeo.2005.04.014

Davies, A. J., Duineveld, G. C. A., Lavaleye, M. S. S., Bergman, M. J. N., Van Haren, H., and Roberts, J. M. (2009). Downwelling and deep-water currents as food supply mechanisms to the cold-water coral *lophelia pertusa* (Scleractinia) at the mingulay reef complex. *Limnol. Oceanography* 54, 620–629. doi: 10.4319/lo.2009.54.2.0620

Davies, J., Guinan, J., Howell, K., Stewart, H., and Verling, E. (2008). MESH south west approaches canyons survey: Final report. *MESH Cruise*.

Davison, J. J., Van Haren, H., Hosegood, P., Piechaud, N., and Howell, K. L. (2019). The distribution of deep-sea sponge aggregations (Porifera) in relation to oceanographic processes in the faroe-Shetland channel. *Deep Sea Res. Part I: Oceanographic Res. Papers* 146, 55–61. doi: 10.1016/j.dsr.2019.03.005

De Clippele, L. H., Huvenne, V. A. I., Orejas, C., Lundälv, T., Fox, A., Hennige, S. J., et al. (2018). The effect of local hydrodynamics on the spatial extent and morphology of cold-water coral habitats at tisler Reef,Norway. *Coral Reefs* 37, 253–266. doi: 10.1007/s00338-017-1653-y

De Leo, F. C., Smith, C. R., Rowden, A. A., Bowden, D. A., and Clark, M. R. (2010). Submarine canyons: Hotspots of benthic biomass and productivity in the deep sea. *Proc. R. Soc. B.: Biol. Sci.* 277, 2783–2792. doi: 10.1098/rspb.2010.0462

De Leo, F. C., Vetter, E. W., Smith, C. R., Rowden, A. A., and Mcgranaghan, M. (2014). Spatial scale-dependent habitat heterogeneity influences submarine canyon macrofaunal abundance and diversity off the main and Northwest Hawaiian islands. *Deep Sea Res. Part II: Topical Stud. Oceanography* 104, 267–290. doi: 10.1016/j.dsr2.2013.06.015

Dell'anno, A., Pusceddu, A., Corinaldesi, C., Canals, M., Heussner, S., Thomsen, L., et al. (2013). Trophic state of benthic deep-sea ecosystems from two different continental margins off Iberia. *Biogeosciences* 10, 2945–2957. doi: 10.5194/bg-10-2945-2013

Demopoulos, A. W. J., Mcclain-Counts, J., Ross, S. W., Brooke, S., and Mienis, F. (2017). Food-web dynamics and isotopic niches in deep-sea communities residing in a submarine canyon and on the adjacent open slopes. *Mar. Ecol. Prog. Ser.* 578, 19–33. doi: 10.3354/meps12231

Domke, L., Lacharité, M., Metaxas, A., and Matabos, M. (2017). Influence of an oxygen minimum zone and macroalgal enrichment on benthic megafaunal community composition in a NE pacific submarine canyon. *Mar. Ecol.* 38, e12481. doi: 10.1111/maec.12481

Duineveld, G. C. A., Jeffreys, R. M., Lavaleye, M. S. S., Davies, A. J., Bergman, M. J. N., Watmough, T., et al. (2012). Spatial and tidal variation in food supply to shallow cold-water coral reefs of the mingulay reef complex (Outer Hebrides, Scotland). *Mar. Ecol. Prog. Ser.* 444, 97–115. doi: 10.3354/meps09430

Duineveld, G. C. A., Lavaleye, M. S. S., Bergman, M. J. N., De Stigter, H., and Mienis, F. (2007). Trophic structure of a cold-water coral mound community (Rockall bank, NE Atlantic) in relation to the near-bottom particle supply and current regime. *Bull. Mar. Sci.* 81, 449–467.

Dullo, W., Flögel, S., and Rüggeberg, A. (2008). Cold-water coral growth in relation to the hydrography of the celtic and Nordic European continental margin. *Mar. Ecol. Prog. Ser.* 371, 165–176. doi: 10.3354/meps07623

Du Preez, C., Curtiz, J., and Clarke, M. (2016). The structure and distribution of benthic communities on a shallow seamount (Cobb seamount, northeast pacific ocean). *PloS One* 11, e0165513. doi: 10.1371/journal.pone.0165513

Fabri, M. C., Bargain, A., Pairaud, I., Pedel, L., and Taupier-Letage, I. (2017). Cold-water coral ecosystems in cassidaigne canyon: An assessment of their environmental living conditions. *Deep Sea Res. Part II: Topical Stud. Oceanography* 137, 436–453. doi: 10.1016/j.dsr2.2016.06.006

Fabri, M. C., Pedel, L., Beuck, L., Galgani, F., Hebbeln, D., and Freiwald, A. (2014). Megafauna of vulnerable marine ecosystems in French mediterranean submarine canyons: Spatial distribution and anthropogenic impacts. *Deep Sea Res. Part II: Topical Stud. Oceanography* 104, 184–207. doi: 10.1016/j.dsr2.2013.06.016

FAO (2008). *Report of the expert consultation on international guidelines for the management of deep-Sea fisheries in the high seas* (Bangkok: FAO Fisheries Report No. 855), 11–14.

FAO (2009). *Management of deep-Sea fisheries in the high seas* (Rome: Food and Agriculture Organization of the United Nations).

Fernandez-Arcaya, U., Ramirez-Llodra, E., Aguzzi, J., Allcock, A. L., Davies, J. S., Dissanayake, A., et al. (2017). Ecological role of submarine canyons and need for canyon conservation: A review. *Front. Mar. Sci.* 4. doi: 10.3389/fmars.2017.00005

Frederiksen, J., and Westerberg, (1992). The distribution of the scleractinian coral lophelia pertusa around the faroe islands and the relation to internal tidal mixing. *Sarsia North Atlantic Mar. Sci.* 77, 157–171.

Guihen, D., White, M., and Lundalv, T. (2013). Boundary layer flow dynamics at a cold-water coral reef. *J. Sea Res.* 78, 36–44. doi: 10.1016/j.seares.2012.12.007

Haalboom, S., de Stigter, H., Duineveld, G., Van Haren, H., Reichart, G., and Mienis, F. (2021). Suspended particulate matter in a submarine canyon (Whittard Canyon,Bay of Biscay, NE Atlantic ocean): Assessment of commonly used instruments to record turbidity. *Mar. Geol.* 434, 106439. doi: 10.1016/j.margeo.2021.106439

Hall, R. A., Alford, M. H., Carter, G. S., Gregg, M. C., Lien, R.-C., Wain, D. J., et al. (2014). Transition from partly standing to progressive internal tides in Monterey submarine canyon. *Deep Sea Res. Part II: Topical Stud. Oceanography* 104, 164–173. doi: 10.1016/j.dsr2.2013.05.039

Hall, R. A., Aslam, T., and Huvenne, V. A. I. (2017). Partly standing internal tides in a dendritic submarine canyon observed by an ocean glider. *Deep Sea Res. Part I: Oceanographic Res. Papers* 126, 73–84. doi: 10.1016/j.dsr.2017.05.015

Hall, R. A., and Carter, G. (2011). Internal tides in Monterey Submarine Canyon. *Journal of Physical Oceanography* 41, 186–20.

Hanz, U., Wienberg, C., Hebbeln, D., Duienveld, G., Lavaleye, M., Juva, K., et al. (2019). Environmental factors influencing benthic communities in the oxygen minimum zones on the Angolan and Namibian margins. *Biogeosciences* 16, 4337–4356. doi: 10.5194/bg-16-4337-2019

Henry, L.-A., and Roberts, J. M. (2007). Biodiversity and ecological composition of macrobenthos on cold-water coral mounds and adjacent off-mound habitat in the bathyal porcupine seabight, NE Atlantic. *Deep Sea Res. Part I: Oceanographic Res. Papers* 54, 654–672. doi: 10.1016/j.dsr.2007.01.005

Henry, L. A., Vad, J., and Roberts, J. M. (2014). Environmental variability and biodiversity of megabenthos on the Hebrides terrace seamount (Northeast Atlantic). *Sci. Rep.* 4, 5589. doi: 10.1038/srep05589

Howell, K., Billett, D. S. M., and Tyler, P. (2002). Depth-related distribution and abundance of seastars (Echinodermata: Asteroidea) in the porcupine seabight and porcupine abyssal plain, N.E. Atlantic. *Deep-Sea Res. I* 49, 1901–1920. doi: 10.1016/S0967-0637(02)00090-0

Howell, K. L., Holt, R., Endrino, I. P., and Stewart, H. (2011). When the species is also a habitat: Comparing the predictively modelled distributions of *Lophelia pertusa* and the reef habitat it forms. *Biol. Conserv.* 144, 2656–2665. doi: 10.1016/j.biocon.2011.07.025

Hunter, W. R., Jamieson, A., Huvenne, V. A. I., and Witte, U. (2013). Sediment community responses to marine vs. terrigenous organic matter in a submarine canyon. *Biogeosciences* 10, 67–80. doi: 10.5194/bg-10-67-2013

Hutchins, L. W. (1947). The bases for temperature zonation in geographical distribution. *Ecol. Soc. America* 17, 325–335. doi: 10.2307/1948663

Huvenne, V. A. I., and Davies, J. S. (2014). Towards a new and integrated approach to submarine canyon research. *Deep Sea Res. Part II: Topical Stud. Oceanography* 104, 1–5. doi: 10.1016/j.dsr2.2013.09.012

Huvenne, V., Tyler, P. D. M., Fisher, D., Hauton, C., Huhnerbach, V., Le Bas, T., et al. (2011). A picture on the wall: Innovative mapping reveals cold-water coral refuge in submarine canyon. *PloS One* 6, e28755. doi: 10.1371/journal.pone.0028755

Huvenne, V., Wynn, R., and Gales, J. (2016). RRS James cook cruise 124-125-126 09 Aug-12 sep 2016. CODEMAP2015: Habitat mapping and ROV vibrocorer trials around whittard canyon and haig fras. *Natl. Oceanography Centre Cruise Rep*. 36.

Ismail, K., Huvenne, V., and Robert, K. (2018). Quantifying spatial heterogeneity in submarine canyons. *Prog. Oceanography* 169, 181–198. doi: 10.1016/j.pocean.2018.03.006

James, M. A., Ansell, A. D., Collins, M. J., Curry, G. B., Peck, L. S., and Rhodes, M. C. (1992). Biology of living brachiopods. *Adv. Mar. Biol.* 28, 175–387. doi: 10.1016/S0065-2881(08)60040-1

Järnegren, J., and Altin, D. (2006). Filtration and respiration of the deep living bivalve *Acesta excavata* (J.C. fabriciu) (Bivalvia; limidae). *J. Exp. Mar. Biol. Ecol.* 334, 122–129. doi: 10.1016/j.jembe.2006.01.014

Jeffree, E. P., and Jeffree, C. E. (1994). Temperature and the biogeographical distributions of species. *Funct. Ecol.* 8, 640–650. doi: 10.2307/2389927

Johnson, M. P., White, M., Wilson, A., Wurzberg, L., Schwabe, E., Folch, H., et al. (2013). A vertical wall dominated by *Acesta excavata* and *Neopycnodonte zibrowii*, part of an undersampled group of deep-sea habitats. *PloS One* 8, e79917. doi: 10.1371/journal.pone.0079917

Kenchington, E. L., Cogswell, A. T., Macisaac, K. G., Beazley, L., Law, B. A., and Kenchington, T. J. (2014). Limited depth zonation among bathyal epibenthic megafauna of the gully submarine canyon, northwest Atlantic. *Deep Sea Res. Part II: Topical Stud. Oceanography* 104, 67–82. doi: 10.1016/j.dsr2.2013.08.016

Larsson, A. I., and Purser, A. (2011). Sedimentation on the cold-water coral *Lophelia pertusa*: Cleaning efficiency from natural sediments and drill cuttings. *Mar. pollut. Bulliton* 62, 1159–1168. doi: 10.1016/j.marpolbul.2011.03.041

Legendre, P., and Gallagher, E. (2001). Ecologically meaningful transformations for ordination of species data. *Oecologia* 129, 271–280. doi: 10.1007/s004420100716

Legendre, P., and Legendre, L. (2012). Numerical ecology. *Elsevier* 24.

Lessard-Pilon, S. A., Podowski, E. L., Cordes, E. E., and Fisher, C. R. (2010). Megafauna community composition associated with *Lophelia pertusa* colonies in the gulf of Mexico. *Deep Sea Res. Part II: Topical Stud. Oceanography* 57, 1882–1890. doi: 10.1016/j.dsr2.2010.05.013

Levin, L. A., Jetter, R., Rex, M., Goodday, R., Smith, C., Pineda, J., et al. (2001). Enviornemntal influences on regional deep-sea species diversity. *Annu. Rev. Ecol. Evol. Syst.* 32, 51–93. doi: 10.1146/annurev.ecolsys.32.081501.114002

Liu, J. T., Wang, Y. H., Lee, I. H., and Hsu, R. T. (2010). Quantifying tidal signatures of the benthic nepheloid layer in gaoping submarine canyon in southern Taiwan. *Mar. Geol.* 271, 119–130. doi: 10.1016/j.margeo.2010.01.016

Lo Iacono, C., Guillén, J., Guerrero, Q., Durán, R., Wardell, C., Hall, R. A., et al. (2020). Bidirectional bedform fields at the head of a submarine canyon (NE Atlantic). *Earth Planetary Sci. Lett.* 542, 116321. doi: 10.1016/j.epsl.2020.116321

Lo Iacono, C., Robert, K., González-Villanueva, R., Gori, A., Gili, J.-M., and Orejas, C. (2018). Predicting cold-water coral distribution in the cap de creus canyon (NW mediterranean): Implications for marine conservation planning. *Prog. Oceanography* 169, 169–180. doi: 10.1016/j.pocean.2018.02.012

Masson, D. G. (2009). RRS James cook cruise 36, 19 jul-28 jul 2009. the geobiology of whittard submarine canyon. *Natl. Oceanography Centre Southampton Cruise Rep.* 41.

Mcclain, C., and Barry, J. (2010). Habitat heterogeneity, disturbance, and productivity work in concert to regulate biodiversity in deep submarine canyons. *Ecology* 91, 964–976. doi: 10.1890/09-0087.1

Mcdougall, T. J., and Barker, P. M. (2011). Getting started with TEOS-10 and the Gibbs seawater (GSW) oceanographic toolbox. *SCOR/IAPSO WG127* 28.

Menzies, R., and George, R. (1972). Hydrostatic pressure–temperature effects on deep-sea colonisation. *Proc. R. Soc. Edinburgh Section B. Biol.* 73, 195–202. doi: 10.1017/S0080455X00002253

Mienis, F., De Stigter, H. C., De Haas, H., and Van Weering, T. C. E. (2009). Near-bed particle deposition and resuspension in a cold-water coral mound area at the southwest rockall trough margin, NE Atlantic. *Deep Sea Res. Part I: Oceanographic Res. Papers* 56, 1026–1038. doi: 10.1016/j.dsr.2009.01.006

Mohn, C., Rengstorf, A., White, M., Duineveld, G., Mienis, F., Soetaert, K., et al. (2014). Linking benthic hydrodynamics and cold-water coral occurrences: A high-resolution model study at three cold-water coral provinces in the NE Atlantic. *Prog. Oceanography* 122, 92–101. doi: 10.1016/j.pocean.2013.12.003

Mueller, C. E., Larsson, A. I., Veuger, B., Middleburg, J. J., and Van Oevelen, D. (2014). Opportunistic feeding on various organic food sources by the cold-water coral *Lophelia pertusa*. *Biogeosciences* 11, 123–133. doi: 10.5194/bg-11-123-2014

Obelcz, J., Brothers, D., Chaytor, J., Brink, U., Ross, S., and Brooke, S. (2014). Geomorphic characterization of four shelf-sourced submarine canyons along the U.S. mid-Atlantic continental margin. *Deep-Sea Res. II* 104, 106–119. doi: 10.1016/j.dsr2.2013.09.013

Orejas, C., Gori, A., Lo Iacono, C., Puig, G. J., and Dale, M. R. T. (2009). Cold-water corals in the cap de creus canyon northwestern Mediterranean: Spatial distribution, density and anthropogenic impact. *Mar. Ecol. Prog. Seres* 397, 37–51. doi: 10.3354/meps08314

Orejas, C., Gori, A., Rad-Menéndez, C., Last, K. S., Davies, A. J., Beveridge, C. M., et al. (2016). The effect of flow speed and food size on the capture efficiency and feeding behaviour of the cold-water coral *Lophelia pertusa*. *J. Exp. Mar. Biol. Ecol.* 481, 34–40. doi: 10.1016/j.jembe.2016.04.002

OSPAR (2008). OSPAR list of threatened and/or declining species and habitats.

Pawlowicz, R., Beardsley, B., and Lentz, R. (2002). Classical tidal harmonic analysis including error estimates in MATLAB using T TIDE. *Computers and Geosciences* 28, 929–937. doi: 10.1016/S0098-3004(02)00013-4

Pearman, T. R. R., Robert, K., Callaway, A., Hall, R., Lo Iacono, C., and Huvenne, V. A. I. (2020). Improving the predictive capability of benthic species distribution models by incorporating oceanographic data – towards holistic ecological modelling of a submarine canyon. *Prog. Oceanography* 184, 102338. doi: 10.1016/j.pocean.2020.102338

Pierdomenico, M., Cardone, F., Carluccio, A., Casalbore, D., Chiocci, F., Maiorano, P., et al. (2019). Megafauna distribution along active submarine canyons of the central Mediterranean: Relationships with environmental variables. *Prog. Oceanography* 171, 49–69. doi: 10.1016/j.pocean.2018.12.015

Pierdomenico, M., Martorelli, E., Dominguez-Carrió, C., Gili, J. M., and Chiocci, F. L. (2016). Seafloor characterization and benthic megafaunal distribution of an active submarine canyon and surrounding sectors: The case of gioia canyon (Southern tyrrhenian Sea). *J. Mar. Syst.* 157, 101–117. doi: 10.1016/j.jmarsys.2016.01.005

Pollard, R. T., Griffrrhs, M. J., Cunningham, S. A., Read, J. F., Irez, F. F., and Rlos, A. F. (1996). Vivaldi 1991 - a study of the formation, circulation and ventilation of Eastern north Atlantic central water. *Prog. Oceanography* 37, 167–172. doi: 10.1016/S0079-6611(96)00008-0

Price, D. M., Robert, K., Callaway, A., Lo Lacono, C., Hall, R. A., and Huvenne, V. A. I. (2019). Using 3D photogrammetry from ROV video to quantify cold-water coral reef structural complexity and investigate its influence on biodiversity and community assemblage. *Coral Reefs*. 38, 1007–1021. doi: 10.1007/s00338-019-01827-3

Puig, P., Palanques, A., and Martín, J. (2014). Contemporary sediment-transport processes in submarine canyons. *Annu. Rev. Mar. Sci.* 6, 53–77. doi: 10.1146/annurev-marine-010213-135037

R_CORE_TEAM (2014). *R: A language and environment for statistical computing* (Vienna, Austria: R Foundation for Statistical Computing).

Reid, G., and Hamilton, D. (1990). A reconnaissance survey of the whittard Sea fan, southwestern approaches, British isles. *Mar. Geol.* 92, 69–86. doi: 10.1016/0025-3227(90)90027-H

Rengstorf, A. M., Yesson, C., Brown, C., Grehan, A. J., and Crame, A. (2013). High-resolution habitat suitability modelling can improve conservation of vulnerable marine ecosystems in the deep sea. *J. Biogeography* 40, 1702–1714. doi: 10.1111/jbi.12123

Robert, K., Huvenne, V. A. I., Georgiopoulou, A., Jones, D. O. B., Marsh, L., Carter, G. D. O., et al. (2017). New approaches to high-resolution mapping of marine vertical structures. *Sci. Rep.* 7, 9005. doi: 10.1038/s41598-017-09382-z

Robert, K., Jones, D., Georgiopoulou, A., and Huvenne, V. (2020). Cold-water coral assemblages on vertical walls from the northeast Atlantic. *Biodiversity Res.* 26, 1–15. doi: 10.1111/ddi.13011

Robert, K., Jones, D. O.B., and Huvenne, V. A.I. (2014). Megafaunal distribution and biodiversity in a heterogeneous landscape: The iceberg-scoured Rockall Bank, NE Atlantic. *Marine Ecology Progress Series* 501, 67–88.

Robert, K., Jones, D. O. B., Tyler, P. A., Van Rooij, D., and Huvenne, V. A. I. (2015). Finding the hotspots within a biodiversity hotspot: Fine-scale biological predictions within a submarine canyon using high-resolution acoustic mapping techniques. *Mar. Ecol.* 36, 1256–1276. doi: 10.1111/maec.12228

Rowe, G., and Menzies, R. J. (1969). Zonation of large benthic invertebrates in the deep-sea off the carolinas. *Deep Sea Res. Oceanographic Abstracts* 16, 531–532. doi: 10.1016/0011-7471(69)90041-2

Ruvalcaba-Aroche, E. D., Filonov, A., Sánchez-Velasco, L., Ladah, L. B., and Cruz-Hernández, J. (2019). Internal tidal waves in Tiburon Basin (Gulf of California, Mexico) modulate fish larvae aggregations. *Continental Shelf Research* 178, 41–50.

Sigler, M. F., Rooper, C. N., Hoff, G. R., Stone, R. P., Mcconnaughey, R. A., and Wilderbuer, T. K. (2015). Faunal features of submarine canyons on the eastern Bering Sea slope. *Mar. Ecol. Prog. Ser.* 526, 21–40. doi: 10.3354/meps11201

Simpson, E. H. (1949). Measurement of diversity. *Nature* 163, 688–688. doi: 10.1038/163688a0

Southward, A. J., Hawkins, S. J., and Burrows, M. T. (1995). Seventy years' observations of changes in distribution and abundance of zooplankton and intertidal organisms in the Western English chaennel in relation to rising sea temperature. *J. Thermal Biol.* 20, 127–155. doi: 10.1016/0306-4565(94)00043-I

Stashchuk, N., and Vlasenko, V. (2021). Internal wave dynamics over isolated seamount and its influence on coral larvae dispersion. *Front. Mar. Sci.* 8, 735358. doi: 10.3389/fmars.2021.735358

Stewart, H. A., Davies, J. S., Guinan, J., and Howell, K. L. (2014). The dangeard and explorer canyons, south Western approaches UK: Geology, sedimentology and newly discovered cold-water coral mini-mounds. *Deep Sea Res. Part II: Topical Stud. Oceanography* 104, 230–244. doi: 10.1016/j.dsr2.2013.08.018

Thiem, Ø., Ravagnan, E., Fosså, J. H., and Berntsen, J. (2006). Food supply mechanisms for cold-water corals along a continental shelf edge. *J. Mar. Syst.* 60, 207–219. doi: 10.1016/j.jmarsys.2005.12.004

Thomsen, L., and Gust, G. (2000). Sediment erosion thresholds and characteristics of resuspended aggregates on the western European continental margin. *Deep Sea Res. Part I: Oceanographic Res. Papers* 47, 1881–1897. doi: 10.1016/S0967-0637(00)00003-0

Tietjen, J. H. (1971). Ecology and distribution of deep-sea meiobenthos off north Carolina. *Deep Sea Res. Oceanographic Abstracts* 18, 941–944. doi: 10.1016/0011-7471(71)90001-5

Valls, M. (2017). Trophic ecology in marine ecosystems from the balearis Sea (Western Mediterranean). *PHD Thesis*, 1–198.

Van Aken, H. (2000). The hydrography of the mid-latitude northeast Atlantic ocean II: The intermediate water masses. *Deep-Sea Res. Part I: Oceanographic Res. Papers*. 47, 789–824. doi: 10.1016/S0967-0637(99)00112-0

Van Den Beld, I. M. J., Bourillet, J.-F., Arnaud-Haond, S., De Chambure, L., Davies, J. S., Guillaumont, B., et al. (2017). Cold-water coral habitats in submarine canyons of the bay of Biscay. *Front. Mar. Sci.* 4. doi: 10.3389/fmars.2017.00118

Van Den Hoek, C. (1982). The distribution of benthic marine algae in relation to the temperature regulation of their life histories. *Biol. J. Linn. Soc.* 18, 81–144. doi: 10.1111/j.1095-8312.1982.tb02035.x

Van Haren, H., Hanz, U., De Stigter, H., Mienis, F., and Duineveld, G. (2017). Internal wave turbulence at a biologically rich mid-Atlantic seamount. *PloS One* 12, e0189720. doi: 10.1371/journal.pone.0189720

Van Haren, H., Mienis, F., and Duineveld, G. (2022). Contrasting internal tide turbulence in a tributary of the whittard canyon. *Contiental Shelf Res.* 236, 104679. doi: 10.1016/j.csr.2022.104679

Van Oevelen, D., Mueller, C. E., Lundälv, T., and Middelburg, J. J. (2016). Food selectivity and processing by the cold-water coral lophelia pertusa. *Biogeosciences* 13, 5789–5798. doi: 10.5194/bg-13-5789-2016

Van Rooij, D., De Mol, L., Le Guilloux, E., Wisshak, M., Huvenne, V. A. I., Moeremans, R., et al. (2010). Environmental setting of deep-water oysters in the bay of Biscay. *Deep-Sea Res. I* 57, 1561–1572. doi: 10.1016/j.dsr.2010.09.002

Vetter, E. W., Smith, C. R., and De Leo, F. C. (2010). Hawaiian Hotspots: Enhanced megafaunal abundance and diversity in submarine canyons on the oceanic islands of Hawaii. *Mar. Ecol.* 31, 183–199. doi: 10.1111/j.1439-0485.2009.00351.x

Vlasenko, V., Stashchuk, N., Inall, M. E., Porter, M., and Aleynik, D. (2016). Focusing of baroclinic tidal energy in a canyon. *J. Geophysical Res.: Oceans* 121, 2824–2840. doi: 10.1002/2015JC011314

Walbridge, S., Slocum, N., Pobuda, M., and Wright, D. (2018). Unified geomorphological analysis workflows with benthic terrain modeler. *Geosci. (Switzerland)* 8, 94. doi: 10.3390/geosciences8030094

Weinbauera, M., and Velimirov, B. (1996). Population dynamics and overgrowth of the Sea fan eunicella cavolini (Coelenterata: Octocorallia). *Estuarine Coast. Shelf Sci.* 42, 583–595. doi: 10.1006/ecss.1996.0038

White, M., and Dorschel, B. (2010). The importance of the permanent thermocline to the cold water coral carbonate mound distribution in the NE Atlantic. *Earth Planetary Sci. Lett.* 296, 395–402. doi: 10.1016/j.epsl.2010.05.025

White, M., Mohn, C., De Stigter, H., and Mottram, G. (2005). Deep-water coral development as a function of hydrodynamics and surface productivity around the submarine banks of the rockall trough, NE Atlantic. *Cold-Water Corals Ecosyst*, 503–514. doi: 10.1007/3-540-27673-4_25

Wilson, M. F. J., O'connell, B., Brown, C., Guinan, J. C., and Grehan, A. J. (2007). Multiscale terrain analysis of multibeam bathymetry data for habitat mapping on the continental slope. *Mar. Geodesy.* 30, 3–35. doi: 10.1080/01490410701295962

Wilson, A. M., Raine, R., Mohn, C., and White, M. (2015). Nepheloid layer distribution in the whittard canyon, NE Atlantic margin. *Mar. Geol.* 367, 130–142. doi: 10.1016/j.margeo.2015.06.002

Wunsch, C. (1975). Internal Tides in the Ocean. *Reviews of Geophysics and Space Physics* 13, 167–182.

Zuur, A., Ieno, N., and Elphick, C. (2010). A protocol for data exploration to avoid common statistical problems. *Methods Ecol. Evol.* 1, 3–14. doi: 10.1111/j.2041-210X.2009.00001.x

Zuur, A., Ieno, E., Walker, N., Saveliev, A., and Smith, G. (2014a). *Mixed effects models and extensions in ecology with r* (New York: Springer-Verlag).

Zuur, A., Saveliev, A., and Ien, E. (2014b). *A beginner's guide to generalised additive mixed models with r* (Highland Statistics Ltd).

frontiers | Frontiers in Marine Science

TYPE Original Research
PUBLISHED 21 April 2023
DOI 10.3389/fmars.2023.1122143

OPEN ACCESS

EDITED BY
Kostas Kiriakoulakis,
Liverpool John Moores University,
United Kingdom

REVIEWED BY
Yibo Liao,
Ministry of Natural Resources, China
Barbara Górska,
Institute of Oceanology (PAN), Poland
Mikołaj Mazurkiewicz,
Institute of Oceanology (PAN), Poland

*CORRESPONDENCE
Chih-Lin Wei
clwei@ntu.edu.tw

SPECIALTY SECTION
This article was submitted to Deep-Sea Environments and Ecology, a section of the journal Frontiers in Marine Science

RECEIVED 12 December 2022
ACCEPTED 28 March 2023
PUBLISHED 21 April 2023

CITATION
Tung C-C, Chen Y-T, Liao J-X and Wei C-L (2023) Response of the benthic biomass-size structure to a high-energy submarine canyon. *Front. Mar. Sci.* 10:1122143. doi: 10.3389/fmars.2023.1122143

Response of the benthic biomass-size structure to a high-energy submarine canyon

Chueh-Chen Tung[1], Yen-Ting Chen[1], Jian-Xiang Liao[1,2] and Chih-Lin Wei[1]*

[1]Institute of Oceanography, National Taiwan University, Taipei, Taiwan, [2]Taiwan Power Research Institute, Taiwan Power Company, Taipei, Taiwan

Introduction: Body size regulates all biological processes, including growth, reproduction, metabolism, trophic interactions, etc., and is the master trait across organisms, populations, and communities. Despite a rich literature on the impacts of human and natural disturbances on body size, a clear knowledge gap is the effect of the submarine canyons on the benthic size structures in the deep sea, hindering our understanding of the ecological processes of these dominant ecosystems on the continental margin.

Methods: Therefore, we conducted repeated sediment sampling to compare meiofauna and macrofauna biomass body-size spectrum, growth, metabolism, and size composition from a high-energy submarine canyon, Gaoping Submarine Canyon (GPSC), and the adjacent continental slope off SW Taiwan. The GPSC is a dynamic ecosystem connected to a high sediment-yield small mountain river subjected to strong internal-tide energy, swift bottom currents, frequent mass wasting events, and high terrestrial sediment inputs.

Results: We found that the meiofauna and macrofauna were characterized by relatively larger individuals dominating on the slope to smaller ones dominating in the canyon. As a result, the community biomass, secondary production, and respiration were depressed with distinctive biomass-size composition in the canyon compared to the non-canyon slope. The environmental factors related to internal tide disturbance (i.e., bottom current velocity, duration of sediment erosion, or low light transmission) substantially influence the body size composition of the canyon benthos, while food supplies (i.e., TOC and C/N ratio) and sediment characters (i.e., grain size and porosity) correlated closely with the slope communities.

Discussion: We concluded that the disturbed condition in the GPSC may have wiped out or depressed the local benthic assemblages, and only the smaller, more resilient species could persist. Our results also highlight that the alterations of the canyon benthic community could be a reference to deep-sea ecosystems under anthropogenic disturbances or global climate change.

KEYWORDS

meiobenthos, macrobenthos, submarine canyon, continental slope, biomass, biomass-size spectrum, secondary production, respiration

1 Introduction

Body size is a master trait affecting all biological processes and interactions among community groups (Elton, 1927; Kleiber, 1932), which is widely used to describe animal population, including growth, reproduction, and mortality (Pepin, 1991; Sukhotin et al., 2002; Moyano et al., 2017). Body size is also a key component of the metabolic theory of ecology (Peters, 1983; Brown et al., 2004) and directly influence metabolic rates, energy demands, and consumption rates of overall populations and communities (Klumpp, 1984; Vranken and Heip, 1986; Sommer et al., 1999). Therefore, animal density, respiration, and productivity in an ecosystem can be expressed through the allometric scaling of individual body size across taxa (Dickie et al., 1987; Boudreau and Dickie, 1989). Furthermore, body size affects energy and matter fluxes in marine sedimentary environments, especially for species that develop biogenic habitats (Norkko et al., 2013). While small individuals may dominate specific ecosystem functions due to their high abundance and rapid turnover, large-size individuals can modify habitats through bioturbations and bioirrigations, altering nutrient and organic matter cycling at the sediment-water interface (Aller, 1978; Volkenborn et al., 2012; Wrede et al., 2019).

In size-based ecosystem modeling, the biomass-size spectrum is the most widely used method to express the size structure of a community (Blanchard et al., 2017). The biomass-size spectrum refers to the distribution of living biomass across the organism size range of a community, estimating biomass in size categories that increase logarithmically and first applied to the planktonic community in the 1960s (Parsons, 1969; Sheldon et al., 1972; Platt, 1985). Usually, a linear relationship emerges when abundance and body mass are plotted on logarithmic scales. This suggests that the abundance is a power law function of body size, with many more small planktonic organisms than large ones. The dome patterns on the biomass size spectrum reveal how individual size governs feeding interactions and biological rates (Rossberg et al., 2019). The changes in body mass or abundance indicate trophic relationships. Changes in abundance and size can alter the slope of the spectrum, which in turn affects trophic interactions and carbon and nutrient cycling in the ecosystem (Petchey and Belgrano, 2010; Blanchard et al., 2017). Other than predator-prey interactions, anthropogenic activities can also affect the size structure. The exploited ecosystem usually has a steeper size-spectrum slope because fishery selectively targets large fish with a slow recovery rate and allows small fish to escape, resulting in a high abundance of small fish relative to large ones in the ecosystem (Shin et al., 2005). Other human-caused disturbances, such as habitat destruction, invasive species, and pollution, may have similar effects by steepening the slope of the biomass-size spectrum in the impacted ecosystems (Petchey and Belgrano, 2010).

The biomass-size spectrum has also been applied in the freshwater and benthic communities (Schwinghamer, 1981; Sprules et al., 1983; Sprules and Bowerman, 1988; Gaedke, 1992), suggesting that the physical environment may affect the communities by creating habitats for organisms of different size classes (Schwinghamer, 1981). The community with specific body size spectrums may carve a distinct niche by influencing the biological processes, including metabolism, respiration, movement, development, trophic interaction, and carbon flux (Sprules et al., 1991; Duplisea and Kerr, 1995; Blanchard et al., 2017). Thus, deviations in the size spectrum may be used to identify environmental impacts. Efforts have been devoted to detect responses of the benthic size spectrum to environmental conditions, such as the oxygen minimum zone (Quiroga et al., 2005), coastal hypoxia (Qu et al., 2015), seasonal input of organic matters (Soltwedel et al., 1996), and declining food supply with depth (Górska et al., 2020). However, some studies have found that the shapes of the size spectrum are not strongly affected by latitudinal temperature (Mazurkiewicz et al., 2020) and water depth variations (Schewe and Soltwedel, 1999).

In soft-sediment ecosystems, the responses to environmental disturbances vary with body sizes (i.e., macrofauna and meiofauna) and life history traits. Larger organisms have higher energetic requirements, slower growth, and lower reproductive output (Brey, 1999) making them more vulnerable to environmental disturbances (Giere, 2009). In addition, macrobenthos is considered more sensitive to physical disturbances (Austen and Widdicombe, 2006) and extinction risks (Solan et al., 2004). For example, in the Bilbao Estuary, Spain, the meiofauna biomass dominated over macrofauna along a pollution gradient (Saiz-Salinas and González-Oreja, 2000). Following the Deepwater Horizon (DWH) oil spill in the Gulf of Mexico, the macrofauna abundance was lowest within 3 km from the blowout site and then increased to the natural background conditions. In contrast, meiofauna abundance and the ratio of the nematode to copepod increased from the strong (< 3 km from the blowout site) to the moderate (17 km towards the southwest and 8.5 km towards the northeast from the blowout site) impacted area (Montagna et al., 2013). In the Arctic, glacial disturbances were reported to shift benthic biomass and production from macrofauna to meiofauna (Górska and Włodarska-Kowalczuk, 2017). Under climate change, organic carbon export and benthic biomass are projected to decline, and biomass loss is expected to be more rapid for macrofauna than for meiofauna (Jones et al., 2014). Despite significant efforts in studying biomass size spectra, to our knowledge, no study has yet to examine the effect of dominant geomorphological features, such as submarine canyons, on benthic-size structures in the deep sea, hindering the understanding of biological processes in the canyon ecosystem.

The seafloor consists of diverse habitats, and the submarine canyon is among the most prominent geological features on the continental margin. The variations in the origin, evolution, morphology, sediment transports and hydrodynamic regimes of canyons contribute to the heterogeneous distribution of benthic communities (Levin and Sibuet, 2012). Due to the organic accumulation in these topographic lows, the submarine canyons are usually hotspots of abundance and diversity (Vetter and Dayton, 1998; Vetter and Dayton, 1999; De Leo et al., 2010; Wei et al., 2012). However, in the southwest Taiwan continental margin, the Gaoping Submarine Canyon (GPSC) is connected to a small mountainous river (Chiang et al., 2020; Chiang and Yu, 2022). The extremely high sediment load, frequent turbidity currents, and strong internal tides within the river-fed GPSC result in a highly disturbed seabed

environment (Chiou et al., 2011; Lin et al., 2013; Liu et al., 2016), suppressing the abundance and diversity of the benthos (Liao et al., 2017; Liao et al., 2020). This study's principal objective was to use a size-based approach to examine community responses under intense disturbances in the submarine canyon. We used the high-energy GPSC as a test bed to compare with the adjacent continental slope at a similar depth. We predict that the biomass and body size of both meiofauna and macrofauna would decrease more rapidly in the disturbed canyons (Austen and Widdicombe, 2006). The changes in benthic size structure are expected to affect ecosystem functioning, including growth, respiration, and size composition, and ultimately the transfer of materials and energy in the food chain and sediment-water interface.

2 Materials and methods

2.1 Study area

GPSC is a major conduit of marine-terrestrial materials between the active Taiwan margin and the deep South China Sea. The deeply-incised canyon head cut into the continental shelf with a clear bathymetric connection to a small mountain river, the Gaoping River, with extremely high sediment loads (Chiang et al., 2020; Chiang and Yu, 2022). Therefore, the entire length of the GPSC is characterized by its meandering, V-shaped, and entrenched thalweg with deep-cutting outer bends (Figure 1). These erosive features are believed to be maintained by turbidity currents triggered by river flooding (Lin et al., 2013; Lin et al., 2016), internal tides (Wang et al., 2008; Lee et al., 2009; Chiou et al., 2011), groundwater discharges (Su et al., 2012), and sediment slumping (Hsu et al., 2008; Su et al., 2012; Gavey et al., 2017). The energy of internal tides is estimated to be 3–7 times greater than that in the well-known Monterey Canyon of similar shape and size (Lee et al., 2009), with a bottom current velocity ranging between 1.4-1.7 m/s and increasing toward the canyon head (Wang et al., 2008). The isothermal displacement by the internal tides can be over 200 meters (Liu et al., 2016), resulting in the benthic nepheloid layer as thick as 100 m with the suspended sediment concentration reaching 30 mg/l (Liu et al., 2010; Liao et al., 2017). The turbulence mixing by internal tides, high suspended-sediment concentrations near the seabed, and frequent turbidity currents suggest that the GPSC is a high-energy and disturbed ecosystem (Liu et al., 2016).

2.2 Sampling design

Four stations in the upper Gaoping Submarine Canyon (GC1 to GC4) and four stations on the adjacent slope (GS1 to GS4) were repeatedly sampled onboard R/V Ocean Researcher 1 (Figure 1; Table 1). The canyon and slope pairs were sampled by depth strata

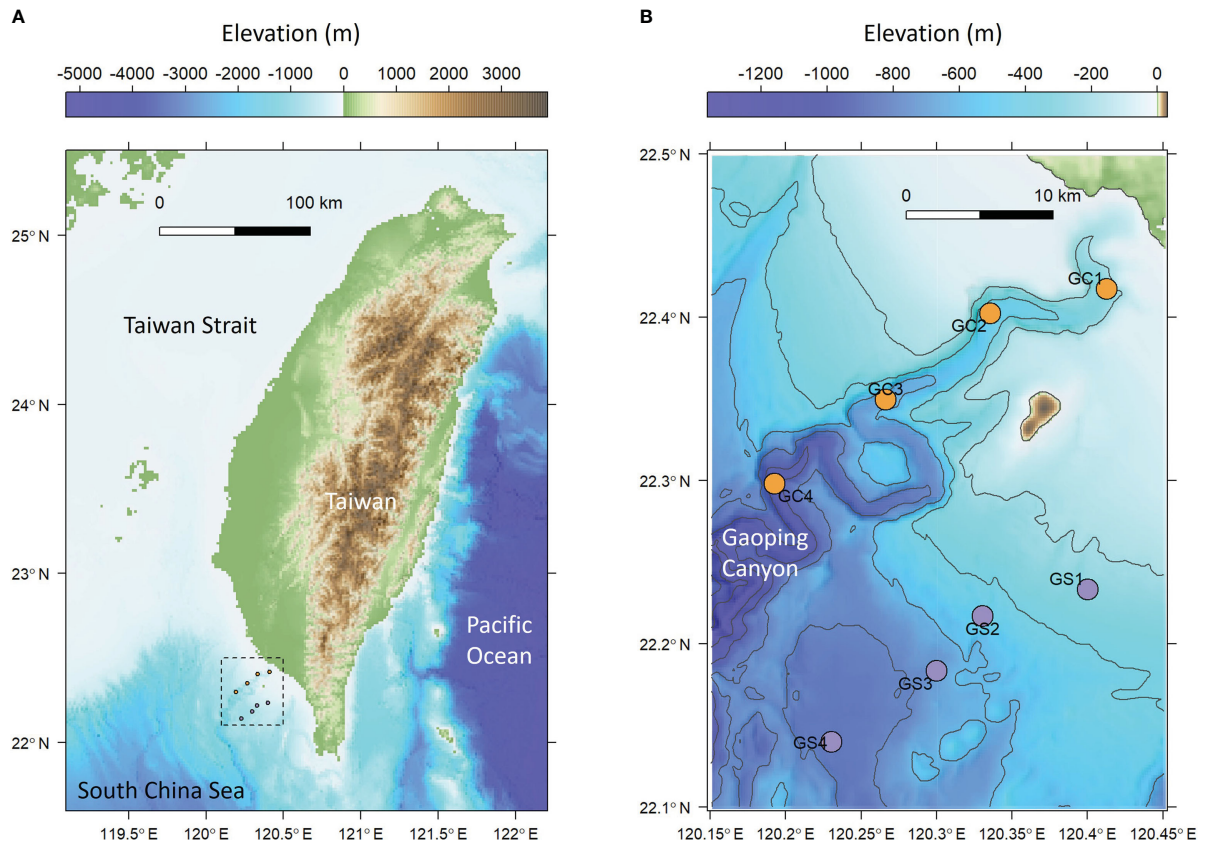

FIGURE 1
Sampling map of meiobenthos and macrobenthos. **(A)** The sampling area off the continental margin of SW Taiwan. **(B)** Sampling transects along the upper Gaoping Submarine Canyon (GC) and Gaoping Slope (GS).

10.3389/fmars.2023.1122143

TABLE 1 Sampling times and locations for boxcorer, multicorer, and CTD.

Habitat	Cruise	Station	Longitude	Latitude	Depth	Date
Canyon	1096	GC1	120.4170	22.4170	222	2014-11-28
		GC2	120.3418	22.4078	462	2014-11-26
		GC3	120.2664	22.3500	655	2014-11-27
	1102	GC1	120.4114	22.4173	323	2015-04-06
		GC2	120.3327	22.4004	482	2015-04-06
		GC3	120.2665	22.3483	653	2015-04-06
		GC4	120.1921	22.2981	1065	2015-04-06
	1114	GC1	120.4114	22.4172	320	2015-08-04
		GC2	120.3348	22.4007	478	2015-08-04
		GC3	120.2665	22.3501	655	2015-08-04
		GC4	120.1928	22.2980	1051	2015-08-05
	1126	GC1	120.4112	22.4175	318	2015-11-21
		GC2	120.3335	22.4003	487	2015-11-21
		GC3	120.2663	22.3492	655	2015-11-20
		GC4	120.1929	22.2982	1068	2015-11-20
Slope	1096	GS1	120.4006	22.2349	270	2014-11-27
		GS2	120.3332	22.2166	465	2014-11-28
		GS3	120.2997	22.1837	692	2014-11-28
	1102	GS1	120.4006	22.2329	279	2015-04-07
		GS2	120.3298	22.2168	464	2015-04-07
		GS3	120.3001	22.1831	682	2015-04-07
		GS4	120.2311	22.1392	840	2015-04-07
	1114	GS1	120.3998	22.2322	279	2015-08-05
		GS2	120.3297	22.2172	462	2015-08-05
		GS3	120.2998	22.1833	690	2015-08-05
		GS4	120.2304	22.1401	848	2015-08-05
	1126	GS1	120.3995	22.2329	277	2015-11-19
		GS2	120.3298	22.2167	463	2015-11-19
		GS3	120.3002	22.1829	690	2015-11-19
		GS4	120.2293	22.1400	848	2015-11-20

(200–400 m, 400–600 m, 600–800 m, and 800–1,100 m). The same stations were visited in November 2014 (OR1-1096), April 2015 (OR1-1102), August 2015 (OR1-1114), and November 2015 (OR1-1126). However, the OR1-1096 only sampled the first three depth strata (200–400 m, 400–600 m, and 600–800 m). We conducted a CTD cast and a boxcorer (November 2014 and April 2015) or multicorer (August 2015 and November 2015) at each station. For the boxcorer, five transparent polycarbonate tubes (i.d. = 67 mm) were inserted into the sample onboard to recover surface sediments. For the multicorer, twelve polycarbonate tubes (i.d. = 105 mm) can be retrieved from a single drop.

2.3 Biological sampling

During Aug 2015 and Nov 2015 cruises, one multicore tube (i.d. = 105 mm) per station was selected for meiofaunal analysis. We used a cut-off syringe (i.d., 28 mm; area 616 mm^2) to take three subsamples (top 5 cm of the sediment) from the recovered core tube; however, only one subsample was retrieved from the deepest canyon station (GC4) during Nov 2015 cruise. Altogether, 46 meiofauna subsamples were retrieved during the two cruises. On average, we selected three tubes from boxcorer (Nov 2014 and Apr 2015 cruises) or multicorer (Aug 2015 and Nov 2015 cruises) for macrofaunal analysis per station. The

top 15 cm of the sediments was extruded and washed with filter seawater (with a 5-μm filter) through a 300-μm sieve. In total, 100 macrofauna samples were retrieved during the four cruises. The sediment samples for meiofauna and macrofauna (after sieving) were fixed in the 5% formalin solution with Rose Bengal for at least one week. Boxcorer is known to create bow waves (Narayanaswamy et al., 2016), possibly resulting in sediment disturbance, loss of associated fauna (Bett et al., 1994), and underestimating macrofauna abundance (Montagna et al., 2017). Nevertheless, our macrofauna densities were comparable between the samples collected by boxcorer and multicorer (see Table A1 in Liao et al., 2017), suggesting that the gear effects are insignificant.

2.4 Body size measurements

The fixed meiofauna samples were washed with tap water through a 1000-μm sieve on top of a 40-μm sieve. The remaining sediments were immersed in Ludox HS40 solution (gravity = 1.18 g/cm^3), centrifuged at 8,000 rpm for 10 min, and repeated three times to extract meiofauna (Danovaro, 2010). After extraction, the fauna samples were transferred to 70% ethanol before sorting and counting under a stereo microscope (Olympus SZ61). From each meiofauna sample, only 100 nematode individuals (or all individuals if fewer than 100 were present) were randomly picked out and transferred to a solution of 5% glycerol and 5% ethanol in water. The mixture evaporated gradually on a warm hotplate, leaving the nematodes in pure glycerol. The nematodes were mounted onto permanent slides, and the length and width of the nematodes were measured by an ocular micrometer mounted on a compound microscope (Olympus BX53). The length and width of the remaining meiofauna and macrofauna specimens were measured by an ocular micrometer under a stereo microscope. We used ImageJ software to measure the macrofauna polychaete length and width from a photo by a camera mounted on a stereo microscope. Both the precisions of the ocular micrometer and image analysis are 1 μm.

The biovolumes of meiofauna and macrofauna specimens were calculated with the formula: $V = L \times W^2 \times C$, where V is the volume, L is the length, W is the width, and C is the taxon-specific conversion factors (Rachor, 1975; Warwick and Gee, 1984; Feller and Warwick, 1988). For the taxa whose conversion factors are unavailable, the biovolumes were calculated from length and width using the nearest geometric shapes (e.g., scaphopods - cone; aplacophorans - cylinder; sipunculans - cylinder; ophiuroids - ellipsoid or cylinder; asteroids - ellipsoid; nemerteans - cylinder). Finally, the biovolumes of meiofauna and macrofauna were converted into wet weight, assuming a specific gravity of 1.13 (Warwick and Gee, 1984).

2.5 Environmental condition

We measured the temperature (*Temp*), salinity (*Salin*), density (*Dens*), dissolved oxygen concentration (*O2*), fluorescence (*Fluo*), and light transmission (*Trans*) of the bottom water using a conductivity-temperature-depth (CTD) recorder (Sea-Bird SBE 911) and other attached sensors (Table 2). Surface sediment grain sizes (non-carbonate fraction), including percent clay, silt, and sand, were measured by a laser diffraction particle size analyzer (Beckman Coulter LS13 320). Total organic carbon (*TOC*) and total nitrogen (*TN*) were analyzed with a Flash EA 1112 elemental analyzer. TOC/TN calculated the C/N ratio. Porosity (*Por*) was estimated from the sediment's wet and dry weight, assuming a dry sediment density of 2.65 g/cm^3. Hourly bottom current velocity at each site was derived from a 3-D, hydrodynamic internal tide model from Chiou et al. (2011). Based on the internal tide model, we calculated the hourly mean velocity of bottom currents (*Spd*) and the duration for which bottom current speed exceeded 20 cm/s for one month preceding the sampling campaign (*Over20*) to estimate the disturbances of near-bottom currents.

We removed the redundant environmental variables (correlations > 0.9) before analyses. For example, the bottom water temperature, density, and dissolved oxygen measured were highly correlated; therefore, the dissolved oxygen (*O2*) was removed because the bottom water was well-oxygenated (O_2 > 2 mg/L), presumably, due to turbulence mixing by internal tides. The density (*Dens*) was removed because it's not known to affect infauna assemblages. We only retained bottom water temperature (*Temp*), salinity (*Salin*), light transmission (*Trans*), percent sand, silt, and clay, sediment TOC and C/N ratio, porosity (*Por*), and mean bottom current speed (*Spd*) and disturbance duration (*Over20*). These variables were logarithm (base of 10) transformed, centered (subtracted from the mean), and normalized (divided by the standard deviation) before use in statistical analyses involving environmental variables.

2.6 Data analysis

2.6.1 Biomass size spectrum

Because not all nematode specimens were measured for their sizes, the observed size measurements (from 100 random individuals) were randomly resampled (with replacement) to scale to the total nematode abundance. Polychaetes and ophiuroids are easy to break off. Therefore, we randomly resampled the measurements of complete specimens to the total abundance in a sample (e.g., polychaete with head and ophiuroids with disk). The individual sizes of meiofauna or macrofauna collected from the GPSC or adjacent slope (across all cruises and stations) were binned by $\log_2$ transformation of their biomass. The biomass within each size bin was $\log_{10}$ transformed and plotted against the $\log_{10}$ midpoint of the size bin to visualize the biomass size spectrum (BSS). For the normalized biomass size spectrum (NBSS), the total biomass of each size bin was divided by the width of the bin. The normalized biomass within each size bin was also $\log_{10}$-transformed and then plotted against the $\log_{10}$ midpoint of the size bin. The slope of the NBSS was estimated by fitting bounded power law (PLB) distribution to individual size distribution (ISD) using maximum likelihood estimation (MLE). The fitted line (with a 95% confidence interval) was plotted on the ISD, which ranks the body size in decreasing order to visualize the fit between the model and size data. The NBSS slope determined by MLE is equivalent to the regression slope of the NBSS; however, comparison studies by

TABLE 2 Environmental data collected along with the biological sampling.

Habitat	Cruise	Station	Temp	Dens	Salin	O2	Fluo	Trans	Clay	Silt	Sand	TOC	TN	CN	Por	Spd	Over20
			°C	kg m-3		mg L-1	µg L-1	%	%	%	%	%	%			m/s	%
Canyon	1096	GC1	15.5	1026.5	34.5	4.7	0.30	0.0	17.5	75.2	7.3	0.4	0.06	5.5	0.50	0.03	0.00
		GC2	8.5	1028.9	34.4	3.6	0.14	0.4	4.1	30.6	65.3	0.2	0.05	4.6	0.47	0.09	0.42
		GC3	9.0	1029.6	34.4	3.7	0.20	0.0	16.2	72.6	11.2	0.3	0.06	5.6	0.52	0.07	0.28
	1102	GC1	14.5	1027.1	34.5	4.6	0.06	21.6	10.0	45.6	44.4	0.3	0.05	5.5	0.42	0.10	6.53
		GC2	8.6	1028.9	34.4	3.6	0.05	32.6	1.1	6.4	92.4	0.2	0.05	4.6	0.27	0.09	6.53
		GC3	7.8	1029.8	34.4	3.5	0.04	43.3	12.7	53.8	33.5	0.4	0.06	6.2	0.45	0.09	0.83
		GC4	4.3	1032.2	34.5	3.2	0.02	66.8	21.7	76.5	1.8	0.6	0.09	6.1	0.55	0.08	1.25
	1114	GC1	13.2	1027.4	34.5	4.3	0.10	4.4	13.3	61.1	25.6	0.4	0.07	5.9	0.64	0.11	8.47
		GC2	8.6	1028.9	34.4	3.5	0.14	1.0	17.9	64.9	17.2	0.4	0.08	6.0	0.64	0.10	7.22
		GC3	8.0	1029.8	34.4	3.4	0.17	0.0	34.1	65.9	0.0	0.5	0.08	6.7	0.69	0.09	1.81
		GC4	4.0	1032.3	34.5	3.1	0.03	49.1	20.3	76.6	3.1	0.6	0.09	6.7	0.76	0.09	1.39
	1126	GC1	12.4	1027.5	34.5	4.4	0.07	19.2	21.0	77.2	1.8	0.4	0.08	5.8	0.61	0.11	4.17
		GC2	7.4	1029.1	34.4	3.5	0.02	42.5	4.7	54.5	40.8	0.3	0.05	5.5	0.54	0.10	7.50
		GC3	7.5	1029.6	34.4	3.5	0.03	61.2	22.3	76.5	1.2	0.4	0.08	5.4	0.74	0.09	1.39
		GC4	4.0	1032.3	34.5	3.2	0.03	51.2	23.6	75.5	0.9	0.6	0.10	5.7	0.78	0.07	0.14
Slope	1096	GS1	14.8	1026.8	34.6	5.0	0.02	84.5	21.2	75.6	3.2	0.5	0.09	5.5	0.59	0.06	0.00
		GS2	9.8	1028.5	34.4	4.0	0.03	75.3	22.7	75.7	1.6	0.6	0.11	5.6	0.64	0.07	0.00
		GS3	6.4	1030.2	34.4	3.2	0.02	87.3	26.4	73.1	0.5	0.6	0.11	5.5	0.64	0.05	0.00
	1102	GS1	14.2	1026.9	34.5	5.0	0.02	87.9	15.4	77.5	7.1	0.6	0.10	5.8	0.57	0.09	2.08
		GS2	9.5	1028.6	34.4	3.8	0.02	86.7	20.7	77.4	1.9	0.7	0.11	5.9	0.66	0.06	0.00
		GS3	7.2	1030.0	34.4	3.3	0.02	89.2	22.3	75.1	2.6	0.6	0.11	5.7	0.63	0.06	0.00
		GS4	5.9	1030.9	34.4	3.1	0.02	85.8	26.1	72.7	1.2	0.7	0.12	6.3	0.67	0.09	0.42
	1114	GS1	13.7	1027.1	34.5	4.6	0.03	76.9	12.6	78.1	9.3	0.5	0.08	6.2	0.67	0.08	1.81
		GS2	10.2	1028.5	34.4	3.9	0.02	87.3	19.8	77.5	2.7	0.7	0.11	6.2	0.78	0.06	0.14
		GS3	6.9	1030.1	34.4	3.2	0.02	86.5	24.3	74.0	1.7	0.8	0.12	6.2	0.77	0.05	0.00
		GS4	5.9	1031.0	34.4	3.0	0.02	83.6	22.4	75.9	1.7	0.8	0.12	6.7	0.84	0.08	0.00
	1126	GS1	13.9	1027.0	34.5	5.0	0.02	83.6	14.7	77.0	8.3	0.6	0.09	6.1	0.73	0.09	1.94
		GS2	9.0	1028.7	34.4	3.8	0.01	84.8	21.3	76.7	2.0	0.7	0.11	5.9	0.74	0.06	0.28
		GS3	6.4	1030.2	34.4	3.3	0.02	87.1	23.9	75.1	1.0	0.6	0.12	5.5	0.74	0.06	0.00
		GS4	5.5	1031.0	34.5	3.2	0.02	86.6	26.0	73.2	0.8	0.8	0.13	6.3	0.81	0.07	0.00

Edwards et al. (2017) concluded that the MLE method provides a better estimate of the NBSS slope.

2.6.2 Production and respiration

Meiofauna production to biomass ratio (P/B) was estimated using the following equation developed by Schwinghamer et al. (1986): $P/B = 0.073 \times M^{-0.337}$, where M is individual body mass [kcal]. We converted the macrofauna individual body mass (in mg wet weight) into energy content [J] using taxon-specific conversion factors from Brey (1999) (Excel table available from http://www.thomas-brey.de/science/DBconversion/datafiles/Conversion03.zip). We estimated macrofaunal annual production to biomass ratio (P/B) and secondary production (P) from three continuous parameters (temperature, water depth, body mass) and 17 categorical parameters (5 taxa, 7 lifestyles, 4 environments, and state of exploitation) using the Artificial Neural Network model (ANN) developed by Brey (2012) using R package BenthicPro (Andresen and Brey, 2018). The macrofauna-size nematode production to biomass ratio was estimated using the same equation from Schwinghamer et al. (1986). We multiplied the biomass of meiofauna and macrofauna with the annual P/B ratio to estimate secondary production.

Mass-specific respiration rates of meiofauna and macrofauna were estimated from body mass and temperature using an empirical

model, $\log_{10}(R/M) = 8.3732 - 0.2073 \times \log_{10}(M) - 2766.0235/T$, based on an extensive database compilated for aquatic invertebrate respiration (< 22000 measurements, > 900 species, > 440 references) by Thomas Brey (available from http://www.thomas-brey.de/science/virtualhandbook/respir/rempirics1.html). In the equation, R/M is the mass-specific respiration (J/J/day), M is individual body mass (J), and T is water temperature (K).

The annual secondary production and daily respiration rate were converted to units in wet weight, joule (J), and organic carbon weight using taxon-specific conversion from Brey (1999) (Tables S1, S2).

2.6.3 Size composition

The individual sizes of meiofauna and macrofauna were binned by the $\log_2$ transformation of their biomass. The total biomass of each size bin and each sample was then calculated as size composition for further multivariate analysis. The biomass in each $\log_2$ size bin and sample (i.e., core tube) was square-root transformed and converted to Bray-Curtis dissimilarity between samples. The same matrix was then subjected to Non-metric Multi-dimensional Scaling (nMDS). The mid-point of the $\log_2$ size bins was projected onto the nMDS plot by the biomass-weighted averages of the ordination scores within each size bin. Distance-based Redundancy Analysis (dbRDA) was used to model the size composition using environmental variables and select the subset of environmental variables which best explained (with the smallest AIC) the size composition. The selected variables were projected as vectors onto the same nMDS ordination, with the length of vectors indicating their correlations with the nMDS ordination scores and the direction of vectors indicating the direction of increasing environmental values.

2.6.4 Statistical test

We used Generalized Least Squares (GLS) modeling to examine the effects of habitat (canyon vs. slope), depth, and sampling time on the mean meiofauna and macrofauna biomass, production, P/B ratio, and respiration (by station). Also, three-way-cross permutation analysis of variance (PERMANOVA) was used to examine the effects of habitat, depth, and sampling time on the average meiofauna and macrofauna size composition. The number of permutations was set to 999. All statistical tests used α-value = 0.05, and pairwise tests used α-value = 0.05/numbers of trials (i.e., Bonferroni correction). All data analyses were conducted using software R version 4.2.1 (R Core Team, 2022). Normalized biomass size spectrum (NBSS), individual size distribution (ISD), and slope of NBSS were computed using R package *sizeSpectra* (Edwards et al., 2017). Multivariate analyses (i.e., nMDS, dbRDA, and PERMANOVA) used the R package *vegan*. Generalized Least Squares (GLS) modeling used the R package *nlme*. All relevant analyses can be reproduced from the R codes and data deposited in an R data package *bsss*, available at https://github.com/chihlinwei/bbbs.

3 Results

3.1 Environmental variations

Liao et al. (2017; Liao et al. 2020) analyzed the environmental data used in this study (Figure S1). Generally, they found that the modeled bottom current velocity (*Spd*) and duration of sediment erosion (*Over20*) increased in the canyon and toward the canyon head. The near-bottom light transmission and sediment *TOC* were lower in the canyon, and both were the lowest at the canyon head due to strong hydrodynamic energy. Furthermore, the bottom water temperature (*Temp*) and dissolved oxygen concentration (*O2*) declined with depth, but the surface *TOC* increased with depth along the canyon and slope transects.

3.2 Size structure

The individual size of meiofauna spanned from ca. 10^{-6} mg to over 1 mg wet weight (Figure 2A). Whereas the macrofauna size ranged from ca. 10^{-4} mg to over 100 mg wet weight. The largest meiofauna (> 0.1 mg) or macrofauna individuals (> 10 mg) occurred on the slope. The canyon meiofauna biomass peaks at mid-size bins (10^{-4} to 10^{-3} mg, Figure 2A), and the slope meiofauna appears to peak at size bins between 10^{-3} and 10^{-1} mg before the biomass dropped slightly and went back up again. Similarly, the biomass of the canyon macrofauna peaked at size bins between 10^{-2} and 10^{-1} mg before the biomass dropped slightly and then went back up again with increasing size bins. For both the meiofauna and macrofauna, the larger size bins contributed the most to the biomass difference between the canyon (orange symbols) and slope communities (purple symbols), and the canyon biomass was consistently lower than the slope biomass (Figure 2A).

The meiofauna and macrofauna NBSS are "dome" shapes, indicating low relative abundance for the smallest and the largest sizes (Figure 2B). When comparing the NBSS of meiofauna between the canyon and slope, a considerable amount of large-size individuals was lost in the canyon. For macrofauna, the relative abundance of the largest and smallest size classes decreased due to the "canyon" effect; however, more individuals were removed from the largest size bins than from the smallest size bins.

For the meiofauna size > 0.001 mg and macrofauna > 0.01 mg, the $\log_{10}$ normalized biomass declined linearly with the $\log_{10}$ mid-point of size bins. The decline of $\log_{10}$ normalized biomass with $\log_{10}$ mid-point of size bins (i.e., NBSS slope, Figure 2C) was more rapid for the canyon (i.e., regression slope = -2.51 and -2.07 for meiofauna and macrofauna, respectively) than for the slope assemblages (i.e., regression slope = -1.99 and -1.56 for meiofauna and macrofauna, respectively), indicating the relative abundance of largest size classes declined as we moved from the slope into the canyon. However, the NBSS slope of the canyon macrofauna was similar to that of the slope meiofauna. The NBSS slopes were

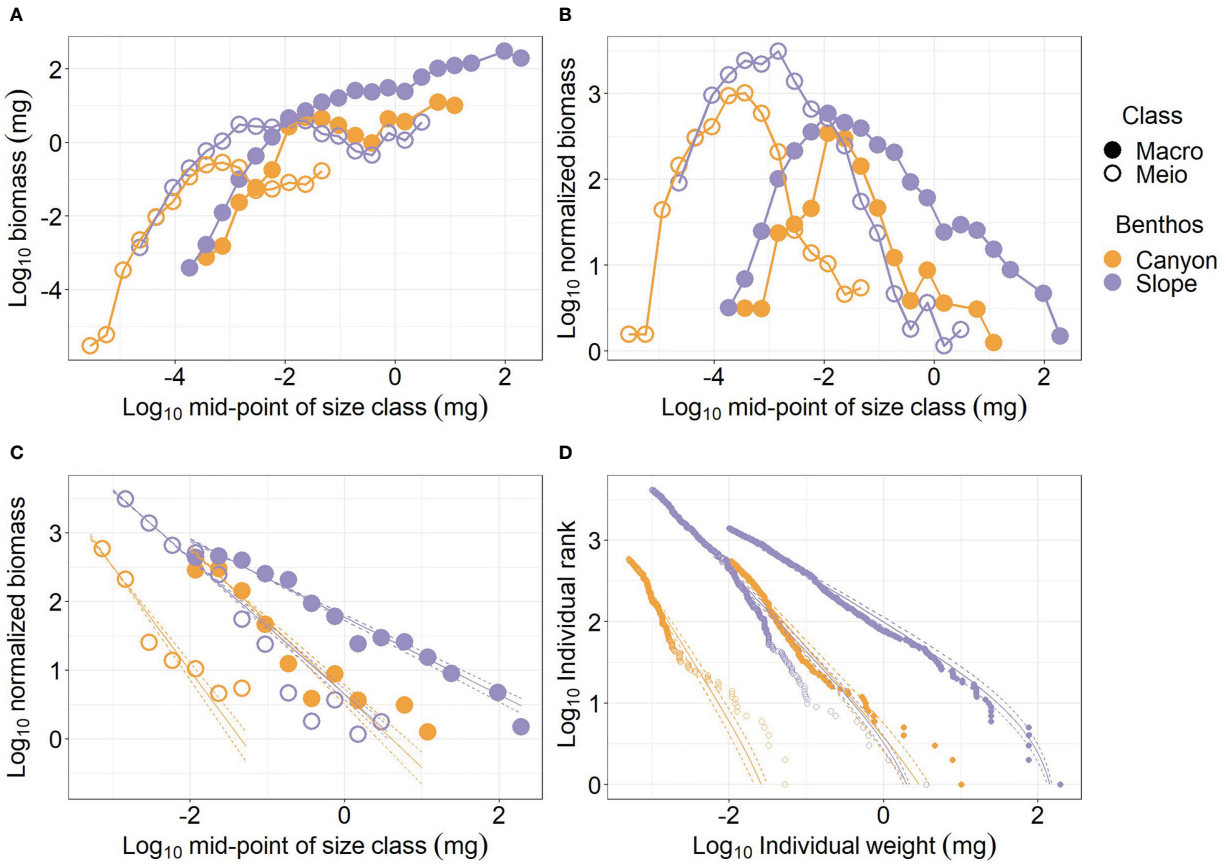

FIGURE 2
Size spectra of meiobenthos and macrobenthos. **(A)** biomass size spectrum (BSS); **(B)** normalized biomass size spectrum (NBSS); **(C)** NBSS excluding small size classes (i.e., meiofauna < 0.001 mg; macrofauna< 0.01 mg) **(D)** Individual sizes distribution (ISD) for panel **(C)**.

estimated from Individual sizes distribution (ISD). Figure 2D shows that the ISDs of the larger meiofauna and macrofauna fitted nicely to bounded power law distributions (PLB). When the size spectra of meiobenthos and macrobenthos are estimated by habitats and cruises (Figure S2), the general patterns are still similar to Figure 2. The NBSS slopes were steeper for larger meiofauna and macrofauna in the canyon. However, the ISDs by habitats and cruises (Figure S2D) did not fit bounded power law distributions (PLB) as well as the ISDs by habitats (Figure 2D).

The meiofauna body size measurements for each subcore (i.d. = 28 mm) were randomly resampled (with replacement) to scale to the coring area of a single multicore tube (i.d. = 105 mm) to examine the effect of different core sizes. Based on the simulated data, a multi-panel figure similar to Figure 2 was presented as Figure S3. Except for a much greater difference in NBSS elevations between the meiofauna and macrofauna, the general patterns (i.e., described in the above paragraph) are similar between the original (Figure 2) and the scaled biomass-size spectra (Figure S3). When the resampled meiofauna merged with the macrofauna size measurements (Figure S4), similar patterns, such as greater biomass on the slope (Figure S4A), "dome" shape NBSS peak ~ 10^{-3} mg (Figure S4B), and steeper NBSS slope in the canyon (Figure S4C), were observed between the merged and separated size spectra (Figure 2).

3.3 Biomass (wet weight)

Average meiofauna biomass on the slope (1,954.5 mg m^{-2}) was more than ten-folds and thus significantly higher than that in the canyon (92.1 mg m^{-2}, Table S1; Figure 3A) (Habitat, $P < 0.001$, Table 3). Despite that macrofaunal biomass appears to increase with depth in the canyon (albeit marginally, $P = 0.06$, Figure 3B), the average biomass on the slope was still nearly ten-fold (3,075 mg m^{-2}, Table S2) and significantly higher than that in the canyon (Habitat, $P < 0.001$, 328 mg m^{-2}, Table 4). On average, the macrofauna contributed 78.1% of the biomass in the canyon but 61.1% of biomass on the slope. Pairwise tests across four depth strata revealed significant habitat effects at depths from 200 to 400 m and from 400 to 600 m ($P < 0.01$) but not at depths from 600 to 800 m and 800 to 1100 m ($P > 0.1$). This discrepancy may have contributed to the significant interaction between habitat and depth in the main test (Habitat: Depth, $P = 0.024$, Table 4).

3.4 Production

The average P/B ratio of meiofauna in the canyon (ca. 9.5 yr^{-1}) was almost two times higher than that on the slope (ca. 4.5 yr^{-1}, Figure 4A; Table S1) (Habitat, $P = 0.04$, Table 3). The macrofaunal

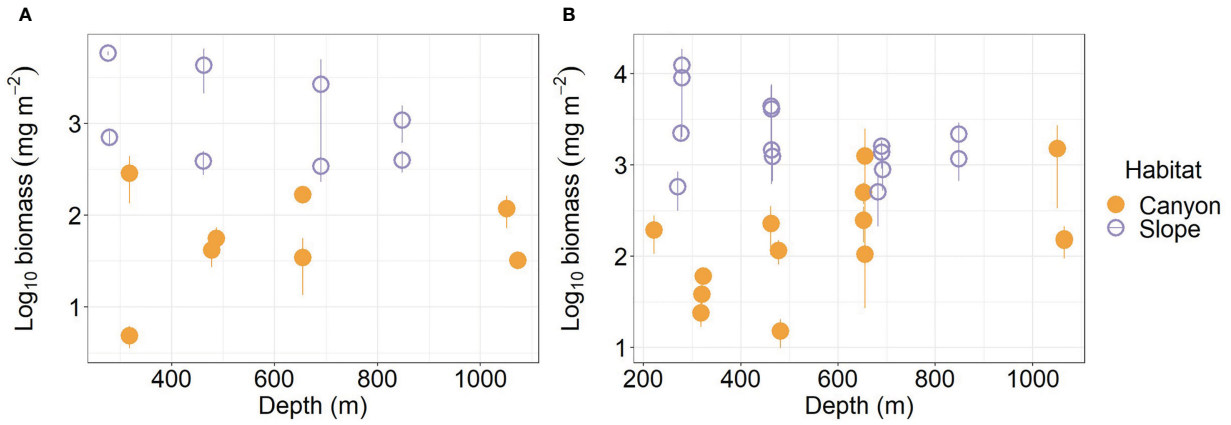

FIGURE 3
Biomass of meiobenthos **(A)** and macrobenthos **(B)** as functions of depth. Error bar shows standard deviation.

TABLE 3 ANOVA table of generalized least square (GLS) modeling on biomass, P/B ratio, production, mess-specific respiration, and respiration of meiofauna, as well as PERMANOVA table on size composition of meiofauna.

	DF	F-value	p-value		DF	F-value	p-value
Biomass				Mass-specific respiration			
(Intercept)	1	363.02	**0.000**	(Intercept)	1	148.09	**0.000**
Habitat	1	27.76	**0.001**	Habitat	1	6.67	**0.030**
Depth	1	0.08	0.780	Depth	1	10.45	**0.010**
Cruise	1	1.25	0.275	Cruise	1	0.19	0.672
Habitat : Depth	1	1.11	0.334	Habitat : Depth	1	0.64	0.445
Habitat : Cruise	1	3.09	0.107	Habitat : Cruise	1	0.64	0.446
Depth : Cruise	1	0.46	0.537	Depth : Cruise	1	0.34	0.573
P/B ratio				Respiration			
(Intercept)	1	119.19	**0.000**	(Intercept)	1	209.27	**0.000**
Habitat	1	15.14	**0.004**	Habitat	1	50.81	**0.000**
Depth	1	0.24	0.639	Depth	1	6.25	**0.034**
Cruise	1	0.90	0.368	Cruise	1	9.60	**0.013**
Habitat : Depth	1	0.95	0.354	Habitat : Depth	1	3.72	0.086
Habitat : Cruise	1	0.99	0.347	Habitat : Cruise	1	6.17	**0.035**
Depth : Cruise	1	1.17	0.307	Depth : Cruise	1	1.19	0.304
Production				Size composition			
(Intercept)	1	4532.57	**0.000**				
Habitat	1	57.70	**0.000**	Habitat	1	3.91	**0.001**
Depth	1	0.86	0.379	Depth	1	1.81	0.073
Cruise	1	14.86	**0.004**	Cruise	1	0.66	0.766
Habitat : Depth	1	3.94	0.078	Habitat : Depth	1	1.31	0.248
Habitat : Cruise	1	15.16	**0.004**	Habitat : Cruise	1	0.81	0.580
Depth : Cruise	1	2.26	0.167	Depth : Cruise	1	1.61	0.125

Bold fonts indicate $P < 0.05$.

TABLE 4 ANOVA table of generalized least square (GLS) modeling on biomass, P/B ratio, production, mess-specific respiration, and respiration of macrofauna, as well as PERMANOVA table on size composition of macrofauna.

	DF	F-value	p-value		DF	F-value	p-value
Biomass				Mass-specific respiration			
(Intercept)	1	919.95	**0.000**	(Intercept)	1	1603.65	**0.000**
Habitat	1	38.79	**0.000**	Habitat	1	0.03	0.866
Depth	1	0.95	0.346	Depth	1	109.33	**0.000**
Cruise	3	0.51	0.682	Cruise	3	1.22	0.337
Habitat : Depth	1	6.29	**0.024**	Habitat : Depth	1	3.90	0.067
Habitat : Cruise	3	1.29	0.315	Habitat : Cruise	3	0.35	0.793
Depth : Cruise	3	0.49	0.691	Depth : Cruise	3	0.09	0.962
P/B ratio				Respiration			
(Intercept)	1	2955.34	**0.000**	(Intercept)	1	123.17	**0.000**
Habitat	1	21.62	**0.000**	Habitat	1	14.81	**0.002**
Depth	1	97.97	**0.000**	Depth	1	5.98	**0.027**
Cruise	3	0.51	0.680	Cruise	3	0.95	0.444
Habitat : Depth	1	2.82	0.114	Habitat : Depth	1	8.33	**0.011**
Habitat : Cruise	3	0.79	0.516	Habitat : Cruise	3	2.39	0.110
Depth : Cruise	3	0.94	0.446	Depth : Cruise	3	1.18	0.352
Production				Size composition			
(Intercept)	1	1878.58	**0.000**				
Habitat	1	15.68	**0.001**	Habitat	1	4.06	**0.003**
Depth	1	3.26	0.091	Depth	1	1.95	0.064
Cruise	3	0.72	0.555	Cruise	3	1.55	0.087
Habitat : Depth	1	6.86	**0.019**	Habitat : Depth	1	0.78	0.635
Habitat : Cruise	3	2.04	0.151	Habitat : Cruise	3	0.87	0.644
Depth : Cruise	3	1.16	0.359	Depth : Cruise	3	1.53	0.076

Bold fonts indicate $P < 0.05$.

P/B ratio declined with depth in both habitats ($P < 0.01$, Figure 4B), but the P/B ratio of the slope assemblage was significantly higher than the canyon assemblage ($P < 0.001$, Table 4).

The average production of meiofauna was 28.4 mg C m^{-2} yr^{-1} in the canyon and 97.8 mg C m^{-2} yr^{-1} on the slope (Table S1). The average macrofauna production was 25 mg C m^{-2} yr^{-1} in the canyon and 72 mg C m^{-2} yr^{-1} on the slope (Table S2). The macrofauna, on average, contributed 47.1% of production in the canyon and 42.5% on the slope. As a result, the meiofaunal and macrofaunal productions were significantly higher on the slope than in the canyon (Production, $P < 0.01$, Tables 3, 4). The secondary production of both meiofauna and macrofauna declined with depth on the slope ($P < 0.05$) but not in the canyon (Figures 4C, D). Nevertheless, significant cruise effect and interaction between habitat and cruise were evident for meiofauna ($P = 0.04$, Table 3). Pairwise tests for meiofauna suggested that the cruise effect was only significant in the canyon (pairwise GLS, $P = 0.013$), and the habitat effect was only significant during Nov 2015 cruise (pairwise GLS, $P = 0.01$). Similarly, macrofauna showed a significant interaction between habitat and depth (Table 4). Pairwise tests suggested that the habitat effect was only marginally significant at depths from 200 to 400 m for macrofauna (pairwise GLS, $P = 0.02$, α-value = 0.05/4).

3.5 Respiration

Mass-specific respiration rate (R/M) for meiofauna declined significantly with depth in the canyon ($P < 0.001$), but the decline was only marginally significant with depth on the slope ($P = 0.05$, Figure 5A). In contrast, the R/M ratio for macrofauna declined significantly with depth in both canyon and slope ($P < 0.001$, Figure 5B). The R/M ratio of canyon meiofauna was significantly higher than that of the slope assemblages (Habitat, $P = 0.03$, Table 3); however, no statistical evidence suggests that the macrofaunal R/M ratio was different between the canyon and slope (Habitat, $P = 0.86$, Table 4).

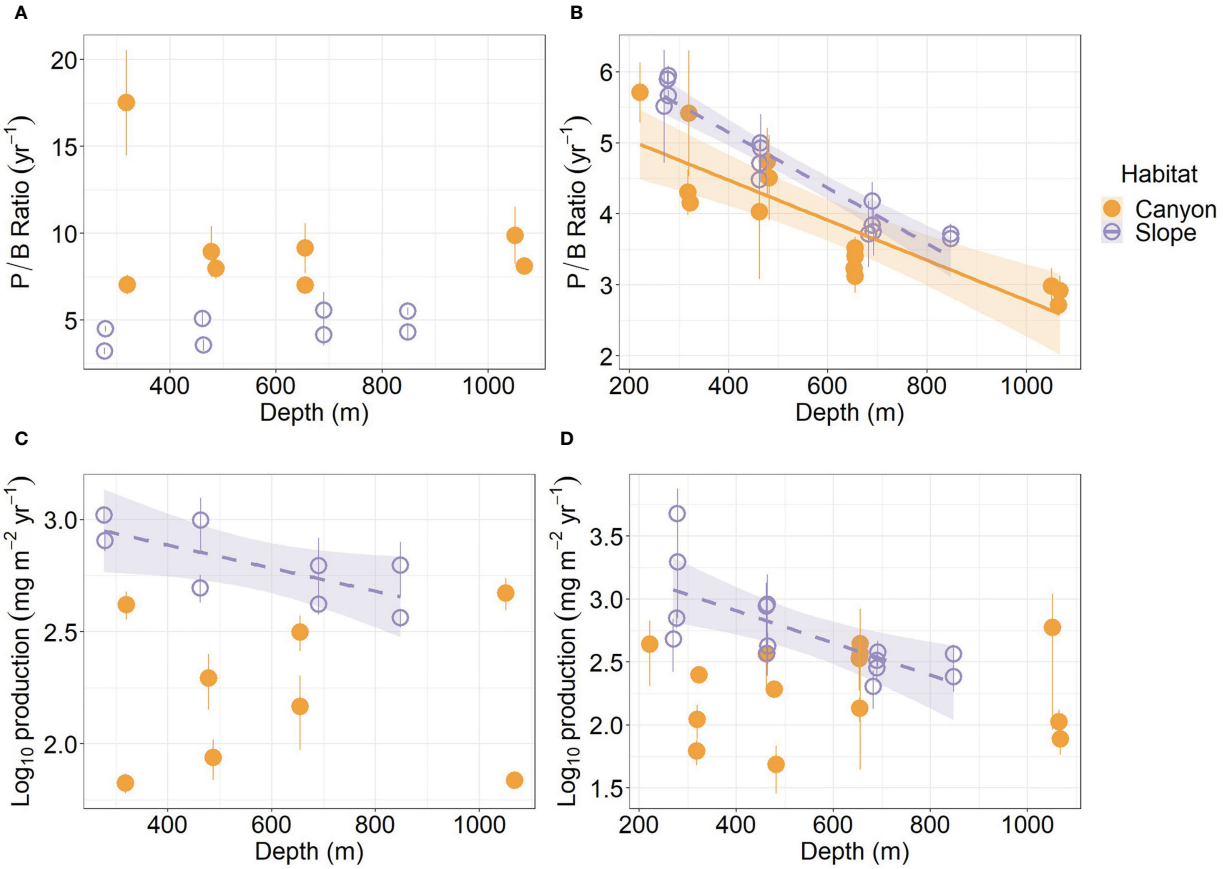

FIGURE 4
Annual P/B ratio and secondary production of meiobenthos **(A–C)** and macrobenthos **(B–D)** as functions of depth. Trend lines show significant relationships with depth based on simple linear regressions (P < 0.05), and shaded areas show 95% confidence intervals. Error bar indicates standard deviation.

The average respiration of meiofauna was 175.8 mg C m^{-2} yr^{-1} in the canyon and 841.7 mg C m^{-2} yr^{-1} on the slope (Table S1). In contrast, the average respiration of macrofauna was 113.8 mg C m^{-2} yr^{-1} in the canyon and 355.3 mg C m^{-2} yr^{-1} on the slope (Table S2). The macrofauna, on average, contributed 39.3% of respiration in the canyon and 29.7% of respiration on the slope. Meiofaunal and macrofaunal respiration declined significantly with depth on the slope (P < 0.02, Figures 5C, D). ANOVA (on GLS) suggests that the meiofaunal and macrofaunal respirations on the slope were significantly higher than that in the canyon (Habitat, P < 0.01, Tables 3, 4); however, there were also interactions between habitat and cruise for meiofauna (Habitat: Cruise, P = 0.04, Table 3) and habitat and depth for macrofauna (Habitat: Depth, P = 0.011, Table 4). For meiofauna, pairwise tests suggest that the habitat effect was only marginal during the August 2015 cruise (P = 0.03, α-value = 0.05/2) but was significant during the November 2015 cruise (P < 0.01). The cruise effect was only significant in the canyon (P = 0.02, α-value = 0.05/2). For macrofauna, pairwise tests suggest that the habitat effect was only marginal at depths between 200 to 400 m (P = 0.02, α-value = 0.05/4).

3.6 Size composition

Habitats were well-separated in the nMDS ordination of meiofaunal size composition (Figures 6A, B). In contrast, the ordination of macrofaunal size composition partly overlapped between the canyon and slope (Figures 6C, D). By projecting the midpoint of the size bins on the nMDS plots, the meiofaunal size bins appear progressively larger from the canyon to the slope (Figure 6A). In contrast, the macrofaunal size bins were clustered around the slope ordinations (Figure 6C), presumably, due to much higher biomass within each size bin on the slope than in the canyon (Figure 2A). Nevertheless, we can still see a clear size transition within the slope ordination for macrofauna (Figure 6C), in which the smaller size bins were closer to the canyon ordination (to the left) and larger size bins away from it (to the right).

The separation of nMDS ordination (whether distinct or partly) was also reflected by a significant between-habitat difference in meiofauna (Habitat, P = 0.001, Table 3) and macrofauna size composition (Habitat, P = 0.002, Table 4) in the PERMANOVA tests. In the meantime, only marginal depth effects were detected for

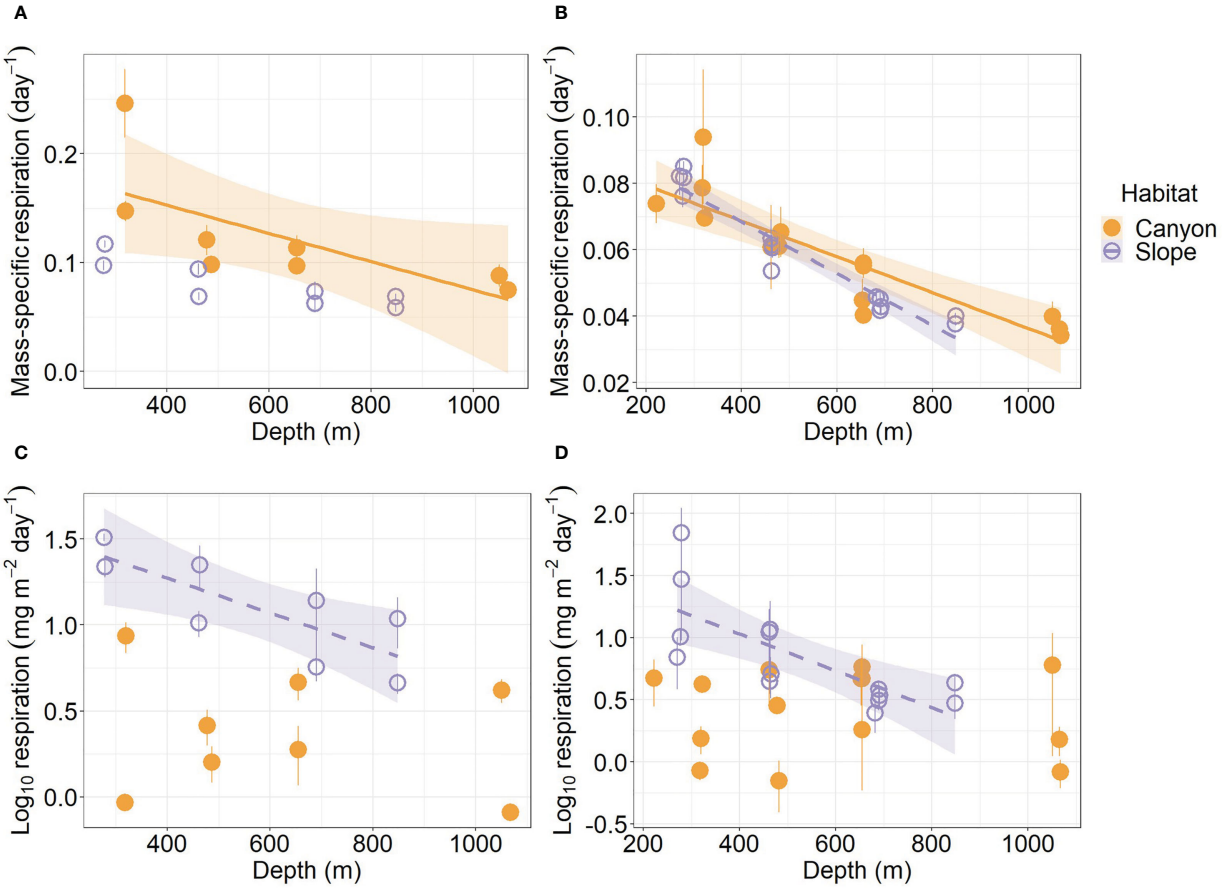

FIGURE 5
Mass-specific respiration and total respiration rate of meiobenthos **(A–C)** and macrobenthos **(B–D)** as functions of depth. Trend lines show significant relationships with depth based on simple linear regressions (P < 0.05), and shaded areas show 95% confidence intervals. The relationship between meiofaunal mass-specific respiration and depth was borderline significant on the slope (P = 0.05); thus, the trend line was not presented. Error bar shows standard deviation.

meiofaunal (Depth, P = 0.073, Table 3) and macrofaunal size composition (Depth, P = 0.064, Table 4).

Based on distance-based redundancy analysis (dbRDA), the best subset of environmental factors explaining meiofauna size composition (adjusted R^2 = 48.1%, p < 0.05) were variables related to 1) internal-tide energy, i.e., *Over20*; 2) food supply, i.e., *TOC*; 3) water masses, i.e., *Temp*; 4) sediment characteristics, i.e., *Silt*, *Clay* and *Por*. These variables are mapped onto the same nMDS plot (Figure 6B) using their correlations with the ordination axes, showing that the canyon assemblages were characterized by increasing *Over20* and the slope assemblages by increasing *TOC*, *Temp*, *Silt*, *Clay*, and *Por*.

For the macrofauna, the best subset of environmental factors explaining the size composition (adjusted R^2 = 27.7%, p < 0.05) were variables related to 1) Internal-tide energy, i.e., *Spd*, *Over20*, and *Trans*; 2) food supply, i.e., *CN*; 3) water masses, i.e., *Temp*; 4) sediment characteristics, i.e., *Por* and *Silt*. These variables are also mapped onto the nMDS plot (Figure 6D), showing that the canyon assemblages were characterized by increasing *Spd* and *Over20* and the slope assemblages by increasing *CN*, *Trans*, *Por*, and *Silt*.

4 Discussion

The localized maximums in normalized biomass size spectra (NBSS), also known as the "dome" patterns, are often observed in the aquatic ecosystem (Boudreau et al., 1991; Quiroga et al., 2014), especially in the pelagic communities (Rossberg et al., 2019). The cause of these "domes" is subject to debate, but the most common explanation is that these "domes" represent the trophic positions on the food chain or different taxonomic groups (Thompson et al., 2013; Kwong and Pakhomov, 2021). The subsequent domes on the NBSS may represent the size ratios between the predator and prey (Yurista et al., 2014; Atkinson et al., 2021). A recent study using a model and empirical data demonstrated that the "dome" patterns in NBSS might be driven by trophic cascade and nutrient availability (Rossberg et al., 2019). In theory, the trophic cascade (or predation) may modulate the community biomass toward the smaller classes, whereas the nutrient enrichment likely increases the density of the larger classes. The interaction between top-down trophic cascade and bottom-up nutrient enrichment is possible to generate the "dome" and "trough" in the NBSS for the theoretical model, which

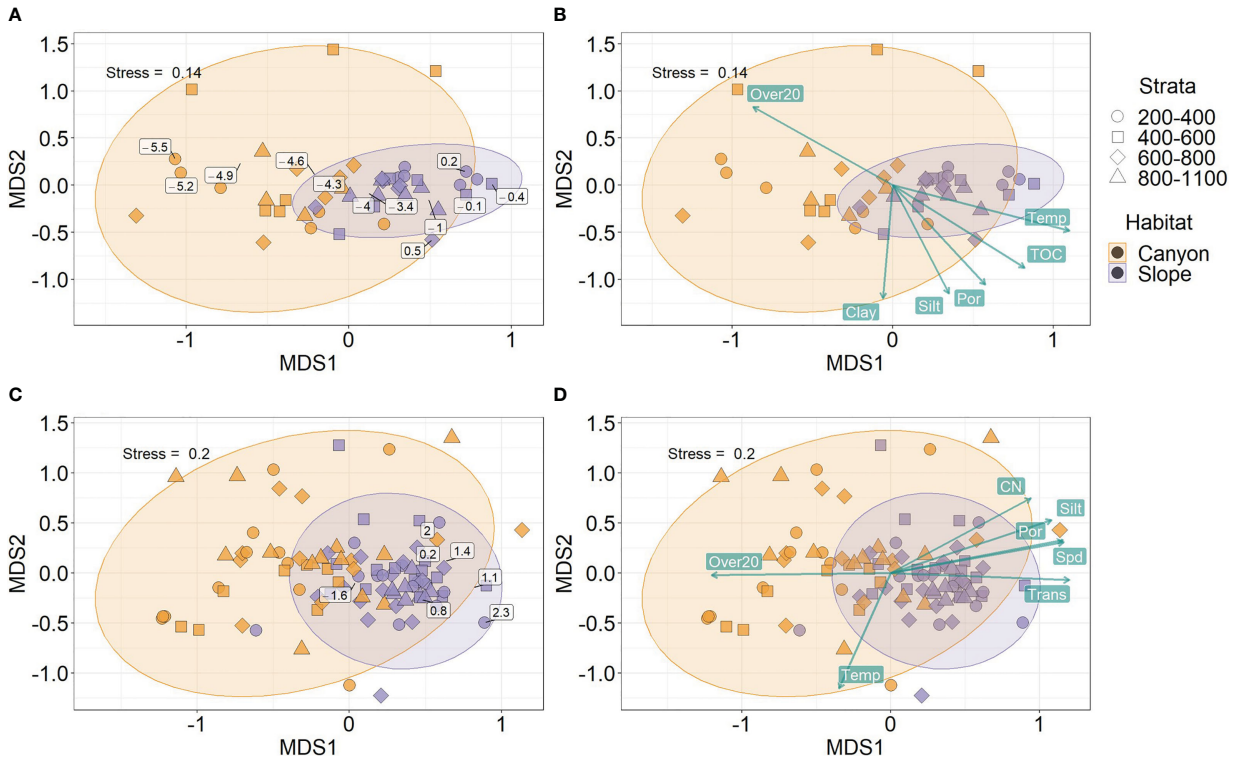

FIGURE 6
Non-metric Multi-dimensional Scaling (nMDS) on body size compositions of meiobenthos **(A, B)** and macrobenthos **(C, D)**. The biomass in each $\log_2$ size bin and sample was square-root transformed and converted to Bray-Curtis dissimilarity between samples before subjecting to nMDS. The text labels on panels **(A–C)** show the mid-point of the $\log_2$ size bins based on the biomass-weighted averages of the ordination scores within each size bin. The text labels on panels **(B–D)** show the best subset of environmental variables selected by Distance-based Redundancy Analysis (dbRDA). The length of vectors on panels **(B–D)** indicates environmental correlations with the nMDS ordination scores. The direction of vectors suggests increasing bottom water temperature (Temp), light transmission (Trans), percent silt and clay, sediment TOC and C/N ratio, porosity (Por), and mean bottom current speed (Spd) and disturbance duration (Over20).

has been validated by the empirical data (Rossberg et al., 2019). Interestingly, our study also observed distinct meiofauna and macrofauna "domes" in the NBSS, supporting the assertion by Rossberg et al. (2019) and others (Thompson et al., 2013; Yurista et al., 2014; Atkinson et al., 2021; Kwong and Pakhomov, 2021) on the trophic origin of the NBSS domes. Moreover, many manipulative and field experiments have confirmed meiofauna as an essential food source for higher trophic levels, including macrofauna (Coull, 1990; Ólafsson, 2003; Schratzberger and Ingels, 2018). Therefore, the trophic interactions between meiobenthos and macrobenthos can potentially result in two NBSS "domes" aligning in a step fashion along a linear trend.

However, the benthic community size structure is known to be less pronounced than the pelagic communities (Shurin et al., 2006). Therefore, to our knowledge, only a handful of benthic studies reported "dome" patterns in their NBSS. For instance, Quiroga et al. (2014) showed "dome" patterns in the NBSS for the Antarctic macrobenthic communities. Mazurkiewicz et al. (2019; Mazurkiewicz et al. 2020) reported consecutive "domes" in the NBSS for the Arctic fjord meiobenthos and macrobenthos, respectively. The bimodal size spectra suggest that meiofauna and macrofauna may be discrete entities (Schwinghamer, 1981; Warwick and Clarke, 1984; Warwick, 2014). Nevertheless, the "dome" patterns reported by these studies were less pronounced than those observed in our study. We did not expect sharp NBSS dips for meiofauna and macrofauna in their smallest and largest sizes, respectively (Figure 2B), because the infauna communities usually have flexible feeding strategies. For example, nearly all benthic carnivores are scavengers (Ruxton and Houston, 2004). Some polychaetes (i.e., *Nereis diversicolor*) can switch among deposit-feeding, scavenging, predation, or suspension-feeding, depending on the flow regimes (Biles et al., 2003). While unintentionally, the deposit-feeding macrofauna may consume meiofauna living in interstitial sediment spaces (Iken et al., 2001; Jumars et al., 2015). Liao et al. (2017; Liao et al. 2020) also examined the feeding strategies of polychaete and nematode specimens from this study. They found the polychaete feeding modes ranging from deposit feeders, carnivores, scavengers, omnivores, and suspension feeders, and nematodes from deposit feeders, epigrowth feeders, and omnivores/predators. Given the flexible feeding guilds of the meiobenthos and macrobenthos, it is likely that trophic cascade (or predation) may not be the only cause of our distinct "dome" patterns in the benthic NBSS.

Using mathematical simulation, Bett (2013) offers an alternative explanation for the "dome" patterns. He showed that the two "domes" and a "trough" in the biomass-size spectra could arise from a continuous size distribution with two hypothetic sieves. In other words, the sampling protocols or sieving artifacts can

contribute to the bimodal biomass-size spectra. Moreover, if we assume that all organisms are perfect spheres. The 40-μm sieve should retain meiofauna larger than 3 x 10^{-4} mg, and the 300-μm sieve should retain macrofauna larger than 1.6 x 10^{-2} mg. These thresholds are close to our cut-off sizes of 0.001 and 0.01 mg (see results for details) to generate linear NBSS for the larger meiobenthos and macrobenthos, respectively. Since most meiobenthos and macrobenthos are not spherical, the sieves might retain even smaller organisms. The retaining sediments can also clog the sieves, keeping the specimens that are supposed to pass the sieves. Still, the numbers of the inadvertently included organisms should decrease with decreasing body size, resulting in the left tail of the "dome" patterns. Nevertheless, it is impossible to determine the relative contributions of trophic position and sieving artifact to the "domes" and "troughs" of our observed NBSS.

We observed linear and negative NBSSs for meiofaunal (> 40 μm) and macrofaunal-size individuals (> 300 μm). Lower intercept and steeper slope of the NBSS were observed in the canyon habitat resulting in lower biomass of the meiofaunal and macrofaunal size individuals. It also means that the "canyon" conditions removed larger individuals with the effect increased toward the larger size classes. Similar patterns (i.e., steeper NBSS slope) have been observed in benthic communities from the coastal hypoxic zone in the Gulf of Mexico (Qu et al., 2015), oxygen minimum zones off Chile (Quiroga et al., 2005), and the Antarctic continental slope (Saiz-Salinas and Ramos, 1999). These studies suggest that the low oxygen conditions and food limitations may impact large organisms more than small ones. Small organisms can better satisfy their metabolic demands (i.e., oxygen demand or nutritional need) due to the relatively large surface area to body volume ratio. Under extreme hypoxia (DO < 1 mg/L), even the small species may decline in abundance, leading to the dominance of medium-sized species (Qu et al., 2015). However, this might not be the case in this study because the medium-size individuals dominated (i.e., dome patterns in Figure 2B) both the disturbed (i.e., canyon) and non-disturbed habitat (i.e., adjacent slope). Other studies using different statistical approaches (i.e., non-NBSS) also report an increasing abundance of smaller individuals (or shift biomass maximum to smaller size classes) due to habitat degradation and fishing (Wilson et al., 2010), glacial sedimentation (Górska and Włodarska-Kowalczuk, 2017), trawling disturbance (Queirós et al., 2006), and pollution (Hargrave and Thiel, 1983; Schwinghamer, 1988; Saiz-Salinas and González-Oreja, 2000). This study demonstrates that the responses of benthic communities to natural disturbances in GPSC may be as strong as the studies mentioned above. We also provide the first evidence for steepening NBSS slopes in a high-energy submarine canyon, suggesting that the physical conditions may be unfavorable for the local infauna communities.

Benthic biomass and production often decline with intensive bottom trawling (Jennings et al., 2001; Duplisea et al., 2002; Queirós et al., 2006), glacial disturbance (Górska and Włodarska-Kowalczuk, 2017), food limitation (Wei et al., 2010a), oxygen deficiency (Diaz and Rosenberg, 1995; Diaz and Rosenberg, 2001; Levin, 2003), and organic pollution (Hargrave and Thiel, 1983; Montagna et al., 2013). We observed similar depressed benthic biomass, production, and respiration in the canyon compared to the adjacent slope. Due to their larger size, macrofauna accounted for more benthic biomass than meiofauna. They contributed even more biomass in the GPSC (~78%) than on the adjacent slope (~61%). The GPSC experiences strong internal tide disturbance and thus was dominated by burrowing, motile, subsurface deposit-feeding polychaetes (i.e., paraonids, capitellids, and cosurrids) (Liao et al., 2017). These specialized animals can burrow deep into the sediments to feed on the organic particles while avoiding being swept away by strong bottom currents. Therefore, the higher contribution by macrofauna biomass in the GPSC could result from adapting life history traits to its unique environmental condition. The body size compositions in the canyon also differed from the non-canyon habitats, indicating that the energetic GPSC not only impacted the body size structure (i.e., steeper NBSS) but also the growth and metabolism of populations and communities (Brey, 1999; Sukhotin et al., 2002; Moyano et al., 2017). Likewise, our results were consistent with the previous studies, showing lower abundance, species diversity, functional diversity, and distinctive species composition in the GPSC compared to the adjacent slope habitat (Liao et al., 2017; Liao et al., 2020). Together, the multifaceted characteristics of community structure from this and previous studies suggest that GPSC is a high-energy and disturbed environment for the local benthic communities.

Interestingly, the canyon meiofauna had higher P/B ratios and mass-specific respiration rates than the slope meiofauna, suggesting that the r-strategists likely dominated the canyon meiofauna community with faster growth and high metabolic rates. This result is in accord with analyses based on nematode buccal and tail morphology and life-history strategies (Liao et al., 2020), in which the non-selective deposit feeders with clavate tail and r-selection strategy dominated the upper GPSC. Nevertheless, the extremely low meiofauna biomass in the canyon (i.e., more than ten folds lower) still resulted in lower meiofauna production and respiration than on the slope. In contrast with the higher meiofauna P/B ratios, the macrofauna P/B ratios were lower in the canyon than on the slope. The contradiction indicates that the extreme condition in the GPSC may negatively affect the macrofauna more than the meiofauna P/B ratios. Given the lower P/B ratio and biomass in the canyon and similar mass-specific respiration rates between the two habitats, it is not surprising that the macrofauna production and respiration were lower in the canyon than on the slope.

Despite the strong habitat effects, the benthic biomass, production, and size composition were not different across depth gradients, suggesting that the habitat difference (i.e., canyon and non-canyon) had greater impacts than the water depth. The individual regression analyses by transects also showed that the benthic production and respiration declined with depth only on the slope but not in the canyon, indicating that these bathymetric variations cannot be generalized across the habitats. Usually, the upper continental margin experiences the greatest depth-related environmental variations, resulting in ubiquitous bathymetric patterns in the benthic communities (Wei et al., 2010a; Wei et al., 2010b). Therefore, the non-depth-related patterns suggest that the high-energy conditions in the GPSC probably smoothed the typical strong bathymetric gradients in the deep-sea sediment.

This study shows that body-size composition can effectively detect the "canyon" effects in meiofauna and macrofauna communities, providing a useful alternative to taxonomical analyses. Since the same data have been analyzed based on taxon (Liao et al., 2017), polychaete family (Liao et al., 2017), nematode species (Liao et al., 2020), and body size compositions (this study), we can assess their "sensitivity" to the disturbed GPSC environment. To compare effect sizes, we calculated the ratio of the effect sum of squares ($SS_{habitat}$) divided by the total sum of squares (SS_{total}) in PERMANOVA (Fritz et al., 2012). The PERMANOVAs based on polychaete families (R^2 = 0.49) and nematode species (R^2 = 0.46) have the largest effect sizes (Table S3). The second highest is the analyses based on macrofauna (R^2 = 0.31) and meiofauna taxa (R^2 = 0.29). The smallest effect sizes are the analyses based on meiofauna (R^2 = 0.2) and macrofauna size compositions (R^2 = 0.12). Hence, while non-taxonomical analysis, such as body size composition, can detect significant habitat effects, they are generally less sensitive than taxonomical or species-level analysis.

The environmental drivers of the body size composition presented in this study are consistent with the previous studies based on taxon and nematode species compositions (Liao et al., 2017; Liao et al., 2020). We show that the meiofauna and macrofauna size compositions can be explained by factors related to internal-tide energy, food supply, temperature, and sediment characteristics. The canyon assemblages were primarily characterized by increasing internal tide energy (i.e., bottom current velocity, duration of sediment erosion, or low light transmission) and the slope assemblages by increasing food supplies (i.e., TOC or C/N ratio). The strong bottom currents may cause intermittent sediment resuspension and transports in the bottom nepheloid layer (Wang et al., 2008; Liu et al., 2010; Chiou et al., 2011). Also, the high internal tide energy can lead to long-lasting sediment winnowing to prevent the organic-rich particles from settling on the seafloor (Liao et al., 2017). Hence, the high-energy condition in the GPSC is a double-edged sword. On the one hand, the hydrodynamic regime erodes the sediment and causes long-term and recurrent disturbances in the local benthic communities. On the other hand, sediment resuspension and transport by the bottom-intensified currents decrease the total organic carbon (TOC) contents and, thus, the food supplies in the sediments.

5 Conclusions

Physical disturbance, food availability, temperature, and sediment characteristics controlled the biomass among size classes (or size bins) in benthic communities of the upper GPSC off SW Taiwan. The biomass-size compositions were distinctively different between the GPSC and adjacent slope. Typical "dome" patterns were observed in the normalized biomass size spectrum (NBSS), possibly due to a combination of factors, including the sampling artifact (i.e., sieve effects), physical disturbance, trophic cascade, food availability, and life-history traits. For the larger meiofauna (> 0.001 mg) and macrofauna (> 0.01 mg), the normalized biomass (or relative abundance) of the size bins decreased linearly with the mid-points of the size bins, in line with the linear normalized biomass size spectra (NBSS) observed elsewhere. These truncated NBSS slopes were steeper in the upper canyon than on the adjacent slope, suggesting that the largest meiofauna and macrofauna were relatively less abundant in the canyon. We hypothesized that the high-energy environment in the Gaoping Canyon (e.g., strong bottom currents and frequent turbidity flow) might have removed the larger-size individuals or favored the re-colonization of smaller individuals.

Nevertheless, the canyon meiofauna had a higher P/B ratio and respiration rate than the slope meiofauna, indicating that the canyon conditions favored the meiofauna with smaller body size and faster growth and metabolism. In contrast, the macrofauna communities in the canyon had a lower P/B ratio than the slope communities, possibly associated with disturbances in the canyon. Moreover, the community-level total biomass, secondary production, and respiration of meiofauna and macrofauna dropped significantly from the slope into the canyon habitats. These findings, along with previous studies (Liao et al., 2017; Liao et al., 2020), show that the energetic GPSC affected the total abundance, taxonomic composition, diversity, total biomass, growth, metabolism, and size composition of the local benthic communities. Understanding the effects of large-scale disturbance (e.g., internal tide and turbidity currents) on the benthic communities and the associated carbon cycling processes (e.g., body size, biomass, growth, and respiration) will enhance our ability to predict the impacts of climate changes in the submarine canyons ecosystems.

Data availability statement

The datasets presented in this study can be found in online repositories. The names of the repository/repositories and accession number(s) can be found below: https://github.com/chihlinwei/bbbs.

Author contributions

C-LW designed and conceived the study, to which all authors contributed ideas and discussion. J-XL and C-LW executed field sampling. J-XL conducted the laboratory work. C-CT, Y-TC, J-XL, and C-LW contributed to data analysis. C-CT, Y-TC, J-XL, and C-LW drafted the manuscript. All authors contributed to the interpretation of results and manuscript revisions. All authors contributed to the article and approved the submitted version.

Funding

This project is part of Fate of Terrestrial/Nonterrestrial Sediments in High Yield Particle-Export River-sea Systems (FATES-HYPERS), sponsored by the National Science and Technology Council (MOST 111-2611-M-002-021).

Acknowledgments

We thank the Institute of Oceanography (IO), the National Taiwan University (NTU), and the National Science and

Technology Council (NSTC) for supporting the fieldwork, analysis, and manuscript preparation. We thank Sen Jan and Ming-Da Chiou for providing the internal tide model. We thank Guan-Ming Chen and Yen-Li Liu for macrofauna body size measurements. We thank the captain, crew members, and technicians of the R/V Ocean Researcher I, as well as the graduate students who participated in the OCEAN 7090 Field Work in Marine Biology. Students collected the majority of samples and data through the field course.

Conflict of interest

The authors declare that the research was conducted in the absence of any commercial or financial relationships that could be construed as a potential conflict of interest.

Publisher's note

Supplementary material

The Supplementary Material for this article can be found online at: https://www.frontiersin.org/articles/10.3389/fmars.2023.1122143/full#supplementary-material

References

Aller, R. C. (1978). "The effects of animal-sediment interactions on geochemical processes near the sediment-water interface," in *Estuarine interactions* (Elsevier), 157–172. doi: 10.1016/B978-0-12-751850-3.50017-0

Andresen, H., and Brey, T. (2018) *BenthicPro: benthic energy flow*. Available at: https://github.com/HenrikeAndresen/BenthicPro.

Atkinson, A., Lilley, M. K. S., Hirst, A. G., McEvoy, A. J., Tarran, G. A., Widdicombe, C., et al. (2021). Increasing nutrient stress reduces the efficiency of energy transfer through planktonic size spectra. *Limnol. Oceanogr.* 66, 422–437. doi: 10.1002/lno.11613

Austen, M. C., and Widdicombe, S. (2006). Comparison of the response of meio-and macrobenthos to disturbance and organic enrichment. *J. Exp. Mar. Biol. Ecol.* 330, 96–104. doi: 10.1016/j.jembe.2005.12.019

Bett, B. J. (2013). Characteristic benthic size spectra: potential sampling artefacts. *Mar. Ecol. Prog. Ser.* 487, 1–6. doi: 10.3354/meps10441

Bett, B. J., van Reusel, A., Vincx, M., Soltwedel, T., Pfannkuche, O., Lambshead, P. J. D., et al. (1994). Sampler bias in the quantitative study of deep-sea meiobenthos. *Mar. Ecol. Prog. Ser.* 104, 197–203. doi: 10.3354/meps104197

Biles, C. L., Solan, M., Isaksson, I., Paterson, D. M., Emes, C., and Raffaelli, D. G. (2003). Flow modifies the effect of biodiversity on ecosystem functioning: an *in situ* study of estuarine sediments. *J. Exp. Mar. Biol. Ecol.* 285–286, 165–177. doi: 10.1016/S0022-0981(02)00525-7

Blanchard, J. L., Heneghan, R. F., Everett, J. D., Trebilco, R., and Richardson, A. J. (2017). From bacteria to whales: using functional size spectra to model marine ecosystems. *Trends Ecol. Evol.* 32, 174–186. doi: 10.1016/j.tree.2016.12.003

Boudreau, P., and Dickie, L. (1989). Biological model of fisheries production based on physiological and ecological scalings of body size. *Can. J. Fisheries Aquat. Sci.* 46, 614–623. doi: 10.1139/f89-078

Boudreau, P. R., Dickie, L. M., and Kerr, S. R. (1991). Body-size spectra of production and biomass as system-level indicators of ecological dynamics. *J. Theor. Biol.* 152, 329–339. doi: 10.1016/S0022-5193(05)80198-5

Brey, T. (1999). Growth performance and mortality in aquatic macrobenthic invertebrates. *Adv. Mar. Biol.* 35, 153–223. doi: 10.1016/S0065-2881(08)60005-X

Brey, T. (2012). A multi-parameter artificial neural network model to estimate macrobenthic invertebrate productivity and production. *Limnol. Oceanogr. Methods* 10, 581–589. doi: 10.4319/lom.2012.10.581

Brown, J. H., Gillooly, J. F., Allen, A. P., Savage, V. M., and West, G. B. (2004). Toward a metabolic theory of ecology. *Ecology* 85, 1771–1789. doi: 10.1890/03-9000

Chiang, C.-S., Hsiung, K.-H., Yu, H.-S., and Chen, S.-C. (2020). Three types of modern submarine canyons on the tectonically active continental margin offshore southwestern Taiwan. *Mar. Geophys Res.* 41, 4. doi: 10.1007/s11001-020-09403-z

Chiang, C.-S., and Yu, H.-S. (2022). Controls of submarine canyons connected to shore during the LGM sea-level rise: examples from Taiwan. *J. Mar. Sci. Eng.* 10, 494. doi: 10.3390/jmse10040494

Chiou, M.-D., Jan, S., Wang, J., Lien, R.-C., and Chien, H. (2011). Sources of baroclinic tidal energy in the gaoping submarine canyon off southwestern Taiwan. *J. Geophys. Res.* 116, C12016. doi: 10.1029/2011JC007366

Coull, B. C. (1990). Are members of the meiofauna food for higher trophic levels? *Trans. Am. Microscopical Soc.* 109, 233–246. doi: 10.2307/3226794

Danovaro, R. (2010). "Chapter 7 abundance of metazoan meiofauna," in *Methods for the study of deep-sea sediments, their functioning and biodiversity* (Boca Raton: CRC Press).

De Leo, F., Smith, C. R., Bowden, D. A., and Clark, M. R. (2010). Submarine canyons: hotspots of benthic biomass and productivity in the deep sea. *Proc. R. Soc. B.* 277, 2783–2792, rspb20100462. doi: 10.1098/rspb.2010.0462

Diaz, R. J., and Rosenberg, R. (1995). Marine benthic hypoxia: A review of its ecological effects and the behavioural responses of benthic macrofauna. *Oceanography Mar. Biol.: Annu. Rev.* 33, 245–303.

Diaz, R. J., and Rosenberg, R. (2001). Overview of anthropogenically-induced hypoxic effects on marine benthic fauna. In: *Coastal hypoxia: Consequences for living resources and ecosystems* (American Geophysical Union). doi: 10.1029/CE058p0129.

Dickie, L., Kerr, S., and Boudreau, P. (1987). Size-dependent processes underlying regularities in ecosystem structure. *Ecol. Monogr.* 57, 233–250. doi: 10.2307/2937082

Duplisea, D. E., Jennings, S., Warr, K. J., and Dinmore, T. A. (2002). A size-based model of the impacts of bottom trawling on benthic community structure. *Can. J. Fish. Aquat. Sci.* 59, 1785–1795. doi: 10.1139/f02-148

Duplisea, D. E., and Kerr, S. R. (1995). Application of a biomass size spectrum model to demersal fish data from the scotian shelf. *J. Theor. Biol.* 177, 263–269. doi: 10.1006/jtbi.1995.0243

Edwards, A. M., Robinson, J. P. W., Plank, M. J., Baum, J. K., and Blanchard, J. L. (2017). Testing and recommending methods for fitting size spectra to data. *Methods Ecol. Evol.* 8, 57–67. doi: 10.1111/2041-210X.12641

Elton, C. (1927). "The animal community," in *Animal ecology* (The Macmillan Company New York), 50–70.

Feller, R. J., and Warwick, R. M. (1988). "Energetics," in *Introduction to the study of meiofauna*. Eds. R. P. Higgins and H. Thiel (Washington, D.C: Smithsonian Institution Press), 181–196.

Fritz, C. O., Morris, P. E., and Richler, J. J. (2012). Effect size estimates: current use, calculations, and interpretation. *J. Exp. psychology: Gen.* 141, 2.

Gaedke, U. (1992). The size distribution of plankton biomass in a large lake and its seasonal variability. *Limnol. Oceanogr.* 37, 1202–1220. doi: 10.4319/lo.1992.37.6.1202

Gavey, R., Carter, L., Liu, J. T., Talling, P. J., Hsu, R., Pope, E., et al. (2017). Frequent sediment density flows during 2006 to 2015, triggered by competing seismic and weather events: Observations from subsea cable breaks off southern Taiwan. *Mar. Geol.* 384, 147–158. doi: 10.1016/j.margeo.2016.06.001

Giere, O. (2009). Meiobenthology: the microscopic motile fauna of aquatic sediments. *2nd* ed. Berlin: Springer. doi: 10.1007/978-3-540-68661-3

Górska, B., Soltwedel, T., Schewe, I., and Włodarska-Kowalczuk, M. (2020). Bathymetric trends in biomass size spectra, carbon demand, and production of Arctic benthos (76-5561 m, fram strait). *Prog. Oceanogr.* 186, 102370. doi: 10.1016/j.pocean.2020.102370

Górska, B., and Włodarska-Kowalczuk, M. (2017). Food and disturbance effects on Arctic benthic biomass and production size spectra. *Prog. Oceanogr.* 152, 50–61. doi: 10.1016/j.pocean.2017.02.005

Hargrave, B. T., and Thiel, H. (1983). Assessment of pollution-induced changes in benthic community structure. *Mar. Pollut. Bull.* 14, 41–46. doi: 10.1016/0025-326X(83)90189-3

Hsu, S.-K., Kuo, J., Lo, C.-L., Tsai, C.-H., Doo, W.-B., Ku, C.-Y., et al. (2008). Turbidity currents, submarine landslides and the 2006 pingtung earthquake off SW Taiwan. *Terrestrial Atmospheric Oceanic Sci.* 19, 767. doi: 10.3319/TAO.2008.19.6.767(PT

Iken, K., Brey, T., Wand, U., Voigt, J., and Junghans, P. (2001). Food web structure of the benthic community at the porcupine abyssal plain (NE atlantic): a stable isotope analysis. *Prog. Oceanogr.* 50, 383–405. doi: 10.1016/S0079-6611(01)00062-3

Jennings, S., Dinmore, T. A., Duplisea, D. E., Warr, K. J., and Lancaster, J. E. (2001). Trawling disturbance can modify benthic production processes. *J. Anim. Ecol.* 70, 459–475. doi: 10.1046/j.1365-2656.2001.00504.x

Jones, D. O. B., Yool, A., Wei, C.-L., Henson, S. A., Ruhl, H. A., Watson, R. A., et al. (2014). Global reductions in seafloor biomass in response to climate change. *Global Change Biol.* 20, 1861–1872. doi: 10.1111/gcb.12480

Jumars, P. A., Dorgan, K. M., and Lindsay, S. M. (2015). Diet of worms emended: An update of polychaete feeding guilds. *Annu. Rev. Mar. Sci.* 7, 497–520. doi: 10.1146/annurev-marine-010814-020007

Kleiber, M. (1932). Body size and metabolism. *Hilgardia* 6, 315–353. doi: 10.3733/hilg.v06n11p315

Klumpp, D. (1984). Nutritional ecology of the ascidian pyura stolonifera: Influence of body size, food quantity and quality on filter-feeding, respiration, assimilation efficiency and energy balance. *Mar. Ecol. Prog. series. Oldendorf* 19, 269–284. doi: 10.3354/meps019269

Kwong, L. E., and Pakhomov, E. A. (2021). Zooplankton size spectra and production assessed by two different nets in the subarctic northeast pacific. *J. Plankton Res.* 43, 527–545. doi: 10.1093/plankt/fbab039

Lee, I.-H., Wang, Y.-H., Liu, J. T., Chuang, W.-S., and Xu, J. (2009). Internal tidal currents in the gaoping (Kaoping) submarine canyon. *J. Mar. Syst.* 76, 397–404. doi: 10.1016/j.jmarsys.2007.12.011

Levin, L. A. (2003). Oxygen minimum zone benthos: adaptation and community response to hypoxia. *Oceanography Mar. Biology: Annu. Rev.* 41, 1:45.

Levin, L. A., and Sibuet, M. (2012). Understanding continental margin biodiversity: A new imperative. *Annu. Rev. Mar. Sci.* 4, 79–112. doi: 10.1146/annurev-marine-120709-142714

Liao, J.-X., Chen, G.-M., Chiou, M.-D., Jan, S., and Wei, C.-L. (2017). Internal tides affect benthic community structure in an energetic submarine canyon off SW Taiwan. *Deep Sea Res. Part I: Oceanographic Res. Papers* 125, 147–160. doi: 10.1016/j.dsr.2017.05.014

Liao, J.-X., Wei, C.-L., and Yasuhara, M. (2020). Species and functional diversity of deep-sea nematodes in a high energy submarine canyon. *Front. Mar. Sci.* 7. doi: 10.3389/fmars.2020.00591

Lin, B.-S., Brimblecombe, P., Lee, C.-L., and Liu, J. T. (2013). Tracing typhoon effects on particulate transport in a submarine canyon using polycyclic aromatic hydrocarbons. *Mar. Chem.* 157, 1–11. doi: 10.1016/j.marchem.2013.07.004

Lin, B.-S., Lee, C.-L., Brimblecombe, P., and Liu, J. T. (2016). Transport and fluxes of terrestrial polycyclic aromatic hydrocarbons in a small mountain river and submarine canyon system. *J. Environ. Manage.* 178, 30–41. doi: 10.1016/j.jenvman.2016.04.039

Liu, J. T., Hsu, R. T., Hung, J.-J., Chang, Y.-P., Wang, Y.-H., Rendle-Buhring, R., et al. (2016). From the highest to the deepest: the gaoping-River-Gaoping submarine canyon dispersal system. *Earth-Science Rev.* 274–300. doi: 10.1016/j.earscirev.2015.10.012

Liu, J. T., Wang, Y. H., Lee, I.-H., and Hsu, R. T. (2010). Quantifying tidal signatures of the benthic nepheloid layer in gaoping submarine canyon in southern Taiwan. *Mar. Geol.* 271, 119–130. doi: 10.1016/j.margeo.2010.01.016

Mazurkiewicz, M., Górska, B., Renaud, P. E., Legeżyńska, J., Berge, J., and Włodarska-Kowalczuk, M. (2019). Seasonal constancy (summer vs. winter) of benthic size spectra in an Arctic fjord. *Polar Biol.* 42, 1255–1270. doi: 10.1007/s00300-019-02515-2

Mazurkiewicz, M., Górska, B., Renaud, P. E., and Włodarska-Kowalczuk, M. (2020). Latitudinal consistency of biomass size spectra - benthic resilience despite environmental, taxonomic and functional trait variability. *Sci. Rep.* 10, 4164. doi: 10.1038/s41598-020-60889-4

Montagna, P. A., Baguley, J. G., Cooksey, C., Hartwell, I., Hyde, L. J., Hyland, J. L., et al. (2013). Deep-sea benthic footprint of the deepwater horizon blowout. *PloS One* 8, e70540. doi: 10.1371/journal.pone.0070540

Montagna, P. A., Baguley, J. G., Hsiang, C.-Y., and Reuscher, M. G. (2017). Comparison of sampling methods for deep-sea infauna. *Limnology Oceanography: Methods* 15, 166–183. doi: 10.1002/lom3.10150

Moyano, M., Illing, B., Christiansen, L., and Peck, M. A. (2017). Linking rates of metabolism and growth in marine fish larvae. *Mar. Biol.* 165, 5. doi: 10.1007/s00227-017-3252-4

Narayanaswamy, B. E., Bett, B. J., Lamont, P. A., Rowden, A. A., Bell, E. M., and Menot, L. (2016). "Corers and grabs," in *Biological sampling in the deep Sea* (Wiley-Blackwell). doi: 10.1002/9781118332535.ch10

Norkko, A., Villnäs, A., Norkko, J., Valanko, S., and Pilditch, C. (2013). Size matters: implications of the loss of large individuals for ecosystem function. *Sci. Rep.* 3, 2646. doi: 10.1038/srep02646

Ólafsson, E. (2003). Do macrofauna structure meiofauna assemblages in marine soft-bottoms? a review of experimental studies. *Vie Milieu / Life Environ.* 53, 249–265.

Parsons, T. (1969). The use of particle size spectra in determining the structure of a plankton community. *J. Oceanographical Soc. Japan* 25, 172–181. doi: 10.5928/kaiyou1942.25.172

Pepin, P. (1991). Effect of temperature and size on development, mortality, and survival rates of the pelagic early life history stages of marine fish. *Can. J. Fish. Aquat. Sci.* 48, 503–518. doi: 10.1139/f91-065

Petchey, O. L., and Belgrano, A. (2010). Body-size distributions and size-spectra: universal indicators of ecological status? *Biol. Lett.* doi: 10.1098/rsbl.2010.0240

Peters, R. H. (1983). *The ecological implications of body size* (Cambridge: Cambridge University Press). doi: 10.1017/CBO9780511608551

Platt, T. (1985). "Structure of marine ecosystems: its allometric basis," in *Ecosystem theory for biological oceanography*., eds. R. E. Ulanowicz and T. Platt. Canadian Bulletin of Fisheries and Aquatic Sciences 213, 55–64.

Qu, F., Nunnally, C., Rowe, G. T., Qu, F., Nunnally, C., and Rowe, G. T. (2015). Polychaete annelid biomass size spectra: the effects of hypoxia stress. *J. Mar. Biology J. Mar. Biol.* 2015, e983521. doi: 10.1155/2015/983521

Queirós, A. M., Hiddink, J. G., Kaiser, M. J., and Hinz, H. (2006). Effects of chronic bottom trawling disturbance on benthic biomass, production and size spectra in different habitats. *J. Exp. Mar. Biol. Ecol.* 335, 91–103. doi: 10.1016/j.jembe.2006.03.001

Quiroga, E., Gerdes, D., Montiel, A., Knust, R., and Jacob, U. (2014). Normalized biomass size spectra in high Antarctic macrobenthic communities: linking trophic position and body size. *Mar. Ecol. Prog. Ser.* 506, 99–113. doi: 10.3354/meps10807

Quiroga, E., Quiñones, R., Palma, M., Sellanes, J., Gallardo, V. A., Gerdes, D., et al. (2005). Biomass size-spectra of macrobenthic communities in the oxygen minimum zone off Chile. *Estuarine Coast. Shelf Sci.* 62, 217–231. doi: 10.1016/j.ecss.2004.08.020

Rachor, E. (1975). Quantitative untersuchungen über meiobenthos der nordostatlantischen tiefsee. *"Meteor" ForschErgebn (Ser. D)* 21, 1–10.

R Core Team (2022). *R: a language and environment for statistical computing* (Vienna, Austria: R Foundation for Statistical Computing). Available at: http://www.R-project.org/.

Rossberg, A. G., Gaedke, U., and Kratina, P. (2019). Dome patterns in pelagic size spectra reveal strong trophic cascades. *Nat. Commun.* 10, 4396. doi: 10.1038/s41467-019-12289-0

Ruxton, G. D., and Houston, D. C. (2004). Energetic feasibility of an obligate marine scavenger. *Mar. Ecol. Prog. Ser.* 266, 59–63. doi: 10.3354/meps266059

Saiz-Salinas, J. I., and González-Oreja, J. A. (2000). Stress in estuarine communities: Lessons from the highly-impacted bilbao estuary (Spain). *J. Aquat. Ecosystem Stress Recovery* 7, 43–55. doi: 10.1023/A:1009919429985

Saiz-Salinas, J., and Ramos, A. (1999). Biomass size-spectra of macrobenthic assemblages along water depth in Antarctica. *Mar. Ecol. Prog. Ser.* 178, 221–227. doi: 10.3354/meps178221

Schewe, I., and Soltwedel, T. (1999). Deep-sea meiobenthos of the central Arctic ocean: distribution patterns and size-structure under extreme oligotrophic conditions. *Vie Milieu/Life Environ.* 49, 79–92.

Schratzberger, M., and Ingels, J. (2018). Meiofauna matters: The roles of meiofauna in benthic ecosystems. *J. Exp. Mar. Biol. Ecol.* 502, 12–25. doi: 10.1016/j.jembe.2017.01.007

Schwinghamer, P. (1981). Characteristic size distributions of integral benthic communities. *Can. J. Fish. Aquat. Sci.* 38, 1255–1263. doi: 10.1139/f81-167

Schwinghamer, P. (1988). Influence of pollution along a natural gradient and in a mesocosm experiment on biomass-size spectra of benthic communities. *Mar. Ecol. Prog. Ser.* 46, 199–206. doi: 10.3354/meps046199

Schwinghamer, P., Hargrave, B. T., Peer, D., and Hawkins, C. (1986). Partitioning of production and respiration among size groups of organisms in an intertidal benthic community. *Mar. Ecol. Progr Ser.* 31, 131–142. doi: 10.3354/meps031131

Sheldon, R., Prakash, A., and Sutcliffe, (1972). The size distribution of particles in the ocean. *Limnol. Oceanogr.* 17, 327–340. doi: 10.4319/lo.1972.17.3.0327

Shin, Y. J., Rochet, M. J., Jennings, S., Field, J. G., and Gislason, H. (2005). Using size-based indicators to evaluate the ecosystem effects of fishing. *ICES J. Mar. Sci.* 62, 384–396. doi: 10.1016/j.icesjms.2005.01

Shurin, J. B., Gruner, D. S., and Hillebrand, H. (2006). All wet or dried up? real differences between aquatic and terrestrial food webs. *Proc. R. Soc. B: Biol. Sci.* 273, 1–9. doi: 10.1098/rspb.2005.3377

Solan, M., Cardinale, B. J., Downing, A. L., Engelhardt, K. A. M., Ruesink, J. L., and Srivastava, D. S. (2004). Extinction and ecosystem function in the marine benthos. *Science* 306, 1177–1180. doi: 10.1126/science.1103960

Soltwedel, T., Pfannkuche, O., and Thiel, H. (1996). The size structure of deep-sea meiobenthos in the north-eastern Atlantic: nematode size spectra in relation to environmental variables. *J. Mar. Biol. Assoc. United Kingdom* 76, 327–344. doi: 10.1017/S0025315400030587

Sommer, U., Meusel, B., and Stielau, C. (1999). An experimental analysis of the importance of body-size in the seastar-mussel predator-prey relationship. *Acta Oecologica* 20, 81–86. doi: 10.1016/S1146-609X(99)80019-8

Sprules, W., and Bowerman, J. (1988). Omnivory and food chain length in zooplankton food webs. *Ecology* 69, 418–426. doi: 10.2307/1940440

Sprules, W. G., Brandt, S., Stewart, D., Munawar, M., Jin, E., and Love, J. (1991). Biomass size spectrum of the lake Michigan pelagic food web. *Can. J. Fisheries Aquat. Sci.* 48, 105–115. doi: 10.1139/f91-015

Sprules, W. G., Casselman, J., and Shuter, B. (1983). Size distribution of pelagic particles in lakes. *Can. J. Fisheries Aquat. Sci.* 40, 1761–1769. doi: 10.1139/f83-205

Su, C.-C., Tseng, J.-Y., Hsu, H.-H., Chiang, C.-S., Yu, H.-S., Lin, S., et al. (2012). Records of submarine natural hazards off SW Taiwan. *Geological Society London Special Publications* 361, 41–60. doi: 10.1144/SP361.5

Sukhotin, A. A., Abele, D., and Pörtner, H.-O. (2002). Growth, metabolism and lipid peroxidation in mytilus edulis: age and size effects. *Mar. Ecol. Prog. Ser.* 226, 223–234. doi: 10.3354/meps226223

Thompson, G. A., Dinofrio, E. O., and Alder, V. A. (2013). Structure, abundance and biomass size spectra of copepods and other zooplankton communities in upper waters of the southwestern Atlantic ocean during summer. *J. Plankton Res.* 35, 610–629. doi: 10.1093/plankt/fbt014

Vetter, E. W., and Dayton, P. K. (1998). Macrofaunal communities within and adjacent to a detritus-rich submarine canyon system. *Deep Sea Res. Part II: Topical Stud. Oceanography* 45, 25–54. doi: 10.1016/S0967-0645(97)00048-9

Vetter, E. W., and Dayton, P. K. (1999). Organic enrichment by macrophyte detritus, and abundance patterns of megafaunal populations in submarine canyons. *Mar. Ecol. Prog. Ser.* 186, 137–148. doi: 10.3354/meps186137

Volkenborn, N., Meile, C., Polerecky, L., Pilditch, C. A., Norkko, A., Norkko, J., et al. (2012). Intermittent bioirrigation and oxygen dynamics in permeable sediments: An experimental and modeling study of three tellinid bivalves. *J. Mar. Res.* 70, 794–823. doi: 10.1357/002224012806770955

Vranken, G., and Heip, C. (1986). The productivity of marine nematodes. *Ophelia* 26, 429–442. doi: 10.1080/00785326.1986.10422004

Wang, Y. H., Lee, I. H., and Liu, J. T. (2008). Observation of internal tidal currents in the kaoping canyon off southwestern Taiwan. *Estuarine Coast. Shelf Sci.* 80, 153–160. doi: 10.1016/j.ecss.2008.07.016

Warwick, R. M. (2014). Meiobenthos and macrobenthos are discrete entities and not artefacts of sampling a size continuum: Comment on bett, (2013). *Mar. Ecol. Prog. Ser.* 505, 295–298. doi: 10.3354/meps10830

Warwick, R. M., and Clarke, K. R. (1984). Species size distributions in marine benthic communities. *Oecologia* 61, 32–41. doi: 10.1007/BF00379085

Warwick, R. M., and Gee, J. M. (1984). Community structure of estuarine meiobenthos. *Mar. Ecol. Prog. Ser.* 18, 97–111. doi: 10.3354/meps018097

Wei, C.-L., Rowe, G. T., Escobar-Briones, E., Boetius, A., Soltwedel, T., Caley, M. J., et al. (2010a). Global patterns and predictions of seafloor biomass using random forests. *PloS One* 5, e15323. doi: 10.1371/journal.pone.0015323

Wei, C.-L., Rowe, G. T., Escobar-Briones, E., Nunnally, C., Soliman, Y., and Ellis, N. (2012). Standing stocks and body size of deep-sea macrofauna: predicting the baseline of 2010 deepwater horizon oil spill in the northern gulf of Mexico. *Deep Sea Res. Part I: Oceanographic Res. Papers* 69, 82–99. doi: 10.1016/j.dsr.2012.07.008

Wei, C.-L., Rowe, G. T., Hubbard, G. F., Scheltema, A. H., Wilson, G. D. F., Petrescu, I., et al. (2010b). Bathymetric zonation of deep-sea macrofauna in relation to export of surface phytoplankton production. *Mar. Ecol. Prog. Ser.* 399, 1–14. doi: 10.3354/meps08388

Wilson, S. K., Fisher, R., Pratchett, M. S., Graham, N., Dulvy, N. K., Turner, R. A., et al. (2010). Habitat degradation and fishing effects on the size structure of coral reef fish communities. *Ecol. Appl.* 20, 442–451. doi: 10.1890/08-2205.1

Wrede, A., Andresen, H., Asmus, R., Wiltshire, K. H., and Brey, T. (2019). Macrofaunal irrigation traits enhance predictability of nutrient fluxes across the sediment-water interface. *Mar. Ecol. Prog. Ser.* 632, 27–42. doi: 10.3354/meps13165

Yurista, P. M., Yule, D. L., Balge, M., VanAlstine, J. D., Thompson, J. A., Gamble, A. E., et al. (2014). A new look at the lake superior biomass size spectrum. *Can. J. Fish. Aquat. Sci.* 71, 1324–1333. doi: 10.1139/cjfas-2013-0596

frontiers | Frontiers in Marine Science

TYPE Original Research
PUBLISHED 18 May 2023
DOI 10.3389/fmars.2023.1180334

OPEN ACCESS

EDITED BY
Jaime Selina Davies,
University of Plymouth, United Kingdom

REVIEWED BY
Chih-Lin Wei,
National Taiwan University, Taiwan
Fabio Cabrera De Leo,
University of Victoria, Canada

*CORRESPONDENCE
Katharine T. Bigham
katie.bigham@vuw.ac.nz

†PRESENT ADDRESS
Arne Pallentin,
Seafloor Maps Ltd., Wellington,
New Zealand

RECEIVED 06 March 2023
ACCEPTED 25 April 2023
PUBLISHED 18 May 2023

CITATION
Bigham KT, Rowden AA, Bowden DA, Leduc D, Pallentin A, Chin C, Mountjoy JJ, Nodder SD and Orpin AR (2023) Deep-sea benthic megafauna hotspot shows indication of resilience to impact from massive turbidity flow.
Front. Mar. Sci. 10:1180334.
doi: 10.3389/fmars.2023.1180334

Deep-sea benthic megafauna hotspot shows indication of resilience to impact from massive turbidity flow

Katharine T. Bigham[1,2*], Ashley A. Rowden[1,2], David A. Bowden[1], Daniel Leduc[1], Arne Pallentin[1†], Caroline Chin[1], Joshu J. Mountjoy[1], Scott D. Nodder[1] and Alan R. Orpin[1]

[1]National Institute of Water and Atmospheric Research (NIWA), Wellington, New Zealand, [2]School of Biological Sciences, Victoria University of Wellington, Wellington, New Zealand

Sediment density flows are large scale disturbances that can have dramatic impacts on seafloor animal communities in the deep sea. Seafloor imagery collected in Kaikōura Canyon (New Zealand), before and after a sediment density flow event that included debris and turbidity flows triggered by a 2016 M_w 7.8 Kaikōura Earthquake, shows the recovery trajectory of the animal community in the canyon head in the weeks, months, and years following the disturbance. The canyon community appears resilient to this event, with models estimating full recovery within a minimum of 4.5–5.1 years and as long as 12 years. The implications of the resilience of this deep-sea community are discussed in the context of the local marine protected area, the surrounding fishery, and global seabed mining.

KEYWORDS

deep sea, morphology, resilience (environmental), megafauna, benthic community, disturbance, canyon, turbidity flow

1 Introduction

Disturbance structures all marine communities by freeing limiting resources (space, refuge, nutrients, etc.) and creating habitat heterogeneity, which influences succession and enhances biodiversity (Sousa, 1984; Willig and Walker, 1999; Sousa, 2001). Subaqueous sediment-density flows are one of the largest and potentially the most pervasive and persistent physical disturbances in the deep sea (Meiburg and Kneller, 2010; Talling et al., 2013; Azpiroz-Zabala et al., 2017; Bigham et al., 2021). Sediment density flows occur when the material in submarine landslides disintegrates and mixes with water creating high-density bodies of turbid water filled with suspended sediment that travel downslope beneath less dense water (Kuenen and Migliorini, 1950; Talling, 2014). Sediment density flows are complex and a single event can contain multiple flow types such as debris flows and turbidity flows (Haughton et al., 2003; Talling et al., 2007; Paull et al., 2018). As such, many terms and classification schemes have been proposed to differentiate flow types, although

confusion around the use of these terms still occurs (Kuenen and Migliorini, 1950; Lowe, 1979; Talling et al., 2012). Here we will mainly use the term "turbidity flow" sensu (Kuenen and Migliorini, 1950) because it is the common overarching term used for sediment density flows in the ecological literature.

Turbidity flows occur worldwide and transport large volumes of sediment and associated organic matter across long distances, from the continental slope to the abyssal plain (e.g., the earthquake-triggered Grand Banks turbidity flow transported and deposited >175 km^3 sediment across an area of 240 000 km^2 (Piper and Aksu, 1987)). These flows impact the benthic faunal communities in their path across a range of spatial scales through both erosional and depositional processes. The immediate pulse-type of impact from the high velocity flows can entrain bottom substrates, leading to mass benthic mortality through dislodgment by erosion, and sediment smothering or transport and burial by sediment deposition as flow velocities wane (Young and Richardson, 1998; Oguri et al., 2013; Bigham et al., 2021). Longer term press-type impacts include persistent turbid waters which can form benthic nepheloid layers (distinct near-bed layers that contain elevated suspended sediment concentrations), which can also be derived from resuspension by secondary disturbances from storms or earthquake aftershocks (Kawagucci et al., 2012; Wakita et al., 2022). Prolonged elevated benthic turbidity can impair feeding and cause mortalities, especially for suspension and filter feeders (Rubenstein and Koehl, 1977; Schönberg, 2016; Abdul Wahab et al., 2017), and can delay an organism's ability to colonize the disturbed patches of the seafloor (Clark et al., 2016) or even, in the case of aftershocks, cause additional mortalities of colonizing fauna (Heezen et al., 1964; Tyler and Ramirez-Llodra, 2002; Harris, 2014). Turbidity flows can also create completely new habitats in the deep sea by uncovering or creating new resources. For example, chemosynthetic communities, unique assemblages of organisms that are fuelled by reduced chemical compounds rather than photosynthetic detritus (Sibuet and Olu, 1998), will occur where there is enough decaying organic material to support reducing conditions (Gooday et al., 1990). Turbidity flows can transport labile organic matter into the deep sea (Stetten et al., 2015; Pruski et al., 2017; Gibbs et al., 2020; Hage et al., 2020) which can in turn initiate the development of reducing habitats, and thus chemosynthetic communities, both through the burial of large volumes of organic material and through exposure of methane-bearing sediments by erosion (Rathburn et al., 2009). In general, whether by transport of coastal and slope sediments, or exposure from down-cutting, turbidity flows can increase the availability of organic matter and create nutrient-enriched environments in the deep sea. The availability of this organic matter has been hypothesized to influence benthic communities at abyssal depths in the deep sea (Heezen et al., 1955).

While it is evident that disturbance from turbidity flows can have an impact on deep-sea benthic communities, it is less clear to what extent these communities are resilient to the impacts of turbidity flows. Here the definition of resilience used is Holing's "ecological resilience" which refers to the amount of disturbance that a system can experience before changing to an alternative state (Holling, 1996) and considers both the community's resistance (how similar it remains to the pre-disturbance state despite the disturbance (Walker et al., 2004)) and recovery (ability to return to pre-disturbance state (Folke et al., 2004)). Studies following the M_w 9.0 2011 Tōhoku Earthquake-triggered turbidity flow showed rapid recovery of the meiofaunal communities (Kitahashi et al., 2014; Kitahashi et al., 2016; Nomaki et al., 2016). In contrast, studies of ancient turbidity flows, hundreds to many thousands of years old, inferred that the impact of flows on mega- and macrofauna communities may still be detectable (Griggs et al., 1969; Huggett, 1987; Briggs et al., 1996). However, studies of older turbidity flows are often confounded by local patterns of organic matter input from surface productivity and/or terrigenous inputs that have occurred in the intervening time (Richardson et al., 1985; Richardson and Young, 1987; Thurston et al., 1994; Thurston et al., 1998). Many studies, even ones of more recent turbidity flows, lack sufficient pre-disturbance data and high temporal resolution post-disturbance data to disentangle the impacts of turbidity flows on benthic communities and assess their likely resilience to these disturbances (Galéron et al., 2009; van Gaever et al., 2009). Kaikōura Canyon off eastern New Zealand is the site of a recent and major earthquake-triggered turbidity flow, with the additional context of pre-event benthic data.

Kaikōura Canyon was identified previously as a globally significant benthic productivity hotspot due to an abundant macro- and megafaunal biological community with biomasses 100 times higher than other (non-chemosynthetic) deep-sea habitats below 500 m water depth (De Leo et al., 2010). The reasons proposed for such a hotspot include habitat heterogeneity, high food availability *via* channelling of pelagic and terrestrial organic matter, and physical disturbance from past submarine landslides and turbidity flows (De Leo et al., 2010). Kaikōura Canyon also supports a distinct meiofaunal community that is believed to reflect high food availability and high frequency of disturbance, and which contributes significantly to regional meiofaunal diversity (Leduc et al., 2014).

On 14th November 2016, the M_w 7.8 Kaikōura Earthquake triggered a 1-in-140 year highly complex "full canyon-flushing event" that reshaped the canyon floor and transported an estimated 850 metric megatons of sediment and 7.5 metric megatons of carbon through the canyon and out along the Hikurangi Channel (Mountjoy et al., 2018). This event included submarine landslides, and other local mass-wasting episodes, as well as debris flow and turbidity flows from the canyon walls and along the canyon floor. Comparison of pre- and post-event multibeam echosounder-derived bathymetric data showed that in some locations up to 50 m of the canyon floor was eroded, while deposition was apparently more localized and at most up to a few metres. Preliminary analysis of camera imagery collected 10 weeks after this event indicated that the turbidity flow had been catastrophic for the once productive benthic community on the canyon floor (Mountjoy et al., 2018). Repeat photographic transects were subsequently collected at previously sampled sites 10 months and 4 years after the event. With these data from before and after the turbidity flow, Kaikōura Canyon provides a unique opportunity to examine the resilience of benthic communities to such large disturbances in the deep sea over time scales of weeks to years.

The aim of the present study is to compare seabed megafauna community structure before and after the Kaikōura Canyon turbidity

flow to determine the community response to the large-scale disturbance. The management implications for the Hikurangi Marine Reserve, which includes most of Kaikōura Canyon, and the region's productive deep-sea fishery are considered, along with the potential of turbidity flows to be used as proxies for predicting the impacts of large physical disturbances caused by global deep-sea mining in the future.

2 Methods

2.1 Study site

Kaikōura Canyon is located off the northeastern coast of New Zealand's South Island (Figure 1). The canyon is 60 km long, ranges in water depth from around 20 m to > 2000 m, is generally U-shaped in profile, and is the primary source for the 1500 km-long Hikurangi Channel, which transports erosional sediments from the Southern Alps to a distal abyssal plain. The head of the canyon cuts deeply into a narrow shelf, bringing it within 500 m of the shore (Lewis and Barnes, 1999). Photographic data used in this study were collected from the head of the canyon, near the beginning of the turbidity flow path and where significant erosion occurred (Figure 1).

2.2 Image collection

Photographic surveys of the seafloor were conducted in Kaikōura Canyon from the R/V *Tangaroa* 10 years before the turbidity flow in November 2006 (De Leo et al., 2010), and 10 weeks, 10 months, and 4 years after the turbidity flow event in February 2017 (Mountjoy et al., 2018), September 2017, and October 2020, respectively. These surveys were all carried out using NIWA's towed camera system, DTIS (deep-towed imaging system) (Hill 2009). DTIS is a battery-powered towed camera frame that records both high-definition video and high definition still images taken every 15 seconds. The downward facing still image camera resolution was 8 megapixels (Canon EOS 350D) in 2006 and 24 megapixels (Nikon D3200) in 2017 and 2020. Target speed and height above seafloor were 0.3-0.5 ms^{-1} and 2-3 m, respectively. Parallel lasers 20 cm apart were projected onto the seabed and used to calculate the seafloor area in each image. Five of the transects conducted in the 2006 survey at the head of the canyon were repeated during the subsequent voyages using the R/V *Tangaroa's* dynamic positioning (Figure 1). Positioning of DTIS is monitored in real time using an acoustic ultra-short baseline (USBL) transponder system (Kongsberg HiPAP). Distance between repeated transects ranged between 0 and 50 m, and was mostly < 20 m. Transects varied in length between 1.02 and 1.52 km and were between water depths of 900 and 1200 m (see Table S4 for transect details).

2.3 Bathymetric data collection

Bathymetric data were collected using hull-mounted multibeam echosounders on the R/V *Tangaroa* 10 years before (Kongsberg EM300) and 8 months after the turbidity flow (Kongsberg EM302). Bathymetric data was also collected 4 years after the turbidity flow

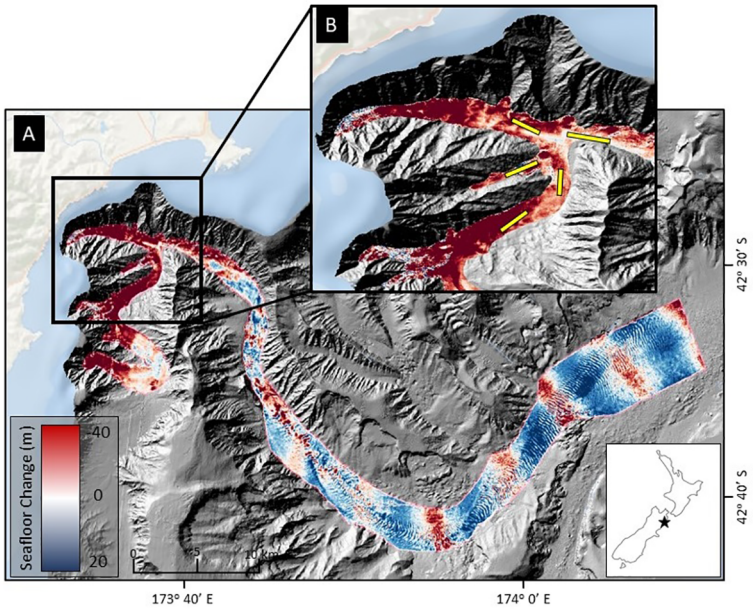

FIGURE 1
Location of photographic transects in upper Kaikōura Canyon overlayed on sediment density flow-induced bathymetry changes, following the November 2016 M_w 7.8 Kaikōura Earthquake. **(A)** Magnitude of erosion (red) and deposition (blue) within Kaikōura Canyon caused by the earthquake-triggered canyon flushing event, measured by the differencing the pre- and post-earthquake bathymetry data sets (Mountjoy et al., 2018). In this figure, the shelf break occurs where the pale blue bathymetry meets the gray canyon edge, generally around 80-100 m. The floor of the canyon ranges between 400 m and 2000 m. **(B)** Location of the time-series of towed camera transects (yellow lines) within the head of Kaikōura Canyon. The floor of the canyon in this figure ranges between 400 and 1200 m. Inset shows the location of Kaikōura Canyon (star) relative to New Zealand.

using a multibeam echosounder mounted on a HUGIN 3000 Autonomous Underwater Vehicle (AUV *RAN*; Kongsberg EM2040) deployed from R/V *Tangaroa*. Processed data were gridded at 25 m cell size resolution and exported to ESRI grid formats for use in ArcGIS Pro. From these grids, using the benthic terrain modeler package (Walbridge et al., 2018) seafloor terrain variables were generated: mean and standard deviation of depth, "Northness" (cosine of the aspect), "Eastness" (sine of aspect), seafloor ruggedness calculated as the vector ruggedness measure (VRM), mean, plan, and profile curvature, and mean and standard deviation of slope. All seafloor terrain variables were generated at five focal means (number of cells: 1 x 1, 3 x 3, 5 x 5, 15 x 15, 25 x 25), and standard deviations and ruggedness measures were calculated at grid sizes of 3 x 3, 5 x 5, 7 x 7, 15 x 15 for each focal mean. Due to AUV-collected bathymetry covering a smaller area than the shipboard multibeam it was not possible to get full overlapping coverage of all computed variables at all focal means for all times.

Pressure values were obtained from a SeaBird MicroCat Conductivity-Temperature-Depth (CTD) instrument (Model: SBE 37) attached to DTIS during each transect. The CTD took measurements at 15 second increments 10 years before, 10 weeks after, and 4 years after, and at 180 second increments 10 months after the turbidity flow. These pressure measurements were converted to depth in metres (+/- 0.01 m).

2.4 Image annotations

The online image analysis tool BIIGLE 2.0 (Langenkämper et al., 2017) was used to annotate all visible megafauna (invertebrates and fish > 2 cm; 40 labels), life traces of both epi- and infauna known as '*lebensspuren*' (tracks, mounds, burrow holes etc; 20 labels), and substrate types (muddy sediment, dark grey sediment, blocky sediment, boulder, cobble, pebble, and bacterial mat; 7 labels) in all images for the five transects repeated at the four times (5,795 images in total). High densities of *lebensspuren* were noted in the canyon prior to the turbidity flow (De Leo et al., 2010). These biogenic structures provide insights into community function such as those related to bioturbation (turnover of sediments and nutrients) (Belley et al., 2010). Bioturbation is a critical controlling factor for oxygen penetration and organic carbon reworking in sediments (Meysman et al., 2006) and including the factor in analysis of community structure provides insight not otherwise attainable from the environmental metrics obtained from the bathymetry or imagery. The abundance of *lebensspuren* believed to not be associated with megafauna also annotated in the imagery (mounded and nested faecal casts and all dwelling traces except for elongated depressions; 9 labels, Table S2) were summed to represent "bioturbation" and included as an environmental factor in subsequent analysis (see below).

Visible fauna were identified to the lowest possible taxonomic level using standard taxonomic guides for the area (Tracey et al., 2011; McMillan et al., 2019) and with the assistance of taxonomists and para-taxonomists (see Acknowledgements). Some of the initial taxa identifications were combined to a higher taxonomic level before the final analysis to ensure consistency of identification across all times (Table S1). Best practices recommended for annotation labels of image- derived data were used where possible (Horton et al., 2021). *Lebensspuren* were identified using a regional guide ((Przeslawski et al., 2012); Table S2), and sediment substrates were categorized according to the Wentworth Scale (Wentworth, 1922). Counting the number of individuals or individual colonies was straightforward for most taxa, except for burrowing ophiuroids and the foraminiferan *Bathysiphon filiformis*. Burrowing ophiuroids were only partially observable, and so counts for this taxon were determined by dividing the number of arms observed above the seafloor by two, the number of arms typically observed above the sediment in aquaria studies (Hollertz et al., 1998). Due to large numbers of *B. filiformis* observed 4 years after the turbidity flow, total counts per image of this species for this time point were determined by making counts from subsets of the image. The images were gridded into nine equal rectangles (3 x 3 grid), and then a sub-set of four of the rectangles were randomly selected using a random number generator. All *B. filiformis* within the four randomly selected rectangles were then counted and the total number of individuals in the images four years after were estimated by scaling up from the subset (i.e., sum of *B. filiformis* in subset was multiplied by 9/4 = 2.25). Four rectangles was chosen as the number to analyze for its balance between sampling enough of the image and the amount of time necessary to obtain a reliable estimate of abundance (based on comparing counts of *B. filiformis* in each rectangle to the total number per image for those images taken before the turbidity flow).

Fauna abundances were standardized to 1 m^2 of the seafloor and substrate area was standardized to percentage of the full image area prior to analysis.

2.5 Image data treatment

Only images from portions of transect that overlapped between surveys and with imaged seafloor areas between 0.5 and 2.5 m^2 were selected from the five transects at the four times (2,768 images in total). The selected image area range was determined by first making plots of the numbers of taxa and individuals annotated per image by the area of each image (for transects collected 10 years before, 10 weeks after, and 10 months after the turbidity flow event). These plots were used to identify the area range where the two univariate community metrics were not influenced by the area of the image analyzed (Figure S1). Images outside this identified range were excluded to reduce any effect of seafloor area on the analysis, including to ensure that smaller organisms only detectable when the camera is close to the seafloor, or in later years when the camera quality improved, did not bias identification and abundance data. Data from 4 years after the turbidity flow event were not used to identify the seafloor area range to use for the data analysis because image analysis had begun before these data were collected.

The contiguous images along the transect were assigned to 'sample groups' with a maximum of ten images and a minimum of four images per group. Sample group membership was determined using a multivariate measure of pseudo standard error known as "MultiSE" (Anderson and Santana-Garcon, 2015) applied to the Kaikōura Canyon megafauna data. MultiSE evaluates the amount

of variation in the position of group centroids in the space of the chosen dissimilarity measure (in this case Bray-Curtis) under repeated sampling. When applied to a series of sample group sizes MultSE can be used to determine when increasing the sample group size no longer results in greater precision (Anderson and Santana-Garcon, 2015). Creating sample groups allows for less computer intensive statistical analyses to be run while still accounting for variation along the transects as opposed to using data for every image in each transect. An alternative could have been to use average data for each transect; however, using average data would have caused issues for some of the selected analyses. For example, using the sample groups was necessary for running the DISTLM analysis (see below) because this analysis cannot be run if the ratio of variables to samples is too low (as would be the case with transect centroids).

Environmental variables derived from the bathymetry layers were extracted for each image based on the latitude and longitude of each image, and the average of these values was taken for each sample group. Water depth measurements derived from the CTD were assigned to each image or sample group (only done for 10 months after the turbidity flow when CTD sampling increment was larger and more aligned with sample group increments then individual image increments) based on timestamps associated with each image/sample group and the CTD measurements.

2.6 Statistical analysis

Unless noted, statistical analyses were carried out using routines in PRIMER 7 (Clarke and Gorley, 2018) with PERMANOVA + (Anderson et al., 2008).

2.6.1 Data treatment

Prior to running statistical tests, data transformation for down-weighting of abundances and the use of a zero-adjusted Bray-Curtis measure were applied to image level data. Down-weighting *via* transformation (square root or fourth root) lowers the influence of highly abundant taxa and makes the influence of rarer taxa to the community structure clearer (Clarke and Green, 1988; Clarke et al., 2006). Fourth root transformation was used for fauna abundances. The zero-adjusted Bray-Curtis measure adds a constant or "dummy species" of uniform abundance (1 individual) to all samples, which results in any comparisons between pairs of samples in which no fauna were recorded yielding zero dissimilarity. This method assumes such samples are that way for the same reason (Clarke and Gorley, 2018). This assumption is reasonable for samples in the Kaikōura Canyon time-series dataset because the samples with no records are primarily from the time point immediately after the turbidity flow and are assumed to be due to the disturbance.

2.6.2 Community structure

Variability in community structure through time was tested using main and pair-wise permutational multivariate analysis of variance (PERMANOVA). Sample group centroids were calculated from the zero-adjusted Bray-Curtis similarities between the transformed fauna abundances from the images providing similarity matrices for multivariate community structure data. The PERMANOVA was run on this sample group centroid similarity matrix with Type III (partial) sums of squares, unrestricted permutation of raw data and 9999 permutations. The results of this multivariate community structure analysis were visualized using three- and two-dimensional non-metric multi-dimensional (nMDS) ordination plots for fauna. The nMDS plots were made using data for sample group centroids and transect centroids. While the centroids allow for faster computation of tests, they also provide multiple ways of visualizing the data cloud and greater clarity of overall patterns. The RELATE, MVDISP, and PERMDISP routines were used to evaluate the patterns observed in the nMDS plot for sample group centroids and were therefore based on these data.

The recovery trajectory of fauna was evaluated with a RELATE test of cyclicity (Correlation method: Spearman rank (ρ), Number of permutations: 9999). This test measures how closely the fauna community structure through time matches a simple cyclical model (H_o: no cyclicity exists, $\rho \approx 0$), i.e., community recovery towards original community state (Clarke and Gorley, 2018). Other patterns of recovery are possible, but in general communities follow a gradual progressive return to their original state that is described by a cyclical model (Holling, 1973).

The MVDISP routine determines the multivariate dispersion of the samples at each time point. This dispersion can be interpreted as the relative amount of heterogeneity or homogeneity at each time point and is an indication of a community's response to disturbance, with higher variability being expected at disturbed sites (Warwick and Clarke, 1993). Permutational Analysis of Multivariate Dispersion (PERMDISP) (Number of permutations: 9999) was used to determine the significance of differences in the multivariate dispersion (Anderson et al., 2008). The SIMPER routine was run on all images and used to determine the contribution of the fauna to within and between community similarity for each time point. It was not possible to run the SIMPER analysis on the sample group centroids since both SIMPER and calculating centroids are run on the abundance matrix and generate a similarity/dissimilarity of the resemblance matrix (Anderson et al., 2008; Clarke and Gorley, 2018). Since centroids are not the same as averages (Anderson et al., 2008), the SIMPER analysis was done on the image level data to match the data used to generate the sample group centroids.

2.6.3 Environmental drivers

Distance-based multivariate linear regression models (DISTLM) were used to assess the relationship between environmental parameters and the faunal community structure for four of the five transects (the Gully site was not used because it lacked bathymetry data from the 4 years after time point). The DISTLM method creates regression models of the relationship between a multivariate data cloud and multiple predictor values (McArdle and Anderson, 2001). Correlation between environmental variables was checked before running the DISTLM using draftsman plots and correlation matrices. When Pearson's r was >0.8 between variables, the variable which was correlated with the greater number of other variables was excluded from the analysis. If more than one variable

correlated with others, the variable with the most correlations was kept and where possible the variable with the least missing data for the sample groups was kept (generally the variable with the smaller focal mean). In addition, variables with missing data for sample groups, primarily those variables at the larger focal means (25x25 and 15x15), were also omitted from the analysis. Values for the sediment and bioturbation variables derived from the images, except for muddy sediment, were transformed by $\log_{10}(0.1+\text{variable})$ to normalize their distribution. Following this process, 27 environmental variables (see bolded variables in Table S3) were used in a DISTLM for megafauna. The DISTLM was run with distance among sample group centroids as input data, stepwise variable selection, the Akaike Information Criterion (AIC) and 9999 permutations. Distance-based redundancy analysis (dbRDA) plots were used on sample group centroids to visualize the results of the DISTLM. dbRDA performs an ordination of fitted data based on the best model proposed by the DISTLM test (Anderson et al., 2008).

2.7 Predicting recovery

To estimate when the post-turbidity flow community in Kaikōura Canyon may recover to be similar to the pre-disturbance community, rates of recovery were predicted by fitting the observed similarities between the pre-turbidity and three post-turbidity communities to three common models of population growth [linear, exponential, logistic; (Lundquist et al., 2010; Solé et al., 2010)] using the generalized linear model and nonlinear least squares functions in R (R Core Team, 2022). Recovery in deep-sea habitats has been best modelled by a variety of population models (Barnthouse, 2004; Sciberras et al., 2018). Individual taxa within a community can display different population growth responses (McClanahan et al., 2007), and therefore to estimate the recovery of communities made up of many populations it is sensible to use a multiple population model approach. Studies generally consider a community recovered when it is no longer statistically different from the pre-disturbance or reference community (Bluhm, 2001; Jones et al., 2012; Wan Hussin et al., 2012; Jones et al., 2017). This recovery threshold has not yet been reached by the Kaikōura Canyon benthic community 4 years after the turbidity flow. Studies of shallow marine environments have found this point to be when the disturbed community is anywhere between 50 and 80% similar to an undisturbed community (Blyth et al., 2004; Smale et al., 2008). Rather than use an arbitrary similarity threshold, for the purposes of this predictive analysis it was assumed that the community could be considered recovered when it at least reaches the level of within-group similarity exhibited by the pre-turbidity flow community (i.e., 60%). That is, the difference between the average similarity of the post-turbidity flow community and the pre-turbidity community should be equivalent or greater than the variation expressed within the community before the disturbance. This recovery threshold is considered a minimum, and the level of similarity achieved when the pre- and post-turbidity are no longer significantly different may be higher.

3 Results

3.1 Community response to the turbidity flow

The Kaikōura Canyon megafauna community is recovering following the impact of the turbidity flow, though it is not identical in structure to the pre-disturbance community. This recovery is illustrated in multivariate ordinations of community similarity that show clustering of megafauna samples by time point (Figures 2A, B). The community was only 11-14% similar to the

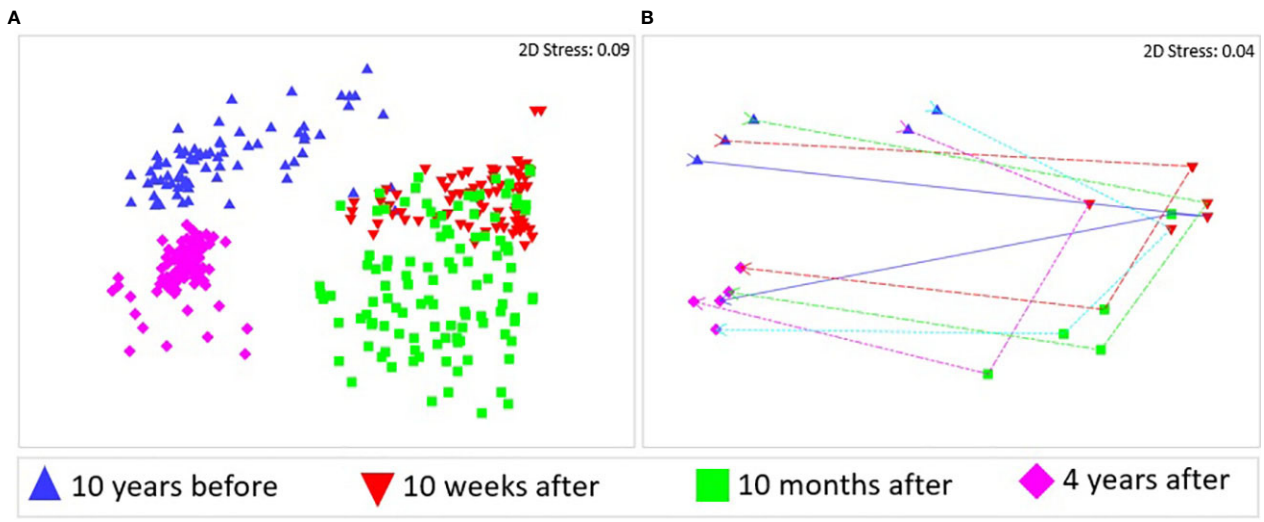

FIGURE 2
Non-metric multidimensional scaling (nMDS) ordinations of megafauna community similarity 10 years before the turbidity flow event and at 10 weeks, 10 months, and 4 years after it. **(A)** using centroids of sample groups (clusters of images), and **(B)** using centroids of transects. The lines follow transects through time. Similarities were calculated from zero adjusted, fourth root transformed fauna abundances and all stress values are <0.2, indicating that the plots are acceptable representations of the similarity patterns.

pre-disturbance community in the weeks and months after the turbidity flow, but by 4 years after the event, the community was 51% similar (Table 1). The recovery appears cyclical in nature in the ordination plots, though not yet complete, which is supported by the result of a test for cyclicity ($\rho = 0.57$, $p < 0.01\%$). The community structure differed significantly between all time points (PERMANOVA, $p<0.0001$ for all comparisons, Table 2). Community variability (dispersion) (Figure 2A) was greatest 10 months after the turbidity flow (1.265), then decreased as recovery progressed towards the pre-earthquake community structure (, 4 years after: 0.628), and was significantly different between all time points (Pseudo-F = 40.721, P(perm) = 0.0001).

3.2 Individual taxa contribution to the observed community response

The foraminiferan *Bathysiphon filiformis* was the only taxon that contributed consistently to the similarity of the communities at each time point. This species was the highest contributor to community similarity both 10 years before and 4 years after the turbidity flow, contributing 60% and 91% of the within time point similarity, respectively (Table 1).

Community dissimilarity among time points was generally explained by two to five taxa. *Bathysiphon filiformis* had the highest contribution to all dissimilarities among times, except for between 10

TABLE 1 SIMPER analysis results.

Time point/ Comparison	Average similarity	Influential fauna	% Contribution	Time 1 Avg. Abundance	Time 2 Avg. Abundance
10 years before, 10 weeks after	59.59	*Bathysiphon filiformis*	60.74	178.51	
		Ophiuroid	28.91	0.02	
	16.53	*Coryphaenoides subserrulatus*	60.50	0.29	
		Bathysiphon filiformis	35.20	0.70	
10 months after, 4 years after	31.23	Holothurian	54.97	5.43	
		Bathysiphon filiformis	24.63	2.18	
	72.77	*Bathysiphon filiformis*	90.68	581.58	
10 years before, 10 weeks after	10.62	*Bathysiphon filiformis*	43.83	178.51	0.70
		Ophiuroid	22.91	0.02	0
		Mysida	8.16	1.96	0.05
10 years before, 10 months after	14.27	*Bathysiphon filiformis*	37.31	178.51	2.18
		Ophiuroid	20.59	0.02	0
		Holothurian spp.	11.89	0	5.43
		Mysida	7.64	1.96	0.09
10 years before, 4 years after	48.80	*Bathysiphon filiformis*	29.77	178.51	581.58
		Ophiuroid	20.59	0.02	0
		Mysida	8.51	1.96	0.25
		Echiuran	6.34	0.61	0.10
		Astropectinidae	5.91	0.05	0.35
10 weeks after, 10 months after	14.17	Holothurian spp.	33.59	0.01	5.43
		Bathysiphon filiformis	26.57	0.70	2.18
		Coryphaenoides subserrulatus	23.28	0.30	0.40
10 weeks after, 4 years after	10.60	*Bathysiphon filiformis*	66.59	0.70	581.58
		Coryphaenoides subserrulatus	5.95	0.30	0.25
10 months after, 4 years after	15.20	*Bathysiphon filiformis*	58.91	2.18	581.58
		Holothurian spp.	10.57	5.43	0.83
		Coryphaenoides subserrulatus	5.85	0.40	0.25

SIMPER analysis results indicating average within and between time point community similarity and the individual megafaunal taxa key to the within or between time point community variation (contributing 70% or more cumulatively). Avg. Abundance is the untransformed average abundance of individuals per m^2.

10.3389/fmars.2023.1180334

TABLE 2 Main and pair-wise PERMANVOA tests results.

Test	Comparison	Psuedo-F/t statistic	P(perm)
Main		189.400	0.0001
Pair-wise	10 years before, 10 weeks after	12.988	0.0001
	10 years before, 10 months after	14.641	0.0001
	10 years before, 4 years after	10.593	0.0001
	10 weeks after, 10 months after	7.847	0.0001
	10 weeks after, 4 years after	16.813	0.0001
	10 months after, 4 years after	18.140	0.0001

PERMANOVA test results for the differences between times for megafauna community structure. Pseudo-F statistic = multivariate analogue to Fisher's F statistic; ratio of the between cluster variation to the within cluster variation. t-statistic = ratio of the difference in group means to the pooled standard error. P(perm) = permutation P-value.

weeks after and 10 months after the turbidity flow, when it was the second highest contributor behind Holothuroidea spp. Other taxa that contributed to the community dissimilarity included Astropectinidae sea stars, Mysida crustaceans, Echiura spoon worms, and the rattail fish *Coryphaenoides subserrulatus* (Table 1). Abundances for *B. filiformis*, Astropectinidae, Mysida, Echiura, and Ophiuroidea decreased in the weeks and months following the turbidity flow and then increased towards recovery 4 years after the event. However, only *B. filiformis* and Astropectinidae abundances increased above pre-event levels (Figure 3A). The two exceptions to the general trend seen in the key taxa were *C. subserralatus* and Holothuroidea spp. Abundance of *C. subserralatus* increased above pre-disturbance levels 10 weeks and 10 months after the turbidity flow before decreasing to around pre-turbidity flow levels by 4 years after the event (Figure 3B). While Holuthuroidea spp. abundances increased considerably 10 months after the turbidity flow and remained higher than pre-event levels by 4 years after the disturbance (Figure 3B).

3.3 Environmental variation related to the benthic community response

The best distance-based multivariate multiple regression model (AIC = 1953.6, R^2 = 0.4910, RSS = 222,860) for megafauna included 18 environmental variables derived from bathymetry, physical oceanography, and imagery data, 14 of which were significantly correlated to the community structure (p-value ≤ 0.05) and explained 49.1% of the sample variation across all time points. The dbRDA visualization of this model is available in the supplementary material

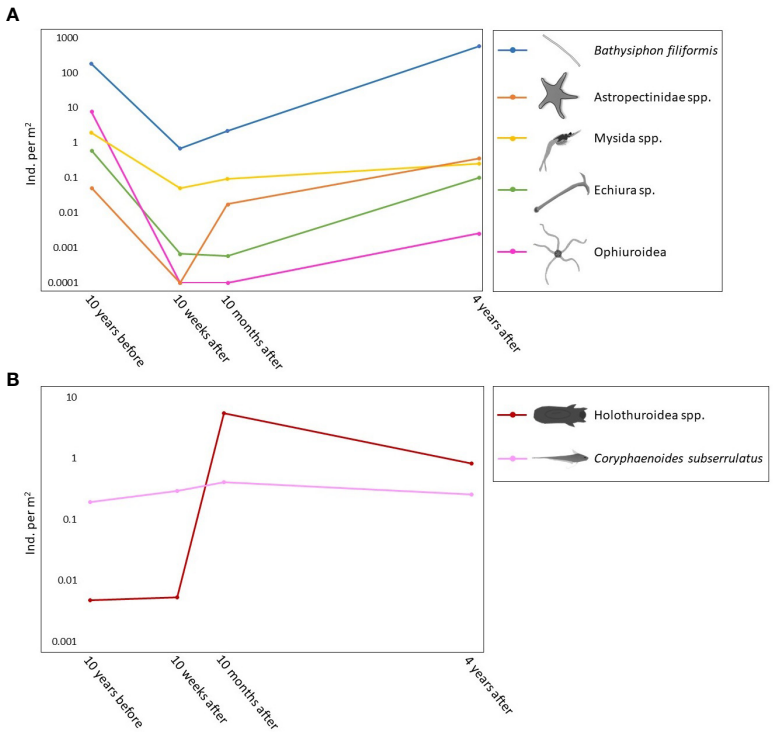

FIGURE 3
Line plots showing the change in abundance of key megafaunal taxa identified by the SIMPER analysis. **(A)** Primary pattern for five of the seven key taxa (*B. filiformis*, Astropectinidae, Mysida, Echiura, and Ophiuroidea); abundances decreased immediately after the turbidity flow but increased towards or above pre-event levels by 4 years after the event. The two exceptions to this pattern were **(B)** the rattail fish *Coryphaenoides subserrulatus*, which increased in abundance above pre-event levels 10 weeks and 10 months after the turbidity flow and Holothuroidea spp. which increased considerably in abundance 10 months after the turbidity flow and remained higher than pre-event levels by 4 years after the event. Scale for both plots is logarithmic.

(Figure S2). Bioturbation and the standard deviation of water depth (FM: 3 x 3, GS: 3 x 3) explained most of the community variation (11.1% and 8.9%, respectively) (Table 3). Bioturbation and standard deviation of depth were much lower and higher (respectively) 10 weeks, 10 months after, and 4 years after the turbidity flow compared to 10 years before the event (Figure 4). While the depth (measured by the seafloor imaging vehicle's onboard Conductivity-Temperature-Depth instrument), and substrate areas and *lebensspuren* (visible life traces of infauna used as proxy for bioturbation) were measured at the same spatial scale as the taxa, there was a discrepancy in spatial scale between the images (meter scale) and the multibeam echosounder-derived bathymetric variables (tens to hundreds of metres scale). This discrepancy may be why the regression model did not account for larger proportion of the total variation, although there are also other possible reasons for the model explaining only half of the variation in community structure across all time points (see Discussion). It must be noted that the highly correlated variables removed from this analysis could also likely explain the same variation in community structure; generally, the variables in Table 3 were correlated with the same variables at higher focal means.

3.4 Predicting the recovery of the megafauna community

Rates of recovery for the megafauna community were estimated using three different population growth models (linear, exponential, and logistic). These models estimate that the impacted benthic community could become as similar to the pre-disturbance community as the pre-disturbance community is to itself (60% within-group similarity) between 4.5 to 5.1 years after the turbidity flow. The shortest time to this predicted recovery threshold is modelled by both exponential and logistic growth and the longest is modelled by linear growth. However, achieving levels of similarity with the pre-disturbance community above this minimum threshold of recovery were predicted to take up to 12 years (Figure 5).

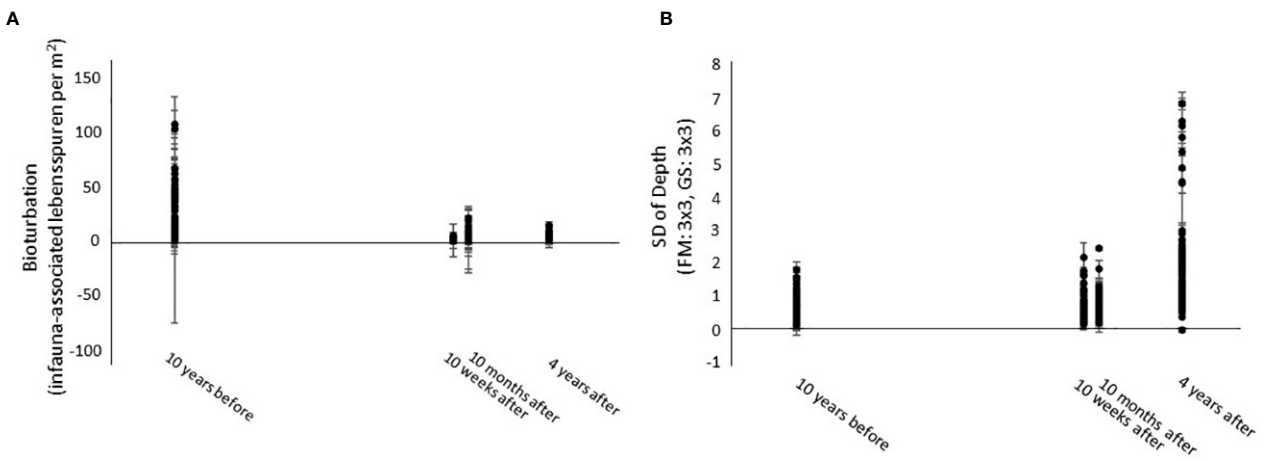

FIGURE 4
Scatter plots of the two most important environmental factors identified by the DISTLM analysis as influencing megafauna community structure. **(A)** Bioturbation (infauna-associated *lebensspuren* per m^2) and **(B)** Standard deviation of depth (FM: 3x3, GS: 3x3).

TABLE 3 DISTLM results.

Variable	AIC	SS (trace)	Pseudo-F	*p*	Prop.	Cumulative Prop.
Fauna						
Bioturbation	2080.3	48423.0	35.564	0.0001	0.1106	0.1106
SD of Depth (FM: 3 x 3, GS: 3 x 3)	2051.9	39079.0	31.791	0.0001	0.0893	0.1999
Slope (FM: 1 x 1)	2030.2	27657.0	24.342	0.0001	0.0632	0.2630
Depth	2020.4	12876.0	11.762	0.0001	0.0294	0.2924
Plan Curvature (FM: 15 x 15)	2013.9	9059.0	8.495	0.0001	0.0207	0.3131

DISTLM results for the sequential tests for the megafauna community structure. Only variables contributing more than 2% to the community variation explained are listed. FM = focal mean, GS = grid size, AIC = Akaike Information Criterion, SS = sum of squares, Pseudo-F = multivariate analogue Fisher's F test, p = p-value, Prop. = indicates the proportion of variation explained by each variable, Cumulative Prop. = cumulative proportion.

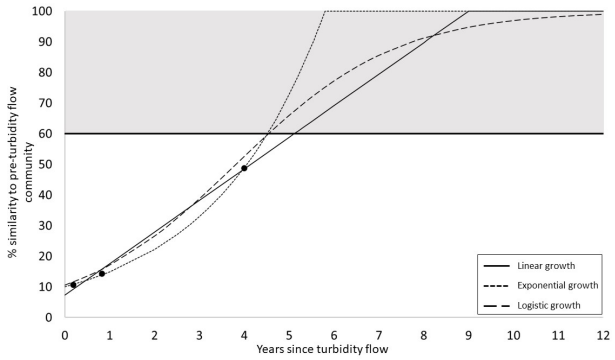

FIGURE 5
Predictions of megafauna community recovery in Kaikōura Canyon. Three hypothetical models of population growth (linear, exponential, and logistic) were used to predict the time to community recovery for the Kaikōura Canyon megafauna community (i.e., indicated by the grey area on the plot, where the lower threshold is defined by the 60% within-group similarity of the pre-turbidity flow community; see Methods for detailed justification for recovery threshold).

4 Discussion

4.1 Impact of the turbidity flow on megafauna community structure

The benthic megafauna community in Kaikōura Canyon was not resistant to disturbance caused by the 2016 Kaikōura Earthquake-triggered turbidity flow, but it appears that the community is resilient because it has begun to recover. Preliminary examination of seafloor imagery taken 10 weeks after the turbidity flow in the canyon suggested that the highly productive deep-sea community had been "wiped out" (Mountjoy et al., 2018). However, a full analysis of these images in the present study showed that while the community was very much affected by the benthic disturbance, occasional patches of the foraminiferan *Bathysiphon filiformis* were observed, as well as white bacterial mats similar to those observed at methane hydrate seeps (Baco et al., 2010), and there was a notable increase in abundance of small rattail fish, particularly *Coryphaenoides subserrulatus*, at 10 weeks after the event. At 10 months after the benthic disturbance event, the primary fauna were a large number of small holothurians, along with the highest abundance of rattails, primarily *C. subserrulatus* along with juvenile *Coelorinchus* spp., observed over the whole the study period (Figure 6C). Four years after the disturbance, the community appeared similar to the pre-disturbance community. However, while several key taxa, such as *B. filiformis* and Astropectinidae sea stars, were still present, they had become the dominant fauna and were observed at higher abundances than before the turbidity flow (Figure 6D). Furthermore. some pre-event fauna had not returned (e.g., ophiuroids, visible in Figure 6A but not in 6D) while other fauna observed were unique to this study's final time point (e.g., sea pens, although not pictured in Figure 6). These findings were supported by the cyclicity correlation test, which indicated recovery was occurring but has not been fully achieved, and by the sample dispersion values, which were lowest 4 years after the event due to an increase in community homogenization over time since the disturbance.

The foraminiferan *B. filiformis* is a key organism for understanding the recovery dynamics from the turbidity flow in Kaikōura Canyon. *Bathysiphon filiformis* were present at all sample

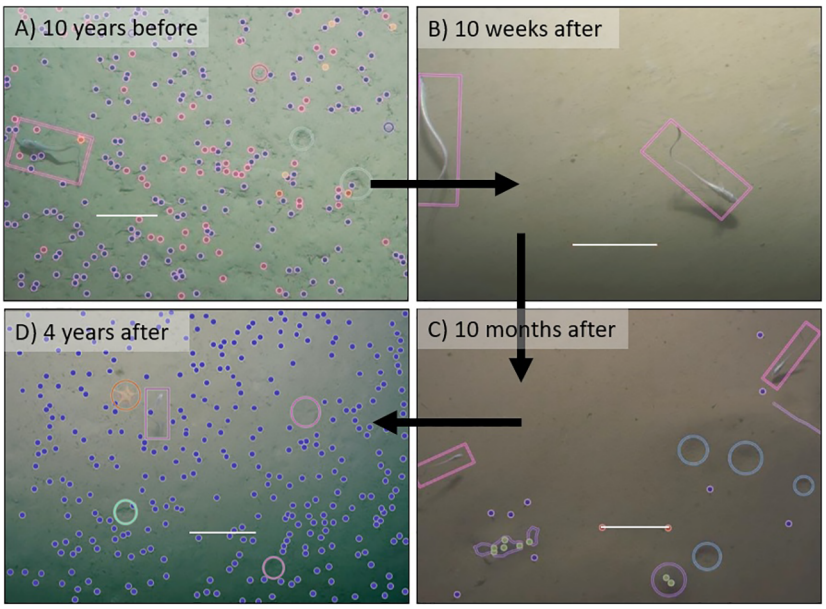

FIGURE 6
Seafloor images taken at the same location in Kaikōura Canyon at times before and after the earthquake-triggered turbidity flow illustrating relative changes in the occurrence and abundance of megafaunal taxa. Scale bars (white line) in all images are 20 cm. Images include annotations. Key: blue dots = *B. filiformis*, magenta dots = burrowing ophiuroid arms, red dots = single burrow, pink rectangles = fish, yellow dots = Mysida crustaceans, dark pink circles = oblique burrow, green circles = rattail feeding marks, cyan circles = large depressions, purple outline = dark grey sediment, green dots = burrow with grey sediment, light pink circles = sea star resting marks, orange circles = sea stars.

times and contributed significantly to the similarity patterns among times. Abundances for *B. filiformis* 10 weeks after the turbidity event were approximately a hundredth of what they were prior to the event (10 years before: 178.51 ind. per m^2, 10 weeks after: 0.7 ind. per m^2) but had increased to greater than pre-event abundances by 4 years after the turbidity flow (581.58 ind. per m^2). This finding may indicate that the canyon is still in a relatively early successional stage, which is generally characterized by high abundances of early arrival taxa (Odum, 1969). *Bathysiphon filiformis* and other *Bathysiphon* species have been found in organic-rich and sometimes low oxygen environments, such as canyons, continental slopes, and methane seeps (Gooday et al., 1992; Hecker, 1994; Hess et al., 2005; Koho et al., 2007; Grupe et al., 2015; Sen et al., 2017), and in stratigraphic studies of turbidites (Crimes and Uchman, 1993; Saja et al., 2009; Grunert et al., 2013), and are considered an indicator of disturbance (Ortiz et al., 2011). As an early colonizer of disturbed environments, *B. filiformis* may be providing important substrate for small and larval fauna (Gooday et al., 1992) and promoting deeper oxygen penetration or reworking of surface organic carbon (Schaff and Levin, 1994).

High abundances of the rattail *C. subserrulatus* 10 weeks and 10 months after the turbidity flow, and juvenile *Coelorinchus* spp. 10 months after, are likely due to these mobile faunas being able to quickly return to the canyon floor habitat after the disturbance (Lefèvre and Bellwood, 2015). Similarly, an increase in fish activity described as a "feeding frenzy" was observed after the Loma Prieta earthquake in the Monterey Canyon (Okey, 1997). However, little is known about the timing of reproduction for *C. subserrulatus* (Neat, 2017), so an increase in individuals due to a local spawning event instead cannot be ruled out. The dominance of smaller rattail species [which eat benthic and benthopelagic macrofauna (Jones, 2008a; Jones, 2008b)] in the weeks and months after the event, while larger rattail species (which eat smaller fish along with macrofauna (Jones, 2008b)) had not returned until 4 years after, suggests challenges for animals feeding at higher trophic levels to find the necessary size or quantity of prey items after the benthic disturbance event.

While overall the megafauna community at the head of Kaikōura Canyon appears to be on the path to recovery, 4 years after the turbidity flow the response of specific taxa was variable. Some taxa such as echiurans (possibly the deposit-feeding echiuran *Alomasoma nordpacificum* noted as a biomass dominant in Kaikoura Canyon prior to the turbidity flow by De Leo et al., 2010, but physical samples were not collected so identification could not be confirmed) and mysids were present but at lower abundance levels than before the turbidity flow event, while other taxa (e.g., burrowing ophiuroids from the family Amphiuridae, an isopod species from the family Arcturidae, and an unidentified polychaete (Polychaete sp. 1)) had yet to return to the upper canyon site even 4 years after the turbidity flow. Furthermore, other taxa (including two unidentified polychaetes (Polychaete sp. 2 and Phyllodocidae sp.), two nemertean species (Nemertea sp. 1 and Nemertea sp. 2), sea pens, and the echinoids *Brissopsis oldhami* and *Paramaretia peloria)* were only observed at the final time point of the present study.

The burrowing ophiuroids and the Arcturidae isopods may not have returned yet because many species within the Amphiuridae family and the Isopoda order are brooders (Hendler, 1975; Hendler and Tran, 2001; Johnson et al., 2001; Tyler and Gage, 2020), meaning that eggs are retained by adults until hatching. Therefore, adult individuals would need to return and reproduce in the canyon before the population could re-establish. Conversely, free-spawning species, such as nemerteans and sea pens (Stricker et al., 2001; Pires et al., 2009; Servetto et al., 2013), which release free swimming larva into the water may have an advantage after a disturbance as both adults and juveniles can independently establish in the 'opened' habitat patches (Grassle and Morse-Porteous, 1987). Another reason that some taxa have not returned may be that other taxa that arrived sooner after the disturbance filled the same niche and outcompeted or prevented the previous taxa from returning (Sousa, 1979). This inhibition may be the case for Polychaete sp. 1, as there were two other unidentified polychaetes that were seen 4 years after but not 10 years before, which may have replaced Polychaete sp. 1. However, there were relatively few nemertean, sea pen, and new polychaete individuals observed, so data from future surveys would be necessary to determine whether or not they become established members of the benthic megafauna community.

In the case of the apparently unique presence of the echinoids *B. oldhami* and *P. peloria* 4 years after the turbidity flow, the observations of these taxa in the images may be more about the change in distribution of nutrients or oxygen in the sediments as an effect of the turbidity flow rather than the arrival of new species. *Brissopsis oldhami* were present in Kaikōura Canyon prior to the turbidity flow but only recorded below the sediment surface in sediment samples taken using grabs (De Leo et al., 2010). Studies of deep-sea imagery and modern ichnofacies (an assemblage of trace fossils that are indicative of habitat conditions) have shown shifts in echinoid foraging behavior in response to high quality food (Wetzel, 2008; Miguez-Salas et al., 2022). Natural sedimentation in the Conway Trough arm of the canyon has been estimated as high as 1.7 m $(1000\ yr)^{-1}$ (Carter et al., 1982), and sediments in Kaikōura Canyon are known to have higher organic matter content than surrounding regions (Leduc et al., 2014). In addition, tens of thousands of shallow terrestrial landslides, also triggered by the Kaikōura Earthquake (Dellow et al., 2017; Massey et al., 2020), may have increased riverine suspended sediment loads and direct sediment flux to the marine environment for a period after the earthquake (Croissant et al., 2019) along with the presumed transport of dead fauna and macroalgae from intertidal waters (resulting from uplift caused by the earthquake (Thomsen et al., 2020)) to deeper waters. Overall, a large amount of sediment and associated organic carbon would likely have been deposited on the canyon floor at the time or soon after the turbidity flow event. Further, oxygen levels are typically quickly depleted where oxidation of organic carbon occurs (Reimers et al., 1986) (Glud, 2008) and bioturbation is the most important vector for oxygen transport into sediments (Revsbech et al., 1980), so it would be expected that sediment oxygen levels would be reduced after the turbidity flow, when higher levels of organic carbon are present and lower levels of bioturbation are reworking the sediment (see below). Therefore, the presence of *B. oldhami* on the seafloor surface 4 years after the turbidity flow (and therefore in images taken by the towed

camera) may be due to organic carbon being more readily available on the surface for deposit feeding and/or they might be avoiding lower oxygen levels at depth within the sediment even 4 years after the turbidity flow. Additionally, the influx of small epibenthic holothurians seen 10 months after the turbidity flow may also have been due to the increased organic carbon availability following the turbidity flow. The relative abundance of the holothurians 10 months after the disturbance rivalled that of all other key taxa (except for *B. filiformis*) at all time points. Similar holothurians have been seen in other canyon systems (ascribed to the Elpidiidae family (Rowe, 1971; Amaro et al., 2015)) where they have been linked to the presences of fresh phytodetritus (Amaro et al., 2015) with reproductive strategies that promote reproduction and recruitment in response to favorable food conditions (FitzGeorge-Balfour et al., 2010).

The presence of fauna not observed before the turbidity flow along with the absence of some taxa observed before the event may indicate that an alternative megafauna community state is forming at the head of the Kaikōura Canyon. Alternative stable states occur when the community crosses an alteration threshold - often attributed to large-scale disturbance (Scheffer et al., 2001) - and state-type shifts occur in species composition (Holling, 1973; May, 1977). However, whether the observed changes in the overall structure of the benthic community following the "full canyon flushing" event represent an alternative stable state rather than a path to the previously observed pre-event state, which itself could be a "relic of a former disaster" (87), remains to be determined by future sampling.

4.2 Time to recovery of the megafauna community

Estimates of the minimum time until recovery for the megafauna community in Kaikōura Canyon were between 4.5-5.1 years, although recovery could take up to 12 years if higher levels of similarity between a pre-disturbance and recovered community are used (e.g., 80%, Blyth et al., 2004) or observed when there is no significance difference between pre- and post-disturbed communities. Previous studies of modern turbidity flows have not focused on megafauna. However, indications of recovery and estimates of minimum time until recovery from the present study are longer than what has been observed in other modern turbidity flow studies of meiofauna (1.5 years; (Kitahashi et al., 2014; Kitahashi et al., 2016; Nomaki et al., 2016)). Recovery indications from the present study, however, are significantly shorter than studies of ancient turbidity flows, which have suggested impacts from the turbidity flows on mega- and macrofauna benthic communities were still observable hundreds to thousands of years later (Griggs et al., 1969; Huggett, 1987; Briggs et al., 1996).

One reason that Kaikōura Canyon megafauna do not fit the previous slow recovery paradigm may be because they are in the head of a physically active canyon in the bathyal zone (905-1190 m) rather than deeper abyssal, submarine fan environments (between 2900-5050 m) which have been the focus of previous studies on ancient turbidity flows. With increasing depth there is a decrease in abundance and size of organisms due to decreased nutrient availability and slower growth rates compared to shallower waters (Thiel, 1992; Rex et al., 2006), and it is therefore probable that communities in abyssal environments may be more susceptible to impact from large-scale disturbances (Radziejewska and Stoyanova, 2000; Stratmann et al., 2018). In addition, submarine canyons are high energy environments that are frequently disturbed by strong bottom currents, internal tidal mixing, and mass wasting events of various sizes (Fernandez-Arcaya et al., 2017), such that communities in these environments are expected to be resilient to physical disturbances on a range of temporal scales (Rowe, 1971). As already noted, full canyon flushing events in Kaikōura Canyon, like the example studied here, might reoccur at centennial intervals (Mountjoy et al., 2018) with smaller, more localized submarine landslides, debris flows, and turbidity flows occurring more often (Lewis and Barnes, 1999; Mountjoy and Micallef, 2018). This difference in disturbance regimes is important to keep in mind when considering our understanding of the broader impact of turbidity flows on deep-sea ecosystems, as many early studies were of distal abyssal, submarine channel, and distil fan environments which are only reached periodically by very large turbidity flows on millennial timescales (Bigham et al., 2021). As such, fauna at these distal sites will likely have experienced less pressure to adapt to regular disturbances than fauna undergoing more frequent disturbance at canyon heads. While beyond the scope afforded by the dataset of the present, there may well be a difference in the impact from the sediment density flow in the head of Kaikōura Canyon, where the primary disturbance was mass erosion, compared to further along the flow path in the Hikurangi Channel or the abyssal submarine fan where it would be expected that the disturbance would be more depositional in nature, and where historical disturbances are typically less frequent.

4.3 Changes in environmental factors and potential influences on megafauna community

Lebensspuren indicative of infauna (not directly counted as visible megafauna) were almost non-existent immediately after the turbidity flow and by 4 years after the event the abundance of these life traces was around half that of pre-disturbance. This finding may mean that the infauna community [such as the biomass dominant, mound building holothurian *Molpadia musculus* sampled by sediment grabs before the turbidity flow (De Leo et al., 2010)] may not be recovering as rapidly as the visible megafauna community and that even 4 years after the turbidity flow, organic carbon in the sediment is not being reworked by the infauna in the way it was 10 years before the event. As such, low rates of bioturbation may be preventing or slowing the recovery of some megafauna. For example, as discussed above, vertical shifts in urchin distribution may be related to the reduced bioturbation that would facilitate organic carbon and oxygen reaching deeper depths. Modelling of the influence of environmental variables on the megafauna community identified 'bioturbation', a factor calculated from the sum of infauna and

faecal *lebensspuren*, as the most important variable. However, it is also possible that the correlation was just coincident with the changes brought about independently in the infauna. Future studies focused on the infauna will hopefully resolve these speculations.

Though the overwhelming change to the seafloor bathymetry at the head of the Kaikōura Canyon was erosional (10s of metres of sediment removed (Mountjoy et al., 2018), the imagery of the seafloor 10 weeks after the event showed a relatively smooth seafloor characteristic of freshly deposited material (for a field of view of between 0.5 and 2.5 m^2). This apparent deposition of sediment may be due to the complex nature of turbidity flows and other components of sediment density flows (Maier et al., 2019; Ge et al., 2022), subsequent sediment deposition from small landslides caused by after-shocks (Völker et al., 2011), or the naturally high sedimentation rate within the canyon driven by the combination of oceanographic processes such as along-shore drift, tidal flows, wave-resuspension, and seaward sediment advection (Thiel, 1992). In general, the turbidity flow increased the rugosity of the canyon floor by increasing the variability in the slope and depth, and from visual observations apparently dislodged large blocks of angular sediment and exposed or redeposited boulders and gravel. These more rugged terrain features were still evident at least 10 months after the disturbance event. While rugged terrain has been identified as a significant environmental factor in structuring faunal communities in other deep-sea environments (du Preez et al., 2016; Post et al., 2017; Gutt et al., 2019), it has typically been due the presence or absence of rocks and other hard substrates. In Kaikōura Canyon there was no evidence of unique fauna associated with the exposed boulders and cobbles on the seafloor, and taxa observed throughout the surveys were all soft sediment taxa. One unique feature observed only 10 weeks after the event was small patches of white bacterial mats, probably indicative of reducing conditions associated with elevated levels of available organic carbon (Baco et al., 2010). These short-lived mats were similar to those seen between 5 months and 1.5 years after the Tōhoku Earthquake-triggered turbidity flow in the Japan Trench, which were fuelled by the breakdown of megafauna carcasses (Tsuji et al., 2013). Despite the presence of hard rocky substrates and bacterial mats soon after the turbidity flow, by 4 years post-event the substrate of within Kaikōura Canyon was predominantly muddy sediments as it was before the event, presumably due to the naturally high sedimentation rates within the canyon.

Overall, the modelling of the influence of environmental variables on the benthic community only accounted for half the variation in the community structure over time, which may be because other unmeasured environmental factors were responsible for the recovery process. These may include: (1) non-local environmental factors that influence recruitment (i.e. larval dispersal) including the distance to nearest undisturbed patch and currents (Lundquist et al., 2010); and, (2) the unmeasured chemical conditions of the sediments and/or overlying water column which can be influenced by infauna bioturbation rates as well as subsequent sediment remobilization by aftershocks or slope instability (*14*).

4.4 Management implications

Many submarine canyons support important deep-sea ecosystems but are subjected to impacts from human activities including fishing, dumping of land-based mine tailings, oil and gas extraction, and litter. As such, some canyons have been designated marine protected areas to conserve their important ecological function (Fernandez-Arcaya et al., 2017). Kaikōura Canyon was designated a part of the Hikurangi Marine Reserve in 2014 due to recognition as a benthic productivity hotspot (De Leo et al., 2010) and of the wider ecosystem services it provides (Fernandez-Arcaya et al., 2017). The reserve is the deepest and largest of New Zealand's marine protected areas on the main islands, and the only one that protects a deep-sea submarine canyon. The full canyon flushing event triggered by the 2016 Kaikōura Earthquake could have impacted the conservation efficacy of this reserve. While the megafauna community in the canyon head is showing clear signs of recovery, the community is yet to reach full recovery 4 years after the event. As such, it is not yet certain whether or not the ecosystem services once provided have returned. The original community may have had a high degree of functional redundancy, and so the return of some taxa may not be critical for maintaining previous functions (Tilman and Downing, 1994). However, previous functions mediated by bioturbation, which apparently remains reduced, have probably yet to fully return. Furthermore, the decreased local diversity and abundances of the megafauna community currently observed during the recovery phase means that the functional redundancy of the benthos is likely much reduced. This likelihood in turn makes the canyon's benthic community, and thereby the marine reserve's efficacy, vulnerable to further impact from subsequent perturbations until full recovery is achieved (Rosenfeld, 2002). Anthropogenic and environmental disturbances are increasing in many ecosystems (Oliver et al., 2015), and the seafloor communities in Kaikōura Canyon will not be immune from such disturbances; for example, riverine sediment input is increasing in other parts of New Zealand due to increased rainfall and land erosion because of climate change (Crozier, 2010). Additionally, while bottom trawling is not allowed in the reserve, it does occur in the surrounding areas (Ministry for Primary Industries, 2022) and studies elsewhere have shown that nearby bottom trawling can focus and increase sedimentation within submarine canyons (Puig et al., 2012; Paradis et al., 2018). Therefore, additional protection of the benthic communities surrounding the reserve may be needed while the full ecosystem services provided by the communities of Kaikōura Canyon are re-established.

Despite the increase in abundance of small and juvenile rattail species in the weeks and months after the turbidity flow, few large rattail species or other fish were observed by the end of the study, which may indicate a temporary decline in the upward trophic movement of organic carbon in the canyon. This potential impact on trophic pathways may be the reason why sperm whales – an important tourist attraction nationally - were absent from the upper canyon and had moved to nearby canyon and gully features to forage for pelagic prey (squid and demersal fish (Gaskin and

Cawthorn, 1967)) for up to a year after the turbidity flow (Guerra et al., 2020). This decline may have also impacted local fisheries, if rattail abundances and sizes are reflective of other benthic and benthopelagic feeding fish. A number of demersal fish species – which are generally carnivorous, feeding on crustaceans, squid, and fish smaller than themselves (Rosecchi et al., 1988; Connell et al., 2010) - are caught in both recreational and commercial fishing around Kaikōura Canyon (Francis, 1979; Doonan and Dunn, 2011; Parker et al., 2011), with rattails being a common New Zealand-wide bycatch species (Ballara et al., 2010).

Debris and turbidity flows create large-scale erosional and depositional disturbances, and thus, could be considered as proxies for some anthropogenic disturbances, such as deep-sea seabed mining. Estimates from this study put recovery of the megafauna community in Kaikōura Canyon within a minimum of 4.5-5.1 years and as long as 12 years. This prediction indicates that the community is likely to be relatively resilient to large-scale disturbances from turbidity flows, which is encouraging for the long-term efficacy of the Hikurangi Marine Reserve. However, studies looking at the small-scale experimental impact of seabed mining type activity on deep-sea fauna have found that megafauna communities can take up to 3-7 years before showing signs of recovery (Bluhm, 2001) or show no signs of recovery two decades after the simulated mining event (Jones et al., 2017). However, there are a number of reasons why the estimate of community recovery from the turbidity flow in Kaikōura Canyon is not a useful proxy for understanding recovery from deep-sea mining. First, locational variation in environment and fauna will play a part in the observed differences in recovery rates noted above (as already discussed), and this difference between indications of benthic community resilience is also likely due to discrepancies in the scale of the two types of disturbances. Erosion and deposition of sediment by the sediment density flow was on the scale of metres to tens of metres (Mountjoy et al., 2018), much greater than the tens of centimetres to metres of erosion (Levin et al., 2001) and millimeters of deposition (Thiel et al., 2001) that are expected to occur from seabed mining. The minimum areal extent of the impact from the turbidity flow in Kaikōura Canyon was approximately 220 km^2 (Mountjoy et al., 2018), which although it is comparable to the hundreds km^2 per year impacted area envisaged for manganese nodule mining in the abyss (Ardron et al., 2019) seabed mining is expected to occur over successive and multiple years, and therefore it may ultimately extend hundreds to thousands of square kilometers (Smith et al., 2008). Large areas of disturbance can take longer to recolonize than smaller ones (Bluhm, 2001). Furthermore, some areas of Kaikōura Canyon were untouched by the disturbance and thereby provide refuge for fauna, and potential sources for faunal recolonization of impacted areas. Commercial mining disturbance is generally expected to be more contiguous than the impact of a turbidity flow, although some mining plans do envisage leaving refuge areas (Wedding et al., 2013). Nonetheless, re-suspension and subsequent settling of sediments *via* the mining vehicle and tailing plume will cause widespread disturbance on surrounding unmined benthic habitats, potentially dispersed up to hundreds of kilometers away (Sharma et al., 2001; Smith et al., 2008).

In conclusion, the megafauna community visible in seafloor imagery from Kaikōura Canyon appears to be a resilient to the 2016 Kaikōura Earthquake-triggered turbidity flow. That is, four years after the event the community has somewhat recovered and is now similar to the once highly productive community present before the turbidity flow. Simple population growth models predict that the community could fully recover in a minimum of 4.5 years, although full recovery may take up to 12 years after the disturbance. Future sampling at the same sites remains key to ascertain if the community is on a trajectory to an identical pre-earthquake state or developing an alternative state. Analysis of the visible *lebensspuren* suggests that the infauna has been impacted more by the turbidity flow and that recovery is not as advanced as for the megafauna. Additional research focused on the infauna will further resolve this provisional observation. While the results of the present study are encouraging for the long-term efficacy of the Hikurangi Marine Reserve, some supportive management actions may still be warranted. Questions remain about the impact of the turbidity flow on the local demersal fishery. And finally, findings from the studies of impacts on benthic communities by turbidity flows are not readily transferable to understanding about the impact of future deep-sea mining.

Data availability statement

The original contributions presented in the study are included in the article/Supplementary Material. Further inquiries can be directed to the corresponding author.

Author contributions

AR, DB, DL, JM, SN, and AO obtained funding for the study and were leads on data collection voyages. AP collected and processed the bathymetric data. CC assisted with the setup of the image annotation environment, annotation troubleshooting, and identified taxa. KB performed the data analysis and wrote the first manuscript draft. AR, DB, and DL advised KB on the analyses and contributed significantly to manuscript revision and preparation. All authors contributed to the article and approved the submitted version.

Funding

Funding for this project came from NOAA Ocean Exploration and NIWA, with co-funding from Woods Hole Oceanographic Institution, Scripps Oceanographic Institution, and the University of Hawaii (TAN0616), New Zealand Ministry for Primary Industries with additional funding from NIWA Strategic Science Investment Fund (SSIF) project COES1701 (TAN1701), NIWA SSIF, NIWA Oceans Centre and TRG (TAN1707, TAN1708), NIWA Marine Geological Processes programme, TRG, and Eurofleets+ (TAN2011). KB was supported by the NIWA-VUW PhD scholarship in marine sciences.

Acknowledgments

We would like to thank the captain, crew, and scientific parties of the five R/V *Tangaroa* voyages TAN0616, TAN1701, TAN1707, TAN1708, and TAN2011. Several NIWA taxonomists and parataxonomists were integral in identifying taxa in the images: Sadie Mills (ophiuroids), Kate Neill (asteroids), Jeff Forman (decapods), and Dennis Gordon (general taxa), as well as Te Papa taxonomist Andrew Stewart (fish). We also thank the two reviewers for providing constructive criticisms on the manuscript.

Conflict of interest

The authors declare that the research was conducted in the absence of any commercial or financial relationships that could be construed as a potential conflict of interest.

Publisher's note

Supplementary material

The Supplementary Material for this article can be found online at: https://www.frontiersin.org/articles/10.3389/fmars.2023.1180334/full#supplementary-material

References

Abdul Wahab, M. A., Fromont, J., Gomez, O., Fisher, R., and Jones, R. (2017). Comparisons of benthic filter feeder communities before and after a large-scale capital dredging program. *Mar. pollut. Bull.* 122, 176–193. doi: 10.1016/j.marpolbul.2017.06.041

Amaro, T., de Stigter, H., Lavaleye, M., and Duineveld, G. (2015). Organic matter enrichment in the whittard channel; its origin and possible effects on benthic megafauna. *Deep Sea Res. 1 Oceanogr Res. Pap* 102, 90–100. doi: 10.1016/j.dsr.2015.04.014

Anderson, M. J., Gorley, R. N., and Clarke, K. R. (2008). *PERMANOVA+ for PRIMER: guide to software and statistical methods* (Plymouth, UK).

Anderson, M. J., and Santana-Garcon, J. (2015). Measures of precision for dissimilarity-based multivariate analysis of ecological communities. *Ecol. Lett.* 18, 66–73. doi: 10.1111/ele.12385

Ardron, J. A., Simon-Lledó, E., Jones, D. O. B., and Ruhl, H. A. (2019). Detecting the effects of deep-seabed nodule mining: simulations using megafaunal data from the clarion-clipperton zone. *Front. Mar. Sci.* 6. doi: 10.3389/fmars.2019.00604

Azpiroz-Zabala, M., Cartigny, M. J. B., Talling, P. J., Parsons, D. R., Sumner, E. J., Clare, M. A., et al. (2017). Newly recognized turbidity current structure can explain prolonged flushing of submarine canyons. *Sci. Adv.* 3. doi: 10.1126/sciadv.1700200

Baco, A. R., Rowden, A. A., Levin, L. A., Smith, C. R., and Bowden, D. A. (2010). Initial characterization of cold seep faunal communities on the new Zealand hikurangi margin. *Mar. Geol* 272, 251–259. doi: 10.1016/j.margeo.2009.06.015

Ballara, S. L., O'Driscoll, R. L., and Anderson, O. F. (2010). *Fish discards and non-target fish catch in the trawl fisheries for hoki, hake, and ling in new Zealand waters* (Wellington).

Barnthouse, L. W. (2004). Quantifying population recovery rates for ecological risk assessment. *Environ. Toxicol. Chem.* 23, 500–508. doi: 10.1897/02-521

Belley, R., Archambault, P., Sundby, B., Gilbert, F., and Gagnon, J. M. (2010). Effects of hypoxia on benthic macrofauna and bioturbation in the estuary and gulf of st. Lawrence, Canada. *Cont Shelf Res.* 30, 1302–1313. doi: 10.1016/j.csr.2010.04.010

Bigham, K. T., Rowden, A. A., Leduc, D., and Bowden, D. A. (2021). Review and syntheses: impacts of turbidity flows on deep-sea benthic communities. *Biogeosciences* 18, 1893–1908. doi: 10.5194/bg-18-1893-2021

Bluhm, H. (2001). Re-establishment of an abyssal megabenthic community after experimental physical disturbance of the seafloor. *Deep Sea Res. 2 Top. Stud. Oceanogr* 48, 3841–3868. doi: 10.1016/S0967-0645(01)00070-4

Blyth, R. E., Kaiser, M. J., Edwards-Jones, G. , and Hart, P. J. B. (2004). Implications of a zoned fishery management system for marine benthic communities. *J. Appl. Ecol.* 41 (5), 951–961. doi: 10.1111/j.0021-8901.2004.00945.x.

Briggs, K. B., Richardson, M. D., and Young, D. K. (1996). The classification and structure of megafaunal assemblages in the Venezuela basin, Caribbean Sea. *J. Mar. Res.* 54, 705–730. doi: 10.1357/0022240963213736

Carter, L., Carter, R. M., and Griggs, G. B. (1982). Sedimentation in the Conway trough, a deep near-shore marine basin at the junction of the alpine transform and hikurangi subduction plate boundary, new Zealand. *Sedimentology* 29, 405–429. doi: 10.1111/j.1365-3091.1982.tb01731.x

Clark, M. R., Althaus, F., Schlacher, T. A., Williams, A., Bowden, D. A., and Rowden, A. A. (2016). The impacts of deep-sea fisheries on benthic communities: a review. *ICES J. Mar. Sci.* 73. doi: 10.1093/icesjms/fsv123

Clarke, K. R., Chapman, M. G., Somerfield, P. J., and Needham, H. R. (2006). Dispersion-based weighting of species counts in assemblage analyses. *Mar. Ecol. Prog. Ser.* 320, 11–27. doi: 10.3354/meps320011

Clarke, K. R., and Gorley, R. N. (2018). Getting started with PRIMER v7. *Primer-E.*

Clarke, K., and Green, R. (1988). Statistical design and analysis for a "biological effects" study. *Mar. Ecol. Prog. Ser.* 46, 213–226. doi: 10.3354/meps046213

Connell, A. M., Dunn, M. R., and Forman, J. (2010). Diet and dietary variation of new Zealand hoki *Macruronus novaezelandiae*. *N Z J. Mar. Freshw. Res.* 44, 289–308. doi: 10.1080/00288330.2010.515232

Crimes, T. P., and Uchman, A. (1993). A concentration of exceptionally well-preserved large tubular foraminifera in the Eocene zumaya flysch, northern Spain. *Geol Mag* 130, 851–853. doi: 10.1017/S0016756800023219

Croissant, T., Steer, P., Lague, D., Davy, P., Jeandet, L., and Hilton, R. G. (2019). Seismic cycles, earthquakes, landslides and sediment fluxes: linking tectonics to surface processes using a reduced-complexity model. *Geomorphology* 339, 87–103. doi: 10.1016/j.geomorph.2019.04.017

Crozier, M. J. (2010). Deciphering the effect of climate change on landslide activity: a review. *Geomorphology* 124, 260–267. doi: 10.1016/j.geomorph.2010.04.009

De Leo, F. C., Smith, C. R., Rowden, A. A., Bowden, D. A., and Clark, M. R. (2010). Submarine canyons: hotspots of benthic biomass and productivity in the deep sea. *Proc. R. Soc. B: Biol. Sci.* 277, 2783–2792. doi: 10.1098/rspb.2010.0462

Dellow, S., Massey, C., Cox, S., Archibald, G., Begg, J., Bruce, Z., et al. (2017). Landslides caused by the Mw7.8 kaikōura earthquake and the immediate response. *Bull. New Z. Soc. Earthquake Eng.* 50. doi: 10.5459/bnzsee.50.2.106-116

Doonan, I. J., and Dunn, M. R. (2011). Trawl survey of mid-East coast orange roughy, march-April 2010. *New Zealand Fisheries Assessment Report 20* (Wellington).

du Preez, C., Curtis, J. M. R., and Clarke, M. E. (2016). The structure and distribution of benthic communities on a shallow seamount (Cobb seamount, northeast pacific ocean). *PloS One* 11. doi: 10.1371/journal.pone.0165513

Fernandez-Arcaya, U., Ramirez-Llodra, E., Aguzzi, J., Allcock, A. L., Davies, J. S., Dissanayake, A., et al. (2017). Ecological role of submarine canyons and need for canyon conservation: a review. *Front. Mar. Sci.* 4. doi: 10.3389/fmars.2017.00005

FitzGeorge-Balfour, T., Billett, D. S. M., Wolff, G. A., Thompson, A., and Tyler, P. A. (2010). Phytopigments as biomarkers of selectivity in abyssal holothurians; interspecific differences in response to a changing food supply. *Deep Sea Res. 2 Top. Stud. Oceanogr* 57, 1418–1428. doi: 10.1016/j.dsr2.2010.01.013

Folke, C., Carpenter, S., Walker, B., Scheffer, M., Elmqvist, T., Gunderson, L., et al. (2004). Regime shifts, resilience, and biodiversity in ecosystem management. *Annu. Rev. Ecol. Evol. Syst.* 35, 557–581. doi: 10.1146/annurev.ecolsys.35.021103.105711

Francis, M. (1979). Checklist of the marine fishes of kaikoura, new Zealand. *Mauri Ora* 7, 63–71.

Galéron, J., Menot, L., Renaud, N., Crassous, P., Khripounoff, A., Treignier, C., et al. (2009). Spatial and temporal patterns of benthic macrofaunal communities on the deep continental margin in the gulf of Guinea. *Deep Sea Res. 2 Top. Stud. Oceanogr* 56, 2299–2312. doi: 10.1016/j.dsr2.2009.04.011

Gaskin, D. E., and Cawthorn, M. W. (1967). Diet and feeding habits of the sperm whale (*Physeter catodon l.*) in the cook strait region of new Zealand. *N Z J. Mar. Freshw. Res.* 1, 156–179. doi: 10.1080/00288330.1967.9515201

Ge, Z., Nemec, W., Vellinga, A. J., and Gawthorpe, R. L. (2022). How is a turbidite actually deposited? *Sci. Adv.* 8. doi: 10.1126/sciadv.abl9124

Gibbs, M., Leduc, D., Nodder, S. D., Kingston, A., Swales, A., Rowden, A. A., et al. (2020). Novel application of a compound-specific stable isotope (CSSI) tracking technique demonstrates connectivity between terrestrial and deep-Sea ecosystems *via* submarine canyons. *Front. Mar. Sci.* 7. doi: 10.3389/fmars.2020.00608

Glud, R. N. (2008). Oxygen dynamics of marine sediments. *Mar. Biol. Res.* 4, 243–289. doi: 10.1080/17451000801888726

Gooday, A. J., Levin, L. A., Thomas, C. L., and Hecker, B. (1992). The distribution and ecology of *Bathysiphon filiformis* sars and b. major de folin (Protista, foraminiferida) on the continental slope off north Carolina. *J. Foraminifer Res.* 22. doi: 10.2113/gsjfr.22.2.129

Gooday, A. J., Turley, C. M., and Allen, J. A. (1990). Responses by benthic organisms to inputs of organic material to the ocean floor: a review. *Philos. Trans. R. Soc. A: Mathematical Phys. Eng. Sci.* 331, 119–138. doi: 10.1098/rsta.1990.0060

Grassle, J. F., and Morse-Porteous, L. S. (1987). Macrofaunal colonization of disturbed deep-sea environments and the structure of deep-sea benthic communities. *Deep Sea Res. Part A Oceanog. Res. Papers* 34, 1911–1950. doi: 10.1016/0198-0149(87)90091-4

Griggs, G. B., Carey, A. G., and Kulm, L. D. (1969). Deep-sea sedimentation and sediment-fauna interaction in cascadia channel and on cascadia abyssal plain. *Deep Sea Res. Oceanog. Abstracts* 16, 157–170. doi: 10.1016/0011-7471(69)90071-0

Grunert, P., Hinsch, R., Sachsenhofer, R. F., Bechtel, A., ćorić, S., Harzhauser, M., et al. (2013). Early burdigalian infill of the puchkirchen trough (North alpine foreland basin, central paratethys): facies development and sequence stratigraphy. *Mar. Pet Geol* 39, 164–186. doi: 10.1016/j.marpetgeo.2012.08.009

Grupe, B. M., Krach, M. L., Pasulka, A. L., Maloney, J. M., Levin, L. A., and Frieder, C. A. (2015). Methane seep ecosystem functions and services from a recently discovered southern California seep. *Mar. Ecol.* 36, 91–108. doi: 10.1111/maec.12243

Guerra, M., Dawson, S., Sabadel, A., Slooten, E., Somerford, T., Williams, R., et al. (2020). Changes in habitat use by a deep-diving predator in response to a coastal earthquake. *Deep Sea Res. 1 Oceanogr Res. Pap* 158. doi: 10.1016/j.dsr.2020.103226

Gutt, J., Arndt, J., Kraan, C., Dorschel, B., Schröder, M., Bracher, A., et al. (2019). Benthic communities and their drivers: a spatial analysis off the Antarctic peninsula. *Limnol Oceanogr* 64, 2341–2357. doi: 10.1002/lno.11187

Hage, S., Galy, V. V., Cartigny, M. J. B., Acikalin, S., Clare, M. A., Gröcke, D. R., et al. (2020). Efficient preservation of young terrestrial organic carbon in sandy turbidity-current deposits. *Geology* 48, 882–887. doi: 10.1130/g47320.1

Harris, P. T. (2014). Shelf and deep-sea sedimentary environments and physical benthic disturbance regimes: a review and synthesis. *Mar. Geol* 353, 169–184. doi: 10.1016/j.margeo.2014.03.023

Haughton, P. D. W., Barker, S. P., and McCaffrey, W. D. (2003). "Linked" debrites in sand-rich turbidite systems - origin and significance. *Sedimentology* 50, 459–482. doi: 10.1046/j.1365-3091.2003.00560.x

Hecker, B. (1994). Unusual megafaunal assemblages on the continental slope off cape hatteras. *Deep-Sea Res. Part II* 41, 809–834. doi: 10.1016/0967-0645(94)90050-7

Heezen, B. C., Ewing, M., and Menzies, R. J. (1955). The influence of submarine turbidity currents on abyssal productivity. *Oikos*, 170–182. doi: 10.2307/3564853

Heezen, B. C., Menzies, R. J., Schneider, E. D., Ewing, M., and Granelli, N. C. L. (1964). Congo Submarine canyon. *Am. Assoc. Pet Geol Bull.* 48, 1126–1149. doi: 10.1306/BC743D7F-16BE-11D7-8645000102C1865D

Hendler, G. (1975). Adaptational significance of the patterns of ophiuroid development. *Integr. Comp. Biol.* 15, 691–715. doi: 10.1093/icb/15.3.691

Hendler, G., and Tran, L. U. (2001). Reproductive biology of a deep-sea brittle star *Amphiura carchara* (Echinodermata: ophiuroidea). *Mar. Biol.* 138, 113–123. doi: 10.1007/s002270000446

Hess, S., Jorrissen, F. J., Venet, V., and Abu-Zied, R. (2005). Benthic foraminiferal recovery after recent turbidite deposition in cap Breton canyon, bay of Biscay. *J. Foraminiferal Res.* 35, 114–129. doi: 10.2113/35.2.114

Hollertz, K., Sköld, M., and Rosenberg, R. (1998). Interactions between two deposit feeding echinoderms: the spatangoid brissopsis lyrifera (Forbes) and the ophiuroid amphiura chiajei forbes. in. *Hydrobiologia*., 287–295. doi: 10.1007/978-94-017-2864-5_23

Holling, C. S. (1973). Resilience and stability of ecological systems. *Future Nature: Doc. Global Change*, 1–24. doi: 10.1146/annurev.es.04.110173.000245

Holling, C. S. (1996). ""Engineering resilience versus ecological resilience,"," in *Foundations of ecological resilence*, 31–44.

Horton, T., Marsh, L., Bett, B. J., Gates, A. R., Jones, D. O. B., Benoist, N. M. A., et al. (2021). Recommendations for the standardisation of open taxonomic nomenclature for image-based identifications. *Front. Mar. Sci.* 8. doi: 10.3389/fmars.2021.620702

Huggett, Q. J. (1987). Mapping the hemipelagic versus turbiditic muds by feeding traces observed in deep-sea photographs. *Geol. Geochem. Abyssal Plains Geological Soc. Special Publ.* 31, 105–112. doi: 10.1144/GSL.SP.1987.031.01.09

Johnson, W. S., Stevens, M., and Watling, L. (2001). Reproduction and development of marine peracaridans. *Adv. Mar. Biol.* 39, 105–260. doi: 10.1016/s0065-2881(01)39009-0

Jones, M. R. L. (2008a). Biology and diet of *Coryphaenoides subserrulatus* and *Etmopterus baxteri* from the puysegur region, southern new Zealand. *N Z J. Mar. Freshw. Res.* 42, 333–337. doi: 10.1080/00288330809509961

Jones, M. R. L. (2008b). Dietary analysis of *Coryphaenoides serrulatus, c. subserruiatus* and several other species of macrourid fish (Pisces: macrouridae) from northeastern chatham rise, new Zealand. *N Z J. Mar. Freshw. Res.* 42, 73–84. doi: 10.1080/00288330809509937

Jones, D. O. B., Gates, A. R., and Lausen, B. (2012). Recovery of deep-water megafaunal assemblages from hydrocarbon drilling disturbance in the faroe-Shetland channel. *Mar. Ecol. Prog. Ser.* 461, 71–82. doi: 10.3354/meps09827

Jones, D. O. B., Kaiser, S., Sweetman, A. K., Smith, C. R., Menot, L., Vink, A., et al. (2017). Biological responses to disturbance from simulated deep-sea polymetallic nodule mining. *PloS One* 12. doi: 10.1371/journal.pone.0171750

Kawagucci, S., Yoshida, Y. T., Noguchi, T., Honda, M. C., Uchida, H., Ishibashi, H., et al. (2012). Disturbance of deep-sea environments induced by the M9.0 tohoku earthquake. *Sci. Rep.* 2, 1–7. doi: 10.1038/srep00270

Kitahashi, T., Jenkins, R. G., Nomaki, H., Shimanaga, M., Fujikura, K., and Kojima, S. (2014). Effect of the 2011 tohoku earthquake on deep-sea meiofaunal assemblages inhabiting the landward slope of the Japan trench. *Mar. Geol* 358, 128–137. doi: 10.1016/j.margeo.2014.05.004

Kitahashi, T., Watanabe, H., Ikehara, K., Jenkins, R. G., Kojima, S., and Shimanaga, M. (2016). Deep-sea meiofauna off the pacific coast of tohoku and other trench slopes around Japan: a comparative study before and after the 2011 off the pacific coast of tohoku earthquake. *J. Oceanogr* 72, 129–139. doi: 10.1007/s10872-015-0323-3

Koho, K. A. A., Kouwenhoven, T. J. J., de Stigter, H. C. C., and van der Zwaan, G. J. J. (2007). Benthic foraminifera in the nazaré canyon, Portuguese continental margin: sedimentary environments and disturbance. *Mar. Micropaleontol* 66, 27–51. doi: 10.1016/j.marmicro.2007.07.005

Kuenen, P. H. H., and Migliorini, C. I. (1950). Turbidity currents as a cause of graded bedding. *J. Geol* 58, 91–127. doi: 10.1086/625710

Langenkämper, D., Zurowietz, M., Schoening, T., and Nattkemper, T. W. (2017). BIIGLE 2.0 - browsing and annotating large marine image collections. *Front. Mar. Sci.* 4. doi: 10.3389/fmars.2017.00083

Leduc, D., Rowden, A. A., Nodder, S. D., Berkenbusch, K., Probert, P. K., and Hadfield, M. G. (2014). Unusually high food availability in kaikoura canyon linked to distinct deep-sea nematode community. *Deep Sea Res. 2 Top. Stud. Oceanogr* 104, 310–318. doi: 10.1016/j.dsr2.2013.06.003

Lefèvre, C. D., and Bellwood, D. R. (2015). Disturbance and recolonisation by small reef fishes: the role of local movement versus recruitment. *Mar. Ecol. Prog. Ser.* 537, 205–215. doi: 10.3354/meps11457

Levin, L. A., Etter, R. J., Rex, M. A., Gooday, A. J., Smith, C. R., Pineda, J., et al. (2001). Environmental influences on regional deep-Sea species diversity. *Annu. Rev. Ecol. Syst.* 32, 51–93. doi: 10.1146/annurev.ecolsys.32.081501.114002

Lewis, K. B., and Barnes, P. M. (1999). Kaikoura canyon, new Zealand: active conduit from near-shore sediment zones to trench-axis channel. *Mar. Geol* 162, 39. doi: 10.1016/S0025-3227(99)00075-4

Lowe, D. R. (1979). Sediment gravity flows: their classification and some problems of application to natural flows and deposits. *Geol. continental slopes*. 27, 75–82. doi: 10.2110/pec.79.27.0075

Lundquist, C. J., Thrush, S. F., Coco, G., and Hewitt, J. E. (2010). Interactions between disturbance and dispersal reduce persistence thresholds in a benthic community. *Mar. Ecol. Prog. Ser.* 413, 217–228. doi: 10.3354/meps08578

Maier, K. L., Gales, J. A., Paull, C. K., Rosenberger, K., Talling, P. J., Simmons, S. M., et al. (2019). Linking direct measurements of turbidity currents to submarine canyon-floor deposits. *Front. Earth Sci. (Lausanne)* 7. doi: 10.3389/feart.2019.00144

Massey, C. I., Townsend, D., Jones, K., Lukovic, B., Rhoades, D., Morgenstern, R., et al. (2020). Volume characteristics of landslides triggered by the MW 7.8 2016 kaikōura earthquake, new Zealand, derived from digital surface difference modeling. *J. Geophys Res. Earth Surf* 125. doi: 10.1029/2019JF005163

May, R. M. (1977). Thresholds and breakpoints in ecosystems with a multiplicity of stable states. *Nature* 269, 471–477. doi: 10.1038/269471a0

McArdle, B. H., and Anderson, M. J. (2001). Fitting multivariate models to community data: a comment on distance-based redundancy analysis. *Ecology* 82, 290–297. doi: 10.1890/0012-9658(2001)082[0290:FMMTCD]2.0.CO;2

McClanahan, T. R., Graham, N. A. J., Calnan, J. M., and MacNeil, M. A. (2007). Toward pristine biomass: reef fish recovery in coral reef marine protected areas in Kenya. *Ecol. Appl.* 17, 1055–1067. doi: 10.1890/06-1450

McMillan, P. J., Francis, M. P., James, G. D., Paul, L. J., Marriott, P., MacKay, E. J., et al. (2019). *New Zealand fishes. a field guide to common species caught by bottom, midwater, and surface fishing* (Ministry for Primary Industries).

Meiburg, E., and Kneller, B. (2010). Turbidity currents and their deposits. *Annu. Rev. Fluid Mech.* 42, 135–156. doi: 10.1146/annurev-fluid-121108-145618

Meysman, F. J. R., Middelburg, J. J., and Heip, C. H. R. (2006). Bioturbation: a fresh look at darwin's last idea. *Trends Ecol. Evol.* 21, 688–695. doi: 10.1016/j.tree.2006.08.002

Miguez-Salas, O., Vardaro, M. F., Rodríguez-Tovar, F. J., Pérez-Claros, J. A., and Huffard, C. L. (2022). Deep-Sea echinoid trails and seafloor nutrient distribution: present and past implications. *Front. Mar. Sci.* 9. doi: 10.3389/fmars.2022.903864

Ministry for Primary Industries (2022) *Kaikōura area fishing rules*. Available at: https://www.mpi.govt.nz/fishing-aquaculture/recreational-fishing/fishing-rules/kaikoura-fishing-rules/ (Accessed May 17, 2022).

Mountjoy, J. J., Howarth, J. D., Orpin, A. R., Barnes, P. M., Bowden, D. A., Rowden, A. A., et al. (2018). Earthquakes drive large-scale submarine canyon development and sediment supply to deep-ocean basins. *Sci. Adv.* 4 (3). doi: 10.1126/sciadv.aar3748

Mountjoy, J., and Micallef, A. (2018). *Submarine geomorphology*. 235–250.

Neat, F. C. (2017). Aggregating behaviour, social interactions and possible spawning in the deep-water fish coryphaenoides rupestris. *J. Fish Biol.* 91, 975–980. doi: 10.1111/jfb.13386

Nomaki, H., Mochizuki, T., Kitahashi, T., Nunoura, T., Arai, K., Toyofuku, T., et al. (2016). Effects of mass sedimentation events after the 2011 off the pacific coast of tohoku earthquake on benthic prokaryotes and meiofauna inhabiting the upper bathyal sediments. *J. Oceanogr* 72, 113–128. doi: 10.1007/s10872-015-0293-5

Odum, E. P. (1969). The strategy of ecosystem development. *Sci. (1979)* 164, 262–270. doi: 10.1126/science.164.3877.262

Oguri, K., Kawamura, K., Sakaguchi, A., Toyofuku, T., Kasaya, T., Murayama, M., et al. (2013). Hadal disturbance in the Japan trench induced by the 2011 tohoku-oki earthquake. *Sci. Rep.* 3, 1–6. doi: 10.1038/srep01915

Okey, T. A. (1997). Sediment flushing observations, earthquake slumping, and benthic community changes in Monterey canyon head. *Cont Shelf Res.* 17, 877–897. doi: 10.1016/S0278-4343(96)00067-2

Oliver, T. H., Heard, M. S., Isaac, N. J. B., Roy, D. B., Procter, D., Eigenbrod, F., et al. (2015). Biodiversity and resilience of ecosystem functions. *Trends Ecol. Evol.* 30, 673–684. doi: 10.1016/j.tree.2015.08.009

Ortiz, S., Alegret, L., Payros, A., Orue-Etxebarria, X., Apellaniz, E., and Molina, E. (2011). Distribution patterns of benthic foraminifera across the ypresian-lutetian gorrondatxe section, northern Spain: response to sedimentary disturbance. *Mar. Micropaleontol* 78, 1–13. doi: 10.1016/j.marmicro.2010.09.004

Paradis, S., Puig, P., Sanchez-Vidal, A., Masqué, P., Garcia-Orellana, J., Calafat, A., et al. (2018). Spatial distribution of sedimentation-rate increases in blanes canyon caused by technification of bottom trawling fleet. *Prog. Oceanogr* 169, 241–252. doi: 10.1016/j.pocean.2018.07.001

Parker, S. J., Paul, L. J., and Francis, M. (2011). Age structure characteristics of hāpuku polyprion oxygeneios stocks estimated from existing samples of otoliths. *New Zealand Fisheries Assessment Report*.

Paull, C. K., Talling, P. J., Maier, K. L., Parsons, D., Xu, J., Caress, D. W., et al. (2018). Powerful turbidity currents driven by dense basal layers. *Nat. Commun.* 9, 4114. doi: 10.1038/s41467-018-06254-6

Piper, D. J. W., and Aksu, A. E. (1987). The source and origin of the 1929 grand banks turbidity current inferred from sediment budgets. *Geo-Mar. Lett.* 7, 177–182. doi: 10.1007/BF02242769

Pires, D. O., Castro, C. B., and Silva, J. C. (2009). Reproductive biology of the deep-sea pennatulacean anthoptilum murrayi (Cnidaria, octocorallia). *Mar. Ecol. Prog. Ser.* 397, 103–112. doi: 10.3354/meps08322

Post, A. L., Lavoie, C., Domack, E. W., Leventer, A., Shevenell, A., and Fraser, A. D. (2017). Environmental drivers of benthic communities and habitat heterogeneity on an East Antarctic shelf. *Antarct Sci.* 29, 17–32. doi: 10.1017/S0954102016000468

Pruski, A. M., Decker, C., Stetten, E., Vétion, G., Martinez, P., Charlier, K., et al. (2017). Energy transfer in the Congo deep-sea fan: from terrestrially-derived organic matter to chemosynthetic food webs. *Deep Sea Res. 2 Top. Stud. Oceanogr* 142, 197–218. doi: 10.1016/j.dsr2.2017.05.011

Przeslawski, R., Dundas, K., Radke, L., and Anderson, T. J. (2012). Deep-sea lebensspuren of the Australian continental margins. *Deep Sea Res. 1 Oceanogr Res. Pap* 65, 26–35. doi: 10.1016/j.dsr.2012.03.006

Puig, P., Canals, M., Company, J. B., Martín, J., Amblas, D., Lastras, G., et al. (2012). Ploughing the deep sea floor. *Nature* 489, 286–289. doi: 10.1038/nature11410

Radziejewska, T., and Stoyanova, V. (2000). Abyssal epibenthic megafauna of the clarion-clipperton area (NE pacific): changes in time and space versus anthropogenic environmental disturbance. *Oceanol. Stud.* 29, 83–101.

Rathburn, A. E., Levin, L. A., Tryon, M., Gieskes, J. M., Martin, J. B., Pérez, M. E., et al. (2009). Geological and biological heterogeneity of the Aleutian margin, (1965-4822 m). *Prog. Oceanogr* 80, 22–50. doi: 10.1016/j.pocean.2008.12.002

R Core Team (2022). *R: a language and environment for statistical computing* (R Foundation for Statistical Computing).

Reimers, C. E., Fischer, K. M., Merewether, R., Smith, K. L., and Jahnke, R. A. (1986). Oxygen microprofiles measured *in situ* in deep ocean sediments. *Nature* 320, 741–744. doi: 10.1038/320741a0

Revsbech, N. P., Sorensen, J., Blackburn, T. H., and Lomholt, J. P. (1980). Distribution of oxygen in marine sediments measured with microelectrodes. *Limnol Oceanogr* 25, 403–411. doi: 10.4319/lo.1980.25.3.0403

Rex, M. A., Etter, R. J., Morris, J. S., Crouse, J., McClain, C. R., Johnson, N. A., et al. (2006). Global bathymetric patterns of standing stock and body size in the deep-sea benthos. *Mar. Ecol. Prog. Ser.* 317, 1–8. doi: 10.3354/meps317001

Richardson, M. D., Briggs, K. B., and Young, D. K. (1985). Effects of biological activity by abyssal benthic macroinvertebrates on a sedimentary structure in the Venezuela basin. *Mar. Geol* 68, 243–267. doi: 10.1016/0025-3227(85)90015-5

Richardson, M. D., and Young, D. K. (1987). Abyssal benthos of the Venezuela basin, Caribbean Sea: standing stock considerations. *Deep Sea Res. Part A. Oceanog. Res. Papers* 34, 145–164. doi: 10.1016/0198-0149(87)90079-3

Rosecchi, E., Tracey, D. M., and Webber, W. R. (1988). Diet of orange roughy, *Hoplostethus atlanticus* (Pisces: trachichthyidae) on the challenger plateau, new Zealand. *Mar. Biol.* 99, 293–306. doi: 10.1007/BF00391992

Rosenfeld, J. S. (2002). Functional redundancy in ecology and conservation. *Oikos* 98, 156–162. doi: 10.1034/j.1600-0706.2002.980116.x

Rowe, G. T. (1971). Observations on bottom currents and epibenthic populations in hatteras submarine canyon. *Deep-Sea Res. Oceanog. Abstracts* 18, 569–581. doi: 10.1016/0011-7471(71)90123-9

Rubenstein, D. I., and Koehl, M. A. R. (1977). The mechanisms of filter feeding: some theoretical considerations. *Am. Nat.* 111, 981–994. doi: 10.1086/283227

Saja, D. B., Pfefferkorn, H. W., and Phipps, S. P. (2009). *Bathysiphon* (foraminiferida) at Pacheco pass, California: a geopetal, paleocurrent, and paleobathymetric indicator in the Franciscan complex. *Palaios* 24, 181–191. doi: 10.2110/palo.2008.p08-037r

Schaff, T. R., and Levin, L. A. (1994). Spatial heterogeneity of benthos associated with biogenic structures on the north Carolina continental slope. *Deep-Sea Res. Part II* 41, 901–918. doi: 10.1016/0967-0645(94)90053-1

Scheffer, M., Carpenter, S., Foley, J. A., Folke, C., and Walker, B. (2001). Catastrophic shifts in ecosystems. *Nature* 413, 591–596. doi: 10.1038/35098000

Schönberg, C. H. L. (2016). "Effects of dredging on benthic filter feeder communities, with a focus on sponges," in *Report of theme 6 - project 6.1.1 prepared for the dredging science node* (Perth, Western Australia: Western Australian Marine Science Institution).

Sciberras, M., Hiddink, J. G., Jennings, S., Szostek, C. L., Hughes, K. M., Kneafsey, B., et al. (2018). Response of benthic fauna to experimental bottom fishing: a global meta-analysis. *Fish Fish.* 19, 698–715. doi: 10.1111/faf.12283

Sen, A., Dennielou, B., Tourolle, J., Arnaubec, A., Rabouille, C., and Olu, K. (2017). Fauna and habitat types driven by turbidity currents in the lobe complex of the Congo deep-sea fan. *Deep Sea Res. 2 Top. Stud. Oceanogr* 142, 167–179. doi: 10.1016/j.dsr2.2017.05.009

Servetto, N., Torre, L., and Sahade, R. (2013). Reproductive biology of the antarctic "sea pen" malacobelemnon daytoni (Octocorallia, pennatulacea, kophobelemnidae). *Polar Res.* 32. doi: 10.3402/polar.v32i0.20040

Sharma, R., Nagender Nath, B., Parthiban, G., and Jai Sankar, S. (2001). Sediment redistribution during simulated benthic disturbance and its implications on deep seabed mining. *Deep Sea Res. 2 Top. Stud. Oceanogr* 48, 3363–3380. doi: 10.1016/S0967-0645(01)00046-7

Sibuet, M., and Olu, K. (1998). Biogeography, biodiversity and fluid dependence of deep-sea cold-seep communities at active and passive margins. *Deep Sea Res. 1 Oceanogr Res. Pap* 45, 517–567. doi: 10.1016/S0967-0645(97)00074-X

Smale, D. A., Barnes, D. K. A., Fraser, K. P. P., and Peck, L. S. (2008). Benthic community response to iceberg scouring at an intensely disturbed shallow water site at Adelaide island, Antarctica. *Mar. Ecol. Prog. Ser.* 355, 85–94. doi: 10.3354/meps07311

Smith, C. R., Levin, L. A., Koslow, A., Tyler, P. A., and Glover, A. G. (2008). ""The near future of the deep-sea floor ecosystems,"," in *Aquatic ecosystems: trends and global prospects*. doi: 10.1017/CBO9780511751790.030

Solé, R. v., Saldaña, J., Montoya, J. M., and Erwin, D. H. (2010). Simple model of recovery dynamics after mass extinction. *J. Theor. Biol.* 267, 193–200. doi: 10.1016/j.jtbi.2010.08.015

Sousa, W. P. (1979). Disturbance in marine intertidal boulder fields: the nonequilibrium maintenance of species diversity. *Ecology* 60, 1225. doi: 10.2307/1936969

Sousa, W. P. (1984). The role of disturbance in natural communities. *Annu. Rev. Ecol. Syst.* 15, 353–391. doi: 10.1146/annurev.es.15.110184.002033

Sousa, W. P. (2001). ""Natural disturbance and the dynamics of marine benthic communities,"," in *Marine community ecology*. Eds. M. D. Bertness, S. D. Gaines and M. E. Hay (Sinauer Associates, Inc), 85–130.

Stetten, E., Baudin, F., Reyss, J. L., Martinez, P., Charlier, K., Schnyder, J., et al. (2015). Organic matter characterization and distribution in sediments of the terminal lobes of the Congo deep-sea fan: evidence for the direct influence of the Congo river. *Mar. Geol* 369, 182–195. doi: 10.1016/j.margeo.2015.08.020

Stratmann, T., Lins, L., Purser, A., Marcon, Y., Rodrigues, C. F., Ravara, A., et al. (2018). Abyssal plain faunal carbon flows remain depressed 26 years after a simulated deep-sea mining disturbance. *Biogeosciences* 15, 4131–4145. doi: 10.5194/bg-15-4131-2018

Stricker, S. A., Smythe, T. L., Miller, L., and Norenburg, J. L. (2001). Comparative biology of oogenesis in nemertean worms. *Acta Zool.* 82, 213–230. doi: 10.1046/j.1463-6395.2000.00080.x

Talling, P. J. (2014). On the triggers, resulting flow types and frequencies of subaqueous sediment density flows in different settings. *Mar. Geol* 352, 155–182. doi: 10.1016/j.margeo.2014.02.006

Talling, P. J., Amy, L. A., Wynn, R. B., Blackbourn, G., and Gibson, O. (2007). Evolution of turbidity currents deduced from extensive thin turbidites: marnoso arenacea formation (Miocene), Italian Apennines. *J. Sedimentary Res.* 77, 172–196. doi: 10.2110/jsr.2007.018

Talling, P. J., Masson, D. G., Sumner, E. J., and Malgesini, G. (2012). Subaqueous sediment density flows: depositional processes and deposit types. *Sedimentology* 59, 1937–2003. doi: 10.1111/j.1365-3091.2012.01353.x

Talling, P. J., Paull, C. K., and Piper, D. J. W. (2013). How are subaqueous sediment density flows triggered, what is their internal structure and how does it evolve? direct observations from monitoring of active flows. *Earth Sci. Rev.* 125, 244–287. doi: 10.1016/j.earscirev.2013.07.005

Thiel, H. (1992). Deep-sea environmental disturbance and recovery potential. *Internationale Rev. der gesamten Hydrobiol. und Hydrograph.* 77, 331–339. doi: 10.1002/iroh.19920770213

Thiel, H., Schriever, G., Ahnert, A., Bluhm, H., Borowski, C., and Vopel, K. (2001). The large-scale environmental impact experiment DISCOL - reflection and foresight. *Deep Sea Res. 2 Top. Stud. Oceanogr* 48, 3869–3882. doi: 10.1016/S0967-0645(01)00071-6

Thomsen, M. S., Metcalfe, I., Siciliano, A., South, P. M., Gerrity, S., Alestra, T., et al. (2020). Earthquake-driven destruction of an intertidal habitat cascade. *Aquat Bot.* 164. doi: 10.1016/j.aquabot.2020.103217

Thurston, M. H., Bett, B. J., Rice, A. L., and Jackson, P. A. B. (1994). Variations in the invertebrate abyssal megafauna in the north Atlantic ocean. *Deep-Sea Res. Part I* 41, 1321–1348. doi: 10.1016/0967-0637(94)90100-7

Thurston, M. H., Rice, A. L., and Bett, B. J. (1998). Latitudinal variation in invertebrate megafaunal abundance and biomass in the north Atlantic ocean abyss. *Deep Sea Res. 2 Top. Stud. Oceanogr* 45, 203–224. doi: 10.1016/S0967-0645(97)00077-5

Tilman, D., and Downing, J. A. (1994). Biodiversity and stability in grasslands. *Nature* 367, 363–365. doi: 10.1038/367363a0

Tracey, D. M., Anderson, O. F., and Naylor, J. R. (2011). *A guide to common deepsea invertebrates in new Zealand waters* (Wellington).

Tsuji, T., Kawamura, K., Kanamatsu, T., Kasaya, T., Fujikura, K., Ito, Y., et al. (2013). Extension of continental crust by anelastic deformation during the 2011 tohoku-oki earthquake: the role of extensional faulting in the generation of a great tsunami. *Earth Planet Sci. Lett.* 364, 44–58. doi: 10.1016/j.epsl.2012.12.038

Tyler, P. A., and Gage, J. D. (2020). ""Reproductive patterns in deep sea ophiuroids from the north East atlantic,"," in *Echinoderms: present and past*. (CRC Press) doi: 10.1201/9781003078913-79

Tyler, P. A., and Ramirez-Llodra, E. (2002). Larval and reproductive strategies on European continental margins. *Ocean Margin Syst.*, 417–421. doi: 10.1007/978-3-662-05127-6_21

van Gaever, S., Galéron, J., Sibuet, M., and Vanreusel, A. (2009). Deep-sea habitat heterogeneity influence on meiofaunal communities in the gulf of Guinea. *Deep Sea Res. 2 Top. Stud. Oceanogr* 56, 2259–2269. doi: 10.1016/j.dsr2.2009.04.008

Völker, D., Scholz, F., and Geersen, J. (2011). Analysis of submarine landsliding in the rupture area of the 27 February 2010 maule earthquake, central Chile. *Mar. Geol* 288, 79–89. doi: 10.1016/j.margeo.2011.08.003

Wakita, M., Watanabe, S., Yoshino, J., Oguri, K., Nomaki, H., Kawagucci, S., et al. (2022). Deep-sea bottom-water environment change caused by sediment resuspension on the continental slope off sanriku, Japan, before and after the 2011 tohoku earthquake. *Prog. Earth Planet Sci.* 9, 56. doi: 10.1186/s40645-022-00515-1

Walbridge, S., Slocum, N., Pobuda, M., and Wright, D. J. (2018). Unified geomorphological analysis workflows with benthic terrain modeler. *Geosci. (Switzerland)* 8. doi: 10.3390/geosciences8030094

Walker, B., Holling, C. S., Carpenter, S. R., and Kinzig, A. (2004). Resilience, adaptability and transformability in social-ecological systems. *Ecol. Soc.* 9. doi: 10.5751/ES-00650-090205

Wan Hussin, W. M. R., Cooper, K. M., Froján, C. R. S. B., Defew, E. C., and Paterson, D. M. (2012). Impacts of physical disturbance on the recovery of a macrofaunal community: a comparative analysis using traditional and novel approaches. *Ecol. Indic* 12, 37–45. doi: 10.1016/j.ecolind.2011.03.016

Warwick, R. M., and Clarke, K. R. (1993). Increased variability as a symptom of stress in marine communities. *J. Exp. Mar. Biol. Ecol.* 172, 215–226. doi: 10.1016/0022-0981(93)90098-9

Wedding, L. M., Friedlander, A. M., Kittinger, J. N., Watling, L., Gaines, S. D., Bennett, M., et al. (2013). From principles to practice: a spatial approach to systematic conservation planning in the deep sea. *Proc. R. Soc. B: Biol. Sci.* 280. doi: 10.1098/rspb.2013.1684

Wentworth, C. K. (1922). A scale of grade and class terms for clastic sediments. *J. Geol* 30, 377–392. doi: 10.1086/622910

Wetzel, A. (2008). Recent bioturbation in the deep south China Sea: a uniformitarian ichnologic approach. *Palaios* 23, 601–615. doi: 10.2110/palo.2007.p07-096r

Willig, M. R., and Walker, L. R. (1999). "Disturbance in terrestrial ecosystems: salient themes, synthesis, and future directions," in. *Ecosyst. World*, 747–768.

Young, D. K., and Richardson, M. D. (1998). Effects of waste disposal on benthic faunal succession on the abyssal seafloor. *J. Mar. Syst.* 14, 319–336. doi: 10.1016/S0924-7963(97)00033-X

frontiers | Frontiers in Marine Science

TYPE Review
PUBLISHED 21 July 2023
DOI 10.3389/fmars.2023.1224859

OPEN ACCESS

EDITED BY
Alessandro Cau,
University of Cagliari, Italy

REVIEWED BY
Giorgio Castellan,
Consiglio Nazionale delle Ricerche (CNR), Italy
Ming Su,
Sun Yat-sen University, China

*CORRESPONDENCE
Martina Pierdomenico
martina.pierdomenico@ias.cnr.it

RECEIVED 18 May 2023
ACCEPTED 22 June 2023
PUBLISHED 21 July 2023

CITATION
Pierdomenico M, Bernhardt A, Eggenhuisen JT, Clare MA, Lo Iacono C, Casalbore D, Davies JS, Kane I, Huvenne VAI and Harris PT (2023) Transport and accumulation of litter in submarine canyons: a geoscience perspective. *Front. Mar. Sci.* 10:1224859. doi: 10.3389/fmars.2023.1224859

Transport and accumulation of litter in submarine canyons: a geoscience perspective

Martina Pierdomenico[1]*, Anne Bernhardt[2], Joris T. Eggenhuisen[3], Michael A. Clare[4], Claudio Lo Iacono[5], Daniele Casalbore[6], Jaime S. Davies[7,8], Ian Kane[9], Veerle A.I. Huvenne[4] and Peter T. Harris[10]

[1]Istituto per lo studio degli Impatti Antropici e Sostenibilità in ambiente marino, Consiglio Nazionale delle Ricerche (IAS-CNR), Rome, Italy, [2]Institute of Geological Sciences, Freie Universität Berlin, Berlin, Germany, [3]Faculty of Geosciences, Utrecht University, Utrecht, Netherlands, [4]Ocean BioGeoscience, National Oceanography Centre, Southampton, United Kingdom, [5]Institut de Ciències del Mar, Spanish National Research Council (CSIC), Barcelona, Spain, [6]Dipartimento di Scienze della Terra, Sapienza Università di Roma, Rome, Italy, [7]School of Marine Science and Engineering, University of Plymouth, Plymouth, United Kingdom, [8]School of Marine and Environmental Science, University of Gibraltar, Gibraltar, Gibraltar, [9]School of Earth and Environmental Sciences, University of Manchester, Manchester, United Kingdom, [10]GRID-Arendal, Arendal, Norway

Marine litter is one of the most pervasive and fast-growing aspects of contamination in the global ocean, and has been observed in every environmental setting, including the deep seafloor where little is known about the magnitude and consequences of the problem. Submarine canyons, the main conduits for the transport of sediment, organic matter and water masses from shallow to abyssal depths, have been claimed to be preferential pathways for litter transport and accumulation in the deep sea. This is supported by ongoing evidence of large litter piles at great water depths, highlighting efficient transfer via canyons. The aim of this article is to present an overview of the current knowledge about marine litter in submarine canyons, taking a geological, process-based point of view. We evaluate sources, transport mechanisms and deposition of litter within canyons to assess the main factors responsible for its transport and accumulation in the deep sea. Few studies relate litter distribution to transport and depositional processes; nevertheless, results from available literature show that canyons represent accumulation areas for both land-based and maritime-based litter. Particularly, accumulation of fishing-related debris is mainly observed at the canyon heads and walls and is related to fishing activities carried out in and adjacent to canyons, while transport and accumulation of general waste and plastic along canyon axes can be related to different mechanisms, encompassing enhanced bottom currents, dense water cascading and turbidity currents, and is related to the proximity of canyons to shore. Global assessment of canyons exposure to riverine plastic inputs and fishing-related debris indicates varying susceptibility of canyons to litter, also highlighting that most of the canyons prone to receive large amounts of anthropogenic debris have not yet been surveyed. Considering that litter research in canyons is still in its infancy, several knowledge gaps need to be filled before the role of canyons as litter traps and the implication for benthic ecosystems can be fully understood.

KEYWORDS

submarine canyons, marine litter, microplastics, fishing-related debris, litter transport, sediment transport, deep-sea litter

Introduction

The input of solid waste into the Global Ocean has become a topic of worldwide concern, due to its negative consequences on marine ecosystems, the economy and potentially human health (Beaumont et al., 2019). As a result of the dramatic increase in waste production and mismanaged disposal over the last half century (Geyer et al., 2017), large quantities of litter have entered the ocean, either from terrestrial sources or directly from ships or other maritime infrastructures (UNEP, 2009). Approximately 10 million tons of land-derived plastic debris ended up in the oceans in 2010 alone (Jambeck et al., 2015); a scenario that is forecast to rise to 53 million metric tons per year by 2030 under a business-as-usual scenario (Borrelle et al., 2020).

Marine litter, defined as 'any persistent, manufactured or processed solid material discarded, disposed or abandoned in the marine and coastal environment' (UNEP, 2005), consists of a great variety of materials, among which plastic predominates, accounting for 60–80% of marine litter worldwide (Derraik, 2002). A significant proportion of the plastic lost in the marine environment consists of microplastics, small (<5 mm) fragments and fibres derived from the breakdown of larger plastic debris and synthetic textiles or originated as manufactured particles (Lebreton et al., 2017; Pabortsava and Lampitt, 2020). Both macro- and microparticles can have adverse impacts on species across trophic levels and threaten habitat integrity in different ways and at different spatial and temporal scales. These pollutants can be ingested by organisms, affecting individual fitness or resulting in direct mortality (Gall and Thompson, 2015). Litter, especially fishing-related debris, can entangle biota, hindering its ability to move, feed and breathe (Kühn et al., 2015; Bruemmer et al., 2023, this issue). Furthermore, plastic debris can act as a dispersal vector for alien species and pathogens (Barnes, 2002; Zettler et al., 2013) or as a source of persistent organic pollutants and toxic compounds (Hartmann et al., 2017), and is also able to alter the physical characteristics of the environment (Carson et al., 2011).

Marine litter and microplastics have now been reported from all environmental settings across the Global Ocean, from beaches and coastal surface waters (Willis et al., 2017; Schmidt et al., 2018) to the most remote environments such as the polar regions (Tekman et al., 2017), oceanic islands (Lavers and Bond, 2017) and the deep seafloor (Ramirez-Llodra et al., 2013; Peng et al., 2018), which is considered the final depositional sink for the majority of anthropogenic litter entering the ocean (Thompson et al., 2004; Pham et al., 2014; Woodall et al., 2015).

The spatial variability of litter abundance and composition in the ocean is driven by the complex interplay of anthropogenic factors linked to litter sources (such as coastal population densities and industrialization, fishing pressure, maritime traffic and tourism) and natural factors including hydrological, geomorphological and sedimentary processes, responsible for its transport and deposition (Ramirez-Llodra et al., 2013; Pham et al., 2014; Lopez-Lopez et al., 2017). Once at sea, buoyant litter can be transported by surface currents and winds and can be stranded on the coastlines or transferred offshore and concentrated by converging surface currents into the so-called floating "garbage patches" (Eriksen et al., 2014; Lebreton et al., 2017). However, estimation of floating plastic represent only a small percentage of global input to the ocean (Van Sebille et al., 2015), while a significant proportion of litter is thought to sink to the deep seafloor, where little is known about the extent, magnitude and impacts of this issue. Despite the increasing number of publications discussing seafloor litter over the last decades (Hernandez et al., 2022), papers on seafloor litter represent less than 15% of all studies on marine litter (Canals et al., 2021).

Furthermore, the physical processes governing the horizontal and vertical transport of anthropogenic debris and its fate on the seafloor, especially in deep-sea environments, are still poorly understood (Kane and Clare, 2019; Waldschläger et al., 2022). Notwithstanding the patchy survey coverage of the deep seafloor, current knowledge highlights an uneven distribution of benthic litter and microplastics (Harris, 2020; Canals et al., 2021; Galgani et al., 2022), which cannot be explained solely by vertical settling from concentrated surface accumulations. Oceanographic and sedimentary processes play a fundamental role in transporting and redistributing litter coming from land across continental margins, focusing it in specific physiographic settings, such as abyssal trenches, submarine canyons, bottom current drift deposits and on deep-sea fans located at the mouths of submarine canyons and channels (Pham et al., 2014; Peng et al., 2018; Kane and Clare, 2019; Kane et al., 2020). On the other hand, the rough topography characterizing geomorphological features such as seamounts and banks may favor entanglement and local accumulation of lost or abandoned fishing gears (Angiolillo et al., 2015; Angiolillo et al., 2021).

Submarine canyons are common erosive features found on all the world's continental margins (Harris and Whiteway, 2011) connecting continental shelves to deep ocean basins and acting as preferential transport routes for sediment, organic matter and water masses (Shepard, 1981; Vetter and Dayton, 1999; Masson et al., 2010; Hage et al., 2022; Pope et al., 2022; Post et al., 2022). Canyons are considered to be important conduits for the transfer and accumulation of litter from land to the deep sea (Galgani et al., 1996; Tubau et al., 2015; Pierdomenico et al., 2019; Zhong and Peng, 2021). At the same time, due to their role in focusing currents and transporting sediment and nutrients and their complex topography, submarine canyons are sites of enhanced biodiversity and productivity (De Leo et al., 2010; Fernandez-Arcaya et al., 2017). As such, submarine canyons are often preferential targets for fishing activities (Puig et al., 2012), and susceptible to the accumulation of fishing-related debris along their course (Mordecai et al., 2011; Cau et al., 2017).

Although submarine canyons may feature among the largest hotspots of litter in the deep sea, research on this topic remains limited, and the processes that control the inputs, distribution and ultimate fate of litter within canyons are poorly understood (Kane and Clare, 2019; Harris, 2020; Canals et al., 2021; Zhong and Peng, 2021). Similarly, it is not clear to what degree canyons may act as sinks or conduits for litter transfer toward deeper areas, which type of canyons may be more susceptible to funnel and/or accumulate litter and on which timescales, as well as what is their potential for

litter burial and sequestration in the sedimentary record (Zhong and Peng, 2021).

The overarching aim of this paper is therefore to assess the occurrence and distribution of macro- and microlitter in submarine canyons based on a review of the existing literature. Given that litter, and particularly plastics, is rapidly becoming a key indicator for the Anthropocene in the sedimentary record (Bancone et al., 2020), this review is presented from a geoscience perspective. We evaluate source, transport mechanism and deposition of litter as a type of anthropogenic 'sediment', and discuss the predisposing factors that may be responsible for their accumulation in and around submarine canyons.

Therefore, we estimate the potential exposure of individual canyons to riverine and maritime-sourced litter on a global scale and discuss how modeling of physical sediment transport processes combined with flume experiments can constrain the spatial variability and abundance of marine litter occurrences in submarine canyon systems. Finally, we identify knowledge gaps and perspectives on future research that could help to better understand the role of canyons as potential litter repositories and conduits to the deep-sea.

Methods

Review of litter assessment and transport processes in submarine canyons

To assess the current state of knowledge on litter in submarine canyons, a literature review was carried out using Google Scholar and the ISI Web of Knowledge. The keywords "litter", "plastic" and "microplastics" in combination with "canyons", were used to generate a list of peer-reviewed papers from 1996 till 2022. All papers dealing with litter in surface waters and the water column were excluded. From the selected paper we extracted information about: the geographical area and specific canyon studied; the method used to assess the presence of litter or microplastics; the number of surveyed sites and the depth range explored; litter abundance within the canyons, its spatial distribution and the dominant litter type. In parallel, selected literature on submarine canyons and their transport processes were used to discuss and infer the role of sedimentary and hydrodynamic processes in litter transfer and distribution.

Estimating the exposure of submarine canyons to plastics delivered by river systems

To identify the regions where submarine canyon heads are exposed to the highest input of river-derived litter, we combined a global model of river macroplastic input into the ocean (Meijer et al., 2021) with a global database of seafloor morphology (Harris et al., 2014; Bernhardt and Schwanghart, 2021a; Bernhardt and Schwanghart, 2021b). We calculated the distance from each submarine canyon head to the adjacent river outlets along the world's coastlines. Then, we divided the modeled floating macroplastic emissions of the closest river outlet (in million metric tons per year (MT/yr)) of Meijer et al. (2021) by the distance from each canyon head to the closest river outlet.

This index is, of course, a simplified metric. It does not account for litter other than macroplastic (e.g., microplastic), the buoyancy of plastic litter and other pathways of litter introduction into the ocean system including coastal inputs, atmospheric deposition, and direct inputs from ships. It omits any oceanographic processes. Moreover, this approach refers to submarine canyons that were mapped on global low-resolution bathymetric data and hence only features large submarine canyons (see details in Harris et al., 2014). Additionally, we restricted this analysis to canyons between 50°N and 50°S and to the main continents including the major islands of the West-Pacific, where data coverage is best. However, we argue that this approach helps to depict highly vulnerable submarine canyons with potential high litter input, canyons with low potential input that may be declared as sanctuaries, and to design future targeted scientific surveys.

Estimating the exposure of submarine canyons to marine fishing debris

To estimate canyon exposure to fishing activity, we used the global compilation of commercial fishing activity (any type) of the NGO "Global Fishing Watch" (available here https://services7.arcgis.com/IyvyFk20mB7Wpc95/arcgis/rest/services/SDG_14_Global_Fishing_Activity_1/FeatureServer). We calculated the mean fishing activity per canyon per year for 4398 canyons of the global canyon database (Harris et al., 2014). All remaining canyons were not covered by fishing activity data. Commercial fishing activity is measured in hours per area (area = grid size = 0.1 x 0.1 degrees) and refers to the annual average of the pre-pandemic year 2019.

Differences in exposure to riverine plastic and to fishing activity between geographical regions have been tested by the non-parametric Kruskal-Wallis test and *post-hoc* pair-wise comparisons with the Wilcoxon method and Bonferroni correction, using the software R (R Core Team, 2016).

To compare observed litter abundances (Supplementary Material S1) with canyon exposure to riverine plastic and to fishing activity, these indices have been estimated in higher detail for selected canyons where litter data were available. Canyon head locations and canyon areas have been remapped using Emodnet bathymetry for European seas (https://emodnet.ec.europa.eu/) and Gebco 2020 bathymetry (https://www.gebco.net) elsewhere, as these bathymetric data sets are of higher resolution (100 m resolution for Emodnet dataset, 15-arc resolution for Gebco 2020 bathymetry) than the SRTM30_PLUS 30-arc second database (Becker et al., 2009) used in the canyon mapping of Harris et al. (2014).

Canyons hosting a prevalence of plastic litter have been compared to the riverine-plastic input exposure, whereas canyon with dominant fishing-related debris have been compared to the exposure factor to fishing pressure.

Research efforts on the study of seafloor litter and microplastics in canyons

Submarine canyons have been the subject of research for a long time. Due to the difficulty of surveying such complex deep-sea environments, our knowledge of canyons has come primarily from remote sensing and sampling, with contributions from various oceanographic disciplines (Inman et al., 1976; Shepard, 1981). Over the last few decades, the advances in marine robotics for mapping, imaging and sampling, coupled with long term time-series from submarine observatories and moorings has shed light on the diverse and complex hydrodynamics and geomorphic processes acting along canyons (e.g., Xu, 2011; Amaro et al., 2016; Chaytor et al., 2016; Carter et al., 2018), showing that active sediment transport during the present sea level highstand may be considerably higher than previously predicted (Puig et al., 2014; Heijnen et al., 2022a) and revealing the widespread occurrence of anthropogenic debris along their course. However, while a handful of individual canyon systems have received considerable attention, most canyons around the world have not yet been studied, or only to a very limited extent. Eleven canyons account for almost 50% of the body of submarine canyon literature (Matos et al., 2018) and these are mostly located along the North American and European continental margins. A similar geographical bias also characterizes the research on litter in canyons, as shown below.

We found 46 studies reporting the occurrence of macrolitter in submarine canyons (Supplementary Material S1). From the selected publications, litter was reported and/or quantified in more than 120 canyons around the world (Figure 1). Over half of the studies featured seafloor litter distribution as the primary research topic, while a large proportion (~40%) addressed the study of canyon habitats, mostly focusing on ecologically relevant communities such as cold-water corals (CWCs), and reported the presence of litter or its relative impacts as secondary aims. In two studies, litter

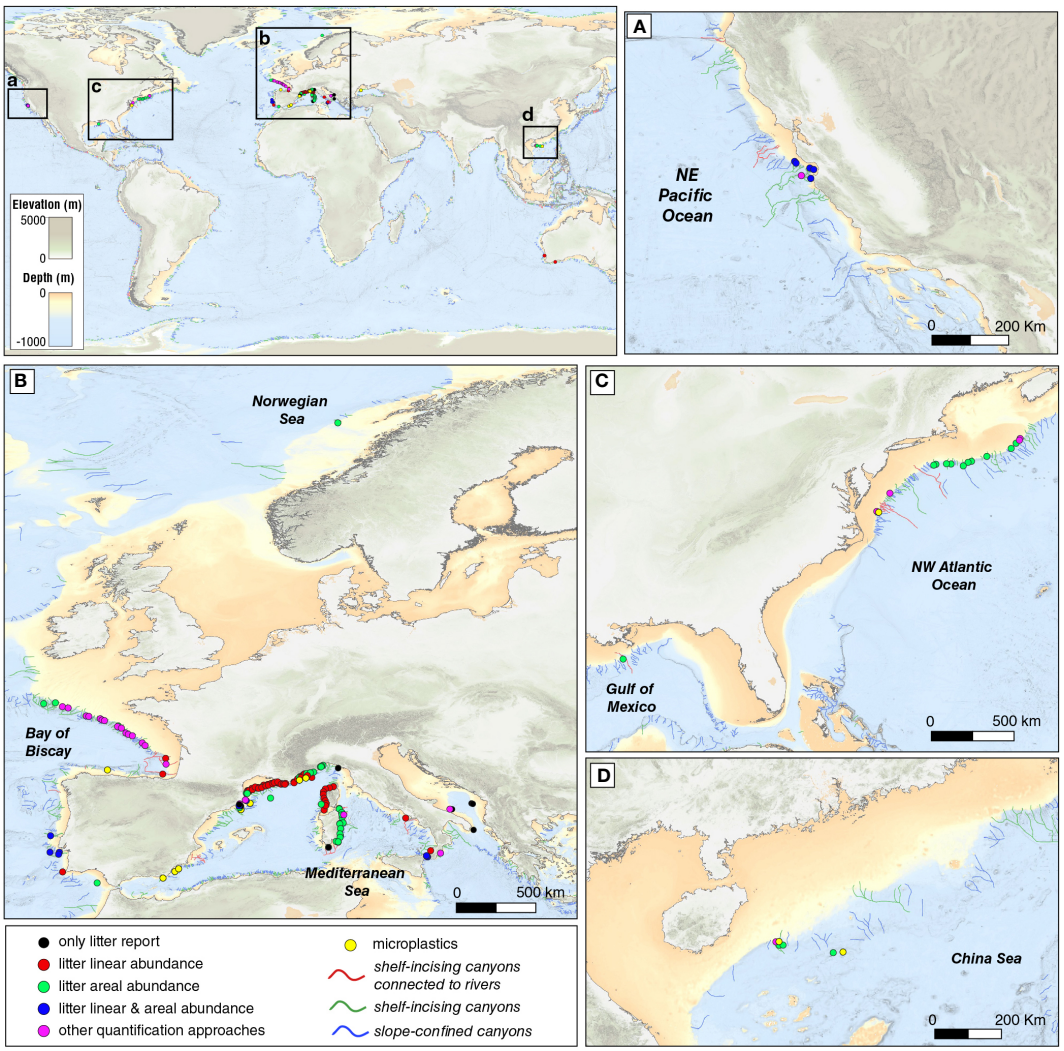

FIGURE 1
Global distribution of studies which quantified or reported litter and microplastics within submarine canyons. a-d. Zoom of geographical areas shown in the inset on the upper left. Bathymetric map has been obtained from GEBCO relief data (https://www.gebco.net). Canyons distribution and classification after Harris and Whiteway, 2011.

accidentally collected in canyons during sampling for other purposes was analyzed to assess colonization of benthic organisms (Aymà et al., 2019; Santín et al., 2020).

Apart from a few cases where litter is collected by trawling (i.e., Wei et al., 2012; Ramirez-Llodra et al., 2013; Pham et al., 2014), the assessment of seafloor litter within submarine canyons is mainly carried out using seafloor imagery, acquired by remotely operated vehicles (ROVs) (e.g., Mordecai et al., 2011; Tubau et al., 2015; Gerigny et al., 2019; Pierdomenico et al., 2019; Angiolillo et al., 2021), towed cameras (e.g., Buhl-Mortensen and Buhl-Mortensen, 2018), or submersibles (e.g., Watters et al., 2010; Peng et al., 2019). These instruments are more appropriate for studies in complex and rugged terrains, such as those occurring in canyons, which are usually inaccessible to bottom trawls. However, these methods do not give information about volumes or weight of litter, which are necessary for estimates of fluxes and mass balance models (Canals et al., 2021). Presence of litter is therefore primarily quantified as abundance (i.e., number of items), although there is a high variability in the units of measure adopted to report its density (see also Hernandez et al., 2022). Both abundance of litter per unit of area and/or abundance per linear distance are commonly used (Figure 1), along with other quantification approaches, such as abundance per time of observation (Schlining et al., 2013), per image frames (van den Beld et al., 2017; Zhong and Peng, 2021), frequency of occurrence (Moccia et al., 2019) or simple enumeration (Jones et al., 2022). The only attempt at mass estimates from video images was performed by Buhl-Mortensen and Buhl-Mortensen (2017), who assumed approximate weights for different items based on their composition.

The presence of microplastics in canyons is much less investigated than that of macrolitter, with only 4 studies reporting microplastics in seafloor sediments collected from 12 canyons around the world (Figure 1; Supplementary Material S1). Although all studies use density-based extraction methods, where lighter plastic particles are separated from sediment by mixing the sample with saturated solutions (Hidalgo-Ruz et al., 2012), the units of measure adopted to report microplastic concentrations are highly variable, encompassing the number of microparticles per unit of weight (Chen et al., 2020; Angiolillo et al., 2021), per unit of volume (Sanchez-Vidal et al., 2018) or per unit of area (Jones et al., 2022).

Distribution of studies: geographical and sampling biases

There is a strong geographic bias to the studies that have been performed to date. Most of the research on seafloor litter and microplastics has focused on Mediterranean canyons (accounting for more than 50% of the canyons where anthropogenic debris has been reported), followed by the northeast and northwest Atlantic canyons (Figure 2A). In the Pacific Ocean, few canyons have been studied for litter assessment, mostly offshore California (Watters et al., 2010; Schlining et al., 2013) and in the South China Sea (Peng et al., 2019; Chen et al., 2020; Zhong and Peng, 2021). Canyons in the Indian Ocean are almost absent from published reports, except for a recent study of two canyon systems on the SW Australian margin (Taviani et al., 2023). The striking differences in coverage by studies are also evident when analyzing the sampling effort (i.e., the number of stations surveyed) for individual canyons (Figure 2B). On average, studies on litter distribution in Mediterranean canyons have analyzed a larger number of samples than canyons in other regions (Figure 2B), especially those in the NW Mediterranean. La Fonera, Cap de Creus and Blanes Canyons on the Catalan margin (Orejas et al., 2009; Ramirez-Llodra et al., 2013; Tubau et al., 2015; Mecho et al., 2018; Dominguez-Carrió et al., 2020) and some canyons of the Gulf of Lyons have been extensively studied (Galgani et al., 1996; Fabri et al., 2014; Fabri et al., 2019; Gerigny et al., 2019), with tens of stations explored per single canyon. Similarly, for a few canyons in the Atlantic Ocean, namely Dangeard, Explorer and Whittard Canyons on the Celtic margin (Pham et al., 2014), Nazaré Canyon off the west coast of Portugal (Mordecai et al., 2011), and Baltimore and Norfolk Canyons off the US coast (Jones et al., 2022) a large number of stations (>10) have been surveyed. However, the assessment of seafloor litter is based in most cases on exploration of only one or two sites of the entire canyon system. This is also true for microplastics assessment, which has been performed mostly based on a single sediment sample, except for a few individual canyons such as Norfolk (Jones et al., 2022) and Blanes Canyons (Sanchez-Vidal et al., 2018) where several samples have been collected. Papers on litter in the Monterey Canyon, one of the most studied canyon systems in the world (Matos et al., 2018), do not report the exact number of sampled sites, although the large number of surveys covering decadal time spans and the availability of a wide database (332 stations for shelf and canyons of Central California as reported in Watters et al. (2010) and 1149 videos in Monterey Bay analyzed by Schlining et al. (2013)) indicate that the sampling effort is likely much higher than all other canyons.

Bathymetric ranges of observations are also highly variable (Figure 2C; Supplementary Material S1). Overall, Mediterranean canyons have been mainly surveyed in their heads or along their upper reaches, and only a few canyons offshore the Spanish and French coasts have been surveyed in their middle or lower reaches at depths >1500 m (Galgani et al., 2000; Ramirez-Llodra et al., 2013; Tubau et al., 2015; Dominguez-Carrió et al., 2020; Angiolillo et al., 2021). Conversely, in the Atlantic Ocean, wider depth ranges have been covered. Canyons of the Bay of Biscay have been surveyed from 300 to 2300 m depth (Galgani et al., 2000; van den Beld et al., 2017), similar to the canyons of the continental margin off the Northeastern US, with observations from 300 to 2100 m depth (Quattrini et al., 2015; Jones et al., 2022). Explorations at greater depths have been carried out in the canyons offshore of Portugal, from 1600 down to 4500 m depth (Mordecai et al., 2011), as well as in the Whittard (Pham et al., 2014) and Mississippi Canyons (Wei et al., 2012), down to 2600 and 2700 m depth, respectively. In the Pacific Ocean, litter and microplastics have been reported from the tributary canyons of the Xisha Trough at around 2000 m depth, with deeper exploration in the trough down to 3300 m depth (Peng et al., 2019; Chen et al., 2020; Zhong and Peng, 2021). Canyons off SW Australia have been surveyed from 180 m down to 3300 m depth (Taviani et al., 2023) (Figure 2C).

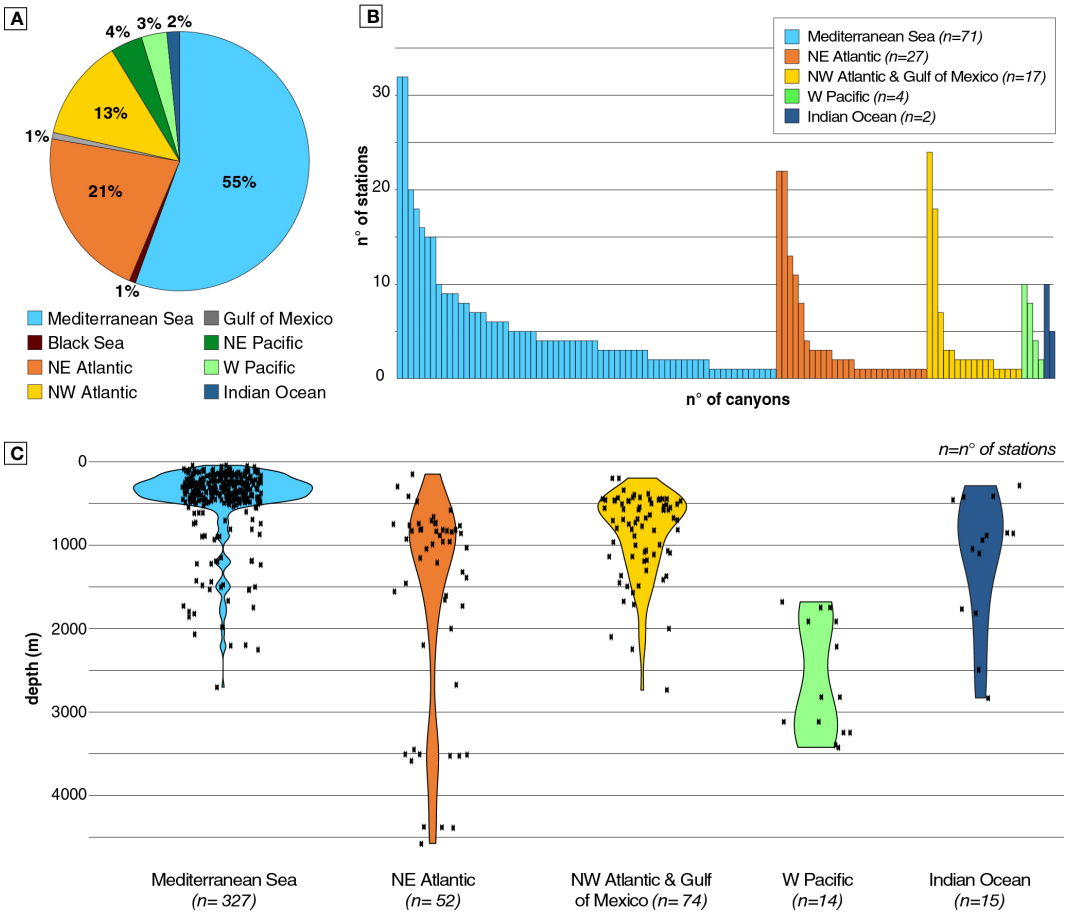

FIGURE 2
Research effort on seafloor litter and microplastics in canyons. **(A)** Pie chart showing the geographical location of publications reporting litter and microplastic in canyons. **(B)** Bar plot of sampling effort (number of stations) per submarine canyon carried out in each of the main geographical regions. **(C)** Violin plots showing the depth ranges covered by surveys in canyons in each of the five main geographical regions. For each available station, the mean depth of ROV transects/trawl hauls and the depth of sediment sampling for microplastic assessment were plotted.

Submarine canyons are hotspots for litter accumulation

Overall, reviews of published data (Galgani et al., 2015; Angiolillo, 2018; Canals et al., 2021; Galgani et al., 2022; Hernandez et al., 2022) and studies covering wide geographic areas indicate that canyons are preferential accumulation areas for anthropogenic debris, often showing higher concentrations compared to the surrounding areas. Large-scale assessments of seafloor litter in European waters found higher litter abundance in canyons than in shelf and slope areas (Galgani et al., 2000), and also compared to other physiographic settings such as seamounts, mounds, ocean ridges and deep basins (Pham et al., 2014). Using a wide dataset of over 1700 video transects collected along the Norwegian margin in the national scientific program Mareano, Buhl-Mortensen and Buhl-Mortensen (2017) observed that litter densities in canyons were more than twice the densities of shelf and slope areas, and lower only than fjords. Trawl surveys in the northern Gulf of Mexico, from the outer continental shelf to the abyssal plain, showed that Mississippi Canyon was a focal point for litter accumulation (Wei et al., 2012). Even on a more local scale and with much limited sampling on the margin, several studies in the Mediterranean Sea and NE Atlantic report increased abundances of litter in canyons compared to the adjacent sectors (e.g., Galgani et al., 1996; Cau et al., 2017; van den Beld et al., 2017; Mecho et al., 2018; Gerigny et al., 2019; Dominguez-Carrió et al., 2020; Pierdomenico et al., 2020).

Canyons have also been shown to represent main hotspots for microplastics contamination, with higher abundances compared to other physiographic settings (Kane and Clare, 2019). This has been further supported by results from a large-scale survey of seafloor sediments in European seas from 42 m down to 3500 m depth, which revealed microplastic abundances in canyons almost twice those of adjacent open slopes (Sanchez-Vidal et al., 2018).

Slope-confined canyons are much less extensively investigated than shelf-indenting canyons, as their transport activity has been traditionally considered reduced during the present highstand of

sea level, despite there is increasing evidence for intermittent sediment transport even in these systems (Yin et al., 2019; Post et al., 2022). Consequently, their role in litter accumulation remains practically unknown. Litter assessment in a slope-confined canyon and comparison with other physiographic domains in the Gulf of Cadiz showed higher abundance of litter within the canyon, with plastic concentrations more than twice than those observed on the adjacent continental slope; litter abundance was only higher in the nearby contouritic channels (Mecho et al., 2020).

Litter supply to canyons: the influence of natural and anthropogenic factors on global abundance and composition

The abundance and composition of litter reported are extremely variable, with spatial densities spanning several orders of magnitude (Figure 3) and no obviously discernible patterns related to geographical location and depth range (Hernandez et al., 2022).

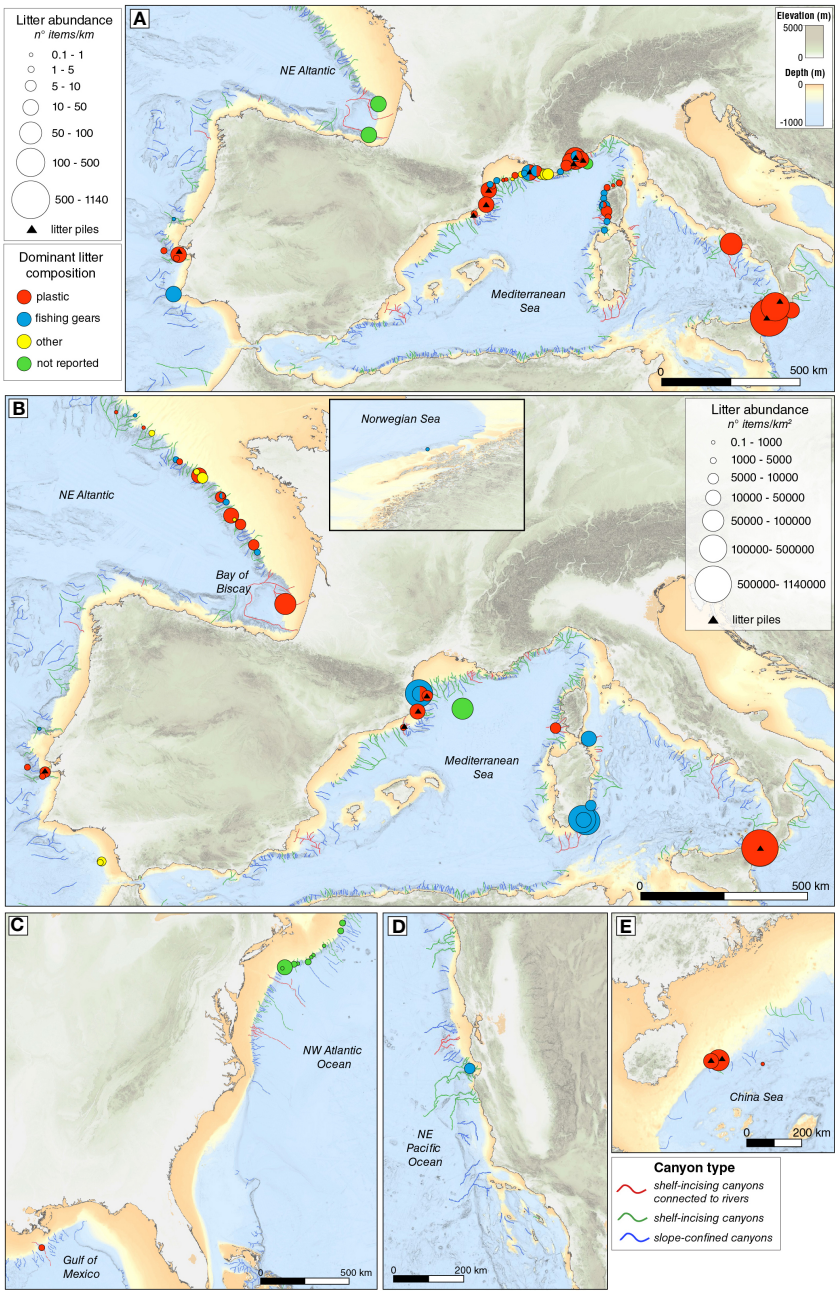

FIGURE 3
Global Abundance and composition of litter in canyons. **(A)** Bubble plot showing the abundance of litter reported as n° items per linear km of video track. **(B-E)** Bubble plots showing the abundance of litter reported as n° items per square km in different geographical areas. The plotted values refer to the mean abundance estimated per each canyon, while the colors of bubbles refer to the dominant type of litter. The black triangles indicate the occurrence of litter accumulation piles. For canyons included in more than one study all the mean abundances reported are plotted in the map.

Such large variability has been observed between canyons of different geographical areas, as well as between nearby canyons along the same margin (e.g., van den Beld et al., 2017; Gerigny et al., 2019; Quattrini et al., 2014). This is linked to the fact that the abundance and composition of litter in canyons is the result of a combination of anthropogenic factors (e.g., sources and litter buoyancy), geomorphological factors and physical transport processes, which may differ between canyons as well as along different reaches of an individual canyon. In addition, the uneven geographical distribution, sampling effort and bathymetric range of studies in canyons, combined with the general lack of standardization of data collection and reporting in the literature (Canals et al., 2021; Hernandez et al., 2022), hinder comparisons between studies and estimates of absolute pollution magnitude. This information is essential to better assess the role of canyons in focusing, distributing and trapping litter and to evaluate the influence of natural and anthropogenic predisposing factors.

Regarding litter composition, canyons can represent accumulation areas for both land-sourced and maritime-sourced litter, which is reflected in the overall types of litter found. A wide variety of objects has been reported from canyons, with plastic items and fishing gears featuring as the most common types of waste (Figure 3). Despite fishing materials currently being largely made of artificial polymers, fishing-related debris is often classified as a separate category because of its origin (Hernandez et al., 2022). It is not easy to ascertain the exact origin for many types of litter, except for specific categories such as fishing gears; however, the majority of plastic, one of the main components of urban waste, is thought to derive from terrestrial and coastal sources, at least on a global basis (Jambeck et al., 2015). Among plastics, single-use items such as bags, packaging and bottles are often the most common categories (e.g., Schlining et al., 2013; Tubau et al., 2015; Peng et al., 2019; Pierdomenico et al., 2019; Angiolillo et al., 2021; Grinyó et al., 2021), which reflects the large contribution of single-use items to the global marine plastic pollution (Schnurr et al., 2018) and highlights the high mobility of these light-weight objects.

The abundance and distribution of litter of terrestrial and maritime origins in canyons may differ due to the different entry points, transport and depositional mechanisms of these types of litter (Galgani et al., 2022). It has been proposed that the efficiency of litter transfer from onshore to the deep sea via canyons is dependent on the physiographic configuration of the continental margin and the connection of the canyon heads to terrestrial sources of sediment (Kane and Clare, 2019), together with the magnitude of litter inputs from inland. In the following paragraphs the main factors determining the connectivity of submarine canyons to a source of sediment are described, together with other maritime sources that may influence the supply of litter to canyons.

Rivers

Canyons which indent the shelf and are connected directly to river systems may be highly efficient at transferring sediment (and potentially litter) directly to the slope, bypassing the shelf. Dense sediment-laden water generated at the river mouth may plunge to form a hyperpycnal flow that can evolve into turbidity currents and supply sediment directly to the canyon (e.g., Var Canyon, NW Mediterranean; Mulder et al., 2003; Gaoping Canyon, Taiwan; Khripounoff et al., 2009; Carter et al., 2012; La Jolla Fan, Romans et al., 2016; Messina Canyons; Pierdomenico et al., 2019). Alternatively, high discharge from these river mouths may lead to rapid sediment accumulation near the river mouth or at the canyon head; these deposits may become flushed offshore as a buoyant river plume before sinking to the seabed (Tubau et al., 2015; van den Beld et al., 2017), or may collapse, to trigger turbidity currents (Carter et al., 2012; Pope et al., 2017; Hizzett et al., 2018; Hage et al., 2019; Talling et al., 2022).

Rivers, globally recognized as the main conveyers and transporting agents of land-based litter (Rech et al., 2014; Lebreton et al., 2017; Meijer et al., 2021), can be responsible for significant inputs of mismanaged anthropogenic waste to the sea, although many uncertainties still exist about the proportion of litter rapidly sinking close to the river mouth versus being transported offshore, and consequently about how riverine outflows may enter and interact with the sedimentary regime in canyons. While the largest discharging rivers have been traditionally considered to contribute almost entirely to the global river emissions (Lebreton et al., 2017; Schmidt et al., 2017), the important role of small (low discharge), heavily polluted urban rivers has been recently reconsidered (Meijer et al., 2021). Direct input from a small river affected by flash-floods and draining a heavily populated area explains the high concentration of litter in the Gioia-Petrace Canyon system, where up to 560 items per linear km of ROV track were observed (Pierdomenico et al., 2020). Even higher densities have been reported from the Messina Strait, ranging from 121,000 to up to 1.3 million items/km^2, making it the most litter-affected canyon and deep-marine environment recorded to date globally (Figure 3, Pierdomenico et al., 2019). These canyons are connected to subaerial drainage networks and are frequently affected by sedimentary gravity flows triggered by river flash-floods, which are able to funnel huge amounts of anthropogenic waste into adjacent canyons. In this area, the high coastal population densities coupled with poor disposal practices likely contribute to the extreme density values observed (Pierdomenico et al., 2019).

The presence of large rivers may influence litter abundance even in canyons separated from land by wide continental shelves, such as observed in the Bay of Biscay, where the higher litter abundances found in the Belle-île and Arcachon Canyons (with maximum densities up to 59,000 items/km^2, comparable to those observed in other Mediterranean coastal canyons), with respect to the other canyons of the margin, have been attributed to the influence of the Loire and Gironde rivers, respectively (van den Beld et al., 2017). In the Gulf of Lyon, despite low litter densities being observed off the mouth of Rhône River (Galgani et al., 1996) and in the upper reach of the Petit Rhône Canyon (Fabri et al., 2014; Gerigny et al., 2019), trawling on the deep-water Rhône fan at 2200 m depth, more than 150 km from the river mouth, revealed litter concentrations of 52,000 items/km^2 (Galgani et al., 2000), suggesting efficient transfer of river-derived waste.

Distance of canyon head from land and coastal urbanization

Submarine canyons that indent the shelf, but that do not have a direct connection to a river mouth, are fed by along-shelf currents and wave and tide action, which redistributes and disperses sediments and litter (Mulder et al., 2012; Schlining et al., 2013; Eidam et al., 2019; Pierdomenico et al., 2020). Natural and anthropogenic debris may be transported along the shelf, until the load is diminished through wave and storm action, or until it meets an intersecting canyon head (e.g., La Jolla or Monterey Canyons, California; Xu et al., 2002; Covault et al., 2007). Particularly, high energy seasonal events that might enhance cross- and along-shelf transport such as storms, dense water shelf cascading, hurricanes or typhoons (e.g., Flemming, 1980; Canals et al., 2006; Harris and Heap, 2009), can be responsible for the transfer of heavy litter from the shelf to canyons (Wei et al., 2012; Tubau et al., 2015; Zhong and Peng, 2021).

Submarine canyons deeply incising the shelf offshore densely populated areas were observed to accumulate substantial amounts of litter, such as the Paillon Canyon offshore Nice (>80 items/km, Galgani et al., 1996), La Fonera and Cap de Creus Canyons (>25,000 items/km^2 Tubau et al., 2015; Dominguez-Carrió et al., 2020) and the Dohrn Canyon, offshore Naples (50 items/km, Taviani et al., 2019) (Figure 3A). Reduced distances between the canyon head and the coastline may also in part explain the higher abundance of anthropogenic waste observed in the Ligurian and Corsica canyons with respect to the offshore Gulf of Lyon canyons (Gerigny et al., 2019). The higher litter abundance reported from the Lisbon Canyon compared to other canyons of the Portuguese margin was also interpreted as due to the proximity to a large population center (Mordecai et al., 2011). On the other hand, the low litter density observed in the canyon systems off southwestern Australia (1 to 1.7 items/km), has been attributed to reduced coastal urbanization in this region compared to other regions worldwide, combined with the national status as marine parks which further limits human activities in these areas (Taviani et al., 2023). Exploration of north-western Atlantic canyons, which are separated from land by a wide continental shelf, revealed an overall low litter abundance, despite anthropogenic debris being observed in most dives (Quattrini et al., 2015; Jones et al., 2022) (Figure 3). Surprisingly, the highest litter densities >10,000 items/km^2 were found in an un-named slope-confined canyon at 1000-1100 m depth (Quattrini et al., 2015).

While the proximity of a canyon's head to land may facilitate the transfer of litter of terrestrial origin from the coast and shelf environments into the canyons, one of the most littered canyons observed to date is the SY82 Canyon, a tributary of the Xisha Trough in the southern China Sea (Peng et al., 2019). This canyon has its head at 350 m depth, being located ~150 km from the coast. Here, large litter accumulations reaching densities >50,000 items/km^2 were found in the middle course of the canyon at 1700-1800 m depth, indicating that the massive transfer of anthropogenic debris to the deep sea via canyons does not necessarily require close proximity of the canyon head to land. Even though it has been proposed that most of the debris came from fishery and navigation activities, the uneven and focused distribution of the litter accumulations indicates subsequent reworking and down-canyon transport of litter (Zhong and Peng, 2021), showing that even canyons indenting wide shelves may become hotspots of litter accumulation.

Global canyon exposure to river-derived plastic

The global maps in Figure 4 and the boxplots in Figure 5A show a highly spatially-variable exposure of canyons to river-supplied plastic fluxes, as confirmed by Kruskal-Wallis test ($p<0.001$) and Wilcoxon pair-wise comparisons (Supplementary Material S2). Overall, the Mediterranean Sea, the North Pacific Ocean and the South Atlantic Ocean show a significantly higher proportion of submarine canyons that are most exposed to plastic contamination when compared to other ocean basins (Figure 5A). Specifically, we infer high exposure of canyons to litter in areas where high macroplastic emission from rivers (Meijer et al., 2021) coincides with short distances between the river outlets and submarine canyon heads. For instance, in the Philippines and India, which are recognized as the largest contributing countries to global plastic emissions (Meijer et al., 2021), tectonics and high rainfall result in high sediment supply (and therefore litter export) to the oceans (Milliman and Meade, 1983). Narrow shelves and the higher percentage of shelf-indenting canyons compared to other margins (Harris and Whiteway, 2011) makes these areas more prone to transfer plastic from land to the deep sea via canyons. Similarly, canyons off West Africa, Central America and Brazil as well as those in the Mediterranean and Black seas are also susceptible to receiving large amounts of river-derived litter, mostly because of rivers draining highly populated coastal areas. They are therefore identified as hotspots for plastic emissions (Meijer et al., 2021).

Our global assessment highlights that most of the canyons highly vulnerable to plastic input are located in areas that have not been yet surveyed for litter (see Figure 1 for comparison). Hence, we are likely far from a comprehensive knowledge of the real magnitude of this worldwide impact. Moreover, it also highlights areas with canyons that are potentially less affected by riverine plastic emissions, such as those located in the North Atlantic Ocean, on the Australian coasts and in the NE Pacific (Figure 4). These canyons, theoretically less impacted by plastic inputs along their course, may host well-preserved and relatively pristine ecosystems, and could be considered as priority areas to concentrate conservation efforts (Fernandez-Arcaya et al., 2017).

Notwithstanding the limitations of this approach (as explained in the methods section), the comparison of the estimated exposure values with litter densities observed in canyons shows an overall increase in litter abundance with increasing exposure values (Figures 5B, C). This supports the validity of the global assessment and stresses the strong role of rivers as main inputs of litter to the Global Ocean (Rech et al., 2014; Jambeck et al., 2015). The increase is more evident for Mediterranean canyons (Figure 5B), which have been more extensively surveyed, especially in their upper reaches, than other canyons worldwide.

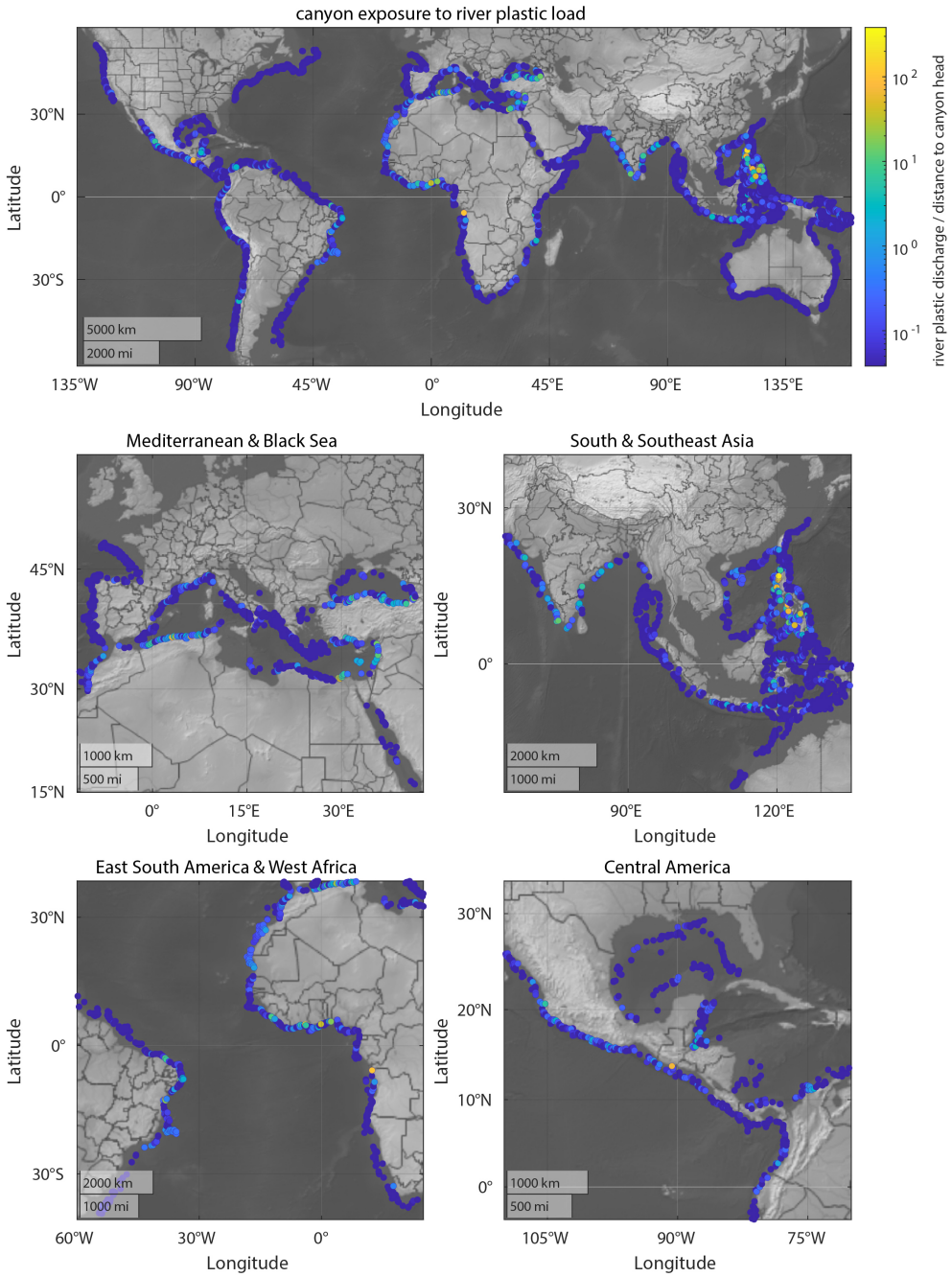

FIGURE 4
Global map showing the canyon head exposure to plastic input from rivers and insets of the regions with canyons most susceptible to receive substantial amount of land-derived plastic.

In canyon systems developed on the edge of wide continental shelves, as in the case of the North Atlantic passive margin, that show highly variable litter abundance for similar exposure values (Figure 5C), complex hydrographic regimes acting over large areas may concur to generate more complex dispersal patterns of litter. Departures from the overall trend could also be related to the fact that river plastic discharge from Meijer et al. (2021) may be not representative of local scenarios. The mismanagement of litter dumped in small torrential rivers may for instance explain the unpredicted higher abundances in the Messina Canyons with respect to other ones with comparable exposure (Pierdomenico et al., 2019).

Fishing and other maritime activities

Although overlooked by many global studies on plastic transport to the ocean, fishing activities can represent an important source of litter in canyons, which can be the dominant source of plastic pollution in some systems. Many canyons are the

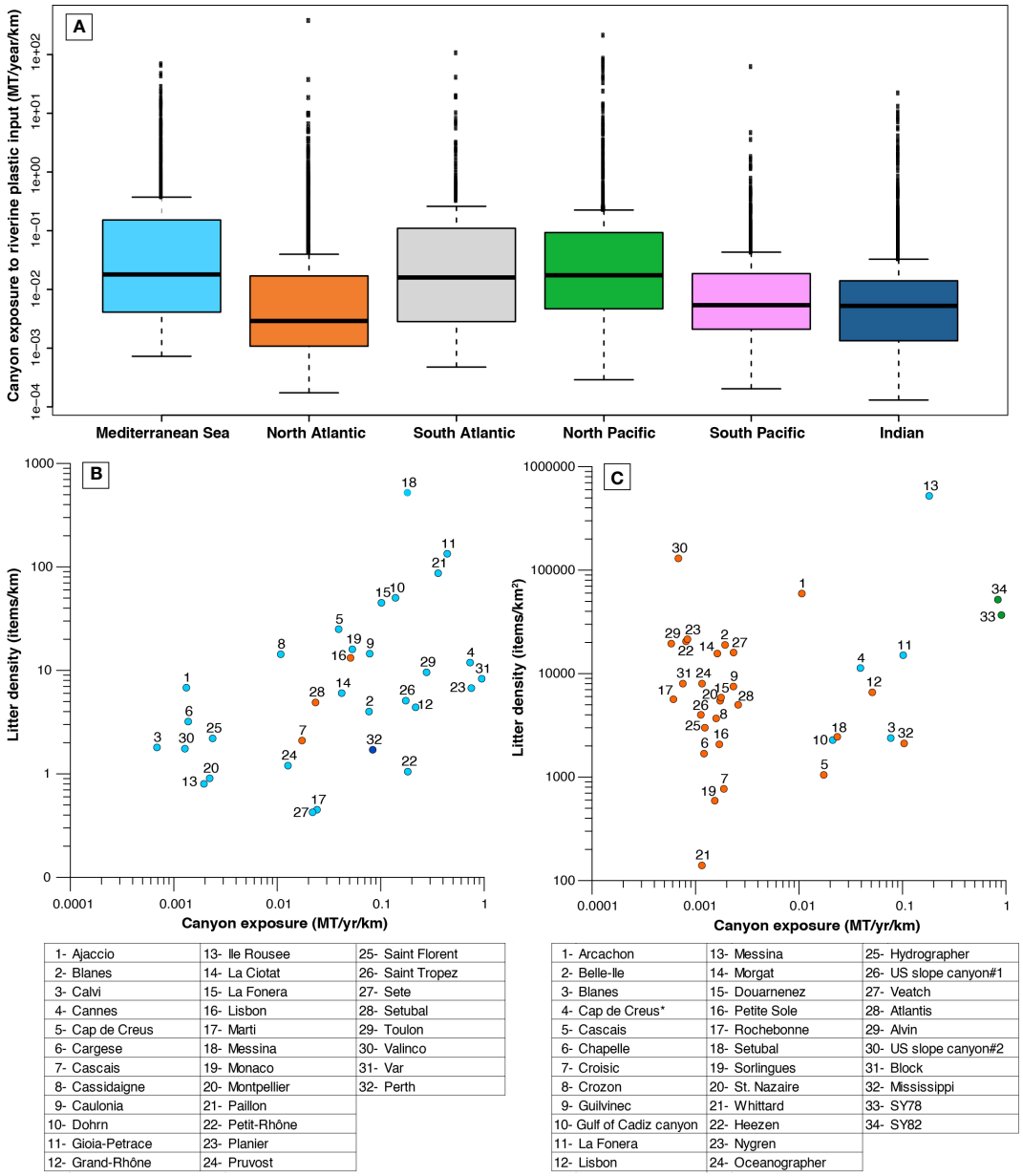

1- Ajaccio	13- Ile Rousee	25- Saint Florent
2- Blanes	14- La Ciotat	26- Saint Tropez
3- Calvi	15- La Fonera	27- Sete
4- Cannes	16- Lisbon	28- Setubal
5- Cap de Creus	17- Marti	29- Toulon
6- Cargese	18- Messina	30- Valinco
7- Cascais	19- Monaco	31- Var
8- Cassidaigne	20- Montpellier	32- Perth
9- Caulonia	21- Paillon	
10- Dohrn	22- Petit-Rhône	
11- Gioia-Petrace	23- Planier	
12- Grand-Rhône	24- Pruvost	

1- Arcachon	13- Messina	25- Hydrographer
2- Belle-Ile	14- Morgat	26- US slope canyon#1
3- Blanes	15- Douarnenez	27- Veatch
4- Cap de Creus*	16- Petite Sole	28- Atlantis
5- Cascais	17- Rochebonne	29- Alvin
6- Chapelle	18- Setubal	30- US slope canyon#2
7- Croisic	19- Sorlingues	31- Block
8- Crozon	20- St. Nazaire	32- Mississippi
9- Guilvinec	21- Whittard	33- SY78
10- Gulf of Cadiz canyon	22- Heezen	34- SY82
11- La Fonera	23- Nygren	
12- Lisbon	24- Oceanographer	

FIGURE 5
(A) Box plots of canyon head exposure to plastic input from rivers across different basins. **(B, C)** Scatter plots of litter density reported in canyons and corresponding canyon head exposure to plastic input from rivers. Canyons are colored according to their location, using the same colors of the geographical areas in **(A)**. **(B)** Canyons with litter density reported as items/km. **(C)** Canyons with litter density reported as items/km2.

sites of intense commercial and artisanal fishery activities (due to the rich commercially-important fauna they host), including bottom trawling along the rims and long-line fisheries on the rocky substrates not accessible to trawling (Puig et al., 2012; Fernandez-Arcaya et al., 2017). Small-scale artisanal fishing activities may have a deep impact on littering in canyons, as indicated by the very high litter densities of 280,000 items/km^2 observed in the East Sardinian canyons (Cau et al., 2017), with abandoned or discarded fishing gears comprising 84 to 100% of litter, approx. three times higher than other geomorphological settings (Cau et al., 2017). Similarly, concentrations of benthic long-line fishing gears of up to 220,000 items/km^2 were observed on rocky outcrops along the flanks of Cap de Creus Canyon (Orejas et al., 2009). During submersible explorations off the Californian margin, hotspots of litter, with densities up to 380 items per linear km of ROV track, were found in Monterey Canyon and the south-western edge of Soquel Canyon at places that are traditionally fished (Watters et al., 2010).

Apart from fishing gear, other maritime activities are also attributed as the source for heavy items found in canyons such as glass, clinker or large metal objects, whose distribution has been tentatively linked to direct dumping from ships and therefore associated with marine traffic and shipping routes (e.g., Ramirez-Llodra et al., 2013; van den Beld et al., 2017). Other local factors

may determine the accumulation of specific litter types, such as the presence of naval bases or military dumping sites, which are thought to be responsible for the large proportion of metal objects observed in some canyons of the Gulf of Lyon (Fabri et al., 2014; Gerigny et al., 2019) and the Gulf of Cadiz (Mecho et al., 2020).

Global canyon exposure to fishing-related debris

The exposure of global canyons to commercial fishing activity was calculated for 4398 large submarine canyons of the 9477 canyons mapped by Harris et al. (2014) (Figure 6). The remaining canyons do not overlap with fishing activity data as such data do not exist for large regions of the global ocean, such as the South and Southern Asia, the Central and South-Eastern America and the Southern Mediterranean Sea (Supplementary Material S3). However, the available results show that the canyons of the Mediterranean Sea are more heavily affected by fishing pressure along their course than canyons in other regions in the world ($p<0.001$). No striking differences in canyon exposure to fishing pressure were observed across the main oceans, except for a slightly higher exposure of canyons in the northern hemisphere, which is significant only for the Mediterranean Sea and the North Atlantic Ocean (Figure 7A; Supplementary Material S2).

Comparison of the observed litter densities with mean commercial fishing activities at submarine canyons, carried out for canyons where the dominant litter type was fishing-related debris, does not show clear trends (Figure 7B). However, along with

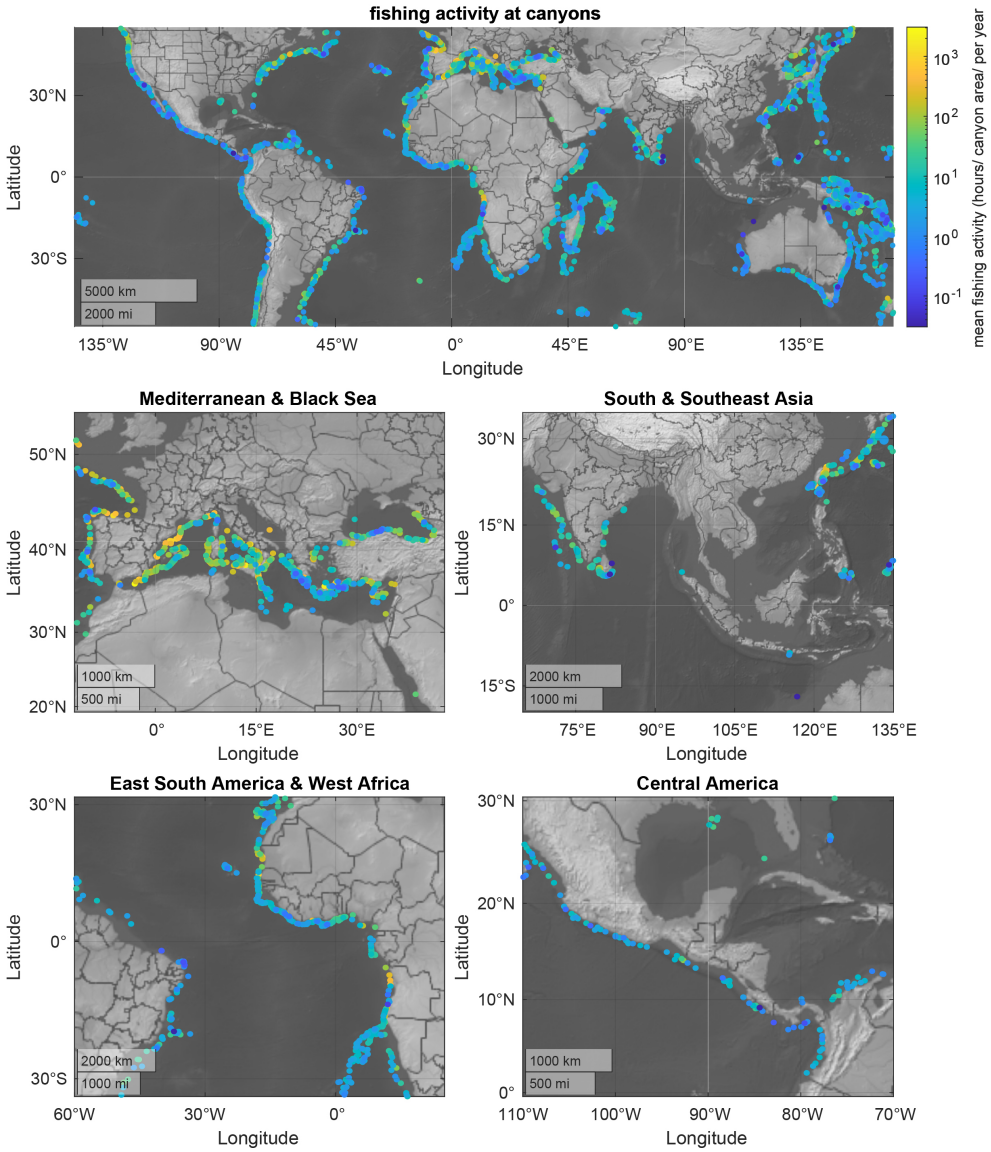

FIGURE 6
Global map showing the canyon exposure to commercial fishing activity and insets of the regions shown in Figure 4 for comparison. Data coverage is inhomogeneous and very sparse around Southeast Asia and the southern Mediterranean Sea where the fishing activity per submarine canyon could not be computed.

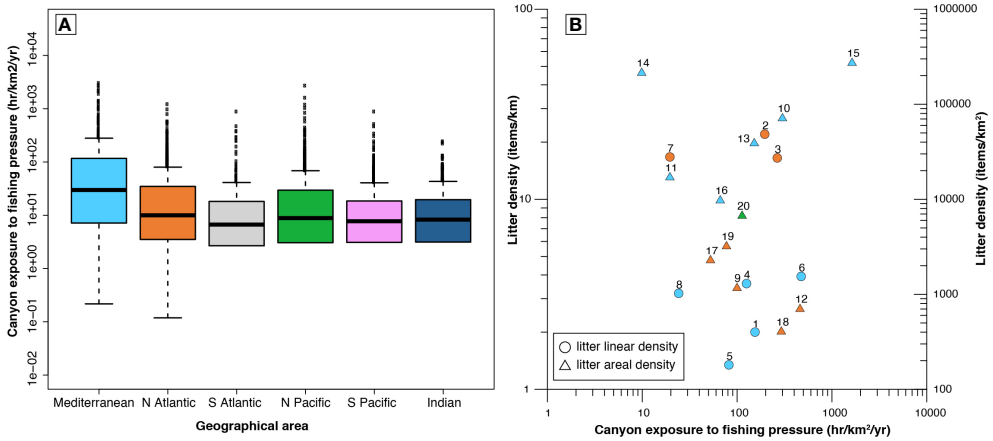

1- Boucart	5- Couronne	9- Ars	13- E-Sardinia #1	17- Lampaul
2- Cape Breton	6- Lacaze-Duthiers	10- Cap de Creus	14- E-Sardinia #2	18- Nazaré
3- Cape Ferret	7- São Vicente	11- Caprera	15- E-Sardinia #3	19- Odet
4- Centuri	8- Stoechades	12- Dangeard & Explorer	16- E-Sardinia #4	20- Monterey

FIGURE 7
(A) Box plots of canyon exposure to fishing activity across different basins. **(B)** Scatter plot of the abundance of fishing-related debris reported in canyons and corresponding canyon exposure to commercial fishing activity. Canyons are colored according to their location, using the same colors of the geographical areas in **(A)**.

the data gaps, it has to be considered that the calculated mean commercial fishing activity may not recognize the artisanal fishery activities, which are regarded as an important source of litter in specific cases (Cau et al., 2017). This may explain, for instance, the high densities of fishing gears in Sardinian canyons (Mediterranean Sea) despite variable fishing activity (Figure 7B). In addition, as the distribution of fishing debris may be largely controlled by the substrate topography and the occurrence of rocky outcrops that favor entanglement, the estimation of fishing-debris concentration may be strongly influenced by the sampling location along the canyon course.

Litter distribution within canyons: transport and deposition

Processes controlling the distribution of terrestrial litter

Plastic and other land-based litter that is funneled into canyon heads can be remobilized and redistributed downslope toward deep-sea areas by a variety of oceanographic and sedimentary processes, including enhanced bottom currents, dense water cascading and sediment gravity flows (Schlining et al., 2013; Tubau et al., 2015; Dominguez-Carrió et al., 2020; Pierdomenico et al., 2019; Pierdomenico et al., 2020; Zhong and Peng, 2021). These processes act at different temporal and spatial scales from the continental margin down to individual canyons and on to small-scale features along the canyon course and can be responsible for the uneven distribution of litter among and within individual canyons. Furthermore, various sediment-transport mechanisms (and by extension litter transport mechanisms) often coexist in a given submarine canyon and along-canyon transport is not a constant or unidirectional process (Puig et al., 2014; Amaro et al., 2016). This means that understanding the magnitude of transport activity and the role of canyons in funneling and accumulating litter in the deep sea is not a trivial task, as it is driven by a complex interplay of natural and anthropogenic factors linked to sources, transport, and depositional mechanisms (Ramirez-Llodra et al., 2013; Maier et al., 2019; Pearman et al., 2020; Pierdomenico et al., 2020).

Local topography and spatial variations in flow energy seem to play an important role in the deposition of litter in canyons. Litter has been observed frequently within the troughs of furrows, behind rock slabs, tree trunks or other obstacles (Figures 8A, B) (Galgani et al., 1996; Tubau et al., 2015; Pierdomenico et al., 2020). Specific types of litter, such as fishing gear, or cables and pipelines lying on the seafloor, can nucleate the formation of small litter accumulation points, where mostly plastic items get trapped (Figure 8C) (Mordecai et al., 2011; Tubau et al., 2015; Biede et al., 2022). On a larger scale, morphological features along the canyon axis such as scours, knickpoints, or changes in thalweg slope, which may interact with flows promoting deposition, can represent important accumulation areas for litter (Pierdomenico et al., 2019; Angiolillo et al., 2021; Zhong and Peng, 2021).

Sediment gravity flows

Sediment gravity flows, principally turbidity currents, are the main agents for sediment transport down canyons and consequently for litter transfer to the deep sea (Pierdomenico et al., 2019; Zhong and Peng, 2021). There are several processes able to trigger sediment gravity flows within canyons (Piper and Normark, 2009), including the evolution of mass-failures along canyon walls (Paull et al., 2010), advection of resuspended shelf sediments by oceanographic currents or storm waves (Xu et al., 2010; Martín et al., 2011) and hyperpycnal flows during pulses of

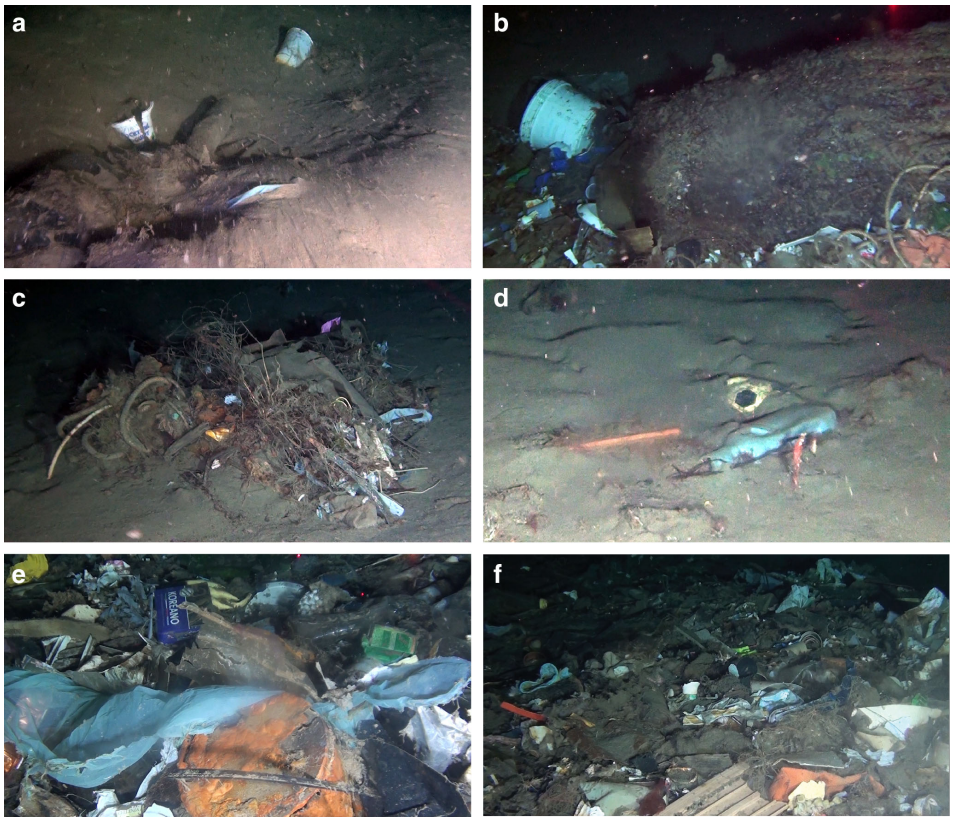

FIGURE 8
Examples of litter on the floor of submarine canyons. **(A)** plastic accumulating within a depression along the thalweg of Gioia Canyon (400 m depth). **(B-F)** accumulation hotspots in the Messina Strait Canyons (200-600 m depth).

river discharge or ice melting (Mulder et al., 2003; Khripounoff et al., 2012; Hizzett et al., 2018; Bailey et al., 2021; Talling et al., 2022). Sediment resuspension induced by bottom trawling can be an additional trigger for the development of turbidity currents along canyons (Puig et al., 2012). However, it is increasingly apparent that major external triggers are not always required for the inception of gravity flows; the key driver appears to be the availability and supply of sediment, which may be sustained or ephemeral in its delivery to canyons (Bailey et al., 2021). While it has been long assumed that during the modern high-stand of sea level, the level of activity of canyons whose heads lie at large distances from terrestrial sediment sources is significantly reduced, recent studies have shown that turbidity flows with high frequencies (i.e., sub-annual) and velocities comparable with highly active coastal canyons, may also affect such land-detached canyons (Heijnen et al., 2022a), with potential implication for the transfer of litter and microplastics in the deep-sea realm via submarine canyons.

Due to the high flow velocities, transport capacity and the potential to run out to significant distances, turbidity currents are able to carry and redistribute significant amount of litter at high depths. In Monterey Canyon, which is frequently affected by powerful turbidity currents (Paull et al., 2010), surveys for litter from 25 to 4000 m depth found the greatest abundance of plastic between 2000 and 4000 m depth (Schlining et al., 2013). The activity of turbidity flows can also lead to the deposition of large litter accumulation hotspots, such as those found in the upper reach of the Messina Strait Canyons (200-600 m depth, Figures 8E, F) (Pierdomenico et al., 2019), in the middle reach of the SY82 Canyon at 1800-1900 m depth (Zhong and Peng, 2021) and at the base of the Monaco Canyon at 2100 m depth (Angiolillo et al., 2021). These accumulation hotspots are a few to tens of meters wide and formed by a mixture of items, whose chaotic arrangement evidences remobilization and emplacement by sediment transport processes (Pierdomenico et al., 2019; Zhong and Peng, 2021). Their composition, dominated by litter of urban origin, primarily plastic, the presence of terrestrial plant debris and the paucity of fishing-related debris further support their link with the action of turbidity flows carrying litter from shallower depths (Angiolillo et al., 2021). Furthermore, the occurrence of large rocky boulders and heavy litter items, such as pieces of furniture, metals sheets and cars, within litter piles testifies to the high transport competence of turbidity currents (Pierdomenico et al., 2019).

Even though it might be expected that turbidity flows (that can travel for hundreds of kilometers), should enable transport of anthropogenic debris to the lowest reaches of canyons, very little is known about potential accumulation at the base of canyons and on deep-sea fans, as these zones have not been extensively surveyed for litter. However, the high concentration of litter found in the Rhône deep-sea fan (Galgani et al., 2000) suggests that litter can be transferred throughout the entire canyon course in systems actively

carrying sediment toward deep-sea fans, where it can eventually be prone to entrainment by bottom currents.

Sediment-gravity flows may also bury litter within the sediment, as indicated by reports of partially buried items in canyon sediments (Figure 8D) (Pierdomenico et al., 2019; Angiolillo et al., 2021). The ability of gravity flows to transport and bury litter is largely unstudied, although flume experiments evidenced that microplastic can be transported and buried by turbidity currents (Pohl et al., 2020). Furthermore, macroplastics enclosed within coarse grained turbidite deposits buried 2.5 m below the seafloor have been recovered from a sediment core in a prodelta channel, further demonstrating the potential of gravity flows in burying litter deeply beneath the sea floor (Pierdomenico et al., 2022).

Oceanographic processes

Oceanographic processes can also be involved in the transport of sediment and litter within canyons. The accumulation of plastic below 1000 m depth in the Cap de Creus Canyon has been linked to the action of dense shelf water cascading that generates strong bottom flows able to erode and entrain seafloor sediment in the upper reach of the canyon (Canals et al., 2006). These flows transport litter from the continental shelf and upper canyon, favoring its settling once the current speed has slowed down (Tubau et al., 2015; Dominguez-Carrió et al., 2020).

Bottom currents are recognized as important agents for the dispersal of microplastics in the deep sea (Kane et al., 2020) and can be steered down- and up-slope through canyons, where they can also transport larger macrodebris. In the Gioia Canyon, almost 40% of total macroplastic found between 50 and 490 m depth was observed drifting above the seafloor, demonstrating the important role of bottom currents in the downward flux of plastic (Pierdomenico et al., 2020). The decrease in the amount of drifting litter downslope suggests trapping of debris in the upper parts of canyons for some period of time.

Internal waves and tidal currents, which are usually amplified by the topographic constraint of submarine canyons, can contribute to sediment resuspension and advection along the canyon axis, sometimes favoring sediment and litter accumulation in specific regions (Hotchkiss and Wunsch, 1982; de Stigter et al., 2011; Pearman et al., 2020). Changes in strength and direction of currents driven by internal tides (Mulder et al., 2012), combined with the occurrence of biologically and geologically complex habitats promoting trapping of litter, are thought to be responsible for the higher abundances observed in specific mid-depth ranges (800-1100 m) in the Bay of Biscay canyons (van den Beld et al., 2017).

Processes controlling the distribution of fishing-related debris

Because of the different entry points and transport mechanisms, litter of terrestrial and maritime origins often shows a different distribution in the different morphological zones of canyons, as observed in the Cap de Creus Canyon (Dominguez-Carrió et al., 2020), the Dohrn Canyon (Taviani et al., 2019; Angiolillo et al., 2023) and the Gioia Canyon (Pierdomenico et al., 2020). In these canyons, fishing-related debris was observed mainly on rocky substrates at the canyon head or along the walls as opposed to general plastic items, which were concentrated within the thalweg. This may be related to the fact that accumulation of fishing debris is linked to the spatial distribution of fishing activities, which are often focused in specific sectors of canyons such as the canyon head and rims (Puig et al., 2012; Tubau et al., 2015). In addition, fishing gear may be too large or heavy to be easily displaced by bottom currents, compared to plastics (van den Beld et al., 2017), and due to their shape can be easily entangled in complex terrains such as rocky outcrops, coral frameworks or other biogenic structures that are common in canyons (Angiolillo et al., 2015). A dominance of fishing gear, especially lines and trammel nets, has been reported in several studies that surveyed the rocky habitats at the canyon head or flanks in the upper canyon reach (e.g., Watters et al., 2010; Oliveira et al., 2015; Cau et al., 2017; Enrichetti et al., 2020), often as additional observations within the assessment of coral communities that thrive in these habitats (Orejas et al., 2009; Cau et al., 2017, Giusti et al., 2019; Fabri et al., 2019; Angiolillo et al., 2023). The presence of fishing gear within the thalweg in the Nazaré Canyon down to 4300 m depth (Mordecai et al., 2011) suggests that fishing-related debris can be also funneled to the canyon thalweg and transported to great depths, although direct dumping by fishermen cannot be excluded. However, the greater abundance of fishing debris at shallower depths, compared to general waste (e.g., Schlining et al., 2013; Tubau et al., 2015; Angiolillo et al., 2021; Taviani et al., 2017; Dominguez-Carrió et al., 2020) and the paucity of fishing gear within the large litter piles found in the middle and lower reach of canyons (Angiolillo et al., 2021; Zhong and Peng, 2021), suggest a relatively lower mobility for this type of litter compared to general plastic items.

Physical transport processes of microplastics

Recent literature addresses transport and burial of microplastics by sediment gravity flows (Ballent et al., 2013; Pohl et al., 2020; Bell et al., 2021), with some attention being paid to interaction with bottom current systems (Kane et al., 2020). The resemblance of microplastics size to the natural sediment present in gravity-driven flows, has motivated application of existing sediment transport hydrodynamics of sediment gravity flows to microplastics transport, specifically the Rouse perspective (Kane and Clare, 2019; Waldschläger et al., 2022). Suspension of dense particles in turbulent environmental fluid flow is understood to result from a balance between downward settling due to gravity and upward mixing due to turbulence. This process was resolved by Rouse nearly a century ago for rivers (Rouse, 1937). In rivers, turbulence is exclusively generated through friction with the floor. Mixing of air into the top of rivers can be neglected. The non-dimensional Rouse number characterizes the ability of river-like flows to suspend particles of different size and density. It can be used to calculate vertical distributions of each particle type suspended in a flow (the Rouse equations). There are fundamental differences between

rivers and turbidity currents due to the presence of ambient sea water above turbidity currents rather than air above rivers: a) the density difference between the flow and its surroundings is 1 to 2 orders of magnitude smaller; b) there is no viscosity discontinuity at the top of turbidity currents, and this generates friction and turbulence at the top of the flow as well as at the bottom; c) as a result of a) and b) ambient water can be mixed into the top of turbidity currents, which dilutes the particle concentration in the top of the flow. These fundamental differences from rivers are widely acknowledged to be problematic for the application of the Rouse equations to turbidity currents, yet Rouse still dominates quantification of particle suspension in turbidity currents (Hiscott, 1994; Hiscott et al., 1997; Straub and Mohrig, 2008; Bolla Pittaluga and Imran, 2014; Jobe et al., 2017; Bolla Pittaluga et al., 2018; Eggenhuisen et al., 2020). Indeed, Rouse equations satisfy observations for dense mineral sand with a Rouse number as low as ≈1/2 in turbidity currents (Eggenhuisen et al., 2020). However, here we test the Rouse equations with the experiments with plastic microfibers of Pohl et al. (2020) to reveal a critical shortcoming when applied to sediment gravity flows: the Rouse number of the microfibers is ≈1/50; yet the observed vertical distribution in the turbidity currents is identical to that of dense mineral sand with a Rouse number of ≈1/2 (Figure 9). This violation of the Rouse equations is a critical barrier to using the Rousean perspective to quantify fluxes of low-density particles such as plastics in sediment gravity flows. Plastic particles that are virtually neutrally buoyant should hardly settle downwards due to gravity, should be easily mixed homogenously throughout the water column, and are therefore unlikely to ever be deposited with dense mineral sand at the base of the flow. Observations of plastic floating in the water column above the seabed (Pierdomenico et al., 2020) are indeed intuitively explained by their approximately neutral buoyancy in sea water. However, the burial of litter beneath the seafloor together with dense mineral sand in both observations (Pierdomenico et al., 2022) and experiments (Pohl et al., 2020; Bell et al., 2021) is not. It appears that a conventional buoyancy and turbulent diffusion treatment does not suffice to treat transport and burial of plastic litter in sediment gravity flows in submarine canyons. Pohl et al. (2020) explain the preferential burial of microplastic fibres relative to microplastic fragments with shape effects. Burial of the fibres is promoted by their larger surface area and length. As one section of the fibre is pushed downwards by settling sediment particles it gets trapped in the seabed, and the rest of the fibre is subsequently buried, despite it still sticking upwards partly above the bed into the ongoing flow. This shape effect does explain predominance of burial of plastic fibres over plastic fragments, and this could extend to explain preferential burial of macrolitter films, sheets, nets, and wires. However, it cannot explain the similarity in transport to natural dense sediment with Rouse numbers of ≈1/2. Furthermore, biological processes such as fouling, consumption and incorporation in fecal material (Choy et al., 2019) could increase density and settling velocities of microparticles. Though further research is needed, provisional treatment of plastic litter in similarity to natural sediment of Ro ≈ ½ is advocated here based on the empiric evidence of our analyses (Figure 9) of the experiments by Pohl et al. (2020).

Testing a sediment process-based model to infer plastic transport in a submarine canyon: the case of the Congo Canyon

Modeling and quantification of physical transport processes of litter in submarine canyons can substantiate extrapolations of spatial occurrence and abundance of litter from sparse observations, and even provide justifications for predictions in systems that are designated as highly vulnerable to litter input,

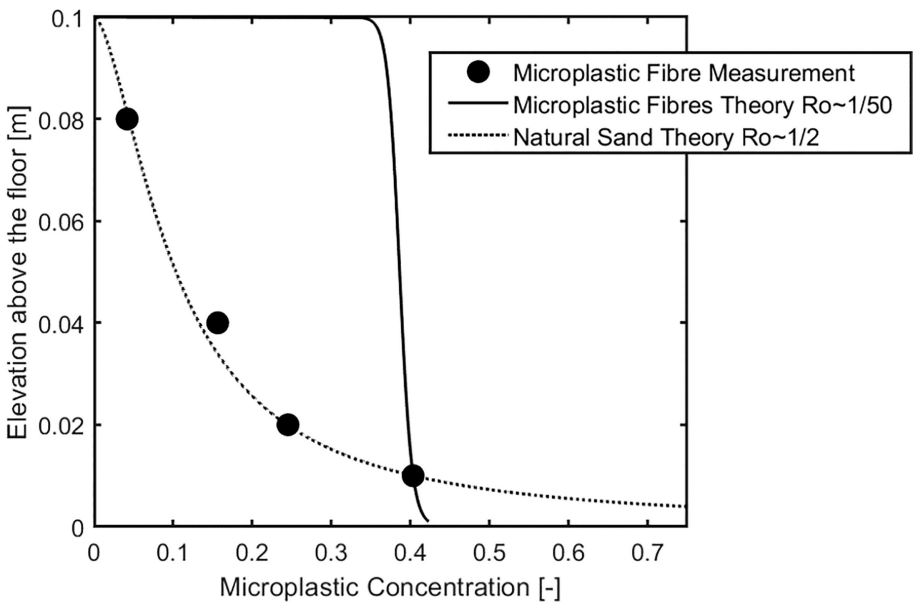

FIGURE 9
The Rouse equation for fine grained quartz sand also predicts the measured concentration of microplastic fibres in an experimental turbidity current. The equations yield incorrect results when calculated with the density and size of the fibres.

but that have not been surveyed yet. As an example of the potential of integrated studies in inferring litter distribution in canyons we apply the Sediment Budget Estimator (SBE) process model (Eggenhuisen et al., 2022) to the Congo Canyon, which we identified as a potential hotspot for plastic litter based on the canyon head exposure parameter to land-derived plastic litter (Figure 4). We assume that plastic is transported in association with natural sediment (Figure 9) in sediment gravity flows. Unfortunately, no direct survey information is available to quantitatively inform this association yet. However, such quantifications are available for the association between natural sediment and Particulate Organic Carbon (POC; Azpiroz-Zabala et al., 2017; Simmons et al., 2020). POC overlaps in density, sizes, and shapes with at least some plastic litter. Furthermore, we suggest that there is a physical similarity between transport of this litter and POC that can be leveraged. The potential for successful process modeling of litter fluxes is illustrated by populating the process model with input conditions (Supplementary Material S4) based on published monitoring studies at 2000 m water depth in the Congo Canyon (Cooper et al., 2013; Azpiroz-Zabala et al., 2017; Simmons et al., 2020), and comparing the simulated POC budgets to the estimates of those studies (Figure 10). The flow-velocity and sediment-concentration profiles of the sediment gravity flows compare well to the ADCP results. More importantly, resulting sediment fluxes closely match the variability observed in the 4 months monitoring deployment (Figure 10C). The simulated estimates for sediment-associated POC fluxes cover the range estimated from ADCP monitoring, though the histogram reveals an overestimation of the top end of the range reported by Azpiroz-Zabala et al. (2017). This success highlights that, when the association between litter and natural sediment is clarified, existing knowledge of sediment gravity flows suffices to quantitatively simulate fluxes and budgets of litter transport and burial down submarine canyons. Various approaches exist in process modeling of sediment gravity flows. The SBE demonstrated here uses a simplified stochastic approach. The benefits of this approach make it uniquely suited to integration with global estimation of canyon-head exposure to river-derived litter (Figure 4) and sparse modeling: input conditions can be based on robust estimates from bathymetric surveys and sparse monitoring results; and ensemble simulations can rapidly be performed for tens of thousands of events in one or more canyons. The modeling results are still critically dependent on direct flow monitoring results, specifically sediment gravity flow

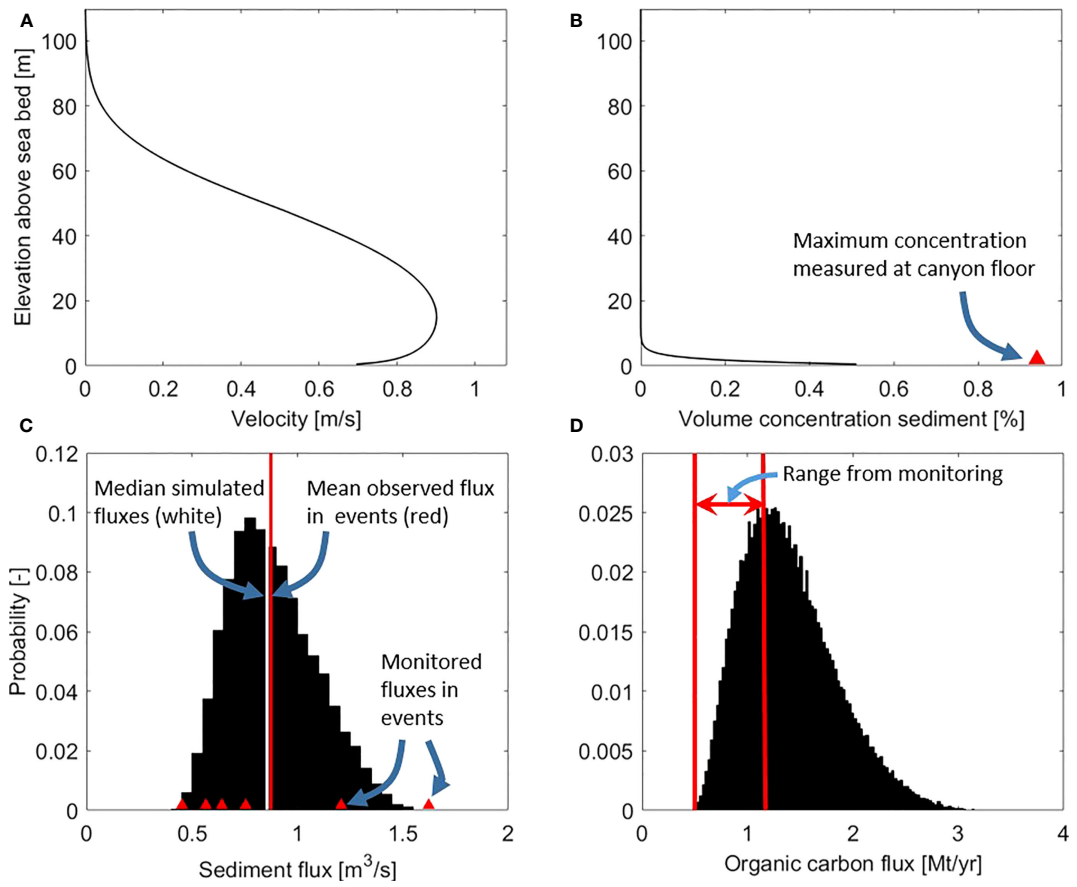

FIGURE 10
(A, B) Velocity and concentration profiles of simulated sediment gravity flow #5 of Azpiroz-Zabala et al. (2017). Maximum concentration at the seabed is from Simmons et al. (2020) whose ADCP backscatter inversion leads to 50% overestimation of concentration relative to the Azpiroz-Zabala et al. (2017) conditions simulated here. **(C)** Histogram of all simulated sediment fluxes, compared to sediment fluxes estimated from ADCP measurements in Azpiroz-Zabala et al. (2017). **(D)** Histogram of simulated POC-flux estimates compared to the range reported by Azpiroz-Zabala et al. (2017).

thickness and natural sediment concentration. This means that at present, process modeling is only feasible in parallel to continued efforts in sea going research. Specifically, there is an urgent need to establish the association of litter and natural sediment in sediment gravity flows and buried deposits.

Final remarks

Although litter research in canyons is still in its infancy, it is clear that these geomorphic features represent preferential area for litter accumulation and that the distribution of litter within canyons may be greatly influenced by the diverse transport routes and processes characterizing them. However, several knowledge gaps exist about the pathways that bring litter and microplastics from their entry-points to the seafloor and into canyons as well as about the interplay of depositional and erosional processes controlling their dispersal, deposition and potential burial. This is not surprising, considering that less than 10% of submarine canyons worldwide have been surveyed so far (Matos et al., 2018), and, out of this estimate, no more than 1% canyons have been studied with focused efforts on marine litter (Hernandez et al., 2022). Particularly, information is missing for most of the canyons that our model highlighted as prone to receiving large litter inputs from land sources. On top of that, our ability to depict distribution patterns is constrained by the sampling strategy, frequently originally planned to address other topics than litter assessment and often targeting specific morphological zones or depth ranges. Beside the difficulties in comparisons between studies linked to the lack of standardized approaches in litter classification and quantification (Canals et al, 2021), the variability of geological settings and of spatio-temporal scales of natural processes within canyons makes local estimates less consistent and representative of the entire source to sink system.

Our work highlights the importance of the connection of canyon heads to terrestrial and maritime sources of litter. However, hydrographic processes, which play a crucial role in litter supply to canyons, are not taken into account in these estimations, due to their high temporal and spatial variability and to the lack of globally available datasets of coastal and shelf currents and sediment transport. Little is also known about the environmental residence times of litter and their final depositional sinks in the deep sea. Canyons are highly dynamic environments where sediment and litter storage is often transient, as also suggested by the shift of microplastic depocentres from the continental shelf to the canyons and then to the lower reach of the Xisha Trough observed within a 40-year time span from 1980s to 2018 (Chen et al., 2020). Gravity-driven flows are generally assumed to decrease in energy both spatially and temporally, although the relationships between event magnitude and frequency and its variation within distance, as well as the resulting depositional/erosional patterns, are not fully clarified (Heijnen et al., 2022a). Litter and sediment transported by high-frequency low-magnitude events could be confined and stored in the upper and middle reach of submarine canyons for decades or centuries, before being flushed further down canyon by high-magnitude events that can deliver material to the basin seafloor (Normark and Piper, 1991; Mas et al., 2010). Repeated burial and excavation over shorter timescales, with stepwise sediment transport and fragmentation by a range of flows with variable run-out has also been proposed (Stacey et al., 2019; Heijnen et al., 2022b). The lower reach of canyons would theoretically represent main depositional areas for litter, as also suggested by the report of large piles at thousands of meters depth, although these zones are largely unexplored for most canyons.

In summary, the geological processes-based approach highlighted in this work helps to elucidate land-to-sea transport and pathways by which litter is transferred and moved throughout canyons in deep-sea areas, but we are aware that a realistic assessment of this issue is still far to be reached. This is due to multiple problems, such as i) the paucity of systematic studies targeted to assess litter distribution in different morpho-sedimentary zones of canyons, ii) the lack of common standards in classification and quantification of litter, as well as of contextual information useful to constrain the depositional environment iii) the paucity of studies dealing with physical transport of litter (except for a few flume experiments targeting microplastics) and the fact that physical (e.g.: dimension, density) and chemical properties (e.g.: composition) of these pollutants can fundamentally differ from those of natural sediment, influencing their behavior and pathways. Considering the paramount role of canyons in funneling litter to the deep sea and the potential threat on deep-sea ecosystems, this issue should be carefully addressed by research communities together with monitoring agencies and policy-makers, to better assess global plastic budgets and to help delineate future mitigation strategies.

Author contributions

Conceptualization, MP, AB, MC, VH, JD, and PH; methodology, MP, AB, and JE; validation, MP, AB, and JD; formal analysis and investigation, MP, AB, and JE; data curation, MP, AB, and JD; writing original draft preparation, MP, AB, and JE; writing review and editing, MC, CLI, DC, JD, IK, VH, and PH. All authors contributed to the article and approved the submitted version.

Funding

MP acknowledges funding from CNR-DSSTTA “SNAPSHOT” Project (CIG Z503B9C139 - CUP B22F20000270001). DC acknowledges funding provided by “Progetto di Ateneo 2021” of University of Rome Sapienza “Morpho-sedimentary characterization of mass-wasting processes along Italian continental margins and insular volcanoes”. VH and MC acknowledge funding from the Natural Environment Research Council (NERC) National Capability Programme (NE/R015953/1) “Climate Linked Atlantic Sector Science”. VH was also funded through the EU H2020 project iAtlantic (Project No 818123) and enjoyed a Fellowship from the Hanse Wissenschaftskolleg Institute for Advanced Study during the final stages of this manuscript. CLI acknowledges funding from the EU-H2020 Marie Sklodowska Curie single action "Eco-hydrodynamics of cold water coral habitats across integrated spatial scales - HABISS" (GA 890815).

Acknowledgments

This work has been carried out in the framework of INCISE network and it has benefited from fruitful discussion of the Marine litter Working group during the 2021 INCISE Conference. The authors are grateful to Pia Urban (FU Berlin) for the global estimation of commercial fishing activity per canyon.

Conflict of interest

The authors declare that the research was conducted in the absence of any commercial or financial relationships that could be construed as a potential conflict of interest.

Publisher's note

Supplementary material

The Supplementary Material for this article can be found online at: https://www.frontiersin.org/articles/10.3389/fmars.2023.1224859/full#supplementary-material

References

Amaro, T., Huvenne, V. A. I., Allcock, A. L., Aslam, T., Davies, J. S., Danovaro, R., et al. (2016). The whittard canyon–a case study of submarine canyon processes. *Prog. Oceanogr.* 146, 38–57. doi: 10.1016/j.pocean.2016.06.003

Angiolillo, M. (2018). "Debris in deep water," in *World seas: an environmental evaluation, 2nd ed.* (Cambridge, MA: Academic Press), 251–268. doi: 10.1016/j.dsr.2023.103963

Angiolillo, M., Bo, M., Toma, M., Giusti, M., Salvati, E., Giova, A., et al. (2023). A baseline for the monitoring of Mediterranean upper bathyal biogenic reefs within the marine strategy framework directive objectives. *Deep Sea Res. Part I: Oceanographic Res. Papers* 194, 103963.

Angiolillo, M., di Lorenzo, B., Farcomeni, A., Bo, M., Bavestrello, G., Santangelo, G., et al. (2015). Distribution and assessment of marine debris in the deep tyrrhenian Sea (NW Mediterranean Sea, Italy). *Mar. pollut. Bull.* 92 (1-2), 149–159. doi: 10.1016/j.marpolbul.2014.12.044

Angiolillo, M., Gérigny, O., Valente, T., Fabri, M. C., Tambute, E., Rouanet, E., et al. (2021). Distribution of seafloor litter and its interaction with benthic organisms in deep waters of the ligurian Sea (Northwestern Mediterranean). *Sci. Total Environ.* 788, 147745. doi: 10.1016/j.scitotenv.2021.147745

Aymà, A., Aguzzi, J., Canals, M., Lastras, G., Mecho, A., and Lo Iacono, C. (2019). "Occurrence of living cold-water corals at Large depths within submarine canyons of the northwestern Mediterranean Sea," in *Mediterranean Cold-water corals: past, present and future* (Cham: Springer), 271–284.

Azpiroz-Zabala, M., Cartigny, M. J., Talling, P. J., Parsons, D. R., Sumner, E. J., Clare, M. A., et al. (2017). Newly recognized turbidity current structure can explain prolonged flushing of submarine canyons. *Sci. Adv.* 3 (10), e1700200. doi: 10.1126/sciadv.1700200

Bailey, L. P., Clare, M. A., Rosenberger, K. J., Cartigny, M. J., Talling, P. J., Paull, C. K., et al. (2021). Preconditioning by sediment accumulation can produce powerful turbidity currents without major external triggers. *Earth Planetary Sci. Lett.* 562, 116845. doi: 10.1016/j.epsl.2021.116845

Ballent, A., Pando, S., Purser, A., Juliano, M. F., and Thomsen, L. (2013). Modelled transport of benthic marine microplastic pollution in the nazaré canyon. *Biogeosciences* 10 (12), 7957–7970. doi: 10.5194/bg-10-7957-2013

Bancone, C. E., Turner, S. D., Ivar do Sul, J. A., and Rose, N. L. (2020). The paleoecology of microplastic contamination. *Front. Environ. Sci.* 8, 574008. doi: 10.3389/fenvs.2020.574008

Barnes, D. K. A. (2002). Invasions by marine life on plastic debris. *Nature* 416, 808–809. doi: 10.1038/416808a

Beaumont, N. J., Aanesen, M., Austen, M. C., Börger, T., Clark, J. R., Cole, M., et al. (2019). Global ecological, social and economic impacts of marine plastic. *Mar. pollut. Bull.* 142, 189–195. doi: 10.1016/j.marpolbul.2019.03.022

Becker, J. J., Sandwell, D. T., Smith, W. H. F., Braud, J., Binder, B., Depner, J. L., et al. (2009). Global bathymetry and elevation data at 30 arc seconds resolution: SRTM30_PLUS. *Mar. Geodesy* 32 (4), 355–371. doi: 10.1080/01490410903297766

Bell, D., Soutter, E. L., Cumberpatch, Z. A., Ferguson, R. A., Spychala, Y. T., Kane, I. A., et al. (2021). Flow-process controls on grain type distribution in an experimental turbidity current deposit: implications for detrital signal preservation and microplastic distribution in submarine fans. *Depositional Rec.* 7 (3), 392–415. doi: 10.1002/dep2.153

Bernhardt, A., and Schwanghart, W. (2021a). Where and why do submarine canyons remain connected to the shore during sea-level rise? insights from global topographic analysis and Bayesian regression. *Geophysical Res. Lett.* 48 (10), e2020GL092234. doi: 10.1029/2020GL092234

Bernhardt, A., and Schwanghart, W. (2021b). Global dataset of submarine canyon heads combined with terrestrial and marine topographic and oceanographic parameters. *GFZ Data Serv.* doi: 10.5880/fidgeo.2021.008

Biede, V., Gates, A. R., Pfeifer, S., Collins, J. E., Santos, C., and Jones, D. O. (2022). Short-term response of deep-water benthic megafauna to installation of a pipeline over a depth gradient on the Angolan slope. *Front. Mar. Sci.* 9, 917. doi: 10.3389/fmars.2022.880453

Bolla Pittaluga, M., Frascati, A., and Falivene, O. (2018). A gradually varied approach to model turbidity currents in submarine channels. *J. Geophysical Research: Earth Surface* 123 (1), 80–96. doi: 10.1002/2017JF004331

Bolla Pittaluga, M., and Imran, J. (2014). A simple model for vertical profiles of velocity and suspended sediment concentration in straight and curved submarine channels. *J. Geophysical Research: Earth Surface* 119 (3), 483–503. doi: 10.1002/2013JF002812

Borrelle, S. B., Ringma, J., Law, K. L., Monnahan, C. C., Lebreton, L., McGivern, A., et al. (2020). Predicted growth in plastic waste exceeds efforts to mitigate plastic pollution. *Science* 369 (6510), 1515–1518. doi: 10.1126/science.aba3656

Bruemmer, A. L., Dissanayake, A., and Davies, J. S. (2023). Marine litter-fauna interactions in submarine canyons: a standardised reporting framework and critical review of the current status of research. *Front. Mar. Sci.*

Buhl-Mortensen, L., and Buhl-Mortensen, P. (2017). Marine litter in the Nordic seas: distribution composition and abundance. *Mar. pollut. Bull.* 125 (1-2), 260–270. doi: 10.1016/j.marpolbul.2017.08.048

Buhl-Mortensen, P., and Buhl-Mortensen, L. (2018). Impacts of bottom trawling and litter on the seabed in Norwegian waters. *Front. Mar. Sci.* 5, 42. doi: 10.3389/fmars.2018.00042

Canals, M., Pham, C. K., Bergmann, M., Gutow, L., Hanke, G., Van Sebille, E., et al. (2021). The quest for seafloor macrolitter: a critical review of background knowledge, current methods and future prospects. *Environ. Res. Lett.* 16 (2), 023001. doi: 10.1088/1748-9326/abc6d4

Canals, M., Puig, P., De Madron, X. D., Heussner, S., Palanques, A., and Fabres, J. (2006). Flushing submarine canyons. *Nature* 444, 354–357. doi: 10.1038/nature05271

Carson, H. S., Colbert, S. L., Kaylor, M. J., and McDermid, K. J. (2011). Small plastic debris changes water movement and heat transfer through beach sediments. *Mar. pollut. Bull.* 62 (8), 1708–1713. doi: 10.1016/j.marpolbul.2011.05.032

Carter, G. D., Huvenne, V. A., Gales, J. A., Iacono, C. L., Marsh, L., Ougier-Simonin, A., et al. (2018). Ongoing evolution of submarine canyon rockwalls; examples from the whittard canyon, celtic margin (NE Atlantic). *Prog. Oceanogr.* 169, 79–88. doi: 10.1016/j.pocean.2018.02.001

Carter, L., Milliman, J. D., Talling, P. J., Gavey, R., and Wynn, R. B. (2012). Near-synchronous and delayed initiation of long run-out submarine sediment flows from a record-breaking river flood, offshore Taiwan. *Geophysical Res. Lett.* 39 (12), L12603. doi: 10.1029/2012GL051172

Cau, A., Alvito, A., Moccia, D., Canese, S., Pusceddu, A., Rita, C., et al. (2017). Submarine canyons along the upper sardinian slope (Central Western Mediterranean) as repositories for derelict fishing gears. *Mar. pollut. Bull.* 123 (1-2), 357–364. doi: 10.1016/j.marpolbul.2017.09.010

Chaytor, J. D., Demopoulos, A. W., ten Brink, U. S., Baxter, C., Quattrini, A. M., and Brothers, D. S. (2016). "Assessment of canyon wall failure process from multibeam bathymetry and remotely operated vehicle (ROV) observations, US Atlantic continental margin," in *Submarine mass movements and their consequences: 7th international symposium* (Switzerland: Springer International Publishing), 103–113.

Chen, M., Du, M., Jin, A., Chen, S., Dasgupta, S., Li, J., et al. (2020). Forty-year pollution history of microplastics in the largest marginal sea of the western pacific. *Geochemical Perspective Lett.* 13, 42–47. doi: 10.7185/geochemlet.2012

Choy, C. A., Robison, B. H., Gagne, T. O., Erwin, B., Firl, E., Halden, R. U., et al. (2019). The vertical distribution and biological transport of marine microplastics across the epipelagic and mesopelagic water column. *Sci. Rep.* 9 (1), 7843. doi: 10.1038/s41598-019-44117-2

Cooper, C., Wood, J., and Andrieux, O. (2013). Turbidity current measurements in the Congo canyon. *In Offshore Technol. Conf. (Vol. 23992* pp, 6–9). doi: 10.4043/23992-MS

Covault, J. A., Normark, W. R., Romans, B. W., and Graham, S. A. (2007). Highstand fans in the California borderland: the overlooked deep-water depositional systems. *Geology* 35 (9), 783–786. doi: 10.1130/G23800A.1

De Leo, F. C., Smith, C. R., Rowden, A. A., Bowden, D. A., and Clark, M. R. (2010). Submarine canyons: hotspots of benthic biomass and productivity in the deep sea. *Proc. R. Soc. B: Biol. Sci.* 277 (1695), 2783–2792. doi: 10.1098/rspb.2010.0462

de Stigter, H. C., Jesus, C. C., Boer, W., Richter, T. O., Costa, A., and van Weering, T. C. E. (2011). Recent sediment transport and deposition in the Lisbon–setúbal and cascais submarine canyons, Portuguese continental margin. *Deep Sea Res. Part II* 58, 2321–2344. doi: 10.1016/j.dsr2.2011.04.001

Derraik, J. G. (2002). The pollution of the marine environment by plastic debris: a review. *Mar. Pollut. Bull.* 44 (9), 842–852.

Dominguez-Carrió, C., Sanchez-Vidal, A., Estournel, C., Corbera, G., Riera, J. L., Orejas, C., et al. (2020). Seafloor litter sorting in different domains of cap de creus continental shelf and submarine canyon (NW Mediterranean Sea). *Mar. pollut. Bull.* 161, 111744. doi: 10.1016/j.marpolbul.2020.111744

Eggenhuisen, J. T., Tilston, M. C., de Leeuw, J., Pohl, F., and Cartigny, M. J. (2020). Turbulent diffusion modelling of sediment in turbidity currents: An experimental validation of the rouse approach. *Depositional Rec.* 6 (1), 203–216.

Eggenhuisen, J. T., Tilston, M. C., Stevenson, C. J., Hubbard, S. M., Cartigny, M. J., Heijnen, M. S., et al. (2022). The sediment budget estimator (SBE): a process model for the stochastic estimation of fluxes and budgets of sediment through submarine channel systems. *J. Sedimentary Res.* 92 (12), 1093–1115. doi: 10.2110/jsr.2021.037

Eidam, E. F., Ogston, A. S., and Nittrouer, C. A. (2019). Formation and removal of a coastal flood deposit. *J. Geophysical Research: Oceans* 124 (2), 1045–1062. doi: 10.1029/2018JC014360

Enrichetti, F., Dominguez-Carrió, C., Toma, M., Bavestrello, G., Canese, S., and Bo, M. (2020). Assessment and distribution of seafloor litter on the deep ligurian continental shelf and shelf break (NW Mediterranean Sea). *Mar. pollut. Bull.* 151, 110872.

Eriksen, M., Lebreton, L. C., Carson, H. S., Thiel, M., Moore, C. J., Borerro, J. C., et al. (2014). Plastic pollution in the world's oceans: more than 5 trillion plastic pieces weighing over 250,000 tons afloat at sea. *PLoS One* 9 (12), e111913. doi: 10.1371/journal.pone.0111913

Fabri, M. C., Pedel, L., Beuck, L., Galgani, F., Hebbeln, D., and Freiwald, A. (2014). Megafauna of vulnerable marine ecosystems in French mediterranean submarine canyons: spatial distribution and anthropogenic impacts. *Deep Sea Res. Part II* 104, 184–207. doi: 10.1016/j.dsr2.2013.06.016

Fabri, M. C., Vinha, B., Allais, A. G., Bouhier, M. E., Dugornay, O., Gaillot, A., et al. (2019). Evaluating the ecological status of cold-water coral habitats using non-invasive methods: an example from cassidaigne canyon, northwestern Mediterranean Sea. *Prog. Oceanogr.* 178, 102172. doi: 10.1016/j.pocean.2019.102172

Fernandez-Arcaya, U., Ramirez-Llodra, E., Aguzzi, J., Allcock, A. L., Davies, J. S., Dissanayake, A., et al. (2017). Ecological role of submarine canyons and need for canyon conservation: a review. *Front. Mar. Sci.* 4, 5. doi: 10.3389/fmars.2017.00005

Flemming, B. W. (1980). Sand transport and bedform patterns on the continental shelf between Durban and port Elizabeth (south-east African continental margin). *Sedimentary Geology* 26 (1-3), 179–205. doi: 10.1016/0037-0738(80)90011-1

Galgani, F., Hanke, G., and Maes, T. (2015). "Global distribution, composition and abundance of marine litter," in *Marine anthropogenic litter*. Eds. M. Bergmann, L. Gutow and M. Klages (Cham: Springer International Publishing), 29–56.

Galgani, F., Leaute, J. P., Moguedet, P., Souplet, A., Verin, Y., Carpentier, A., et al. (2000). Litter on the sea floor along European coasts. *Mar. pollut. Bull.* 40 (6), 516–527. doi: 10.1016/S0025-326X(99)00234-9

Galgani, F., Michela, A., Gérigny, O., Maes, T., Tambutté, E., and Harris, P. T. (2022). "Marine litter, plastic, and microplastics on the seafloor," in *Plastics and the ocean: origin, characterization, fate, and impacts*. Andrady A.L Ed. (John Wiley & Sons), 151–197.

Galgani, F., Souplet, A., and Cadiou, Y. (1996). Accumulation of debris on the deep sea floor off the French Mediterranean coast. *Mar. Ecol. Prog. Ser.* 142, 225–234. doi: 10.3354/meps142225

Gall, S. C., and Thompson, R. C. (2015). The impact of debris on marine life. *Mar. pollut. Bull.* 92 (1-2), 170–179. doi: 10.1016/j.marpolbul.2014.12.041

Gerigny, O., Brun, M., Fabri, M. C., Tomasino, C., Le Moigne, M., Jadaud, A., et al. (2019). Seafloor litter from the continental shelf and canyons in French Mediterranean water: distribution, typologies and trends. *Mar. pollut. Bull.* 146, 653–666. doi: 10.1016/j.marpolbul.2019.07.030

Geyer, R., Jambeck, J. R., and Law, K. L. (2017). Production, use, and fate of all plastics ever made. *Sci. Adv.* 3 (7), e1700782. doi: 10.1126/sciadv.1700782

Giusti, M., Canese, S., Fourt, M., Bo, M., Innocenti, C., Goujard, A., et al. (2019). Coral forests and derelict fishing gears in submarine canyon systems of the ligurian Sea. *Prog. Oceanography* 178, 102186.

Grinyó, J., Chevaldonné, P., Schohn, T., and Le Bris, N. (2021). Megabenthic assemblages on bathyal escarpments off the west Corsican margin (Western Mediterranean). *Deep Sea Res. Part I: Oceanographic Res. Papers* 171, 103475.

Hage, S., Cartigny, M. J., Sumner, E. J., Clare, M. A., Hughes Clarke, J. E., Talling, P. J., et al. (2019). Direct monitoring reveals initiation of turbidity currents from extremely dilute river plumes. *Geophysical Res. Lett.* 46 (20), 11310–11320. doi: 10.1029/2019GL084526

Hage, S., Galy, V. V., Cartigny, M. J., Heerema, C., Heijnen, M. S., Acikalin, S., et al. (2022). Turbidity currents can dictate organic carbon fluxes across river-fed fjords: an example from Bute inlet (BC, Canada). *J. Geophysical Research: Biogeosciences* 127 (6), e2022JG006824. doi: 10.1029/2022JG006824

Harris, P. T. (2020). The fate of microplastic in marine sedimentary environments: a review and synthesis. *Mar. pollut. Bull.* 158, 111398. doi: 10.1016/j.marpolbul.2020.111398

Harris, P. T., and Heap, A. (2009). Cyclone-induced net sediment transport pathway on the continental shelf of tropical Australia inferred from reef talus deposits. *Continental Shelf Res.* 29 (16), 2011–2019. doi: 10.1016/j.csr.2008.12.006

Harris, P. T., Macmillan-Lawler, M., Rupp, J., and Baker, E. K. (2014). Geomorphology of the oceans. *Mar. Geology* 352, 4–24. doi: 10.1016/j.margeo.2014.01.011

Harris, P. T., and Whiteway, T. (2011). Global distribution of large submarine canyons: geomorphic differences between active and passive continental margins. *Mar. Geology* 285, 69–86. doi: 10.1016/j.margeo.2011.05.008

Hartmann, N. B., Rist, S., Bodin, J., Jensen, L. H., Schmidt, S. N., Mayer, P., et al. (2017). Microplastics as vectors for environmental contaminants: exploring sorption, desorption, and transfer to biota. *Integrated Environ. Assess. Manage.* 13 (3), 488–493. doi: 10.1002/ieam.1904

Heijnen, M. S., Clare, M. A., Cartigny, M. J., Talling, P. J., Hage, S., Pope, E. L., et al. (2022b). Fill, flush or shuffle: how is sediment carried through submarine channels to build lobes? *Earth Planetary Sci. Lett.* 584, 117481. doi: 10.1016/j.epsl.2022.117481

Heijnen, M. S., Mienis, F., Gates, A. R., Bett, B. J., Hall, R. A., Hunt, J., et al. (2022a). Challenging the highstand-dormant paradigm for land-detached submarine canyons. *Nat. Commun.* 13 (1), 3448. doi: 10.1038/s41467-022-31114-9

Hernandez, I., Davies, J. S., Huvenne, V. A., and Dissanayake, A. (2022). Marine litter in submarine canyons: a systematic review and critical synthesis. *Front. Mar. Sci.* 1615. doi: 10.3389/fmars.2022.965612

Hidalgo-Ruz, V., Gutow, L., Thompson, R. C., and Thiel, M. (2012). Microplastics in the marine environment: a review of the methods used for identification and quantification. *Environ. Sci. Technol.* 46 (6), 3060–3075. doi: 10.1021/es2031505

Hiscott, R. N. (1994). Loss of capacity, not competence, as the fundamental process governing deposition from turbidity currents. *J. Sedimentary Res.* 64, 209–214. doi: 10.2110/jsr.64.209

Hiscott, R. N., Hall, F. R., and Pirmez, C. (1997). "Turbidity-current overspill from the Amazon channel: texture of the silt/sand load, paleoflow from anisotropy of magnetic susceptibility, and implications for flow processes," in *Proceedings-ocean drilling program scientific results* (Texas: National Science Foundation), 53–78.

Hizzett, J. L., Hughes Clarke, J. E., Sumner, E. J., Cartigny, M. J. B., Talling, P. J., and Clare, M. A. (2018). Which triggers produce the most erosive, frequent, and longest runout turbidity currents on deltas? *Geophysical Res. Lett.* 45 (2), 855–863. doi: 10.1002/2017GL075751

Hotchkiss, F. S., and Wunsch, C. (1982). Internal waves in Hudson canyon with possible geological implications. *Deep Sea Res. Part I* 29, 415–442. doi: 10.1016/0198-0149(82)90068-1

Inman, D. L., Nordstrom, C. E., and Flick, R. E. (1976). Currents in submarine canyons: an air-sea-land interaction. *Annu. Rev. fluid mechanics* 8 (1), 275–310. doi: 10.1146/annurev.fl.08.010176.001423

Jambeck, J. R., Geyer, R., Wilcox, C., Siegler, T. R., Perryman, M., Andrady, A., et al. (2015). Plastic waste inputs from land into the ocean. *Science* 347 (6223), 768–771. doi: 10.1126/science.1260352

Jobe, Z., Sylvester, Z., Bolla Pittaluga, M., Frascati, A., Pirmez, C., Minisini, D., et al. (2017). Facies architecture of submarine channel deposits on the western Niger delta slope: implications for grain-size and density stratification in turbidity currents. *J. Geophysical Research: Earth Surface* 122 (2), 473–491. doi: 10.1002/2016JF003903

Jones, E. S., Ross, S. W., Robertson, C. M., and Young, C. M. (2022). Distributions of microplastics and larger anthropogenic debris in Norfolk canyon, Baltimore canyon, and the adjacent continental slope (Western north Atlantic margin, U.S.A.). *Mar. pollut. Bull.* 174, 113047. doi: 10.1016/j.marpolbul.2021.113047

Kane, I. A., and Clare, M. A. (2019). Dispersion, accumulation, and the ultimate fate of microplastics in deep-marine environments: a review and future directions. *Front. Earth Sci.* 7, 80. doi: 10.3389/feart.2019.00080

Kane, I. A., Clare, M. A., Miramontes, E., Wogelius, R., Rothwell, J. J., Garreau, P., et al. (2020). Seafloor microplastic hotspots controlled by deep-sea circulation. *Science* 368 (6495), 1140–1145. doi: 10.1126/science.aba5899

Khripounoff, A., Crassous, P., Bue, N., Dennielou, B., and Jacinto, R. S. (2012). Different types of sediment gravity flows detected in the var submarine canyon

(northwestern Mediterranean Sea). *Prog. Oceanography* 106, 138–153. doi: 10.1016/j.pocean.2012.09.001

Khripounoff, A., Vangriesheim, A., Crassous, P., and Etoubleau, J. (2009). High frequency of sediment gravity flow events in the var submarine canyon (Mediterranean Sea). *Mar. Geology* 263 (1-4), 1–6. doi: 10.1016/j.margeo.2009.03.014

Kühn, S., Bravo Rebolledo, E. L., and van Franeker, J. A. (2015). "Deleterious effects of litter on marine life," in *Marine anthropogenic litter*. Bergmann, Lutow, Klages (Eds) (Berlin: Springer Nature), 75–116.

Lavers, J. L., and Bond, A. L. (2017). Exceptional and rapid accumulation of anthropogenic debris on one of the world's most remote and pristine islands. *Proc. Natl. Acad. Sci.* 114 (23), 6052–6055. doi: 10.1073/pnas.1619818114

Lebreton, L. C. M., van der Zwet, J., Damsteeg, J. W., Slat, B., Andrady, A., and Reisser, J. (2017). River plastic emissions to the world's oceans. *Nat. Communication* 8, 1–10. doi: 10.1038/ncomms15611

Lopez-Lopez, L., González-Irusta, J. M., Punzón, A., and Serrano, A. (2017). Benthic litter distribution on circalittoral and deep sea bottoms of the southern bay of Biscay: analysis of potential drivers. *Continental. Shelf Res.* 144, 112–119. doi: 10.1016/j.csr.2017.07.003

Maier, K. L., Rosenberger, K. J., Paull, C. K., Gwiazda, R., Gales, J., Lorenson, T., et al. (2019). Sediment and organic carbon transport and deposition driven by internal tides along Monterey canyon, offshore California. *Deep Sea Res. Part I* 153, 103108. doi: 10.1016/j.dsr.2019.103108

Martín, J., Palanques, A., Vitorino, J., Oliveira, A., and De Stigter, H. C. (2011). Near-bottom particulate matter dynamics in the nazaré submarine canyon under calm and stormy conditions. *Deep Sea Res. Part II* 58, 2388–2400. doi: 10.1016/j.dsr2.2011.04.004

Mas, V., Mulder, T., Dennielou, B., Schmidt, S., Khripounoff, A., and Savoye, B. (2010). Multiscale spatio-temporal variability of sedimentary deposits in the var turbidite system (North-Western Mediterranean Sea). *Mar. Geology* 275, 37–52. doi: 10.1016/j.margeo.2010.04.006

Masson, D. G., Huvenne, V. A. I., De Stigter, H. C., Wolff, G. A., Kiriakoulakis, K., Arzola, R. G., et al. (2010). Efficient burial of carbon in a submarine canyon. *Geology* 38 (9), 831–834. doi: 10.11 30/G30895.1

Matos, F. L., Ross, S. W., Huvenne, V. A. I. I., Davies, J. S., and Cunha, M. R. (2018). Canyons pride and prejudice: exploring the submarine canyon research landscape, a history of geographic and thematic bias. *Prog. Oceanogr.* 169, 6–19. doi: 10.1016/j.pocean.2018.04.010

Mecho, A., Aguzzi, J., De Mol, B., Lastras, G., Ramirez-Llodra, E., Bahamon, N., et al. (2018). Visual faunistic exploration of geomorphological human-impacted deep-sea areas of the north-western Mediterranean Sea. *J. Mar. Biol. Assoc. United Kingdom* 98 (6), 1241–1252. doi: 10.1017/S0025315417000431

Mecho, A., Francescangeli, M., Ercilla, G., Fanelli, E., Estrada, F., Valencia, J., et al. (2020). Deep-sea litter in the gulf of cadiz (Northeastern Atlantic, Spain). *Mar. pollut. Bull.* 153, 110969.

Meijer, L. J., van Emmerik, T., van der Ent, R., Schmidt, C., and Lebreton, L. (2021). More than 1000 rivers account for 80% of global riverine plastic emissions into the ocean. *Sci. Adv.* 7 (18), eaaz5803. doi: 10.1126/sciadv.aaz5803

Milliman, J. D., and Meade, R. H. (1983). World-wide delivery of river sediment to the oceans. *J. Geology* 91 (1), 1–21. doi: 10.1086/628741

Moccia, D., Cau, A., Alvito, A., Canese, S., Cannas, R., Bo, M., et al. (2019). New sites expanding the "Sardinian cold-water coral province" extension: a new potential cold-water coral network? *Aquat. Conservation: Mar. Freshw. Ecosyst.* 29 (1), 153–160. doi: 10.1002/aqc.2975

Mordecai, G., Tyler, P. A., Masson, D. G., and Huvenne, V. A. I. (2011). Litter in submarine canyons off the west coast of Portugal. *Deep Sea Res. Part II* 58, 2489–2496. doi: 10.1016/j.dsr2.2011.08.009

Mulder, T., Syvitski, J. P. M., Migeon, S., Faugères, J. C., and Savoye, B. (2003). Marine hyperpycnal flows: initiation, behaviour and related deposits. a review. *Mar. Petroleum Geology* 20 (6-8), 861–882. doi: 10.1016/j.marpetgeo.2003.01.003

Mulder, T., Zaragosi, S., Garlan, T., Mavel, J., Cremer, M., Sottolichio, A., et al. (2012). Present deep-submarine canyons activity in the bay of Biscay (NE Atlantic). *Mar. Geology* 295, 113–127. doi: 10.1016/j.margeo.2011.12.005

Normark, W. R., and Piper, D. J. W. (1991). "Initiation processes and flow evolution of turbidity currents: implications for the depositional record," in *From shoreline to abyss: contributions in marine geology in honor of Francis Parker Shepard* (Tulsa, OK: SEPM), 207–230.

Orejas, C., Gori, A., Lo Iacono, C., Puig, P., Gili, J. M., and Dale, M. R. T. (2009). Cold-water corals in the cap de creus canyon, northwestern Mediterranean: spatial distribution, density and anthropogenic impact. *Mar. Ecol. Prog. Ser.* 397, 37–51. doi: 10.3354/meps08314

Oliveira, F., Monteiro, P., Bentes, L., Henriques, N. S., Aguilar, R., and Gonçalves, J. M. (2015). Marine litter in the upper são Vicente submarine canyon (SW portugal): Abundance, distribution, composition and fauna interactions. *Mar. pollut. Bull.* 97 (1-2), 401–407.

Pabortsava, K., and Lampitt, R. S. (2020). High concentrations of plastic hidden beneath the surface of the Atlantic ocean. *Nat. Commun.* 11 (1), 1–11. doi: 10.1038/s41467-020-17932-9

Paull, C. K., Ussler, W.III, Caress, D. W., Lundsten, E., Covault, J. A., Maier, K. L., et al. (2010). Origins of large crescent-shaped bedforms within the axial channel of Monterey canyon, offshore California. *Geology* 6 (6), 755–774. doi: 10.1130/GES00527.1

Pearman, T. R. R., Robert, K., Callaway, A., Hall, R., Iacono, C. L., and Huvenne, V. A. (2020). Improving the predictive capability of benthic species distribution models by incorporating oceanographic data–towards holistic ecological modelling of a submarine canyon. *Prog. Oceanography* 184, 102338. doi: 10.1016/j.pocean.2020.102338

Peng, X., Chen, M., Chen, S., Dasgupta, S., Xu, H., Ta, K., et al. (2018). Microplastics contaminate the deepest part of the world's ocean. *Geochemical Perspective Lett.* 9, 1–5. doi: 10.7185/geochemlet.1829

Peng, X., Dasgupta, S., Zhong, G., Du, M., Xu, H., Chen, M., et al. (2019). Large Debris dumps in the northern south China Sea. *Mar. pollut. Bull.* 142, 164–168. doi: 10.1016/j.marpolbul.2019.03.041

Pham, C. K., Ramirez-Llodra, E., Alt, C. H., Amaro, T., Bergmann, M., Canals, M., et al. (2014). Marine litter distribution and density in European seas, from the shelves to deep basins. *PLoS One* 9 (4), e95839. doi: 10.1371/journal.pone.0095839

Pierdomenico, M., Casalbore, D., and Chiocci, F. L. (2019). Massive benthic litter funnelled to deep sea by flash-flood generated hyperpycnal flows. *Sci. Rep.* 9, 1–10. doi: 10.1038/s41598-019-41816-8

Pierdomenico, M., Casalbore, D., and Chiocci, F. L. (2020). The key role of canyons in funnelling litter to the deep sea: a study of the gioia canyon (Southern tyrrhenian Sea). *Anthropocene* 30, 100237. doi: 10.1016/j.ancene.2020.100237

Pierdomenico, M., Ridente, D., Casalbore, D., Di Bella, L., Milli, S., and Chiocci, F. L. (2022). Plastic burial by flash-flood deposits in a prodelta environment (Gulf of patti, southern tyrrhenian Sea). *Mar. pollut. Bull.* 181, 113819. doi: 10.1016/j.marpolbul.2022.113819

Piper, D. J. W., and Normark, W. R. (2009). Processes that initiate turbidity currents and their influence on turbidites: a marine geology perspective. *J. Sedimentary Res.* 79 (6), 347–362. doi: 10.2110/jsr.2009.046

Pohl, F., Eggenhuisen, J. T., Kane, I. A., and Clare, M. A. (2020). Transport and burial of microplastics in deep-marine sediments by turbidity currents. *Environ. Sci. Technol.* 54, 4180–4189. doi: 10.1021/acs.est.9b07527

Pope, E. L., Heijnen, M. S., Talling, P. J., Jacinto, R. S., Gaillot, A., Baker, M. L., et al. (2022). Carbon and sediment fluxes inhibited in the submarine Congo canyon by landslide-damming. *Nat. Geosci.* 15 (10), 845–853. doi: 10.1038/s41561-022-01017-x

Pope, E. L., Talling, P. J., Carter, L., Clare, M. A., and Hunt, J. E. (2017). Damaging sediment density flows triggered by tropical cyclones. *Earth Planetary Sci. Lett.* 458, 161–169. doi: 10.1016/j.epsl.2016.10.046

Post, A. L., Przeslawski, R., Nanson, R., Siwabessy, J., Smith, D., Kirkendale, L. A., et al. (2022). Modern dynamics, morphology and habitats of slope-confined canyons on the northwest Australian margin. *Mar. Geology* 443, 106694. doi: 10.1016/j.margeo.2021.106694

Puig, P., Canals, M., Company, J. B., Martín, J., Amblas, D., Lastras, G., et al. (2012). Ploughing the deep sea floor. *Nature* 489 (7415), 286–289. doi: 10.1038/nature11410

Puig, P., Palanques, A., and Martín, J. (2014). Contemporary sediment-transport processes in submarine canyons. *Annu. Rev. Mar. Sci.* 6, 53–77. doi: 10.1146/annurev-marine-010213-135037

Quattrini, A. M., Nizinski, M. S., Chaytor, J. D., Demopoulos, A. W., Roark, E. B., France, S. C., et al. (2015). Exploration of the canyon-incised continental margin of the northeastern United States reveals dynamic habitats and diverse communities. *PloS One* 10 (10), e0139904. doi: 10.1371/journal.pone.0139904

Ramirez-Llodra, E., De Mol, B., Company, J. B., Coll, M., and Sardà, F. (2013). Effects of natural and anthropogenic processes in the distribution of marine litter in the deep Mediterranean Sea. *Prog. Oceanogr.* 118, 273–287. doi: 10.1016/j.pocean.2013.07.027

Rech, S., Macaya-Caquilpán, V., Pantoja, J. F., Rivadeneira, M. M., Madariaga, D. J., and Thiel, M. (2014). Rivers as a source of marine litter–a study from the SE pacific. *Mar. pollut. Bull.* 82 (1-2), 66–75.

R Core Team (2016). *R: a language and environment for statistical computing* (Vienna, Austria: R Foundation for Statistical Computing). Available at: http://www.R-project.org/.

Romans, B. W., Castelltort, S., Covault, J. A., Fildani, A., and Walsh, J. P. (2016). Environmental signal propagation in sedimentary systems across timescales. *Earth-Science Rev.* 153, 7–29. doi: 10.1016/j.earscirev.2015.07.012

Rouse, H. (1937). Modern conceptions of the mechanics of turbulence. *Trans. Am. Soc. Civil Engineers* 102 (1), 463–543. doi: 10.1061/TACEAT.0004872

Sanchez-Vidal, A., Thompson, R. C., Canals, M., and De Haan, W. P. (2018). The imprint of microfibres in southern European deep seas. *PloS One* 13 (11), e0207033. doi: 10.1371/journal.pone.0207033

Santín, A., Grinyó, J., Bilan, M., Ambroso, S., and Puig, P. (2020). First report of the carnivorous sponge lycopodina hypogea (Cladorhizidae) associated with marine debris, and its possible implications on deep-sea connectivity. *Mar. pollut. Bull.* 159, 1–7. doi: 10.1016/j.marpolbul.2020.111501

Schlining, K., Von Thun, S., Kuhnz, L., Schlining, B., Lundsten, L., Stout, N. J., et al. (2013). Debris in the deep: using a 22-year video annotation database to survey marine litter in Monterey canyon, central California, USA. *Deep Sea Res. Part I* 79, 96–105. doi: 10.1016/j.dsr.2013.05.006

Schmidt, C., Krauth, T., and Wagner, S. (2017). Export of plastic debris by rivers into the sea. *Environ. Sci. Technol.* 51 (21), 12246–12253.

Schmidt, N., Thibault, D., Galgani, F., Paluselli, A., and Sempéré, R. (2018). Occurrence of microplastics in surface waters of the gulf of lion (NW Mediterranean Sea). *Prog. Oceanography* 163, 214–220. doi: 10.1016/j.pocean.2017.11.010

Schnurr, R. E., Alboiu, V., Chaudhary, M., Corbett, R. A., Quanz, M. E., Sankar, K., et al. (2018). Reducing marine pollution from single-use plastics (SUPs): A review. *Mar. pollut. Bull.* 137, 157–171.

Shepard, F. P. (1981). Submarine canyons: multiple causes and long-time persistence. *Aapg Bull.* 65 (6), 1062–1077. doi: 10.1306/03B59459-16D1-11D7-8645000102C1865D

Simmons, S. M., Azpiroz-Zabala, M., Cartigny, M. J. B., Clare, M. A., Cooper, C., Parsons, D. R., et al. (2020). Novel acoustic method provides first detailed measurements of sediment concentration structure within submarine turbidity currents. *J. Geophysical Research: Oceans* 125 (5), e2019JC015904. doi: 10.1029/2019JC015904

Stacey, C. D., Hill, P. R., Talling, P. J., Enkin, R. J., Hughes Clarke, J., and Lintern, D. G. (2019). How turbidity current frequency and character varies down a fjord-delta system: Combining direct monitoring, deposits and seismic data. *Sedimentology* 66 (1), 1–31.

Straub, K. M., and Mohrig, D. (2008). Quantifying the morphology and growth of levees in aggrading submarine channels. *J. Geophysical Research: Earth Surface* 113, F03012. doi: 10.1029/2007JF000896

Talling, P. J., Baker, M. L., Pope, E. L., Ruffell, S. C., Jacinto, R. S., Heijnen, M. S., et al. (2022). Longest sediment flows yet measured show how major rivers connect efficiently to deep sea. *Nat. Commun.* 13 (1), 1–15. doi: 10.1038/s41467-022-31689-3

Taviani, M., Angeletti, L., Canese, S., Cannas, R. I.T.A., Cardone, F., Cau, A M., et al (2017). The "Sardinian cold-water coral province" in the context of the Mediterranean coral ecosystems. *Deep Sea Res. Part II: Topical Studies Oceanography* 145, 61–78.

Taviani, M., Angeletti, L., Cardone, F., Montagna, P., and Danovaro, R. (2019). A unique and threatened deep water coral-bivalve biotope new to the Mediterranean Sea offshore the Naples megalopolis. *Sci. Rep.* 9 (1), 3411. doi: 10.1038/s41598-019-39655-8

Taviani, M., Foglini, F., Castellan, G., Montagna, P., McCulloch, M. T., and Trotter, J. A. (2023). First assessment of anthropogenic impacts in submarine canyon systems off southwestern Australia. *Sci. Total Environ.* 857, 159243. doi: 10.1016/j.scitotenv.2022.159243

Tekman, M. B., Krumpen, T., and Bergmann, M. (2017). Marine litter on deep Arctic seafloor continues to increase and spreads to the north at the HAUSGARTEN observatory. *Deep Sea Res. Part I* 120, 88–99. doi: 10.1016/j.dsr.2016.12.011

Thompson, R. C., Olsen, Y., Mitchell, R. P., Davis, A., Rowland, S. J., John, A. W., et al. (2004). Lost at sea: where is all the plastic? *Science* 304 (5672), 838–838. doi: 10.1126/science.1094559

Tubau, X., Canals, M., Lastras, G., Rayo, X., Rivera, J., and Amblas, D. (2015). Marine litter on the floor of deep submarine canyons of the northwestern Mediterranean Sea: the role of hydrodynamic processes. *Prog. Oceanography* 134, 379–403. doi: 10.1016/j.pocean.2015.03.013

UNEP (2005). *UNEP 2005 marine litter, an analytical overview* (Nairobi: UNEP), 47.

UNEP (2009). *Marine litter: A global challenge* (Nairobi: UNEP), 232.

van den Beld, I. M. J., Guillaumont, B., Menot, L., Bayle, C., Arnaud-Haond, S., and Bourillet, J. F. (2017). Marine litter in submarine canyons of the bay of Biscay. *Deep Sea Res. Part II* 145, 142–152. doi: 10.1016/j.dsr2.2016.04.013

Van Sebille, E., Wilcox, C., Lebreton, L., Maximenko, N., Hardesty, B. D., Van Franeker, J. A., et al. (2015). A global inventory of small floating plastic debris. *Environ. Res. Lett.* 10 (12), 124006. doi: 10.1088/1748-9326/10/12/124006

Vetter, E. W., and Dayton, P. K. (1999). Organic enrichment by macrophyte detritus, and abundance patterns of megafaunal populations in submarine canyons. *Mar. Ecol. Prog. Ser.* 186, 137–148. doi: 10.3354/meps186137

Waldschläger, K., Brückner, M. Z., Almroth, B. C., Hackney, C. R., Adyel, T. M., Alimi, O. S., et al. (2022). Learning from natural sediments to tackle microplastics challenges: a multidisciplinary perspective. *Earth-Science Rev.* 228, 104021. doi: 10.1016/j.earscirev.2022.104021

Watters, D. L., Yoklavich, M. M., Love, M. S., and Schroeder, D. M. (2010). Assessing marine debris in deep seafloor habitats off California. *Mar. pollut. Bull.* 60, 131–138. doi: 10.1016/j.marpolbul.2009.08.019

Wei, C. L., Rowe, G. T., Nunnally, C. C., and Wicksten, M. K. (2012). Anthropogenic "Litter" and macrophyte detritus in the deep northern gulf of Mexico. *Mar. pollut. Bull.* 64, 966–973. doi: 10.1016/j.marpolbul.2012.02.015

Willis, K., Denise Hardesty, B., Kriwoken, L., and Wilcox, C. (2017). Differentiating littering, urban runoff and marine transport as sources of marine debris in coastal and estuarine environments. *Sci. Rep.* 7, 1–9. doi: 10.1038/srep44479

Woodall, L. C., Robinson, L. F., Rogers, A. D., Narayanaswamy, B. E., and Paterson, G. L. J. (2015). Deep-sea litter: a comparison of seamounts, banks and a ridge in the Atlantic and Indian oceans reveals both environmental and anthropogenic factors impact accumulation and composition. *Front. Mar. Sci.* 2, 3. doi: 10.3389/fmars.2015.00003

Xu, J. P. (2011). Measuring currents in submarine canyons: technological and scientific progress in the past 30 years. *Geosphere* 7, 868–876. doi: 10.1130/GES00640.1

Xu, J. P., Noble, M., Eittreim, S. L., Rosenfeld, L. K., Schwing, F. B., and Pilskaln, C. H. (2002). Distribution and transport of suspended particulate matter in Monterey canyon, California. *Mar. Geology* 181 (1-3), 215–234. doi: 10.1016/S0025-3227(01)00268-7

Xu, J. P., Swarzenski, P. W., Noble, M., and Li, A. C. (2010). Event-driven sediment flux in hueneme and mugu submarine canyons, southern California. *Mar. Geology* 269, 74–88. doi: 10.1016/j.margeo.2009.12.007

Yin, S., Lin, L., Pope, E. L., Li, J., Ding, W., Wu, Z., et al. (2019). Continental slope-confined canyons in the pearl river mouth basin in the south China Sea dominated by erosion 2004–2018. *Geomorphology* 344, 60–74. doi: 10.1016/j.geomorph.2019.07.016

Zettler, E. R., Mincer, T. J., and Amaral-Zettler, L. A. (2013). Life in the "plastisphere": microbial communities on plastic marine debris. *Environ. Sci. Technol.* 47, 7137–7146. doi: 10.1021/es401288x

Zhong, G., and Peng, X. (2021). Transport and accumulation of plastic litter in submarine canyons–the role of gravity flows. *Geology* 49, 581–586. doi: 10.1130/G48536.1

frontiers | Frontiers in Marine Science

TYPE Review
PUBLISHED 19 September 2023
DOI 10.3389/fmars.2023.1225114

OPEN ACCESS

EDITED BY
Cinzia Corinaldesi,
Marche Polytechnic University, Italy

REVIEWED BY
Lucy Cheryl Woodall,
University of Oxford, United Kingdom
Francesco Tiralongo,
University of Catania, Italy
Zaira Da Ros,
Polytechnic University of Marche, Italy

*CORRESPONDENCE
Jaime Selina Davies
Jaime.Davies@unigib.edu.gi

RECEIVED 18 May 2023
ACCEPTED 03 August 2023
PUBLISHED 19 September 2023

CITATION
Bruemmer AL, Dissanayake A and Davies JS (2023) Marine litter-fauna interactions: a standardised reporting framework and critical review of the current state of research with a focus on submarine canyons. *Front. Mar. Sci.* 10:1225114. doi: 10.3389/fmars.2023.1225114

Marine litter-fauna interactions: a standardised reporting framework and critical review of the current state of research with a focus on submarine canyons

Alice Lauren Bruemmer[1], Awantha Dissanayake[1] and Jaime Selina Davies[1,2]*

[1]School of Marine Science, University of Gibraltar, Gibraltar, Gibraltar, [2]School of Marine Science and Engineering, University of Plymouth, Plymouth, United Kingdom

Litter is ubiquitous in the ocean, interacting with fauna and causing impacts that are unquantified at present. Mainly sourced from land, marine litter is very persistent, and undergoes slow degradation upon settling on the ocean floor. Submarine canyons contain more litter than other oceanographic features due to hydrological processes, but study of litter in canyons is made difficult by logistical requirements. Monitoring and quantification of marine litter often do not consider interactions between fauna and litter, meaning impacts are largely unconsidered and unknown. Among publications that have reported litter-fauna (L-F) interactions in canyons, the large majority occur in the Mediterranean Sea, and the most reported interaction is of corals entangled in fishing gear. When it occurs, the reporting of L-F interactions is unstandardised, resulting in a lack of global comparison and trend analysis. A standardised, comprehensive framework for the reporting of L-F interactions has been created and includes 6 major categories: entanglement, ingestion, smothering, habitat provision, adaptive behaviour, and encountering (entanglement and smothering occur on abiotic features as well). Use of the framework will aid in research collaboration and creation of a global dataset of L-F interactions. Impacts resulting from interactions are plentiful, most coming from entanglement and smothering.

KEYWORDS

marine litter, benthic fauna, litter-fauna interaction, submarine canyon, seafloor

Introduction

Marine litter is becoming increasingly prevalent, causing effects often unknown and unquantified (Canals et al., 2021). Defined by the United Nations Environment Programme (UNEP), marine litter is "any persistent, manufactured or processed solid material discarded, disposed of or abandoned in the marine and coastal environment"

(United Nations Environment Programme [UNEP], 2009). The focus of this review is marine litter larger than micro-litter, which is sized at over 5 mm in diameter and includes meso-, macro-, and mega-litter (Joint Group of Experts on the Scientific Aspects of Marine Environmental Protection [GESAMP], 2019); these categories will be collectively referred to as 'marine litter'. Most marine litter comes from land-based sources such as coastal landfills, industrial pollution and storm water discharge (Katsanevakis, 2008); but some, especially fishing gear, originates from the ocean via boats, offshore platforms, and aquaculture (United Nations Environment Programme [UNEP], 2009; Galgani et al., 2015). Once in the ocean, litter is transported by currents before sinking to the seabed and accumulating (Watters et al., 2010), sometimes thousands of kilometres from its point of origin (Ryan and Moloney, 1993). The degradation of marine litter is slow, especially in the deep sea, where there is a lack of ultraviolet light, temperatures are cold, and oxygen is limited (Andrady, 2015). Plastic, which makes up the majority of marine litter (Derraik, 2002; Katsanevakis, 2008; Galgani et al., 2015) is essentially non-degradable in the cool, dark deep sea (Ryan and Moloney, 1993; Gregory, 2009; Nevill, 2011). Abandoned, lost or otherwise discarded fishing gear (ALDFG) is a type of marine plastic litter that is very prevalent, especially due to increases in fishing activity and gear durability over the last 50 years (Macfadyen et al., 2009; Watson, 2012). Approximately 1% of fishing gear per ship is lost each year (Gilman et al., 2016), being transported through currents before snagging or sinking (Katsanevakis, 2008). Rocks and coralline structures provide habitat for diverse species and thus are often heavily fished, so fishing gear is found to concentrate on such rugose features (Savini et al., 2014; Tubau et al., 2015; Melli et al., 2017; van den Beld et al., 2017; Consoli et al., 2018a; Angiolillo et al., 2022). Even if inputs decrease, marine litter already in the ocean will remain prevalent, snagged on features and resting on the seafloor (Keller et al., 2010). As such, the persistence of marine litter means transport can occur over long time periods, causing impacts through its movement and settlement (Vieira et al., 2014).

Marine litter may interact with fauna while travelling via ocean currents and after descending to the seafloor. For purposes of research, when an organism comes into contact with litter, it is termed a litter-fauna (L-F) interaction. The organism may or may not be affected by such interactions. Litter-fauna interactions began to be reported in the 1960s, mainly as entanglement and ingestion, which are the easiest to observe and quantify (Ryan, 2015; Bajaj et al., 2021). Reports in the 1970s described litter providing habitat through colonisation by algae and bryozoans (Carpenter and Smith, 1972; Venrick et al., 1973; Holmström, 1975). By the 1980s, more interactions had been observed, and the impacts of marine litter presence became a concern, so solutions started to be explored (Ryan, 2015; Bajaj et al., 2021). Since then, further research and quantification has occurred, with new focus on microplastics and toxin transfer from plastics to seawater and into the food chain (Ryan, 2015). In 1997, there were 267 species reported to be either entangled by or to have ingested marine litter (Laist, 1987); by 2015, Kühn et al. (2015) tallied 557 interacting species, while Gall and Thompson (2015) found 693. Gall and Thompson (2015) further reported that plastic resulted in the majority of interactions: synthetic rope and netting caused entanglement, and plastic fragments were ingested. Additionally, 17% of interactions reported had occurred to near-threatened, vulnerable, endangered, or critically endangered species, according to the IUCN Red List (Gall and Thompson, 2015).

Research on L-F interactions is limited at present and is often reported peripherally in studies with other purposes. In order to quantify and compare global occurrence of L-F interactions, a standardised reporting framework is needed. Currently, research papers reporting interactions vary in level of detail; often, the observed litter, interaction, and species type are not quantified. Some researchers have created their own categories for data categorisation purposes, but non-uniformity means global comparison between datasets is an arduous task. Table 1 displays the L-F interactions categories that have so far been used in reporting. While not standardised, themes exist; for example, entanglement, coverage, and colonisation or habitat provision are often reported (Gall and Thompson, 2015; Kühn et al., 2015).

While the prevalence of L-F interactions has been noted, research on such interactions is still limited at present (Ramirez-Llodra, 2020), and may continue to be so while a standardised framework is not widely utilised. Through conduction of a critical literature review, a litter-fauna interactions framework is proposed with the goal of promoting standardised reporting and, thus, creation of a dataset of L-F interactions that are occurring in all ocean zones. The described quantification of the number and type of species interacting with litter will help create sensitivity and vulnerability assessments to understand the true impact of litter on benthic marine ecosystems.

Litter-fauna interactions result in impacts that harm species, but 'harm' is so far unquantified, and due to non-standardised measurement methods, impacts are not fully monitored or even considered (Galgani et al., 2013; Sherrington et al., 2016). For example, between the two most commonly reported interactions, entanglement and ingestion, assessment inabilities result in discrepancies in impact count. It is reported that 79% of entanglement interactions, but only 4% of ingestion interactions, result in direct harm or death, possibly due to difficulties in observing ingestion and quantifying its sublethal effects (Gall and Thompson, 2015). Even the most plainly visible L-F interactions are undercounted; it is estimated that 80% of seals that are entangled die and do not wash up on shore (Fowler, 1982). Due to difficulties in observation and reporting, sporadic individual interactions do not represent population-level effects (Gall and Thompson, 2015; Kühn et al., 2015; Galgani et al., 2018). On the floor of the deep sea especially, the lack of litter data means that effects on deep-sea fauna are unknown and largely unstudied (Canals et al., 2021). However, while widespread impacts are not well understood, that does not mean they do not exist (Koelmans et al., 2013). Endangered or threatened species can be easily impacted by interactions (Macfadyen et al., 2009) whose effects may result in biodiversity loss (Galgani et al., 2013).

Legislation has been enacted to reduce the input of marine litter, largely targeting ocean-based sources. For example, Annex V of the International Convention for the Prevention of Pollution from Ships, (International Maritime Organization [IMO], 1997), regulates dumping of litter from ships, completely banning the disposal of plastics at sea. The London Protocol, adopted in 1996 and entered

TABLE 1 Reporting categories utilised in litter-fauna interactions reporting by individual research teams, ordered chronologically.

L-F Interaction Categories	Location	Source

- Covering
- Abrasion
- Hanging
- Lying
- Colonisation:
  - None (0 taxa)
  - Moderate (1-3 taxa)
  - Heavy (>3 taxa)
	Tyrrhenian Sea benthic zone, including canyon heads	Angiolillo et al. (2015)

Entanglement: - Simple Entanglement - Benthic Scraping - Ghost Fishing	Atlantic and Indian Ocean seamounts, banks, and ridges	Woodall et al. (2015)
- No Effect - Entanglement/Coverage - Physical Damage	Northwest Adriatic Sea rocky shore	Melli et al. (2017)
- Contact - Colonisation - Other	HAUSGARTEN Arctic Deep Sea Observatory	Tekman et al. (2017)
- Entanglement/Coverage - Damage - High Fouling (= 50% coverage by epibionts)	Straits of Sicily coasts	Consoli et al. (2018a)
- No Effect - Entanglement/Coverage (no visible damage) - Physical Damage	Southwest Sicily coasts	Consoli et al. (2018b)

No Interaction:
- Hanging Litter
- Laying Litter
Interaction:
- Coverage/Smothering
- Entanglement
- Ghost Fishing
- Colonisation:
  - Refuge/Shelter
  - New Substrate
  - Adaptive Behaviour
	Malta benthic zone	Consoli et al. (2020)

- Entanglement - Ghost Fishing - Coverage - Behavioural - Substratum - Incorporation	Literature Review (not primary data)	Angiolillo and Fortibuoni (2020)
- Covering - Entanglement - Colonisation - Refuge - Epibiont Fouling	South Tyrrhenian Sea Basin, Tiberio Seamount, Marettimo Bank	Angiolillo et al. (2021a)
- Covering - Entanglement - Colonisation - Refuge - Adaptive Behaviour - Fouling	Ligurian Sea seamounts and canyons	Angiolillo et al. (2021b)

into force in 2006, to which 53 countries adhere, bans most ship-based dumping (International Maritime Organization [IMO], 2019). The accumulation of litter along open-ocean shipping routes (Gjerde, 2006) means the targeting of ocean-based litter sources can be beneficial. However, since the initial writing of the two described pieces of legislation, it has been discovered that up to 80% of marine litter comes from land (North Pacific Fishery Management Council [NPFMC], 2011). Land-sourced litter legislation occurs on a country-by-country or even city-by-city basis. Successful methods to reduce land-sourced marine litter include educational campaigns, increased waste receptacles, improved waste management plans, and beach clean-up activities (Matthews and Doyle, 2012).

While policy increasingly regulates general marine litter, legislation to decrease L-F interactions specifically is lacking. The Marine Strategy Framework Directive (MSFD), which was created to protect European marine ecosystems, calls its member states to achieve Good Environmental Status (GES) in their waters. There are 11 descriptors to be met for achievement of GES, and marine litter is one. As such, achievement of GES requires there to be minimal marine litter presence. To assess GES based on marine litter, impacts due to interactions are monitored, namely impacts of ingestion (EC, 2010) and of entanglement (EC, 2022). As described, L-F interactions are beginning to be considered important benchmarks for marine litter presence and environmental health, but further analysis and policy creation will be necessary to better regulate L-F interactions.

Submarine canyons contain significantly more litter than any other oceanographic feature (Pham et al., 2014; Tubau et al., 2015). Described as keystone structures for their provision of habitat heterogeneity and facilitation of nutrient upwelling, submarine canyons are V-shaped valleys with steep walls incised into continental shelves and margins (Vetter et al., 2010; Fernandez-Arcaya et al., 2017). Submarine canyons are formed by mass slumping, landslides, and turbidity currents, and they act as conduits for the transport of sediment, debris, and anthropogenic litter from canyon heads to their deep-sea floors (Fernandez-Arcaya et al., 2017; Ramirez-Llodra, 2020). Linear litter items such as ropes, fishing lines, and nets are commonly found snagged on rugose canyon walls, while rounded objects such as plastic fragments, bottles, and cans are transported to canyon floors (Lastras et al., 2016). Canyons closer to shore and populated cities contain the highest litter densities (Galgani et al., 2000; Pham et al., 2014; Pierdomenico et al., 2019); however, marine litter is still found in offshore canyons, even those in protected, no-fishing zones (Marin and Aguilar, 2012).

The abundance of marine litter in submarine canyons and the general occurrence of marine L-F interactions suggests that interactions and impacts are occurring within submarine canyons. However, financial, logistical, and technical implications make research of submarine canyons and the deep sea challenging compared to that of shallow-water areas (Barnes et al., 2009; Galgani et al., 2015; Tekman et al., 2017; Canals et al., 2021). Such challenges leave the deep sea, which makes up half of the surface of the earth, grossly understudied (Barnes et al., 2009; Ramirez-Llodra et al., 2011; Galgani et al., 2015); over 95% of the deep sea is unexplored (van den Beld, 2017). As such, there is a need for increased research into submarine canyon L-F interactions.

The current research aims to fill gaps in knowledge in two ways. Firstly, a standardised L-F interactions framework is proposed, sourced from interaction types reported ocean-wide, and will help increase the ability for global interactions comparisons found in all oceanic zones. Additionally, the current documentation of L-F interactions occurring in submarine canyons will be presented, categorised using the standardised framework, providing both L-F interactions knowledge at present and a baseline dataset to be augmented upon further L-F interactions observations within canyons.

Methods

A critical literature review was undertaken following the PRISMA methodology (Page et al., 2021) to amalgamate L-F interactions and impacts reported to occur in all ocean zones, from which the L-F interactions framework was derived. Additionally, papers reporting marine L-F interactions within submarine canyons were used to complete a synthesis review of the current state of research. The body of papers read was derived from three separate groupings, the first two resulting from keywords searches using Google Scholar, and the third resulting from relevant citations found within papers read. The first, general keywords search was conducted by entering the keywords 'marine AND debris* AND/OR litter* AND/OR interact* AND/OR seafloor* AND/OR seabed* AND fauna AND -micro' into Google Scholar. In order to find additional papers focusing on canyons, a second, specific keywords search was undertaken by using the terms from the first search plus AND canyon* AND "deep sea*" AND/OR "deep-sea". The final search was performed on 7th May, 2023. See Figure 1 for a decision tree depicting the creation of the body of papers to be read, starting with all papers found in the general and specific keywords search, and selecting for papers with relevant data. Peer-reviewed publications with data on L-F interactions with micro-litter or in simulated laboratory experiments were excluded from the primary data categories. Relevant citations within the publications from the keywords searches were recorded and read. The literature review was deemed exhaustive when all relevant citations in each paper read had already been included in the review.

All L-F interactions mentioned or reported were categorised by type. Synonyms describing the same type of interaction were recorded using the most common term, and similar interactions were amalgamated into groups. Overarching categories of interactions were finalised into groupings of the main types of marine L-F interactions that occur, creating a framework. Each description of an impact resulting from an interaction was likewise categorised by type. Impact types were combined to be written as one term if synonymic, and similar types of impacts were grouped together; primary, secondary, and tertiary impacts were recorded as such. Primary impacts occur as direct results of interactions, secondary impacts occur as direct results of primary impacts, and tertiary impacts occur as direct results of secondary impacts.

From papers reporting primary data on L-F interactions and impacts within submarine canyons, the following information was recorded for comparison and analysis:

- taxa (categorised by phylum, the most specific level possible)/ features affected,
- type of litter,
- type of interaction,
- global canyon location,
- location of interaction within the canyon,
- maximum depth range of study, and
- initial intention of data collection.

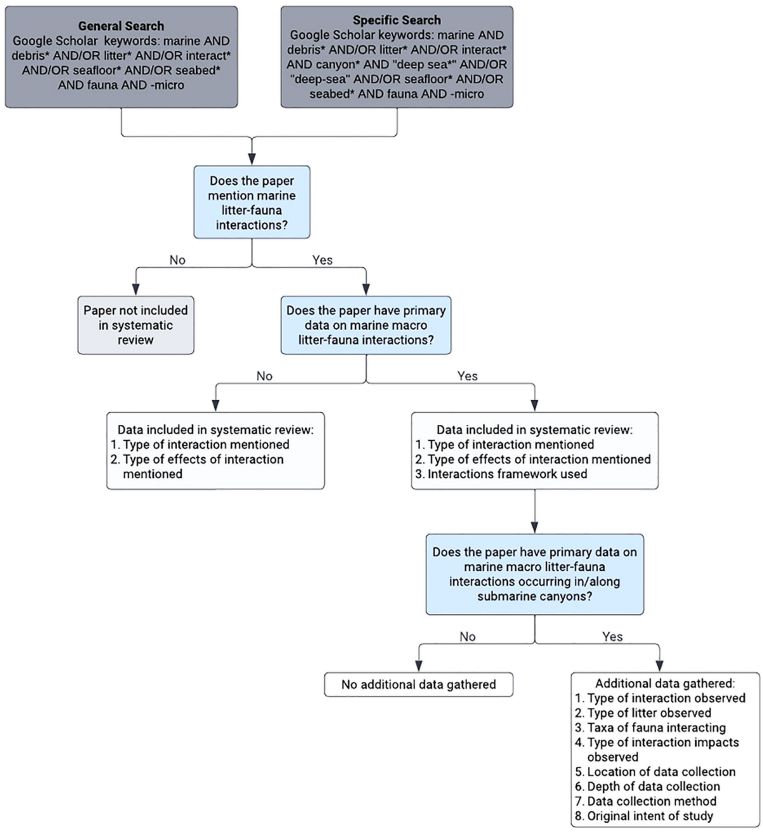

FIGURE 1
Criteria for inclusion or exclusion in the systematic review of papers resulting from the keywords searches and data gathered from each evidence source.

As canyons are complex systems with transport and mixing throughout, all locations within canyons were considered in data extraction.

Results

The critical literature review produced a body of scientific articles and grey literature that provides background on the current state of L-F interactions, with an emphasis on submarine canyons. A total of 4,086 papers resulted from the two keywords searches, of which 222 mentioned L-F interactions and were retained for the next stage of screening (Figure 2). An additional 137 papers which mentioned L-F interactions were found through in-text citations while reviewing the literature from the two keyword searches, which were used to build the L-F interactions framework. Almost two-thirds (n=221) of papers mentioning or reporting L-F interactions have been published in the past 10 years, starting in 2013 (Figure 3). Out of 359 papers found that mentioned L-F interactions, 23 contained primary data of such interactions occurring in submarine canyons (Figure 2). All 23 of those papers have been published in the past 14 years, since 2009 (Figure 3).

Litter-fauna interactions framework

A comprehensive L-F interactions framework has been devised, based on categorisation of L-F interactions in all ocean zones mentioned in the literature review. The six litter-fauna interaction categories are as follows: entanglement, ingestion, smothering, habitat provision, adaptive behaviour, and encountering. While biotic interactions are most often mentioned, a smaller framework for interactions between litter and abiotic features consists of entanglement and smothering. Abiotic features are those that are not living and are not derived from organisms that were once living. If no biotic or abiotic L-F interaction is observed, the piece of litter should be reported as such. See Table 2 for L-F interactions framework, including synonyms and common examples.

Entanglement

Entanglement in marine litter is defined as fauna becoming ensnared by a piece of litter (Figures 4A–C). An entangled individual may remain mobile or become immobilised. Also reported as tangling and entrapment, entanglement occurs largely due to fishing gear and

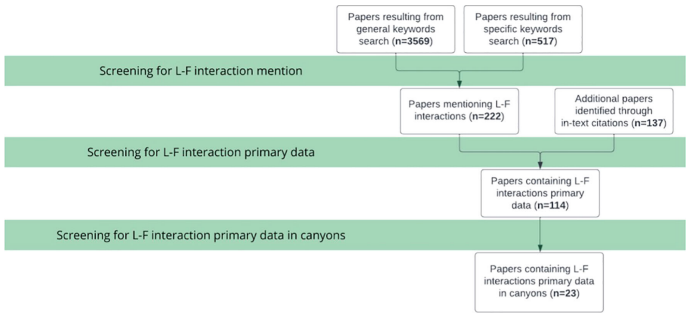

FIGURE 2
Screening process for papers to be included in the critical literature review and number of papers included at each step, following the PRISMA methodology (Page et al., 2021).

packing bands (United Nations Environment Programme [UNEP] and National Oceanic and Atmospheric Administration [NOAA], 2012; Morris and Seasholes, 2014). Impacts are mainly mechanical, and include reduced feeding and difficulty breathing, as suggested in *Rhizoprionodon lalandii* sharks in southeast Brazil found emaciated with plastic debris collars (Sazima et al., 2002), increased metabolic rate, seen in captive *Callorhinus ursinus* fur seals from St. Paul Island, Alaska (Feldkamp et al., 1988), wounds or abrasions, as seen in Asia-Pacific coral reefs (Lamb et al., 2018), and even drowning and death, which are difficult to observe (Fowler, 1982). Abiotic entanglement occurs when litter snags on ocean features, degrading, altering, or obstructing habitat (Gilman et al., 2021).

Ingestion

Ingestion of marine litter is defined as fauna consuming marine litter (Table 3). The main source of ingestion is degraded micro-litter (United Nations Environment Programme [UNEP] and National Oceanic and Atmospheric Administration [NOAA], 2012); it can, therefore, be difficult to observe ingestion as it occurs. Ingestion may occur purposefully or inadvertently, and impacts include digestion blockages, as seen in *Chelonia mydas* sea turtles in southeastern Brazil (Di Beneditto and Awabdi, 2014), internal injuries, as suggested by Gramentz (1988) in species of loggerhead sea turtles, false senses of satiation, as seen in albatross chicks on Midway Atoll (Auman et al., 1997), and transport of chemical pollutants adsorbed to ingested litter, as suggested by Rochman et al. (2013) in *Oryzias latipes* fish.

Smothering

Smothering by marine litter is defined as litter settling on top of fauna and blocking water flow (Figures 4D, E). Also reported as 'covering,' smothering is mainly caused by wide pieces of litter, such as bags, fabric, and sheets of various materials (United Nations Environment Programme [UNEP] and National Oceanic and Atmospheric Administration [NOAA], 2012). Smothering can also occur on abiotic features where no fauna is discernible.

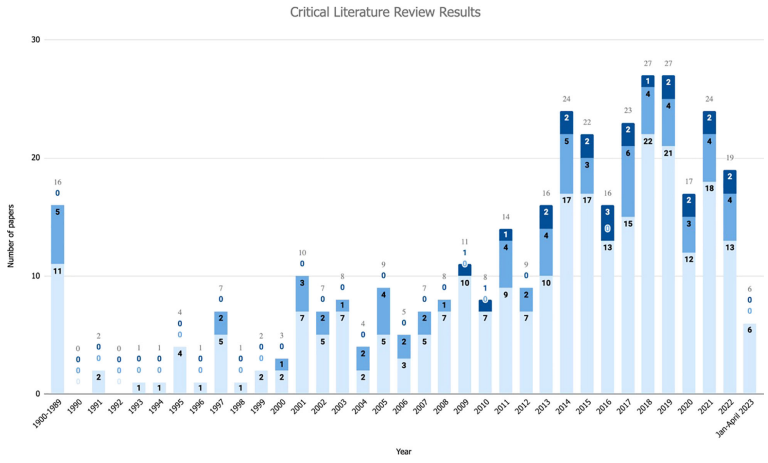

FIGURE 3
Publication year of papers that were included in the critical literature review, delineated by type of paper. Light blue: number of papers that mention Litter-fauna (L-F) interactions but have no primary interaction data. Medium blue: number of papers with primary data on L-F interactions, not including micro-litter ingestion or simulated experiments. Dark blue: number of papers with primary data on L-F interactions in or along submarine canyons, not including micro-litter ingestion.

TABLE 2 Litter-fauna interactions categories with common synonyms and examples.

	Entanglement *biotic + abiotic	Ingestion	Smothering *biotic + abiotic	Habitat Provision	Adaptive Behaviour	Encountering
Synonyms	• Snagging • Entrapment • Tangling • Wrapping	• Swallowing • Consumption	• Occlusion • Crushing • Covering			
Examples	• Ghost fishing (netting, trapping, potting, hooking) • Stationary entanglement (mobile species held in place) • Mobile entanglement (mobile species moving with litter attached)	• Partial ingestion (stuck in mouth/ throat) • Complete ingestion (entrance into intestinal tract/ excretion)	• Feeding obstruction • Habitat homogenization	• Shelter provision (e.g. sheltering in litter cavities, burrowing under litter, use as mobile habitat) • Substrate provision (e.g. colonisation, encrusting, fouling)	• Carrying • Overgrowing • Camouflage/ covering body with litter for protection • Use as egg laying substrate • Use as aggregation site • Use as a den feature	• Contact (e.g. touching, collision) • Non-contact (i.e. within a radius of 2 lengths of the fauna)

All categories may occur between litter and biotic features, those that are living or are derived from features that were once living. Entanglement and smothering may also occur between litter and abiotic features, those that are not living and were not derived from features that were once living. * identifies those categories which can both be biotic and abiotic, while the remaining categories are biotic only.

Impacts include preventing filter feeders from feeding, as suggested in sponges by Bergmann and Klages (2012), and creation of anoxic sediment, as exemplified by plastic bags placed in intertidal waters off the coast of Dublin, Ireland (Green et al., 2015).

Habitat provision

Habitat provision by marine litter is defined as litter acting as either substrate or shelter for fauna (Figures 4F, G). Substrate provision occurs when sessile and encrusting species grow on pieces of litter, as seen in the settlement of sea anemones, hydroids, and crinoids on litter in the Arctic deep sea (Bergmann and Klages, 2012), and in the settlement of species on a shipping container not typically found in the soft sediment of the area (Taylor et al., 2014). Shelter provision occurs when species take cover in the cavities of litter, either temporarily or permanently, such as *Munida* crustaceans making burrows of plastic and cloth in the Bay of Biscay (van den Beld et al., 2017). In the use of litter as substrate or shelter, species may settle on mobile materials that are transported by currents, potentially causing the spread of invasive species; in the review by Gall and Thompson (2015), there were 259 species reported to use litter as rafts, and 6 of those were invasives.

Adaptive behaviour

Adaptive behaviour to marine litter is defined as the adaptation of a species to the presence of litter, using it in ways other than habitat provision. Examples include use as egg laying substrates, as seen in *Sepia officinalis* cuttlefish and *Loligo vilgaris* squid in the Northern Adriatic Sea (Moschino et al., 2019), aggregation sites, exemplified by *Cidaris cidaris* and *Pleisionika* species being often found around litter accumulations in submarine canyons south of Italy (Pierdomenico et al., 2018), and carrying litter, as seen by *Paromola cuvieri* off the southern coast of Sardinia (Figure 9, Image E: Taviani et al., 2017). Impacts include alteration of natural systems and behaviours, with so far unquantified effects. Adaptive behaviour is the least understood of all the L-F interactions (Barros et al., 2020).

Encountering

Encountering marine litter is defined as a species coming across litter but not interacting with it in any of the 5 ways listed above (Figures 4H–J). Examples of encountering include touching, collision, or general disturbance from litter, and impacts may include altered behaviour or wounds. While the interaction 'encountering' is not often reported as such, Tekman et al. (2017) reported contact between litter and fauna to occur in 80% of its 60 observed interactions on the Arctic seafloor, largely with suspension feeders. When any part of a species is within two of its body lengths of a piece of litter, it is considered to have encountered the litter in a non-contact manner. Impacts of non-touching encountering include proximity to toxin leaching from the litter and increased likelihood of one of the other types of interactions.

Impacts of L-F interactions

Interactions do not occur in isolation but cause ensuing impacts on fauna. For examples, see Katsanevakis (2008); Barreiros and Raykov (2014); Lamb et al. (2018) and Angiolillo and Fortibuoni (2020). Connections between interactions and their primary, secondary, and tertiary impacts, as discovered in the literature review, have been amalgamated using common standardised terminology. Entanglement and smothering resulted in the largest number of possible primary impacts, with 6 each in biotic interactions, and 2 and 5, respectively, in abiotic interactions. See

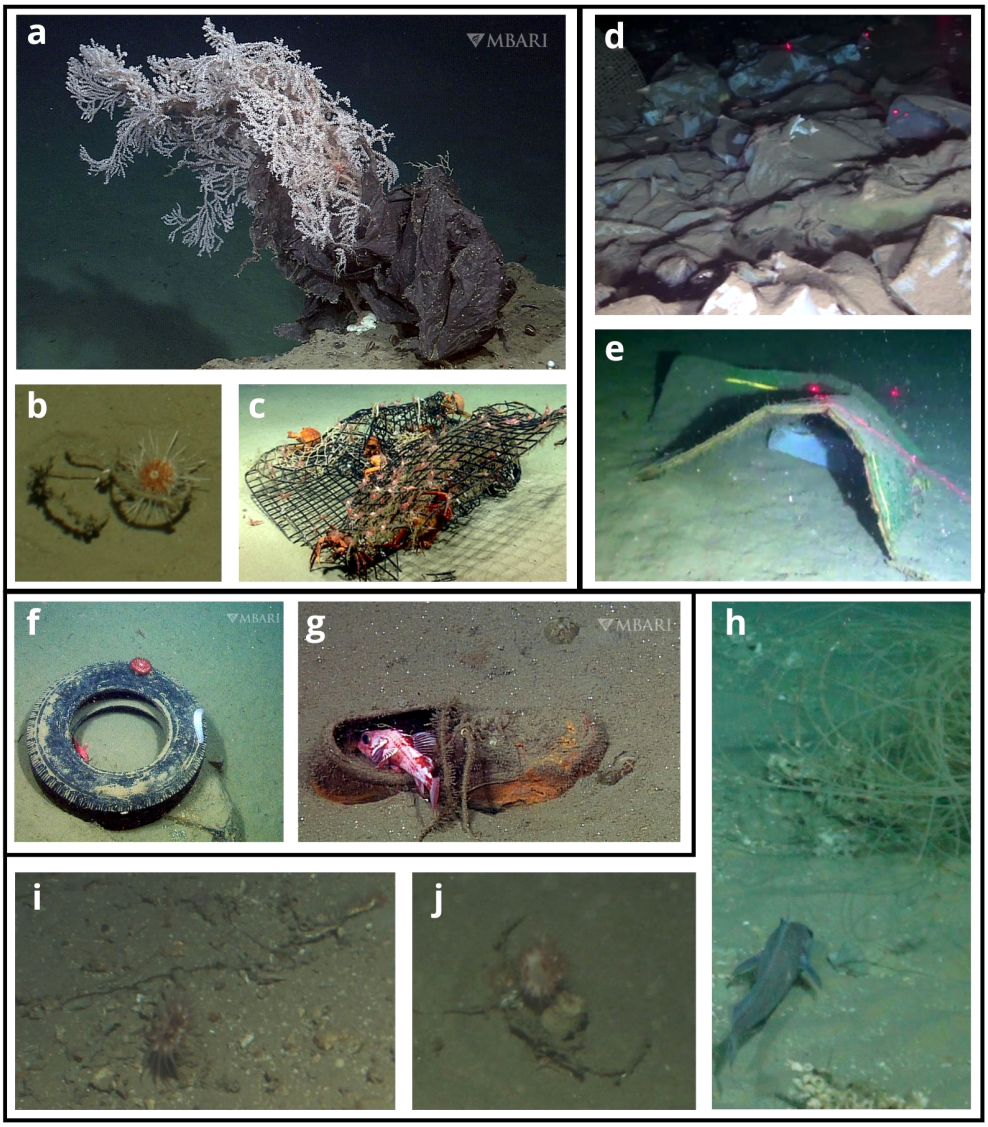

FIGURE 4
Litter-fauna entanglement, smothering, habitat provision, and encountering examples. Entanglement: **(A)** Plastic bag snagged on a deep-sea gorgonian (source: Schlining et al., 2013 © MBARI 2006). **(B)** Echinoid entangled (mobile entanglement) in rope (© JNCC/Cefas, 2017). **(C)** Ghost trapping of red crabs and banded shrimp (source: Quattrini et al., 2015). Smothering: **(D)** Abiotic smothering: plastic bags smothering the seafloor (source: Taviani et al., 2019). **(E)** Abiotic smothering: mattress smothering the seafloor (source: Taviani et al., 2019). Habitat provision: **(F)** Tire serving as substrate for an anemone and sea cucumber, shelter for a rockfish (source: Schlining et al., 2013 © MBARI 2009). **(G)** Shoe serving as shelter for a rockfish (source: Schlining et al., 2013 © MBARI 2010). Encountering: **(H)** Fish *Lepidion eques* within 2 body lengths of monofilament fishing line (© JNCC/Cefas, 2017). **(I)** Anemone *Actinauge richardi* within 2 body lengths of rope (© JNCC/Cefas, 2017). **(J)** Two individuals of *A richardi* and one *Munida* (small lobster opposite rope from the right-most anemone) touching rope (© JNCC/Cefas, 2017).

TABLE 3 Litter-fauna ingestion examples within publications.

Description of Image	Source and Image
Loggerhead sea turtle (*Caretta caretta*) found dead after swallowing a longline with hooks	Barreiros and Raykov (2014) Figure 2, image a
Harbour porpoise (*Phocoena phocoena*) having partially ingested a bracelet	Unger et al. (2017) Figure 2, image c
Loggerhead sea turtle (*C. caretta*) having partially ingested a crown cork bottle cap	Gramentz (1988) Figure 4

Figure 5 for chord diagrams of the relationship between biotic and abiotic interactions and their respective resulting primary effects on marine ecosystems.

L-F interactions in submarine canyons

Information extracted from the 23 papers reporting primary data on L-F interactions within submarine canyons is displayed in Figure 6. See Table 4 for further details on country, phylum, litter category, and interaction type from the 23 papers. Papers included in the matrix are referred to in Appendix A.

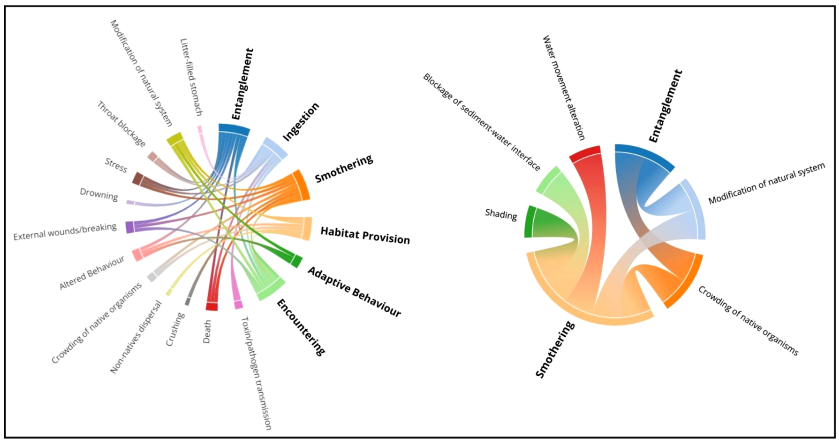

FIGURE 5
Left: Litter-fauna interactions (bold) and their respective primary impacts on fauna. Number of primary impacts from each interaction: Entanglement-6; Ingestion-5; Smothering-6; Habitat Provision-4; Adaptive Behaviour-2; Encountering-3 (not including the potential for occurrence of the other interaction types). Right: Abiotic litter interactions (bold) and their respective impacts on fauna and ocean features. Number of primary impacts from each interaction: Entanglement-2; Smothering-5. Diagrams created using datasmith.org.

Survey logistics

The categories of survey method and data collection method were each dominated by one type (Figure 6). ROVs were used in 19 of the 23 papers, making them the most commonly used survey tool to encounter L-F interactions in submarine canyons. Of the 23 papers, 15 collected data indirectly, meaning L-F interactions were observed incidentally during a survey that had other aims. Of those papers, 13 occurred at the time of surveying, and 2 occurred retrospectively, upon reviewing the footage for another purpose. Of the 8 reports that directly intended to search for litter-fauna interactions, 5 were retrospective and 3 had the initial goal of quantifying litter-fauna interactions.

L-F interactions reported

Among all taxa, entanglement and habitat provision were most commonly observed, each reported at least once by 19 papers (Figure 6). Smothering and adaptive behaviour were each reported 3 times, 4 papers observed encountering, and ingestion was never reported. The most commonly observed interactions took place between plastic and Cnidarians; 21 papers reported at least one instance of plastic interacting with fauna, and 19 papers reported at least one instance of the phylum Cnidaria interacting with litter. In total, 15 of the 23 papers reported corals entangled by fishing nets or lines, making coral entanglement with plastic fishing gear the most commonly reported L-F interaction in submarine canyons.

Canyon locations

Globally, the majority of litter-fauna interactions occurring in canyons were reported from Europe, mainly in the Mediterranean Sea (Figure 7). At 7 papers, Italy has produced the largest number of such publications by a single country. Within the canyons, maximum survey depth and location of interactions vary. Of the 23 papers analysed, 19 presented results from deep sea surveys, while 2 occurred largely outside of the zone of the deep sea, with maximum depths under 250 m. All papers reported on benthic interactions except

	Max. Survey Depth					Location Within Canyon							Survey Type				Data Collection			Phylum Affected									Interaction Observed						Litter Type						
Country	0-250 m	250-500 m	500-750 m	750-1000 m	>1000 m	Flanks	Heads	Floors	Slopes	Thalwegs	Multiple Locations	Not Specified	ROV	Manned Submersible	Towed Camera	Trawl	Indirect	Direct	Retrospective, Indirect	Retrospective, Direct	Cnidaria	Chordata	Arthropoda	Echinodermata	Porifera	Annelida	Mollusca	Abiotic Features	Bryozoa	Brachiopoda	Entanglement	Habitat Provision	Smothering	Adaptive Behavior	Encountering	Ingestion	Plastic	Metal	Rubber	Glass/Ceramics	Natural Products/Clothes	Miscellaneous
Italy	2	5	2	0	0	3	4	1	0	1	0	2	8	0	1	0	6	1	0	2	9	4	4	2	3	2	1	2	1	0	9	7	2	2	0	0	9	3	0	1	2	1
Spain	0	2	2	0	1	2	1	0	1	0	1	0	4	1	0	1	4	0	0	1	3	1	1	0	1	1	1	1	0	1	3	4	0	0	1	0	4	1	0	1	1	0
USA	0	1	0	0	3	1	0	1	1	0	1	0	2	1	0	0	1	1	2	0	3	3	4	2	1	1	1	1	0	0	3	3	0	0	1	0	3	1	2	0	1	1
France	0	0	1	0	2	0	1	0	0	0	2	0	3	1	1	0	0	1	0	2	3	2	2	2	2	3	3	1	1	0	2	3	0	1	1	0	3	1	0	0	1	1
Portugal	0	0	0	0	1	0	0	0	0	0	0	1	1	0	0	0	1	0	0	0	1	1	0	1	0	0	0	1	0	0	1	1	1	0	0	0	1	1	0	0	0	0
Australia	0	0	0	0	1	0	0	0	0	0	1	0	1	0	0	0	1	0	0	0	0	0	1	0	1	0	0	1	1	0	1	1	0	0	1	0	1	0	0	0	0	0
Total	2	8	5	0	8	6	6	2	2	1	5	3	19	3	2	1	13	3	2	5	19	11	12	7	8	7	6	7	3	1	19	19	3	3	4	0	21	7	2	2	5	3

FIGURE 6
Trends in canyon litter-fauna interactions reporting, categorised by country of research, with each category organised from L to R. Maximum survey depth categorised by depth (metres); location within canyon is organised by most commonly observed location of interaction in each publication, followed by 'multiple locations' and 'not specified'; survey type is organised by most commonly used method; data collection is organised by category; phylum affected is organised by most commonly affected phylum; interaction observed is categorised by most commonly observed interaction; litter type is organised according to the framework used by the MSFD (Source: Hanke et al., 2013).

10.3389/fmars.2023.1225114

TABLE 4 Primary reports of litter-fauna interactions in submarine canyons detailed by country, phylum with Cnidaria order (Cnidaria is the most commonly observed interacting phylum), litter category with plastic type [categories from the MSFD framework (Hanke et al., 2013)], and interaction type.

Citation	Country	Phylum	Order (if Cnidaria)	Litter Category	Type (if Plastic)	Interaction Type
Orejas et al. (2009)	Spain	Cnidaria	Scleractinia	plastic	fishing line (entangled)	Entanglement
Watters et al. (2010)	USA	Arthropoda		plastic	crates and containers (fishing trap)	entanglement
		Abiotic Features		plastic	fishing line (monofilament); fishing net	encountering
		Chordata		not specified		habitat provision
Mordecai et al. (2011)	Portugal	Cnidaria	Actiniaria	plastic	fishing line (monofilament); fishing net	habitat provision
		Cnidaria	Brisingida	metal		habitat provision
		Cnidaria	Hydrozoa	metal		habitat provision
		Cnidaria	Alcyonacea, Hydrozoa	metal		habitat provision
		Chordata		metal		habitat provision
		Echinodermata		plastic	fishing line (entangled)	entanglement
		Abiotic Features		plastic	Bag	smothering
Ramirez-Llodra et al. (2013)	Spain	Brachiopoda		natural products/ clothes		habitat provision
Schlining et al. (2013)	USA	Arthropoda		miscellaneous		entanglement
		Cnidaria	Alcyonacea	plastic	Bag	entanglement
		Chordata		natural products/ clothes		habitat provision
		Chordata, Cnidaria, Echinodermata	Actiniaria	rubber		habitat provision
		Porifera		miscellaneous		habitat provision
Fabri et al. (2014)	France	Cnidaria	Alcyonacea	plastic	fishing line (entangled); fishing net	entanglement
		Abiotic Features		plastic	fishing line (entangled)	entanglement
		Annellida, Mollusca, Cnidaria	Scleractinia	plastic	fishing line (monofilament)	habitat provision
Taylor et al. (2014)	USA	Annelida, Arthropoda, Cnidaria, Echinodermata, Mollusca, Chordata	Cnidaria order not specified	metal		habitat provision
Angiolillo et al. (2015)	Italy	Cnidaria, Porifera	Antipatharia	plastic	fishing net, other	smothering
		Annelida		metal, natural products/ clothes		habitat provision
		Cnidaria	Alcyonacea, Actiniaria, Scleractinia	plastic	not specified	habitat provision

(Continued)

10.3389/fmars.2023.1225114

TABLE 4 Continued

Citation	Country	Phylum	Order (if Cnidaria)	Litter Category	Type (if Plastic)	Interaction Type
		Cnidaria	Alcyonacea	plastic	fishing net, other	habitat provision
		Echinodermata		plastic	fishing net	habitat provision
		Chordata, Arthropoda, Echinodermata, Mollusca		not used		habitat provision
Quattrini et al. (2015)	USA	Cnidaria	Scleractinia; Alcyonacea	plastic, rubber	fishing net, crates and containers (fishing trap)	entanglement
		Arthropoda		plastic	crates and containers (fishing trap)	entanglement
Lastras et al. (2016)	Spain	Cnidaria	Scleractinia	plastic	fishing net, fishing line (monofilament)	entanglement, habitat provision
Cau et al. (2017)	Italy	Cnidaria	Alcyonacea, Antipatharia, Scleractinia	plastic	fishing net, fishing line (entangled)	entanglement
		Annelida, Porifera, Chordata, Bryozoa, Cnidaria	Zoantharia, Hydrozoa	plastic	fishing net, fishing line (monofilament)	habitat provision
		Cnidaria	Cnidaria order not specified	plastic	bag, fishing net	entanglement
		Arthropoda		plastic	fishing net	entanglement
D'Onghia et al. (2017)	Italy	Cnidaria	Scleractinia	plastic	fishing line (entangled), other	entanglement
Taviani et al. (2017)	Italy	Arthropoda		plastic	Other	adaptive behaviour
		Cnidaria	Scleractinia	plastic	Bag	entanglement
		Arthropoda		plastic	fishing net	entanglement
		Cnidaria	Scleractinia	metal		habitat provision
van den Beld et al. (2017)	France	Cnidaria	Scleractinia	plastic, natural products/ clothes	Other	habitat provision
		Cnidaria	Actiniaria	plastic, metal	fishing line (monofilament), fishing net, crates and containers (fishing trap)	habitat provision
		Porifera, Annelida		metal		habitat provision
		Mollusca		metal		habitat provision
		Echinodermata		plastic, metal	Other	encountering
		Echinodermata		plastic	fishing net	encountering
		Echinodermata		plastic	fishing net	entanglement
		Echinodermata		metal		habitat provision
		Arthropoda		plastic, natural products/ clothes	Other	habitat provision
		Arthropoda, Chordata		plastic	fishing net, fishing line (monofilament)	encountering

(Continued)

10.3389/fmars.2023.1225114

TABLE 4 Continued

Citation	Country	Phylum	Order (if Cnidaria)	Litter Category	Type (if Plastic)	Interaction Type
		Chordata		plastic	fishing net, fishing line (monofilament)	encountering
Pierdomenico et al. (2018)	Italy	Cnidaria, Echinodermata	Alcyonacea	plastic	Other	entanglement
		Cnidaria	Alcyonacea	glass/ceramics		habitat provision
		Echinodermata, Arthropoda		not used		adaptive behaviour
		Arthropoda		plastic	Other	adaptive behaviour
		Chordata		plastic	Bag	habitat provision
Giusti et al. (2019)	Italy	Cnidaria	Alcyonacea, Scleractinia	plastic, natural products/ clothes	fishing line (entangled), fishing net	entanglement
Taviani et al. (2019)	Italy	Abiotic Features		plastic	Bag	smothering
		Cnidaria	Cnidaria order not specified	plastic	fishing line (monofilament)	habitat provision
		Not specified		plastic	fishing net, fishing line (entangled)	entanglement
		Abiotic Features		plastic	fishing line (entangled)	entanglement
Enrichetti et al. (2020)	Italy	Cnidaria	Alcyonacea	plastic	fishing line (entangled)	entanglement
		Abiotic Features		plastic	fishing net	entanglement
		Cnidaria	Alcyonacea	plastic	fishing net	entanglement
		Chordata		plastic	crates and containers (fishing pot)	entanglement
		Porifera		metal		habitat provision
Santín et al. (2020)	Spain	Porifera		plastic	synthetic rope	habitat provision
Angiolillo et al. (2021b)	France	Porifera, Cnidaria, Annelida, Bryozoa	Actiniaria, Alcyonacea, Scleractinia, Zoantharia, Hydrozoa	not specified		habitat provision
		Arthropoda, Chordata		not specified		habitat provision
		Arthropoda		plastic	Sheet	adaptive behaviour
		Cnidaria, Porifera, Mollusca	Alcyonacea, Scleractinia, Antipatharia	plastic, miscellaneous	fishing line (entangled)	entanglement
Moccia et al. (2021)	Italy	Cnidaria	Antipatharia, Alcyonacea	plastic	fishing line (entangled)	entanglement
		Cnidaria	Alcyonacea	plastic, miscellaneous	fishing net, other	entanglement
		Not specified		plastic, miscellaneous	fishing net, fishing line (monofilament)	habitat provision
Cerrillo-Escoriza et al. (2023)	Spain	Mollusca, Cnidaria, Arthropoda, Chordata	Hydrozoa	not specified		habitat provision
		Annelida		glass/ceramics		habitat provision

(Continued)

TABLE 4 Continued

Citation	Country	Phylum	Order (if Cnidaria)	Litter Category	Type (if Plastic)	Interaction Type
		Cnidaria, Abiotic Features	Scleractinia	plastic	fishing line (entangled)	entanglement, encountering
		Chordata, Arthropoda		plastic, metal	not specified	habitat provision
Taviani et al. (2023)	Australia	Arthropoda		plastic	Other	habitat provision
		Porifera, Bryozoa		plastic	fishing line (monofilament)	habitat provision
		Abiotic Features		plastic	fishing line (entangled)	entanglement
		Bryozoa		plastic	fishing line (monofilament)	encountering

Santín et al. (2020), which found sponges colonising plastic entangled in ROV rope as it was pulled up from a canyon. Among benthic surveys, the most common locations of L-F interactions were canyon flanks and heads, each with 6 reports.

Discussion

Current state of submarine canyon L-F interactions research

Submarine canyons provide habitat and harbour biodiversity, especially for vulnerable slow-growing species like cold-water corals (CWCs), meaning the pressure of litter can cause long-lasting physical damage (Giusti et al., 2019; Lartaud et al., 2020). At present, research on L-F interactions in submarine canyons is extremely limited, with reports coming from 23 scientific publications, only 8 of which whose primary aim was to investigate L-F interactions. The amount of deep-sea litter research is disproportionate to the number of canyons that exist. Globally, at least 9,477 submarine canyons are found in the ocean, making up approximately 11% of the area of continental slopes (Harris et al., 2014). The prevalence of submarine canyons, combined with their provision of habitat and transport of materials such as litter to the deep sea, means that the minimal data on L-F interactions likely does not signify a lack of interactions, but a lack of research.

Submarine canyon research is made difficult by constraints such as equipment, financing, and logistics (Barnes et al., 2009; Galgani et al., 2015; Tekman et al., 2017; Canals et al., 2021). Trawl surveys are commonly used in benthic litter analyses due to low costs and litter retrieval ability, but L-F interactions are disturbed during the trawling process, thus minimising the advantages of this method (Angiolillo and Fortibuoni, 2020). The benefits of manoeuvrability and access to the deep sea make ROVs the best option for submarine canyon L-F interactions research, but their cost and variation in image resolution can be limiting factors (Canals et al., 2021). Among the 23 papers with L-F interactions in canyons, inconsistencies in taxon level reported required fauna to be compared at the phylum level, making for poor taxonomic resolution. In order to quantify and classify marine litter and L-F interactions, a combination of visual and trawling surveys may

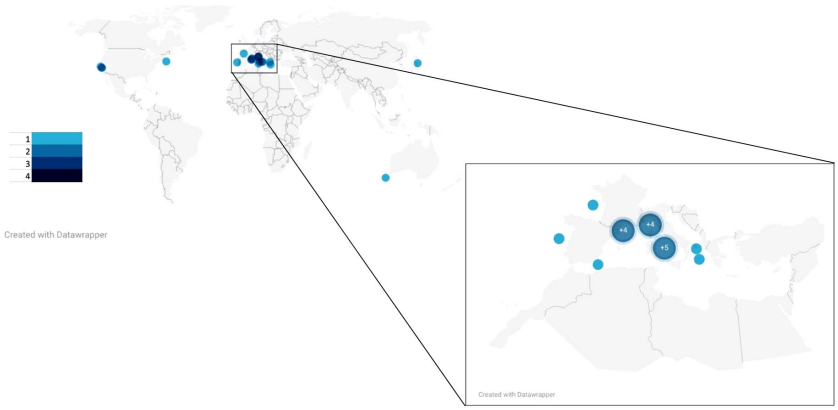

FIGURE 7
Global locations of the 23 reports of litter-fauna interactions occurring in submarine Canyons. Legend indicates the dot colour based on the number of scientific publications. Inset depicts European locations of litter-fauna interactions occurring in submarine canyons, making up 18 out of 23 total global reports. Each bubble indicates one scientific publication, unless otherwise labelled.

provide the most comprehensive results (Tubau et al., 2015). With increasingly descriptive data, even if total global reports stay low, impacts of L-F interactions on fauna and ecosystems may begin to be hypothesised and assessed. In order to better understand the existence and impacts of litter in submarine canyons, standardised reporting of litter in general (Hernandez et al., 2022), and of L-F interactions specifically, will help to start compiling standardised datasets and allow for global comparability and elucidation of trends and true ecological impact. For example, currently under negotiation is the Global Plastics Treaty, which aims to address plastic pollution worldwide (Plastics Europe, 2023); the binding legislature proposed by this treaty could benefit from a standardised framework to help in reporting and monitoring.

Marine litter mitigation

Litter finds its way to the ocean due to unsustainable, linear production and consumption processes (Thompson et al., 2011). Producers are not concerned with the end of a product's life, proper recycling centres are few and far between, and there is a disconnect between product use and far away disposal, promoting irresponsible waste practices (Thompson et al., 2011). When litter originates at sea, such as ALDFG, dumping may occur due to costliness of repairing damaged nets (Macfadyen et al., 2009), or boats not even being equipped to bring deep sea fishing nets back to shore (Brown et al., 2005). Both small- and large-scale policy and action will be required to reduce the presence of, and therefore faunal interactions with, marine litter. Mitigation strategies generally follow one of two paths: remove what is already present or stop the input of new litter, the latter of which is widely considered to be more advantageous, being more cost-effective and sustainable (United Nations Environment Programme [UNEP], 2009; Consoli et al., 2019; Hohn et al., 2020). While it will take further research to globally quantify marine litter impacts, it is advantageous to take action now to mitigate marine litter and prevent further harm than is already occurring (National Research Council [NRC], 2009; Kühn et al., 2015). A comprehensive strategy is needed that combines public-facing advocacy with shifts to circular production and consumption cycles, global litter prevention policies, and improved recycling technology, all while ensuring that each effort is conducted in a sustainable, long-lasting manner (Borrelle et al., 2020).

Limitations

Several limitations of this research must be considered to increase transparency. The literature review, though deemed exhaustive using the keywords search method, potentially missed reports of L-F interactions within submarine canyons if such reports had misaligned keywords or a lack of keywords entirely. Future literature reviews of the same topic may prevent the issue by utilising more than one search method. Of the papers read, all but one reported L-F interactions within canyons in the Northern Hemisphere, providing potential bias in trend analyses. The limited location of studies was corroborated by the results found by Hernandez et al. (2022), so a potential solution is seemingly to collate ongoing research on litter in submarine canyons and grow the dataset.

Global applicability of framework

At present, any marine L-F interactions reported globally are sporadic in timescale and in quantity of data presented. The overwhelming majority of primary data on L-F interactions in submarine canyons comes from the Mediterranean Sea. The global locations of general marine litter surveys at depths greater than 50 m presented by Hernandez et al. (2022) corroborate this finding: most sites were in the Mediterranean Sea, and research sites specifically in submarine canyons solely existed in the Northern Hemisphere. The first assessment of anthropogenic impact in Australian canyons was reported in 2022 (Taviani et al., 2023). In creating a standardised L-F interactions framework, the ease of reporting will be increased, thus encouraging L-F interactions observed to be studied and recorded. With reports from additional locations and even depths, a global dataset can begin to be compiled, helping track trends and make comparisons worldwide. Further, L-F interaction data will be critical in the creation of sensitivity and vulnerability assessments for marine flora and fauna, as the ubiquitous nature of litter in the ocean suggests impacts on biota that are not yet quantified.

The L-F interactions framework proposed and tested within the present research has the potential to be applied globally, increasing the breadth of marine litter data while encouraging standardised reporting approaches and, thus, connectivity between researchers. The body of evidence that contributed to the design of the framework reported on L-F interactions occurring in all ocean zones, from the surface to the benthos and from the shore to the open ocean. As such, the framework is applicable for use in all aquatic research, not just those studying submarine canyons. The framework is intentionally broad, providing 6 main categories of interactions, 2 of which also occur with abiotic features. Each interaction category was designed through comprehensive review of reported interactions and categories used previously. Additionally, impacts were considered in the delineation of categories; specific types of interactions within each of the 6 groupings cause similar impacts to the fauna or features involved.

Within each broad category, there is potential for subdivision based on interactions observed, which will provide higher data resolution. For example, in a location with a high incidence of encountering, such interactions may be split into the categories of contact and non-contact. Within the wide auspice of entanglement, ghost fishing or coral snagging may be separated; within the umbrella term of habitat provision, shelter vs. substrate provision may be specified. The L-F interactions framework may be added to or receive alterations as it is utilised by researchers, strengthening it for increased global applicability. Overall, we propose a 'call to action' to the submarine canyon and deep-sea researcher

community-at-large with the goal being implementation of the litter-fauna interaction framework to kickstart connectivity and comparability between researchers observing L-F interactions all over the world. Without this standardised reporting method and analysis of global trends, the types and scale of the long-term ecological impacts of marine litter cannot truly be assessed.

Author contributions

AB: research, framework creation, manuscript draft JD: conception and design of the study, manuscript editing AD: conception and design of the study, manuscript editing. All authors contributed to the article and approved the submitted version.

Conflict of interest

The authors declare that the research was conducted in the absence of any commercial or financial relationships that could be construed as a potential conflict of interest.

Publisher's note

All claims expressed in this article are solely those of the authors and do not necessarily represent those of their affiliated organizations, or those of the publisher, the editors and the reviewers. Any product that may be evaluated in this article, or claim that may be made by its manufacturer, is not guaranteed or endorsed by the publisher.

References

Andrady, A. L. (2015). "Persistence of plastic litter in the oceans," in *Marine anthropogenic litter*. Eds. M. Bergmann, L. Gutow and M. Klages (Cham: Springer), 57–72. doi: 10.1007/978-3-319-16510-3_3

Angiolillo, M., and Fortibuoni, T. (2020). Impacts of marine litter on mediterranean reef systems: From shallow to deep waters. *Front. Mar. Sci.* 7. doi: 10.3389/fmars.2020.581966

Angiolillo, M., Giusti, M., Rossi, L., and Tunesi, L. (2022). A dendrophyllia ramea population in the ionian sea (Central mediterranean sea) threatened by anthropogenic impacts. *Front. Mar. Sci.* 9. doi: 10.3389/fmars.2022.838274

Angiolillo, M., La Mesa, G., Giusti, M., Salvati, E., Di Lorenzo, B., Rossi, L., et al. (2021a). New records of scleractinian cold-water coral (CWC) assemblages in the southern Tyrrhenian Sea (western Mediterranean Sea): Human impacts and conservation prospects. *Prog. Oceanography* 197, 1–21. doi: 10.1016/j.pocean.2021.102656

Auman, H. J., Ludwig, J. P., Giesy, J. P., and Colborn, T. (1997). 'Plastic ingestion by Laysan Albatross chicks on Sand Island, Midway Atoll, in 1994 and 1995'. *Albatross Biol. Conserv.*, 239–244.

Bajaj, R., Kulkarni, N., Raut, R., and Garg, S. (2021). Sea debris: A review of marine litter detection techniques. *Int. J. Innovative Res. Technol.* 7 (8), 119–125.

Barnes, D. K. A., Galgani, F., Thompson, R. C., and Barlaz, M. (2009). Accumulation and fragmentation of plastic debris in global environments. *Philos. Trans. R. Soc. B* 364, 1985–1998. doi: 10.1098/rstb.2008.0205

Barreiros, J. P., and Raykov, V. S. (2014). Lethal lesions and amputation caused by plastic debris and fishing gear on the loggerhead turtle Caretta caretta (Linnaeus, 1758). Three case reports from Terceira Island, Azores (NE Atlantic). *Mar. pollut. Bull.* 86, 518–522. doi: 10.1016/j.marpolbul.2014.07.020

Barros, F., Santos, D., Reis, A., Martins, A., Dodonov, P., and Nunes, J. A. C. C. (2020). Choosing trash instead of nature: Sea urchin covering behavior. *Mar. pollut. Bull.* 155, 1–4. doi: 10.1016/j.marpolbul.2020.111188

Bergmann, M., and Klages, M. (2012). Increase of litter at the Arctic deep-sea observatory HAUSGARTEN. *Mar. pollut. Bull.* 64, 2734–2741. doi: 10.1016/j.marpolbul.2012.09.018

Borrelle, S. B., Ringma, J., Law, K. L., Monnahan, C. C., Lebreton, L., McGivern, A., et al. (2020). Predicted growth in plastic waste exceeds efforts to mitigate plastic pollution. *Science* 369, 1515–1518. doi: 10.1126/science.aba3656

Brown, J., Macfadyen, G., Huntington, T., Magnus, J., and Tumilty, J. (2005). *Ghost fishing by lost fishing gear, institute for european environmental policy*. Available at: https://citeseerx.ist.psu.edu/viewdoc/download?doi=10.1.1.114.8547&rep=rep1&type=pdf.

Canals, M., Pham, C. K., Bergmann, M., Gutow, L., Hanke, G., van Sebille, E., et al. (2021). The quest for seafloor macrolitter: a critical review of background knowledge, current methods and future prospects. *Environ. Res. Lett.* 16 (2), 1–29. doi: 10.1088/1748-9326/abc6d4

Carpenter, E. J., and Smith, K. L. Jr. (1972). Plastics on the sargasso sea surface. *Science* 175, 1240–1241. doi: 10.1126/science.175.4027.1240

Consoli, P., Andaloro, F., Altobelli, C., Battaglia, P., Campagnuolo, S., Canese, S., et al. (2018a). Marine litter in an EBSA (Ecologically or Biologically Significant Area) of the central Mediterranean Sea: Abundance, composition, impact on benthic species and basis for monitoring entanglement. *Environ. pollut.* 236, 405–415. doi: 10.1016/j.envpol.2018.01.097

Consoli, P., Falautano, M., Sinopoli, M., Perzia, P., Canese, S., Esposito, V., et al. (2018b). 'Composition and abundance of benthic marine litter in a coastal area of the central Mediterranean Sea'. *Mar. pollut. Bull.* 136, 243–247. doi: 10.1016/j.marpolbul.2018.09.033

Consoli, P., Romeo, T., Angiolillo, M., Canese, S., Esposito, V., Salvati, E., et al. (2019). Marine litter from fishery activities in the Western Mediterranean Sea: The impact of entanglement on marine animal forests. *Environ. pollut.* 249, 472–481. doi: 10.1016/j.envpol.2019.03.072

Consoli, P., Sinopoli, M., Deidun, A., Canese, S., Berti, C., Andaloro, F., et al. (2020). The impact of marine litter from fish aggregation devices on vulnerable marine benthic habitats of the central Mediterranean Sea. *Mar. pollut. Bull.* 152, 1–8. doi: 10.1016/j.marpolbul.2020.110928

Derraik, J. G. B. (2002). The pollution of the marine environment by plastic debris: a review. *Mar. pollut. Bull.* 44, 842–852. doi: 10.1016/S0025-326X(02)00220-5

Di Beneditto, A. P. M., and Awabdi, D. R. (2014). Marine debris, megafauna, fish, turtle, dolphins, Brazilian coastal area. *Mar. pollut. Bull.* 88 (1-2), 86–90. doi: 10.1016/j.marpolbul.2014.09.020

European Commission (2010). EU Commission Decision of 1 September 2010 on criteria and methodological standards on good environmental status of marine waters. (2010/477/EU) *Off. J. Eur. Union* 232, 1424.

European Commission (2022) *D10 Marine litter*. Available at: https://mcc.jrc.ec.europa.eu/main/dev.py?N=28&O=223&titre_chap=D10+Marine+litter.

Feldkamp, S. D., Costa, D. P., and DeKrey, G. K. (1988). Energetic and behavioral effects of net entanglement on juvenile northern fur seals, callorhinus ursinus. *Fishery Bull.* 87, 85–94.

Fernandez-Arcaya, L., Ramirez-Llodra, E., Aguzzi, J., Allcock, A. L., Davies, J. S., Dissanayake, A., et al. (2017). Ecological role of submarine canyons and need for canyon conservation: A review. *Front. Mar. Sci.* 4. doi: 10.3389/fmars.2017.00005

Fowler, C. W. (1982). "Interactions of Northern Fur seals and commercial fisheries', in Kenneth Sabol (ed.) *Transactions of the forty-third North American Wildlife and Natural Resources Conference*. Washington, DC: United States Department of Commerce. pp. 278-292.

Galgani, F., Hanke, G., and Maes, T. (2015). "Global distribution, composition and abundance of marine litter," in *Marine anthropogenic litter*. Eds. M. Bergmann, L. Gutow and M. Klages (Springer Open), 29–56. doi: 10.1007/978-3-319-16510-3_2

Galgani, F., Hanke, G., Werner, S., and De Vrees, L. (2013). Marine litter within the European Marine Strategy Framework Directive. *ICES J. Mar. Sci.* 70 (6), 1055–1064. doi: 10.1093/icesjms/fst122

Galgani, F., Leaute, P., Moguedet, P., Souplet, A., Verin, Y., Carpentier, A., et al. (2000). Litter on the sea floor along European coasts. *Mar. pollut. Bull.* 40 (6), 516–527. doi: 10.1016/S0025-326X(99)00234-9

Galgani, F., Pham, C. K., Claro, F., and Consoli, P. (2018). Marine animal forests as useful indicators of entanglement by marine litter. *Mar. pollut. Bull.* 135, 735–738. doi: 10.1016/j.marpolbul.2018.08.004

Gall, S. C., and Thompson, R. C. (2015). The impact of debris on marine life. *Mar. pollut. Bull.* 92, 170–179. doi: 10.1016/j.marpolbul.2014.12.041

Gilman, E., Chopin, F., Suuronen, P., and Kuemlangan, B. (2016). *Abandoned, lost and discarded gillnets and trammel nets: Methods to estimate ghost fishing mortality, and the status of regional monitoring and management* (Rome, Italy: Food and Agriculture Organization of the United Nations).

Gilman, E., Musyl, M., Suuronen, P., Chaloupka, M., Gorgin, S., Wilson, J., et al. (2021). Highest risk abandoned, lost and discarded fishing gear. *Sci. Rep.* 11, 1–11. doi: 10.1038/s41598-021-86123-3

Gjerde, K. M. (2006). "Ecosystems and biodiversity in deep waters and high seas," in *UNEP regional seas report and studies* (Switzerland: UNEP/IUCN).

Gramentz, D. (1988). Involvement of loggerhead turtle with the plastic, metal, and hydrocarbon pollution in the central mediterranean. *Mar. pollut. Bull.* 19 (1), 11–13. doi: 10.1016/0025-326X(88)90746-1

Green, D. S., Boots, B., Blockley, D. J., Rocha, C., and Thompson, R. (2015). Impacts of discarded plastic bags on marine assemblages and ecosystem functioning. *Environ. Sci. Technol.* 49 (9), 1–37. doi: 10.1021/acs.est.5b00277

Gregory, R. M. (2009). Environmental implications of plastic debris in marine settings –entanglement, ingestion, smothering, hangers-on, hitch-hiking and alien invasions. *Philos. Trans. R. Soc. B* 364, 2013–2025. doi: 10.1098/rstb.2008.0265

Hanke, G., Galgani, F., Werner, S., Oosterbaan, L., Nilsson, P., Fleet, D., et al. (2013). Guidance on Monitoring of Marine Litter in European Seas. *EUR 26113* Luxembourg (Luxembourg): Publications Office of the European Union. JRC83985 doi: 10.2788/99475

Harris, P. T., Macmillan-Lawler, M., Rupp, J., and Baker, E. K. (2014). 'Geomorphology of the oceans'. *Mar. Geology* 352, 4–24. doi: 10.1016/j.margeo.2014.01.011

Hernandez, I., Davies, J. S., Huvenne, V. A. I., and Dissanayake, A. (2022). Marine litter in submarine canyons: A systematic review and critical synthesis. *Front. Mar. Sci.* 9. doi: 10.3389/fmars.2022.965612

Hohn, S., Acevedo-Trejos, E., Abrams, J. F., de Moura, J. F., Spranz, R., and Merico, A. (2020). The long-term legacy of plastic mass production. *Sci. Total Environ.* 746, 1–8. doi: 10.1016/j.scitotenv.2020.141115

Holmström, A. (1975). Plastic films on the bottom of the Skagerack. *Nature* 255, 622–623. doi: 10.1038/255622a0

International Maritime Organization [IMO] (1997). *MARPOL 73/78: consolidated edition 1997* (London: International Maritime Organization), 349–355. Available at: https://vdoc.pub/download/marpol-73-78-33i5ha4808d0.

International Maritime Organization [IMO] (2019) *Convention on the prevention of marine pollution by dumping of wastes and other matter*. Available at: https://www.imo.org/en/OurWork/Environment/Pages/London-Convention-Protocol.aspx.

Joint Group of Experts on the Scientific Aspects of Marine Environmental Protection [GESAMP] (2019). *Guidelines for the monitoring and assessment of plastic litter in the ocean* (UNEP).

Katsanevakis, S. (2008). "Marine debris, a growing problem: sources, distribution, composition, and impacts," in *Marine pollution: new research*. Ed. T. N. Hofer (New York, NY: Nova Science Publishers, Inc.), 53–100.

Keller, A. A., Fruh, E. L., Johnson, M. M., Simon, V., and McGourty, C. (2010). Distribution and abundance of anthropogenic marine debris along the shelf and slope of the US West Coast. *Mar. pollut. Bull.* 60, 692–700. doi: 10.1016/j.marpolbul.2009.12.006

Koelmans, A. A., Gouin, T., Thompson, R., Wallace, N., and Arthur, C. (2013). Plastics in the marine environment. *Environ. Toxicol. Chem.* 33 (1), 5–10. doi: 10.1002/etc.2426

Kühn, S., Bravo Rebolledo, E. L., and van Franeker, J. A. (2015). "Deleterious effects of litter on marine life," in *Marine anthropogenic litter*. Eds. M. Bergmann, L. Gutow and M. Klages (Springer), 75–116.

Laist, D. W. (1987). Overview of the biological effects of lost and discarded plastic debris in the marine environment. *Mar. pollut. Bull.* 18, 319–326. doi: 10.1016/S0025-326X(87)80019-X

Lamb, J. B., Willis, B. L., Fiorenza, E. A., Couch, C. S., Howard, R., Rader, D. N., et al. (2018). Plastic waste associated with disease on coral reefs. *Science* 359 (6374), 460–462. doi: 10.1126/science.aar3320

Lartaud, F., Meistertzheim, A. L., Reichert, J., Ziegler, M., Peru, E., and Ghiglione, J. F. (2020). "Plastics: an additional threat for coral ecosystems," in *Perspectives on the marine animal forests of the world*. Eds. S. Rossi and L. Bramanti (Switzerland: Springer), 469–485. doi: 10.1007/978-3-030-57054-5_14

Macfadyen, G., Huntington, T., and Cappell, R. (2009). *Abandoned, lost or otherwise discarded fishing gear* (Rome: United Nations Environment Programme (UNEP) and Food and Agriculture Organization of the United Nations (FAO). Available at: https://wedocs.unep.org/bitstream/handle/20.500.11822/13603/rsrs185r.pdf?sequence=1&amp%3BisAllowed.

Marin, P., and Aguilar, R. (2012). "Mediterranean submarine canyons 2012: pending protection," in *Mediterranean submarine canyons*. Ed. M. Würtz (Gland, Switzerland and Málaga, Spain: IUCN), 191–205.

Matthews, T. R., and Doyle, E. (2012). Marine litter in the caribbean: Five case studies. *Proc. 64th Gulf Caribbean Fisheries Institute*, 64, 172–179.

Melli, V., Angiolillo, M., Ronchi, F., Canese, S., Giovanardi, O., Querin, S., et al. (2017). The first assessment of marine debris in a Site of Community Importance in the north-western Adriatic Sea (Mediterranean Sea). *Mar. pollut. Bull.* 114 (2), 821–830. doi: 10.1016/j.marpolbul.2016.11.012

Morris, J., and Seasholes, B. (2014). *How green is that grocery bag ban? An assessment of the environmental and economic effects of grocery bag bans and taxes* (Reason Foundation). Available at: https://reason.org/wp-content/uploads/2014/06/how_green_bag_ban.pdf.

Moschino, V., Riccato, F., Fiorin, R., Nesto, N., Picone, M., Boldrin, A., et al. (2019). Is derelict fishing gear impacting the biodiversity of the Northern Adriatic Sea? An answer from unique biogenic reefs. *Sci. Total Environ.* 663, 387–399. doi: 10.1016/j.scitotenv.2019.01.363

National Research Council [NRC] (2009). *Tackling marine debris in the 21st century* (Washington, D.C: The National Academies Press).

Nevill, J. (2011). *Submission to the select committee on marine parks in south Australia* (Victoria, Australia: OnlyOnePlanet Consulting). Available at: http://www.onlyoneplanet.com/marineSAsubmissionMPAs_2011.pdf.

North Pacific Fishery Management Council [NPFMC] (2011). *Appendix C: non-fishing effects on EFH in the arctic* (Arctic FMP). Available at: https://media.fisheries.noaa.gov/dam-migration/arctic1-fmp-akr.pdf.

Page, M. J., McKenzie, J. E., Bossuyt, P. M., Boutron, I., Hoffmann, T. C., Mulrow, C. D., et al. (2021). The PRISMA 2020 statement: an updated guideline for reporting systematic reviews. *BMJ* 372 (71). doi: 10.1136/bmj.n71

Pham, C. K., Ramirez-Llodra, E., Alt, C. H. S., Amaro, T., Bergmann, M., Canals, M., et al. (2014). Marine litter distribution and density in European seas, from the shelves to deep basins. *PloS One* 9 (4), 1–13. doi: 10.1371/journal.pone.0095839

Pierdomenico, M., Casalbore, D., and Chiocci, F. L. (2019). Massive benthic litter funnelled to deep sea by flash-flood generated hyperpycnal flows. *Sci. Rep.* 9, 1–10. doi: 10.1038/s41598-019-41816-8

Plastics Europe (2023) *The global plastics treaty*. Available at: https://plasticseurope.org/changingplasticsforgood/global-plastics-treaty/.

Ramirez-Llodra, E. (2020). "Deep-sea ecosystems: biodiversity and anthropogenic impacts," in *The law of the seabed*. Ed. C. Banet (Netherlands: Brill-Nijhoff), 36–60. doi: 10.1163/9789004391567_004

Ramirez-Llodra, E., Tyler, P. A., Baker, M. C., Bergstad, O. A., Clark, M. R., Escobar, E., et al. (2011). 'Man and the last great wilderness: Human impact on the deep sea'. *PloS One* 6 (7), 1–25. doi: 10.1371/journal.pone.0022588

Rochman, C. M., Browne, M. A., Halpern, B. S., Hentschel, B. T., Hoh, E., Karapanagioti, H. K., et al. (2013). Classify plastic waste as hazardous. *Nature* 494, 169–171. doi: 10.1021/es303700s

Ryan, P. G. (2015). "A brief history of marine litter research," in *Marine anthropogenic litter*. Eds. M. Bergmann, L. Gutow and M. Klages (Cham: Springer), 1–25. doi: 10.1007/978-3-319-16510-3_1

Ryan, P. G., and Moloney, C. L. (1993). Marine litter keeps increasing. *Nature* 361, 23. doi: 10.1038/361023a0

Savini, A., Vertino, A., Marchese, F., Beuck, L., and Freiwald, A. (2014). Mapping Cold-Water Coral Habitats at Different Scales within the Northern Ionian Sea (Central Mediterranean): An Assessment of Coral Coverage and Associated Vulnerability. *PloS One* 9. doi: 10.1371/journal.pone.0087108

Sazima, I., Gadig, O. B. F., Namora, R. C., and Motta, F. S. (2002). Plastic debris collars on juvenile carcharhinid sharks (*Rhizoprionodon lalandii*) in southwest Atlantic. *Mar. pollut. Buletin* 44, 1147–1149. doi: 10.1016/S0025-326X(02)00141-8

Sherrington, C., Darrah, C., Hann, S., Cole, G., and Corbin, M. (2016). "Study to support the development of measures to combat a range of marine litter sources," in *Report for european commission DG environment*. Available at: https://www.kosmopedia.org/wp-content/uploads/2020/09/MSFD-Measures-to-Combat-Marine-Litter.pdf.

Tekman, M. B., Krumpen, T., and Bergmann, M. (2017). Marine litter on deep Arctic seafloor continues to increase and spreads to the North at the HAUSGARTEN observatory. *Deep-Sea Res. I* 120, 88–99. doi: 10.1016/j.dsr.2016.12.011

Thompson, R. C., La Belle, B. E., and Bouwman, H. (2011). "Marine debris: defining a global environmental challenge," in *A STAP advisory document* (Nairobi: UNEP), 1–28. Available at: https://www.thegef.org/sites/default/files/council-meeting-documents/C.40.Inf_.14_Marine_Debris.pdf.

Tubau, X., Canals, M., Lastras, G., Rayo, X., Rivera, J., and Amblas, D. (2015). Marine litter on the floor of deep submarine canyons of the Northwestern Mediterranean Sea: The role of hydrodynamic processes. *Prog. Oceanography* 134, 379–403. doi: 10.1016/j.pocean.2015.03.013

Unger, B., Herr, H., Benke, H., Böhmert, M., Burkhardt-Holm, P., Dähne, M., et al. (2017). Marine debris in harbour porpoises and seals from German waters. *Mar. Environ. Res.* 130, 77–84. doi: 10.1016/j.marenvres.2017.07.009

United Nations Environment Programme [UNEP] (2009). *Marine litter: A global challenge* (Nairobi: UNEP), 1–234.

United Nations Environment Programme [UNEP] and National Oceanic and Atmospheric Administration [NOAA] (2012) *The Honolulu Strategy: A global framework for prevention and management of marine debris*. Available at: https://wedocs.unep.org/20.500.11822/10670.

van den Beld, I. (2017). *Coral habitats in submarine canyons of the Bay of Biscay: distribution, ecology and vulnerability* (Université de Bretagne Occidentale).

Venrick, E. L., Backman, T. W., Bartram, W. C., Platt, C. J., Thornhill, M. S., and Yates, R. E. (1973). Man-made objects on the surface of the central North Pacific ocean. *Nature* 241, 271. doi: 10.1038/241271a0

Vetter, E. W., Smith, C. R., and De Leo, F. C. (2010). Hawaiian hotspots: enhanced megafaunal diversity in submarine canyons on the oceanic islands of Hawaii. *Mar. Ecol.* 31, 183–199. doi: 10.1111/j.1439-0485.2009.00351.x

Vieira, R. P., Raposo, I. P., Sobral, P., Gonçalves, J. M. S., Bell, K. L. C., and Cunha, M. R. (2014). Lost fishing gear and litter at Gorringe Bank (NE Atlantic). *J. Sea Res.* 100, 91–98. doi: 10.1016/j.seares.2014.10.005

Watson, M. (2012). *Marine debris along the florida keys reef tract- mapping, analysis and perception study* (University of Miami).

Woodall, L. C., Robinson, L. F., Rogers, A. D., Narayanaswamy, B. E., and Paterson, G. L. J. (2015). Deep-sea litter: a comparison of seamounts, banks and a ridge in the Atlantic and Indian Oceans reveals both environmental and anthropogenic factors impact accumulation and composition. *Front. Mar. Sci.* 2 (3). doi: 10.3389/fmars.2015.00003

Appendix A Systematic review references

Angiolillo, M., di Lorenzo, B., Farcomeni, A., Bo, M., Bavestrello, G., Santangelo, G., et al. (2015). Distribution and assessment of marine debris in the deep Tyrrhenian Sea (NW Mediterranean Sea, Italy). *Mar. pollut. Bull.* 92, 149–159. doi: 10.1016/j.marpolbul.2014.12.044

Angiolillo, M., Gérigny, O., Valente, T., Fabri, M.-C., Tambute, E., Rouanet, E., et al. (2021b). Distribution of seafloor litter and its interaction with benthic organisms in deep waters of the Ligurian Sea (Northwestern Mediterranean). *Sci. Total Environ.* 788, 1–20. doi: 10.1016/j.scitotenv.2021.147745

Cau, A., Alvito, A., Moccia, D., Canese, S., Pusceddu, A., Rita, C., et al. (2017). Submarine canyons along the upper Sardinian slope (Central Western Mediterranean) as repositories for derelict fishing gears. *Mar. pollut. Bull.* 123, 357–364. doi: 10.1016/j.marpolbul.2017.09.010

Cerrillo-Escoriza, J., Lobo, F. J., Puga-Bernabéu, Á., Rueda, J. L., Bárcenas, P., Sánchez-Guillamón, O., et al. (2023). Origin and driving mechanisms of marine litter in the shelf-incised Motril, Carchuna, and Calahonda canyons (northern Alboran Sea). *Front. Mar. Sci.* doi: 10.3389/fmars.2023.1098927

D'Onghia, G., Calculli, C., Capezzuto, F., Carlucci, R., Carluccio, A., Grehan, A., et al. (2017). Anthropogenic impact in the Santa Maria di Leuca cold-water coral province (Mediterranean Sea): Observation and conservation straits. *Deep Sea Res. Part II: Topical Stud. Oceanography* 145, 87–101. doi: 10.1016/j.dsr2.2016.02.012

Enrichetti, F., Dominguez-Carrió, C., Toma, M., Bavestrello, G., Canese, S., and Bo, M. (2020). Assessment and distribution of seafloor litter on the deep Ligurian continental shelf and shelf break (NW Mediterranean Sea). *Mar. pollut. Bull.* 151, 1–14. doi: 10.1016/j.marpolbul.2019.110872

Fabri, M.-C., Pedal, L., Beuck, L., Galgani, F., Hebbeln, D., and Freiwald, A. (2014). Megafauna of vulnerable marine ecosystems in French mediterranean submarine canyons: Spatial distribution and anthropogenic impacts. *Deep Sea Res. Part II: Topical Stud. Oceanography* 104, 184–207. doi: 10.1016/j.dsr2.2013.06.016

Giusti, M., Canese, S., Fourt, M., Bo, M., Innocenti, C., Goujard, A., et al. (2019). Coral forests and Derelict Fishing Gears in submarine canyon systems of the Ligurian Sea. *Prog. Oceanography* 178, 1–16. doi: 10.1016/j.pocean.2019.102186

Lastras, G., Canals, M., Ballesteros, E., Gili, J.-M., and Sanchez-Vidal, A. (2016). Cold-water corals and anthropogenic impacts in la fonera submarine canyon head, Northwestern mediterranean sea. *PloS One* 11 (5), 1–36. doi: 10.1371/journal.pone.0155729

Moccia, D., Cau, A., Bramanti, L., Carugati, L., Canese, S., Follesa, M. C., et al. (2021). Spatial distribution and habitat characterization of marine animal forest assemblages along nine submarine canyons of Eastern Sardinia (central Mediterranean Sea). *Deep Sea Res. Part I: Oceanographic Res. Papers* 167. doi: 10.1016/j.dsr.2020.103422

Mordecai, G., Tyler, P. A., Masson, D. G., and Huvenne, V. E. I. (2011). Litter in submarine canyons off the west coast of Portugal. *Deep-Sea Res. II* 58, 2489–2496. doi: 10.1016/j.dsr2.2011.08.009

Orejas, C., Gori, A., Lo Iacono, C., Puig, P., Gili, J.-M., and Dale, M. R. T. (2009). Cold-water corals in the Cap de Creus canyon, northwestern Mediterranean: spatial distribution, density and anthropogenic impact. *Mar. Ecol. Prog. Ser.* 397, 37–51. doi: 10.3354/meps08314

Pierdomenico, M., Cardone, F., Carluccio, A., Casalbore, D., Chiocci, F., Maiorano, P., et al. (2018). Megafauna distribution along active submarine canyons of the central Mediterranean: relationships with environmental variables. *Prog. Oceanography* 171, 49–69. doi: 10.1016/j.pocean.2018.12.015

Quattrini, A. M., Nizinski, M. S., Chaytor, J. D., Demopoulos, A. W. J., Roark, E. B., France, S. C., et al. (2015). Exploration of the canyon-incised continental margin of the Northeastern United States reveals dynamic habitats and diverse communities. *PloS One* 10 (10), 1–32. doi: 10.1371/journal.pone.0139904

Ramirez-Llodra, E., De Mol, B., Company, J. B., Coll, M., and Sardà, F. (2013). Effects of natural and anthropogenic processes in the distribution of marine litter in the deep Mediterranean Sea. *Prog. Oceanography* 118, 273–287. doi: 10.1016/j.pocean.2013.07.027

Santín, A., Grinyó, J., Bilan, M., Ambroso, S., and Puig, P. (2020). First report of the carnivorous sponge *Lycopodina hypogea* (Cladorhizidae) associated with marine debris, and its possible implications on deep-sea connectivity. *Mar. pollut. Bull.* 159, 1–7. doi: 10.1016/j.marpolbul.2020.111501

Schlining, K., von Thun, S., Kuhnz, L., Schlining, B., Lundssten, L., Stout, N. J., et al. (2013). Debris in the deep: Using a 22-year video annotation database to survey marine litter in the Monterey Canyon, central California, USA. *Deep-Sea Res. I* 79, 96–105. doi: 10.1016/j.dsr.2013.05.006

Taviani, M., Angeletti, L., Canese, S., Cannas, R., Cardone, F., Cau, A., et al. (2017). The "Sardinian cold-water coral province" in the context of the Mediterranean coral ecosystems. *Deep-Sea Res. II* 145, 61–78. doi: 10.1016/j.dsr2.2015.12.008

Taviani, M., Angeletti, L., Cardone, F., Montagna, P., and Danovaro, R. (2019). A unique and threatened deep water coral-bivalve biotope new to the Mediterranean Sea offshore Naples megalopolis. *Sci. Rep.* 9 (1), 1–12. doi: 10.1038/s41598-019-39655-8

Taviani, M., Foglini, F., Castellan, G., Montagna, P., McCulloch, M. T., and Trotter, J. A. (2023). First assessment of anthropogenic impacts in submarine canyon systems off southwestern Australia. *Sci. Total Environ.* 857 (1), 1–12. doi: 10.1016/j.scitotenv.2022.159243

Taylor, J. R., DeVogelaere, A. P., Burton, E. J., Frey, O., Lundsten, L., Kuhnz, L. A., et al. (2014). Deep-sea faunal communities associated with a lost intermodal shipping container in the Monterey Bay National Marine Sanctuary, CA. *Mar. pollut. Bull.* 83 (1), 92–106. doi: 10.1016/j.marpolbul.2014.04.014

van den Beld, I. M. J., Guillaumont, B., Menot, L., Bayle, C., Arnaud-Haond, S., and Bourillet, J.-F. (2017). Marine litter in submarine canyons of the Bay of Biscay. *Deep-Sea Res. II* 145, 142–152. doi: 10.1016/j.dsr2.2016.04.013

Watters, D. L., Yoklavich, M. M., Love, M. S., and Schroeder, D. M. (2010). Assessing marine debris in deep seafloor habitats off California. *Mar. pollut. Bull.* 60, 131–138. doi: 10.1016/j.marpolbul.2009.08.019

Frontiers in Marine Science

Explores ocean-based solutions for emerging global challenges

The third most-cited marine and freshwater biology journal, advancing our understanding of marine systems and addressing global challenges including overfishing, pollution, and climate change.

Discover the latest Research Topics

See more →

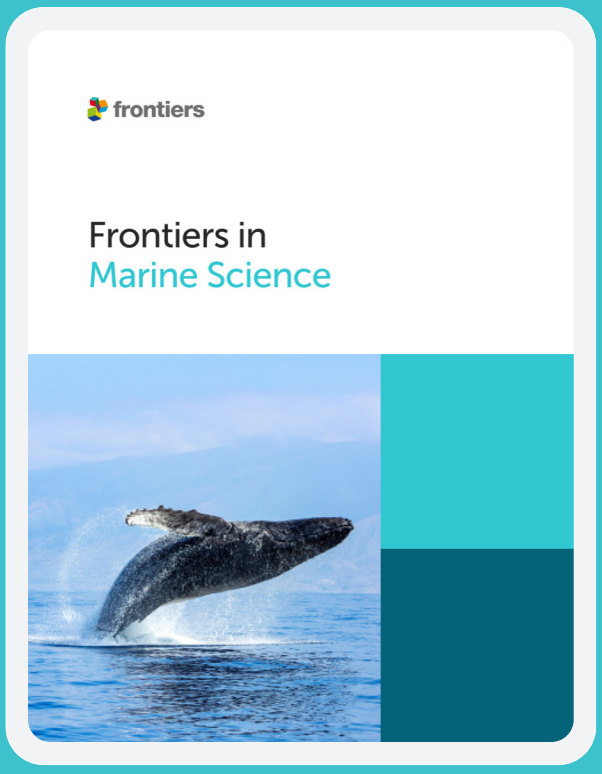

Frontiers

Avenue du Tribunal-Fédéral 34
1005 Lausanne, Switzerland
frontiersin.org

Contact us

+41 (0)21 510 17 00
frontiersin.org/about/contact